Tectonic-sedimentary evolution of the northern margin of Gondwana during Late Palaeozoic – Early Cenozoic time in the Eastern Mediterranean region: evidence from the Central Taurus Mountains, Turkey.

Peter W. Mackintosh

Thesis submitted for the degree of Doctor of Philosophy

The University of Edinburgh

2008

I declare that this thesis has been written by myself and is the result of my own research, except where contributions have been stated and duly acknowledged.

Peter W. Mackintosh

Abstract

The Taurus Mountains are an E-W trending mountain range in southern Turkey, with an elevation of up to 3500 m. In the south central Taurides, the Beyşehir-Hoyran-Hadim nappes, a series of thrust sheets of Palaeozoic to Early Cenozoic age, are emplaced onto a relatively autochthonous Tauride platform, known as the Geyik Dağ. These thrust sheets consist of a variety of discrete tectonostratigraphic units of continental platform, rifted margin and oceanic (ophiolitic) origin. It is generally accepted that the relatively autochthonous Tauride platform and the associated thrust sheets restore as a north-facing passive margin during Jurassic–Cretaceous time; however, the Triassic and earlier tectonic setting of the Tauride units is contentious. New data (mainly structural and sedimentological) presented here tests contrasting tectonic models of Late Palaeozoic – Early Mesozoic Tethys ocean evolution. Also, new light is shed on the Late Cretaceous and Early Cenozoic break-up and emplacement of the Tauride units during closure of Tethys.

The Late Palaeozoic Tauride stratigraphy consists of shallow-marine carbonate, sandstone and mudstone, characteristic of a proximal passive margin. Detailed stratigraphic logging, facies interpretation, compositional analysis and geochemical evidence supports a passive margin setting, with sediment derived from the Tauride "basement". Early – Middle Triassic mixed siliciclastic/carbonate sediments are interpreted as representing rifting and subsidence. Late Triassic coarser terrestrial clastics (Çayır Formation) are considered to represent a pulse of rift-related flexural uplift. Sediment provenance during this time was from the underlying Tauride platform to the north of the studied area. A previous hypothesis that a Palaeotethyan ocean closed in this area during latest Triassic "Cimmerian" orogenesis is discounted. Instead, structural and sedimentary data suggest that all of the deformation relates to Late Cretaceous – Early Cenozoic southward emplacement of the Beyşehir-Hoyran-Hadim nappes. A first phase of thrusting (thin-skinned) emplaced ophiolite and distal margin units, whilst a second phase (thick-skinned) thrust platform lithologies southwards onto the foreland. Evidence is also summarised, notably from the Palaeozoic – Early Mesozoic Konya Complex to the north, which illustrates the relation of the Tauride platform to other geological terranes in Turkey and elsewhere in the Alpine-Himalayan orogenic belt. This thesis increases understanding of large-scale tectonic and sedimentary processes associated with continental margins and orogenic development.

Acknowledgements

There are many people whom without this project would not be a success.

Firstly, thank you Alastair Robertson for your supervision, enthusiasm, patience and teaching which has moulded me into a geologist; working with you in the field was an absolute pleasure, and taught me more than any textbook could.

Thank you to my other Edinburgh-based supervisors, John Dixon and John Underhill, for useful discussion and advice. Thanks to Hugh Sinclair for being my advisor of studies.

My fieldwork in Turkey would not be possible without the help of Ulvi Can Ünlügenç and his family. Thank you for making me so welcome in Adana, for all the logistical support, and for getting me out of some awkward situations!

A huge thank you to my Turkish field assistants – Mustafa Kavuzlu, Turgut Aksu and Özcan Aşik – it was great to make such good friends. At Çukurova Üniversitesi, thank you to Ozman Parlak, Fatih Karaoğlan and numerous other scientists who offered help and advice. Thank you also to Timur Ustaömer at Istanbul Üniversitesi for valuable discussion. At Mersin Üniversitesi, thank you to Kemal Tasli, Nurdan İnan and Hayati Koç.

Back in Edinburgh, thanks to Nic Odling for teaching me geochemical techniques; Mike Hall for preparation of thin-sections; and to all the other members of staff who have helped me at some point or another. Thank you Mark Hempton for useful discussions.

Thank you to the rest of the Tethyan research group for all the good times: Tim Kinnaird, Gillian McCay, Sarah Boulton, Sam Rice and Steve Nairn. Thanks Ciaran for 'pimping' my palaeocurrent data! Many thanks to my proof-readers, and all the other PhD students in the department for making the last three-and-a-bit years so enjoyable.

This project was funded by NERC, with additional sponsorship from Shell; to both I am extremely grateful.

A huge thanks to all my family for supporting me during my extensive University career.

Finally, and most importantly, thank you Claire for all your love and support.

Contents

1 Introduction

1.1 Rationale

The Eastern Mediterranean region provides valuable insights of important geological processes such as continental rifting, passive margin subsidence, active margin subduction-accretion, ophiolite genesis and obduction and continental collision. It also documents the development and evolution of a key orogenic belt. In this region, the interaction between tectonics, sedimentation, magmatism and metamorphism are crucial to our understanding of tectonic processes. Despite extensive work in the Eastern Mediterranean region by numerous authors over several decades, debate still arises over its tectonic evolution, especially from Palaeozoic to present. An important juncture has been reached whereby conflicting models now require critical testing to increase our understanding of major tectonic events. In particular, debate arises over Gondwana-related terranes, and whether they were formed in an active or passive continental margin setting.

Continental margins contain information on a variety of sedimentary environments, ranging from terrestrial to deep-sea. For example, they record interactions between faulting and sedimentation, and the effects of sea-level changes. They can also document compression-or extension-related magmatism and deformation. This thesis will focus on the tectono-stratigraphic development of the ancient Tauride continental margin, a Gondwana-related terrane which is preserved in the Tethyan orogenic belt of southern Turkey. Critical new information from both autochthonous and allochthonous units will be used to test conflicting tectonic models of Tethys evolution, and to restore the Tauride continental margin to its original pre-orogenic setting. This thesis hopefully broadens our understanding of large-scale tectonic processes associated with continental margins and orogenic development.

1.2 Geology of Turkey

Turkey is part of the Alpine-Himalayan orogenic belt which stretches from southern Spain to China (Fig. 1.1). It is located between the Eastern Mediterranean Sea in the south and the Black sea in the north (Fig. 1.2). This orogen, or 'suture zone', contains the remnants of the Tethys ocean, a Palaeozoic – Early Cenozoic westward-narrowing ocean that separated the ancient supercontinents of Eurasia in the north and Gondwana in the south. Within the orogen are a huge variety of geological terranes including rifted margins, continental fragments, accretionary complexes, arcs, foreland basins and ophiolites.

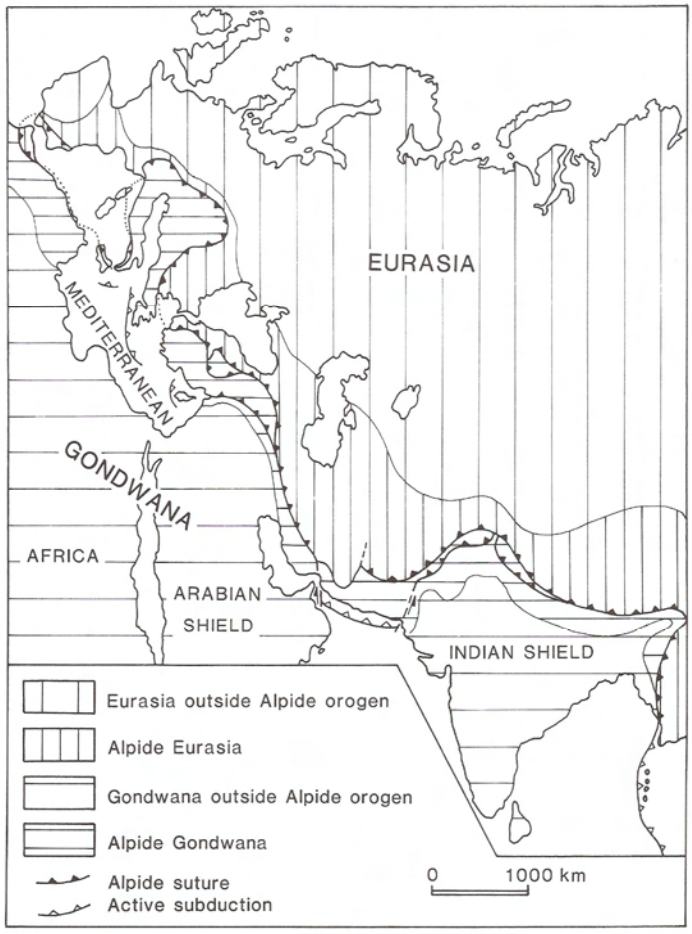

Fig. 1.1. The Alpine-Himalayan orogenic belt, with major sutures indicated. Diagram from Pickett (1994).

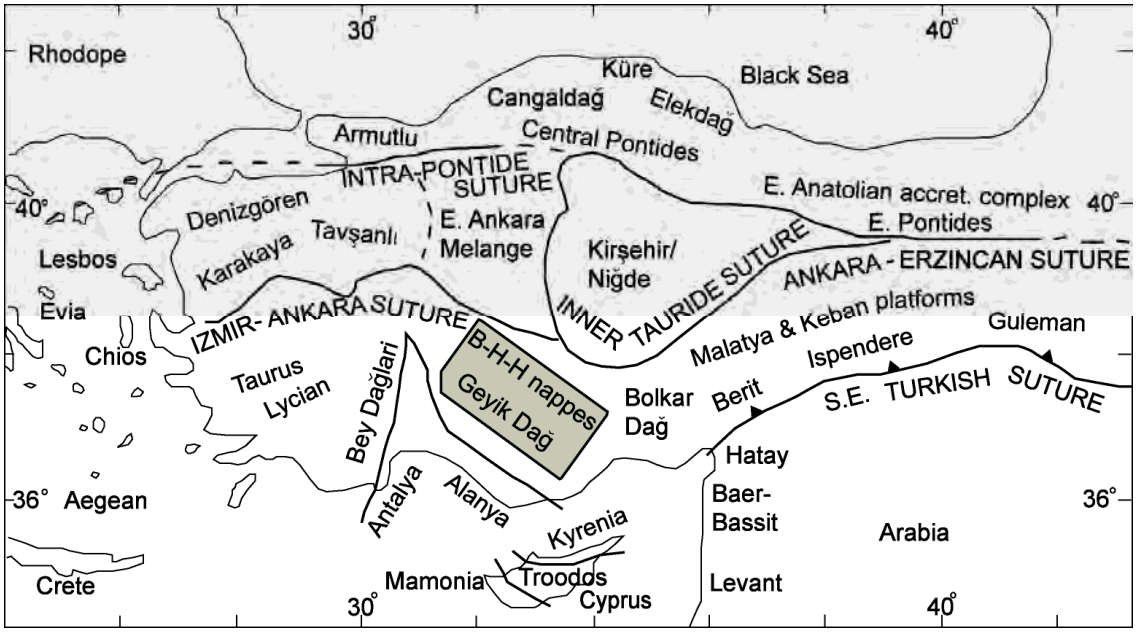

Fig. 1.2. The main tectonic zones in the Eastern Mediterranean region, with the study area in the Central Taurides highlighted (shaded box). 'B-H-H' stands for 'Beyşehir-Hoyran-Hadim'. Modified from Robertson et al. (2006).

The Taurus Mountains, also known as the Toros Dağları, are an E-W trending mountain range in the south of Turkey, with an elevation of up to 3500 m. In the south-central Taurus, the Beyşehir-Hoyran-Hadim nappes represent a series of thrust sheets of Palaeozoic to Early Cenozoic age that were emplaced onto the relatively autochthonous Tauride platform, known as the Geyik Dağ. These nappes consist of a variety of discrete tectonostratigraphic units of carbonate platform, marginal and oceanic (e.g. ophiolitic) origins. It is generally accepted that the relatively autochthonous Tauride platform and associated thrust sheets restore as a north-facing passive margin, at least during Jurassic–Cretaceous time (Şengör and Yılmaz, 1981; Robertson and Dixon, 1984; Dercourt et al., 1993; Stampfli et al., 2001; Andrew and Robertson, 2002; Göncüoğlu et al., 2003; Okay et al., 2006). However, the Triassic and earlier tectonic setting of these Tauride units is contentious. This study focuses on the structure and sedimentology of the Beyşehir-Hoyran-Hadim nappes and the regional autochthon between the towns of Beyşehir and Hadim (Fig. 1.3), with the aim of reconstructing the tectonic setting of the Tauride continental margin during two critical periods: Carboniferous and Triassic. This thesis

will also investigate the Late Cretaceous and Early Cenozoic deformation and emplacement of the Tauride platform during closure of the Tethys ocean.

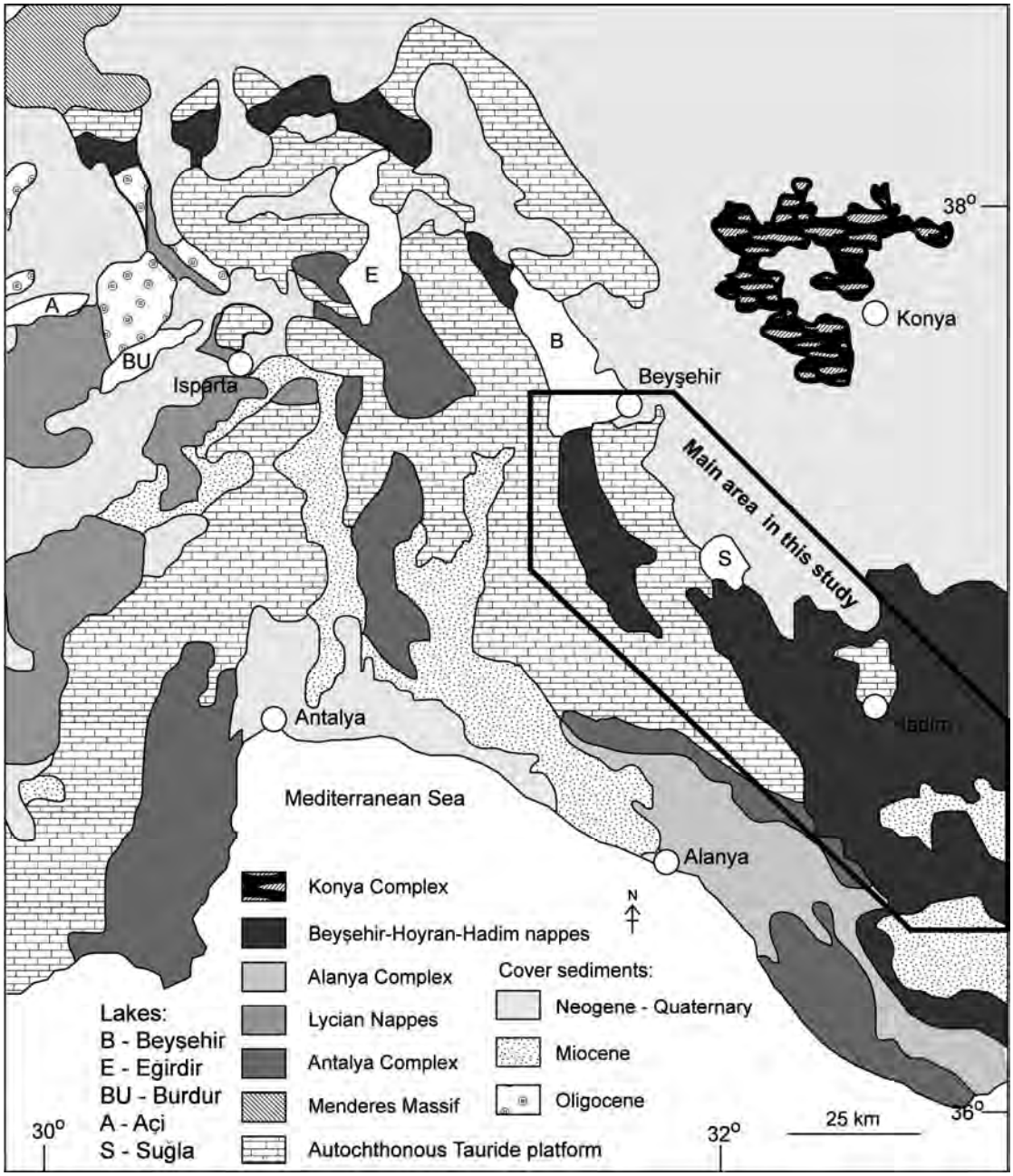

Fig. 1.3. Distribution of main tectonostratigraphic units and age of cover sediments in the south-central Tauride mountains. The main study area highlighted in box.

1.3 Alternative Tethyan models

Tethyan nomenclature has, until recently, been somewhat confusing due to oceanic basins of the same age being called different names. The terms 'Palaeotethys' and 'Neotethys', in particular, mean different things to different authors. This thesis will use a nomenclature suggested by Robertson and Mountrakis (2006) whereby 'Palaeotethys' refers to oceanic crust of Late Palaeozoic – Early Mesozoic age, whereas 'Neotethys' refers to oceanic basins that are Early Mesozoic or younger.

A variety of models exist for the Late Palaeozoic – Early Cenozoic evolution of Tethys. At the beginning of each chapter, the applicable models for each time period (Carboniferous; Triassic; Late Triassic; Late Cretaceous – Early Cenozoic) will be introduced. It is useful to set the scene here by describing the four most currently discussed Tethyan tectonic reconstructions (Fig. 1.4).

In one model (Şengör et al., 1984), a Palaeotethyan ocean was subducted southwards beneath an active Gondwanan margin during Late Palaeozoic – Early Mesozoic, which resulted in back-arc rifting. A large continental fragment known as "Cimmeria" drifted northwards during the Triassic opening a "Neotethys ocean" to the south. By the Late Triassic, continuous southward subduction of Palaeotethys had resulted in the suturing of the Eurasian margin with the Cimmerian continental fragment (Fig. 1.4a). The Tauride unit was part of a continental terrane known as the Tauride-Anatolide platform, which sutured with the Cimmerian continent in the Late Triassic. During the Jurassic – Cretaceous there was a switch to northwards subduction both in an intra-oceanic setting, and along the Eurasian margin. This is the only model which involves southward subduction as the dominant tectonic regime during Late Palaeozoic – Mesozoic.

In other tectonic models, subduction polarity was predominantly northwards beneath the Eurasian continental margin. In a second model (Dercourt et al., 1993), the Tethys ocean formed a single oceanic basin during the Mesozoic (Fig. 1.4b). The Gondwana margin remained passive during the Late Palaeozoic – Early Mesozoic, whilst northwards subduction occurred beneath Eurasia. The Tauride platform was part

of the Gondwana margin from the Late Palaeozoic to Cretaceous, before rifting separated a series of microcontinents from the margin in the Upper Cretaceous. In this model Jurassic and Cretaceous ophiolites were all derived from a single ocean ridge (Ricou, 1996).

In a third model (Stampfli, 2000; Stampfli et al., 2001; Stampfli and Borel, 2002), Palaeotethyan oceanic crust was subducted northwards beneath Eurasia during the Late Palaeozoic. A "Cimmerian" continental fragment, including the Tauride platform, rifted from the north-east margin of Gondwana, opening a wide southern Neo-Tethys ocean during the Late Permian – Early Triassic time (Fig. 1.4c), whilst northerly subduction continued. An "Anatolide" block, a Eurasian-derived continental margin unit, drifted southwards opening a back-arc basin (Küre basin) during Middle–Late Triassic time. Palaeotethys was sutured during the Late Triassic (Fig. 1.4c), when Eurasian and Gondwanan derived continental fragments collided during a so called "Cimmerian orogeny". Northward subduction continued during the Jurassic – Cretaceous and Early Cenozoic.

In a fourth model (Robertson et al., 2004) a Palaeozoic Tethys ocean subducted northwards under Eurasia from Late Palaeozoic to Triassic (Fig. 1.4d). A combined Tauride–Anatolide platform was separated from Gondwana by a small oceanic basin to the south during the Triassic (Southern Neotethys). Further north, continental fragments drifted across Palaeotethys (e.g. Çal unit of the Karakaya complex) until they collided with the Eurasian active margin prior to latest Triassic. During the Mesozoic, the south Tethys ocean was characterised by a series of oceanic basins and microcontinents. The Tauride-Anatolide unit, however, remained in a southerly location and experienced a rift-related passive margin evolution within this evolving Tethys ocean.

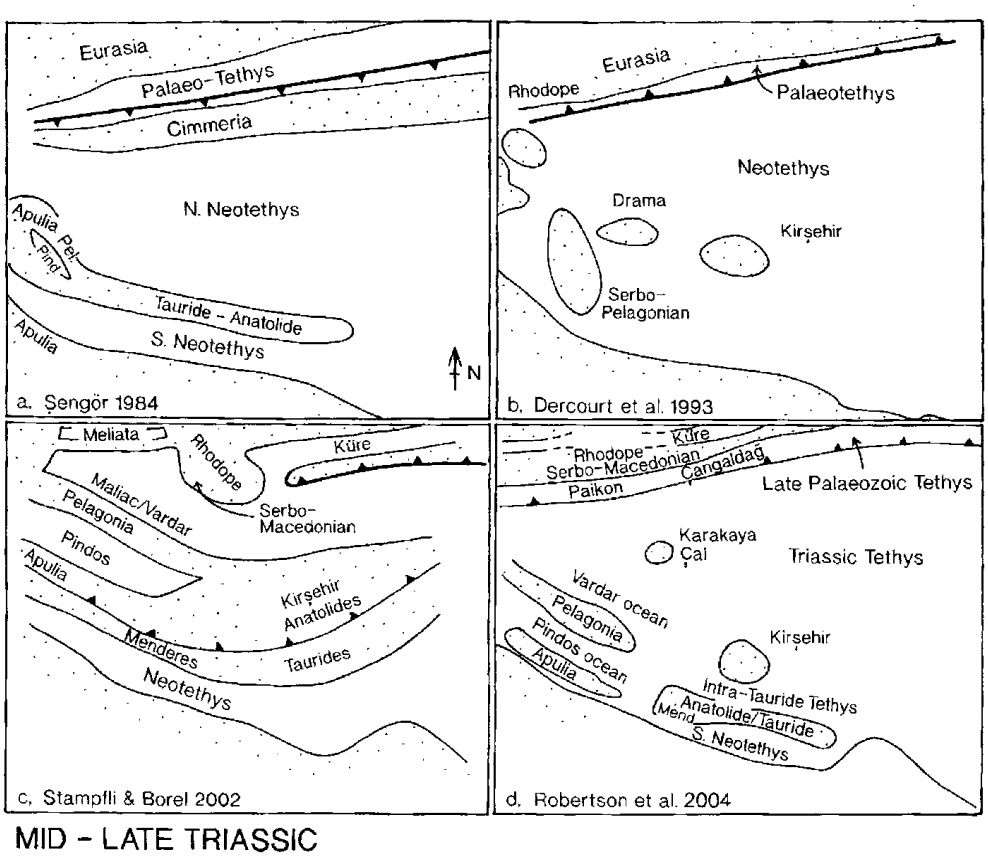

Fig. 1.4. Alternative tectonic models of Tethys in the Eastern Mediterranean during Middle – Late Triassic, from Robertson and Mountrakis (2006). a. Şengör et al., 1984. b. Dercourt et al., 1993. c. Stampfli & Borel, 2002. d. Robertson et al., 2004.

1.4 Methodology

This project is based on new fieldwork undertaken in the central Tauride mountains over 6 months between 2004 – 2006. Field investigation included the production of new geological maps, stratigraphic logging, structural and sedimentological data measurement, sample collection and field checking of previous literature. In addition, literature resources and maps were accessed at Çukurova Üniversitesi in the city of Adana, Turkey. Laboratory work on samples was carried out at the University of Edinburgh, including X-ray fluorescence, X-ray diffraction and thin-section analysis.

Thin sections that contained microfossils were sent to Mersin Üniversitesi in Turkey, where they were dated by the palaeontologists Kemal Tasli and Nurdan İnan.

1.5 Thesis Organisation

Each chapter in this thesis has been written with the intention of being submitted for publication. For this reason, each starts with an introduction to the related aspect of Tethyan evolution, and different models are discussed. Following relevant data presentation, each chapter has a self-contained discussion which includes regional literature and relevant comparisons. It is thus intended that each chapter can be read as a 'stand-alone' article. This means that the discussion chapter at the end of this thesis is an extended summary and review, rather than a 'traditional' discussion of the whole thesis.

Chapter 2 introduces the regional tectonostratigraphy of the central Tauride mountains. A review of the previous literature introduces the tectonic units and correlates them across the study area. Formation names, ages, basic structural and stratigraphic relationships and fauna are reviewed; however, detailed descriptions are provided in subsequent chapters.

Chapter 3 discusses the Late Palaeozoic evolution of the Tauride platform, with particular emphasis on the Carboniferous period. **Chapter 4** concerns the Triassic evolution of the platform, primarily providing new sedimentary facies evidence.

Chapter 5 covers the emplacement and structural history of the Tauride platform, and includes an integrated study of sedimentological and structural data.

Chapter 6 is an extended summary and review of the previous chapters, that also provides critical regional evidence to support individual chapter conclusions. A model of regional Tethyan evolution is presented based on the findings of this thesis. **Chapter 7** itemises the conclusions. **References** follow, plus an **Appendix.** The Appendix includes a complete manuscript of a paper that is currently in review in *Tectonophysics* (Mackintosh and Robertson, submitted) based on work presented elsewhere in the thesis.

1.6 Turkish pronunciation

These are some of the more common pronunciations of Turkish words in the thesis, along with sounds produced by individual letters, some of which that are not in the English alphabet.

Letters:

c/C: pronounced 'j' as in judge.

ç/Ç: pronounced "ch", as in church.

ğ/Ğ: essentially a silent "g", and lengthens the sound of the preceding vowel.

ı/I: pronounced "i" as in cousin.

i/İ: pronounced "i" as in git.

ö/Ö: pronounced "e" as in Bert.

ş/Ş: pronounced "sh" as in flash.

ü/Ü: pronounced "oe" as in shoe.

Towns / key words:

Beyşehir: pronounced *Bay-sh-here*.	Town name; *şehir* translates as 'city'.
Çayır: pronounced *Chai-err*.	Key Formation name.
Dere: pronounced *Deh-Reh*	Translates as 'river/stream'.
Deniz: pronounced *Deh-neez.*	Translates as 'sea'.
Geyik Dağ: pronounced *Gay-ik Daa*.	*Dağ* / *Dağları* translates as 'mountain'.
Göl: pronounced *Guhl*.	Translates as 'lake'.
Köy: pronounced *Keuy*	Translates as 'village'.
Seydişehir: pronounced *Say-dish-eh-here*.	Town name.
Tepe: pronounced *Teh-peh.*	Translates as 'hill'.
Taşkent: pronounced *Tash-kent*.	Town name; *Taş* translates as 'stone'.

2 Tectonostratigraphy of the Central Taurides

2.1 Introduction

This chapter introduces the regional tectonostratigraphy of the Central Taurus Mountains. The study area consists of an autochthonous continental platform overlain by a series of NW-SE trending allochthonous units. These tectonic units have been assigned different names by different authors, and in this chapter the units will be correlated across the mountain belt and the regional terminology will be revised. The basic structural relationships, sedimentology and age of the units will be outlined, before being covered in more detail in subsequent chapters. A revised tectonic map of the study area is included here. The time scale of Gradstein (2004) is used throughout.

2.2 Previous work

The first geological descriptions of the region are from the 19th century (Hamilton, 1836), when a report described Cenozoic sedimentary rocks near the towns of Bozkir and Beyşehir (Fig. 2.1). The first detailed mapping was undertaken by Blumenthal (1947; 1951; 1956; 1960-1963), which included a 1/200,000 geological map of the Beyşehir-Seydişehir region. During this time a commercial study of bauxite within the autochthonous carbonate platform was documented (Wippern, 1962).

The most detailed and important stratigraphic interpretations were undertaken in the late 1970s and early 1980s. The area between Beyşehir and Akseki was mapped at 1:10,000 scale (Monod, 1977), and his associated PhD thesis includes detailed sedimentary logging and palaeontological dating. A correlation between this area and other parts of the central Taurides put the Beyşehir-Hoyran-Hadim nappe stack into a regional context (Gutnic et al., 1979). The area between Bozkir and Hadim/Taşkent was investigated by Özgül (1976; 1983; 1984; 1997), with much information being provided on the stratigraphy and palaeontology of each tectonic unit. Other detailed studies on aspects of the central Tauride stratigraphy were carried out by Demirkol (1981; 1982), Önder (1984), Tekin (1999), and Turan (2000). A geological map of the region (1:500,000) was produced by the Turkish MTA (General Directorate of Mineral Research and Exploration) in 2002 (Fig. 2.1).

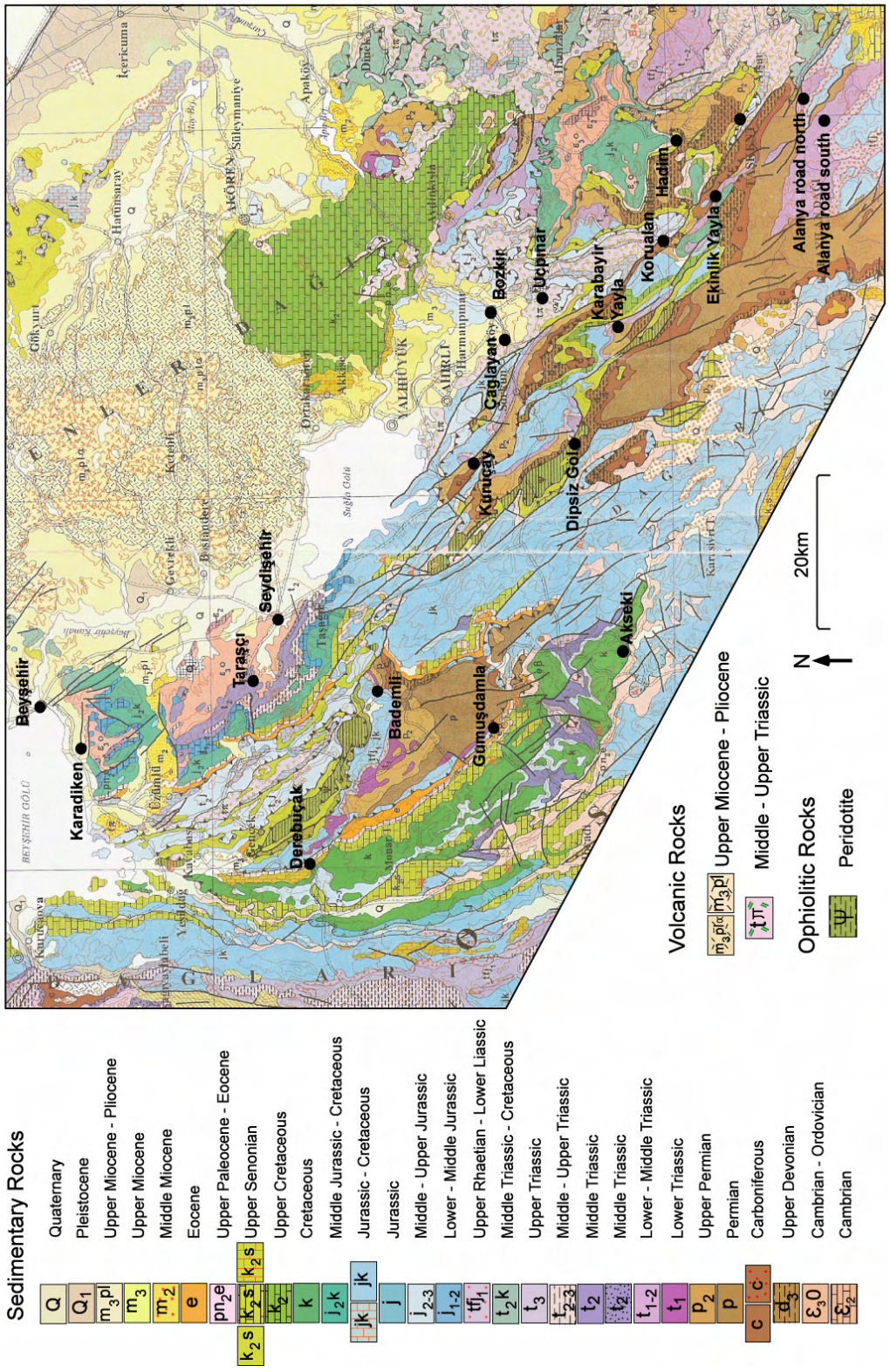

Fig. 2.1. Geological map of the study area showing some of the key locations discussed in this thesis. Map modified after MTA (2002).

The most recent detailed work on the region was carried out by Andrew (2003). His PhD study was a detailed investigation of distal margin and ophiolitic-derived units in the region (Beyşehir, Hoyran and Bozkir nappes). The reconstruction of these nappes was discussed by Andrew and Robertson (2002). The geological maps and existing literature, particularly those of Monod (1977), Özgül (1984; 1997) and Andrew (2003) were used as a basis for this study.

2.3 Tectonic units

The study area consists of a series of allochthonous units emplaced onto a relatively autochthonous continental platform. The autochthon is known as the Geyik Dağ across the whole area studied (Özgül, 1976; Monod, 1977). In the northern part of the study area between the towns of Beyşehir (in the north) and Akseki (in the south), the allochthonous units are known as the Beyşehir-Hoyran[1]-Hadim nappes (Monod, 1977). In the southerly part of the study area, near the towns of Bozkir and Hadim/Taşkent, the nappes are known as the Hadim (Aladağ), Bolkar Dağı and Bozkir nappes (Özgül, 1976; 1984). Many of these tectonic units can be correlated across the study area, although the nappe stacking order is variable.

A tectonic map of the region shows the simple distribution of the tectonic units (Fig. 2.2). The Beyşehir nappes and Bozkir nappes have been grouped together as one tectonic unit on this map, even though they are composed of several different thrust sheets. Extensive work has correlated these thrust sheets along strike (Andrew, 2003), and they are outside the scope of this study. The Hadim nappe is observed in both the northern and southern part of the study area, but the Bolkar Dağı nappe is only observed in the southern part. The term 'Bolkar Dağı' can cause some confusion, as a large mountain range within the Taurides to the east of this region (north of Mersin city) is referred to as the Bolkar Dağı (Bolkar Mountains). Throughout this study, the unit will be referred to simply as the 'Bolkar nappe' or the 'Bolkar unit'. Similarly, the Hadim nappe has been referred to in the literature as the 'Aladağ nappe' (e.g. Özgül, 1997). The Aladağ Mountains are found in the eastern Taurus Mountains (Tekeli et al., 1984),

[1] The 'Hoyran' nappes are found to the north of lake Beyşehir, and are outside the scope of this study.

several hundred kilometres to the east of this study area. To avoid confusion, the 'Aladağ unit' within this study area will be referred to from here on as the 'Hadim nappe' or 'Hadim unit'.

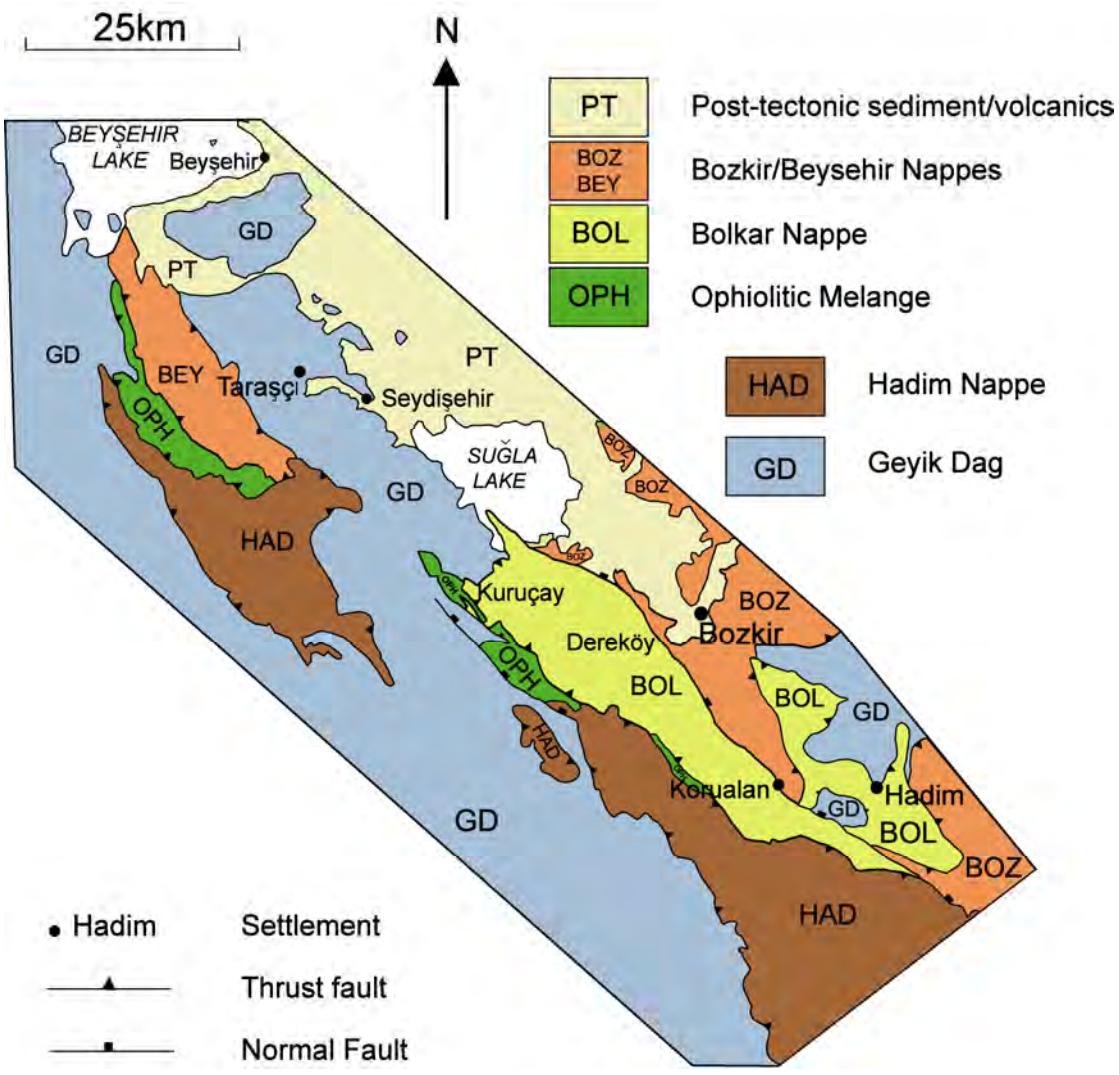

Fig. 2.2. Simplified tectonic map of the study area showing the distribution of tectonostratigraphic units.

A summary of the nappe stacking order and simplified stratigraphy of each tectonic unit in the northerly part of the study area is shown in Fig. 2.3 (after Monod, 1977). The Huğlu, Gencek and Boyali Tepe units, along with the ophiolitic melange, are

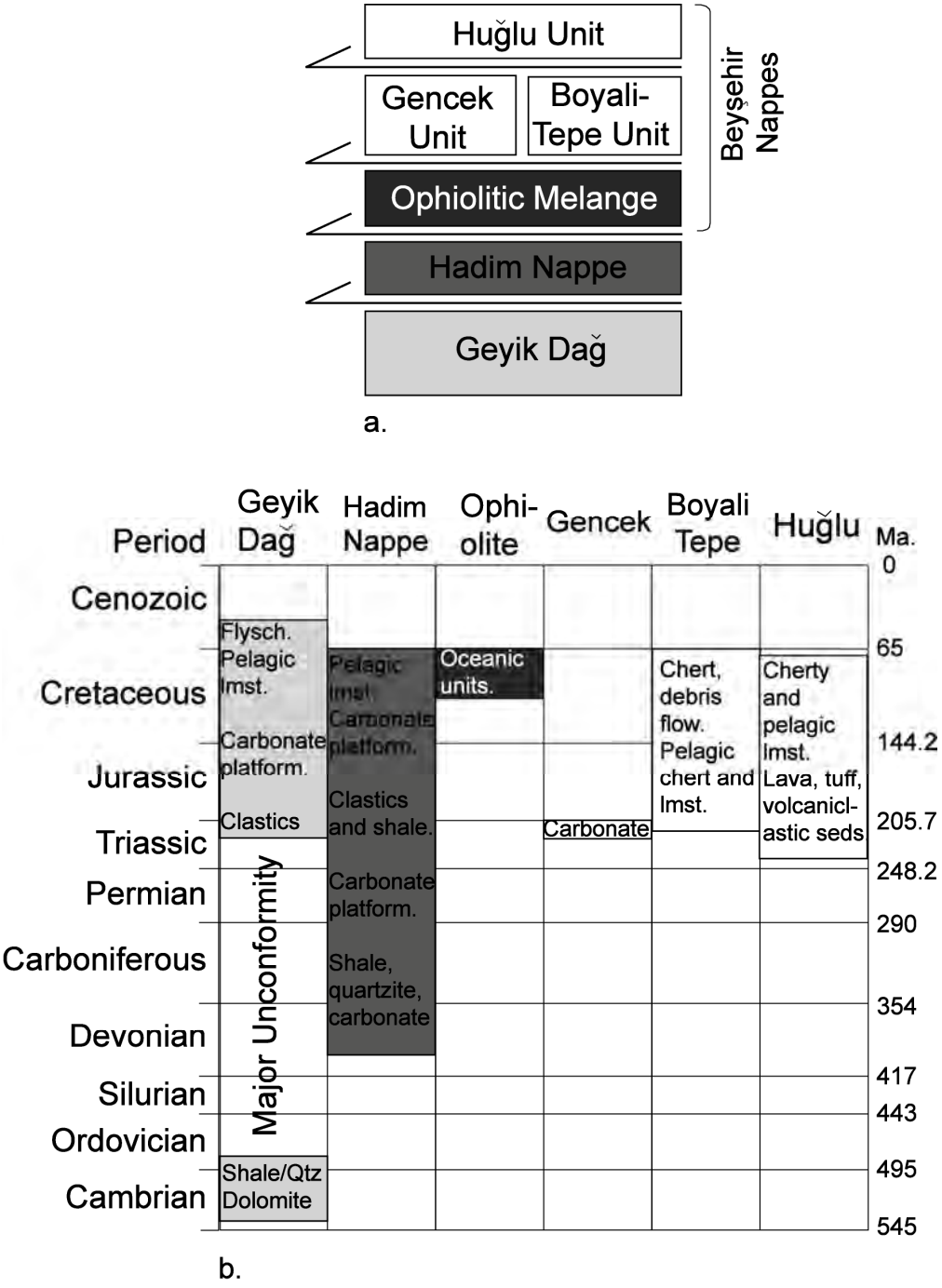

Fig. 2.3. a. Nappe stacking order of the Beyşehir-Hadim nappes in the northern part of the study area (after Monod, 1977); b. Simplified tectonostratigraphy in the northern part of the study area (after Andrew, 2003).

referred to as the Beyşehir nappes (after Andrew, 2003). However, on the tectonic map the ophiolitic melange is distinguished separately (Fig. 2.2). The autochthonous Geyik Dağ is tectonically overlain by the Hadim nappe, which, in turn, is tectonically overlain by the ophiolitic melange unit (Fig. 2.3a). The Gencek and Boyali Tepe nappes are thrust over the ophiolitic melange unit, and the highest thrust sheet is the Huğlu nappe. From the simplified tectonic framework (Fig. 2.3b) it can be seen that the Geyik Dağ and Hadim nappe both contain Palaeozoic aged rocks, whilst the other tectonic units are all of Mesozoic – Early Cenozoic age.

In the southern part of the study area, there are six allochthonous units emplaced over the autochthonous Geyik Dağ (Fig. 2.4). The Boyali Tepe, Huğlu and the Korualan units are commonly known as the Bozkir nappes (after Özgül, 1984); however, they are essentially the more south-easterly equivalent of the Beyşehir nappes. Andrew (2003) also refers to the Bozkir nappes as the Beyşehir nappes. The Geyik Dağ is tectonically overlain by the ophiolitic melange, which, in turn, is overthrust by the Hadim and Bolkar nappes (Fig. 2.4a). These are then tectonically overlain by the higher Bozkir thrust sheets. The Bolkar nappe has a similar age range and composition as the Hadim nappe, as shown in the simplified tectonostratigraphy (Fig. 2.4b). As in the northerly part of the study area, all units are Mesozoic or younger, apart from the Geyik Dağ, Hadim and Bolkar units. The Korualan unit of the Bozkir nappes is the lateral equivalent of the Gencek unit (Andrew, 2003).

2.4 Geyik Dağ autochthon

The Geyik Dağ unit ranges from Cambrian to Early Cenozoic. A summary diagram shows the stratigraphy of the Geyik Dağ unit in the northern (Fig. 2.5) and southern parts (Fig. 2.6) of the study area. There are subtle variations in upper and lower limits of the unit, which will now be discussed.

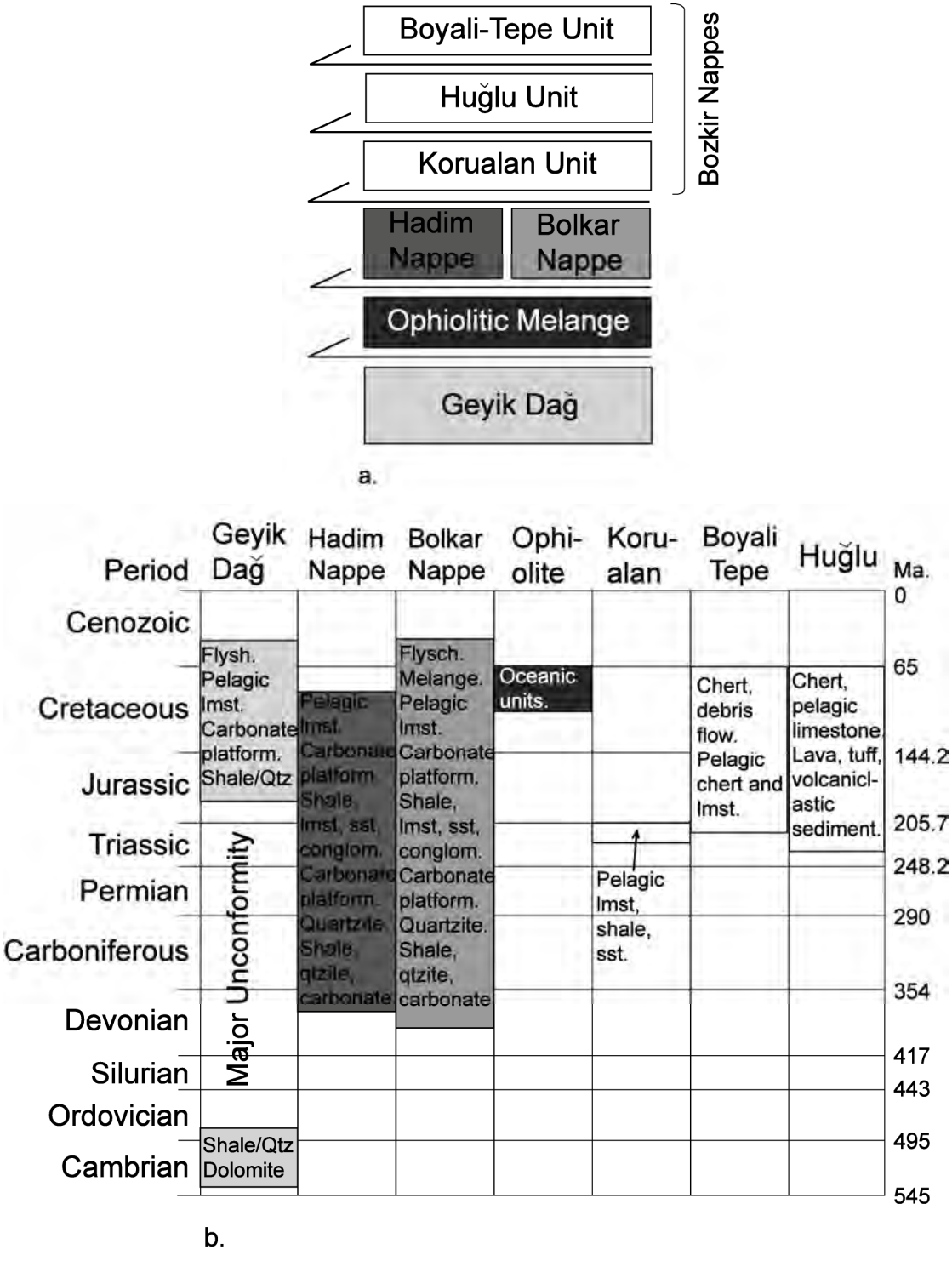

Fig. 2.4. a. Nappe stacking order of the Hadim-Bolkar-Bozkir nappes in the southern part of the study area (after Ozgul, 1984). b. Simplified tectonostratigraphy in the southern part of the study area (after Andrew, 2003).

2.4.1 Northerly part of study area

The Palaeozoic units of the Geyik Dağ are divided into the **Çal Tepe Formation** (Lower–Middle Cambrian), the **Seydişehir Formation** (Middle Cambrian–Ordovician) and the **Sobova Formation** (Late Arenig) (after Monod, 1977). The **Çal Tepe Formation** is composed of dolomite, bioclastic limestones, nodular limestone and some mudstone, and is ~125 m thick. These sediments are dated as Lower to Middle Cambrian (545-505 Ma) from the trilobites *Protolenidae*, *Agraulos* and *Corynexochus*, amongst others (Monod, 1977). The **Seydişehir Formation** primarily consists of a thick succession (>1000 m) of interbedded mudstones and quartzites. The lowermost beds, which include some carbonate horizons, contain the Middle Cambrian (518-505 Ma) trilobite *Paradoxoides* (Monod, 1977). The top of the formation contains the brachiopods *Alimbella* sp., *Hesperethis* sp. amd *Scaphorthis* sp. which are dated as Arenig (485-470 Ma) in age (Dean and Monod, 1970). The Late Arenig (c. 478-470 Ma) **Sobova Formation** overlies the Seydişehir shales and consists of various interbedded lithologies (limestone, shale, sandstone) containing the trilobites *Agerina* sp., *Carolinites* sp., *Ilaenus* sp., *Niobe* sp. and *Symphysurus* sp. (Dean and Monod, 1970). It is only ~30 m thick near the town of Seydişehir, but is >50 m thick elsewhere in the region.

An unconformity exists between the Ordovician and Triassic within the Geyik Dağ. The Triassic sediments (~80 m thick) above the unconformity are Anisian (c. 241-234 Ma) carbonates (**Calcaires de Tarasçi**), disconformably overlain by Carnian (c. 227-220 Ma) shales and sandstones, <100 m thick at Seydisehir (**Saplar Dere Formation**) (Gutnic et al., 1979). Near the village of Karadiken these sediments were reported to be Middle – Upper Triassic (c. 242-205 Ma) (Monod and Akay, 1984), although no faunal information is available. The uppermost Triassic sequence near Akseki consists of terrestrial clastics of the **Çayır Formation** (Late Triassic – Early Jurassic, c. 227-180 Ma), that vary in thickness from 20-120 m. Another unconformity occurs between Triassic shales and Middle Jurassic carbonates in the Beyşehir-Seydişehir area (Monod, 1977). The Jurassic to Cretaceous stratigraphy (**Sarakmana Formation, Teperasi Dolomite, Série Carbonate Principale**) is dominated by thick-

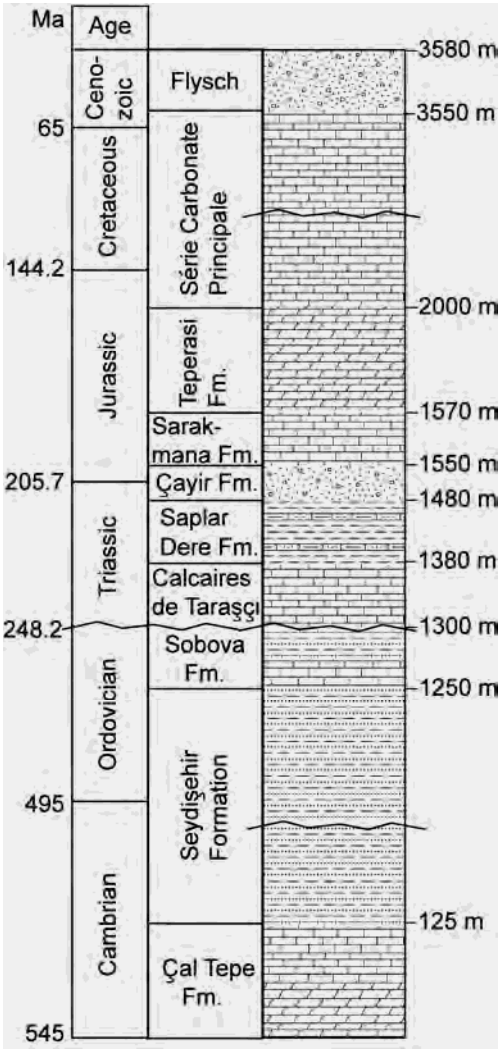

Fig. 2.5. Stratigraphy and formation names of the northerly part of the Geyik Dağ Unit from the Beyşehir – Seydişehir region.

bedded, to massive, platform carbonates (up to 2000 m thick), which continue into the Early Cenozoic. The succession is mainly composed of grainstones and wackestones, with limited age-diagnostic fauna (Andrew, 2003). Bauxite horizons and minor stratigraphic gaps occur in the latest Cretaceous (Monod, 1977).

The uppermost Cretaceous (Maastrichtian) to Palaeocene succession (c. 71-55 Ma) is composed of bioclastic limestones, grainstones and calcareous mudstones, of laterally variable thickness (Monod, 1977; Andrew, 2002). Overlying this are Lower to

Middle Eocene (c. 55-41 Ma) limestones (~30 m-thick) containing *Nummulites* (benthic foraminifera), locally capped by a hardground (Monod, 1977; Andrew, 2002). The top of the succession is calcareous sandstones and siltstones, interpreted as turbidites, and dated as Middle Eocene (c. 49-37 Ma) (Monod, 1977; Andrew, 2003) owing to the presence of benthic foraminifera, e.g. *Asterocyclina stellatus*.

2.4.2 Southerly part of study area

Lower Palaeozoic units in the southerly part of the Geyik Dağ are similar to those described from the north. The Lower to Middle Cambrian (c. 545-505 Ma) **Hazamlar Formation** consists ~300 m of interbedded shales and siltstones (Özgül, 1997) (Fig. 2.6). Above this, the **Çal Tepe Formation** (~100 m) consists of limestones including the trilobites *Agraulos* sp., *Corynexochus* sp. and *Paradoxides* sp. (Özgül, 1997) that indicate a Middle to Late Cambrian age (c. 518-495 Ma). These carbonates pass into the **Seydişehir Shale Formation** of Ordovician age (495-443 Ma), ~770 m-thick.

There are no Triassic sediments within the Geyik Dağ sequence in the south (Fig. 2.6), and the Jurassic **Polat Formation** unconformably overlies the Seydişehir Formation. The oldest Jurassic carbonates are dated as Middle Jurassic (Bajocian, c. 177-169 Ma) particularly owing to the presence of the foraminifera *Amijiella amiji* and *Sellioporella donzelli* (Özgül, 1977). The youngest sediments within this sequence are Cretaceous in age (Aptian-Cenomanian, c. 121-94 Ma) and contain the benthic foraminifera *Dicyclina schulumbergeri* and *Nummoloculuna heimi* (Özgül, 1997; Andrew, 2003). The total thickness of the Polat Formation is ~560 m.

The overlying **Çataloluk Limestone Formation** (Fig. 2.6) contains corals, gastropods and benthic foraminifera including *Orbitoides media* and *Lepidorbitoides minor* at the base, and *Rapydionina* at the top, giving an age range for the formation of Maastrichtian – Palaeocene (c. 71-55 Ma) (Özgül, 1997; Andrew, 2002). Overlying this the **Çobanağaci Formation** is Palaeocene – Middle Eocene (c. 65-41 Ma), and composed of sandstones and debris flows. The base of this unit includes the planktonic foraminifera *Nummulites* sp., *Discocyclina* sp., and *Assilina* sp. (Özgül, 1997). The upper horizons of this sequence contain the Leutetian foraminifera *Assilina cf. exponens*

(Sovverby), and *Orbulinoides cf. beekmanni* (Saido) (Özgül, 1997). The combined thickness of these units is ~400 m.

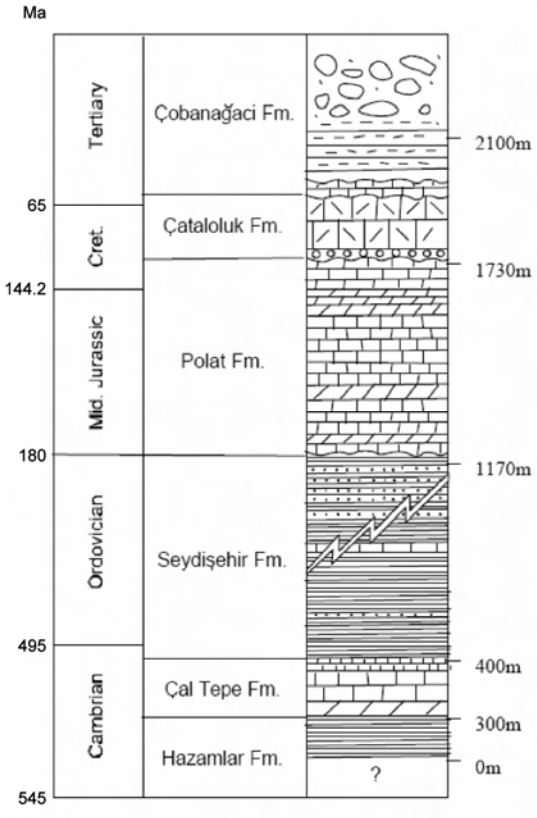

Fig. 2.6. Stratigraphy and formation names of the southerly part of the Geyik Dağ Unit from the Hadim region. Figure modified from Andrew (2003), originally from Özgül (1997).

2.5 Hadim Nappe

The Hadim nappe consists of a complete stratigraphic sequence through the Late Palaeozoic and the Mesozoic. In the northern part of the study area, a detailed description of the Hadim nappe was provided by Monod (1977), whilst in the south it was described by Özgül (1976; 1984; 1997). It is possible to correlate the stratigraphy, ages and formation names between the north and the south (Fig. 2.7).

2.5.1 Northern part of the study area

The oldest rocks in the Hadim nappe are best exposed at the village of Bademli (Fig. 2.1). The **Bademli Unit** refers to a Late Palaeozoic sequence, with the oldest sediments being Middle – Upper Devonian in age (391-354 Ma). These units contain the brachiopods *Cyrtospirifer*, *Platyspirifer*, *Zdimir*, *Schizophoria* and *Reticularia* and the trilobite *Phacops* (Monod, 1977; Andrew, 2003). Exposure of the Devonian sequence, mainly shales and quartzites with some limestone intercalations, is limited in the northern part of the study area (<100 m). The Lower Carboniferous (c. 354-327 Ma) of the Bademli unit is composed of dark shales and limestone at the base, which contain the brachiopods *Inlatia* and *Ovatia* (Monod, 1977). Up-sequence, Middle Carboniferous (c. 327-311 Ma) carbonates and dolomites contain the foraminifera *Archaediscidae* and *Rectodiscus rotundus*. The top of the Carboniferous succession consists of quartzites and carbonates which contain algae (*Dvinella* sp.) and foraminifera (*Fusiella*) of Late Carboniferous age (c. 311-303 Ma) (Monod, 1977). The complete Carboniferous succession is ~300 m thick. The Permian (c. 290-248 Ma) succession is a thick sequence (~500 m) of dark-grey carbonates, the base of which contains the foraminifera *Triticites* and the algae Girvanella. The top of the Upper Permian sequence (and top of the Bademli Unit) contains the foraminifera *Globivalvulina* and *Dagmarita chanakchiensis* (Monod, 1977).

The Triassic **Medi Ova Formation** is a thin (~220 m) succession of mudstones, limestones and sandstones that overlie the Upper Palaeozoic sequence. Limited fauna have been recovered from this succession; however, the brachiopod *Unionites*, the gastropod *Natiria costata* and foraminifera *Glomospirella* have been dated as Lower Triassic in age (c. 248-242 Ma) (Monod, 1977). The overlying **Derebuçak Formation** (<50 m-thick) is a succession of red clastics containing no fauna, but is inferred by stratigraphic association to be Late Triassic – Early Jurassic (c. 227-180 Ma) in age (Monod and Akay, 1984). The remainder of the Mesozoic succession is dominated by thick-bedded fossiliferous carbonates, the **Calcaires de Çamlik** (~700 m). The oldest sediments in this unit are Liassic in age (c. 206-180 Ma), and were dated by the algae

Palaeodasycladus (Monod, 1977). The youngest carbonates contain rudist bivalves and the echinoderm *Orbitoides*, which are of Late Cretaceous age (c. 99-65 Ma). The uppermost part of the Calcaires de Çamlik are pelagic limestones which contain pelagic foraminifera *Globotruncana* (Monod, 1977). Overlying the carbonates succession is a '**wild-flysch**', up to 100 m-thick. This is a syn-tectonic unit of turbidites and debris flows ("flysch"), formed during the emplacement of the Beyşehir-Hoyran-Hadim nappe.

2.5.2 Southern part of the study area

The Late Palaeozoic sequence of the Hadim nappe in the more southerly part of the study area is considerably thicker than in the northerly part. A Devonian succession, known as the **Gölboğazi Formation** (after Özgül, 1997), is composed of quartzitic sandstone, shale and limestone (<1000 m) which contain the brachiopod *Cyrtospirifer* sp. and *Leptaena* sp. of Upper Devonian age (370-354 Ma). The overlying Carboniferous succession (**Yarıcak Formation**) consists of black shales containing the foraminifera *Earlandia minor* and the brachiopod *Rhipidomella*, which are dated as Tournaisian (354-342 Ma) (Özgül, 1997). A thick Middle to Upper Carboniferous (342-290 Ma) limestone succession overlying the shales contains the foraminifera *Profusulinella* sp., *Schwagerinidae* and *Endothyra* sp. in the uppermost beds. The total thickness of the Carboniferous is estimated in this study to be ~300 m.

The Permian **Çekiç Dağ Formation** consists of a thick succession of grey limestones, ranging from 500-1500 m-thick. The lowermost beds of this formation contains *Quasifusulina* sp. and *Braduna samarica* of Early Permian (Asselian, 290-282 Ma) age, whilst the uppermost beds contain the foraminifera *Cornuspira* of Late Permian age (c. 256-248 Ma) (Özgül, 1997). These sediments are then overlain by the Triassic **Gevne Formation** (~500 m thick), which is composed of interbedded shales, limestones and sandstones. The beds at the base of this formation are thick-bedded algal limestones, and contain the calcareous foraminifera *Rectocornuspira kalhori* and *Elisonian Triassica* of Lower Triassic age (c. 248-242 Ma) (Özgül, 1997). Anisian (c. 242-234 Ma) carbonates, containing *Endothyranella wirzi,* indicate the top of the Gevne

Formation. Overlying clastics of the **Çayır Formation** (<130 m) were thought to be Late Triassic in age (Norian-Rhaetian, c. 221-206Ma) (Ozgul, 1997), although no faunal evidence was available.

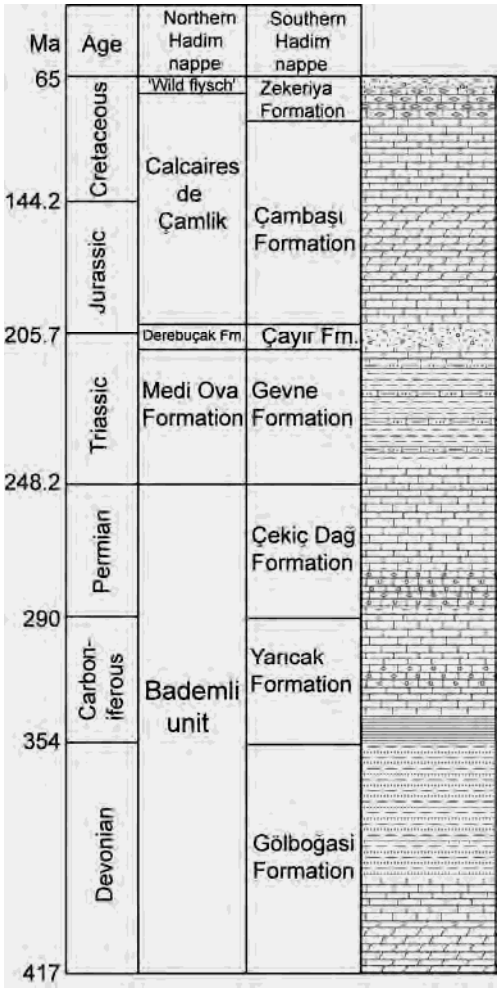

Fig. 2.7. Simplified stratigraphy of the Hadim nappe, with the names and ages of units in the northern Hadim nappe (after Monod, 1977) and the southern Hadim nappe (after Özgül, 1997).

The Jurassic – Cretaceous **Çambaşı Formation** is composed of thick-bedded carbonates (<1500 m), which contains a variety of benthonic foraminifera and algae that give an age range of Liassic – Albanian/Cenomanian (c. 206-94 Ma) (Özgül, 1997). The uppermost beds of this formation contain the algae *Spirolina* sp. and the foraminifera *Peneroplis*

turonicus. The Late Cretaceous (c. 99-65 Ma) sediments in this sequence (**Zekeriya Formation**) consists of polymict debris flows (<120 m thick). Within this succession are detached blocks ("olistoliths") of pelagic limestone and "ophiolitic" material (Özgül, 1997).

2.6 Bolkar nappe

The Bolkar nappe is only found in the more southerly part of the study area. This tectonic unit has a comparable stratigraphy and age range as the Hadim nappe (Fig. 2.8). The Devonian interval is known as the **Hocalar Formation** (Özgül, 1997) and is primarily composed of sandstones and shales, with rare limestone beds, up to 500 m thick. The limestone beds contain a variety of fauna, such as the brachiopods *Spirifer* sp. and *Cyrtospirifer* sp. which give an age range of Middle – Upper Devonian (c. 391-354 Ma) (Ozgul, 1997) for the formation. The overlying **Kongul Formation** (200 m) is Carboniferous in age and consists of dark shales at the base, and thick-bedded carbonates in the middle and upper part of the succession. The lowermost beds are dated as Lower Carboniferous (Visean, 342-327 Ma) due to the presence of the foraminifera *Eostafella* sp. and *Archaediscus* sp., whilst the upper limits of the Kongul formation are characterised by carbonates with *Endothyra* sp. and *Globivalvulina* sp. of Upper Carboniferous age (311-303 Ma) (Özgül, 1997).

A disconformity exists at the top of the Carboniferous succession, above which the Permian **Taşkent Formation** (400-700 m) consists of thick-bedded dark-grey carbonates. The oldest rocks in this sequence are Lower Permian (c. 290-256 Ma) and contain the large foraminifera *Parafusulina* sp. (Özgül, 1997). The youngest Permain carbonates are microbial limestones which contain the foraminifera *Yabeina globosa* and *Neoschwagerina*, dated as Upper Permain (c. 256-248 Ma). These are, in turn, overlain by Lower Triassic (c. 248-242 Ma) dolomites of the **Ekinlik Formation** (~300-400 m), which contain the foraminifera *Paradunbarula* sp. and *Nankinella* sp., amongst others (Özgül, 1997). The mid part of the Triassic sequence consists of interbedded shales, quartzitic sandstones and thin limestones. A thick horizon of neritic limestone dated as

Middle Triassic (Ladinian, c. 234-227 Ma) contain the benthic foraminifera *Glomospira sinensis* and *Glomospirella vulgaris*. These carbonates are unconformably overlain by clastic sediments of the **Morbayır Formation** (<50 m), which lack fauna but are inferred to be Late Triassic – Early Jurassic (c. 227-180 Ma) in age based on lithological comparisons (Özgül, 1997).

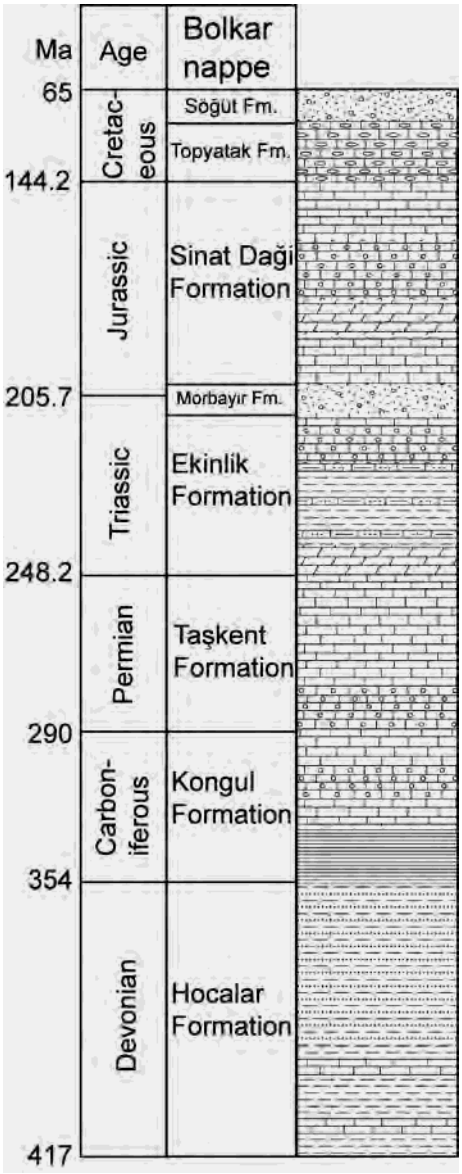

Fig. 2.8. Simplified stratigraphy of the Bolkar nappe, with the names and ages of units (after Özgül, 1997).

The Jurassic **Sinat Dağı Formation** – Liassic to Tithonian (c. 206-144 Ma) – consists of thick-bedded neritic limestone and dolomite <800 m thick. The Liassic carbonates that overlie the Morbayir Formation contain the algae *Cayeuxia* sp. and foraminifera *Reophax* sp. amongst others (Özgül, 1997). The top of the Sinat Dagi limestone contains foraminifera including *Pseudoeggerella* sp. and *Trocholina* sp. A stratigraphic break in the sequence exists above the Sinat Dağı Formation, above which the **Topyatak Formation** consists of pelagic carbonate of Upper Cretaceous (Cenomanian – Turonian, c. 99-89 Ma) age (<80 m). These sediments contain pelagic fauna, including the foraminifera *Favusella washitensis* and *Marginotruncana* sp. (Özgül, 1997). The **Sögüt Formation** is the uppermost unit in the Bolkar nappe, and consists of pelagic limestone, turbidites and debris flows (<100 m). Clastic sediments within the formation do not contain any datable fauna; however, pelagic limestones at the base have yielded *Globotruncana* sp. of Maastrichtian age (c. 71-65 Ma) (Özgül, 1997).

2.7 Beyşehir / Bozkir nappes

The Beyşehir / Bozkir nappes is a collective name for the higher thrust sheets within the the study area. They extend north of lake Beyşehir (known as the Hoyran nappes) and to the southeast of this study area (Ermenek – Karaman area). Much of the original mapping and terminology was founded in the north by Monod (1977) and in the south by Özgül (1976; 1984; 1997), whilst the most recent work on these units was provided by Andrew (2003) and Andrew and Robertson (2002). This section will provide a brief overview of the individual nappe units.

2.7.1 Ophiolitic Melange

The ophiolitic melange unit is composed of a dismembered ophiolite, notably serpentinised peridotite, along with an associated volcano-sedimentary ophiolitic melange (Andrew, 2003). The melange unit contains blocks ("olistoliths") of serpentinite, limestone, radiolarian chert, tuff, amphibolite, hartzburgite, pelagic limestone and altered volcanics. Ophiolite genesis is assumed to be Late Cretaceous (c.

99-65 Ma) (Monod, 1977; Andrew, 2003), consistent with other southern Turkey ophiolites. Local blocks of neritic limestone within the melange contain an Upper Permian *Fusilinid* fauna; these block are thought to originate from the Tauride platform (Andrew, 2003).

2.7.2 Gencek Unit

The Gencek unit is a broken formation of Triassic (c. 248-206 Ma) neritic limestone set in a tectono-sedimentary melange (Andrew, 2003). The carbonates contain a variety of macrofauna including bryozoa and coral fragments, algae and disarticulated bivalve shells. It tectonically overlies the ophiolitic melange unit in the northern part of the study area (Andrew, 2003). The large Megalodon *Conchodon infraliasicus* has been recovered from within the Gencek unit, dating it as Rhaetian (c. 210-206 Ma) (Monod, 1977; Andrew, 2003).

2.7.3 Korualan Unit

The Korualan unit is the lowest unit in the southerly part of the study area, and consists of a variety of neritic, hemi-pelagic and pelagic sediments, mainly carbonates, up to 200 m-thick (Andrew, 2003). A lower dolomite unit is overlain by interbedded mudstone, siltstone, sandstone, calcarenite and micritic limestone. Above this pelagic limestones and cherty horizons contain small bivalves. The uppermost part of the sequence consists of a less coherent melange type sequence (undated), with variable oceanic derived sediment and volcanic blocks set in a fine-grained silty matrix (Andrew, 2003). The bivalve *Halobia* sp. and foraminifera *Glomospira* sp. indicate a Middle to Upper Triassic age (c. 242-206 Ma) (Özgül, 1997).

2.7.4 Boyali Tepe Unit

The Boyali Tepe unit tectonically overlies the ophiolitic melange, and is at a similar structural level to the Gencek unit (Andrew, 2003). It consists of a neritic carbonate unit of Late Triassic age (c. 227-206 Ma), overlain by Lower Jurassic – Upper Cretaceous

pelagic carbonates, altogether several hundred metres thick. This unit can also be described as large-scale broken formation. The oldest carbonates contain the foraminifera *Involutina* of Rhaetian age (c. 210-206 Ma) (Monod, 1997; Andrew, 2003). A fossiliferous pink nodular limestone horizon has yielded ammonites including *Dactilioceras* sp. and *Phylloceras* sp. of Lower – Middle Toarcian age (c. 190-180 Ma) (Gutnic et al., 1970; Monod, 1977; Özgül, 1997). Overlying ribbon radiolarites are undated. The youngest sediments in the unit are pelagic limestones with foraminifera (e.g. *Globotruncana* sp.) of Albian – Santonian age (c. 112-84 Ma) (Andrew, 2003).

2.7.5 Huğlu Unit

This unit is the highest thrust sheet within the Beyşehir nappes in the north, but in the southern Bozkir nappes it is overlain by the Boyali Tepe unit. It can be subdivided in a lower volcano-sedimentary unit and an upper pelagic limestone unit (Andrew, 2003). The lower unit consists of siliceous volcanic debris flows, siliceous tuff, chert and rare redeposited neritic limestone, interbedded locally with mudstones and redeposited limestone. The upper unit stratigraphically overlies the volcanic unit and consists of well-bedded pelagic micritic limestone containing the pelagic bivalve *Daonella*, of Anisian – Ladinian (c. 242-227 Ma) age at the base (Monod, 1977). Higher in the sequence the planktonic foraminifera *Globotruncana* indicate an Upper Cretaceous age (c. 99-65 Ma) (Andrew, 2003). The thickness of the unit is ~250 m.

2.8 Summary

1) The study area within the Central Tauride mountain consists of a series of allochthonous units (Hadim, Bolkar, Beyşehir and Bozkir nappes) and an ophiolitic melange unit which were all emplaced onto an autochthonous continental platform (Geyik Dağ unit).

2) Different names exist for each tectonostratigraphic unit and individual formations, but the ages and stratigraphy can be correlated along strike. However, the nappe stacking order changes between the north and the south of the studied area. In the northern part of the study area, the Hadim nappe is the lowest allochthonous unit, tectonically overlain by the ophiolitic melange, in turn overlain by the Beyşehir nappes. In the southern part of the study area, the ophiolitic melange is the lowest allochthonous unit, tectonically overlain by the Hadim and Bolkar nappes, with the Bozkir nappes in the highest structural position.

3) The relatively autochthonous Geyik Dağ consists of a Cambrian-Ordovician succession of dolomites and carbonates overlain by interbedded quartzitic sandstone and shale. A major unconformity exists between the Ordovician and Triassic. Triassic siliciclastics are overlain by a thick Jurassic – Cretaceous carbonate succession, and then by pelagic limestones and gravity deposits in the Late Cretaceous – early Cenozoic.

4) The allochthonous Hadim unit consists of a complete stratigraphic sequence from Devonian – Cretaceous. A predominantly carbonate and fine siliciclastic succession is interrupted in the Late Triassic – Early Jurassic by a coarse clastic horizon, the Çayır Formation. The Late Cretaceous consists of pelagic limestones.

5) The stratigraphy of the allochthonous Bolkar unit is comparable to the Hadim nappe; however, this unit is only observed in the south of the study area. It consists of Devonian

– Cretaceous carbonates and siliciclastics, with a Late Cretaceous pelagic sequence. The Bolkar stratigraphy is slightly thinner than the Hadim stratigraphy.

6) The ophiolitic melange unit consists of disorganised slices of a variety of volcanic, volcaniclastic, neritic and pelagic carbonate lithologies. The ophiolite is inferred to be of Late Cretaceous age.

7) The Beyşehir and Bolkar nappes are collective names for the higher thrust sheets in the north and south of the study area respectively. The Boyali Tepe and Huğlu units can be traced along strike and are composed of Late Triassic – Cretaceous limestone, pelagic sediments and volcanics. The Gencek unit is a large-scale broken formation of Triassic neritic carbonate. The Korualan unit is a the lowest structural level in the southerly part of the study area, and is composed of slope deposits.

3 Palaeozoic evolution of the Tauride platform

3.1 Introduction

This chapter will investigate the Upper Palaeozoic sedimentology of the Tauride platform. Upper Palaeozoic rocks are found within the Hadim nappe and the Bolkar nappe (Fig. 3.1); however, they are not observed in the Geyik Dağ autochthon, where an unconformity exists between Ordovician and Triassic units (see chapter 2). Previous work on the Palaeozoic of the Hadim nappe and Bolkar nappe was carried out regionally by Blumenthal (1947, 1951, 1956, 1960-1963), Monod (1977) and Özgül (1976, 1984, 1997). All of the existing formation names are retained from the literature. Work by previous authors (e.g. logs, type sections) was field checked and revised where necessary. A geological map of the study area is provided in Fig. 3.1, showing all the key localities discussed in this chapter.

3.2 Alternative models of Late Palaeozoic tectonic setting

During the Late Palaeozoic, the Tauride platform is thought to have formed part of an extensive continental margin adjacent to the supercontinent Gondwana (Şengör et al., 1984; Robertson et al., 1991; Okay et al., 2006). However, the tectonic setting of the north Gondwana margin during this period is contentious. It is generally accepted that the Tauride platform separated from the north Gondwana margin during Late Permian – Early Mesozoic rifting (Şengör and Yılmaz, 1981; Demirtaşlı, 1984a; Robertson and Dixon, 1984; Stampfli et al., 2001; Andrew and Robertson, 2002; Stampfli and Borel, 2002; Göncüoğlu et al., 2003; Göncüoğlu et al., 2004; Robertson, 2007). It is also inferred that northward subduction of Palaeotethyan oceanic crust occurred along the opposing Eurasian margin during the Late Palaeozoic (Şengör and Yılmaz, 1981; Robertson and Dixon, 1984; Dercourt et al., 1993; Ustaömer and Robertson, 1993; Stampfli and Borel, 2002; Okay et al., 2006; Robertson and Mountrakis, 2006). However, it is still debatable as to whether the Gondwana margin was active or passive during Late Palaeozoic time.

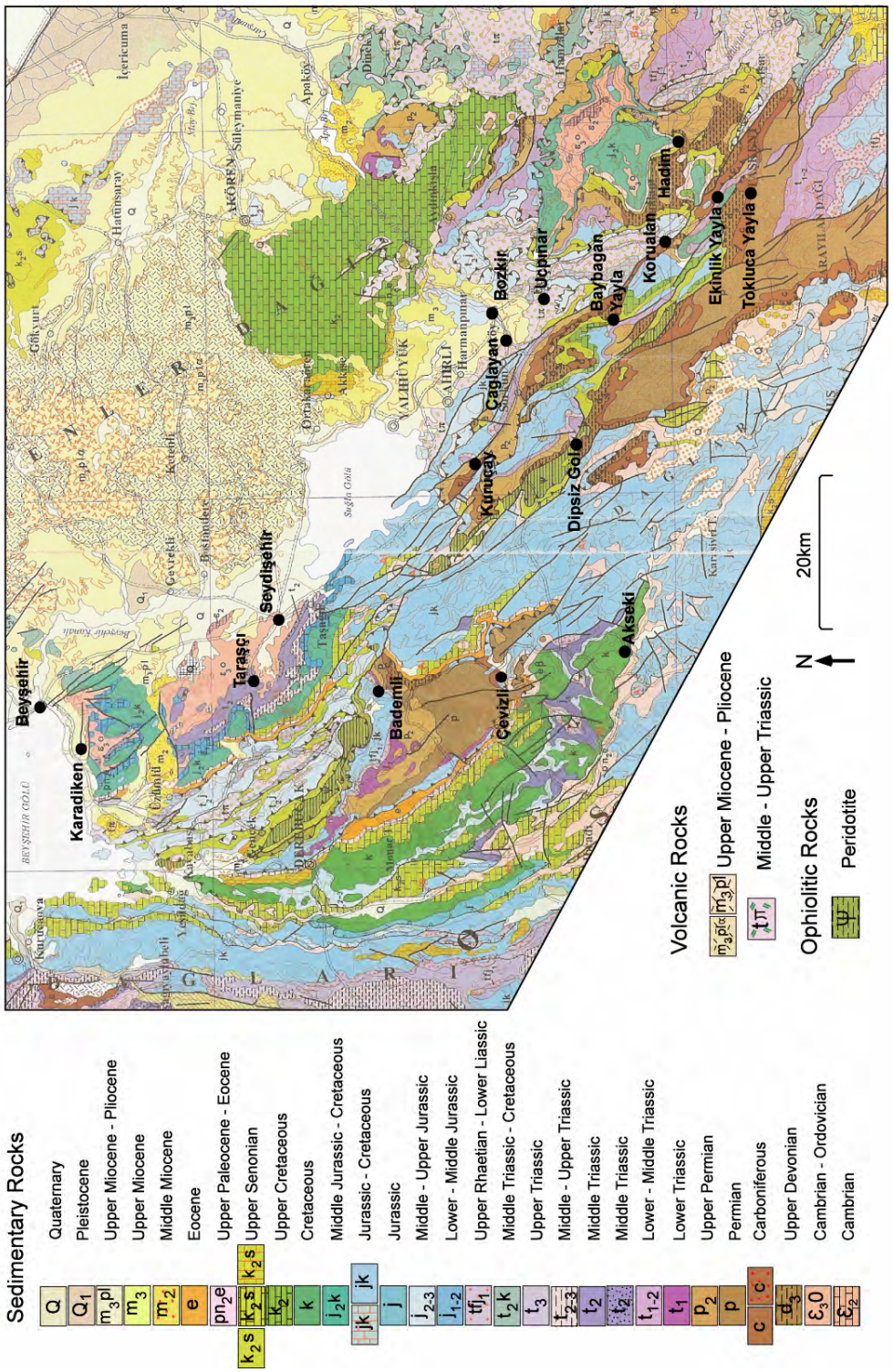

Fig. 3.1. Geological map of the study area showing key localities discussed in the Palaeozoic chapter. Figure modified after MTA (2002).

In one model (Göncüoğlu et al., 2000; Kozur and Göncüoğlu, 2000; Göncüoğlu et al., 2004; Göncüoğlu et al., 2007), the Cambrian to Late Devonian period was represented by stable continental platform deposition along the north-Gondwana margin. Southward subduction of Palaeotethyan oceanic crust took place beneath Gondwana in the Lower Carboniferous, resulting in back-arc rifting and associated volcanism (Fig. 3.2). An arc unit (Sakarya) was separated from Gondwana by a narrow oceanic basin (Göncüoğlu et al., 2007). In the northerly part of the Tauride-Anatolide platform a volcanic rift zone (Konya rift) separated the Bolkar Dağ Unit and the Aladağ Unit (including the Hadim "shallow shelf"). A small rifted basin, with extension-related volcanism, separated the Aladağ Unit from the southerly Geyik Dağ unit. However, the Konya rift did not result in the formation of oceanic crust, and was filled with a regressive sedimentary sequence which was finally 'sealed' during the earliest Late Permian.

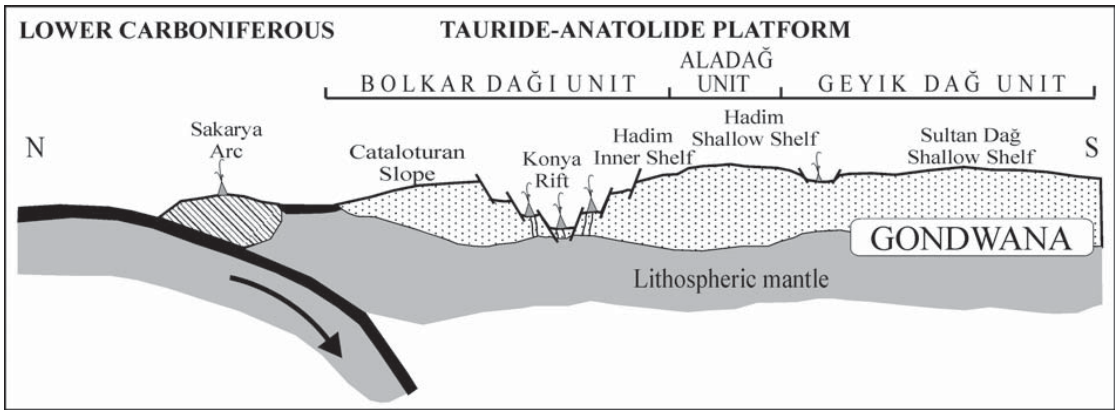

Fig. 3.2. Lower Carboniferous tectonic reconstruction of the north Gondwana margin, showing the inferred locations of the Bolkar Dağı, Hadim and Geyik Dağ units (Göncüoğlu et al., 2007).

A second model suggests that the northern part of the Tauride-Anatolide platform (the Geyik Dağ, Sultan Dağ[2], Hadim and Bolkar units) experienced a passive margin evolution during the Late Palaeozoic (Robertson and Dixon, 1984; Dercourt et al., 1986; Dercourt et al., 1993; Stampfli, 2000; Stampfli et al., 2001; Stampfli and

[2] The Sultan Dağ (Sultan Mountain) is in the northern Central Taurides, and represents the northern continuation of the relatively autochthonous Geyik Dağ unit.

Borel, 2002; Eren et al., 2004; Robertson et al., 2004). In this model, subduction of Palaeotethyan oceanic crust was exclusively northwards beneath the Eurasian continental margin (Fig. 3.3). "Tauride" units rifted from the northerly Gondwana margin during the Late Permian, and sutured with the Eurasian margin during the Late Triassic – Early Jurassic (see chapter 4).

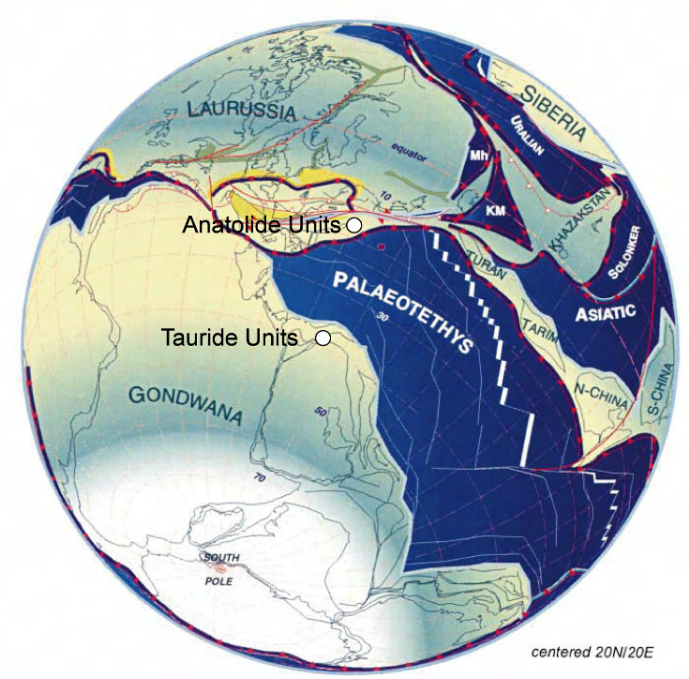

Fig. 3.3. Carboniferous reconstruction of Palaeotethys, modified after Stampfli and Borel (2002). Tauride units are found along the northern Gondwana margin, whilst the Anatolide units (including the Konya Complex) a derived from the Eurasian margin.

The central Tauride mountains preserve critical evidence concerning the tectonic setting of the Late Palaeozoic Gondwana margin. If southward subduction or back-arc rifting occurred, evidence of rift-related subsidence and volcanism should be recorded in the Tauride platform succession. In particular, sedimentary successions within the Hadim, Bolkar and Geyik Dağ units should show evidence of active margin processes. This chapter will consider the Late Palaeozoic stratigraphy of the Central Taurides in order to assess the viability of the two models presented above.

3.3 Palaeozoic sedimentology

In the alternative tectonic models above, the critical time period is the Lower Carboniferous. This study concentrated on collecting detailed information on Carboniferous sequences; however, Devonian and Permian units were also studied. This section will provide detailed descriptions, based on a combination of new fieldwork evidence and literature reviews, of the Upper Palaeozoic successions within the study area.

3.3.1 Devonian

Exposures of Devonian units are found in the Hadim nappe and the Bolkar nappe (Fig. 3.1). There are no Devonian units in the autochthonous Geyik Dağ, as mentioned previously in this thesis. A review of the stratigraphy at three localities within the nappe stack is now presented.

3.3.1.1 Locality 1: Bademli. GPS reference 388490 4129840.

This locality is the type locality of Upper Palaeozoic rocks in the northerly part of the Hadim nappe (Monod, 1977). The exposed Devonian succession is approximately 100 m thick, and is composed of 45% shale, 40% sandstone and 15% limestone. Brown-orange shales and quartzitic sandstone, interbedded with dark limestones, are best exposed along a temporary forestry track that cuts across the hillside to the east of Bademli village. Sandstone beds are medium-thick bedded, interbedded with thin (5cm) shale intercalations. These are heavily recrystallised, locally with thin millimetre-scale laminations, and are quartzitic in composition. Shale is also finely laminated, and can be found as relatively thick (~5 m) uninterrupted horizons, as well as thin interbeds. Dark-grey limestone makes up about 15% of the sequence. This is medium-bedded, with abundant bioclastic material, most notably in situ tabulate coral colonies, up to 30 cm in diameter. Brachiopod shells from the limestone beds have yielded fossils including Middle to Upper Devonian *Cyrtospirifer*, *Zdimir* and *Reticularia*, along with Lower Devonian *Phacops* trilobites (Monod, 1977; Andrew, 2003).

3.3.1.2 Locality 2: Çaglayan. GPS reference 427280 4110580

This locality, 10 km south of Çaglayan village within the Bolkar nappe (Fig. 3.1), has not been documented in the previous literature. Reasonable exposure of Devonian rocks can be found in a temporary road cutting adjacent to a river gorge. Despite heavy faulting and folding, the main lithologies can be identified, as follows.

Middle- to thick-bedded recrystallised quartzitic sandstone is variably light grey, orange or brown in colour (Fig. 3.4). This shows parallel lamination on a millimetre-scale. Sand grains are typically fine- to medium-grained. These quartzitic sandstones form a laterally continuous horizon, 120 m thick, towards the lower part of the exposed succession, rarely interrupted by limestone beds. Overlying this thick horizon is an interbedded sequence, up to 200 m thick, of quartzitic sandstone, shale and limestone, with rare dolomite. These units are thin- to medium-bedded, and the sandstone/shale is variably grey, grey-green, brown and orange in colour. The limestone units contain bioclastic material, namely broken brachiopod shells, crinoids, algae, bryozoan and tabulate corals. Fauna identified included Middle to Upper Devonian *Favosites* sp. coral, and Middle Devonian *Cyrtospirifer* sp. brachiopods (Özgül, 1997). Özgül (1984, 1997) noted that Devonian shales in the Bolkar nappe show initial greenschist metamorphism. According to Özgül (1997), shales contain the metamorphic minerals chlorite, muscovite, zeolite and epidote; however, the sediments observed at this locality were sheared, but not obviously metamorphosed. It is unclear if these minerals are detrital or not.

Fig. 3.4. Thick-bedded Devonian quartzitic sandstone with thin shale intercalations from the Çaglayan Locality.

3.3.1.3 Locality 3: Tokluca Yayla. GPS reference 446100 4088460

Tokluca Yayla is found within the southerly part of the Hadim nappe (Fig. 3.1), and is the best exposed sequence of Devonian units within the study area. A measured log through this succession is shown in Fig. 3.5. The lowermost 100 m of the succession contains primarily dolomite, dolomitic limestone, platform carbonate and shale. Dolomite beds are medium- to thick-bedded, light-grey, or white in colour, and heavily recrystallised. Limestones are variably light- to dark-grey or brown, medium-bedded, and recrystallised. Several limestone horizons contain coral structures (tabulate) and microbial laminations. Interbedded shales throughout this succession are grey or brown and laminated on a 1-2 mm-scale.

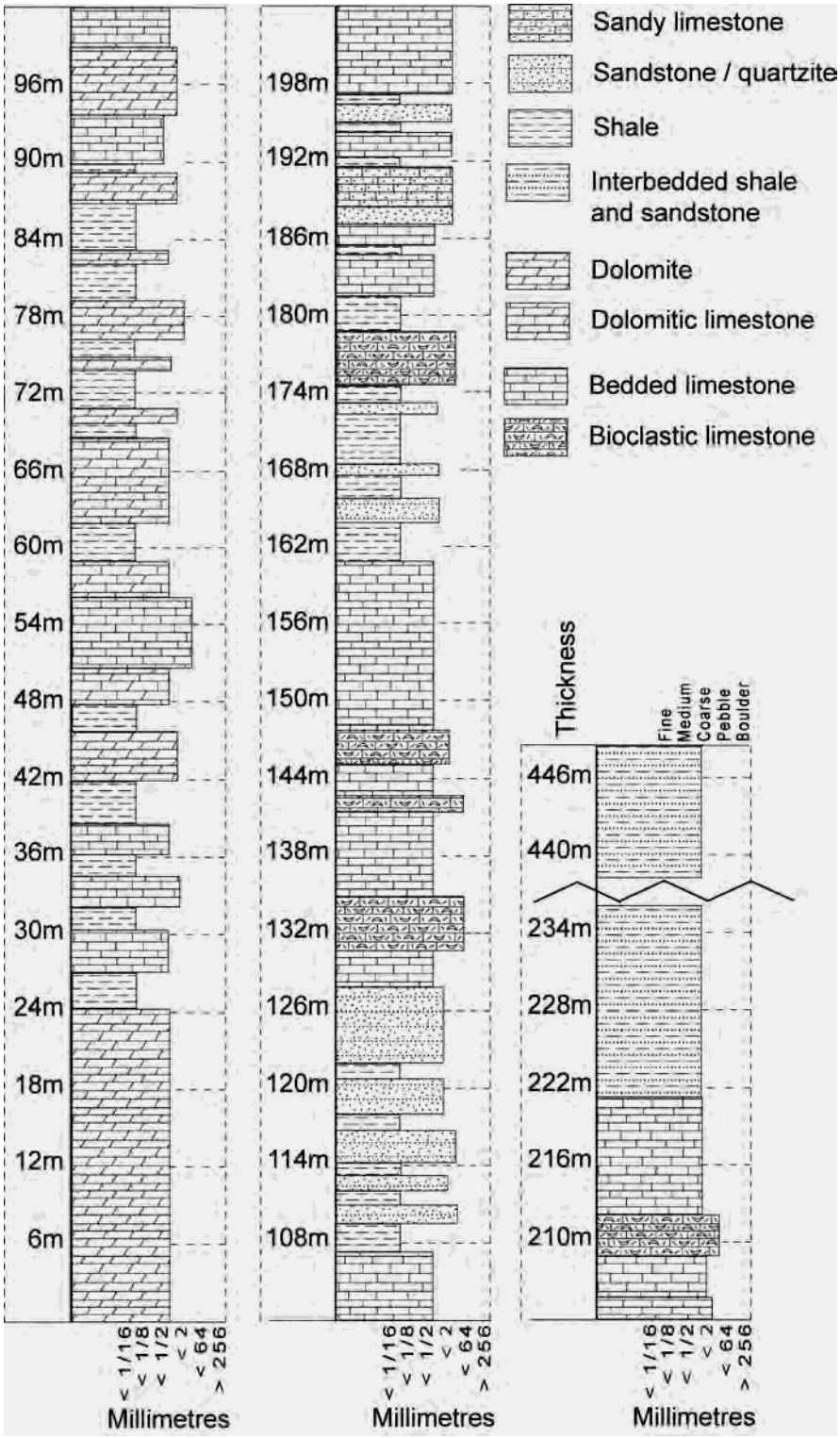

Fig. 3.5. Measured log through the Devonian succession at Tokluca Yayla.

Moving up sequence, dolomite becomes less abundant and the middle part of the succession is composed of shale, quartzitic sandstone and carbonates (Fig. 3.5, 100-220 m). Sandstones are medium- to thick-bedded, recrystallised, hard, and variably white to grey-brown. These beds have fine parallel lamination, and are interbedded with brown shales. Limestone beds are locally coarse and bioclastic, and contain broken shells (particularly brachiopods), crinoids, bryozoans and tabulate coral. These beds are usually fine- to medium-bedded and light grey, and can form moderately thick, uninterrupted horizons within the succession. Rare microbial limestone beds were observed, which are thinly-bedded in comparison to the rest of the sequence.

The uppermost part of the succession is composed of interbedded shale (45%), recrystallised quartzitic sandstone (40%) and dark limestone (15%) (Fig. 3.5, 220-450 m). This part of sequence weathers to a light brown-orange colour, and is comparable to the Devonian units described at Bademli and Çaglayan localities. The quartzite is thin- to medium-bedded, white to light-grey in colour, and typically fine- to medium-grained. A thin (4 m) pebbly sandstone horizon from the top of the succession contains clasts of quartzite (95%) and haematite (5%) (Özgül, 1997). The shales are light-grey and finely laminated. Fossil content is limited, though the brachiopods *Cyrtospirifer* sp. and *Leptaena* sp. have been reported from the mid part of the succession, giving an Upper Devonian (Frasnian to Famennian) age (Özgül, 1997).

3.3.2 Carboniferous

Carboniferous sequences are exposed in both the Hadim and Bolkar nappes (Fig. 3.1). Previous work identified type sections for the Carboniferous within the northerly part of the Hadim nappe (at Bademli village) (Monod, 1977), the southerly part of the Hadim nappe (at Tokluca Yayla) (Özgül, 1997), and the Bolkar nappe (at Baybağan Yayla) (Özgül, 1997). The existing stratigraphic framework for these type sections, in particular the palaeontological data, was exceptionally useful during this study. These three localities will now be discussed, along with three further localities within the study area where Carboniferous units were identified.

3.3.2.1 Locality 1: Bademli. GPS reference 388490 4129840.

Bademli village is located ~35 km north of Akseki town, and ~50 km south of Beyşehir (Fig. 3.1). A well exposed section through the Upper Palaeozoic sequence of the northerly part of the Hadim nappe was found to the northeast of the village (Fig. 3.6, Fig. 3.7). The Lower Carboniferous succession was logged in detail, whilst the Middle and Upper Carboniferous was field checked after Monod (1977).

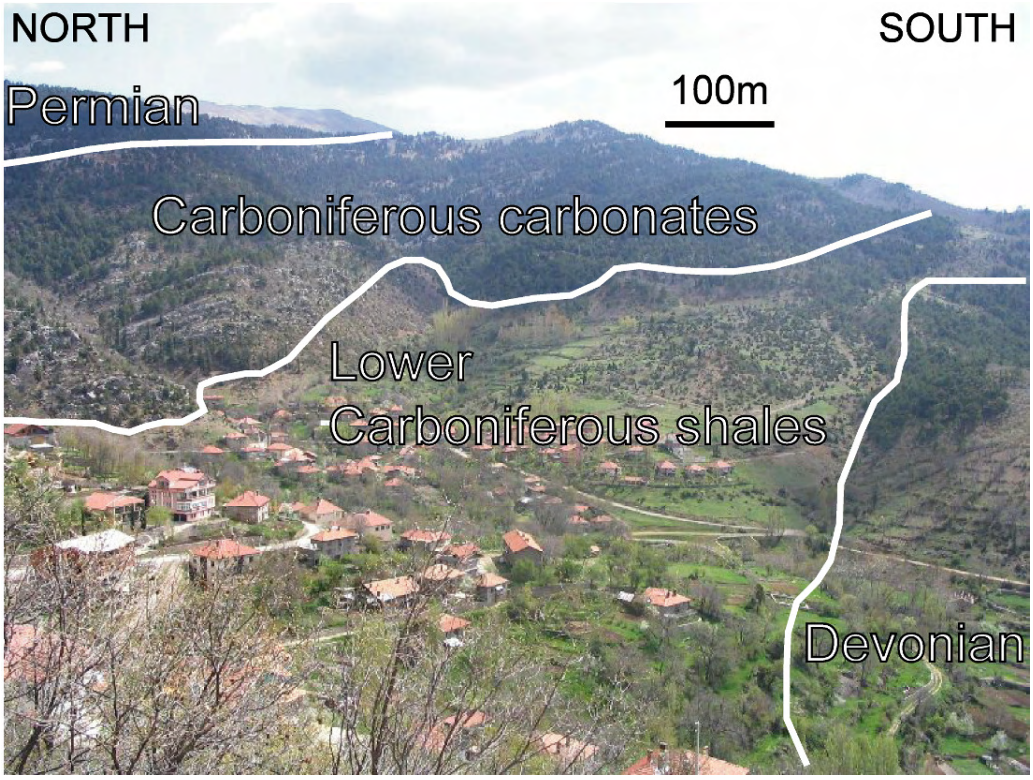

Fig. 3.6. View to the east over Bademli village. Devonian and Lower Carboniferous shales are found in the valley adjacent to the village. Carboniferous and Permian carbonates make up the higher mountains to the north of the village.

Earlier studies have constrained the age of the Carboniferous sediments (Monod, 1977), and the succession at Bademli can be divided into 5 units: (i) 'Schists Noir' (Tournaisian-Visean); (ii) 'Calcaires de Bademli' (Visean-Serpukhovian?); (iii) Dolomite Unit (Serpukhovian-Bashkirian); (iv) Quartzite Unit (Moscovian-Kasimovian?) (v) 'Calcaire de Çevizli' (Gzelian and Permian). This terminology can be

misleading; for example, the 'Schist Noir' translates into English as 'black schists', but this unit is actually composed of shales rather than schists. For the purposes of this study, the 'Schist Noir' will be referred to as the 'Bademli Shales'; the 'Calcaires de Bademli' will be known as 'Bademli Limestone', and the 'Calcaire de Çevizli' will be called the 'Çevizli Limestone'.

The Bademli Shales are represented in the measured section from 0-57 m (Fig. 3.7). A Tournaisian age is constrained by the presence of the Brachiopods *Inflatia*, *Cyrtospirifer*, *Reticularia* and *Schizophoria* (Monod, 1977), although the sequence between 42-57 m may be Lower Visean in age. This Bademli Shale unit is characterised by dark-grey / black fissile shale, locally interbedded with thin horizons of brown quartzitic sandstone and dark-grey carbonate. The quartzite is fine- to medium-grained, and beds are generally <1 m thick, although a 5 m thick horizon (medium-bedded) is observed at 38 m on the measured section (Fig. 3.7, Fig. 3.8a). These sandstones are quartzose in composition, and show fine parallel lamination. Carbonate beds are thin (<50 cm thick) and typically sandy in composition, with some broken shelly fragments (brachiopods). Towards the top of the Bademli Shale succession, thin-bedded carbonates become more abundant. The relative proportions of lithologies in this lowermost sequence are 80% shale, 5% quartzitic sandstone, 5% limestone and 5 % sandy limestone.

The boundary between the Bademli Shale unit and Bademli Limestone unit is represented by a ~15 m transitional zone (Fig. 3.7, 57-72 m). Shale becomes less abundant while sandy limestone and dark grey carbonates become the dominant lithology, interbedded with rare horizons of brown quartzite (Fig. 3.8b). The units are thin-medium bedded (15-50 cm), and become coarser-grained up sequence. Sandy limestone is the dominant lithology between 72-78 m on the measured section (Fig. 3.7). A coarse-grained bed of pebbly calcareous sandstone containing small (<3 cm) reworked black chert clasts, is observed at 75 m (Fig. 3.8c). Many of these beds are laterally variable in thickness, and some of the thinner horizons are lens-shaped, indicative of channelling.

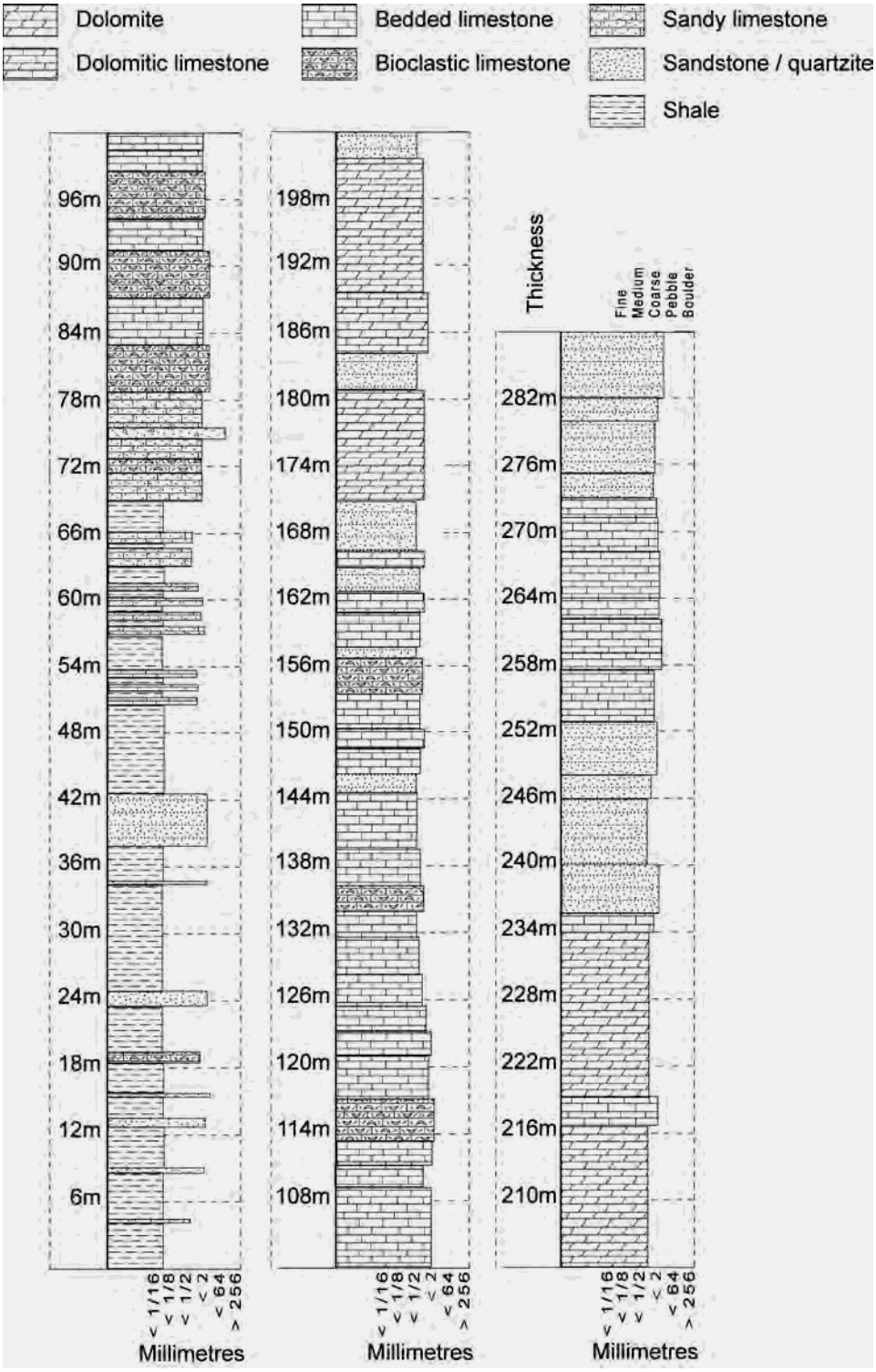

Fig. 3.7. Measured log through the Carboniferous succession at Bademli village. The upper part of the measured section is field checked after Monod (1977).

This transitional zone is overlain by thick-bedded carbonates of the Bademli Limestone unit (Fig. 3.7, 72- 170m). Bioclastic limestone at the base of this sequence contains bivalves, gastropods, brachiopods and echinoderm debris, with the gastropod *Mediocris*, the foraminiferas *Rectodiscus rotundus* and *Archaediscus stilus*, dated as Lower Visean (Monod, 1977). The dark grey Bademli Limestones consist of neritic carbonates including bioclastic limestone, calcarenite, grainstone, packstone, oolitic limestone and some interbedded quartzitic sandstone. As well as shells and echinoderms, the coarser limestone beds contain bryozoan, trilobite fragments, microfossils (foraminifera) and calcareous algae (Monod, 1977). A thicker grey quartzitic sandstone horizon at the top of the Bademli Limestone (Fig. 3.7, 169 m) contains bivalves and some reworked ooids. Limestone intercalated with the quartzite has yielded the foraminifera *Archaediscidae* of Upper Visean – Lower Serpukhovian age (Monod, 1977).

The remainder of the Carboniferous succession is composed of dolomite, dolomitic limestone and quartzitic sandstone. The 'Dolomite unit' (Monod, 1977) is observed from 170-234 m in the measured section (Fig. 3.7) and contains less fauna than the fossiliferous Bademli Limestone. Basal facies are thick-bedded, dark-grey, coarse-grained and heavily recrystallised dolomites. Occasional interbedded quartzitic sandstone horizons are medium-bedded, medium-grained and exhibit parallel lamination. A dolomitic limestone bed at the base of the unit contains the calcareous foraminifera *Globivalvulina moderata* and *Eolasiodiscus* sp. of Serpukhovian age (Monod, 1977). Towards the top of the unit, beige massive dolomites are interbedded with rare black limestone beds. These units yield green algae *Beresella* sp. and *Epimastopora* amongst others, giving an age of Upper Bashkirian (Monod, 1977). During this study, the foraminifera *Climacammina* sp. and *Schwagerinidae* were recovered from higher beds of the 'Dolomite unit', which were subsequently dated as Upper Carboniferous (N. İnan and K. Tasli, pers. comm., 2006).

The Quartzite unit (Monod, 1977) consists of a thick succession of thick-bedded quartzitic sandstone, interbedded with medium- to thick-bedded limestone (Fig. 3.7,

234-288 m). Quartzite is variably fine-, to medium-, to coarse-grained, and has a distinctive orange-red colour. Locally, the quartzite is intercalated with thin-bedded sandy limestone. Midway through the quartzite unit is a sequence of grey-pink-yellow nodular limestone, locally interbedded with limestone breccia and sandstone (Fig. 3.7, 252-274m).

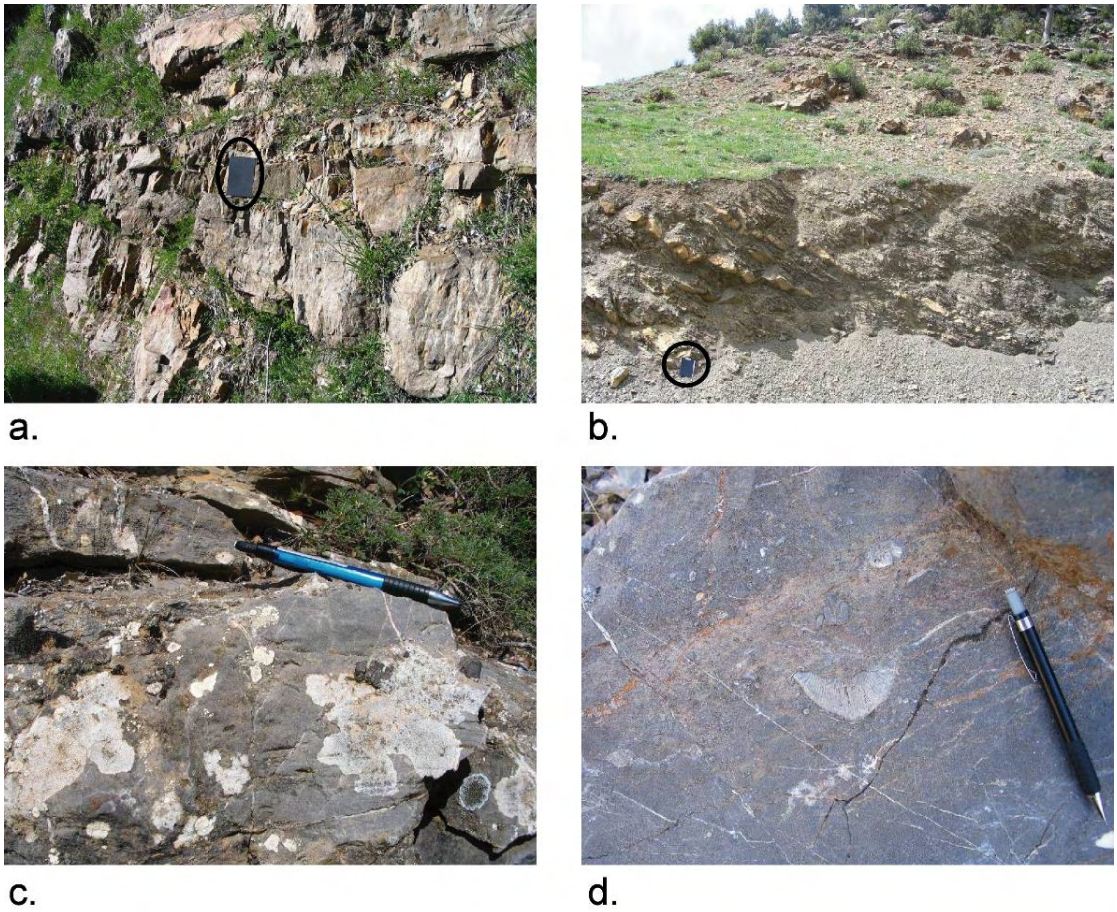

Fig. 3.8. a. Recrystallised quartzitic sandstone horizon from the Lower Carboniferous succession at Bademli. Clipboard circled for scale; b. Transitional facies of interbedded shale, limestone and sandy limestone between Bademli Shales and Bademli Limestone. Clipboard circled for scale; c. Sandy limestone containing small angular clasts of black chert (5 cm below pencil); d. Fossiliferous limestone bed from Upper Carboniferous at Bademli village containing large brachiopod and crinoid fragments.

Many of these limestone beds are fossiliferous grainstone and packstone, containing micro- and macro-fauna including brachiopods, cephalopods and fusilinid foraminifera (Monod, 1977) (Fig. 3.8d). Algae (*Dvinella* sp.) and foraminifera (*Fusiella*)

have yielded a Moscovian age for this carbonate horizon. It is suspected that the uppermost quartzite beds in the succession are Kasimovian in age, and that a thin horizon of carbonate overlying the 'Quartzite unit' may be Gzelian in age based on the presence of the fusilinid foraminifera *Schubertella* (Monod, 1977).

3.3.2.2 Locality 2: Çevizli. GPS reference 391170 4118190

A localised exposure of Carboniferous units were observed in a road cutting to the northeast of Çevizli village, within the northern part of the Hadim nappe (Fig. 3.1). The main lithologies there are medium- to thick-bedded quartzitic sandstone, dark bioclastic limestone and shale.

The stratigraphically lowest sediments exposed at this locality are heavily recrystallised quartzitic sandstones, which are bedded on a 35-100 cm scale. These sedimentary rocks weather to orange-brown, but fresh surfaces are dark-grey. The sandstone is medium- to coarse-grained; grains are sub-rounded to angular, and are 90% quartz and 10% lithic fragments. Locally, the sand is finely laminated. The exposed succession is heavily fractured, possibly due to proximity to a large reversed fault. The interbedded shales are grey-brown in colour and generally thin-bedded, although horizons are locally up to 1 m thick. Thin lenses (5 cm) of fine-grained sandstone are observed within the shale sequence, which is 15 m thick. Stratigraphically overlying the quartzite-shale succession are coarse-grained bioclastic limestones. Most of this material is broken and reworked, and includes coral, brachiopod, bivalve and crinoid fragments. The beds include dense clast-supported packstones.

3.3.2.3 Locality 3: Çaglayan. GPS reference 427280 4110580.

Çaglayan village is found ~8km west of the town of Bozkir (Fig. 3.1). To the south of the village, a permanent dirt track run in a N-S orientation along a small river gorge. A normal fault separates the Bozkir nappes from Palaeozoic – Triassic units of the Bolkar nappe. The Bolkar succession is heavily folded at this locality, and has not been documented in previous literature. Despite an attempt to constrain the ages of the

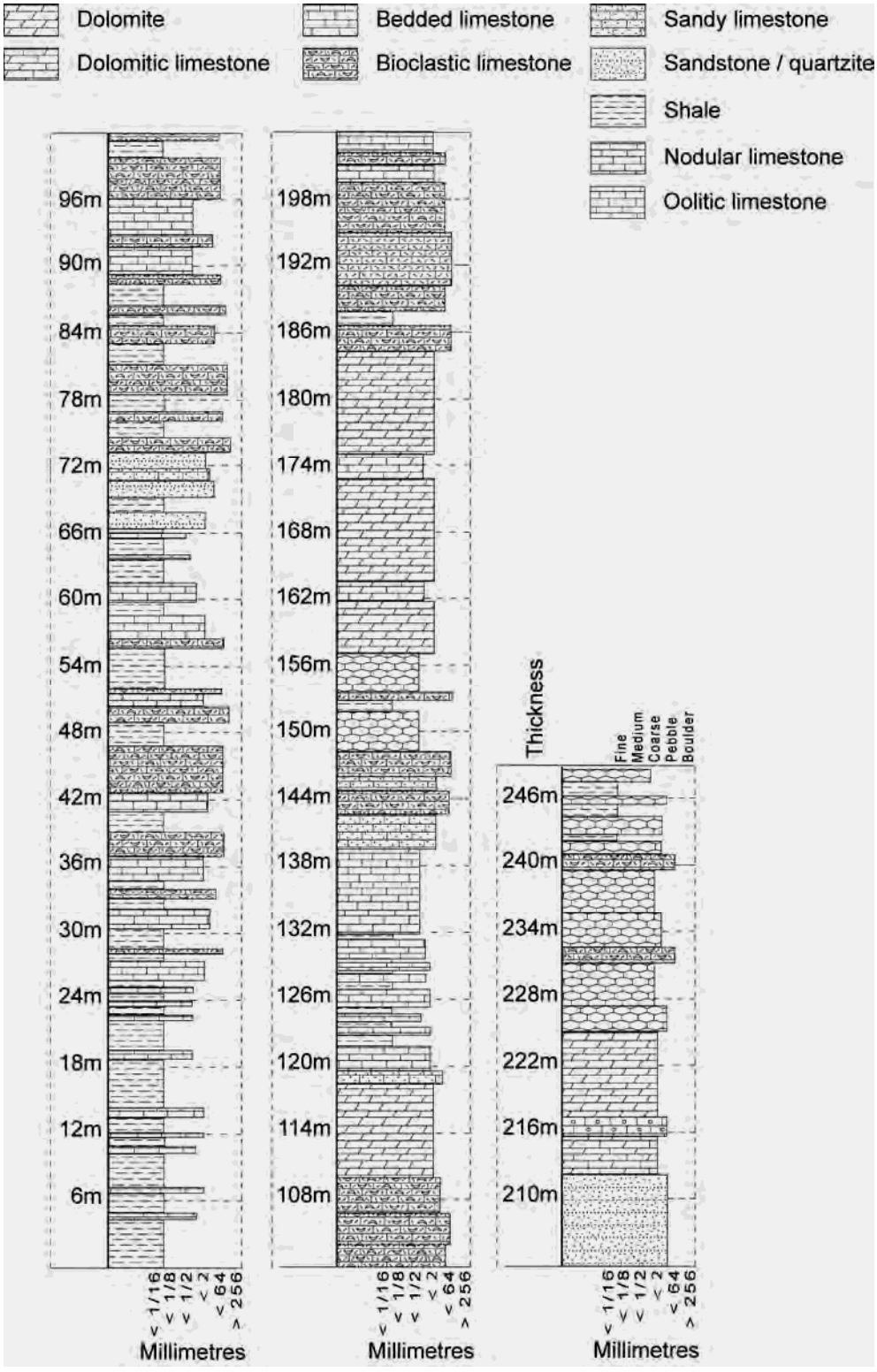

Fig. 3.9. Measured log of the Carboniferous succession south of Çaglayan village.

succession during this study, only limited fauna were identified. The base of the Carboniferous succession is separated from Devonian units by an imbricate thrust, while the top of the succession passes into Permian thick-bedded limestones.

The lowermost sediments within the Carboniferous succession are dark-grey and black micaceous shales (Fig. 3.9), which are heavily foliated on a 2-5 mm-scale. This shale-dominated sequence is ~25 m-thick, and interbedded with thin-bedded dark-grey coarse bioclastic limestone beds. These limestones are only 2-10 cm thick, and contain broken crinoids, brachiopods, coral and bryozoan. Between 24-66 m on the measured section (Fig. 3.9), shale and carbonates continue to be interbedded, with bioclastic limestone the dominant lithology. Limestones vary from thin- to medium- to thick-bedded (5-95 cm), and are often grain-supported packstones composed of reworked crinoids, shell fragments, spicules and corals (Fig. 3.10a). The limestone are very dark-grey or black in colour, partially recrystallised and veined with calcite. In some beds bioclastic material is seen to fine-upwards.

Overlying this is a horizon of medium- to thick-bedded recrystallised quartzitic sandstone, interbedded with shale (Fig. 3.9, 66-74m). The sandstone weathers a distinctive brown-yellow. It is medium-grained, predominantly quartzose, but with some lithic fragments. Overlying are further interbedded shales and limestone (Fig. 3.9, 74-102 m). The abundance of shale varies but typically makes up about 45% of this sequence. Dark-grey limestone beds are typically medium- to thick-bedded, and again contain an abundance of coarse bioclastic material. Locally, thin-beds of limestone contain brachiopods up to 3 cm in size.

Shale becomes less common up sequence, and the remainder of the Carboniferous succession is dominated by thick-bedded carbonates and dolomites, with subordinate quartzitic sandstone and shale horizons. Prominent dolomitic limestone and dolomite successions are found between 110-118 m, 156-184 m, and 212-224 m on the measured section (Fig. 3.9). These horizons are white, recrystallised, and are thick-bedded to massive. Bioclastic limestones contain large Rugosa corals, locally up to 10 cm in size, along with broken crinoid and shelly fragments (Fig. 3.10b). There is also a distinctive recrystallised limestone conglomerate horizon (Fig. 3.9, 190-195 m) which

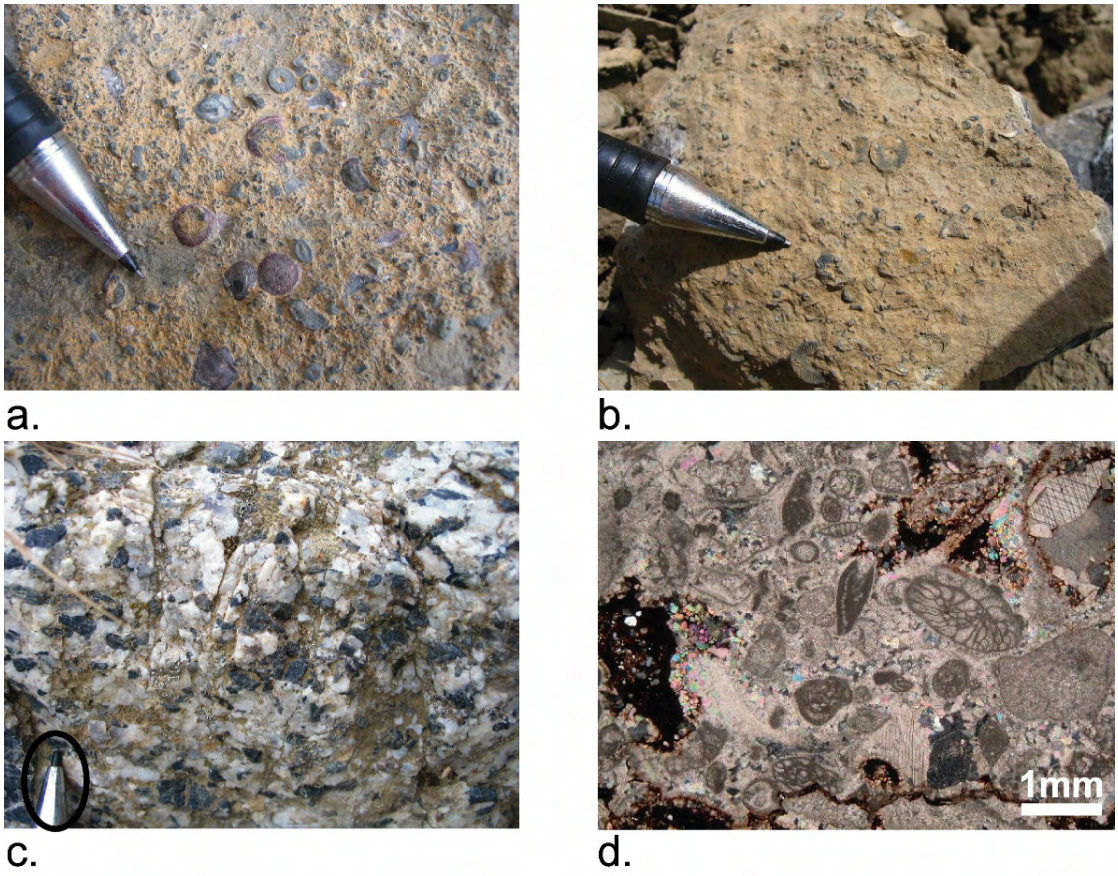

Fig. 3.10. a. Grain-supported packstone containing crinoids, shell fragments and corals from the Carboniferous succession at Çaglayan; b. Bioclastic limestone bed from Middle – Upper Carboniferous at Çaglayan; c. Crystalline white quartzitic sandstone containing angular black chert clasts. Pencil nib circled for scale; d. Photomicrograph of foraminifera bearing nodular limestone of Upper Carboniferous – Lower Permian age.

locally has a red fine-grained muddy limestone matrix. A prominent coarse sandstone horizon is found from 204-210 m in the measured section (Fig. 3.9). The unit is medium- to thick-bedded and composed of a white crystalline quartzitic matrix, with black angular grains of chert (Fig. 3.10c). A single oolitic limestone bed is observed with carbonate grains up to 5 mm in size. In the uppermost part of the succession there are several horizons of nodular limestone. These are recrystallised and dark-grey to grey-red in colour, often with large fossils including coral and Amminoids. At the top of the succession, nodular limestones, containing bryozoan and brachiopod fragments, are interbedded with shales. Fauna recovered from these units (Fig. 3.10d) were identified as

the foraminifera *Ozawainella* sp., *Climacammina* sp. and *Schwagerinidae*, with an age range of Upper Carboniferous to Lower Permian (N. İnan and K. Tasli, pers. comm., 2006).

3.3.2.4 Locality 4: Baybağan. GPS reference 431950 4102560.

Baybağan Yayla is a remote mountain location 10 km south of Uçpinar town (Fig. 3.1), within the Bolkar nappe. The Carboniferous sequence at this locality tectonically overlies Upper Cretaceous syn-tectonic sediments, because Palaeozoic units were thrust southwards during internal deformation of the Bolkar nappe (see chapter 5). Despite tectonic imbrication, intensive faulting and folding, a section through the Lower to Middle Carboniferous is reasonably well exposed. This locality was described by Özgül (1997) as the type section for Carboniferous of his "Bolkar Dağı unit". However, during this study a large fault was observed to truncate the sequence, and a complete Carboniferous section could not be constructed. A summary of the Lower – Middle Carboniferous sequence is shown in Fig. 3.11.

Much of the lower ~50 m of the measured succession consists of dark-grey shale, heavily foliated on a 2-5 mm scale (Fig. 3.11). These sediments are interbedded with thin carbonate beds, often only 1-2 cm thick, but locally up to 30 cm thick. Dark-grey limestone beds are very fine-grained, laminated, and contain no bioclastic material. They are also heavily veined, and have a platy, almost foliated, fabric. The sequence contains randomly distributed siderite nodules and lenses, which are ~10 cm thick and ~20-80 cm wide. These nodules weather to orange-brown, and locally stain the adjacent sediments. Within the lower 50 m of the log, ~90% of the succession is composed of shale, ~9% carbonate and ~1% siderite.

Towards the upper part of the measured section (Fig. 3.11), dark-grey shale is still relatively abundant, however, thick-bedded horizons of limestone are increasingly common in places. A prominent horizon of medium-bedded bioclastic limestone, at 56 m on the measured section (Fig. 3.11), contains crinoids, coral, brachiopods and disarticulated shelly fragments, along with ooids and peloids.

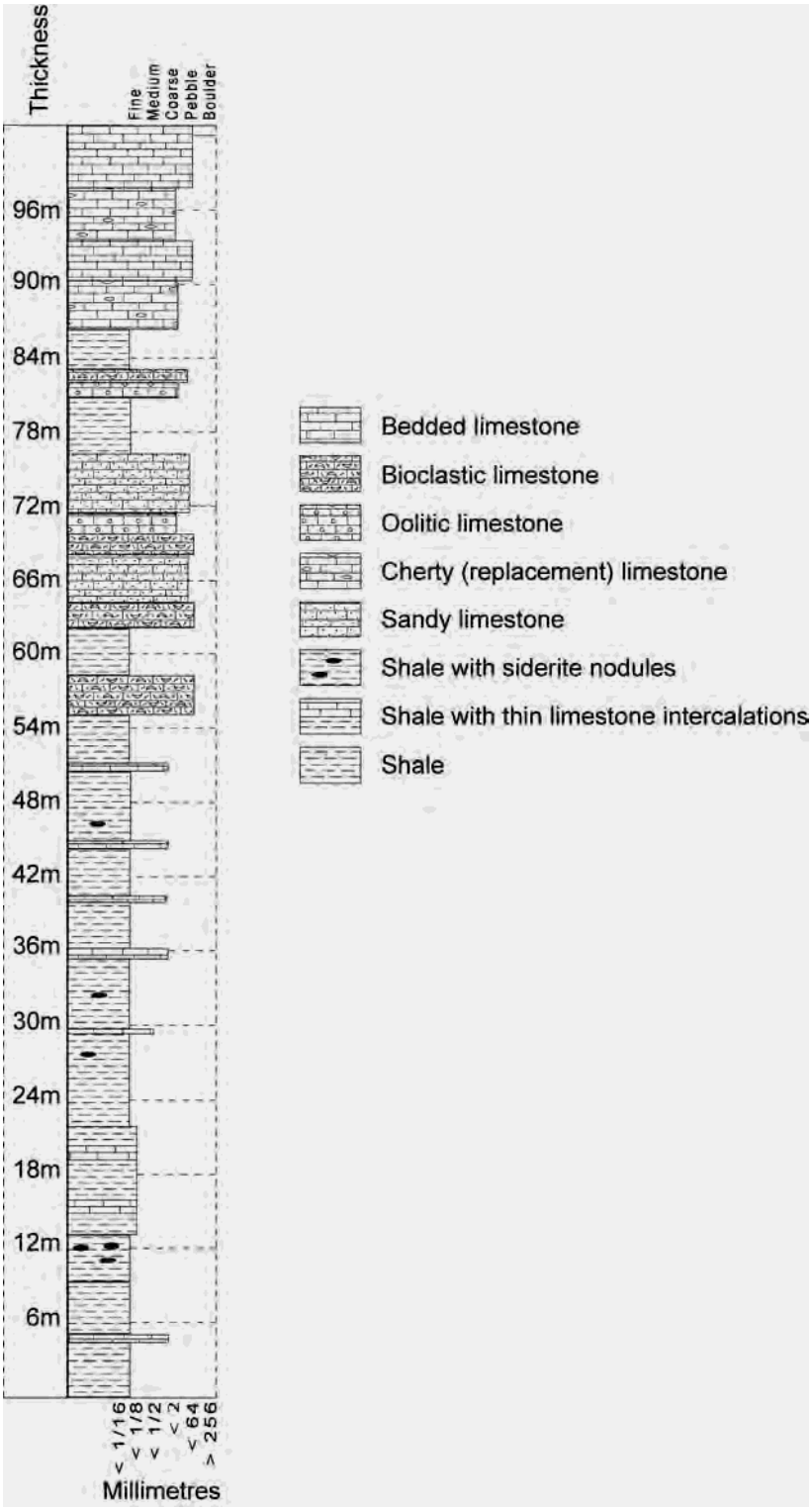

Fig. 3.11. Measured log through the Lower to Middle Carboniferous sequence at Baybağan Yayla. A large fault truncates the section at 100 m.

Foraminifera from these bioclastic beds (e.g. *Archaediscus* sp. and *Permodiscus* sp.) have been dated as Visean-Serpukhovian (Özgül, 1997). A laterally continuous horizon of interbedded grey sandy limestone, oolitic limestone and bioclastic limestone (62-76 m, Fig. 3.11) contains brachiopods, crinoid fragments and Rugosa corals ~5 cm in size. The sandy limestone is closely associated with very thin beds of calcareous sandstone which has a sparry calcite cement and small carbonate concretions.

At the top of the succession, a shale horizon with thin interbeds of oolitic and bioclastic limestone is overlain by medium-bedded, dark-grey, fine-grained recrystallised limestone with black chert nodules of replacement diagenetic type (Fig. 3.11). These sediments are thought to be Bashkirian-Moscovian in age (Özgül, 1997) based on fauna including the calcareous red algae *Rhodophyta* (genus: *Ungdarella*). The uppermost Carboniferous sequence is characterised by white massive recrystallised limestone, adjacent to a reversed fault that separates the sequence from Devonian units.

3.3.2.5 Locality 5: Dedemli Gorge. GPS reference 437570 4197590.

Dedemli Gorge is a E-W trending river gorge located 5 km to the NW of Korualan village. A partial Carboniferous sequence is exposed, bounded to the east by a large normal fault, and underlying an imbricate thrust fault; hence the Carboniferous units are heavily deformed. Despite extensive folding and faulting, the main lithologies were observed. Medium- to thick-bedded, dark-grey limestones are interbedded with thin-bedded heavily foliated shales. The limestone contains small coral fragments and other broken shelly pieces. Small reworked ooids were observed locally. Some limestone beds, that are a lighter grey colour, contain rhomb shaped crystals (seen under a hand lens) of dolomite. Limestones are heavily recrystallised and cross-cut by calcite veins of variable thickness. Dark-grey shales, finely foliated on 2 mm scale, make up about 35% of the succession.

3.3.2.6 Locality 6: Tokluca Yayla. GPS reference 446800 4086010.

The Tokluca Yayla locality is found ~15 km S/SW of Hadim, and is within the southerly part of the Hadim nappe (Fig. 3.1). The Carboniferous units are located close to the tectonic contact between the Hadim nappe and the Bolkar nappe at Ekinlik Yayla. There is significant faulting and folding within this area, particularly imbricate thrusting which has tectonically thickened the lower part of the Carboniferous succession. The base of the Lower Carboniferous overlies Devonian shale/quartzite, whereas the Upper Carboniferous is overlain by Permian thick-bedded carbonates. The distributions of Lower, Middle and Carboniferous units are shown in Fig. 3.12. This locality was described as the type section of the Carboniferous within the Hadim nappe (Özgül, 1977), and during this study a complete section was measured (Fig. 3.13).

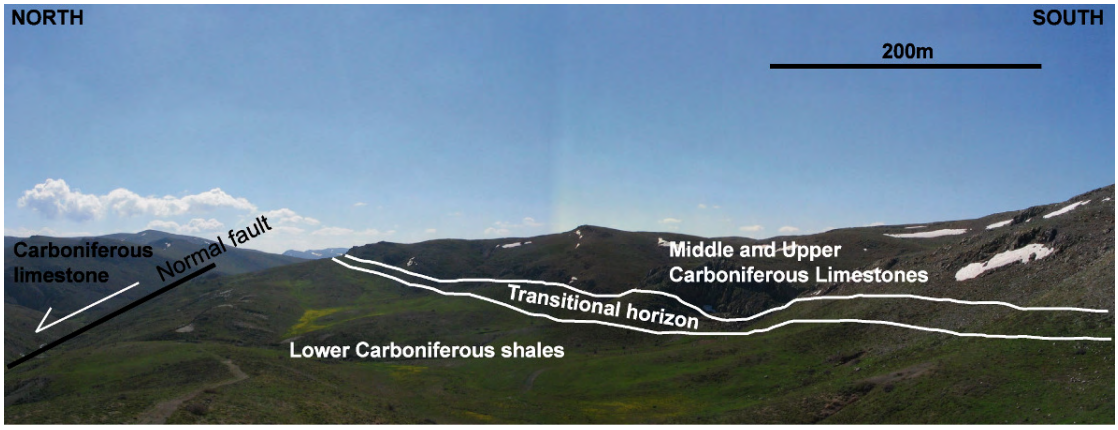

Fig. 3.12. Annotated photograph showing the distribution of Carboniferous units at Tokluca Yayla.

The lowermost part of the measured section is dominated by dark-grey/black micaceous shales (Fig. 3.13, ~0-100 m). These sediments are foliated on a 1cm-scale and very finely laminated, with a slaty fabric. Throughout the sequence the shales are interbedded with very fine-grained dark-grey limestone beds, which are 3-8 cm thick. Occasionally, these limestone beds contain reworked bioclastic material, including brachiopods, corals, bryozoan and crinoids. Siderite nodules, ~10 cm in size, were observed in the shale sequence. Also interbedded with the shales are medium-bedded sandy limestone and quartzitic sandstone, which locally contain clasts of dark black

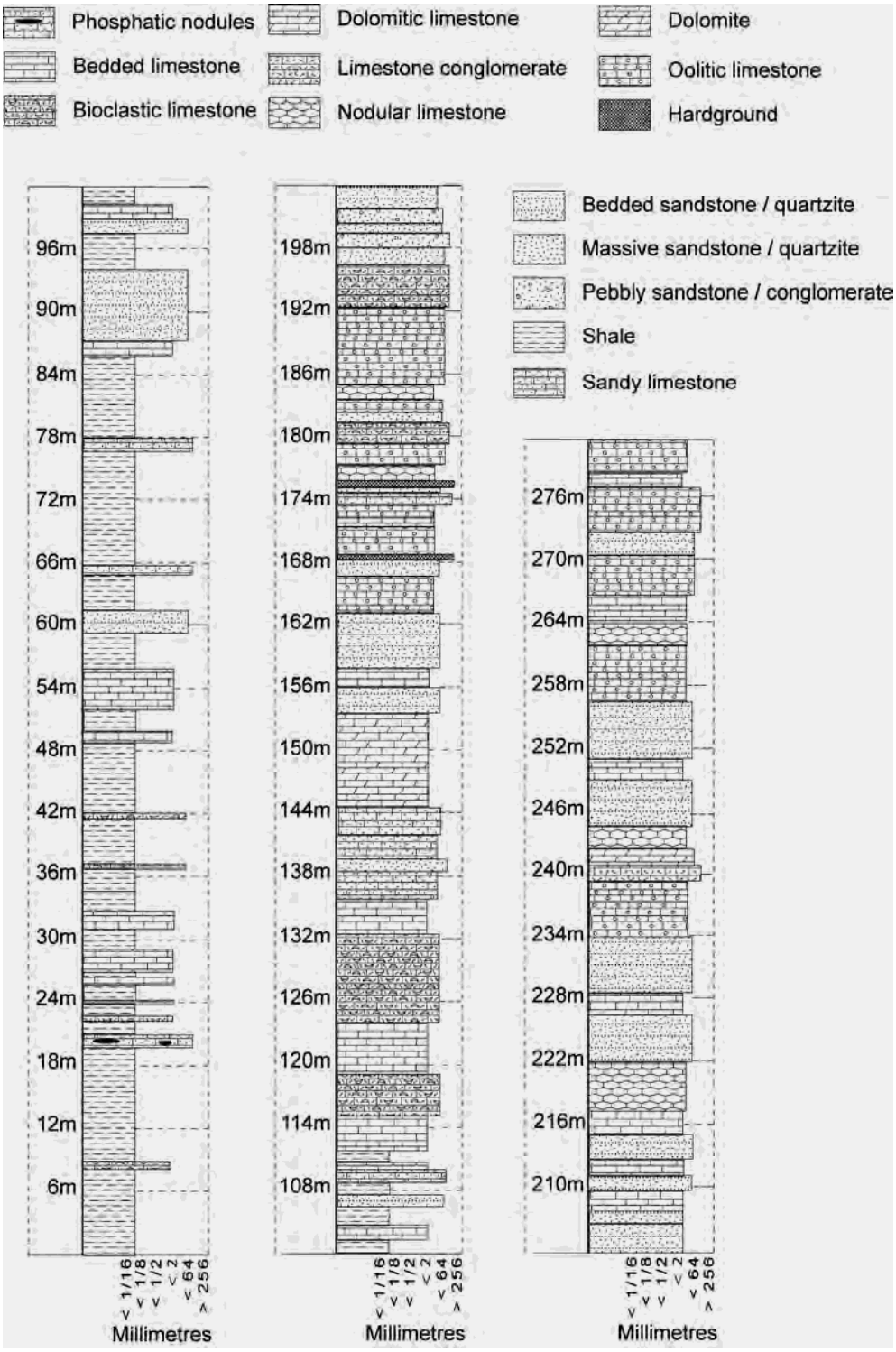

Fig. 3.13. Measured log through the Carboniferous succession at Tokluca Yayla, to the SW of Hadim town.

material. The sand is quartzose, fine- to medium-grained, with angular to sub-rounded black clasts (4-30 mm). The clasts occur towards the base of beds which fine upwards. During this study, these clasts were extracted from the matrix and analysed using X-ray diffraction; this showed that they are primarily composed of fluorapatite (Fig. 3.14). Planar cross-bedding is also observed in these sandy beds which locally indicate palaeocurrent flow to the south (Fig. 3.15a). Fauna identified in this lowermost shale succession include the foraminifera *Earlandia minor* and the brachiopod *Rhipidomella*, which have been dated as Tournaisian (Özgül, 1997).

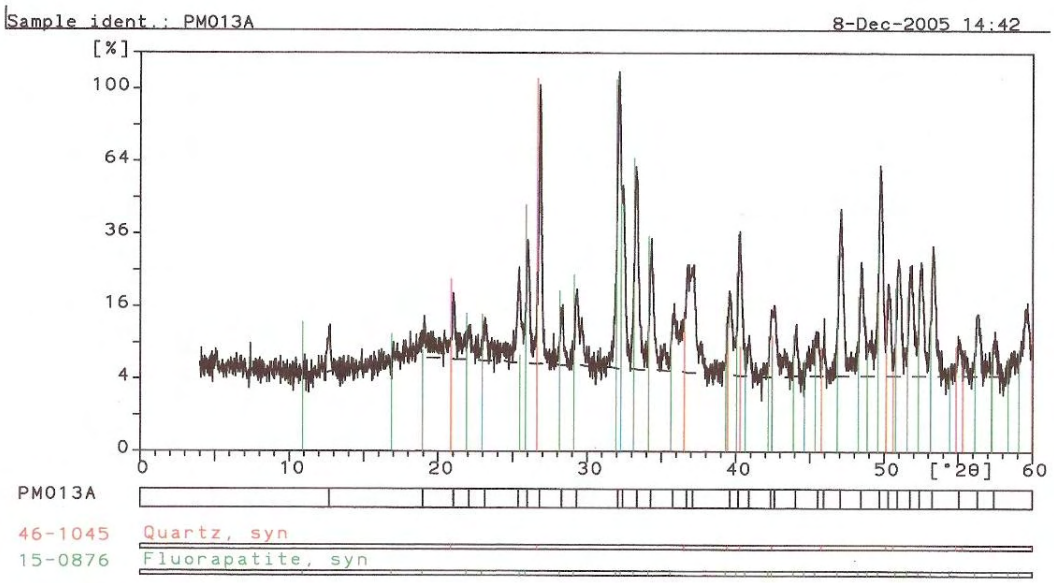

Fig. 3.14. X-ray diffraction analysis of phosphatic nodules from the Lower Carboniferous sequence. Minerals identified were quartz (matrix) and fluorapatite.

A thick horizon of quartzitic sandstone is found towards the upper levels of the shale succession (Fig. 3.13, 86-94 m). This is composed of light-grey (weathering to brown-orange), medium-bedded (60-85 cm), medium-grained, and laterally continuous strata. Overlying this horizon is a transitional sequence in which interbedded shale, limestone, sandstone and sandy limestone pass upwards into a thick bedded carbonate succession (Fig. 3.13, 96-114m). At the base of this succession, medium- to thick-bedded bioclastic limestones contain current-imbricated shells. Large Rugosa corals (10

cm) are present, along with crinoid fragments, bryozoa and gastropods (Fig. 3.15b). These horizons contain evidence of horizontal and vertical burrowing.

Overlying these sediments is a succession of sandy limestone with interbedded quartzitic sandstone (Fig. 3.13). These are thick-bedded (~1 m), quartzose, fine-grained and yellow-grey, with sub-rounded to sub-angular grains. These beds display hummocky cross-bedding (Fig. 3.15c) on a 20-50 cm-scale. Local palaeocurrents indicate flow to the north/northwest. Some of the sandstone beds are lens shaped (15 m-wide, 1 m-high), and contain calcareous concretions within the sandy limestone beds. Optical microscope examination of these units (Fig. 3.15d, e) revealed brachiopod shell fragments, and echinoderm spines and debris, along with various microfossils.

The foraminifera *Endothyra* sp., *Archaeodiscus* sp. and *Pseudolituotubidae* were identified during this study by N. İnan and K. Tasli (pers. comm., 2006), which date the sandstone and sandy limestone units as Early Carboniferous (Fig. 3.13, 136-144 m). Correlation between the stratigraphic descriptions and palaeontological data documented by Özgül (1997), suggests that these units are of Middle Visean age.

A sequence of thick-bedded dolomitic limestone overlies the cross-bedded sandy limestone, followed by purple quartzitic sandstone (Fig. 3.13, 144-162 m). The sandstone is finely laminated, medium-grained, and well cemented / indurated. Some beds contain coarse reworked bioclastic debris. The overlying ~30 m of the measured section is dominated by oolitic limestone, with lesser amounts of sandstone, bioclastic limestone and nodular limestone. Ooids are 1-3mm in size, and recrystallised. Bioclastic beds contain gastropods, crinoids, brachiopods, and redeposited ooids. Within this sequence are also two horizons, 30 cm thick, that have a nodular surface with a dark Fe-Mg rich matrix (Fig. 3.13, 168 m and 175 m). These could be condensed metal-enriched deposits formed during lithification of the sea floor during a period of non-deposition. Özgül (1997) documented this oolitic limestone-dominated part of the succession as containing the foraminifera *Eostaffella* and *Archaediscus* sp. of Upper Visean age.
Overlying this oolitic succession here is a thick succession of quartzitic sandstone and various carbonates, with sandstone making up about 55% of the sequence

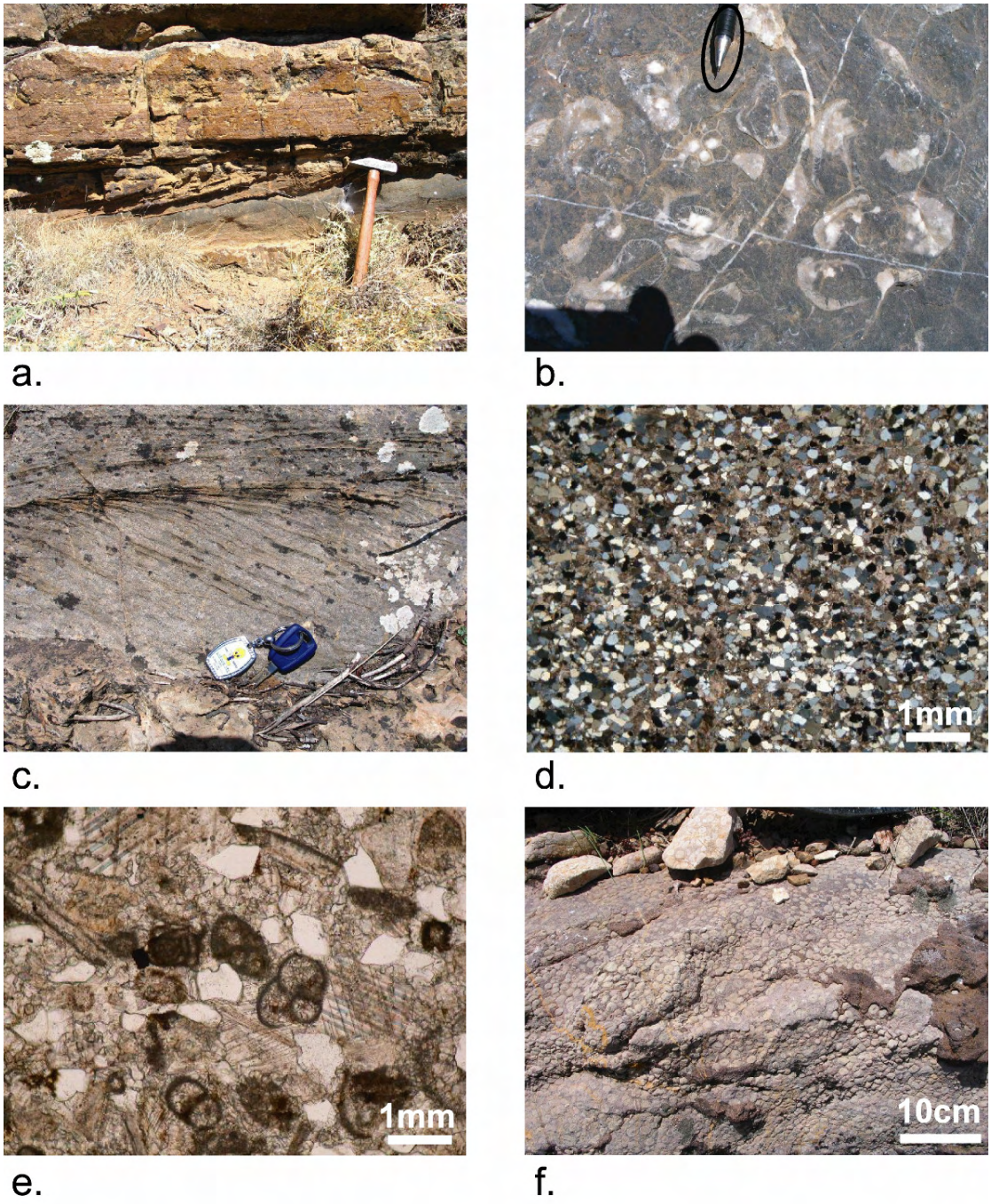

Fig. 3.15. a. Interbedded sandy limestone and quartzitic sandstone, with planar cross-bedding showing palaeocurrent flow to the south; b. Rugosa coral, gastropod, crinoid and bryozoan bearing bioclastic limestone. Pen nib circled for scale; c. Hummocky cross-bedding within sandy limestone horizons of Lower Carboniferous at Tokluca Yayla. Car key for scale; d. Photomicrograph of fine-grained Carboniferous quartzitic sandstone; e. Photomicrograph of foraminiferal-bearing sandy limestone dated as Lower Carboniferous; f. Pisolitic limestone in the Upper Carboniferous succession with pisoids up to 1 cm in size.

(Fig. 3.13, 195-257 m). Sandstones are typically medium-bedded, recrystallised, purple, quartzose and parallel-laminated. Locally some pebbly sandstone / conglomerate beds contain clasts of limestone, quartzite and black chert, ranging from 1-4 cm in size. Interbedded with this limestone is oolitic / pisolitic limestone, with some carbonate grains, up to 1 cm in size. Grey recrystallised nodular limestone and occasional dolomitic beds, along with non-descript grey medium-bedded limestone, and a 1.5 m-thick limestone conglomerate horizon, complete this sequence. There is lateral interfingering of quartzitic and carbonate horizons. Microfossils from the carbonate beds within the sequence, including the foraminifera *Globivalvulina moderata*, indicate a Serpukhovian-Bashkirian age for this interbedded sandstone and carbonate sequence (Özgül, 1997).

The uppermost 25 m of the Carboniferous succession consists of oolitic and pisolitic limestone, interbedded with sandstone, nodular limestone and recrystallised grey limestone (Fig. 3.13, 257-282 m). Some of the pisolitic limestone is very coarse, with pisoids up to 1 cm in size (Fig. 3.15f). An oolitic horizon with a pink limestone matrix at 260 m on the measured section (Fig. 3.13) contains fragments of brachiopod shells and spines with large forams, visible to the naked eye, which were subsequently identified as *Profusulinella* sp., *Schwagerinidae*, and *Endothyra* sp. (Fig. 3.16) (N. İnan and K. Tasli, pers. comm., 2006). These Upper Carboniferous fossils can be correlated with fauna of Bashkirian-Moscovian age that Özgül (1997) recovered from the same oolitic horizon. The youngest sediments in the Carboniferous sequence are identified as Moscovian, and are conformably overlain by thick-bedded dark grey Permian limestones (Özgül, 1997). For this reason there may be a stratigraphic break in the sequence as no sediments of Upper Carboniferous Kasimovian and Gzelian ages sediments are recorded. However, only limited palaeontological information has been published on the succession, and the boundary between Upper Carboniferous – Early Permian sediments is not well constrained.

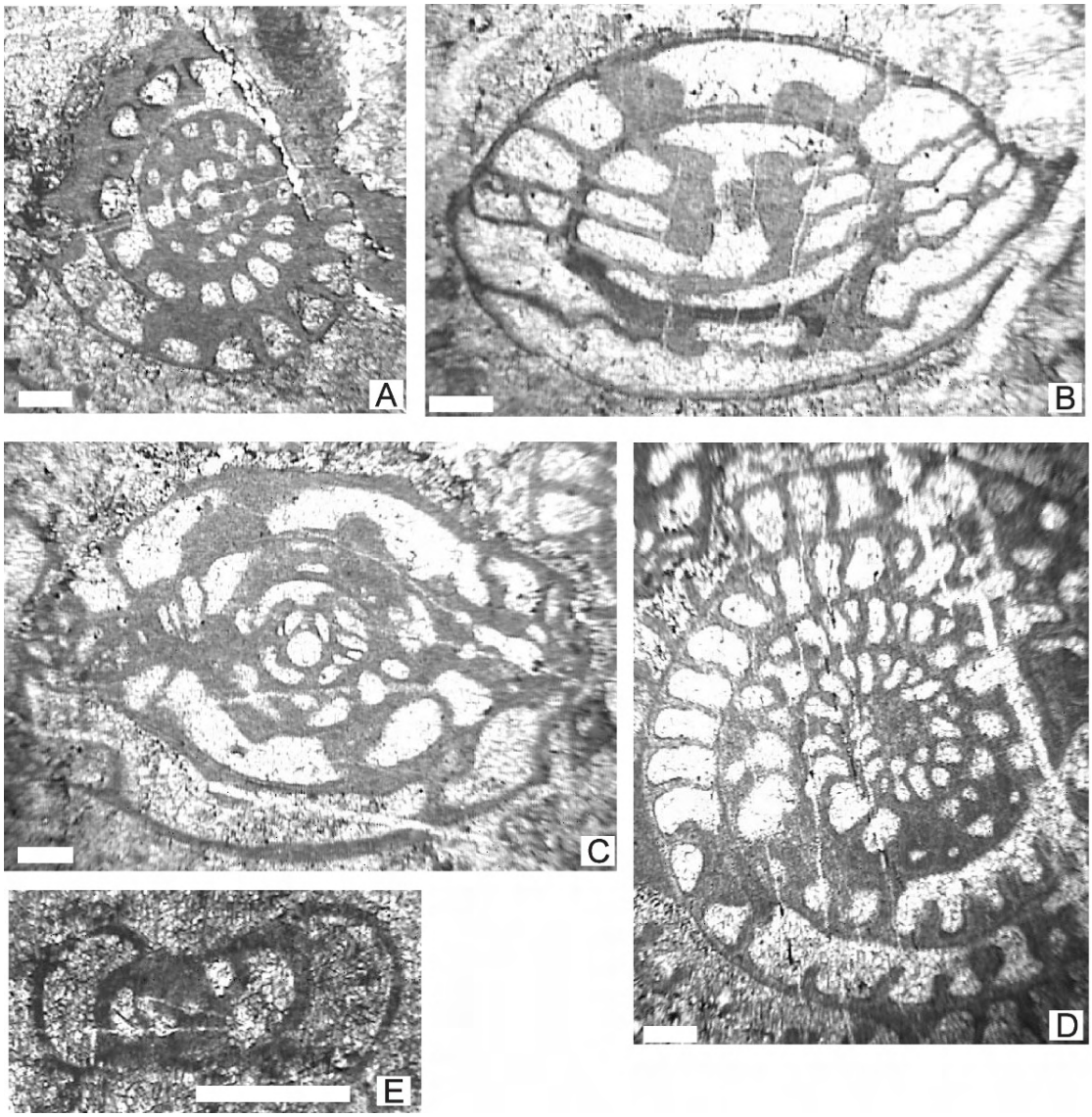

Fig. 3.16. Microfossils of Upper Carboniferous age obtained from the upper part of the Tokluca Yayla sequence. a., b., c. *Profusulinella* sp.; d. *Schwagerinidae*; e. *Endothyra* sp.. Scale bar in each plate is 1 mm in size.

3.3.3 Permian

Permian successions are exposed in the Hadim and Bolkar nappes. The Permian is dominated by thick-bedded grey limestones, with the thickness ranging from <500 m in the north (Bademli area, after Monod, 1977) to a reported 2000 m in the south (Hadim area, after Özgül, 1997). The thickness of Permian units in the Hadim area could not be

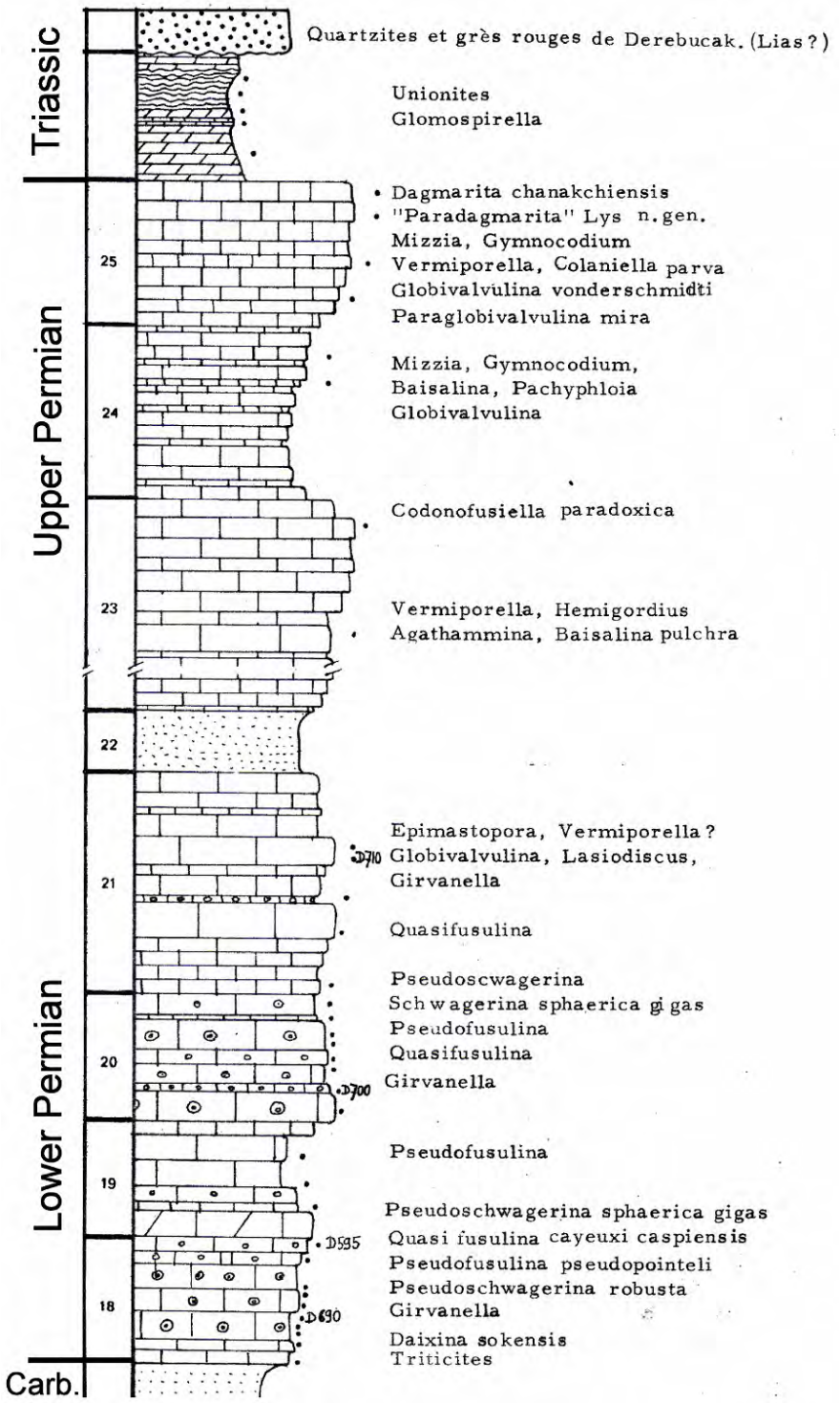

Fig. 3.17. Log through the Permian Çevizli Limestone at the village of Bademli, within the Hadim nappe. Figure scanned and modified from Monod (1977).

confirmed in this study, and it is suspected that the thickness previously suggested is inaccurate due to local tectonic thickening of the stratigraphy. During this study, type sections, as described by Monod (1977) and Özgül (1997), were observed, although no new detailed logging was undertaken. A measured section of the Permian succession, along with fauna identified, is shown in Fig. 3.17 (Monod, 1977).

In the northerly part of the Hadim nappe, the best exposure is found near Bademli village. The Permian there is known as the Çevizli Limestone (Monod, 1977), 400-500 m thick. The oldest Permian sediments are dated as Early Permian (Asselian) in age, whilst the youngest sediments are Late Permian (Kazanian to Tantarian) (Monod, 1977). The lowermost Permian units are medium- to thick-bedded oolitic limestones, which overlie Carboniferous sandstones, that are clearly identifiable in the field. The Lower Permian succession is dominated by oolitic limestone, bioclastic limestone (packstone and wackestone), nodular limestone and microbial limestone. These units contain abundant shelly fauna (e.g. brachiopods, bivalves, gastropods), crinoids and corals (especially Rugosa). A distinctive horizon of white recrystallised quartzitic sandstone is found in the middle of the Permian sequence. Overlying this is a thick succession of Middle Upper Permian thick-bedded, dark-grey limestone, with rare shale horizons towards the top of the formation. In the southerly Hadim nappe, the Permian stratigraphy is very similar in composition to that at Bademli. In the Bolkar nappe, the Permian succession is reported as 820 m thick at the type locality, 10 km NE of Korualan village (Özgül, 1997).

3.4 Sedimentation rate

Subsidence and sedimentation rates can provide useful information on the tectonic evolution of sedimentary basins and continental margins. Quantitative analysis of subsidence rates requires the decompaction of stratigraphic units to their thickness at the time in question (Allen and Allen, 1990). No attempt was made here to provide accurate subsidence rates for the studied units; however, calculations using the measured stratigraphic sections provide an indication of the relative rates of sedimentation for different units during the Late Palaeozoic. This highlights differences between time

periods and stratigraphic units. These relative rates, calculated using the data provided above, are presented in Fig. 3.18.

	Hadim Nappe *(mm/kyr)*	Bolkar Nappe *(mm/kyr)*
Devonian	7.11	n/a
Carboniferous	4.33	3.91
Tournaisian	6.05	6.67
Visean	6.39	4.53
Serpukhovian	12.75	9.50
Bashkirian	2.25	1.50
Moscovian	5.50	3.25
Kasimovian	1.14	2.28
Gzelian	1.33	0.66
Permian	11.90	19.52*
Triassic	11.62**	n/a

Fig. 3.18. Semi-quantitative sedimentation rate estimates for the Upper Palaeozoic of the Hadim and Bolkar Nappes (based on post-compaction thicknesses). *Based on an estimated Permian thickness of 820 m; **Disconformity between Middle and Upper Triassic sediments represents unknown period of non-deposition/erosion.

Significant error may occur due to difficulties in determining stratigraphic boundaries within the Upper Palaeozoic sequences. Also, these sedimentation rates take no account of stratigraphic disconformities. However, it can be tentatively concluded that sedimentation rates remain fairly constant from Devonian to Upper Carboniferous time, followed by an increase during the Permian and Triassic. Also, the sedimentation rate in the Hadim nappe and Bolkar nappes are roughly the same.

3.5 Facies associations and depositional environments

As documented in the introduction to the Late Palaeozoic tectonic setting of the Tauride platform (section 3.2), the critical time period for the regional tectonic setting is the Early Carboniferous. In this section, particular emphasis will be placed on Carboniferous facies associations and inferred depositional environments.

One of the most important influences on sedimentary facies variations at continental margins is relative sea-level rise and fall. In particular, the distribution of siliciclastic sediments can be influenced be even minor changes in global sea-level. As

sea-level regresses, siliciclastic sediment could be transported to more distal parts of the shelf; likewise, marine transgression can result in the landward migration of a marine siliciclastic belt. Sea-level change can be affected by a variety of geological mechanisms, such as growth and decay of ice sheets, variation in sedimentation and large-scale tectonic processes (Fig. 3.19) (Miller et al., 2005). Global sea-level change during the Late Palaeozoic will be considered for each of the main time periods.

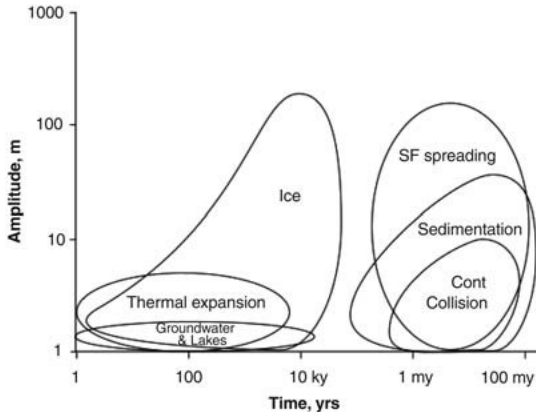

Fig. 3.19. Timing and amplitudes of geologic mechanisms of sea-level change; from Miller et al. (2005).

3.5.1 Devonian

The Devonian succession can be divided up into three facies associations. The **dolomite unit** is found in the lower levels of the Devonian succession. This unit is only observed in the southerly Hadim nappe, where the base of the dolomite sequence tectonically overlies Mesozoic rocks of the Bolkar nappe. The unit consists of medium- to thick-bedded dolomite, interbedded with recrystallised limestone and shale. It is overlain by the quartzite unit. The **quartzite unit** is found in the mid part of the succession, and is best exposed at Çaglayan (section 3.3.1.2). It consists of medium- to thick-bedded, recrystallised quartzitic sandstone, with parallel lamination, locally intercalated with shale. This unit varies from 120 m-thick at Çaglayan, to 20 m thick at Tokluca Yayla. At Tokluca Yayla (section 3.3.1.3), the quartzite unit overlies the dolomite unit, and is overlain by the **interbedded sandstone, shale and limestone unit**. This interbedded

unit is found towards the upper part of the Devonian succession and is overlain by Lower Carboniferous shales. The thickness varies considerably from 100 m at Bademli, to >200 m at Tokluca. This unit is composed of variable, thin to thick beds of quartzitic sandstone, shale and carbonate.

The dolomite and limestone units contain abundant coral, shelly fauna, crinoids and bryozoan. This is indicative of a carbonate reef in a warm-water, shallow-marine environment (<10-20 m) (e.g. Sellwood, 1986; Einsele, 1992). The coralline and algal limestone could represent patch reefs on a gently sloping carbonate shelf. Interbedded with these units are fine-grained sandstones and mudstones, indicative of a low energy environment (Özgül, 1997). Mudstone can form in a variety of shallow-marine settings, such as a nearshore mud belt (Tucker, 1985; Tucker, 1991; Dalrymple, 2005).

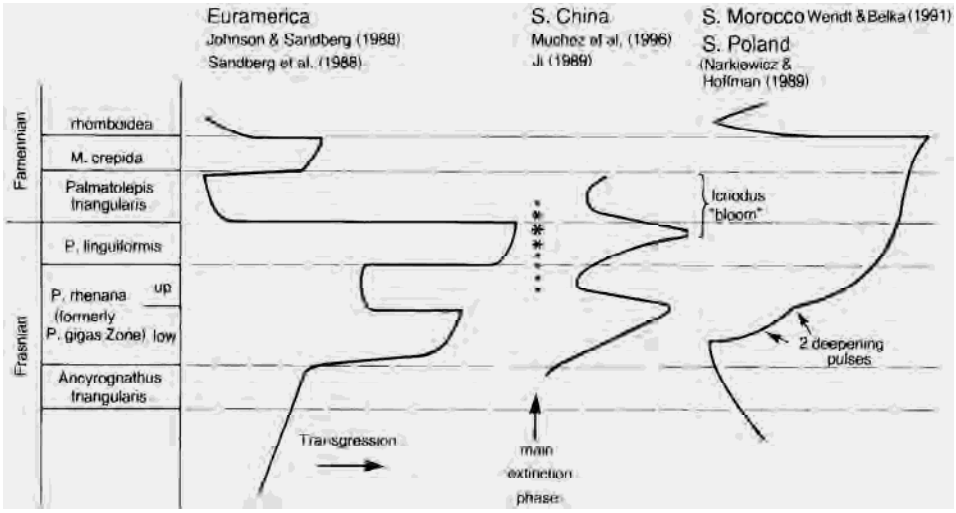

Fig. 3.20. Comparison of eustatic sea-level curves for the Late Devonian. From Hallam and Wignall (1999).

The variations between facies could be related to eustatic sea-level change and also marine transgression and regression (Demirtaşlı, 1984a). Fluctuations in global sea level have been documented for the Late Devonian (Frasnian – Framennian), as shown in Fig. 3.20 (Hallam, 1992; Hallam and Wignall, 1999). The three sea-level curves show there is debate on whether or not the Frasnian – Framennian boundary represents a major

regression; either way, it is evident that significant sea-level transgression – regression occurred during the Late Devonian. A lack of faunal data for the Devonian sequences makes it difficult to correlate siliciclastic sedimentation with any particular regression/transgression event. However, it is likely that the fluctuations in clastic input during the Devonian were related to global sea-level change.

3.5.2 Carboniferous

The Carboniferous type section at Bademli (section 3.3.2.1) has been divided into four main stratigraphic units (Monod, 1977): (i) Bademli Shales; (ii) Bademli Limestones; (iii) Dolomite Unit; (iv) Quartzite Unit. Also, the lowermost beds of the Permian Çevizli Limestone may be uppermost Carboniferous in age (Monod, 1977). Through a combination of palaeontological data and facies association, these stratigraphic units can be correlated across the study area (Fig. 3.21). Subtle variations in the lithology are observed across the study region.

3.5.2.1 Bademli Shales

This facies association is the lowermost unit within the Carboniferous succession, and directly overlies Upper Devonian quartzites, shales and limestone. The thickness across the study area is relatively constant, ranging from 70-100 m. The age is constrained by palaeontological data as Tournaisian – Lower Visean (Monod, 1977; Özgül, 1997). This unit is characterised by very dark shales, interbedded with thin intercalations of carbonate and occasional quartzitic sandstone horizons. The unit contains limited fauna, which could be indicative of a reduced salinity environment. The brachiopod assemblage is indicative of normal or reduced salinity environments (e.g. *Cyrtospirifer*). The presence of sandstone beds with reworked phosphatic nodules is critical to understanding the depositional setting. Marine phosphorite forms in environments with low depositional rates, such as distal continental shelves (Tucker, 1991). Upwelling of cold, nutrient-rich waters from an the oceanic basin results in increased organic activity at the shelf margin, and the formation of phosphatic-rich sediments. Such ‘phosphatic pavements’ can be laterally continuous across much of the shelf during marine

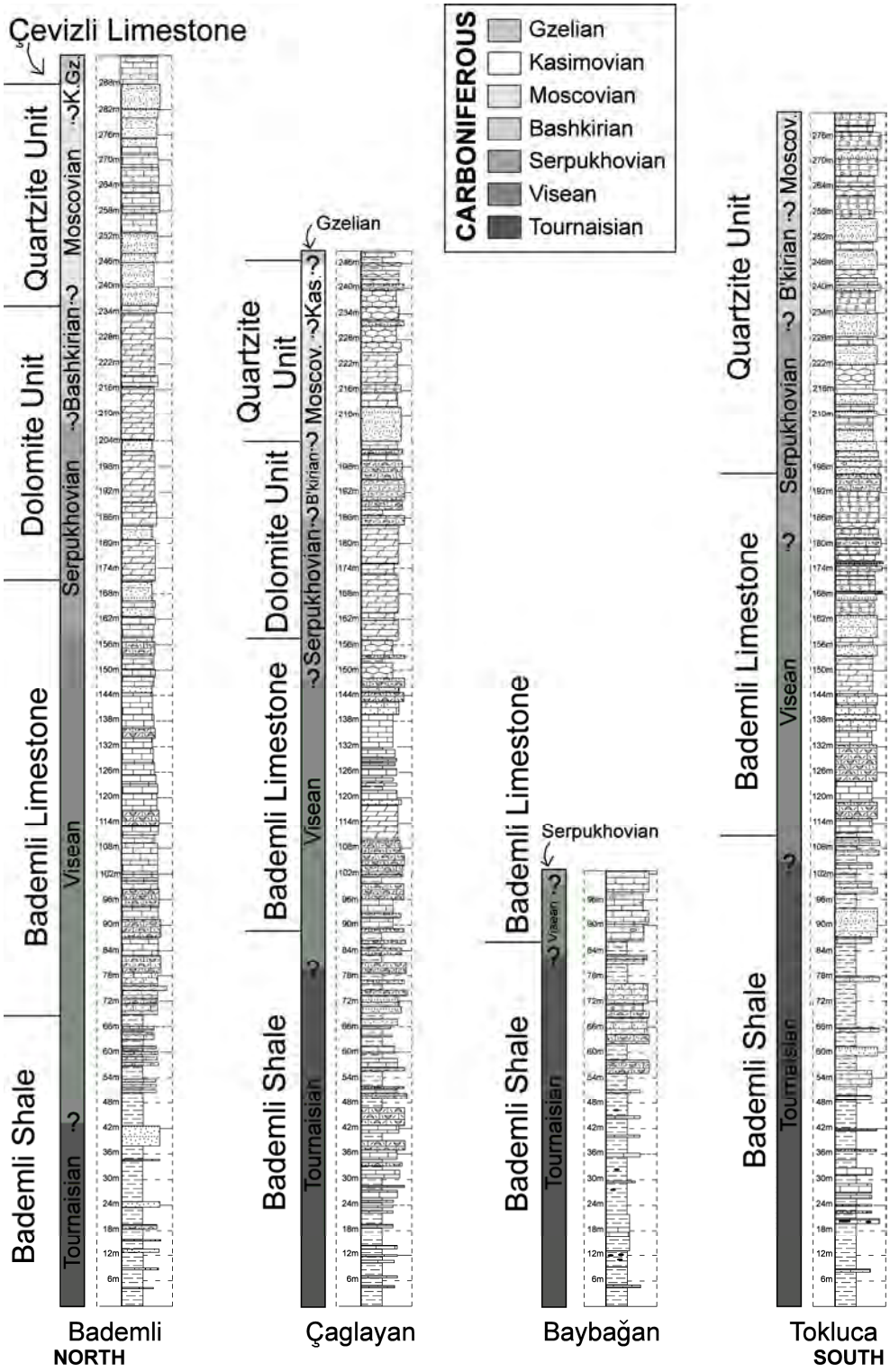

Fig. 3.21. Correlation of Carboniferous stratigraphic units, facies associations and ages across the study area. Stratigraphic units based on classification of Carboniferous type section at Bademli (Monod, 1977).

transgression (Tucker, 1991). These are often closely related to organic-rich mudstones, since fine-grained sediment is transported further across the continental shelf (Fig. 3.22) (Einsele, 1992). It is, therefore, possible that these units were deposited in an outer shelf setting. Also, the lack of sedimentary structures is consistent with deposition below the wave base, which in a storm influenced environment could represent tens of metres water depth. An alternative is that they were deposited in a protected setting.

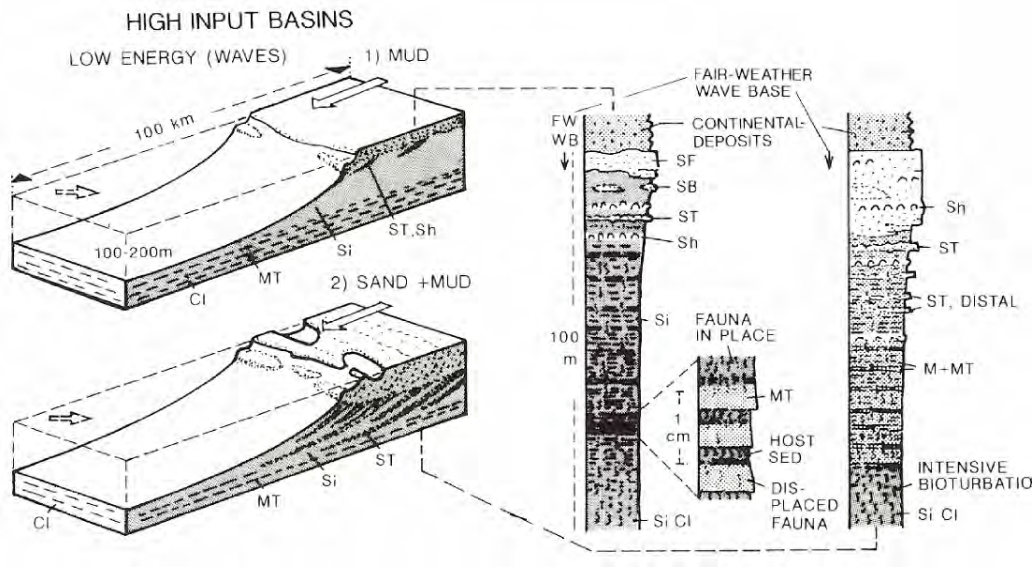

Fig. 3.22. Typical basin setting where terrigenous mud and sand is deposited in a distal shelf setting (Einsele, 1992).

The end-Devonian (Hangenberg) extinction event affected goniatites and placoderms, whilst bryozoan, rugose and tabulate corals were relatively unaffected (Hallam and Wignall, 1999). It is thought that this extinction event was related to fluctuations in global sea-level. The youngest Famennian interval is marked by rapid sea-level transgression and the deposition of anoxic black shale facies globally (Caplan and Bustin, 1999). This was followed by a rapid regression, and the Devonian – Carboniferous boundary is often marked by an erosive surface, for example, in the Rhine slate mountains (Van Steenwinkel, 1992). Rapid transgression at the base of the Carboniferous then resulted in more black shale deposition. It is believed that these short-term, high-amplitude changes were related to a glacioeustatic driving mechanism

(Hallam and Wignall, 1999). It is, therefore, likely that the onset of black shale deposition in the Early Carboniferous was related to global sea-level transgression-regression.

3.5.2.2 Bademli Limestone

This facies association overlies the Bademli Shale, and is, in turn, overlain by the Dolomite Unit. Its thickness is relatively constant across the study area (80-100 m), and its age range is well constrained by palaeontology as Lower Visean – Lower Serpukhovian (Monod, 1977).

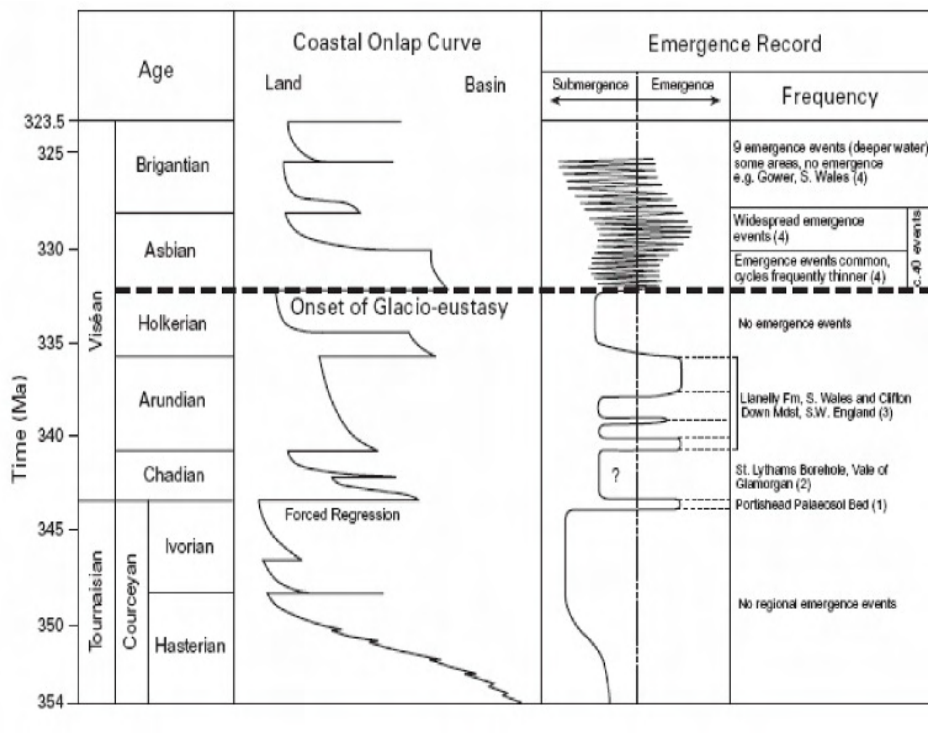

Fig. 3.23. Synthesis of the Lower Carboniferous sea-level and climatic record. Diagram from Wright and Vanstone (2001).

The grey Bademli Limestones consist of neritic carbonates including bioclastic limestone, calcarenite, grainstone, packestone, oolitic limestone and some interbedded quartzitic sandstone. The unit contains abundant micro- and macro-fauna, and represents a change to a highly productive shallow-marine carbonate sedimentary environment.

These thick-bedded carbonates are indicative of a stable shallow-marine platform depositional environment (Sellwood, 1986; Tucker, 1991; Einsele, 1992). Sandy limestone and sandstone horizons which show hummocky cross-bedding (Fig. 3.15c) are indicative of tempestites (Einsele, 1992).

The correlation of Carboniferous units across the study area (Fig. 3.21) shows that the onset of Bademli Limestone deposition probably occurred in the Early Visean. An integrated study of Tournaisian and Visean sediments elsewhere suggests that a major phase of glacioeustatic sea-level change began in the Mid Visean (Fig. 3.23) (Wright and Vanstone, 2001). Initial onset of Visean glacioeustacy appears to cause a sudden marine-regression (Fig. 3.23), which could be factor for the change from deposition of Bademli Shales to Bademli Limestone.

3.5.2.3 Dolomite Unit

The Dolomite unit overlies the Bademli Limestone unit; however, it is not observed in the southerly part of the study area, hence this facies association is laterally discontinuous. This unit is 55-65 m thick at the two localities where it is present (Bademli and Çaglayan), and its age is constrained as Lower Serpukhovian to Upper Bashkirian (Monod, 1977). The unit is composed of medium- to thick-bedded dolomite, dolomitic limestone and rare quartzitic sandstone horizons. The depositional environment was similar to the Bademli Limestone, i.e. a shallow-marine platform. Quartzitic horizons are indicative of clastic input to the system, possibly related to minor sea-level change or marine currents.

3.5.2.4 Quartzite Unit

The quartzite unit stratigraphically overlies the dolomite unit, where present, and is constrained as Upper Bashkirian to Kasimovian in age. The thickness of this unit is variable, ranging from 50 m to 90 m. It is composed of quartzitic sandstone, interbedded with mudstone, dolomite, dolomitic limestone, and various other shallow-marine carbonates. The variability in sedimentary facies suggests that the depositional

environment was sensitive to subtle changes in terrigenous sediment input (Einsele, 1992). It is again likely that changes in sedimentary facies are related to high-frequency sea-level changes, possibly related to low-latitude glaciation on Gondwana during the Late Palaeozoic (e.g. Hallam, 1992). Estimates of Carboniferous sea-level fluctuations from the extent of the Gondwana ice sheet suggests changes of ~60 m (Crowley and Baum, 1991). Ice is considered to have short-term, high-amplitude effects on sea-level change (Fig. 3.19). It is reported that the Gondwana ice sheet was sensitive to forced variations in solar insolation, with sea level oscillations occurring on a ~100 ka periodicity (Wright and Vanstone, 2001). Eustatic sea-level change is, therefore, a viable mechanism for changing sedimentary facies seen throughout the Carboniferous.

3.5.3 Permian

The Permian Çevizli Limestone is a thick succession of shallow-marine carbonates, which formed in a stable shelf environment. The lowermost beds may be upper Carboniferous in age (Monod, 1977), and the base of the succession overlies the Upper Carboniferous Quartzite Unit sequence. The relative lack of terrigenous material in this unit suggests it was deposited on a large carbonate platform. The succession contains abundant fauna indicative of a highly productive marine setting (e.g. Tucker, 1985). Sedimentation throughout the Permian is very constant, especially in comparison to the Carboniferous. If sea-level rise and fall is the cause of facies variation in the Devonian and Carboniferous, this would suggest sea-level remained relatively stable throughout the Permian. Sea-level curves suggest that the Permian was, in general, represented by marine regression (Miller et al., 2005). It is also suggested that the Permian is defined by low sea-level stand (Hallam, 1984), although sea-level curves can be conflicting (Fig. 3.20).

3.6 Sediment composition

Representative photomicrographs are shown in Fig. 3.24. A Devonian sandstone from the Çaglayan locality (Fig. 3.24a) is composed of fine-grained, angular monocrystalline

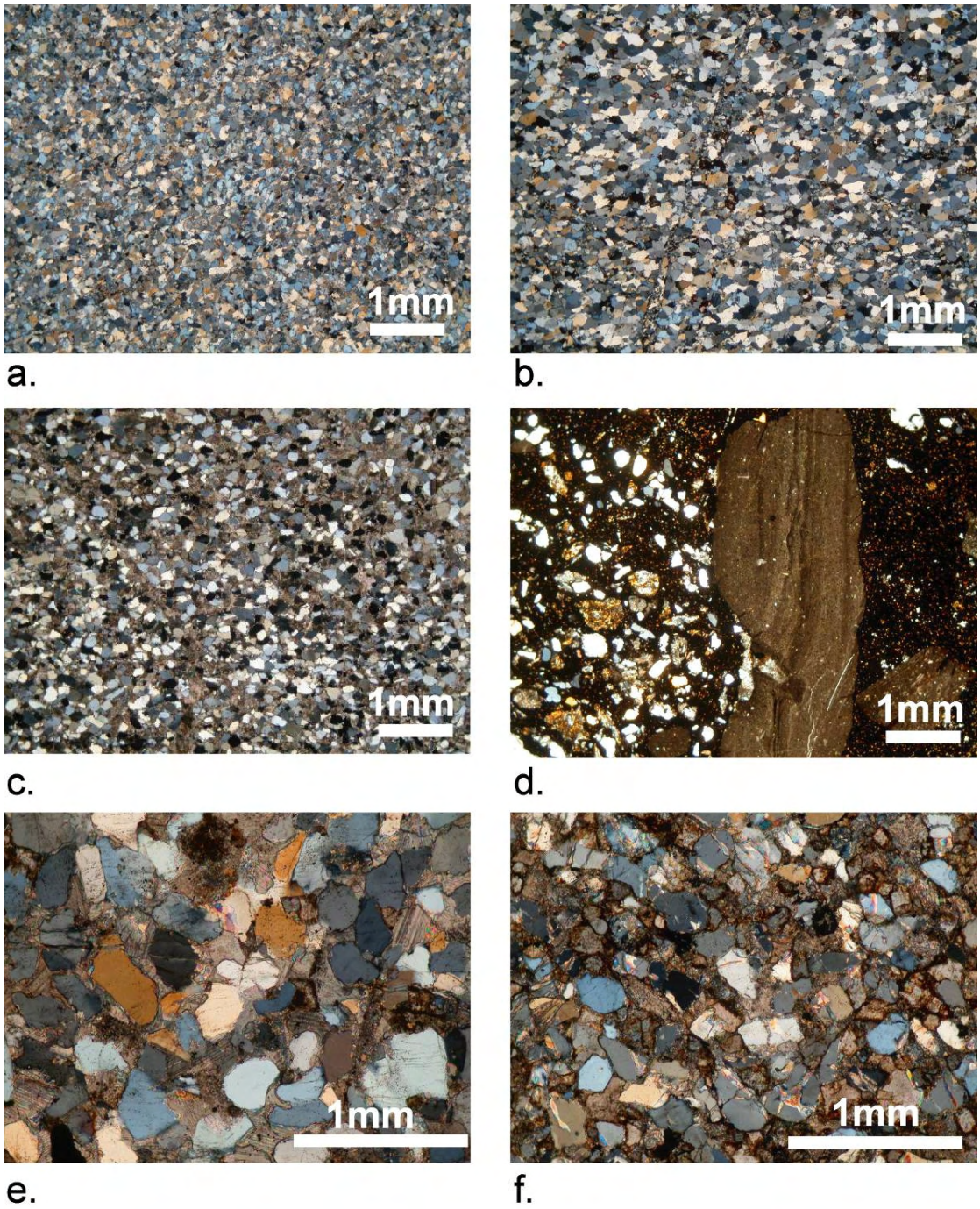

Fig. 3.24. a. Devonian sandstone from Çaglayan locality; b. Recrystallised sandstone from the Lower Carboniferous Bademli Shales at Bademli; c. Sandstone/sandy limestone from Bademli Shales at Baybağan; d. Phosphatic bed within Lower Carboniferous succession at Tokluca Yayla. Large clast is a phosphatic nodule showing growth banding; e. Sandstone / sandy limestone from Bademli Limestone at Tokluca Yayla; f. Sandy limestone from lower Bademli Limestone unit at Bademli village.

quartz with an altered siliceous cement. Recrystallised quartzitic sandstone from the Lower Carboniferous Bademli Shale at Bademli village (Fig. 3.24b) is fine-grained, with sub-angular to sub-rounded grains. It is primarily composed of monocrystalline quartz, with rare polycrystalline and composite quartz grains. Rare altered feldspar grains were observed, along with sub-rounded altered carbonate. The cement is variably calcitic and phosphatic. An equivalent sandstone horizon in the Bademli Shale, at Baybağan (Fig. 3.24c), is very similar in composition to that at Bademli, but with a higher percentage of calcite cement. A horizon within the Bademli Shales, at Tokluca Yayla, contains small pebbles of reworked phosphatic nodules, together with medium-grained quartz, set in a dark red-brown phosphatic matrix (Fig. 3.24d). Sandy limestone units from the Bademli Limestone are illustrated from Tokluca Yayla (Fig. 3.24e) and Bademli (Fig. 3.24f). This sandstone is fine-grained and well-sorted, with variable angular to rounded grains. It is composed, nearly exclusively, of monocrystalline quartz, with rare altered siliceous grains.

3.7 Shale Geochemistry

Mudstone geochemistry can help to indicate the tectonic setting and provenance of fine-grained sediment. During this study, eight representative samples of shale were analysed by X-ray fluorescence (XRF) for major and trace elements at the School of GeoSciences, University of Edinburgh, as specified by Fitton et al. (1998). Shales were collected from Ordovician, Devonian, Carboniferous and Triassic sequences in order to highlight any variation in composition. A summary of the sample localities and ages is provided in Fig. 3.25, whilst an interpretation is given in section 3.8.4. It should be stressed that the geochemical work undertaken here is intended as a pilot study, and primarily aims to show differences (if any) in the geochemical signature of shales of different ages.

Sample	Age	Locality	Description
S1	Carboniferous	Dedemli Gorge	Small quarry located 50 m up hill side adjacent to mud track at the E of the gorge. Quarry exposes succession of dark-grey Lower Carboniferous shales of the Bademli Shale unit, within the Bolkar nappe. (Section 3.3.2.5).
S2	Carboniferous	Tokluca Yayla	Type section of Carboniferous units in the Hadim nappe. Thick succession of Lower Carboniferous shales (Bademli Shale unit); sample taken from middle of shale sequence. (Section 3.3.2.6)
S3	Triassic	Alanya Road South	Road cutting through Lower to Middle Triassic shales within the southerly part of the Hadim nappe. Shales are a distinctive pink-red. (Section 4.3.2.3).
S4	Ordovician	Agilönü	Sample of Seydişehir Shales unit from Agilönü, near Beyşehir, within the autochthonous Geyik Dağ unit. (Section 5.7.1)
S5	Carboniferous	Bademli	Bademli Shale unit from Lower Carboniferous succession within the Hadim nappe (Section 3.3.2.1). Sample taken from lowermost part of succession to the west of village, 20 m from the base of the measured section.
S6	Carboniferous	Bademli	Bademli Shale unit of Lower Carboniferous within the Hadim nappe. Sample taken from temporary road that transects the higher ground to the east of Bademli village. (Section 3.3.2.1).
S7	Devonian	Bademli	Shales collected from the same access road as S6 within the Hadim nappe. Poorly exposed succession in hillside to east of the village. (Section 3.3.1).
S8	Ordovician	Agilönü	Lower Ordovician within the Geyik Dağ autochthon. There was ~250 m distance between the sample site for S8 and S4. (Section 5.7.1).

Fig. 3.25. Description of localities from which shale samples were collected for geochemical analysis.

3.7.1 Multi-element spider diagrams

The concentration of selected major and minor elements from the analysed shales were plotted on spider diagrams (Fig. 3.26; Fig. 3.27). The shales analysed in this study were 'normalised' against the Upper Continental Crust (UCC) composite (McLennan et al., 2006). Subtle variations in the distribution of elements are observed between shale samples of different ages.

Major elements were plotted on a spider diagram (Fig. 3.26) normalised against UCC composite (McLennan et al., 2006). The diagrams shows that the Devonian,

Carboniferous and Triassic shales are all significantly enriched in Ca, but that the Ordovician shale is depleted in Ca in relation to UCC. All of the samples are depleted in Na in relation to UCC. Weathering can affect the trends of Ca, Na, K, and Mn, but during this pilot study the effect of weathering has not been quantified. However, in general, the major element concentration is similar between all seven samples.

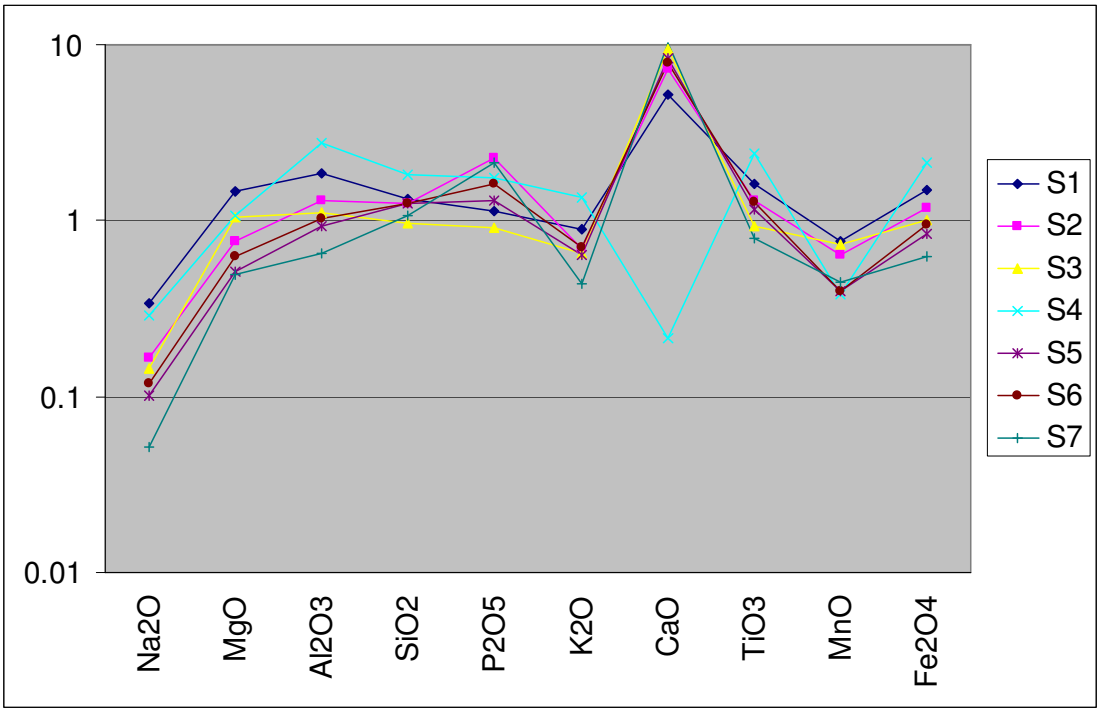

Fig. 3.26. Multi-element plot of major elements for shales normalised against Upper Continental Crust composite (McLennan et al.. 2006). S1: Carboniferous, Dedemli Gorge; S2 Carboniferous, Tokluca Yayla; S3: Triassic, Alanya road south; S4: Ordovician, Agilönü; S5: Carboniferous, Bademli; S6: Carboniferous, Bademli; S7: Devonian, Bademli.

Selected minor elements, normalised against UCC composite (McLennan et al., 2006), are plotted on Fig. 3.27. The Ordovician shale sample has a relatively flat profile, without any notable enrichment or depletion in any elements (plot S4, Fig. 3.27). The Devonian shale has a relative enrichment in Sr, and a depletion in Ba and Sc (plot S7, Fig. 3.27). The Carboniferous samples (plots S1, S2, S5, S6, Fig. 3.27) all have a small enrichment in Sr, but depletion in Ba. Two of the Carboniferous samples (from Bademli village) show a pronounced depletion in Sc. The Triassic shale (plot S3, Fig. 3.27) has a

depletion in Sc and an enrichment in Sr. This shows that the Ordovician shale is the only one to be relatively depleted in Sr, and the only sample that is not depleted in Ba. This diagram also illustrates the pronounced depletion of Sc in two of the Carboniferous samples; however, the unusually low depleted values of Sc suggest this could be close to the detection limit of the X-ray Spectrometer, and hence is likely to be a calibration error. Elements associated with organic-rich black shales (Cu, V, U, Ni) showed only minor enrichment or depletion (Fig. 3.27).

Sr enrichment could reflect the presence of interbedded calcium carbonate-rich rocks within the Devonian, Carboniferous and Triassic sequences. The Ordovician unit, which has a small Sr depletion, comes from a sequence of interbedded shales and quartzites without any limestone. Enrichment of Cr and Ni can indicate a basic / ultrabasic igneous provenance; however, these elements have a 'normal' abundance in all samples. Ba concentration is though to be controlled by feldspar and titanite (Rollinson, 1993); hence, a depletion in Ba in all but the Ordovician sample suggests that these two minerals were not abundant in the source region. Sc concentration is controlled by ferromagnesian minerals (amphiboles, pyroxenes, olivines) (Rollinson, 1993), and the depletion in two of the Carboniferous samples of these elements may indicate a lack of ferromagnesian minerals in the source area.

However, another possibility is that these minerals could have been destroyed during erosion and sediment transport, and hence the presence of these minerals in the source area cannot be ruled out. In this pilot study it is acknowledged that any effects of weathering have not been quantified. In contrast, a relative abundance of these minerals could be a cause of minor Sc enrichment in the Ordovician sample. Critically, despite minor variations, there is no significant change in the geochemical signature between shales of different ages.

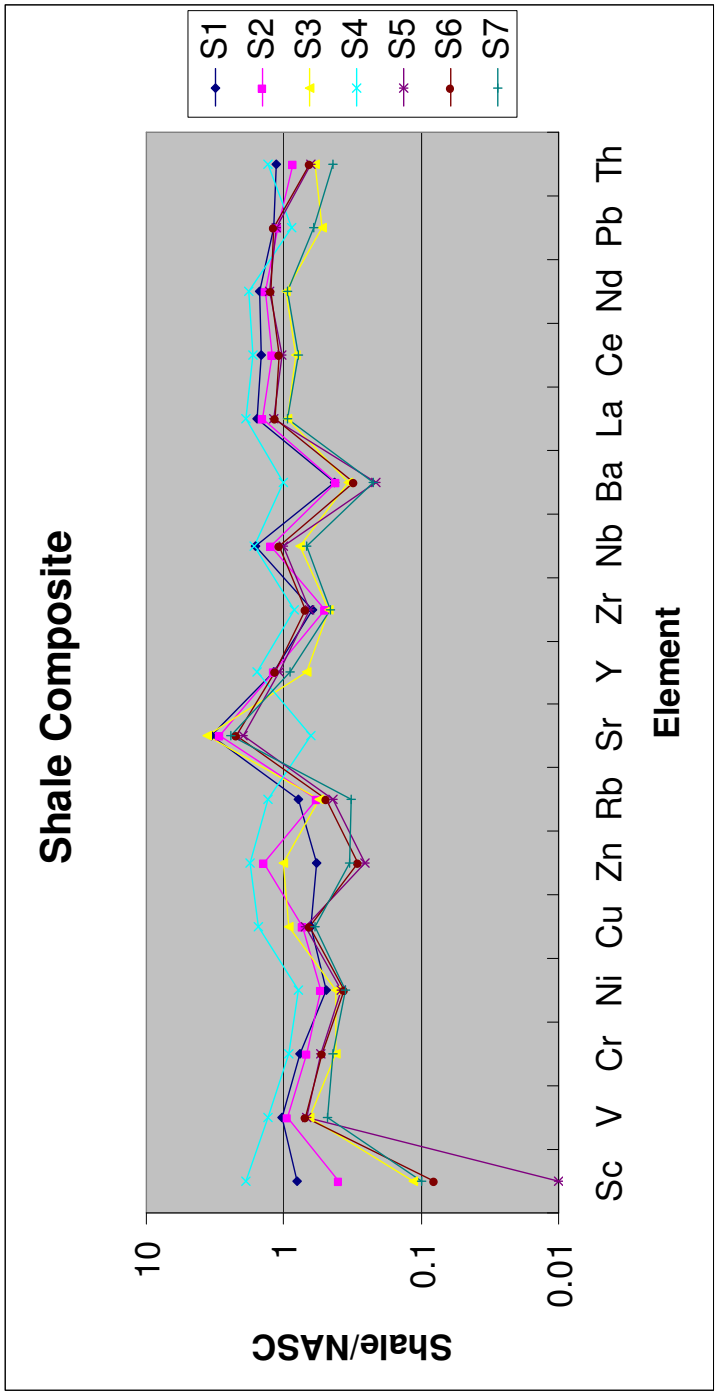

Fig. 3.27. Multi-element plot of minor elements for shales normalised against Upper Continental Crust composite (McLennan et al.. 2006). S1: Carboniferous. Dedemli Gorge; S2 Carboniferous, Tokluca Yayla; S3: Triassic, Alanya road south; S4: Ordovician, Agilönü; S5: Carboniferous, Bademli; S6: Carboniferous, Bademli; S7: Devonian, Bademli.

3.8 Discussion

In this section, information obtained from sedimentary facies analysis, proposed depositional environments, sediment composition and shale geochemistry will be combined to provide an interpretation of the possible Upper Palaeozoic tectonic setting.

3.8.1 Sedimentary facies and depositional environment

The Late Palaeozoic stratigraphy of the area studied is consistent with a shallow-marine shelf depositional environment. The most important factor in determining sedimentary facies during this period was global sea-level change, greatly influenced by Gondwana glaciation (Crowley and Baum, 1991; Hallam, 1992; Hallam and Wignall, 1999; Miller et al., 2005). The Gondwana ice sheet was at its maximum extent during the Late Devonian, Upper Carboniferous and Early Permian (e.g. Ziegler et al., 1997; Scotese et al., 1999). Several sea-level curves exist for the Phanerozoic (Fig. 3.29), which, in some cases, present conflicting results for the Late Palaeozoic time.

Devonian shales, quartzitic sandstone and limestones are indicative of a shallow-marine shelf environment, as inferred by several previous authors (Monod, 1977; Demirtaşlı, 1984a; Özgül, 1984; Özgül, 1997). It is likely that fluctuations in sea-level were responsible for variation in siliciclastic and carbonate facies in the Devonian sequence. During sea-level transgression, fine-grained mudstones represent distal sedimentary deposits; during sea-level regression, coarser-grained sands and carbonates are more common. Unfortunately, a lack of information on the precise age of Devonian units in the studied area means that they cannot be correlated directly with Upper Palaeozoic glacioeustatic cycles. However, relatively high frequency periodicity, as seen in sea-level cycles in the Late Devonian (Frasnian-Frammenian) (Hallam and Wignall, 1999), is a likely control on sedimentary facies.

A combination of palaeontological information and facies associations allow correlation of the Carboniferous sequences across the study area (Fig. 3.28). Most of the recognised sedimentary units can be traced laterally, but the Dolomite unit was not

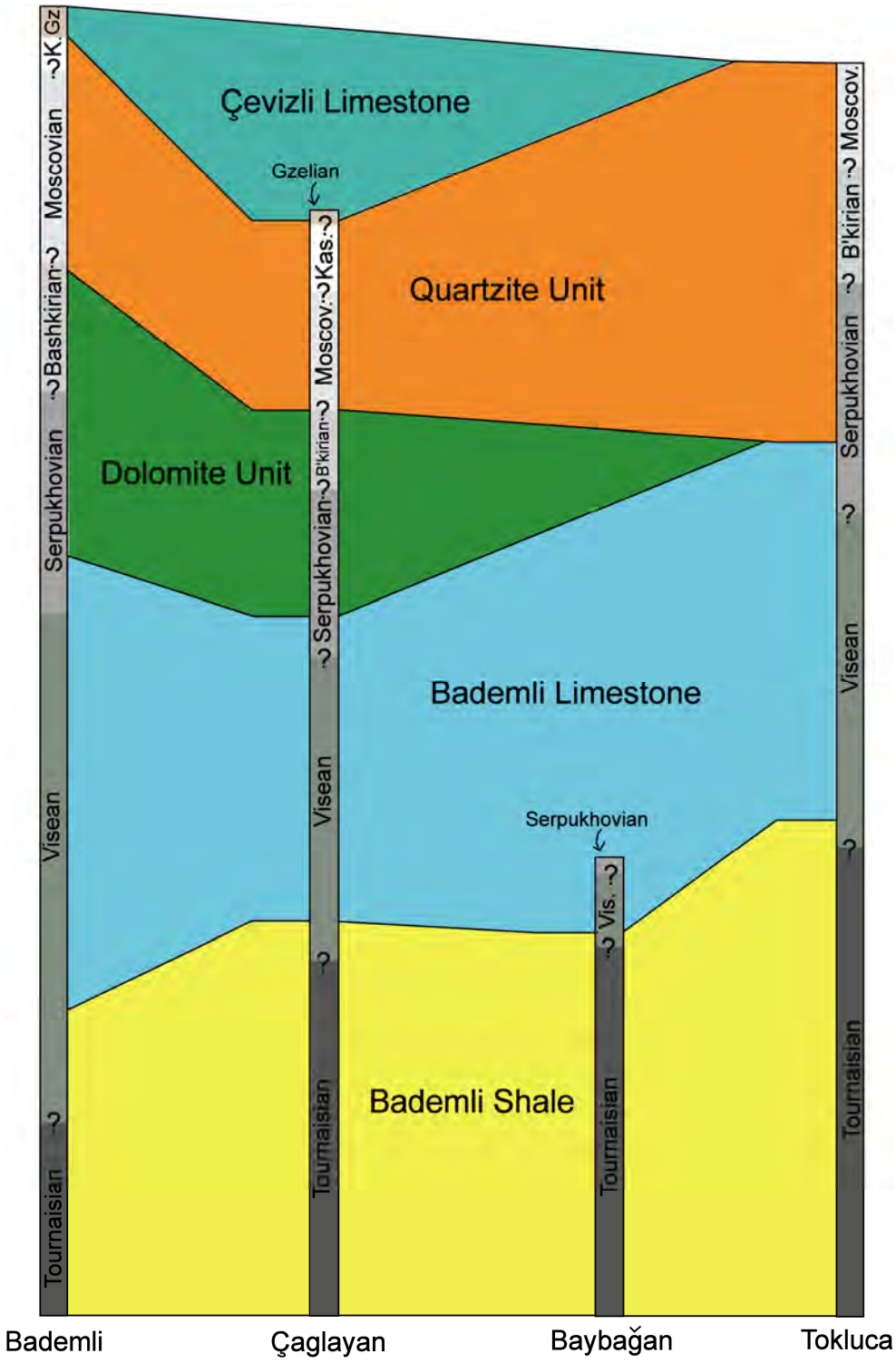

Fig. 3.28. Distribution of stratigraphic units across the study area. Bademli is located in the most northerly position; Tokluca is the most southerly.

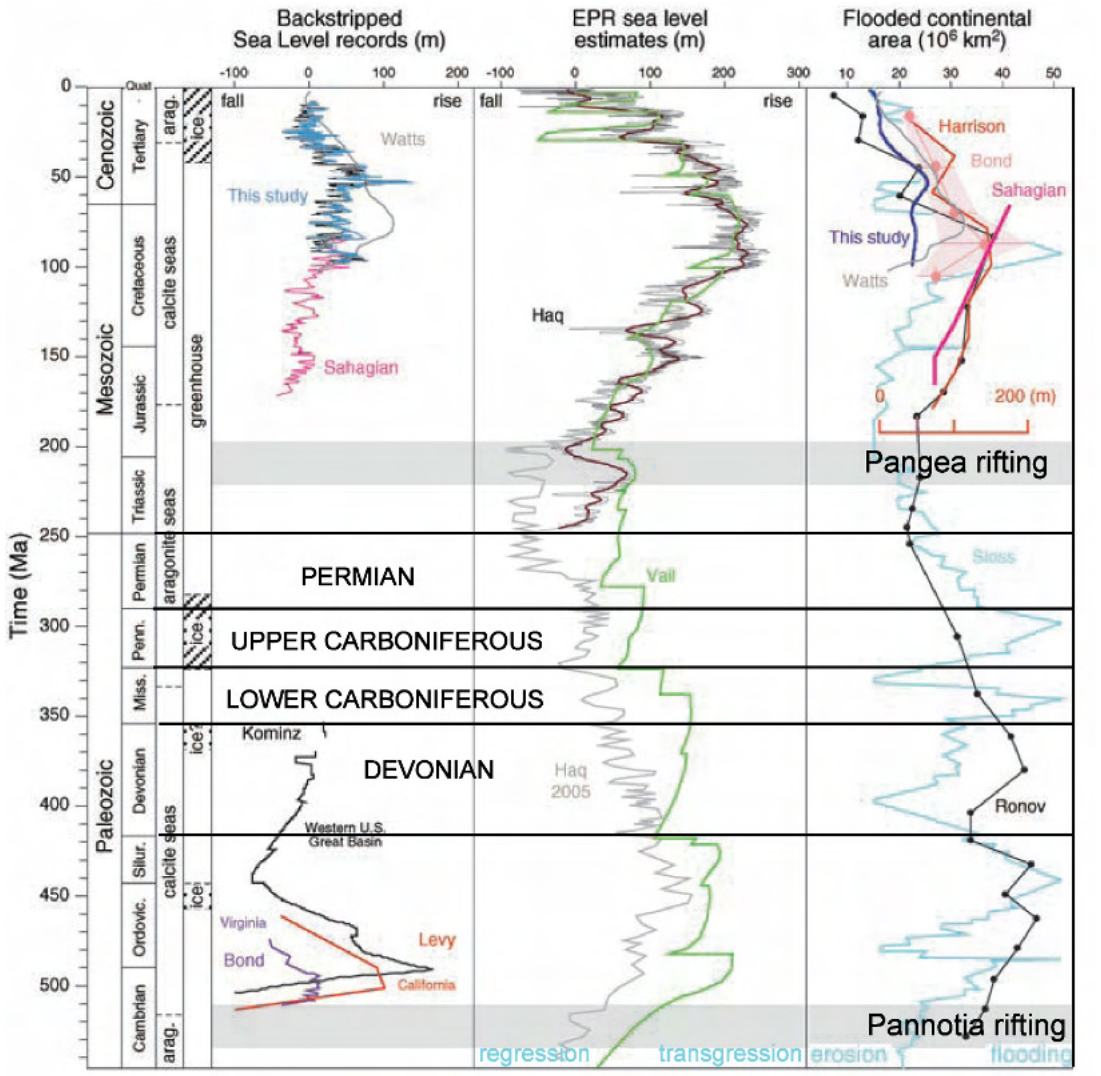

Fig. 3.29. Comparison of Phanerozoic global sea-level estimates, modified from Miller et al. (2005).

recognised at the Tokluca Yayla locality. Correlation of these units was achieved through a combination of stratigraphic comparison and palaeontological dating; as a result, subtle changes in the lithologies found in each sediment package across the study area.

The Bademli Shale unit represents a low-energy, sub-wave base, relatively distal unit on a continental shelf setting. The presence of phosphorite sediments suggests deposition on a submerged continental shelf, where cold nutrient-rich water meets warmer shelf water (Tucker, 1991) (Fig. 3.30). A shelf setting would receive low

sediment input, represented by the dark shales which dominate the sequence, particularly during sea-level high-stand. Mud-sized terrigenous particles were transported to relatively distal settings within a typical continental shelf setting, whilst coarser sediments (e.g. sands) were deposited in more proximal settings (Reading, 1986; Einsele, 1992). Studies of phosphatic deposits, for example, in Patagonia shows that such sediments were deposited in a shallow-marine, storm-dominated setting (Scasso and Castro, 1999). The sandstone beds interbedded with the Bademli Shales could be storm-related deposits, although they lack some of the characteristic sedimentary structures of tempestites (e.g. hummocky cross-bedding). A major global sea-level transgression, starting at the Devonian – Carboniferous boundary (Fig. 3.29), is considered to have been the cause of widespread deposition of black shales (Van Steenwinkel, 1992; Caplan and Bustin, 1999; Hallam and Wignall, 1999).

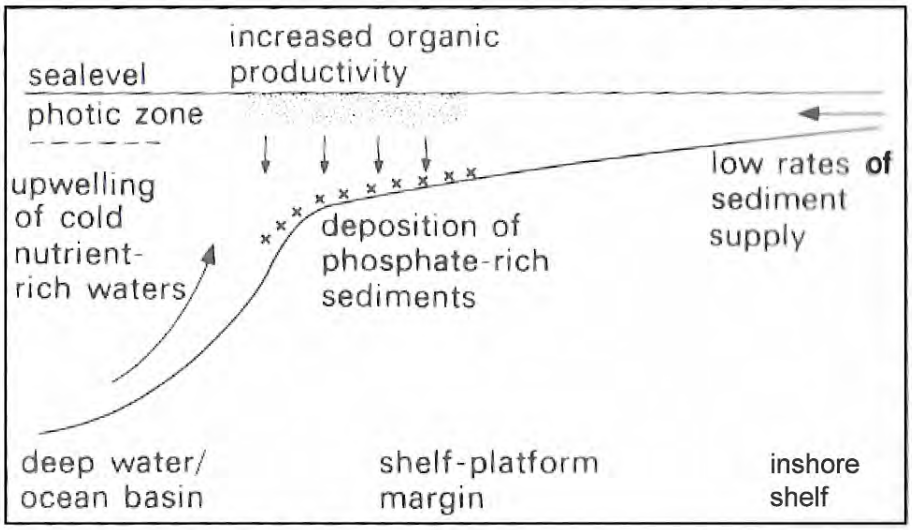

Fig. 3.30. Model for formation of marine phosphorites at a shelf-platform margin (Tucker, 1991).

The Bademli Limestones represent a shallower, more productive carbonate shelf depositional setting. Many of the lithologies (e.g. oolitic limestone, microbial limestone) and fossil assemblages (e.g. corals) are indicative of water depths of less than 5 m (Sellwood, 1986). During the Visean, onset of glacioeustatic sea-level change began with marine regression (Wright and Vanstone, 2001). The change from Bademli Shales

to Bademli Limestones represents, in the simplest of terms, relative sea-level fall. The Bademli Limestones and the overlying Quartzite Unit and the Dolomite Unit do not represent a fundamental change in depositional environment. The Quartzite unit probably represents an Upper Carboniferous marine regression, allowing sand to be transported to more distal areas of the shallow-marine shelf. During this time, the Gondwana ice sheet was at its maximum extent, and hence transgression-regression should be glacioeustatic. Thick sandstone horizons are not traceable laterally throughout the study area; instead, these interfinger with carbonates vertically and horizontally. This suggests that a mixed shallow-marine siliciclastic – carbonate shelf existed. It is likely that the sedimentary facies were controlled by a combination of relative sea-level change, variability in shelf conditions and changing sediment source area and currents. By the Late Carboniferous and Permian, a stable carbonate shelf environment had become established, represented by the Çevizli Limestone. Sea-level curves for the Permian vary (Fig. 3.29); however, the Permian represents low-stand in comparison to the Carboniferous. It is unlikely that this had a significant effect on Permian sedimentary facies, which show little variation during this period.

3.8.2 Sedimentation rate

The sedimentation rates calculated in section 3.4 have obvious errors (e.g. thickness not decompacted; stratigraphic boundaries not well constrained; disconformities not considered). Nevertheless, two important trends can be identified. First, the sedimentation rates are very similar for the Hadim and Bolkar nappes. Second, the sedimentation rate is similar for Devonian and Carboniferous[3] units, but increases for the Permian and Triassic, possibly related to rifting of a southerly strand of the Neotethys ocean in Late Permian – Early Triassic along the north-Gondwana margin (Şengör and Yılmaz, 1981; Demirtaşlı, 1984b; Robertson and Dixon, 1984; Dercourt et al., 1993; Okay et al., 2006). The stratigraphy of the Antalya / Alanya units to the south of the study area is of Late Permian – Early Triassic rifted margin (Özgül, 1983). There is no

[3] It is considered here that the relatively high sedimentation rate for the Serpukhovian is inaccurate, probably due to the lack of palaeontological constraints for the lower and upper boundaries of this age.

evidence that sedimentation rates were altered by Early Carboniferous supposed tectonic events (see section 3.8.5).

3.8.3 Sediment composition

Devonian sandstones are quartzitic in composition, with minor amounts of reworked Palaeozoic carbonate. Lower Carboniferous terrigenous sediments divide into shale and sandstone components. The shales are very dark grey, and were described as 'black shales' (Monod, 1977; Göncüoğlu et al., 2007). Black shales are rich in organic carbon, sulphide and organic matter, and typically contain unusual concentrations of the trace elements U, V, Cu and Ni. The XRF analyses of Carboniferous shales showed no distinctive enrichment or depletion in U, V and Ni relative to the Upper Continental Crust composite (McLennan et al., 2006). Furthermore, the Cu values for Lower Carboniferous shales in this study (15-18 ppm; see appendix for values) were significantly lower than black shales from, for example, Gabon, which average between 3 and 208 ppm (Mossman et al., 2005). In situ fossils within the shales (e.g. brachiopods) suggest the sea-water was oxic. This suggests that the black shales have a relatively high organic content (<1%) compared to, for example, Devonian shales; however, they do not have a high concentration of organic matter or trace elements compared to sapropels and true black shales. The sandstone units of the Lower Carboniferous succession are primarily composed of quartz and are very similar in composition to the Devonian sandstones. This information combined shows that there was no obvious change in sediment provenance during the Lower Carboniferous, consistent with the passive margin model.

3.8.4 Geochemical evidence

Care must be taken when studying multi-element spider diagrams of minor and major trace elements in assessing sediment provenance. In contrast to igneous rocks, trace-element discrimination is considered be of limited use in determining depositional setting (Rollinson, 1993). The assumption in geochemical discrimination studies is that plate tectonic setting and sediment provenance are intrinsically associated. However,

uncertainty arises when sediments are reworked from an ancient tectonic setting into a contrasting modern tectonic setting (Rollinson, 1993). Also, the chemical composition may be influenced by differential erosion in the source area and the effects of sediment transport. Finally, differential mobility of some elements (e.g. large ion lithophile elements) may have affected these sediment which have undergone deep burial diagenesis. The study conducted in this thesis was only a pilot study, and the issues described above are, outwith the scope of this work. For this reason caution is advised when studying these data.

Nevertheless, the results support the hypothesis that sediment was not derived from a volcanic source. Most of the elements have values close to the Upper Continental Crust composite (McLennan et al., 2006). An enrichment in Ca on the major element spider plot corresponds with an enrichment in Sr. Elements that could indicate a basic igneous provenance (e.g. Cr, Ni) show no enrichment. A depletion in Ba and Sc suggest a source area poor in feldspar and ferromagnesian minerals (Rollinson, 1993); such constituents would, however, be found in an intra-plate volcanic rocks. It is also evident that there is little change in geochemical signature between Ordovician, Devonian, Carboniferous and Triassic shales, and that, therefore, there was little change in provenance during this time.

It is likely that the source area for sediment is the Pan-African craton to the south of the Gondwana margin. This craton consists of a variety of Proterozoic – Palaeozoic terranes of convergent (ocean-ocean, oceanic-continent, continent-continent) and divergent (oceanic basin, rift, passive margin) origin (Dalziel, 1997; Meert and Van Der Voo, 1997). The Sandıklı Basement Complex of western Central Anatolia consists of Late Precambrian to Cambrian meta-sediments and meta-igneous rocks (Göncüoğlu and Kozlu, 2000; Gürsu and Göncüoğlu, 2001; Gürsu et al., 2004). The meta-sediments include siliciclastics, chert and cherty-dolomite, and are intruded by meta-rhyolites and quartz-porphyry rocks. The geochemistry of felsic igneous rocks in the complex, and depositional features of the sediments, suggests the complex related to a post-collisional "back-arc" extension event in NW Gondwana (Gürsu et al., 2004). The Sandıklı Complex, in the western Tauride-Menderes platform, is an example of a Pan-African

basement source for the Late Palaeozoic units, although it is not known whether this particular terrane contributed sediment the Palaeozoic sequence. Studies of similar Pan-African derived shales elsewhere in the Tauride orogenic belt show similar geochemical signatures to those in this study (e.g. Baer-Bassit, N Syria) (Al-Riyami and Robertson, 2002; Robertson, 2006b).

3.8.5 Tectonic setting

A review of the stratigraphic, sedimentological, compositional and geochemical analysis of the Tauride units allows the relative merits of the 'active margin' (Göncüoğlu et al., 2007) and 'passive margin' (Stampfli and Borel, 2002) models to be reviewed.

In the first model (Fig. 3.31a) (Göncüoğlu et al., 2007), it would be anticipated that the "Aladağ Unit", which in this study is referred to as the Hadim and Bolkar nappes/units, should show evidence of active margin processes. This could include extension related volcanism, volcaniclastic sedimentation, rift-related subsidence of the platform, erosion of the basement, flexural uplift relating to crustal thinning, or syn-sedimentary faulting (Robertson, 1994). However, during this study no such evidence was observed in the Hadim, Bolkar, and Geyik Dağ units.

In the active margin model, extensional rift zones with associated volcanism should exist to the north and the south of the northern Tauride platform (Fig. 3.31a). It would be expected that volcaniclastic sediment, or reworking of some volcanic material, would be incorporated into sediments of Lower Carboniferous age. There is no evidence of any volcanic-derived sediment within Lower Carboniferous units of the Hadim or Bolkar nappes.

On the other hand, volcanic rocks within the autochthonous Tauride platform are documented very locally from within the Sultan Dağ Unit in Central Anatolia to the northwest of the study area (Göncüoğlu et al., 2007). This area restores as the northern basement of the Geyik Dağ autochthonous unit, which was to the south of the Hadim and Bolkar nappes. In the Sultan Dağ, the Upper Tournaisian – Lower Visean Harlak Formation (Kuz member) contains rare bands and lenses of metatuffs and basic lavas are reported (Göncüoğlu et al., 2007). Unfortunately, no geochemical data are available for

these lavas. Elsewhere, in the eastern Taurides, where the Aladağ mountains are an eastward continuation of the Tauride platform (Tekeli et al., 1984), the Upper Palaeozoic stratigraphy consists mostly of limestones and terrigenous clastics, together with deeper-water sequences (i.e. cherty limestone, turbidites) which contain volcanic material. It has been suggested that these deeper-water sequences relate to localised volcanic-related subsidence within a large continental shelf (Tekeli et al., 1984). However, volcanism on a continental margin does not imply that subduction has occurred, as volcanics is also a feature of many Eastern Tethyan rifted margins (e.g. Himalayas, Oman, Eastern Mediterranean) (Robertson, 2007) and intra-plate settings (e.g. Central North Africa) (Bosworth and McClay, 2001; Guiraud et al., 2001).

a.

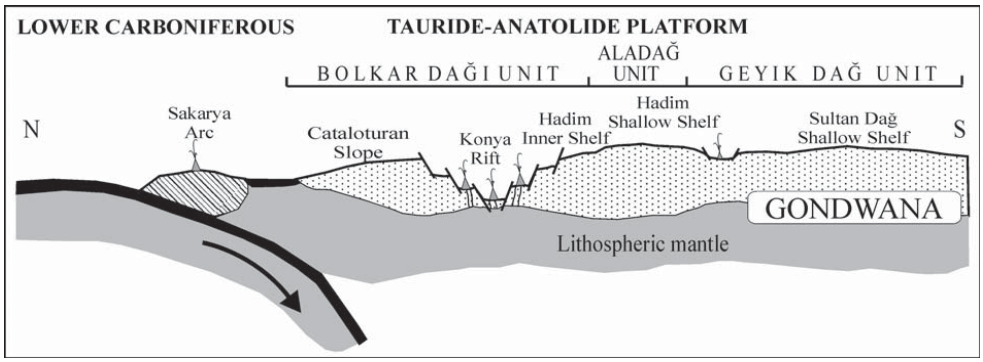

b.

Fig. 3.31. Alternative models for the tectonic setting of the Tauride units during the Lower Carboniferous, after (a) Göncüoğlu et al. (2007); and (b) Stampfli and Borel (2002).

In the alternative model (Fig. 3.31b) (Stamplfi and Borel, 2002; Eren et al., 2004), the Tauride units would have experienced a more simple passive margin related evolution during the Late Palaeozoic period. The stratigraphy of the Geyik Dağ, Hadim unit and Bolkar unit, as documented in this study, are suggestive of a simple subsiding passive margin, dominated by shelf deposits. The variation over time of siliciclastic sediment within the stratigraphy was probably caused by global sea-level change rather than tectonic events. In this model, sediment would be expected to be derived from the Pan-African continental basement of the Taurides in the south (remnant north Africa). However, this model of an entirely passive tectonic setting does not explain the presence of volcanic-related units in the Sultan Dağ.

A major point of contention between the alternative tectonic models concerns the nature of the Konya Complex, which is discussed in Chapter 6.

3.9 Conclusions

1) Sedimentological investigation of Devonian units in the Hadim and Bolkar nappe suggest that sandstones, shales and limestones were deposited in a shallow-marine continental shelf environment. Glacioeustatic changes in the Upper Devonian are likely to have been an important control on sedimentary facies.

2) Detailed stratigraphic logging of Carboniferous units has allowed four main stratigraphic units (Bademli Shales; Bademli Limestones; Dolomite unit; Quartzite unit) to be traced laterally across the study area, with exception of the dolomite unit which is not seen in the southernmost part of the Hadim nappe.

3) The Carboniferous sediments were deposited in a shallow-marine shelf environment, that was influenced by global sea-level changes. Lower Carboniferous black shales, with associated phosphatic nodules, may have been deposited near the shelf margin where organic productivity was high. The dark shales can be correlated with a major global sea-level transgression at the Carboniferous – Devonian boundary.

4) Shallow-marine carbonate deposition continued in the Permian, with an increase in sedimentation rate possibly related to rifting and subsidence along the Gondwana margin.

5) X-ray fluorescence studies of Ordovician, Devonian, Carboniferous and Triassic shales show that there is little change in the geochemical signature between shales of different ages. Regional evidence suggests that sediment provenance was from a variety of different tectonic settings, with the likely source being the Pan-African craton of the Palaeozoic Gondwana supercontinent. This is supported by thin-section analysis of Late Palaeozoic quartzitic sandstones.

6) The evidence is consistent with a passive margin setting for the Hadim and Bolkar nappes throughout Late Palaeozoic time. However, this needs to be considered further in the regional context, which is a subject of the following Discussion Chapter.

4 Triassic evolution of the Tauride platform

4.1 Introduction

This chapter will discuss the Triassic stratigraphy of the Tauride platform. Triassic sediments can be observed within the autochthonous Geyik Dağ, the Hadim nappe and the Bolkar nappe (Fig. 4.1). Exposure of Triassic rocks within the Geyik Dağ is limited due to unconformable relationships between Ordovician and Triassic units, and between Triassic and Jurassic units. The thickest sediments exposed in the Geyik Dağ are observed near the town of Seydişehir and the village of Taraşçı (Fig. 4.1). A much thinner sequence can be observed near the village of Karadiken, to the southwest of Beyşehir. In the southerly part of the study area (Bozkir – Hadim region) the regional unconformity is between Ordovician and Middle Jurassic units, and the Triassic is not present. The Geyik Dağ has been significantly deformed by the emplacement of the Beyşehir-Hoyran-Hadim nappes, and the Triassic sequence is commonly strongly folded and faulted.

Within the Hadim nappe, the Triassic succession is present in both the northerly and southerly study areas. In the northerly part of the Hadim nappe, a complete Triassic sequence is found between the villages of Bademli and Derebuçak (Fig. 4.1), although exposure is poor. There is also limited exposure near the village of Gumuşdamla. In the southerly part of the Hadim nappe, a well exposed Triassic sequence is observed on the road between Taşkent and Alanya. The Hadim nappe is moderately deformed (see chapter 5), and commonly the Triassic sequence is tectonically imbricated, resulting in stratigraphic repetition. Also, folding and faulting are widespread within the Hadim nappe.

The Bolkar nappe (only found in the southerly study area, as described in chapter 2) has been regionally folded, imbricated and heavily deformed during Alpine nappe emplacement. This makes finding a complete Triassic sequence difficult. Some Triassic sediments can be seen near the villages of Korualan and Kuruçay, as well as near Dipsiz Göl and Karabayır Yayla (Fig. 4.1). Triassic sediments are also exposed in a road cutting south of Çağlayan village; however, local deformation and limited palaeontological data

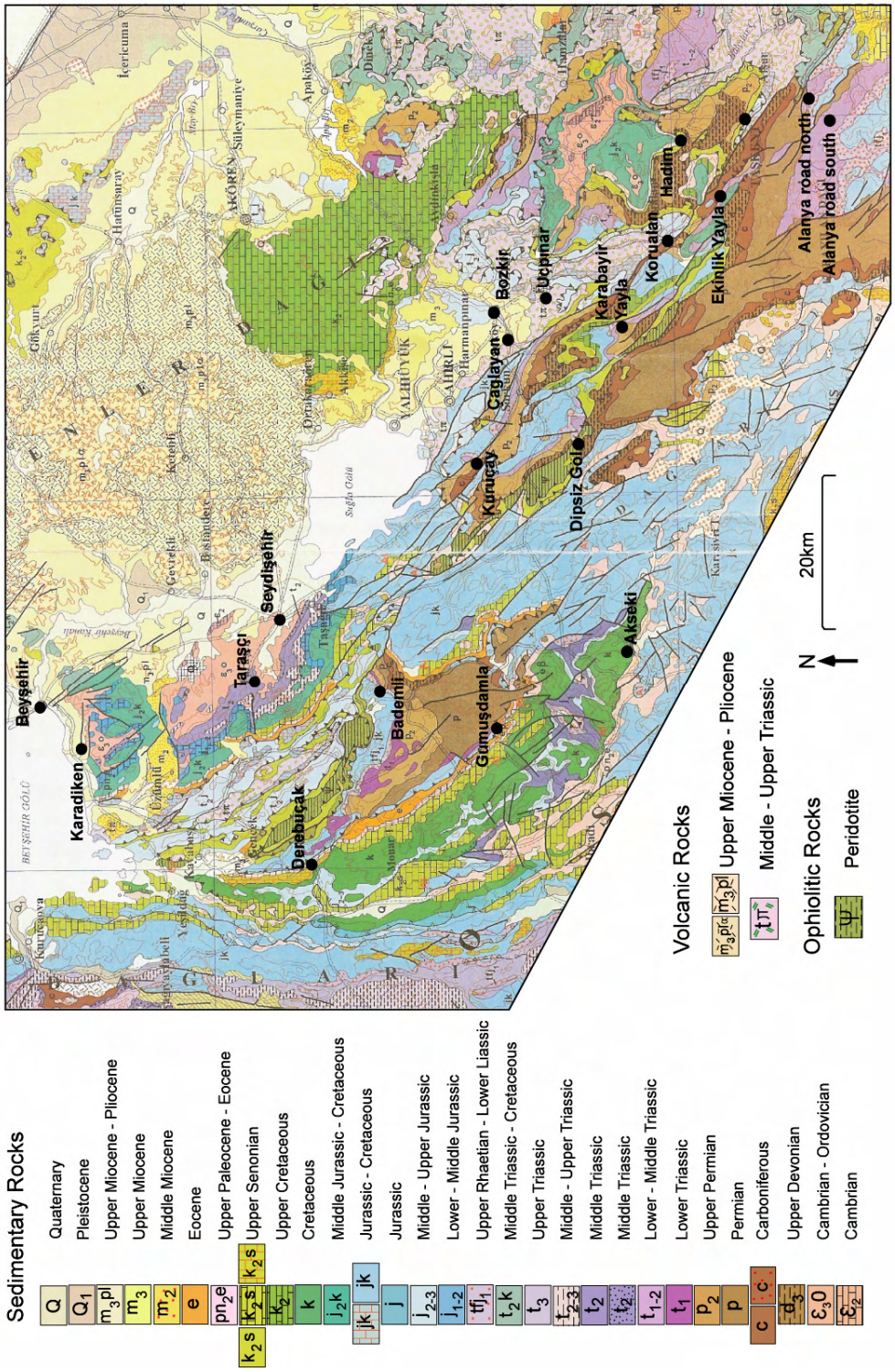

Fig. 4.1. Geological map of the studied area (modified after MTA, 2002), with the main towns and localities discussed in this chapter highlighted.

make identification of Triassic units difficult. The best sequence in the Bolkar nappe is near the town of Hadim.

Previous work on the Triassic of the Geyik Dağ, Hadim nappe and Bolkar nappe was carried out regionally by Blumenthal (1947, 1951, 1956, 1960-1963), Monod (1977), Önder (1984) and Özgül (1976, 1984, 1997). All formation names are retained from the literature. Work by previous authors (e.g. logs, type sections) was field checked and revised where necessary.

4.2 Alternative models of the Triassic tectonic setting

It is generally accepted that the relatively autochthonous Tauride platform and associated thrust sheets restore as a north-facing passive margin, at least during Jurassic–Cretaceous time (Şengör and Yılmaz, 1981; Robertson and Dixon, 1984; Stampfli et al., 2001; Andrew and Robertson, 2002; Robertson et al., 2004; Okay et al., 2006). However, the Triassic and earlier tectonic setting of these Tauride units is contentious (Fig. 4.2).

In one model (Şengör et al., 1984) a Palaeotethyan ocean subducted southwards beneath an active Gondwanan margin during Late Palaeozoic – Early Mesozoic, which resulted in back-arc rifting. A large continental fragment known as "Cimmeria" drifted northwards opening a "Neotethys ocean" to the south. By the Late Triassic, continuous southward subduction of Palaeotethys had resulted in the suturing of the Eurasian margin with the Cimmerian continental fragment. The Tauride unit was part of a continental terrane known as the Tauride-Anatolide platform, separated from Gondwana by a small oceanic basin (Fig. 4.2a). This is the only model which incorporates southward subduction during the Triassic. In other tectonic models, subduction polarity was northwards beneath the Eurasian continental margin. In a second model (Dercourt et al., 1993), the Gondwana margin remained passive during the Late Palaeozoic – Early Mesozoic (Fig. 4.2b). The Tethys ocean was a single oceanic basin during the Triassic, situated to the north of several Gondwana-derived micro-continents. The Tauride

platform remained adjacent to the Gondwana margin during the Triassic, and rifting of the Tauride block from Gondwana occurred much later during the Cretaceous.

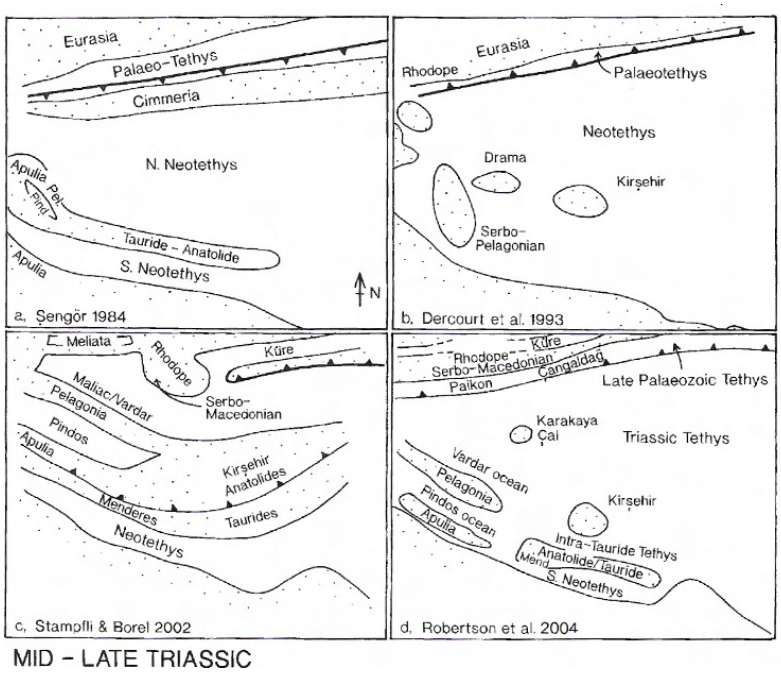

Fig. 4.2. Alternative tectonic models of Tethys in the Eastern Mediterranean during Middle – Late Triassic, from Robertson and Mountrakis (2006). a. Şengör et al., 1984. b. Dercourt et al., 1993. c. Stampfli & Borel, 2002. d. Robertson et al., 2004.

In a third model (Stampfli, 2000; Stampfli et al., 2001; Stampfli and Borel, 2002) a "Cimmerian" continental fragment, including the Tauride platform, rifted from the north-east margin of Gondwana, opening a southern Neo-Tethys ocean during the Late Permian–Early Triassic time. Simultaneously, a more northerly Palaeotethys ocean subducted northwards beneath the Eurasian margin. An "Anatolide" block, a Eurasian-derived continental margin unit, drifted southwards opening a back-arc basin (Küre basin) during Middle–Late Triassic time. Suturing of Palaeotethys occurred during the Late Triassic (Fig. 4.2c), when the "Anatolide" block collided with the Tauride block to the south.

In a fourth model (Robertson et al., 2004) a Palaeozoic Tethys ocean subducted northwards under Eurasia from Late Palaeozoic to Triassic (Fig. 4.2d). A combined

Tauride–Anatolide platform was separated from Gondwana by a small oceanic basin to the south during the Triassic (Southern Neo-Tethys). Further north, continental fragments drifted across Palaeotethys (e.g. Çal unit of the Karakaya complex) until they collided with the Eurasian active margin prior to latest Triassic. The Tauride-Anatolide unit, however, remained in a southerly location and experienced a rift-related Triassic evolution.

4.3 Lower – Middle Triassic sedimentology

This section will discuss the sedimentology of the Triassic, excluding the Upper Triassic Çayır Formation.

4.3.1 Stratigraphic age

The Triassic stratigraphy has been described and dated by several authors (Blumenthal, 1947; Monod, 1977; Gutnic et al., 1979; Önder, 1984; Özgül, 1984; Özgül, 1997; MTA, 2002; Andrew, 2003). During this study, the pre-existing literature on the Triassic was used as a field guide, and the stratigraphy was field-checked and logged in detail. Only limited additional dates were obtained during this study, and for this reason the following guide to the age of the Triassic sediments is based primarily on the work of previous authors stated. The thickness and age of the Triassic sediments vary considerably both across the study area, and between different autochthonous and allochthonous units.

In the autochthonous Geyik Dağ, near the village of Taraşçı (Fig. 4.1), the oldest Triassic sediments are dated as Anisian (Formation de Pınarbaşı) due to the presence of the bivalve *Myophoria* sp. (Monod, 1977; Gutnic et al., 1979). Landinian ages for the 'Calcaire de Taraşçı' and 'Calcaire de Toptaş' groups were determined based on fauna including *Protrachyceras* sp. and *Frankites* sp. (Monod, 1977; Gutnic et al., 1979). The youngest Triassic sediments at Taraşçı (Formation du Sarpiar Dere) are mid-Carnian in age. The Triassic sediments exposed in the Geyik Dağ near Karadiken village (Fig. 4.1)

are dated as Middle – Late Triassic (Monod and Akay, 1984), and Middle Triassic (MTA, 2002); however, the fauna on which these ages were based are not documented.

Within the allochthonous Hadim nappe, different ages for Triassic sediments have been determined for the northerly and southerly areas. In the north, at the village of Bademli (Fig. 4.1), the 'Formation de Mediova' was dated as Scythian in age based on the presence of the bivalves *Unionites and Natiria,* and the foraminifera *Glomospirella* (Monod, 1977). These sediments are unconformably overlain by Upper Triassic sandstones of the Derebuçak Formation, Middle Triassic sediments are not observed. The Triassic units between the villages of Bademli and Derebuçak (Fig. 4.1) have also been dated as Lower Triassic (MTA, 2002). In the southerly Hadim nappe, Triassic units south of Taşkent village (Fig. 4.1) are dated as Lower to Middle Triassic, overlain by Late Triassic clastics (Önder, 1984), but no firm age constraints are given. However, detailed facies analysis and ages are provided from this locality by Özgül (1997). The oldest Triassic sediments, dated as Scythian, include the bivalve *Unionites fassensis.* The youngest Triassic sediments identified are Rhaetian in age, and contain the large foraminifera *Glomospirella rosetta*, and *Auloconus permodiscoides*. During this study, the bivalve *Halobia* sp. was identified in sediments at this locality, and dated the units as Lower to Middle Triassic age.

In the allochtonous Bolkar nappe, the only dates were obtained by Özgül (1997) from a locality to the west of Hadim (Fig. 4.1). The oldest Triassic units are described as Scythian; however this age was inferred from stratigraphic relationships as no fossils were identified. The oldest Triassic fauna, identified are Upper Scythian – Anisian foraminifera, includes *Earlandia* sp. and *Glomospira sinensis*. The youngest Triassic sediments are dated as Landinian, and contain the foraminifera *Aulotortus parvus-minutus* and *Duostaminidae.*

4.3.2 Sedimentary data

Complete Triassic sequences are uncommon within the central Taurides. Within the Geyik Dağ, most of the Triassic sediments are missing because a regional unconformity

that between the Ordovician and the Triassic. The Bolkar nappe is heavily deformed, so although Triassic sediments are identified, complete successions are rare. The Hadim nappe contains the best exposure of Triassic sediments within the region.

The sedimentary facies of each locality studied will now be discussed. Throughout this section, field observations made during this study are integrated with faunal date from the work of Özgül (1997), which is referenced where appropriate.

4.3.2.1 Locality 1: Ekinlik Yayla. GPS reference 447750 4088950. Fig. 4.1.

Ekinlik Yayla is ~10 km to the SW of Hadim village (Fig. 4.1). The Triassic sequence at this locality was described by Özgül (1976; 1983; 1984; 1997) and was studied as the type section within his "Bolkar Dağı unit". The Bolkar nappe is extensively deformed at this locality, with regional folding and tectonic imbrication apparent (see chapter 5: structural history of the platform). A log through the Ekinlik Yayla Triassic sequence is shown in Fig. 4.3. The regional dip of the sediments at this locality is 25-45º to the WSW. The base of the Triassic section tectonically overlies deformed Palaeozoic shale and limestone, and the basal dolomitic horizon locally shows tectonic brecciation.

The lowermost ~40 m of the sequence is characterised by grey-green-brown thick-bedded dolomite interbedded with mudstone and shale. There are local clastic beds towards the bottom of the sequence. Some beds contain small straight shelly fragments, identified as Triassic *Halobia* sp. bivalves. Dolomite and dolomitic limestone are locally interbedded with oolitic limestone, and in places bioclastic and foraminiferous packstone-wackestone (Özgül, 1997). Moving up sequence, thick-bedded fine-grained purple quartzose sandstones are observed. The sequence becomes more mudstone dominated between ~50-100 m (Fig. 4.3) and the succession is infrequently interrupted by dolomite or sandstone horizons. Within the mudstone horizon, slump structures were described by Özgül (1997); however, these were not identified during this study. Thicker bedded dolomite at ~112 m in the succession is light-grey/green, and is locally interbedded with easily eroded muddy layers ~15-30 cm thick. These beds are heavily veined and recrystallised, and contain black chert nodules of diagenetic replacement

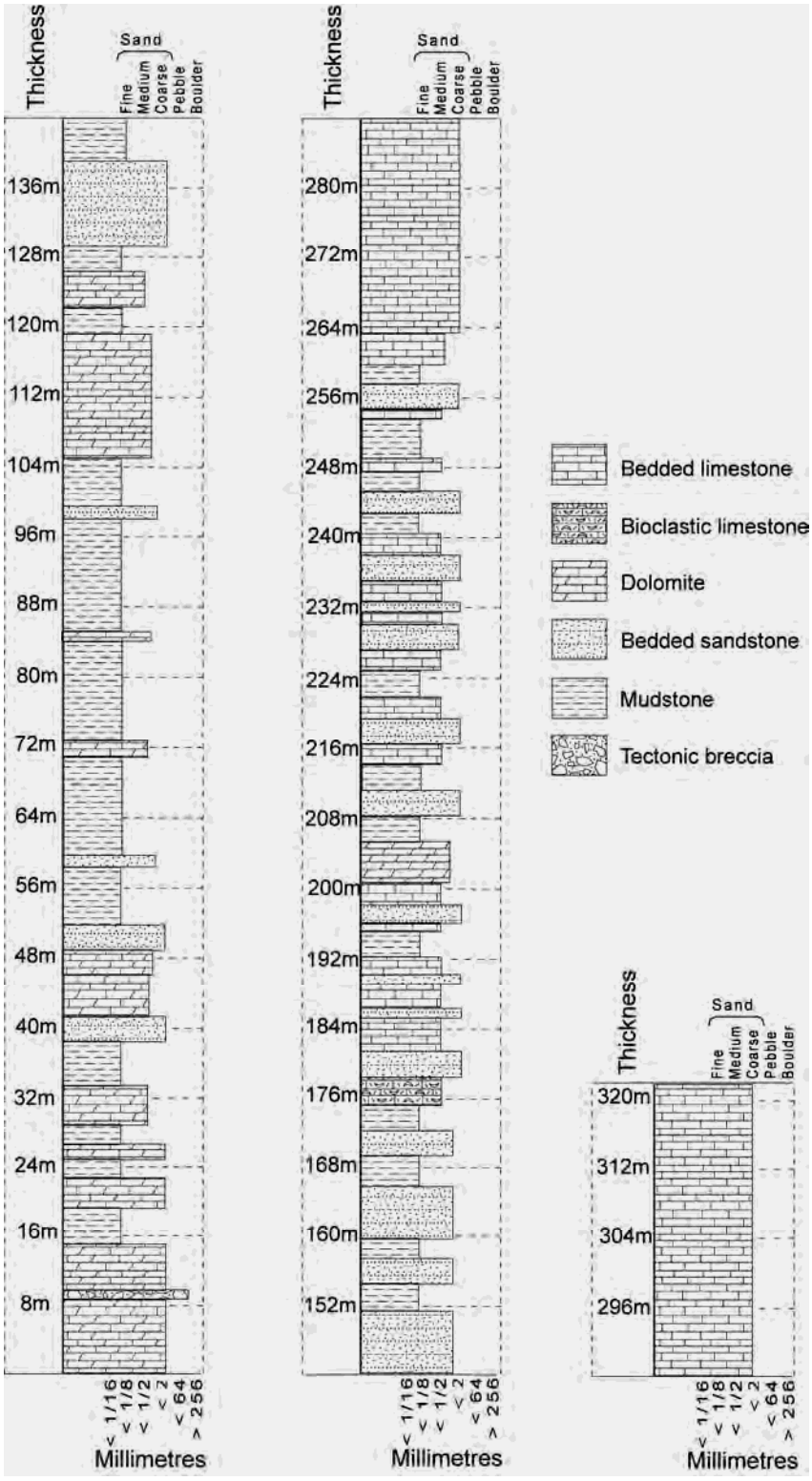

Fig. 4.3. Log of the Triassic succession at locality 1: Ekinlik Yayla.

type. Özgül (1997) describes thin horizons of stromatolitic bindstone with fenestrae interbedded with this dolomite, along with rare bioclastic and bivalve-bearing wackestone horizons. The mudstone horizons are documented as containing ostracods (Özgül, 1997). Overlying this is a ~45 m succession of interbedded mudstone and medium-bedded sandstone (Fig. 4.4a). The lithologies are poorly exposed, but are all deep-red / purple. The sandstone is fine-grained, purple-brown, well indurated, quartzose, and normally recrystallised to quartzite.

The measured section continues with ~80 m of medium- to thick-bedded sandstone, limestone, dolomite and mudstone. Medium-bedded, dark-grey bioclastic limestone is interbedded with thick-bedded, fine-grained quartzose sandstone at 180 m on the measured section (Fig. 4.3). Above this, purple sandstone, grey quartzite, brown sandstone and brown/grey mudstone are interbedded on a metre scale. Sandstone beds have a variable amount of matrix, with some beds containing >15% mud (Özgül, 1997). Bed thickness in this interval of the log varies considerably. The mudstone and clastic lithologies are overlain by a ~60 m sequence of massive, to thick-bedded, shallow-water carbonate and dolomite, which contains mudstone intercalations at the base. In the transitional zone, the limestone is stromatolitic and bivalve bearing in places (Özgül, 1997). The uppermost 50 m of the log contains coralline, algal, and bioclastic horizons (Özgül, 1997). These are heavily recrystallised and partially karstified. The thickness of this limestone sequence is laterally discontinuous due to an overlying tectonic contact with Devonian units of the Hadim nappe. The total thickness of the Triassic sequence measured in this section is 321 m.

4.3.2.2 Locality 2: Alanya road north. GPS reference 456370 4079470. Fig. 4.1.

The term ‘Alanya road’ refers to a road that runs roughly north–south between the village of Taşkent and the Mediterranean coast near the town of Alanya (Fig. 4.1). The road runs perpendicular to the regional strike of Permian – Cretaceous rocks in the region, and exposes the Triassic sequence of the Hadim nappe in road-cuttings. Despite some regional faulting, tectonic imbrication and localised folding, a cross-section through the Triassic sequence can be observed at this locality (Fig. 4.5).

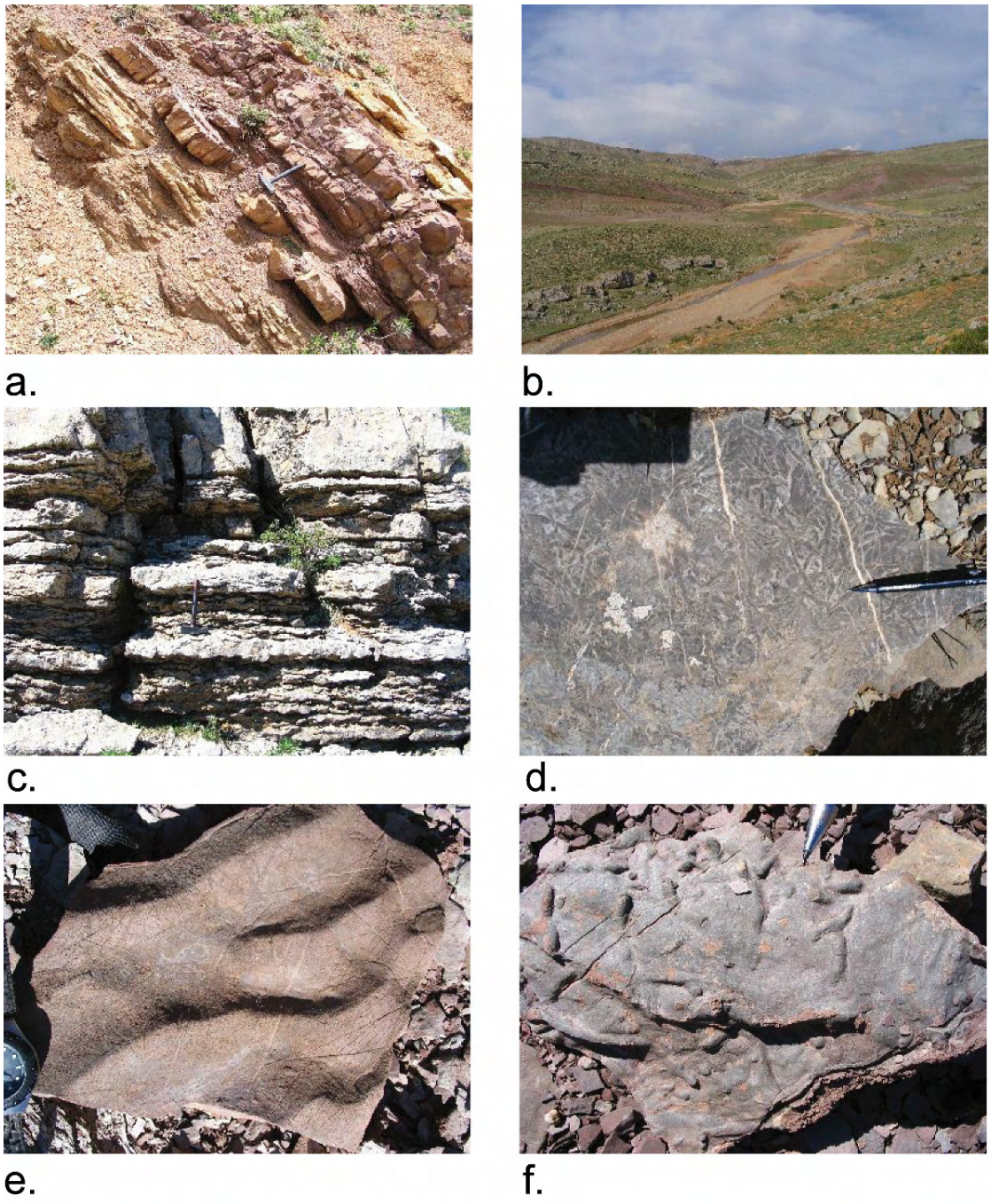

Fig. 4.4. a. Interbedded mudstone and sandstone of the Middle Triassic at locality 1: Ekinlik Yayla; b. View SW over the Middle Triassic succession at locality 3: Alanya road south; c. Lower Triassic stromatolitic / algal limestone at Alanya road south; d. Middle Triassic bioturbated limestone at Alanya road south; e. Symmetrical ripples preserved in Middle Triassic sandstone – mudstone sequence, Alanya road south; f. Prod / groove marks and bioturbation in Middle Triassic sandy-limestone, Alanya road south.

This locality has not been previously documented in the literature. The regional dip of the sediments is 20-40º to the south. The base of the Triassic sequence is marked by a large reverse fault and there is a 4 m horizon of tectonically brecciated and recrystallised limestone adjacent to the fault (Fig. 4.5). Overlying this is an alternating sequence of reworked and recrystallised oolitic and bioclastic limestones. Locally, the oolitic limestones are cross-laminated. Reworked bioclastic horizons contain fragments of bryozoans and crinoids. Overlying this is a ~15 m interval of medium-bedded recrystallised dolomite and fine-grained quartzitic sandstone. At 32 m on the measured section (Fig. 4.5) there is a poorly exposed horizon of mudstone, overlain by a 4 m interval of limestone. Above this is a medium-bedded succession of medium- to coarse-grained sandstone, with well-rounded grains. This sandstone is purple-brown and predominantly quartzose in composition.

Between 53-64 m on the measured section (Fig. 4.5) there is a horizon of cross-bedded oolitic limestone, which has a lenticular geometry. Ooids are 3-4 mm in size. Overlying this, with a planar contact is a 6 m horizon of fine-grained quartzose sandstone. The top of this horizon is planar, above which is a ~50 m succession of thick-bedded, nodular, micritic limestone, alternating with a light-grey nodular recrystallised limestone. The micritic limestone is brown to light-grey, and contains some shelly and muddy beds. The nodular limestone is light-grey to brown, and contains beds with fine shelly fragments and broken crinoids. Above this, 8 m of poorly exposed marly-mudstone is overlain by fine-grained oolitic limestone with some reworked shelly fragments. Nodular limestone between 137-151 m on the log (Fig. 4.5) is recrystallised, and sparry-calcite filled vugs represent replaced bioclastic material. This is followed by a 7 m horizon of fine-grained clastic limestone. Towards the top of the sequence, marly mudstone is interbedded with yellow-grey sandy limestone that contains plant debris. Overlying this is a nodular limestone horizon containing stylolites and thin wavy laminations, which may be microbial in origin. The top of the succession is characterised by mudstone and sandy limestone beds. The total thickness logged is 196 m, considerably less than the other two sections. It is, therefore, suggested that the fault at the base of the succession cuts-out 150 m of the lower Triassic sequence.

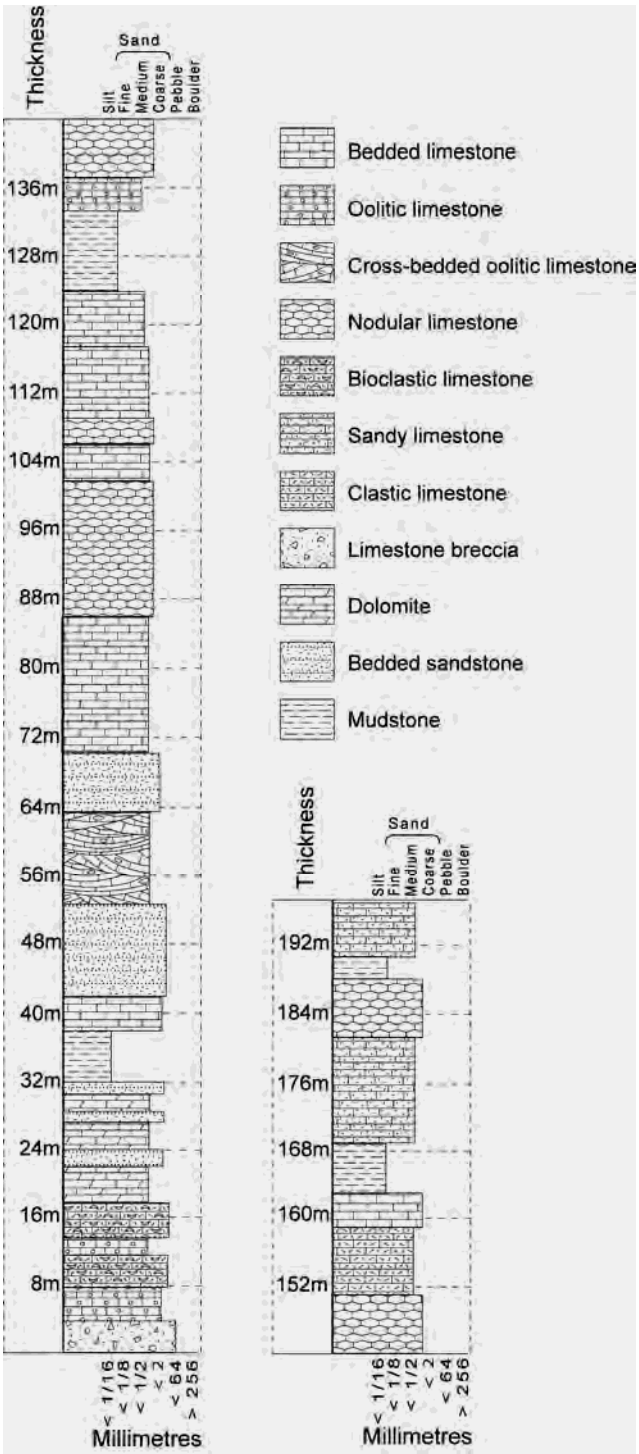

Fig. 4.5. Log of the Triassic section at locality 2: Alanya road north.

4.3.2.3 Locality 3: Alanya road south. GPS reference 455510 4077800. Fig. 4.1.

The second Alanya road locality is the best exposed section of Triassic rocks within the area studied (Fig. 4.1, Fig. 4.4b). The section was documented by Özgül (1997) and Önder (1984) as the type section of the Triassic within the Hadim nappe. Both the contact of the Triassic with the underlying Permian carbonates, and the contact with the Çayır Formation above, can be seen.

The succession begins with 10 m of thin-bedded algal/stromatolitic limestone (Fig. 4.4c) with thin wavy laminations (Fig. 4.6). A 2 m horizon of nodular limestone is overlain by massive, to thick-bedded, limestone with some wavy laminations. The succession then passes into a ~30 m sequence of thin- to medium-bedded mudstone, fossiliferous limestone, oolitic limestone, stromatolitic limestone and micritic limestone. The mudstones are brown-orange in colour, whilst the oolitic limestone contain ooids ~1-2 mm in size. Locally, a horizon of clastic limestone contains limestone pebbles up to 3cm in diameter. Original microbial mats have been recrystallised.

A predominantly mudstone/shale succession exists between 56m – 180m on the measured section (Fig. 4.6), interbedded with thin-bedded horizons of limestone and sandstone. Thin- bedded purple shale is interbedded with fine-grained sandstone and thin limestone beds, which have vertical and horizontal burrows (Fig. 4.4d). Fine-grained purple quartzose sandstone exhibits symmetrical and asymmetrical ripples (Fig. 4.4e), as well as some sole structures (Fig. 4.4f). Coarse, reworked bioclastic limestone and oolitic beds are 3–7 cm thick, and locally contain plant fragments. Limestone horizons contain small *Halobia* sp. bivalve shells. Locally, packstone beds contain high concentrations of ooids, peloids, broken shells and limestone pebbles, all of which have been reworked. Most individual limestone beds have a nodular upper surface. Thinly-bedded grey marls with thin laminations are also observed. Sandy and clastic horizons become more common at ~176 m on the measured section (Fig. 4.6).

This predominantly mudstone sequence is then overlain by a 35 m succession of limestone conglomerate, grainstone, bioclastic limestone, oolitic limestone and marly-shale. Limestone conglomerates are medium-bedded and contain rounded clasts, up to 4

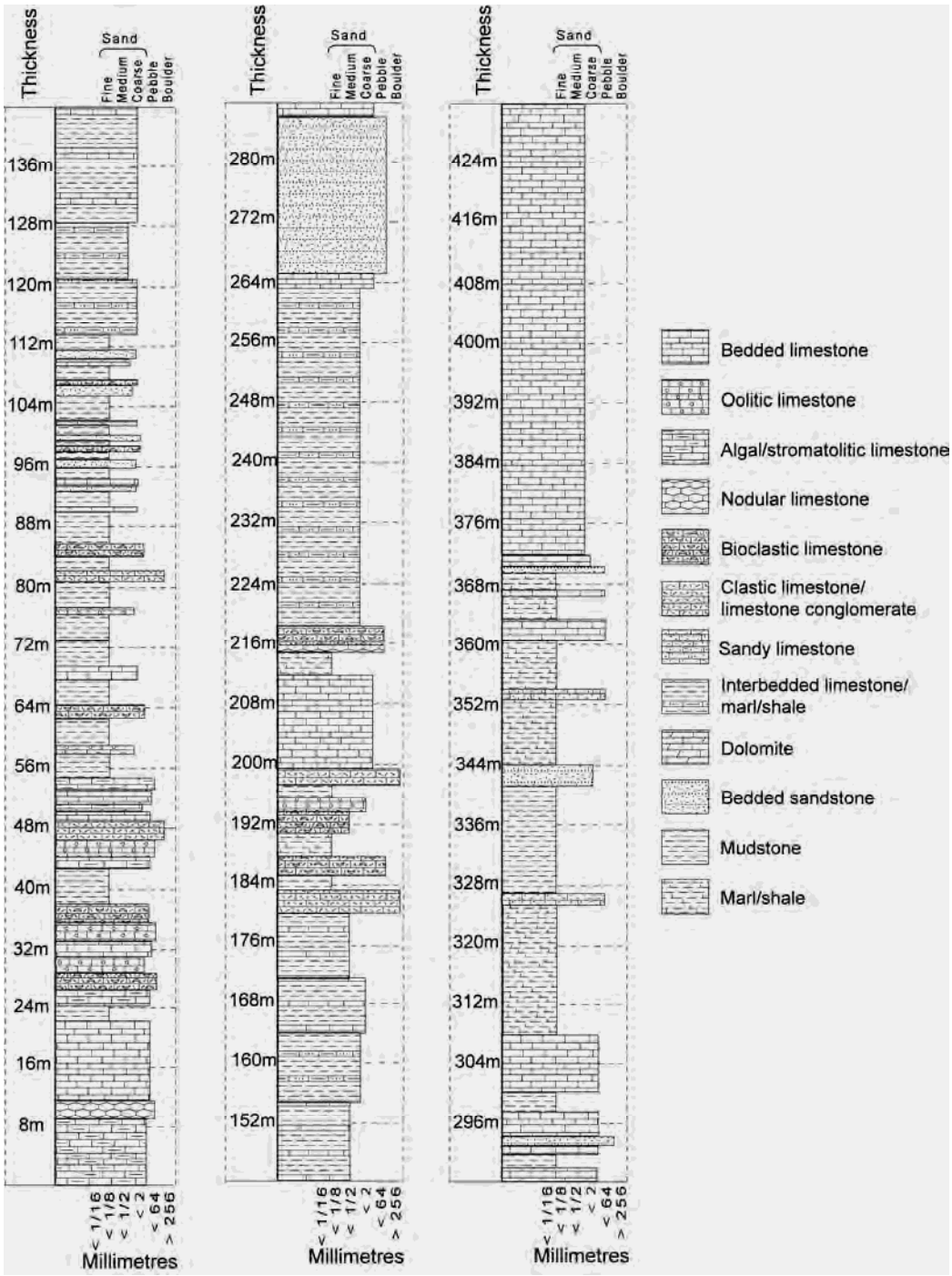

Fig. 4.6. Log of the Triassic section at locality 3: Alanya road south.

cm in size. Özgül (1997) notes that this conglomeratic marker horizon is cross-bedded in places and has a siliceous cement. Fine- to medium-bedded grainstones contain disarticulated shells, such as bivalves. This horizon also contains ammonites, crinoids and gastropods (Özgül, 2007). A 12 m horizon of beige micritic limestone, followed by marly-mudstone and a nodular bioclastic limestone horizon, are then overlain by a thick sequence (~45 m) of finely-laminated, light beige mudstone/marl, with occasional thin beds of micritic limestone. A 1 m horizon of yellow-grey dolomitic limestone is documented at the top of this succession (Özgül, 1997).

At 262 m on the log (Fig. 4.6), a thick horizon of medium- to thick-bedded quartzose sandstone occurs. Bedding is planar, and the sandstone is finely laminated. The sand is generally medium-grained (locally coarse-grained), with sub-rounded to sub-angular grains, moderately- to well-sorted, and with the occasional small sub-rounded pebbles. The cement is calcareous and "lime-clay bearing" (Özgül, 1997). There is also plant debris in thinner-bedded and finer-grained horizons. Overlying this clastic horizon is a ~80 m succession of interbedded mudstone/shale, limestone and sandstone. The mudstone/shale is grey-brown, and is laminated on a millimetre scale. Sandy limestone intercalations are dark-grey and organic rich, containing plant material. They can also contain abundant broken and reworked bivalve shells (2-3 cm in size). Fine-grained sandstone and sandy limestone beds interrupt mainly marly-shale interbeds towards the top of this sequence.

The uppermost part of the succession, 60m thick in places, is made up of thick-bedded micritic limestone (Fig. 4.6). These sediments form inaccessible cliffs in the section studied. This micritic limestone overlain by the Late Triassic Çayır Formation red clastics (section 4.4). The total thickness of the Triassic succession at this locality is 432 m. The three Triassic localities documented above are all in the allochthonous units (i.e. Bolkar nappe and Hadim nappe) which are located in the south of the studied area. As mentioned in the introduction to this chapter, limited Triassic sequences can also be observed in the northerly Hadim nappe and the Geyik Dağ, which will now be described.

4.3.2.4 Geyik Dağ

Triassic exposure in the Geyik Dağ is observed near the village of Tarasçi, ~10 km NW of Seydişehir (Fig. 4.1). An unconformable relationship between Ordovician and Triassic–Jurassic units is poorly exposed in a road section ~250 m north of Taraşçı village. The base of the Triassic succession consists of weakly foliated, varicoloured purple to brown micaceous sandy-shales. The thickness of the purple shales varies from 15-20 m in the road section, to 50-100 m to the west of Taraşçı village. The shales pass up into thinly bedded (10-15 cm), moderately sheared, medium-dark grey recrystallised limestones, thickening upwards to medium-thick bedded over a 5-10 m interval. These beds contain nodules of black chert formed by diagenetic silica replacement. The sequence continues for >50 m and passes into thin-bedded microbial limestones, interbedded with shales and thick-bedded bioclastic limestones. The succession then passes upwards into medium- to thick-bedded carbonates of Triassic age (Monod, 1977), interbedded with thin shale horizons, in all ~300 m thick.

A much thinner horizon of Triassic sediments is exposed ~2 km to the SW of Karadiken village, near the town of Beyşehir (Fig. 4.1). These sediments exhibit a deep red-purple colour, and outcrop over an area 500 m x 750 m. They consist predominantly of shales interbedded with grey medium-grained well indurated quartzose sandstone, bioturbated grey limestone and less indurated purple sandstone. Locally, the purple colour has been leached out and the sediments are a brown-beige. The total thickness of the Triassic at this locality is 25 m. This succession has been dated as Middle – Late Triassic (Monod and Akay, 1984; MTA, 2002), however, the fauna that were identified to obtain this date have not been published.

4.3.2.5 Northerly Hadim nappe

The Triassic sequence in the northerly area of the Hadim nappe is not particularly well exposed. The type section (Monod, 1977) is at the Medi Ova plain, ~12 km W of Bademli (Fig. 4.1). The base of the succession is represented by medium- to thick-bedded dolomite, overlain by bioclastic and bioturbated limestone. Dolomitised oolitic

limestone is overlain by a sequence of interbedded red mudstone, oolitic limestone and bioclastic limestone. Mudstone is abundant within this sequence, so that exposure is poor. The top of the sequence is represented by 25 m of grainstones containing ooids, algae, and other bioclastic fragments (Monod, 1977), overlain by 20 m of marine mudstone. Monod (1977) dated the entire Triassic sequence at this locality as Lower Triassic (Scythian). Late Triassic Çayır Formation sediments unconformably overlie this sequence. The total thickness of this succession is 220 m.

Triassic sediments have also been identified along the western margin of the Hadim nappe near the village of Gumuşdamla (Fig. 4.1). Tracing the Triassic sediments laterally is very difficult because of regional faulting. At Gumuşdamla, red mudstone is interbedded with medium-bedded brown-yellow limestone. Above this thin-bedded dark grey recrystallised limestone is interbedded with dark mudstone/shale. Limestones become more abundant up section, and medium- to thick-bedded carbonates are interbedded with thin shale horizons. It is estimated that approximately 100 m of the Triassic sequence is present.

4.3.3 Sediment composition and provenance

The clastic sediments within the Lower to Middle Triassic succession are believed to have been derived from the underlying Tauride platform stratigraphy. Field observations of sandstone, pebbly sandstone and conglomerate indicated that most clastic sediment was texturally mature and quartzose in composition. Clasts of micritic limestone and quartzose sandstone were derived from adjacent / underlying beds within the Triassic sequence. Any erosion of the Triassic succession was limited, without creating any angular discordance. Examination of Triassic sandstones in thin section confirmed that they are quartzose. The majority of grains are monocrystalline quartz, with minor polycrystalline and composite quartz grains. The only lithic grains observed were microcrystalline silica / chert, and occasionally an altered feldspar grain.

4.3.4 X-ray fluorescence analysis of shales

During this study a sample of shale from the Middle Triassic sequence at Alanya road south was analysed using X-ray fluorescence (XRF) technique for major and trace elements at the School of Geosciences, University of Edinburgh, as specified by Fitton et al. (1998). Multi element plots can be used to indicate the variation of major and trace elements in mudstone (Gromet et al., 1984; Rollinson, 1993), and hence can provide insights into sediment sources.

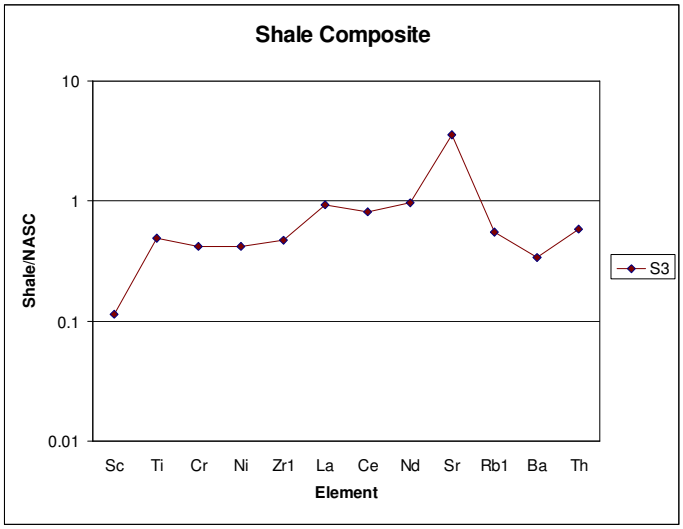

Fig. 4.7. Average shale normalised multi element spidergram of Middle Triassic shale (sample S3) from the Alanya road south locality. Normalising values from Gromet et al. (1984).

The Triassic shale analysed in this study shows a composition that is quite close to the average North American Shale composition (Gromet et al., 1984), with neither depletion nor enrichment in light REE or mafic elements (e.g.. Cr, Ni). The sample is depleted in Sc relative to the NASC. The only element which does show relative enrichment is Sr, which reflects the abundance of calcium carbonate rocks within the Triassic sequence. The XRF analysis suggests that the mudstone is derived from a typical continental crust, without any signs of a local mafic or acidic provenance.

4.4 Upper Triassic Çayır Formation

This section will discuss the Upper Triassic – Lower Jurassic Çayır Formation. The Çayır Formation was studied at 15 localities within the Geyik Dağ, Hadim nappe and Bolkar nappe during this study (Fig. 4.8). The Çayır Formation is thought to be a consequence of "Cimmerian" uplift of the Tauride platform.

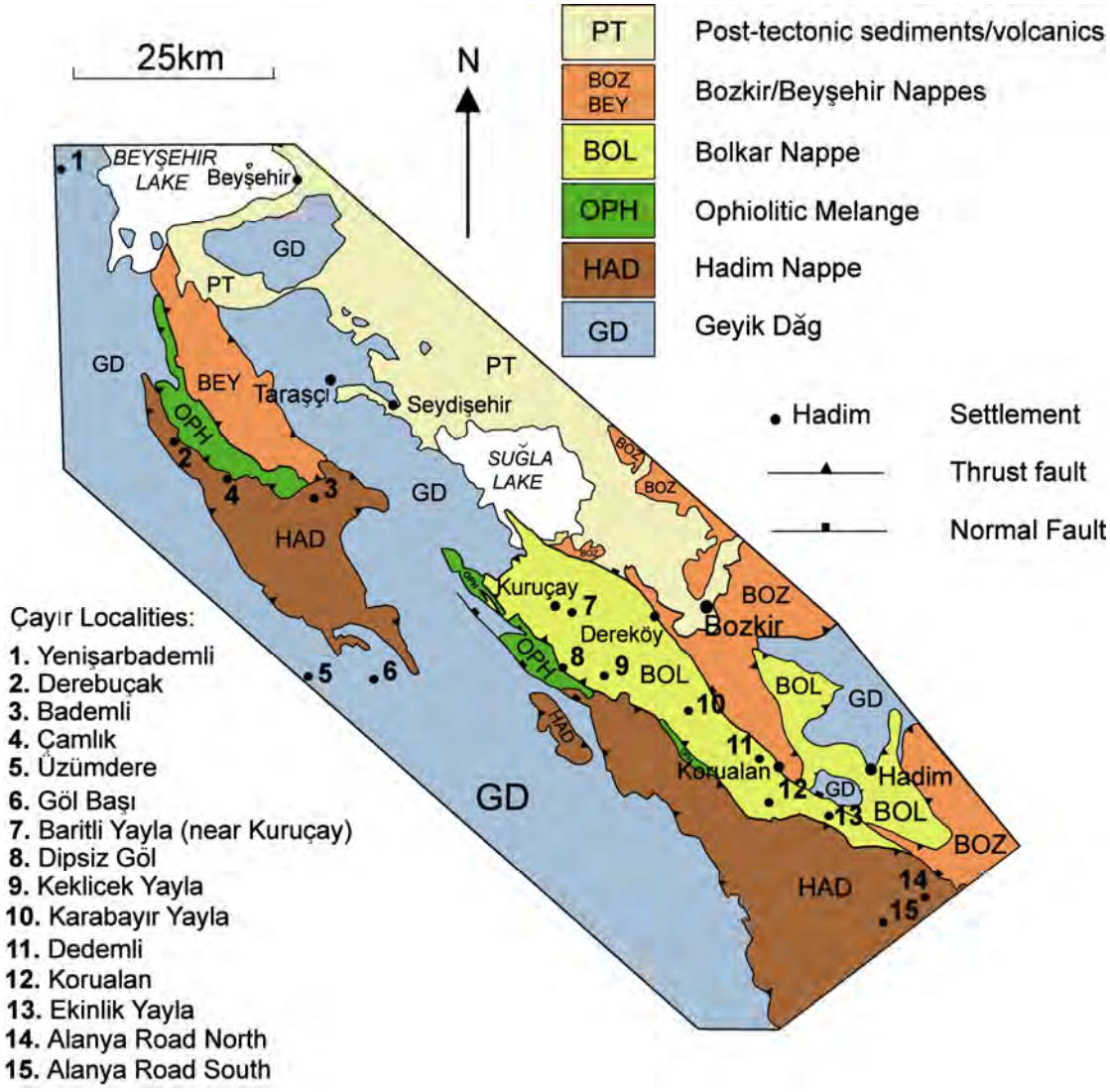

Fig. 4.8. Simplified tectonic map of the study area showing the location of studied Çayır Formation successions documented in section 4.5.2.

4.4.1 Age

Determining the age of the Çayır Formation is difficult owing to a paucity of datable fossils. Monod and Akay (1984) cited ages ranging from Late Triassic to Middle Jurassic, based on local stratigraphic relationships and limited palaeontological data (e.g. Foraminifera *Triasina hantkeni* of Upper Norian age; Algae *Paleodasycladus mediterraneus* of Middle to Upper Liassic age). Özgül (1997) inferred a general Anisian-Norian age, because limestones overlying the clastics were dated as Norian-Rhaetian, and hence the Çayır sediments were inferred to be older. In the Hadim nappe, clastic facies of the Çayır Formation pass conformably into Upper Liassic limestones and dolomites (Gutnic et al. 1979). The base of the Çayır Formation rests unconformably on Upper Triassic shallow-marine platform carbonates at a locality 15 km south of Taşkent village (Önder, 1984). A recent geological map of the region indicates the Çayır Formation as Late Rhaetian – Early Liassic in age (MTA, 2002); however, evidence on what this is based on is unavailable. During this work fossiliferous limestone horizons in the mid-part of the succession yielded the benthic foraminifera *Siphovalvulina variabilis* Septfontaine, *Amijiella amiji* (Henson), *Orbitopsella primaeva* (Henson), *Planiinvoluta* sp., *Valvulina* sp., *Thaumatoporella parvovesiculifera* (Raineri), implying a Middle Liassic age (N. İnan and K. Taslı, pers. comm., 2007).

4.4.2 Sedimentary data

Where studied by us, the Çayır Formation is typically a fining-upward succession, <200 m thick, of continental clastics and shales intercalated with shallow-marine limestones. The basal part of the Çayır Formation is usually composed of coarse conglomerates and sandstones. At some localities conglomerates are not present and the succession as a whole is represented by fine-grained sandstone/shale. Shale and limestone becomes more abundant upwards and typically passes into Jurassic shallow-marine platform carbonates. The following section will discuss the sedimentary facies of the Çayır Formation at 15 studied localities.

4.4.2.1 Locality 1: Yenişarbademli. Grid Reference 354080 4175440.

The village of Yenişarbademli is within the Geyik Dağ regional autochthon, located west of Lake Beyşehir (Fig. 4.8). The formation consists of ~30 m of interbedded sandstone and mudstone, with the top 10 m having interbedded limestone beds (Fig. 4.9a). Sandstone is medium-bedded, purple-red, fine- to medium-grained, and moderately- to well-sorted. Rarely, coarser lenses contain pebbles (1 cm – 3 cm in size) which are sub-angular to sub-rounded. Finer-grained beds exhibit parallel lamination. Sandstone is composed of quartzose grains with varying amounts of muddy / silty matrix. Interbedded mudstone layers are finely laminated and in some cases lightly foliated. Small rip-up clasts locally were diagenetically altered to a yellow colour. Medium-bedded (30-60cm) light-grey limestone beds at the top of the succession are partially recrystallised, veined and fractured. Locally, sandy-limestone interbeds are fine- to medium-grained. There is a lack of fauna to constrain the age.

4.4.2.2 Locality 2: Derebuçak. Grid reference 369260 4139410.

The village of Derebuçak is located in the northerly study area, 40 km SW of Beyşehir on the western margin of the Hadim nappe (Fig. 4.8). To the east of the village, an exposure of coarse red clastics is observed in a road cutting. The Hadim nappe is documented as forming a west-facing recumbent anticline at this locality (Monod, 1977), with its fold axis running through the Çayır Formation. The Çayır sequence is therefore deformed, and half of the sequence is inverted. A log though the complete Çayır sequence is shown in Fig. 4.9b.

The base of the formation is represented by medium- to thick-bedded (50-180 cm) conglomeratic beds showing lateral variation in thickness. Conglomerates are red-grey, very poorly sorted, with angular to sub-rounded clasts. Clast size is variable, ranging from 1 cm to 15 cm, with the average ~3 cm. The matrix is medium to coarse grained lithiclastic sand. Most conglomerates are clast supported. Beds are lithified with a calcitic cement, well indurated, and have low porosity. Localised clast imbrication and cross-bedding is observed. Clast composition is discussed in section 4.4.4.

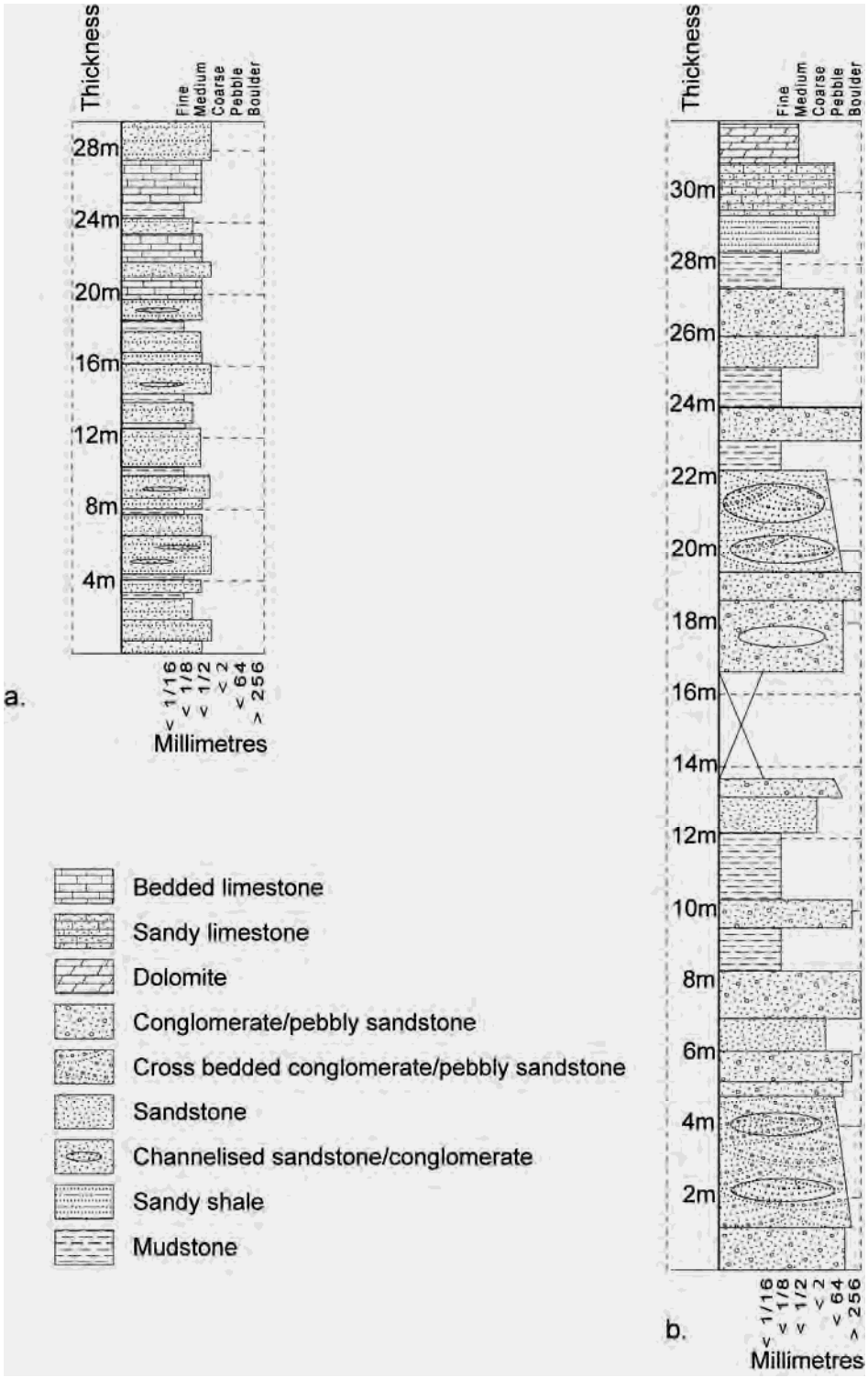

Fig. 4.9. Sedimentary logs through the Late Triassic Çayır Formation. a. Locality 1: Yenişarbademli; b. Locality 2: Derebuçak.

Red-purple and grey mudstones, interbedded with thin-bedded (15 cm) fine-grained sandstone, interrupt the coarse clastic sequence between 8-12 m on the measured section (Fig. 4.9b). Some fine lamination can be seen, but generally exposure is poor. The mudstone has a low organic content. Thin- to thick- bedded sandstone (30-150 cm) and pebbly sandstone is interbedded with conglomerate throughout the whole interval. The sandstone varies from red-grey to beige-yellow, medium- to coarse-grained, moderately- to poorly-sorted, with angular to sub-rounded sand grains. These sandstones are quartzose with varying proportions of lithic fragments. A variety of sedimentary structures, including parallel lamination, fining-upwards beds, and pebbly channels/lenses. Calcite cementation has created well-indurated sandstone with a low porosity.

The sequence fines towards the top of the measured section (Fig. 4.9b) where sandy-mudstone, mudstone, and siltstone beds are more abundant than at the base of the sequence. Above this there is a sandy-limestone horizon, fine- to medium-grained with occasional small (2 cm) limestone pebbles. Overlying this is a thick-bedded, to massive, light grey dolomite which passes upwards into a thick, continuous sequence of Mesozoic carbonates. The total thickness of the Çayır Formation at the Derebuçak locality is ~30 m.

4.4.2.3 Locality 3: Bademli. Grid reference 387370 4129380.

Bademli village is ~40 km south of Lake Beyşehir, on the road between the towns of Beyşehir and Akseki (Fig. 4.8), within the Hadim nappe. Little of the Early – Middle Triassic sequence is exposed, in part owing to local faulting. However, the Late Triassic Çayır Formation can be observed to the SW of the village in several road cuttings.

The Çayır Formation overlies interbedded shales and limestones of the Triassic Medi Ova Formation (described earlier in this chapter, section 4.3.2.5). Medium-bedded (40-80 cm) purple/pink-yellow calcareous sandstone is locally interbedded with pebbly sandstone (Fig. 4.10a). These sandstones are well-sorted, medium-grained, with sub-rounded to sub-angular grains and rounded pebbles (where observed). These sandstones

are quartzitic, with a calcitic cement, and are thus very well indurated. Fine parallel lamination and cross lamination is seen in some beds. Pebbly sandstone horizons are poorly sorted, with clasts from 0.2 cm to 3 cm in size. Clast composition is documented in section 4.4.4.

Poorly exposed mudstone midway through the sequence is purple-red, non-fissile, with a low organic content. Locally, mudstone is thinly interbedded with fine-grained sandstone. Between 22-48 m on the measured section (Fig. 4.10a), the sequence is dominated by medium-bedded (40-50cm) deep-purple calcareous sandstone. Well-sorted, quartzose sandstones are locally interbedded with thin mudstone. The sandstones are medium-grained, and show parallel lamination, and in some places cross-lamination. Overlying the clastic sequence is a thick-bedded, grey, Liassic dolomitic limestone succession, with reworked shelly fragments in the lowermost beds.

4.4.2.4 Locality 4: Çamlık. Grid reference: 378600 4132050.

Çamlik village is located on the road between Derebuçak and Bademli (Fig. 4.8). A dirt track ~1 km to the west of the village runs south ~3 km and emerges on the Medi Ova plain. The Triassic succession is poorly exposed, but the main lithologies of the Çayır Formation can be identified (Fig. 4.10b). Due to poor exposure in this region, Fig. 4.10b is not actually a measured log of the succession, but an interpolated log based on relative abundances of sedimentary facies. The exposure is within the northerly area of Hadim nappe.

The coarsest sediments in the succession are coarse-grained purple/grey/yellow sandstones, containing limestone clasts up to ~2 cm in size. These are matrix supported and quartzitic in composition. Sandstone horizons are laminated, recrystallised, medium-grained, quartzose and range from grey to purple. The remainder of the succession is made up of red/purple mudstone and sandy-mudstone. The thickness of this succession is ~ 35 m (Fig. 4.10b).

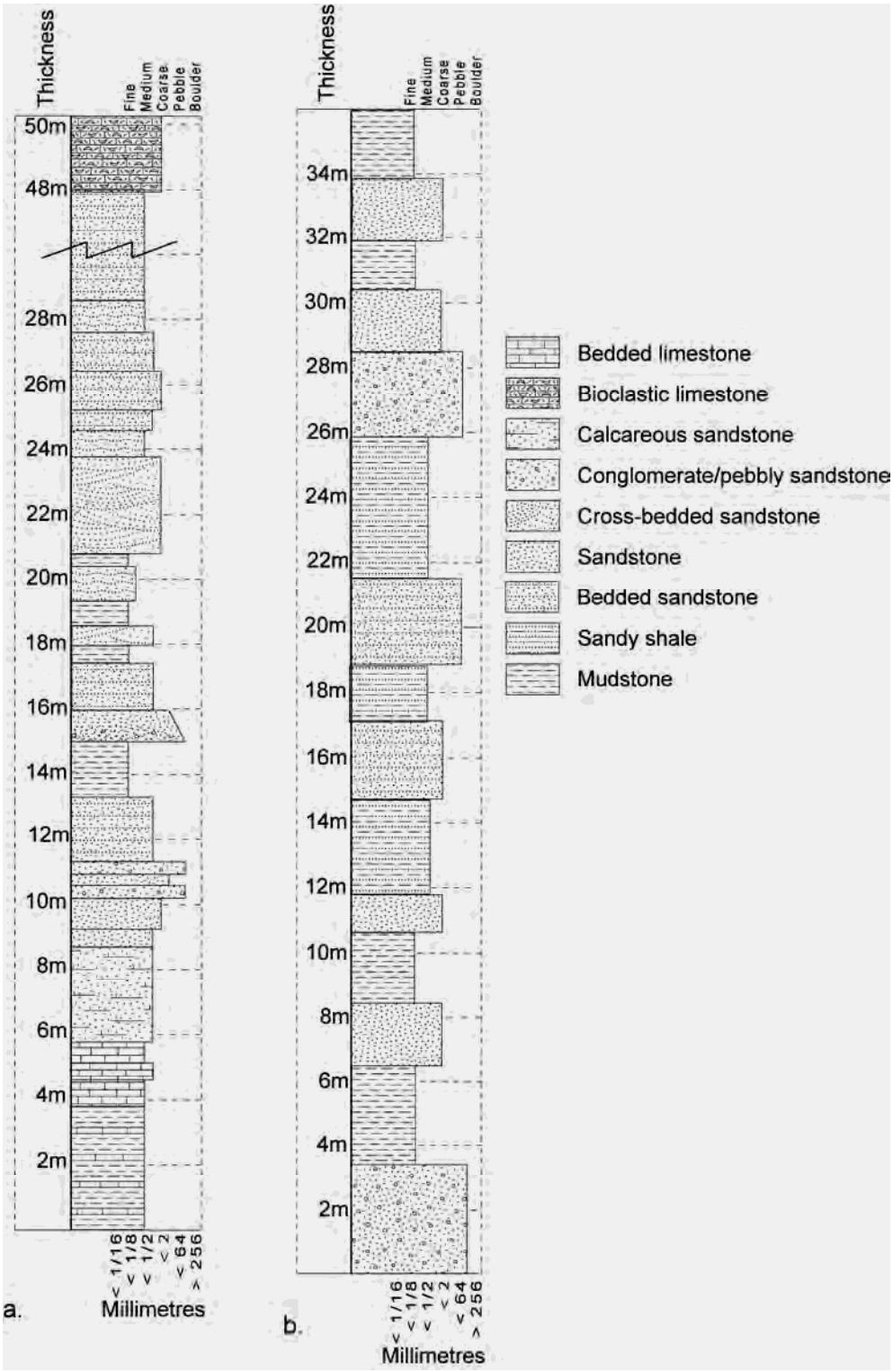

Fig. 4.10. Sedimentary logs through the Late Triassic Çayır Formation. a. Locality 3: Bademli; b. Locality 4: Çamlık.

4.4.2.5 Locality 5: Üzümdere. Grid reference 383780 4109640.

Üzümdere village is located in a spectacular v-shaped valley, ~10 km NW of Akseki (Fig. 4.8). The valley sides are largely covered in limestone scree from high Mesozoic cliffs; however, some good exposure of the Çayır Formation is found towards the NE of the valley. This locality is within the Geyik Dağ autochthon. A summary log of the succession is shown in Fig. 4.11a.

Most of the succession is composed of medium- to thick-bedded, deep purple sandstone, locally intercalated with mudstone (Fig. 4.11a). The sandstone is fine- to medium-bedded (15-60 cm), fine- to medium-grained, and moderately- to well-sorted (Fig. 4.12a). Grains are angular to sub-rounded, largely quartzose in composition, but with a significant proportion of lithic grains in some beds. The matrix is a muddy-sandstone, and porosity is low. Both sandstone and mudstone show parallel lamination, and in some places lens-shaped bodies of pebbly sandstone were observed.

The coarsest sediments within the sequence are medium- to thick-bedded (<70 cm) conglomerates (Fig. 4.12b). These are poorly sorted, with clasts ranging from 1 cm to 12 cm; average size ~2.5 cm. These conglomerates are clast supported, with a medium-grained quartzose sandstone matrix. Sedimentary structures include fining upwards sequences, clast imbrication, erosional channels, sandy lenses, cross-lamination and rip-up clasts. Clast composition at this locality is documented in section 4.4.4. The total measured thickness of the formation at this locality was 22 m; however, it is likely that a much thicker sequence was partially obscured by scree.

4.4.2.6 Locality 6: Göl Başı. Grid reference 393310 4108820.

Göl Başı is found in the Geyik Dağ autochthon ~10 km north of Akseki (Fig. 4.8). Extensive faulting in the area made finding a complete section through the Çayır Formation difficult. A composite log of the stratigraphic sections that were accurately measured is shown in Fig. 4.11b.

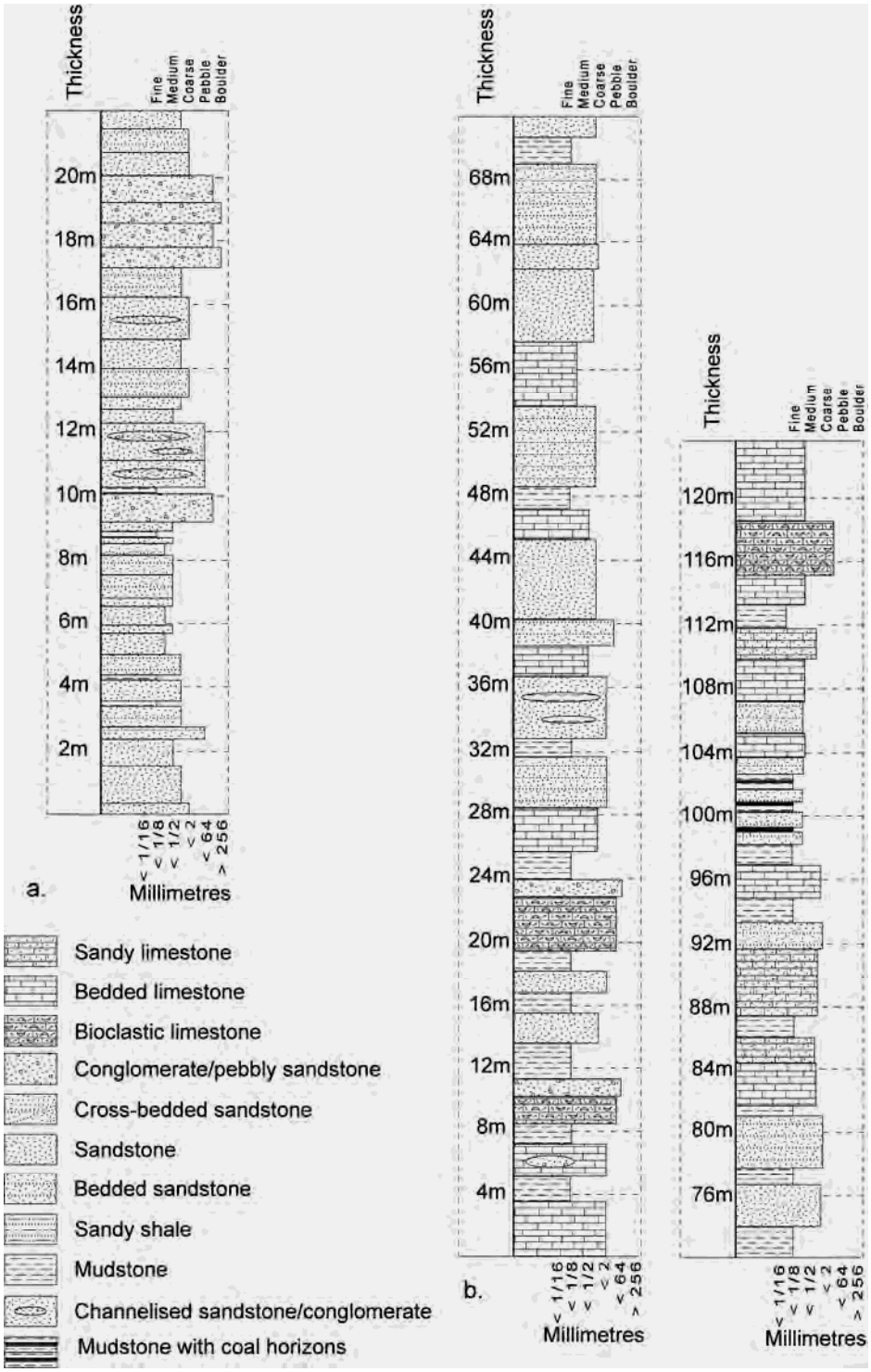

Fig. 4.11. Sedimentary logs through the Late Triassic Çayır Formation. a. Locality 5: Üzümdere; b. Locality 6: Göl Başı.

The basal 25 m of the log (Fig. 4.11b) consists of an interbedded succession of limestone, sandstone and mudstone. Limestone beds are medium- to thick-bedded, partially recrystallised, grey/brown/green, and locally contain significant amounts of bioclastic material (broken bivalve shells). There is also a prominent limestone conglomerate at 11 m on the measured section (Fig. 4.11b). Sandstone is medium-bedded, and variably fine- to medium- to coarse-grained. There is also a prominent muddy debris flow with small clasts, <3 cm at 24 m on the log. Mudstone/shale is fissile, and grey/brown in colour.

Moving up sequence the formation is dominated by medium- to thick-bedded to massive, sandstone, interbedded with medium-bedded limestone with thin-bedded mudstone/shale horizons (Fig. 4.12c). The sandstone is variable in composition and grain size, with some beds containing high percentages of lithic grains, whilst others are quartzitic in composition. Some sandstones are calcareous and may contain abundant carbonate grains, along with a calcite cement. There are local fining-upwards sequences over 3-5 m thick, from medium-grained sandstone to limestone and finally mudstone. Sandy limestone beds were also observed.

Towards the top of the succession, a sandstone/mudstone succession contains thin coal-bearing horizons (10-15 cm thick). Recrystallised limestone and calcareous sandstone are abundant at the top of the formation, with bioclastic limestone containing large bivalves (megalodonts). Through facies association, this is thought to be the base of the overlying Jurassic platform carbonates (Akseki platform). The total thickness of the Çayır Formation at this locality is 112 m.

4.4.2.7 Locality 7: Baritli Yayla. Grid reference 418830 4116120.

Baritli Yayla is located on the road between Bozkir and Akseki, ~5 km to the east of Kuruçay village (Fig. 4.8). This locality is within the Bolkar nappe. Exposure is poor, and dense vegetation makes finding a complete section through the Çayır Formation difficult. However, the main lithologies are exposed on a forestry path to the north of the main road, allowing a composite log of the succession to be made (Fig. 4.13a).

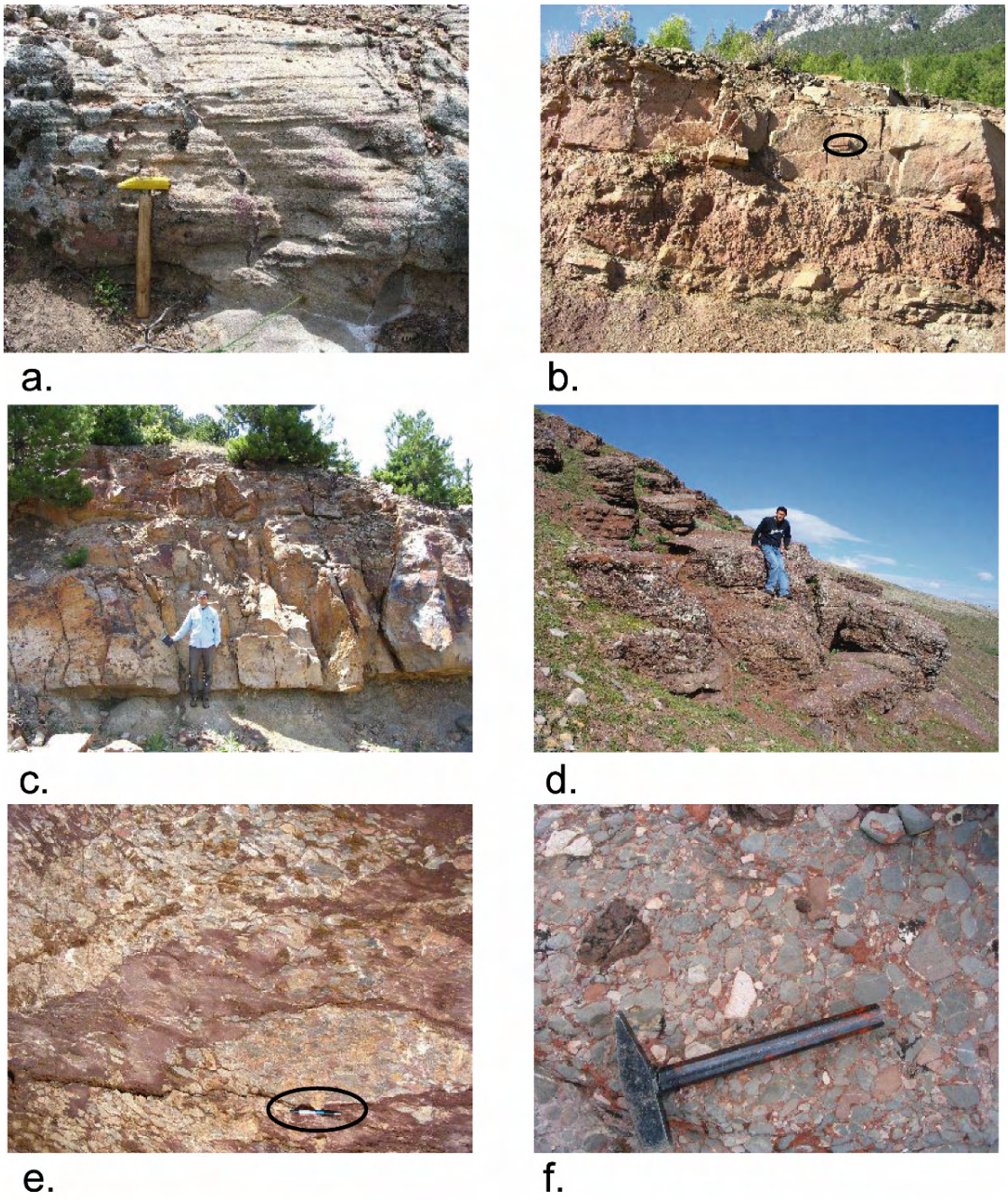

Fig. 4.12. a. Coarsely laminated purple sandstone of the Çayır Formation at locality 5: Üzümdere; b. Medium- to thick-bedded conglomerate and sandstone succession at Üzümdere. Hammer circled for scale; c. Thick-bedded, to massive, sandstone overlying mudstone, Çayır Formation, locality 6: Göl Başı; d. Thick-bedded purple conglomerate of the Çayır Formation at locality 9: Keklicek Yayla; e. Heavily sheared debris-flow / conglomerate at locality 11: Dedemli. Note that despite shearing, clast-supported horizons (light colour) are concentrated in channels. Pencil circled for scale; f. Clast-supported debris-flow / conglomerate at locality 12: Korualan. Clast composition is almost entirely grey limestone.

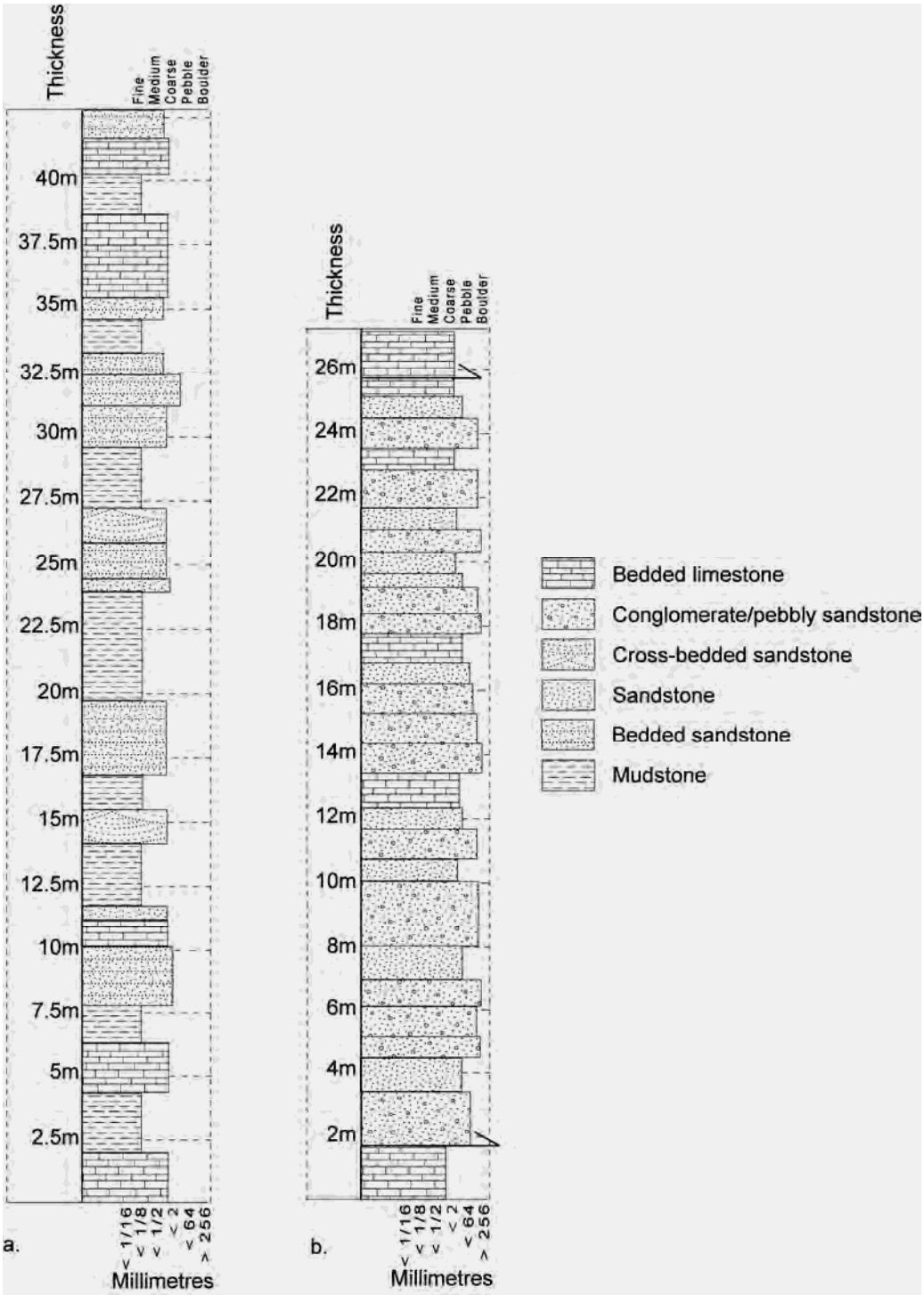

Fig. 4.13. Sedimentary logs through the Late Triassic Çayır Formation. a. Locality 7: Baritli Yayla; b. Locality 8: Dipsiz Göl.

Deep-purple, recrystallised sandstone makes up ~55% of the succession. This is thin- to medium-bedded (15-50 cm), finely laminated and well indurated. The sand is quartzose in composition, with a siliceous cement (locally calcitic). Grains are sub-rounded, fine-, to medium-grained, and generally well sorted. Locally beds have been diagenetically altered to a light-grey/yellow colour. Mudstone is the second most abundant lithology, comprising ~30% of the formation (Fig. 4.13a). This is very fine-grained with fine laminations. However, it is also strongly weathered and poorly exposed. The rest of the succession is composed of fine- to medium-bedded limestone. This weathers to a dirty-yellow colour; however, internally, the limestone is medium- to dark-grey, well indurated, and often contains sandy-limestone horizons. Bioclastic material is absent. Limestone beds are confined to the lower 5 m and upper 10 m of the formation. There is occasional evidence of palaeocurrents, with cross-lamination showing current flow to the south. Locally the formation is folded, and strike-slip faulting is observed. The total thickness at this locality is 35-38 m (Fig. 4.13a).

4.4.2.8 Locality 8: Dipsiz Göl. Grid Reference 415650 4109090.

Dipsiz Göl is a well documented locality due to an excellent exposure of ophiolitic melange (Özgül, 1984; Andrew, 2003). This locality is ~20 km WSW of the town of Bozkir, and is only accessible via temporary dirt tracks (Fig. 4.8). This Çayır Formation sequence is located within the Bolkar nappe, close to the tectonic contact with the Dipsiz Göl ophiolitic melange. As a result, the Çayır Formation forms a heavily faulted and sheared imbricate slice within the Bolkar nappe, itself largely a broken formation (see chapter 5).

The succession is dominated by coarse clast-supported conglomerate and pebbly sandstone (Fig. 4.13b). Conglomerate beds are medium - to thick - bedded and laterally variable in thickness. Clast size ranges from 0.2 cm to 13 cm, the average being 3.5 cm. Clasts are sub-rounded to rounded; their composition is discussed in section 4.4.4. Occasional fining-upward sequences are observed, with conglomerate passing into pebbly sandstone and then into coarse sandstone. The laterally discontinuous geometry of sediment packages is probably indicative of channel features; however, no other

sedimentary structures were observed. Occasional limestone within the succession is heavily recrystallised and sheared, suspected to be imbricate slices of a different age. The total thickness is ~25 m.

4.4.2.9 Locality 9: Keklicek Yayla. Grid Reference 420490 4108250.

Keklicek Yayla is located in a remote area, close to the Dipsiz Göl ophiolitic melange (Fig. 4.8), only accessible via dirt tracks. This locality has not been documented in previous literature, but it is undoubtedly the best exposure of the Çayır Formation within the heavily deformed Bolkar nappe. The total thickness of the succession is 44 m (Fig. 4.14a).

The succession is dominated by coarse-conglomerate, pebbly sandstone and sandstone, with rare mudstone horizons (Fig. 4.14, Fig. 4.12d). Bedding is typically medium- to thick-bedded, ranging from 50-150 cm. Many horizons vary in thickness laterally, lens-shaped bodies being common. Fining-upward packages are seen, with conglomerates grading into pebbly-sandstone and then sandstone over 5-10 m. The contact with underlying Triassic carbonates is not observed; however, the top of the clastic succession is transgressed by thick-bedded Jurassic carbonates (Fig. 4.14a).

Conglomerate clast size ranges from <1 cm to 18 cm; clasts are well rounded to sub-angular, with a majority of clasts being sub-rounded. Clast composition is discussed in section 4.4.4. Clast imbrication is observed, and palaeocurrents are discussed in section 4.4.3. The matrix is a medium- to coarse-grained lithiclastic sandstone. Sandstone is variably fine- to medium- to coarse-grained, and is dominantly a distinctive purple colour (locally grey). It is planar-bedded, sometimes with fine parallel lamination, and cross-lamination locally. Primary current lineation, and clast alignment within pebbly-sandstone horizons is observed. Sandstone beds are usually quartzose, although some beds are composed of lithoclastic sandstone. Where mudstone is present, it typically overlies fine-grained sandstone, and is part of a larger scale fining-upwards sequence (Fig. 4.14a). Mudstone is purple in colour.

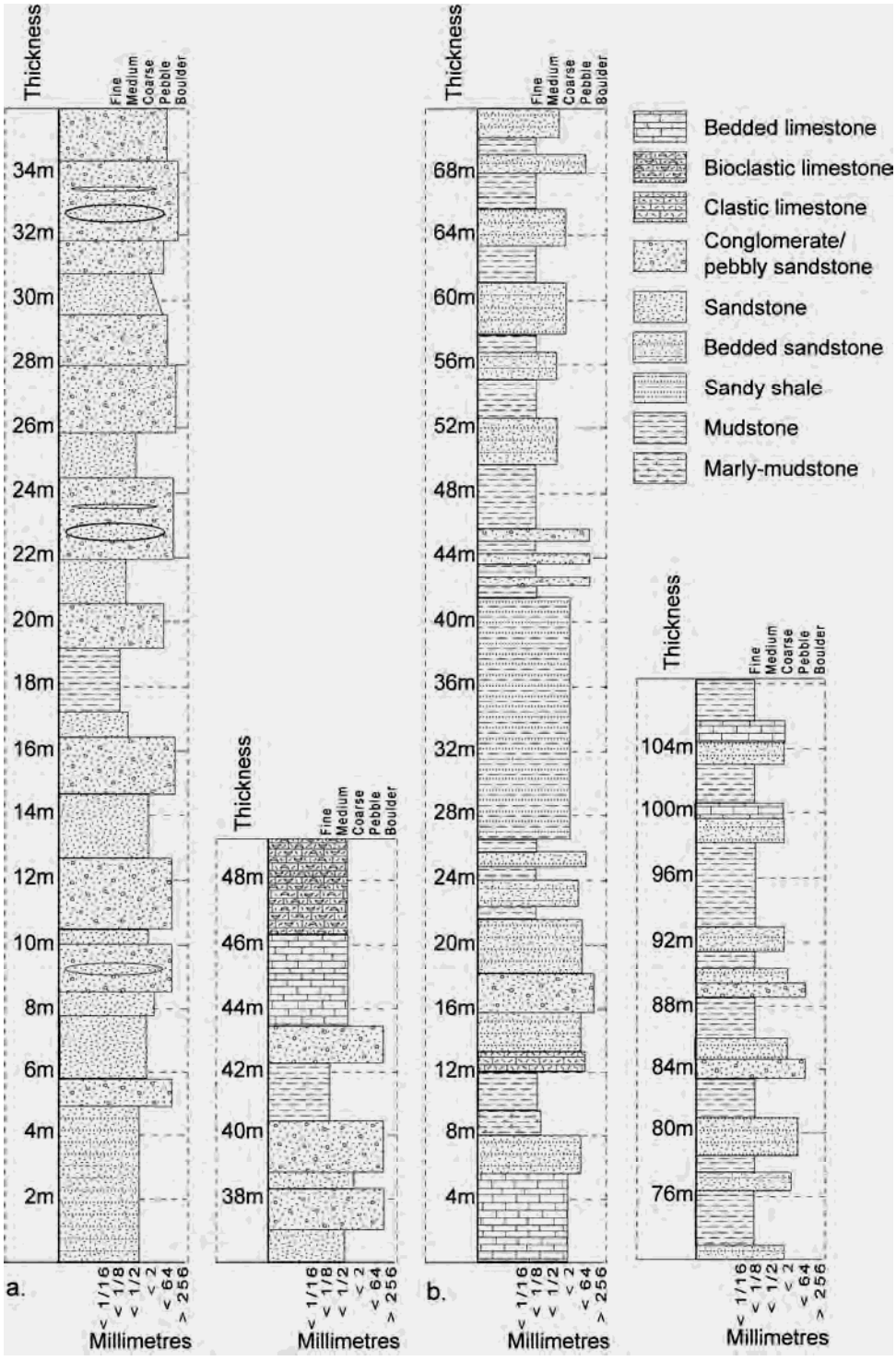

Fig. 4.14. Sedimentary logs through the Upper Triassic Çayır Formation. a. Locality 9: Keklicek Yayla; b. Locality 10: Karabayır Yayla.

4.4.2.10 Locality 10: Karabayır Yayla. Grid reference 430520 4101920.

The Karabayır Yayla locality is situated within the Bolkar nappe (Fig. 4.8), and is accessible via dirt tracks from the village of Uçpınar, on the road between Hadim and Bozkir. The succession lies close to a large thrust fault that separates Triassic sediments from Late Cretaceous pelagic sediments. The Çayır Formation is, however, undeformed, not withstanding its proximity to a thrust. The relatively fine-grained succession here is ~100 m thick, and overlies thick-bedded to massive Middle to early-Late Triassic limestone (Fig. 4.14b).

The sedimentary sequence is dominated by fine- to medium-grained sandstones and mudstone, with limited conglomerate (Fig. 4.14b). Sandstone is predominantly brown or grey, and quartzose. Local pebbly sandstone horizons contain angular to sub-rounded clasts, generally <1-2 cm in size. Sandstone horizons are in places recrystallised and very well indurated. Locally, lithoclastic sandstone is interbedded with subordinate conglomerates. Conglomerate beds contain sub-angular to sub-rounded clasts 2.5 cm in average size, that are composed of limestone and quartzitic sandstone.

Significant proportions of the sequence are interbedded fine sandstone and mudstone (Fig. 4.14b). The mudstone is finely-laminated and varies from brown to purple in colour. Limestone horizons that appear in the sequence near the top of the succession are medium- to dark-grey, moderately recrystallised, muddy, and show bioturbation.

4.4.2.11 Locality 11: Dedemli. Grid reference 437850 4096530.

Dedemli village is located on the western boundary of the Bolkar nappe, on the road between Hadim and Bozkir (Fig. 4.8). An east-west trending gorge cuts through a tectonically imbricated and regionally folded Mesozoic succession of the Bolkar nappe. Faulted coarse red clastics are exposed in a road cutting, overlain by a thick sequence of Jurassic – Cretaceous platform carbonates, in turn overlain by Upper Cretaceous pelagic sediments. The whole succession, locally obscured by landslip, is ~30 m thick (Fig. 4.15a).

The sedimentary sequence mainly consists of thick-bedded debris-flow/conglomerates and sandstones (Fig. 4.12e). Conglomerate clasts range from 1.5 cm to 15 cm, are very poorly sorted, and are predominantly sub-angular in shape. The clasts are either limestone, or purple quartzitic sandstone (see section 4.4.4). The matrix is a deep-purple sandy mudstone, locally forming lenses within the conglomerates. The succession is heavily sheared and no primary sedimentary structures were observed. However, elongate lenses of conglomerate, 3-4 m in width, cross-cut sandstones, indicative of channels.

The top of the formation includes more sandstone and less conglomerate than the base. The sandstone is sheared (with a shear fabric developed locally), fine-grained, purple in colour, and has a muddy matrix. Some horizons contain coarser grains, with small sub-rounded pebbles. The succession overlies sheared micaceous shales and is overlain by light-grey, recrystallised, Mesozoic limestone (Fig. 4.15a).

4.4.2.12 Locality 12: Korualan. Grid reference 441340 4091650.

Korualan village is found on the road between Hadim and Bozkir, approximately 12 km NW of Hadim (Fig. 4.8). The Çayır Formation is best exposed in a valley and adjacent plateau ~3 km to the south-west of Korualan. This locality is within the Bolkar nappe. Tectonic imbrication and associated stratigraphic repetition was observed. The Upper Triassic sediments overlie thick-bedded Triassic carbonates, and are overlain by massive Jurassic carbonates. Total thickness of the Çayır Formation at this locality is 34 m (Fig. 4.15b).

The succession is monotonous, with medium- to thick-bedded (60-120 cm) conglomerate dominating the whole sequence. These are clast supported and poorly sorted (Fig. 4.15, Fig. 4.12f). The whole formation is a pink to purple-red, due to a muddy matrix; however, many clasts are grey. Clast size ranges from 0.5 cm to 25 cm, with an average clast size of ~3.5 cm. Clasts are sub-angular to sub-rounded, with more clasts being sub-angular.

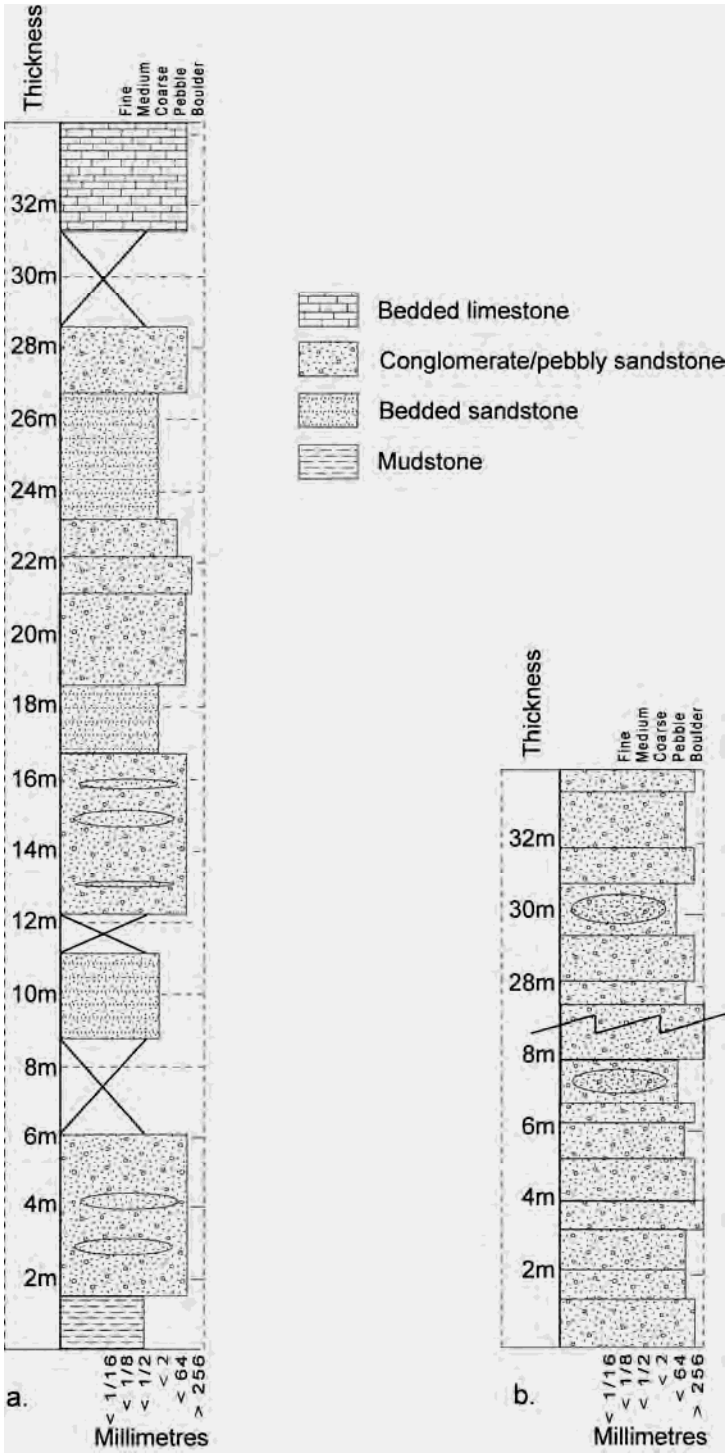

Fig. 4.15. Sedimentary logs through the Upper Triassic Çayır Formation. a. Locality 11: Dedemli; b. Locality 12: Korualan.

Nearly the whole of the unit is clast supported, and the matrix is a poorly-sorted purple/red sandy-mudstone. The clasts are composed of 80 % undifferentiated limestone, and 20 % quartzose sandstone, as described in section 4.4.4. Occasionally, matrix-supported pebbly sandstone horizons occur as lenses within the conglomerates. These Çayır Formation sediments are often found adjacent to shear zones as horizons of relative weakness within the Mesozoic succession.

4.4.2.13 Locality 13: Ekinlik Yayla. Grid reference 446370 4088630.

Ekinlik Yayla is located near the town of Hadim, as documented on earlier in this chapter (section 4.3.2.1). The Triassic succession is found within the Bolkar nappe, adjacent to a tectonic contact with Devonian sediments of the Hadim nappe. Competent Mesozoic carbonates in the area are relatively undeformed; however, the less competent Çayır Formation clastics have been sheared heavily, and only a thin sequence (~10 m) is exposed (Fig. 4.16a).

The base of the Çayır Formation succession overlies thick-bedded, grey, sheared and recrystallised Middle to Upper Triassic limestone (Fig. 4.16a). Above this is a 4 m sequence of heavily sheared shale and debris-flow/conglomerate. The conglomerate contains clasts ranging from 1 cm to 15 cm, with an average clast size of 3 cm. The clasts are angular to sub-rounded, and it was noted that all of the clasts are elongate.

Debris-flow/conglomerate beds are densely packed and clast supported, with a purple muddy-sandstone matrix. Clasts are composed of grey limestone (50%), pink limestone (30%), and sandstone/quartzite (20%). The interbedded shale is purple/grey and foliated. A faulted contact separates the shale/conglomerate succession from heavily sheared, tectonically brecciated limestone (Fig. 4.16a). It is not clear whether this limestone is part of the sequence, or whether it is a tectonic imbricate of a different-aged unit. Tectonically overlying this is thick-bedded Mesozoic limestone with shell fragments and local tectonically-brecciated beds.

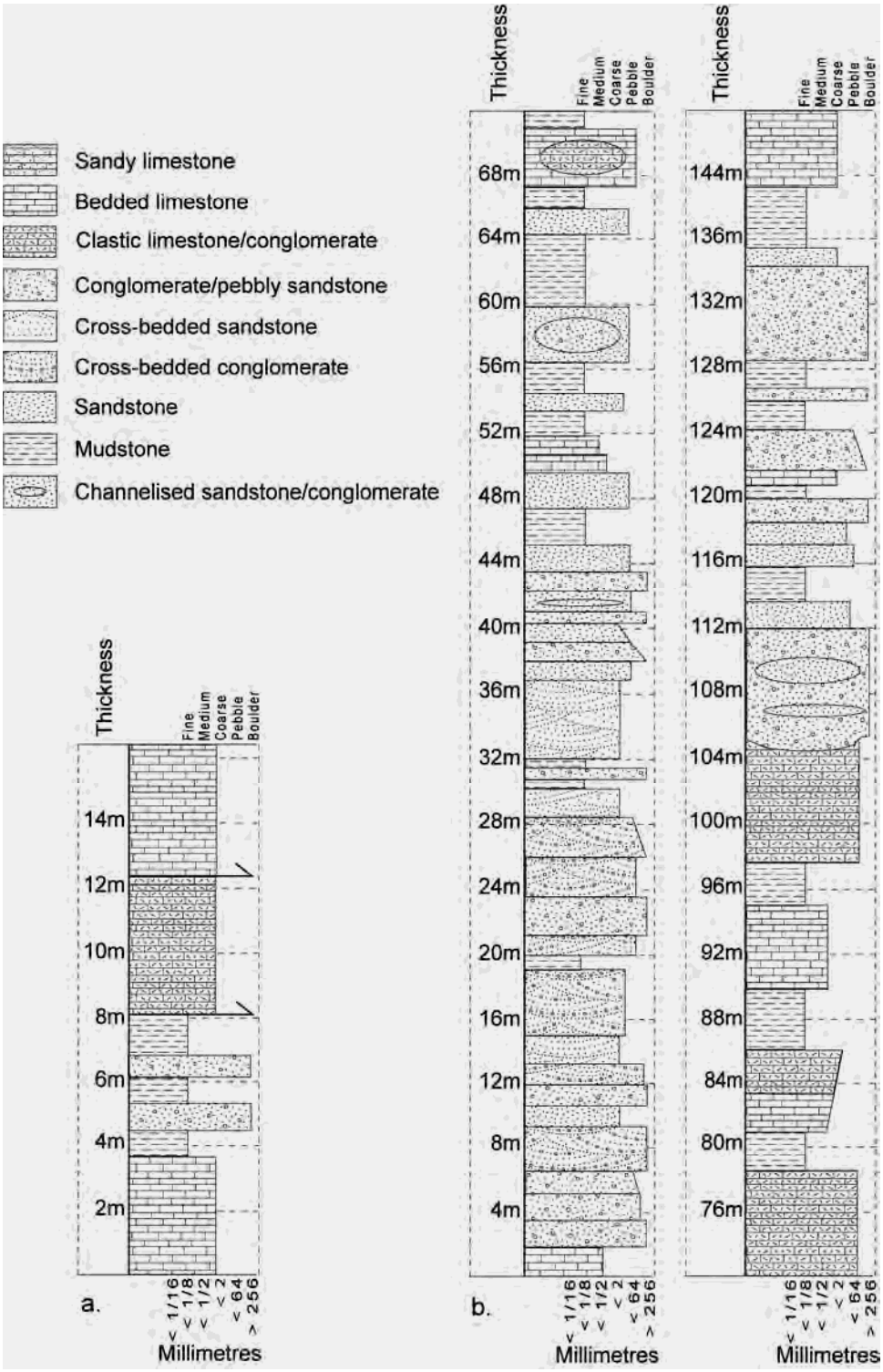

Fig. 4.16. Sedimentary logs through the Upper Triassic Çayır Formation. a. Locality 13: Ekinlik Yayla; b. Locality 14: Alanya road north.

4.4.2.14 Locality 14: Alanya road north. Grid reference 456370 4079470.

The Alanya road north locality shows good exposure of part of the Triassic succession within the southerly part of the Hadim nappe, as documented earlier in this chapter (Fig. 4.5). The sequence is significantly thicker than most other localities documented, totalling ~140 m. The sediments are locally folded and inverted on a ~25 metre scale. A log through the succession is shown in Fig. 4.16b.

The basal 30 m of the succession (Fig. 4.16b) is dominated by medium- to thick-bedded (50-100 cm) cross-bedded conglomerate and sandstone. Fining-upward sequences are common, with conglomerate grading-up into pebbly sandstone and then into sandstone over 2 m intervals. The conglomerates are poorly sorted, with clast sizes ranging from 0.5 cm to 15 cm, with an average size of 3.5 cm (Fig. 4.17a). Clasts are sub-angular to sub-rounded, with more clasts being sub-rounded, although black chert clasts are sub-angular. The matrix is a poorly sorted lithiclastic sandstone. Sedimentary structures include fine parallel lamination, cross lamination, planar- and trough- cross-bedding. Sandstone lenses and erosive channel-like features are also preserved. Sandstone horizons are quartzitic, with varying amounts of lithic grains.

From 28-44 m on the measured section (Fig. 4.16b) there is less conglomerate and more sandstone than at the base. The sandstone has lenses and channelised features, is poorly sorted, and is very coarse-grained (1-2 mm). Pebbly sandstone horizons contain sub-rounded pebbles, up to 2 cm in size. From 44-68 m (Fig. 4.16), the succession is dominated by mudstone with fewer horizons of sandstone and conglomerate, and occasional limestone intercalations. Clastic limestone and limestone conglomerate (Fig. 4.17b) becomes abundant in the mid-part of the measured section, often as laterally discontinuous horizons channelling into mudstone. These limestone conglomerate beds are poorly sorted, matrix supported, with clasts ranging from 1.5 cm to 4 cm in size; most clasts are rounded to sub-rounded. The matrix in most beds is micritic limestone, although some beds are clast supported. Conglomerate bodies vary in geometry, ranging from 3 m thick and 15 m wide, to >10 m thick and 75 m wide. Micritic limestone intervals are recrystallised and light-grey/white in colour.

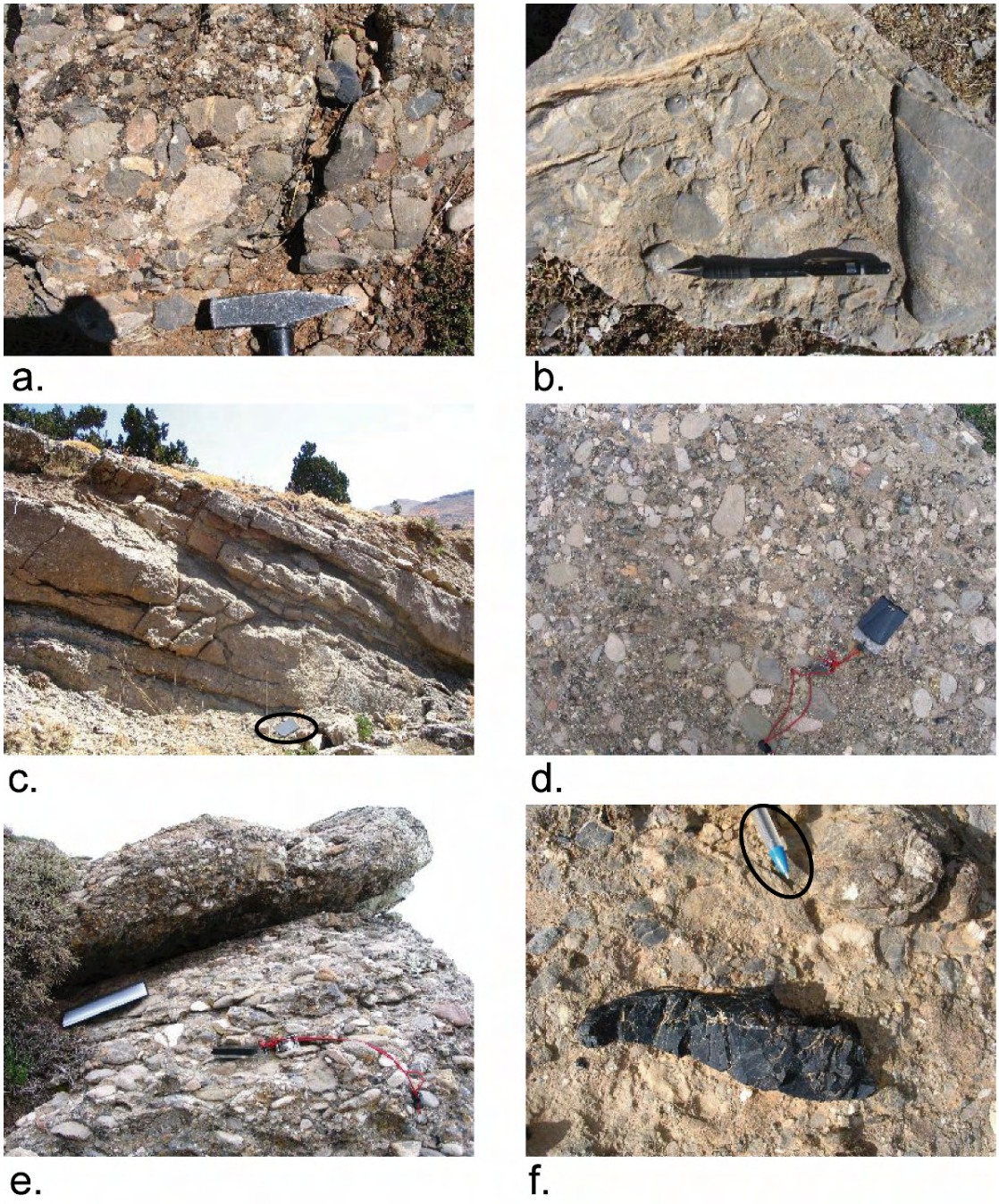

Fig. 4.17. a. Poorly-sorted conglomerate of the Çayır Formation at locality 14: Alanya road north; b. Coarse limestone conglomerate horizon from middle part of the succession at Alanya road north; c. Laterally discontinuous conglomerate and sandstone horizons of the Çayır Formation at locality 15: Alanya road north. Clipboard for scale is circled; d. Clast-supported conglomerate bed from locality 15: Alanya road south; e. Clast imbrication within conglomerate horizon at Alanya road south; f. Angular black chert clast within conglomerate horizon at Alanya road south. Majority of clasts within the same bed are sub-rounded. Pen nib for scale is circled.

An interesting relationship is seen at 104 m in the succession (Fig. 4.16b) where limestone conglomerate is cross-cut by a lithoclastic conglomerate body. Laterally, lithoclastic conglomerates erode down to the base of the limestone conglomerate and directly overlie mudstone. The uppermost 30 m of this succession is composed of interbedded conglomerate, sandstone, micritic limestone and mudstone. The Çayır Formation is transgressed by wackestone and micritic limestone (Fig. 4.16b).

4.4.2.15 Locality 15: Alanya road south. Grid reference 453110 4076930.

The Alanya road south locality, as documented earlier in the chapter (Fig. 4.6), is a excellent cross-section through the complete Triassic sequence of the Hadim nappe, and in the author's view is fairly regarded as the type section for the Triassic of the Tauride platform (in agreement with Özgül, 1997). Due to their close proximity, there are similarities between the facies observed at this locality, with those at Alanya road north (locality 14). Some faulting is evident; however, the base and top of the Çayır formation can both be observed.

The main lithologies within the formation are conglomerate/pebbly sandstone, sandstone and mudstone, with occasional micritic limestone horizons (Fig. 4.18). The base of the succession overlies Middle Triassic carbonates with an angular discordance. Bedding thickness varies throughout the formation, but is mainly medium- to thick-bedded (50-100 cm). Conglomerate horizons are often laterally discontinuous and channelised (Fig. 4.17c), and intergradation between pebbly sandstone and sandstone is common. Clast size ranges from 1 cm to 10 cm, with an average clast size of 3-4 cm (Fig. 4.17d). Conglomerates are poorly sorted, and clasts are sub- to well-rounded. Sandstone is coarse-grained, quartzitic in composition but contains lithic grains as well. Clastic sediments are typically cross-bedded/laminated. Pebble imbrication is evident in many conglomerate beds (Fig. 4.17e). The composition of the clasts is discussed in section 4.4.4. Sandstone is well indurated and has low porosity due to a calcitic cement. Towards the top of the sequence, black chert becomes more abundant, and clasts are more platy and angular than at the base (Fig. 4.17f).

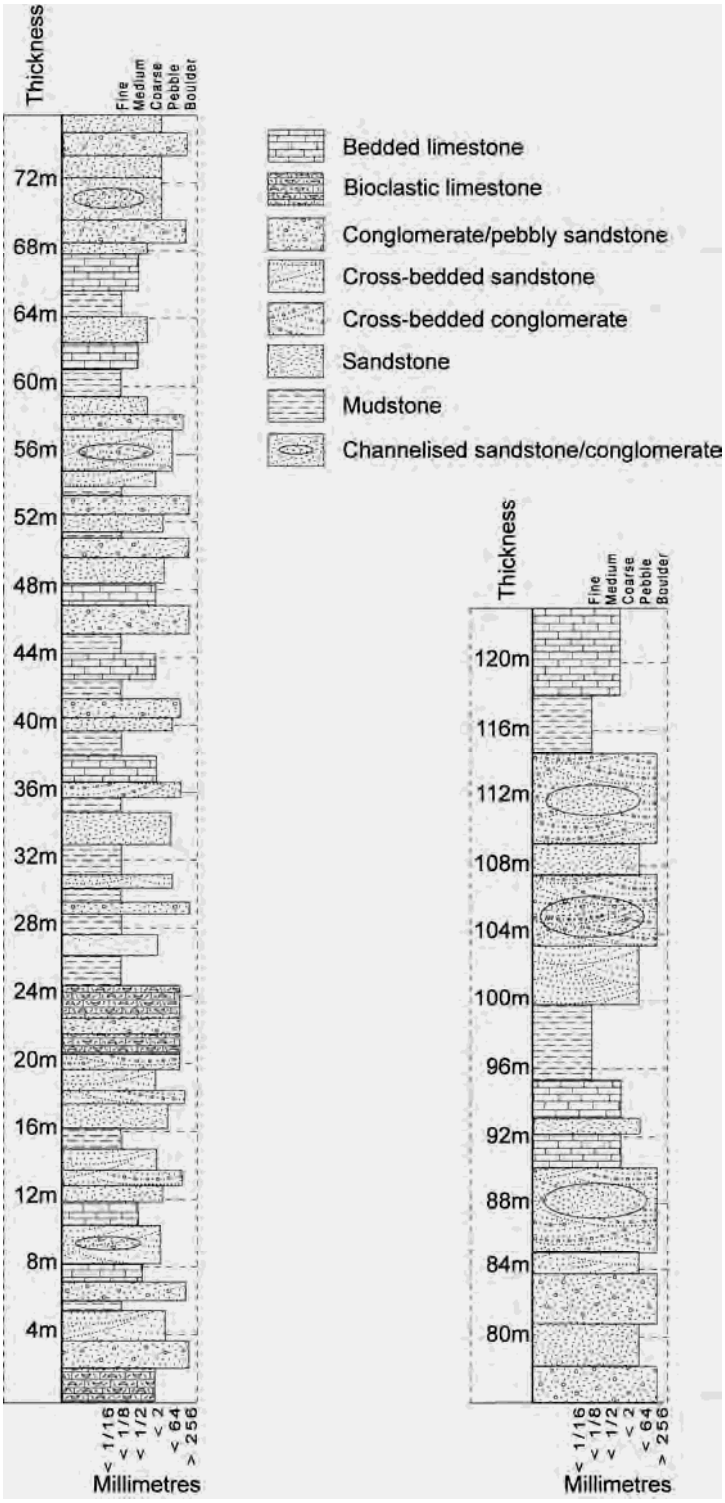

Fig. 4.18. Sedimentary log through the Late Triassic Çayır Formation at locality 15: Alanya road south.

Conglomerate horizons are grey-red, whilst sandstone is grey-brown, and mudstone is red-orange. The limestone intercalations range from limestone conglomerate, bioclastic limestone (near the base of the succession), to micritic limestone (near the top of the succession). Limestone is light-grey, to yellow, to pink, and laterally continuous. Most of the limestone is recrystallised and no palaeontological data was obtained. Some sandstone beds were found to contain plant debris. The succession is transgressed by thick-bedded to massive Mesozoic platform carbonates which are hundreds of metres thick (Fig. 4.18).

4.4.3 Palaeocurrent evidence

Where possible during this study, palaeocurrent evidence was collected from the Çayır Formation. Palaeocurrents are useful to reconstruct the regional topography during the Late Triassic, as well as to help identify possibly sources of sediment. Some sedimentary facies are more likely to contain palaeocurrent evidence than others; for example, cross-bedded sandstone and conglomerate contain abundant palaeocurrents, whilst planar-bedded sandstone and mudstone lack palaeocurrents. For this reason, palaeocurrents could be measured at only 7 out of the 15 Çayır Formation localities documented in section 4.4.2 (Fig. 4.19). However, at some localities, such as Alanya road south (locality 15, section 4.4.2.15), palaeocurrent data could be collected over a large area, allowing data to be grouped into several 'sub-localities' (Fig. 4.19).

Palaeocurrent data were obtained from conglomerate clast imbrication, planar cross-bedding, trough cross-bedding and cross-lamination (Fig. 4.20). All of this data were corrected for the regional dip of the sediments in the study area. At some localities there are complexities when measuring palaeocurrents. For example, at Derebuçak (Fig. 4.19a) the Çayır Formation has been folded into a large west-facing recumbent anticline. Although great care was taken to determine on which limb of the fold the palaeocurrent data were measured, it is possible that faulting and folding may have rotated part of the succession, rendering the data inaccurate. There is also a possibility that the Beyşehir-Hoyran-Hadim nappes may have been rotated about a vertical axis during emplacement

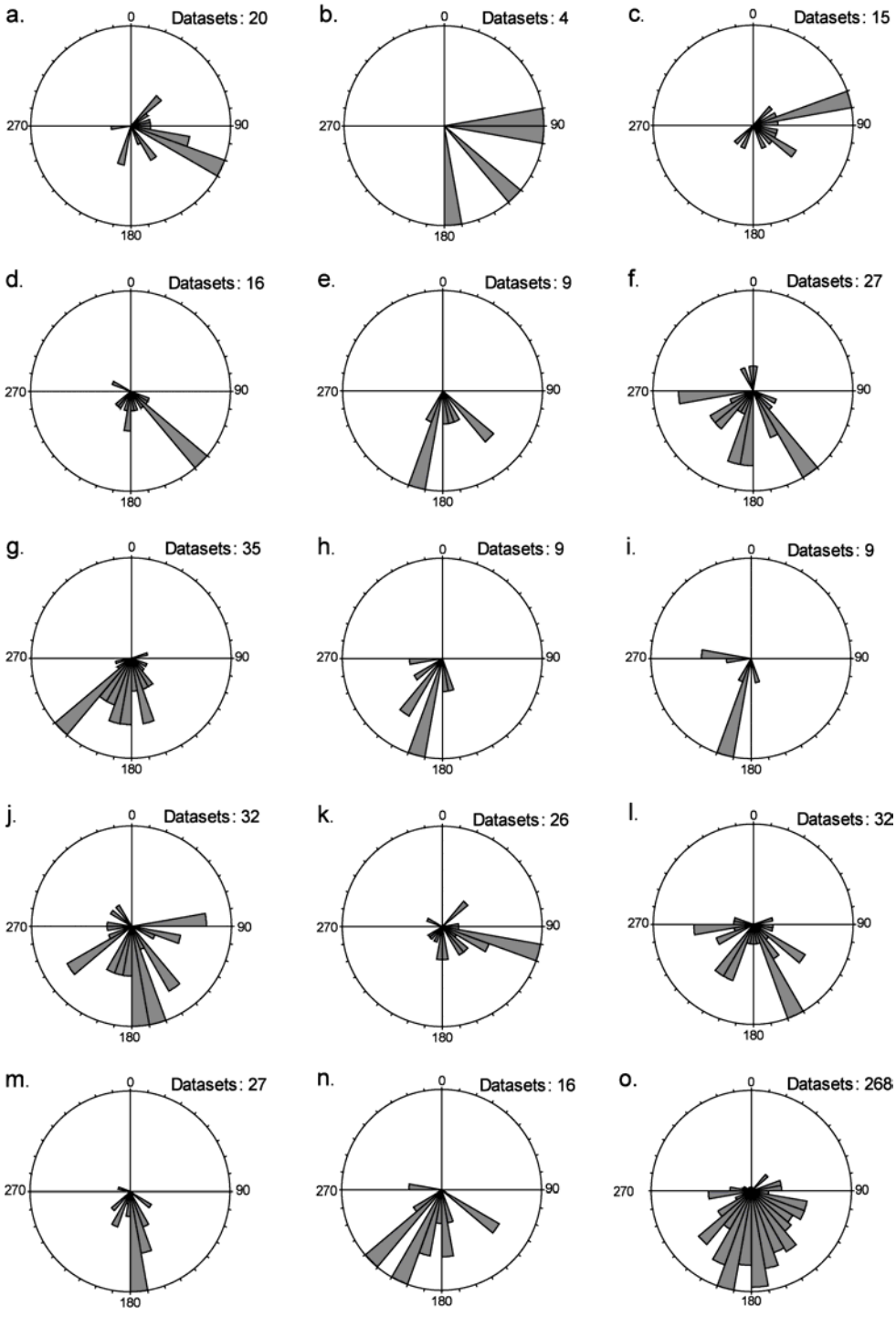

Fig. 4.19. Palaeocurrent data from the Çayır Formation. a. Locality 2: Derebuçak; b. Locality 3: Bademli; c. and d. Locality 4: Üzümdere 1 and 2; e. Locality 6: Göl Başı; f. Locality 9: Keklicek Yayla; g. and h. Locality 14: Alanya road north 1 and 2; i. – n. Locality 15: Alanya road south 1 – 6; o. Consolidated data from 14 localities.

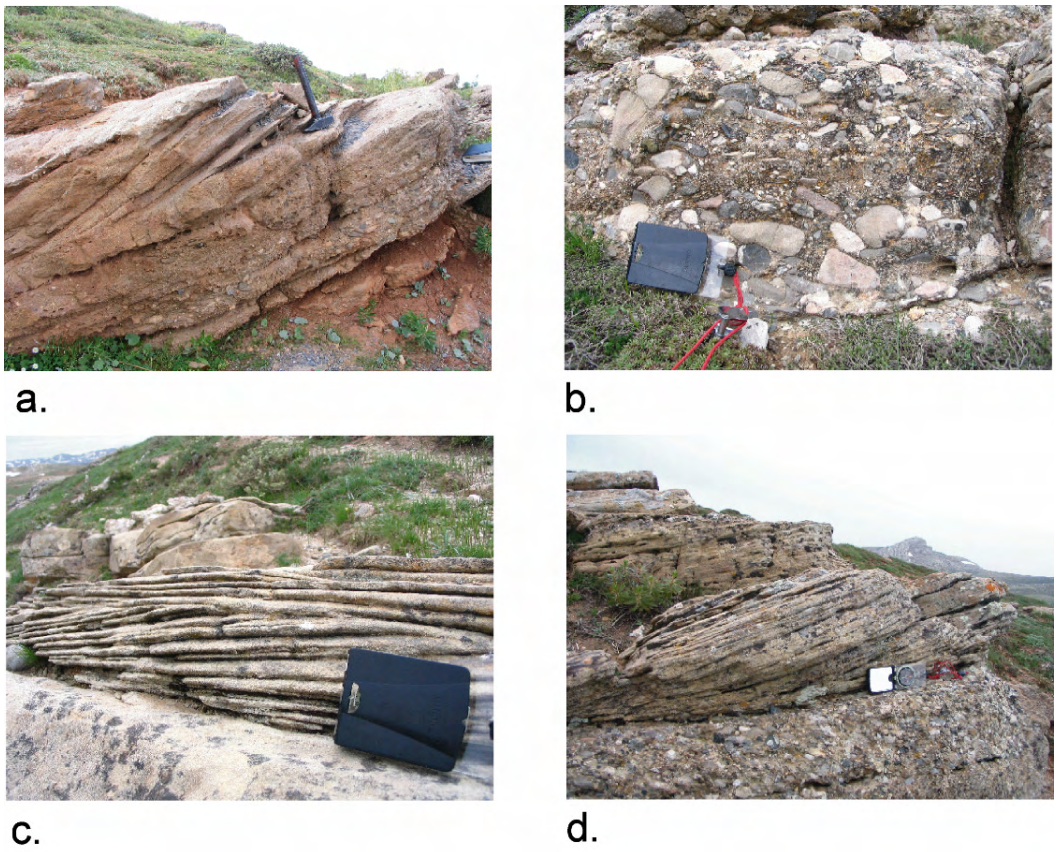

Fig. 4.20. Sedimentary structures within the Çayır Formation that yield palaeocurrent data. a. Planar cross-bedded sandstone/conglomerate; b. Clast imbrication in conglomerate; c. Cross-lamination in sandstone; d. Trough cross-bedding in sandstone/conglomerate.

in the Late Cretaceous – Early Cenozoic. The palaeocurrent data provided is accurate to our best knowledge. However, most localities provide data that appears to be regionally consistent.

The data in Fig. 4.19 show that palaeocurrents are locally variable, but that there is a regional trend towards the south. As we will see in the next section, most of the data were collected from localities where the sedimentary facies analysis has suggested a terrestrial braided river depositional environment. This implies that currents were flowing predominantly from north to south. This also suggests that there was a regional topographic high towards the north of the Tauride platform in latest Triassic time. The variation in flow direction could be explained by fluctuating stream paths, typical of

braided streams. It is also possible that some of the measured structures do not indicate the downstream direction; for example, foresets can develop on the side of sand bars in braided systems, with laminae dipping perpendicular to the actual river flow.

4.4.4 Sediment composition

To determine the provenance of the Çayır Formation, the compositions of conglomerate clasts were determined in the field, and sandstone composition was studied in the laboratory using optical microscopy (Fig. 4.21, Fig. 4.22, Fig. 4.23). Clast counts were only possible at localities where conglomerates or pebbly sandstone are present. Clast composition was found to vary between localities and also between different beds within the same succession.

Combined data from all of the localities (Fig. 4.22e), in decreasing order of abundance, the sedimentary rock clasts are: light grey recrystallised limestone, well-indurated recrystallised quartzose sandstone (quartzite), dark grey recrystallised limestone, red limestone, micritic limestone, weakly-lithified quartzose sandstone, black chert ("lydite"), wackestone, crystalline white limestone, dolomite and oolitic limestone (Fig. 4.22e). In addition, a small numbers of clasts were found of altered metamorphic/volcanic rock (e.g. mica schist, basalt), limestone breccia, quartz vein and packestone.

Black chert ("lydite") is particularly common at some localities, such as Derebuçak (Fig. 4.22a) and Üzümdere (Fig. 4.22d), but completely absent at others, such as Keklicek Yayla (Fig. 4.22f). It can also be variable within individual successions, such as Alanya road north (Fig. 4.22a. and b.), where a conglomerate horizon 24 m above the base of the Çayır Formation contained >8% black chert (Fig. 4.22a), whilst another bed at 132 m on the log yielded no black chert clasts (Fig. 4.22b). Similar variation is observed for different clast compositions, such as quartz vein and crystalline white limestone. This suggests that the source area for Çayır Formation sediment was variable, and that the braided rivers that were eroding and transporting "basement" material from different stratigraphic horizons at different times during the Late Triassic.

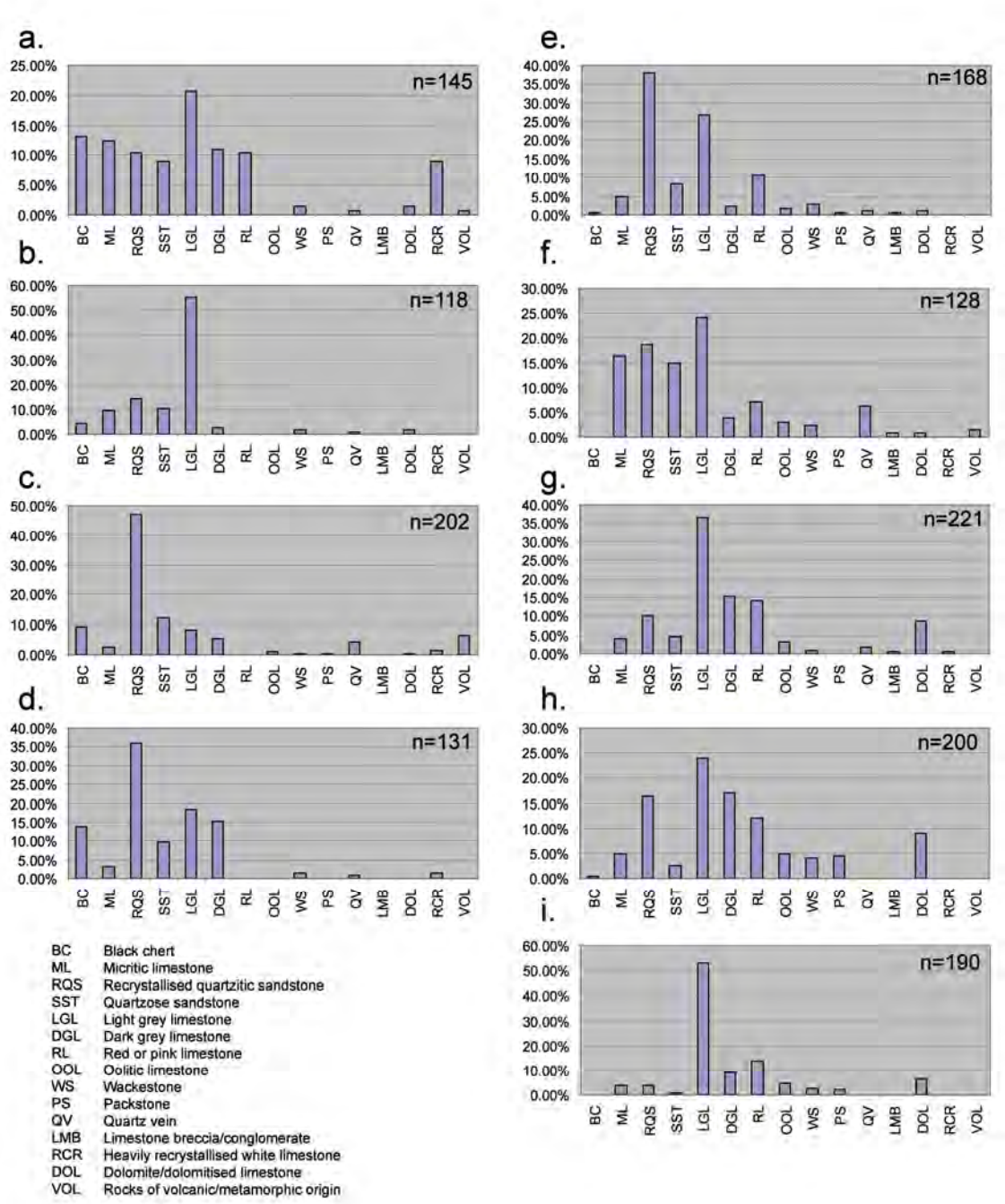

Fig. 4.21. Clast count data for the Çayır Formation. a. Locality 2: Derebuçak; b. Locality 3: Bademli; c. and d. Locality 5: Üzümdere 1 and 2; e. Locality 8: Dipsiz Göl; f. Locality 9: Keklicek Yayla; g. Locality 11: Dedemli; h. and i. Locality 12: Korualan 1 and 2.

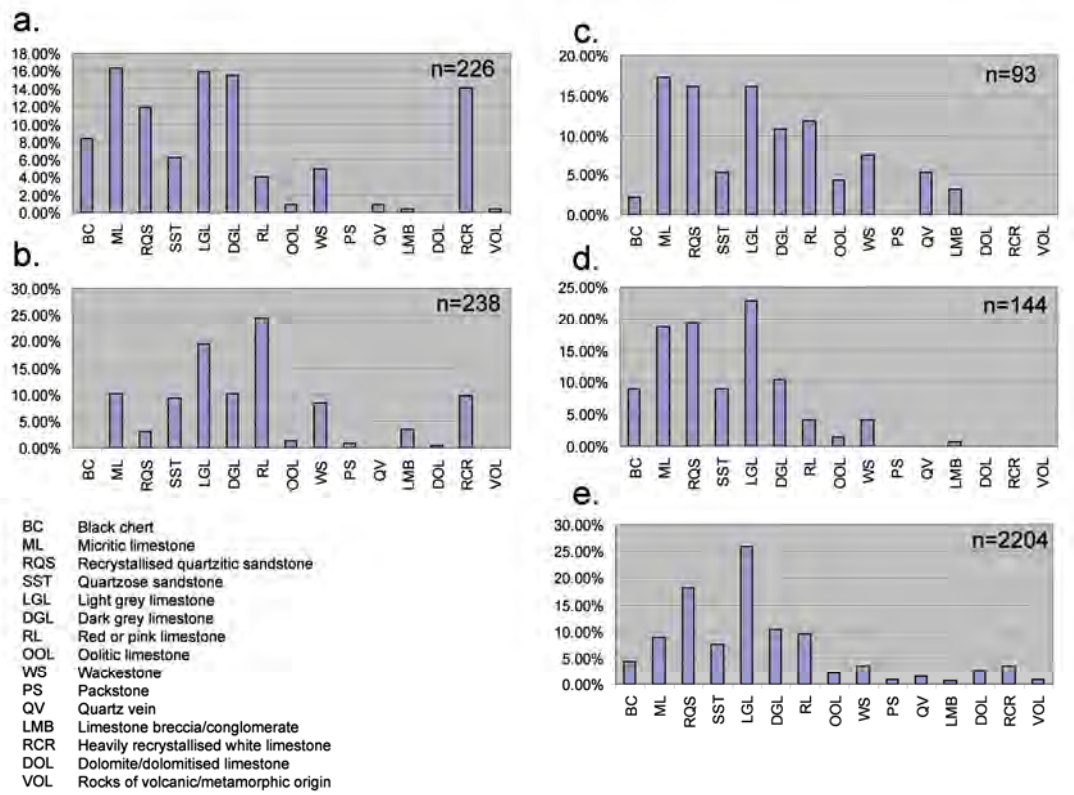

Fig. 4.22. Clast count data for the Çayır Formation. a. and b. Locality 14: Alanya road north 1 and 2; c. and d. Locality 15: Alanya road south 1and 2; e. Combined data from all localities.

Point counting of sandstone horizons from eight Çayır Formation localities shows that grain composition ranges from siliciclastic, to lithiclastic (Fig. 4.23). The grains identified, in decreasing order of abundance, are: monocrystalline quartz, polycrystalline quartz, microcrystalline quartz, sheared composite quartz, altered light limestone, altered dark limestone, micritic limestone, altered feldspar, radiolarian chert. In addition, a small number of altered metamorphic/volcanic grains were observed (Fig. 4.23).

At some localities, for example, Bademli, there are no lithic grains within the analysed sample, and the sandstone has a siliciclastic composition of quartz and chert (Fig. 4.23b). In contrast, other localities, such as Alanya road north, contain siliciclastic grains and lithic grains such as carbonate (variable), radiolarian chert, altered feldspar,

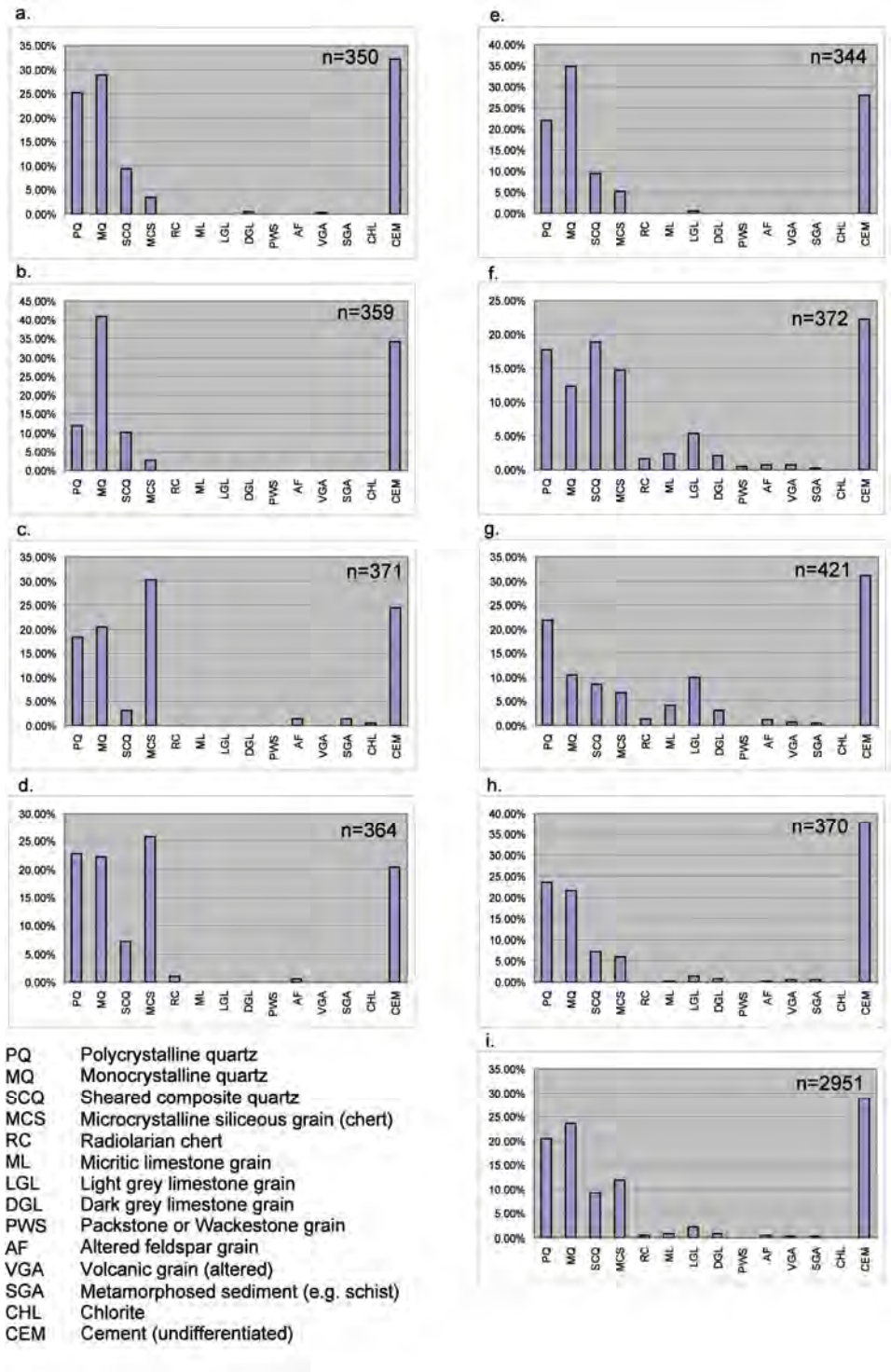

Fig. 4.23. Point count data for the Çayır Formation. a. Locality 2: Derebuçak; b. Locality 3: Bademli; c. Locality 5: Üzümdere; d. Locality 6: Göl Başı; e. Locality 9: Keklicek Yayla; f. Locality 14: Alanya road north; g. and h. Locality 15: Alanya road south; i. Combined data from all localities documented.

altered volcanic and metamorphic grains (Fig. 4.23g). The thin sections analysed had a high percentage of cement (~28 %), ranging from sparry calcite, microcrystalline calcite, fibrous calcite, silica, to iron-rich. Cement is undifferentiated on the plots presented below (Fig. 4.23).

The age of the clasts can rarely be determined directly from evidence of fossils within them. Radiolarians present within chert grains are recrystallised and have not been dated. Micritic limestone clasts locally contain the bivalve *Halobia* sp. that indicates a Triassic age. Also, the large foraminifera *Fusulinia* sp. in some limestone clasts suggests a Palaeozoic, possibly Permian age. In addition, the ages of the clasts and grains can be inferred by a lithological correlation with the various successions exposed in the area. This allows the following inferences: the micritic limestone, red limestone, dolomite and light grey limestones (including wackestone, oolitic limestone, packstone) were derived from the Triassic succession subjacent the Çayır Formation; the weakly-lithified sandstones came from middle part of the Triassic succession; the dark fusilinid-bearing limestones were derived from the Permian shallow-water carbonate succession, locally exposed in the Taurides (Özgül, 1984) and the Konya area further north (Özcan et al., 1988; Robertson et al., 2007). The well-indurated quartzose sandstone, crystalline white limestone and quartz veins are known in the Cambrian-Ordovician succession exposed in the north (Seydişehir–Beyşehir area) and also further south in the Tauride autochthon (Geyik Dağ). There are also thick successions of well-indurated quartzose sandstone within the Carboniferous and Permian sequences of the allochthonous Hadim nappe and Bolkar nappe (Monod, 1977; Özgül, 1984). Black chert (lydite) of Carboniferous age is known in the Konya area beneath a Permo-Triassic unconformity (Özcan et al., 1988; Eren et al., 2004). Finally, metamorphic rocks (e.g. mica schist) are locally found in the Precambrian "basement" of the Taurides, as exposed in the Sultan Dağ further west (Gutnic et al., 1979).

4.5 Facies associations and depositional environments

In this section, the Triassic sedimentology, described in sections 4.3 and 4.4, will be interpreted as a series of facies associations that characterise sedimentary environments. Individual facies provide information on the depositional setting of any particular strata; however, these cannot necessarily be traced laterally, and significant variations exist over large areas (such as this study). Interpreting the context of a facies within the stratigraphy as a whole is essential before proposing an environmental interpretation (Reading, 1986). In light of the previous literature, the facies associations described here will be used to identify depositional environments with reference to modern day sedimentary environments and processes.

4.5.1 Early – Mid Triassic

During this study the sedimentary rocks were divided into four main facies associations: (i) thick-bedded neritic carbonate and dolomite; (ii) medium-bedded shallow-marine clastics and carbonates; (iii) thin-bedded mudstone, shale and marly mudstone; (iv) interbedded mudstone, shale, sandstone, marly mudstone and carbonate. A summary of the facies associations for Early to Mid Triassic time is shown in Fig. 4.24.

4.5.1.1 Thick-bedded neritic carbonate and dolomite

Facies Association: This facies association includes medium- to thick-bedded recrystallised limestone and dolomite, oolitic limestone, microbial limestone, bioclastic limestone, nodular limestone, and in some cases sandy limestone. These units are typically found as thick successions (15 – 60 m) in the lowermost part of the Triassic sequence, and towards the top of the measured sections (underlying the Upper Triassic clastics). The thicknesses of these sediments vary laterally, both locally and regionally. This is one of the most common facies associations in the Early – Mid Triassic sequence, making up ~25% of the thickness of the succession. The two fundamental features of the sedimentary facies identified are that: (i) the sediments are composed primarily of carbonate material of bioclastic origin; (ii) the sediments contain little or no

Facies Association	Lithofacies	Description	Interpretation
1	Thick-bedded neritic carbonate and dolomite	Medium- to thick-bedded carbonate and dolomite, including oolitic limestone, microbial limestone and bioclastic limestone. Locally cross-bedded and rippled bedding surfaces; contains benthic fauna.	Deposited on shallow-marine continental shelf. Warm water, <30 m water depth, high biogenic activity. Wave currents created sedimentary structures.
2	Medium-bedded shallow-marine clastics and carbonates	Thick-bedded sandstone interbedded with thin-bedded limestone and mudstone. Sands contain reworked bioclastic shells and ooids. Sediments show cross-lamination and wave ripples. Contains benthic foraminifera.	Deposited on a shallow-marine shelf. The environment received terrigenous sand and mud from a deltaic source. Intra-tidal as sedimentary structures formed by waves/currents.
3	Thin-bedded fine-grained mudstone, shale and marly mudstone	Fine-grained sediments, mainly mudstone, interbedded with some calcareous marls. Can be thick sequences that are laterally continuous. Bioturbation and broken shells present. Wave ripples and prod / grove marks observed on bedding surfaces.	Deposited in a shallow-marine environment, possibly the nearshore mud belt. May represent the more distal part of a large continental shelf. Water depth up to 50 m.
4	Interbedded mudstone, shale, sandstone, marly mudstone and carbonate	Variable thin- to thick-bedded. Mudstone is the dominant lithology, but interbedded with sandstone and limestone. Pebbly sandstone is rare. Ripples, bioturbation, cross-lamination, grading and channels all observed. Contains benthic foraminifera.	Shallow-marine continental shelf setting, with sporadic inputs of terrigenous sand and mud. Environment influenced by fluctuating sea-level. Mudstone interbeds suggest a relatively distal setting.

Fig. 4.24. Summary of facies associations and interpretations of Triassic sediments. See text for details.

terrigenous material. The carbonate rocks are composed of allochems, carbonate mud, cement and, very locally, siliciclastic sediment. The generally thick-bedded nature of the facies suggests that periods of sediment accumulation was prolonged, and occurred in a stable sedimentary environment. The variable carbonate lithologies described above interchange readily within the sequence. Localised cross-bedding and symmetrical and asymmetrical ripples indicate current influence during deposition. Most of the units contain a variety of microfauna and macrofauna, such as the bivalve *Unionites* sp., which are indicative of shallow-water benthic marine communities (Fraiser and Bottjer, 2007).

Previous Interpretation: Thick-bedded Triassic carbonates have been described as tidal and lagoonal deposits, in a low-energy sub-wave-base shelf environment (Özgül, 1984; Özgül, 1997). However, the cross-bedding, wave ripples and ooids observed during this study suggest that the platform was, at times, current influenced. Other work (Önder, 1984) suggests that the Triassic rocks of the Alanya road south section represent a tidal lagoon. Some modern lagoonal environments are found to contain clayey and silty sediment, with no physical sedimentary structures (Schmidt et al., 2007). However, open-marine lagoonal environments may also be influenced by tidal and wave-influenced currents (Einsele, 1992).

Depositional Environment: These sediments are likely to have been deposited on a shallow-marine continental shelf setting, consistent with modern and ancient examples (Tucker, 1985). The main zone of carbonate accumulation in modern depositional settings is in the 'subtidal carbonate factory', between the shoreline and the shelf-slope break, <30 m water depth (James, 1984). Oolitic limestone is indicative of a warm-water shallow-marine platform, with constant reworking of ooids under wave or current (e.g. tidal) action. Ooids typically form in waters <5 m deep (Sellwood, 1986). The close association with bioclastic limestone (locally reworked) is indicative of high biogenic productivity on a shallow-marine shelf (Tucker, 1991). Microbial (stromatolitic) limestone is evidence of low-energy shallow-water conditions, which suggests a calm,

near-shore protected tidal-flat (Tucker, 1991). The scheme of standard facies belts (Wilson, 1975) shows the variety in lithologies and facies that can exist in a shallow-marine shelf environment (Fig. 4.25). Sandy limestone could have resulted from increased energy on the platform (e.g. storms), or proximity to a siliciclastic sediment source (e.g. delta). Localised cross-bedding, symmetrical and asymmetrical ripples, and laterally discontinuous beds all indicate that the platform experienced disturbance by currents and waves. Nodular limestone and dolomitic limestone are of diagenetic origin.

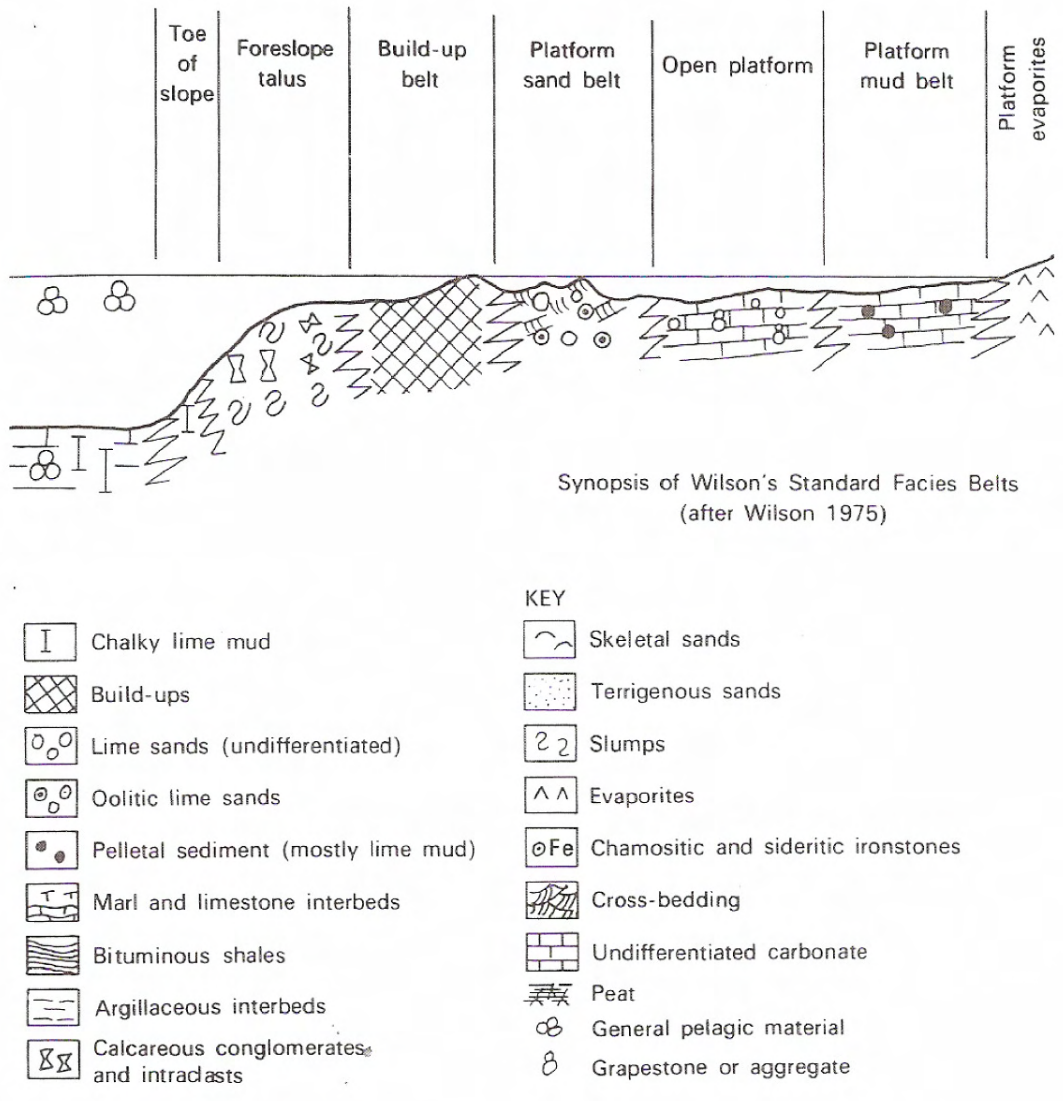

Fig. 4.25. The scheme of standard facies belts after Wilson (1975). Figure redrawn by Sellwood (1986).

4.5.1.2 Medium-bedded shallow-marine clastics and carbonates

Facies Association: This facies association typically consists of thick-bedded sandstone horizons interbedded with thin-bedded limestone and mudstone/marl. These sediments are typically found in the mid-part of the measured succession; thicknesses range from 10-30 m. They are laterally discontinuous on a regional scale. This facies association makes up ~15% of the Triassic sequence. Quartzose sandstone is typically medium-bedded, although locally it can be thin- or thick-bedded. Sandstone beds contain bioclastic material (e.g. reworked shells and ooids), and fine-grained beds locally exhibit symmetrical (wave influenced) or asymmetrical ripples and cross-lamination. Sands are usually moderate- to well-sorted, with predominantly sub-rounded grains. Reworked plant debris was observed locally.

Previous Interpretation: It was suggested that this clastic sedimentation occurred on a unstable shelf, which at times experienced emergence (Özgül, 1997). Özgül (1997) also inferred that some sands could have accumulated in a beach setting. and that relative sea-level rise and fall may be a factor. No evidence of an aeolian influence was observed (e.g. mud cracks, caliche); any emergence of a platform would have been localised and short-lived. In another interpretation (Önder, 1984) suggested that terrigenous material was transported into a lagoon by rivers flowing from an elevated hinterland. Lagoonal deposits would be expected to be carbonate and mud dominated, with shelly fauna, peloids and intensive bioturbation (Tucker, 1991); however, such features are not apparent.

Depositional Environment: Fauna from carbonate interbeds, such as the benthic Foraminifera *Glomospirrella*, along with broken shell fragments and reworked ooids in sandstones, suggest these sediments were formed in a shallow-marine environment (Tomašových, 2004). Sedimentary structures (e.g. cross-stratification, wave ripples) are indicative of a sea-floor affected by currents. Sandstones are typically well-sorted and medium- to fine-grained; a lack of conglomerates suggests there was limited erosion of

the platform. Interbedding of the sand with carbonates shows that clastic input to the system was sporadic. A modern example could be an offshore shelf environment sporadically receiving clastic input from a deltaic source, where terrigenous sediment is transported to a marine environment by rivers (Einsele, 1992) (Fig. 4.26). However, in this study, deltaic facies, such as channels and tidal flats, were not observed.

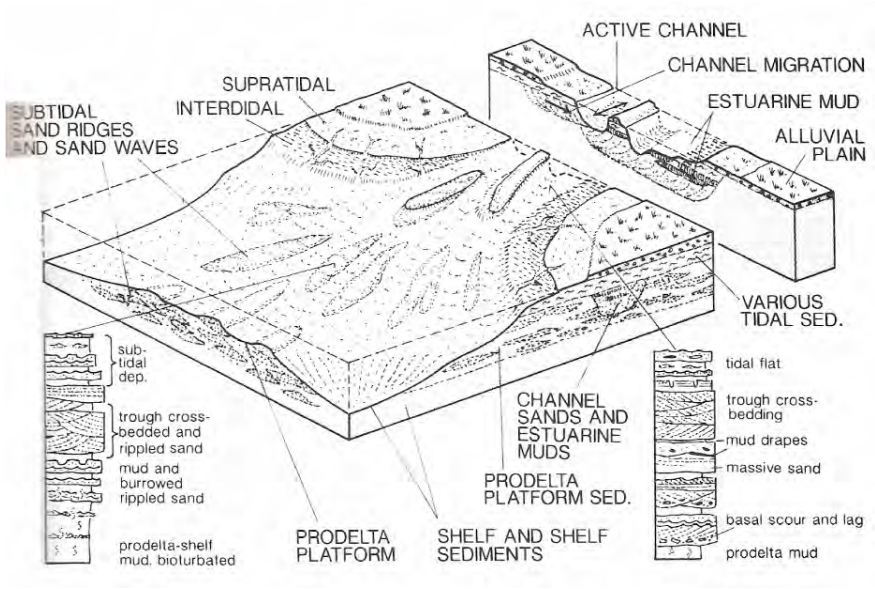

Fig. 4.26. Conceptual model of a tide-dominated delta, with vertical sections of channel fill and tidal sand ridge on pro-delta platform. Figure from Einsele (1992).

4.5.1.3 Thin-bedded fine-grained mudstone, shale and marly mudstone

Facies Association: This facies association consists of fine-grained sediments, primarily mudstone and shale, with some marly mudstone. These rocks are found throughout the mid-part of the Triassic succession, and commonly overlie thick-bedded neritic carbonates at the base of the sequence. Mudstone accumulations, up to 30-40 m, are relatively laterally continuous; these thick sequences are locally interbedded with limestone or quartzose sandstone. This facies association represents approximately 20% of the thickness of the complete Lower to Mid Triassic succession. The sediment is well sorted, with rare sandy-mudstone present. Mudrocks range from non-fissile to fissile, dependent on variations in clay and silt content, and the degree of compaction and

diagenesis. Where calcareous mudrocks exist, there are localised beds of marly-mudstone. Sedimentary structures include small-scale ripples (symmetrical and asymmetrical) and, in places, prod/groove marks, which are strongly suggestive of a wave or current (e.g. tidal) induced disturbance of the surface. Small, flattened cylindrical burrows were observed, which could be *Palaeophycus*, interpreted as a feeding and dwelling burrow (Pemberton and Frey, 1982). There is a relative lack of terrigenous material. Fauna from this facies association are rare, although some broken bivalve fragments were observed.

Previous Interpretation: It was suggested that the mudstone was deposited in a low-energy sub-wave-base environment (Özgül, 1997). The sedimentary structures of the mudstones, however, suggest that currents affected deposition. Önder (1984) suggested that shales were derived from the same uplifted hinterland that supplied the quartzitic sandstone. In his model it was postulated that sedimentation extended into a lagoonal environment, separated from the open sea by a barrier reef. A reef build-up would have a framework of, for example, coral, algae, sponges and shelly fauna. There is no evidence for this within this facies association. Lagoonal deposits can contain much mud, but an abundance of current-induced sedimentary structures (e.g. ripples, groove marks), as observed here, would only be expected in an wide, open lagoon.

Depositional Environment: Mudrocks can develop in a variety of shallow- to deep-water marine environments (Tucker, 1991). Given the close association of the mudrock with neritic carbonate and clastic horizons, this sediment is likely to have been deposited in a relatively shallow-marine environment (Einsele, 1992). A likely depositional setting is a nearshore mud belt (Tucker, 1991). Coarser-grained terrigenous material settles closest to the shoreline, whilst terrigenous mud is transported further onto the shelf, possibly in deeper waters, followed by deposition from suspension. Water depth could be 5-20 m (Tucker, 1991), and the sediment is likely to be affected by tidal currents and storms, explaining the sedimentary structures observed. Relative sea-level change (or other factors, such as variable sediment supply) allows the mud belt to migrate over

time, resulting in interfingering with other neritic carbonate and clastic sediments. Observations of modern deltaic settings suggest that a nearshore mud belt is typically 40-50 km wide, and the water-depth is <50 m (Dalrymple, 2005). A selection of modern day shelf profiles showing typical distributions of sand and mud is shown in Fig. 4.27 (Johnson and Baldwin, 1986).

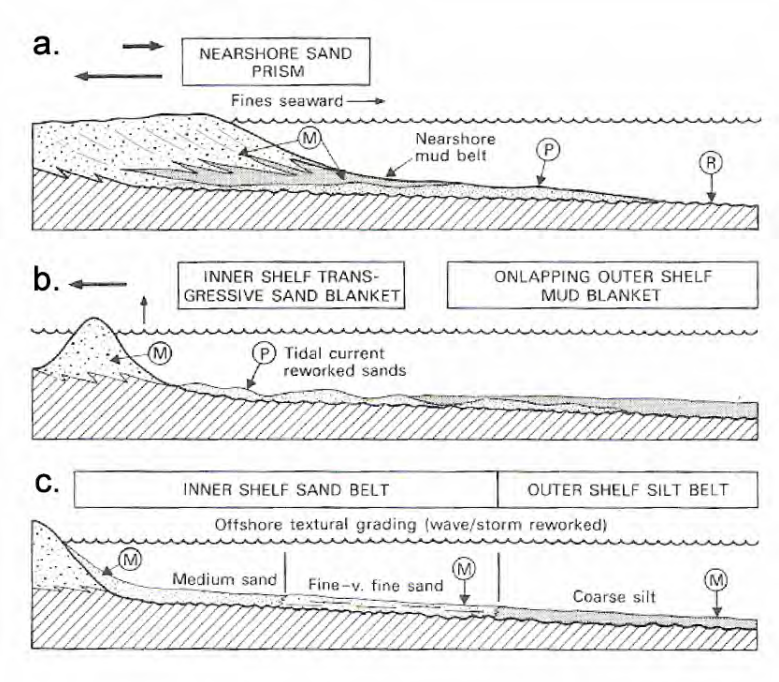

Fig. 4.27. Different types of modern-day shelf profiles, illustrating distribution of sediment cover across the shelf. a. Nearshore sand prism and nearshore mud belt; b. Inner shelf transgressive sand blanket with outer shelf mud blanket; c. Inner shelf sand belt and outer shelf silt belt. Figure from Johnson and Baldwin, (1986).

4.5.1.4 Interbedded mudstone, shale, sandstone, marly mudstone and carbonate

Facies Association: This facies association, which represents ~40% of the thickness of the Lower – Mid Triassic succession, is a narrowly-spaced, repetitively interbedded compilation of all the main lithologies described in facies associations (i) – (iii). These units are found throughout the Triassic succession, but are most abundant in the mid-part of the sequence. Bed thickness is highly variable, ranging from 15-20 cm, to >1 m thick.

A typical sequence consists of a 4 m-thick mudstone horizon (50%), interbedded with quartzose sandstone beds ~50 cm thick (20%), with micritic limestone intercalations ~30 cm thick (20%), and occasional bioclastic limestone or marly-mudstone horizon. Occasional horizons of pebbly-sandstone or conglomerate are present. Sedimentary structures include ripples, bioturbation, cross-lamination, grading and occasional channel features. Typically this facies association is laterally discontinuous on a kilometre-scale. Fauna found within these units are indicative of benthic conditions (e.g. *Glomospirella*); however, these microfossils could have been redeposited.

Previous Interpretation: The interbedded mudstone, shale, sandstone and carbonate sequence was interpreted as turbiditic in origin (Özgül, 1984; Özgül, 1997), passing laterally into reef limestone and dolomite. The sediments do not show classic turbiditic features (e.g. Bouma sequences, scouring, channelling, slumping), but instead exhibit shelf-like features (e.g. wave ripples, bioturbation). These "turbiditic" sediments were inferred to have resulted from tectonic activity on the undulating platform (Özgül, 1997). In contrast, Önder (1984) believed that all of the sedimentation took place in a lagoonal environment, with deltaic systems bringing terrigenous material into the lagoon. Also, Önder (1984) proposed that a carbonate tidal barrier, transected by tidal channels, separated lagoonal and deeper sea environments. The clastic sediment in the sequence was inferred to have been deposited in deltas originating from the tidal barrier itself. However, an obvious problem with this interpretation is the source of the siliciclastic material, unless the tidal barrier was siliciclastic in composition (for which there is no evidence).

Depositional environment: This facies association is indicative of a shallow-marine continental shelf setting, with terrigenous input of sand and mud (Einsele, 1992). The symmetrical ripples observed indicate that the depositional setting was above the wave base. The interbedded nature of these facies is indicative of a depositional environment that could have been greatly influenced by changes in relative sea-level, climatic change in source the area, or autocyclic switching of distributaries.

Predominantly fine-grained deposition in a distal part of the margin could have been interrupted by marine transgression, clastic input from a delta, or a storm-influenced disturbance of the platform (Reading, 1986; Einsele, 1992). A limited diversity and abundance of fauna suggests that the depositional setting was far from the productive nearshore environment that leads to thick carbonate build-up. The association of sandstone and mudstone intercalations is documented at other distal continental shelf settings (Machent et al., 2007).

4.5.2 Late Triassic

Late Triassic sediments of the Çayır Formation, probably extending into the Early Jurassic, are subdivided into 4 facies associations: (i) Coarse-grained conglomerate and sandstone; (ii) Fine-grained mudstone and sandstone; (iii) calcareous sandstone, mudstone and limestone; (iv) Limestone conglomerate / debris flow. A summary of Çayır Formation facies associations is provided in Fig. 4.28, and an illustrative representation of Late Triassic sedimentary environments is shown in Fig. 4.31.

4.5.2.1 Coarse-grained conglomerate and sandstone

Facies Association: This facies association is found in the Çayır Formation in the Geyik Dağ, Hadim nappe and Bolkar nappe, at the following localities: 2 (Derebuçak); 5 (Üzümdere); 8 (Dipsiz Göl); 9 (Keklicek Yayla); 14 (Alanya road north); 15 (Alanya road south). Laterally discontinuous lens-shaped conglomerate bodies are interbedded with trough and planar cross-bedded sandstone and less abundant mudstone horizons. These sediments are typically found as thick sequences towards the base of the Çayır Formation, although they are also observed locally in the middle to upper part of the succession. At most localities, the coarse-grained clastics overlie Middle Jurassic platform carbonates and grade upwards into mudstones and limestones. Conglomerates and sandstones are typically well sorted and clasts are rounded; however, in some cases sediments are coarser and less well sorted, with a large number of angular clasts. The

Facies Association	Lithofacies	Description	Interpretation
1	Coarse-grained conglomerate and sandstone	Laterally continuous interbedded conglomerate and sandstone. Thick successions towards base of Çayır Formation. Cross-bedded, with clast imbrication and graded bedding. Lens-shaped (channelised) sediment packages common.	High-energy terrestrial braided river depositional environment. Conglomerates represent channel fill, whilst sands are inter-channel banks. Rare mudstone could be overbank deposits.
2	Fine-grained mudstone and sandstone	Fine-grained mudstones and sandy-mudstones interbedded with irregular, thin-bedded, medium-grained sandstones. Planar beds with parallel laminations. Rare coarse-grained lenses.	Low-energy depositional environment, such as a silt and mud dominated distal braided river. Sands and muds deposited as sheets across large floodplain.
3	Calcareous sandstone, mudstone and limestone	Medium- to thick-bedded calcareous sandstone, interbedded with thin-bedded mudstone and limestone. Carbonate horizons containing bivalve fragments are bioturbated, and locally contain benthic forams. Some cross-bedding observed.	Marginal siliciclastic shallow-marine shoreline environment, possibly deltaic. Susceptible to changes in sea-level, hence constantly changing sedimentary facies.
4	Limestone conglomerate and debris flow	Debris-flows and conglomerate exclusively composed of limestone clasts with a pink muddy matrix. Limestone conglomerates formed in situ; i.e. limestone clasts with a micritic limestone matrix. Laterally variable in thickness.	Deposited in a marine environment, probably due to mass-movement on a slope. In a shallow-marine setting this could be due to active faulting, or instability on delta slope.

Fig. 4.28. Summary of facies associations and interpretation of the Late Triassic Çayır Formation. See text for details.

thickness of all of these coarse clastic deposits varies considerably along strike. In some instances conglomerates form laterally discontinuous horizons surrounded by mudstone. Other sedimentary structures are common such as clast imbrication, graded bedding, parallel and cross-lamination and primary current lineation. No fauna were found in this facies association.

Previous Interpretation: Özgül (1984) suggested that these clastic sediments were terrestrial in origin. In a later study, Özgül (1997) interpreted these as braided stream deposits developed on a nearshore platform (it is unclear whether these were interpreted as terrestrial or shallow-marine). For Önder (1984), the depositional environment was coastal marine with "rugged" hinterland and sea cliffs. An intermittent river drained the hinterland and transported clastic sediment into a deltaic, shallow-marine setting. In this model, the clastic sediments would be expected to be interbedded with marine mudstones and carbonates (Einsele, 1992). However, the conglomerate and sandstone observed are only locally interbedded with mudstones. There is also a lack of marine fauna within this facies association.

Depositional Environment: This facies association is likely to represent a high-energy terrestrial braided river depositional environment. The sedimentary architecture is, for example, comparable to the main depositional facies of the Buntsandstein, Central Spain (Fig. 4.29) (Ramos et al., 1986; Miall, 1996). Cross-bedding, channels, clast imbrication and lateral discontinuity of beds are all indicative of a braided river system (Einsele, 1992; Miall, 1996). The coarser conglomerate beds are interpreted as channel fill, whilst sandstone horizons represent sand banks proximal to the braided system (Fig. 4.30a, b, c). The rare mudstone beds could represent overbank deposits, or episodes of drought within a channel system. Some of the coarser and less well sorted deposits are thought to represent terrestrial alluvial fan deposits, comparable to fan deposits in South America (Mather and Hartley, 2005). It is possible that some of the conglomerates and sandstones at these localities could be marine (near-shore) or deltaic (Einsele, 1992).

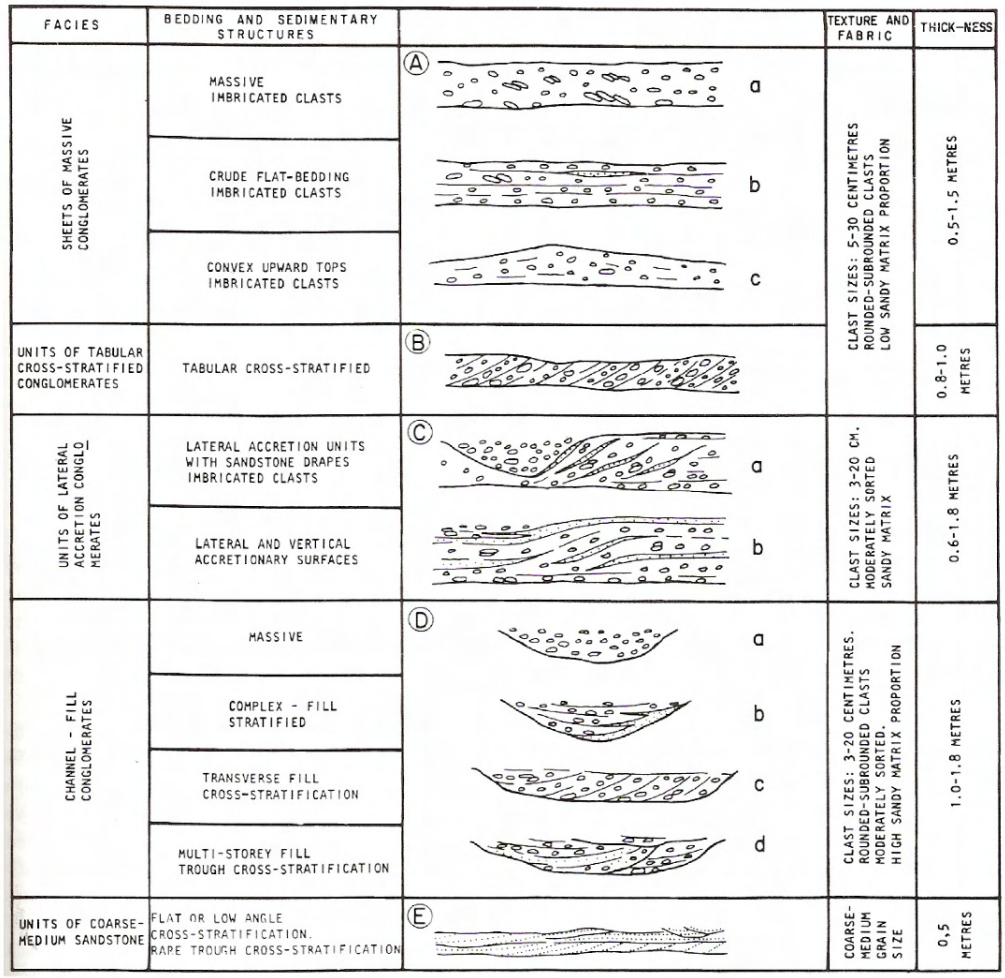

Fig. 4.29. Main depositional facies of the Buntsandstein fluvial sediments, Central Spain (Ramos, 1986).

4.5.2.2 Fine-grained mudstone and sandstone

Facies Association: Fine-grained mudstone and sandstone successions are found in the Geyik Dağ (e.g. locality 1: Yenişarbademli), the Hadim nappe (e.g. locality 4: Çamlik) and the Bolkar nappe (e.g. locality 10: Karabayır Yayla). Fine-grained mudstones and sandy-mudstones are interbedded with irregular, thin-bedded, medium-grained sandstones. These deposits are planar in geometry and are characterised by fine parallel laminations. Occasionally, coarser-grained lenses are observed, such as pebbly sandstone, which is typically only 2-3 m wide. At some localities this facies association constitutes the entire Çayır Formation thickness (e.g. Yenişarbademli), whilst at others it

overlies coarser conglomerate and sandstone horizons. Limestone horizons are interbedded locally towards the top of the sequence. The thickness of this facies association varies from ~5-45 m. No fauna were recovered from these sediments.

Previous Interpretation: Önder (1984) suggested that the red siltstones and the fine-grained sediments could have been deposited on the landward side of inter-tidal mud flats. The main problem with this interpretation is the susceptibility of this depositional environment to sea-level change. Regular interbeds of marine sediments would be expected; however, these are generally not seen.

Depositional Environment: This facies association represents a low-energy depositional environment, such as a silt and mud dominated distal braided river (Fig. 4.30). These environments are common in arid climates, where sediment accumulation is controlled by flash floods over a broad river plain which has shallow channels (Fig. 4.30d,f) (Einsele, 1992). As the flow diminishes, sands and muds are deposited as sheets with horizontal laminations (Einsele, 1992). The coarser pebbly sandstone deposits represent occasional channelised flows within the floodplain. The facies model for these distal braidplain deposits is known as Bijou Creek type (Miall, 1985; Miall, 1996). Fine-grained distal lithofacies similar to this have been described from, for example, a Quaternary alluvial fan in the Abarkoh Basin, Central Iran (Arzani, 2005). There is a close correlation between this facies association, and the coarse conglomerate and sandstone facies association.

4.5.2.3 Calcareous sandstone, mudstone and limestone

Facies Association: Interbedded sandstone, mudstone and limestone are found in the Hadim nappe (e.g. locality 3: Bademli), the Geyik Dağ (e.g. locality 6: Göl Başı) and the Bolkar nappe (e.g. locality 7: Baritli Yayla). At these localities the entire Çayır Formation consists of this facies association, whilst at others it is a minor component. The thickness varies considerably over the studied area. Medium- to thick- bedded

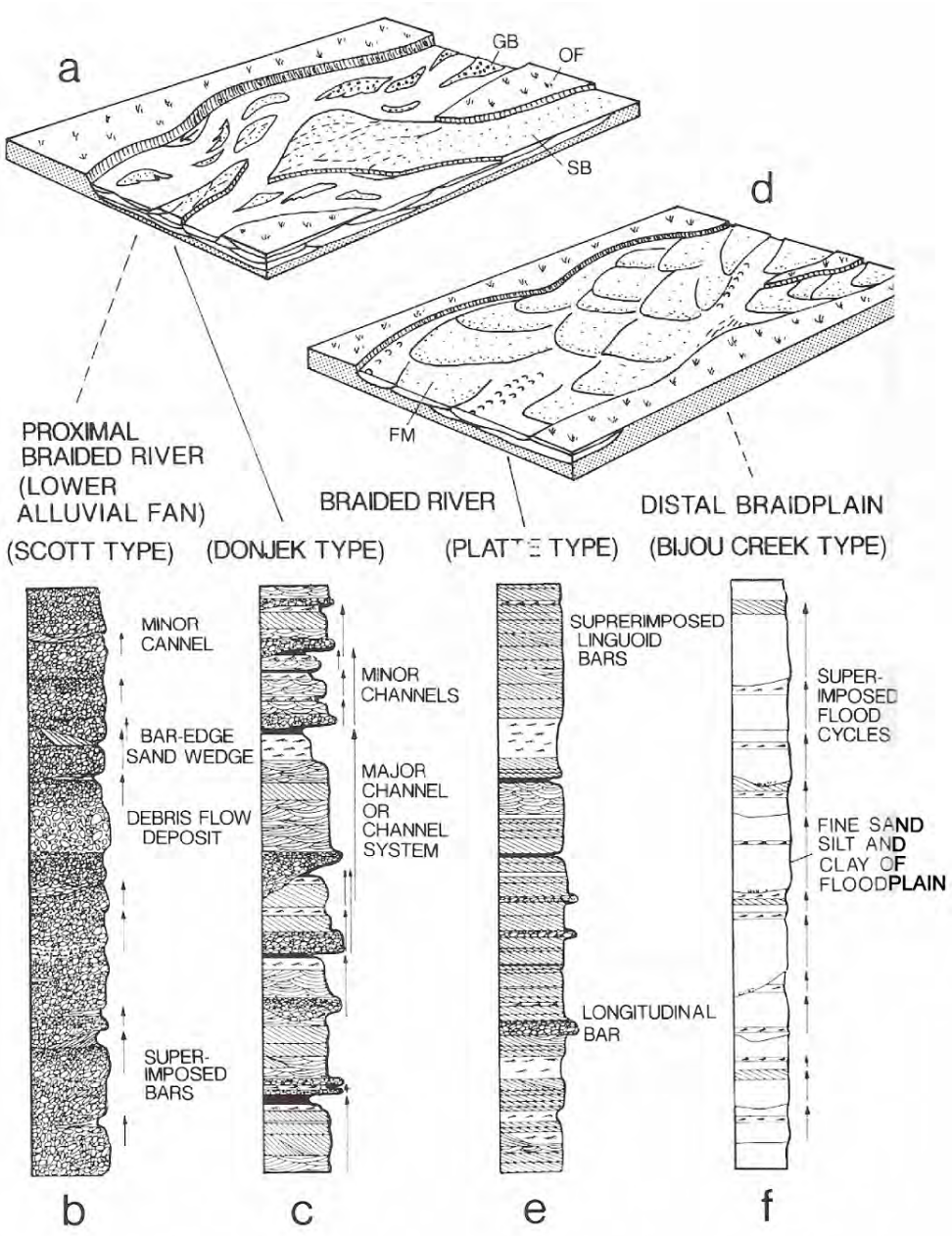

Fig. 4.30. Braided river systems. a. Proximal to middle reaches; b. gravel dominated; c. sand dominated; d. Distal, sand-dominated system; e. Wide channels and flat, linguoid sand bars; f. Wide floodplain inundated by flash floods. Figure after Miall (1985); modified by Einsele (1992).

sandstones (typically calcareous) are interbedded with fine-grained mudstones and medium-bedded shallow-marine limestones. The sediments stratigraphically overlie Upper Triassic thick-bedded carbonates. Towards to top of the Çayır Formation, the

interbedded sediments are typically transgressed by thick-bedded shallow-marine carbonates. Calcareous intercalations occur throughout the sequence, which contain bivalve fragments and are bioturbated. During this study, benthic Foraminifera such as *Planiinvoluta* sp. and *Valvulina* sp. were identified (N. İnan and K. Taslı, pers. comm., 2007). Clastic sediments are locally cross-bedded, but channel features are less common. Fining- and coarsening-upward sequences were observed. Thick-bedded to massive planar sandstones are laterally continuous, and have a sheet-like geometry.

Previous Interpretation: Limestone within the Çayır Formation has been interpreted as having accumulated in a small shallow-marine lagoon that interfingered with a siliciclastic shoreline (Özgül, 1997). The absence of fauna was interpreted as representative of a high-salinity environment. However, in this study, large broken bivalve shells (species unknown) were recognised. Also, the benthic foraminifera identified are generally thought to represent a normal-salinity environment (Márquez, 2005). Another explanation is that the calcareous sandstone was deposited in a coastal setting, subject to wave reworking (Önder, 1984). Changing rates of tectonic subsidence are identified as a cause of marine flooding of tidal flats, and deposition of carbonates.

Depositional Environment: This facies association is interpreted as a marginal-marine siliciclastic near-shore deposit, susceptible to rise and fall of sea level. This would explain the variety of clastic, mud and carbonate sediments (Einsele, 1992). A delta could have transported terrigenous material into a very shallow-marine setting, which would be sensitive to sea-level change. Within such a depositional setting, shelf mud, shoreface sand and lime mud could be deposited (Tucker, 1991; Einsele, 1992). Neritic fauna and bioturbation are indicative of a relatively productive setting; however, this would be reduced during episodic terrigenous input (possibly tectonically induced). Fining- and coarsening-upward sequences are suggestive of marine transgression / regression (Einsele, 1992), and the cross-bedding could result from tidal or channel currents.

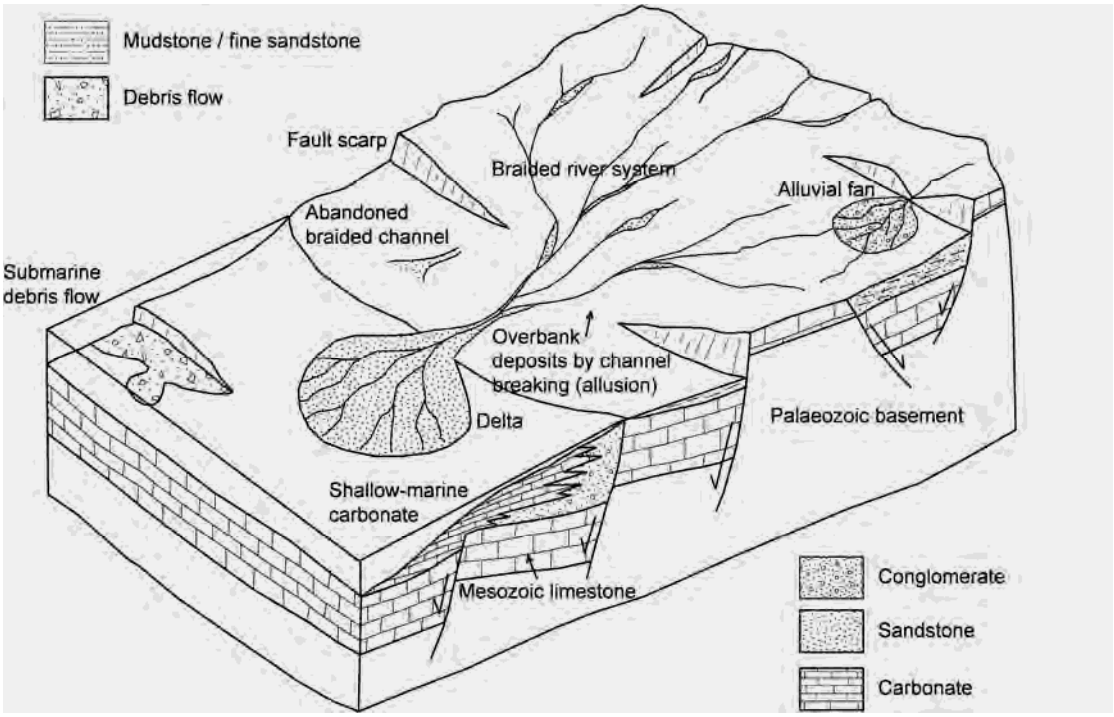

Fig. 4.31. Schematic diagram illustrating the range of depositional environments in which the Çayır Formation sediments were deposited.

4.5.2.4 Limestone conglomerate / debris flow

Facies Association: This facies association is the dominant lithology at localities 11 (Dedemli), 12 (Korualan) and 13 (Ekinlik Yayla), within 10 km of each other in the Bolkar nappe (Fig. 4.8). Limestone conglomerates were also observed as thin horizons at localities 14 and 15 (Alanya road south and north), towards the top of the Çayır Formation sequence, overlying facies associations 1 and 2 (above). At localities 11 and 12, these sediments occur within a thick-bedded Mesozoic limestone succession. At one particular locality (Korualan), a 35 m-thick conglomeratic sequence stratigraphically overlies >60 m of Upper Triassic limestone, and is, in turn, overlain by Jurassic neritic carbonate >300 m thick. The conglomerates are exclusively composed of limestone clasts, set in a marine mudstone matrix. Clasts are poorly sorted, sub-angular, and very densely packed; no sedimentary structures were observed. In some cases the

conglomerate is closely associated with sandstones (e.g. Dedemli), and with mudstone at others (e.g. Ekinlik Yayla). The thickness of these sediments is variable throughout the studied area. During this study, no fauna could be found within the sediments.

Previous Interpretation: Although this facies association has not been specifically identified before, Önder (1984) suggested deposition in a coastal environment, along with wave reworking of sediments. This could explain the rounding of limestone clasts, but not the actual mode of deposition, as there is very little terrigenous material in the matrix.

Depositional Environment: This facies association was deposited in a shallow-marine environment, where high-energy channels cross-cut shallow-marine sediments (Einsele, 1992). At some localities, where the underlying and overlying sediments are marine carbonates, it is difficult to envisage a change from a shallow-marine to a terrestrial environment without the presence of intermediate facies, for example, lagoonal or aeolian deposits. It is, therefore, likely that the conglomerates formed in a sub-marine setting on a carbonate platform. Submarine channels are typical of turbidity currents and are commonly deposited in deep-sea environments (Tucker, 1991; Einsele, 1992). However, the overlying and underlying neritic carbonate suggest these formed in a shallow-marine setting. This could be related to fault activity (Einsele, 1992) which creates a gradient. An example of normal faulting in a shallow-marine environment is documented from the Hammam Faraun fault block, in the Suez Rift, Egypt (Jackson et al., 2005). The deposition of shallow-marine conglomerates, mudstone and limestone is controlled by the localised movement on basin boundary faults. Alternatively, progradation of a shallow-marine fan delta can result in the formation of debris-flows (Tamura and Masuda, 2003); as previously discussed, some of the Çayır Formation may be deltaic in origin.

4.6 Discussion

This section synthesises the data presented in the previous sections with other literature to provide an overall interpretation of the Triassic tectonic setting of the Tauride platform.

4.6.1 Sedimentary Facies and Depositional Environment

The tectonic setting of the Early to Middle Triassic plays an important part in interpreting the Mesozoic tectonic setting and evolution of the Tauride platform. Of the four models proposed in section 4.2 (Fig. 4.2), three suggest an extensional rift-related setting for the Tauride platform, whilst one suggests it bordered a oceanic basin that was closing prior to continental collision. Using the sedimentary evidence and facies association provided in this chapter, along with literature examples, a model of the tectonic setting will be proposed.

4.6.1.1 Early to Middle Triassic

The facies associations identified in section 4.5.1 were: (i) thick-bedded neritic carbonate and dolomite; (ii) medium-bedded shallow-marine clastics and carbonates; (iii) thin-bedded mudstone, shale and marly-mudstone; (iv) interbedded mudstone, shale, sandstone, marly-mudstone and carbonate. The distribution of these facies associations between the measure logs are shown in Fig. 4.32. Comparisons can be made between the Triassic succession described in section 4.3.2.

Firstly, thick-bedded neritic carbonates and dolomites represent the lowest part of the succession (Fig. 4.32, Loc. 1 and 3). These are inferred to be of Early Triassic age, representing a period of relative platform stability. This horizon is not seen at Loc. 2. as the Lower Triassic sequence is not present due to localised emplacement-related thrusting (Fig. 4.5). The underlying Permian sequence is characterised by neritic carbonate deposition (Özgül, 1984; Özgül, 1997), and it is reasonable to assume this stable environment continued into the Early Triassic.

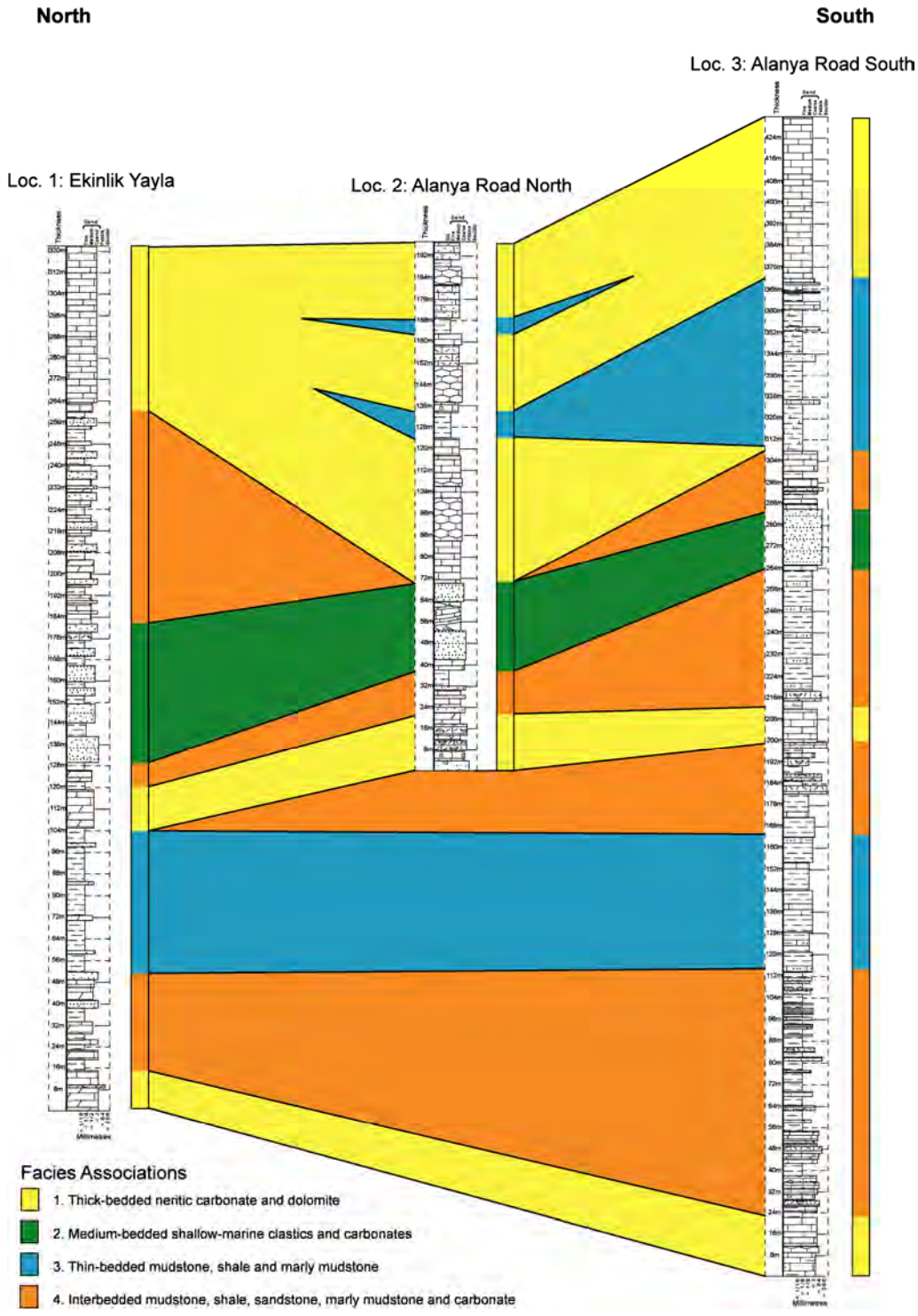

Fig. 4.32. Distribution of Triassic facies associations described in section 4.5.1 between the measured Triassic logs, described in section 4.3.2.

Overlying the thick-bedded carbonates is a sequence of interbedded mudstone, shale, sandstone, marly mudstone and carbonate (facies association 4, Fig. 4.32). This abrupt change in facies association, and the interbedded nature of various lithologies, indicates that the platform was unstable during this time. This interval is laterally variable in thickness, ranging from 35 m in the north (Loc. 1), to 90 m in the south (Loc. 3). Rates of sedimentation across the platform clearly varied, possibly related to differential subsidence, relative sea-level change, or variable sediment supply.

Above comes a laterally continuous sequence of thin-bedded mudstone, shale and marly mudstone (Fig. 4.32, Loc. 1 and 3). This is ~55 m thick across the studied area, which suggests that the depositional setting of the platform remained relatively stable during this period. However, unlike the neritic carbonates at the base of the succession, this facies association is primarily composed of fine-grained terrigenous sediment (mudstone). The likely depositional setting is a shallow-marine environment (nearshore mud-belt), possibly in a more distal setting on a continental shelf, with water depths of up to 50 m (see section 4.5.1.3).

This lower part of the Triassic succession, therefore, shows a change from a neritic shallow-marine carbonates (facies association 1), to interbedded mudstone, shale, sandstone, marly mudstone and carbonate (facies association 4), and then into fine-grained mudstones and marls (facies association 3). This is often characteristic of a deepening-upwards sequence, representative of sea-level rise and marine transgression (Johnson and Baldwin, 1986; Reading, 1986; Sellwood, 1986; Einsele, 1992). In this scenario the sedimentary facies become more distal up-sequence, and there is an increase in terrigenous sediment entering the system.

Continuing up-sequence, the fine-grained sediments (facies association 3) are overlain by interbedded terrigenous sediments and carbonates (facies association 4) in the south, whereas in the north they are overlain by neritic carbonates and dolomitic carbonates (facies association 1) (Fig. 4.32). In the south, the interbedded sequence (facies association 4) is, in turn, overlain by neritic sediments. These units are inferred to be of late Lower Triassic to Middle Triassic age (Monod, 1977; Önder, 1984; Özgül, 1984; Özgül, 1997). The interbedded sediments are laterally discontinuous, and are not

present in the northerly sequence (Fig. 4.32, Loc. 1). However, the neritic units have a constant thickness and can be traced across the whole study area.

In contrast to the deepening-upwards succession in the lower part of the Triassic, this interval represents a transition from fine-grained sediments (facies association 3), to interbedded sediments (facies association 4), and then to neritic shallow-marine carbonates (facies association 1). This represents a typical shallowing-upward succession, indicative of a marine regression (Johnson and Baldwin, 1986; Reading, 1986; Sellwood, 1986; Einsele, 1992).

Overlying the neritic carbonates and dolomites is thick, but laterally variable, sequence of interbedded terrigenous sediments and carbonates (facies association 4), overlain by an abrupt, laterally continuous horizon of shallow-marine clastics and carbonates (facies association 2) (Fig. 4.32). These are, in turn, overlain by a further laterally variable horizon of interbedded terrigenous sediments and carbonates (facies association 4). The variability in facies throughout this period is indicative of platform instability, and relative sea-level change. The succession of shallow-marine clastics and carbonates (facies association 2) and the sustained input of clastic material may be indicative of a relatively proximal setting on a deltaic system (section 4.5.1.2) (Einsele, 1992), with variable marine inundation and erosion. During this time period various parts of the platform experienced different depositional settings. For example, the thickness of facies association 4 can vary from ~80 m in the north (Fig. 4.32, Loc. 1), to ~24 m in the south (Fig. 4.32., Loc. 3), to non-existent in the middle of the study area (Fig. 4.32, Loc. 2).

This variability across the platform is again demonstrated in the upper parts of the measured sections (Fig. 4.32). The top of the Triassic succession is predominantly composed of neritic carbonates (facies association 1), suggestive of a shallow-marine, stable platform setting. However, this is sporadically interrupted by laterally discontinuous horizons of fine-grained mudstone, shale and marl (facies association 3). This could be indicative of a prograding carbonate platform, with an interfingering nearshore mud belt and carbonate build-up (Einsele, 1992). Alternatively, it could

represent a distal, but still shallow-water, setting on a continental platform, too far removed from the shoreline to receive coarser grained terrigenous material.

The sedimentary successions described above were all measured within the Hadim nappe solely in the south of the study area. However, it is useful to consider the variability in Triassic thickness across the whole study area, ranging from the northerly and southerly areas of the Hadim nappe. At the village of Çamlik (section 4.3.2.5) in the northerly area, the Lower Triassic sequence is ~ 200 m thick, and an unconformity exists in the Middle Triassic, with the Upper Triassic Çayır Formation directly overlying Lower Triassic sediments. In contrast, in the southerly area, the Triassic sequence is >400 m thick at locality 15 (Alanya road south). If, as is likely, the two nappes in question restore to a single contiguous continental margin, there must be significant intra-platform variability in depositional setting.

The variability in sedimentary facies and thicknesses of sediment packages across the Tauride platform is a consequence of relative sea-level rise and fall and autocyclic processes. However, sequence stratigraphic studies show that during rhythmic sea-level rise and fall, sedimentary packages develop a cyclicity and a well-defined series of sequences relative to changes in sea-level (Tucker, 1985; Einsele, 1992). A simple sequence stratigraphy model does not take into consideration influences on sedimentary dispersal, for example, tectonic instability or a changing sediment source. The sedimentary facies analyses above cannot be adequately explained simply by rhythmic sea-level changes.

4.6.1.2 Late Triassic

The facies associations identified in the Upper Triassic Çayır Formation (section 4.5.2) are: (i) coarse-grained conglomerate and sandstone; (ii) fine-grained mudstone and sandstone; (iii) Calcareous sandstone, mudstone and limestone; (iv) Limestone conglomerate and debris flow. The measured Çayır Formation sections were divided into facies associations, and a diagram showing the variation in thickness and distribution of these facies associations is shown in Fig. 4.33. The Çayır Formation was

studied in the Geyik Dağ, Hadim nappe and Bolkar nappe. In this study it is proposed these three tectonic units restore in the early Triassic as a single north-facing rifted margin (see chapters 5 and 6 for further discussion). The data presented in Fig. 4.33 have, therefore, been subdivided to show the variations in thickness and facies association of the Upper Triassic sediments within the original restored Tauride platform (**Fig. 4.34**). Data presented in these two diagrams provides crucial insight into the Late Triassic tectonic setting and depositional environment. It should be noted that due to lack of fauna, no stratigraphic time correlations can be made between the Upper Triassic successions.

Fig. 4.33 shows the variety in facies associations and thickness of sediments within the Çayır Formation. The average thickness of the Çayır Formation is 55 m. However, the majority of sequences are between 25 and 50 m thick, with four anomalously thick sequences >100 m thick. The thinnest sequence at locality 13 (Ekinlik Yayla) is tectonically sheared, and thus, therefore, not a true thickness. At other localities (e.g. Üzümdere) the maximum thickness is not exposed.

In some places the Çayır Formation is composed of a single facies association (e.g. Loc. 3 and 6, Fig. 4.33), whilst at others it is composed of several related facies associations (e.g. Loc. 14 and 15, Fig. 4.33). Firstly, this indicates that the Upper Triassic depositional environment was laterally variable across the Tauride platform. Secondly, the depositional environment was stable in some parts of the platform, but unstable in others. And thirdly, as a consequence, the thickness of accumulated sediments was laterally variable from one locality to another. Within the much thicker Early – Middle Triassic sequence, facies associations could be traced laterally between the different measured sections (Fig. 4.32); however, this was not possible in Upper Triassic sequences. This suggests that even greater instability and disturbance of the platform occurred during the Late Triassic period.

The distribution of facies associations relative to their tectonic position within the Tauride platform (**Fig. 4.34**) shows the lateral variations of the Çayır Formation in more detail. Sediments within the Geyik Dağ are predominantly fine-grained terrigenous sediments and limestones (facies associations 2 and 3), although there are some coarse-

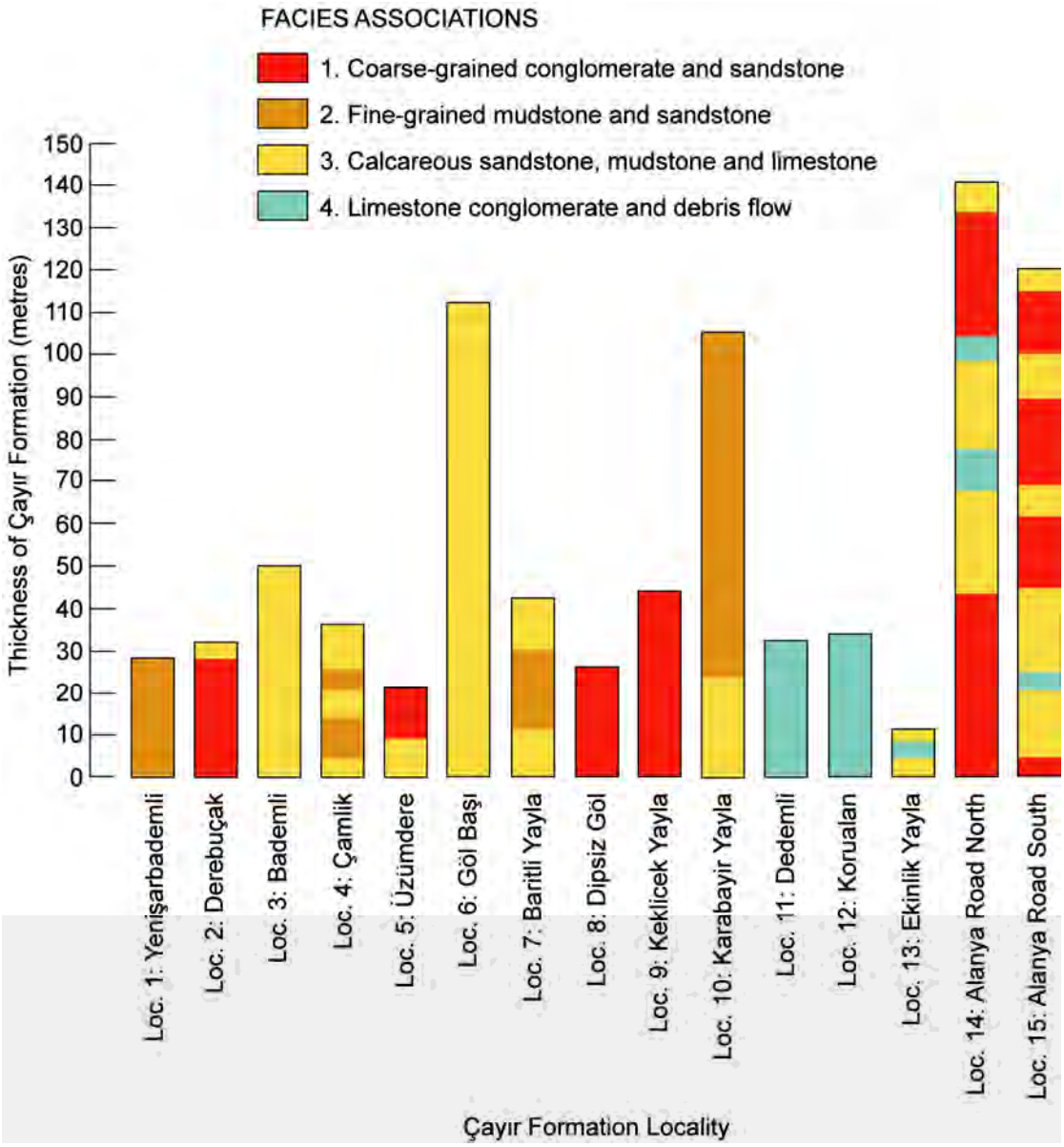

Fig. 4.33. Distribution of thickness of the four facies associations identified within Late Triassic Çayır Formation sediments (from section 4.5.2).

grained conglomerates and sandstones (facies association 1) at locality 5. Facies association 2 is thought to represent a distal braided river environment, and facies association 3 a shallow-marine siliciclastic environment (see section 4.5.2). This suggests that the depositional environment interchanged between terrestrial and marine within this part of the platform.

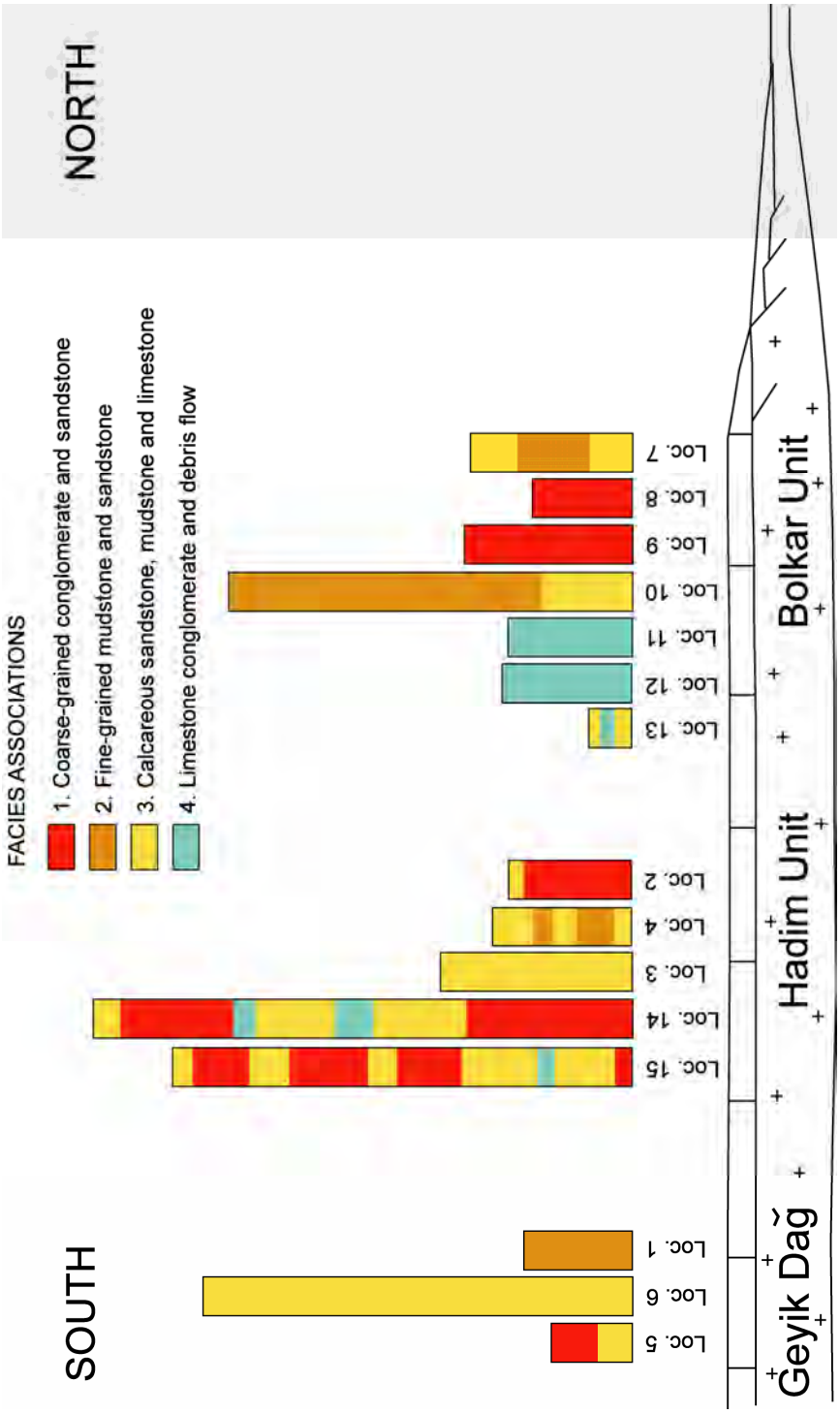

Fig. 4.34. Distribution and thickness of facies associations of Çayır Formation sediments within restored Early Triassic north-facing Tauride rifted margin. Localities are distributed relative to the tectonic unit in which they were observed, and to their present day position within these units (see Fig. 4.8).

Within the Hadim unit there is a higher percentage of coarse-grained sediments (facies association 1 and 4) than fine-grained sediments (**Fig. 4.34**). There is a high abundance of inferred terrestrial braided river deposits (facies association 1) at three localities within this unit; however, the presence of limestone conglomerates and debris flows (facies association 4) within the two thickest successions indicates that the environment interchanged between marine and terrestrial. Another point to note is that the thickness of sediments increases gradually further south in the Hadim unit (with the exception of locality 14).

Within the Bolkar unit, there is a variety of coarse-grained terrestrial sediments (facies association 1), and finer-grained terrestrial and marine sediments (facies associations 2 and 3), and coarse-grained marine sediments (facies association 4) (**Fig. 4.34**). There are no obvious trends to these data; however, towards the south of the Bolkar unit there appears to be more marine conglomerate / debris flow (facies association 4), whilst in the north of the unit there are more terrestrial coarse-grained sediments (facies association 1). It is evident, however, that the depositional environment interchanged between a marine and terrestrial across the Bolkar unit throughout the Late Triassic.

Due to a lack of age constraints it is not possible to determine if facies associations and depositional settings identified can be correlated from one tectonic unit to another. However, the lateral variation in facies observed allows the following inferences to be made with regards to the platform during the Late Triassic.

First, the Tauride platform potentially is hundreds of kilometres wide, and was divided into several sub-basins, which would explain the variable sediment thicknesses and facies associations across the platform. Einsele (1992) describes how depositional environments can vary within relatively small areas, influenced by tectonics, basin morphology, peri-basin characteristics, climate conditions and relief (Fig. 4.35). It is also likely that terrestrial and marine environment could co-exist in different parts of the Tauride platform. Accordingly, several sub-basins possibly existed, and topographic relief is likely to have varied significantly across the platform. The palaeocurrent data presented earlier in this chapter show that the regional topographic high was to the north.

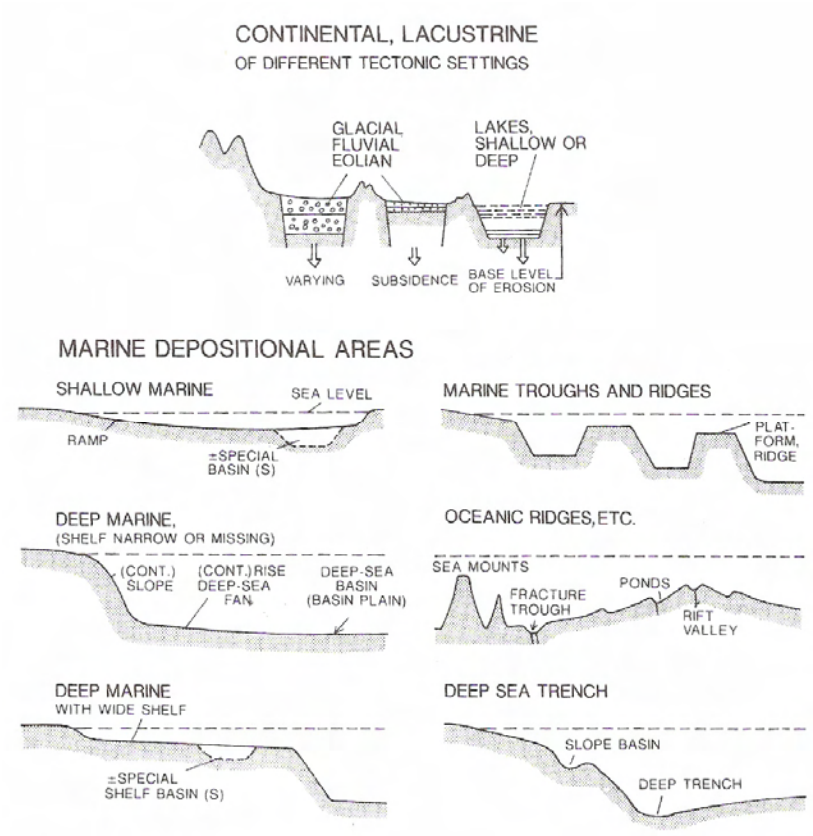

Fig. 4.35. A selection of continental and marine depositional environments, where the basin morphology is influenced by local tectonics, relief, subsidence, and relative sea-level. The amount of terrigenous sediment entering the basin is affected in these circumstances. Figure modified from Einsele (1992).

Einsele (1992) notes syn-depositional tectonic movements can control the thickness of fluvial and shallow-marine sediments and generate a basin-fill structure, without actually forming a morphological basin (Fig. 4.36). This is comparable to Jurassic rift of the high Atlas mountains, when during rift-related subsidence there was little or no change in the relief of the basin, and neritic carbonates were deposited throughout the rifting episode (Warme, 1988).

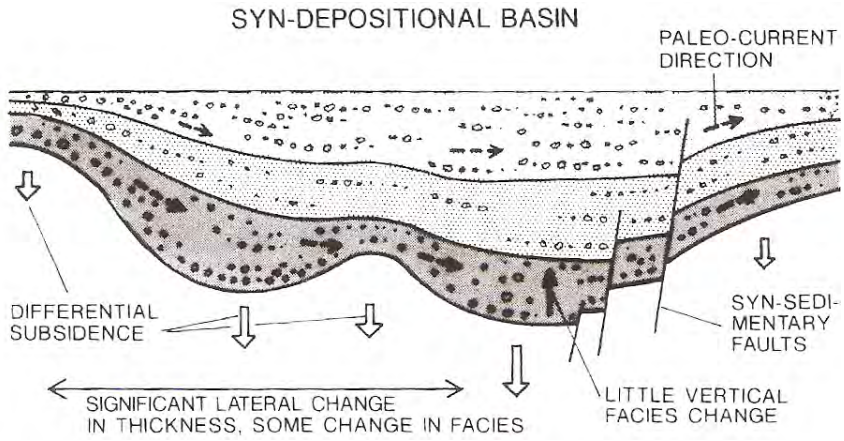

Fig. 4.36. Syn-depositional tectonic movements can influence the thickness of fluvial and shallow-marine sediments, and generate a basin fill structure, even though a morphological basin hardly exists. From Einsele (1992).

4.6.2 Tectonic setting

4.6.2.1 Rifting and rift-related flexural uplift

The tectonic facies concept was introduced by Robertson (1994) as a systematic method of recognising past tectonic settings, particularly those that are of orogenic belts. Sedimentary facies analysis and interpretation is fundamental to this process. In many cases it is not just the presence of particular facies, but also the absence of others, which are crucial when restoring an orogenic belt.

All of the Triassic facies in the Geyik Dağ, Hadim nappe and Bolkar nappe are interpreted as being deposited in shallow-marine, or terrestrial environments. A recent study of the Beyşehir and Bozkir nappes (Andrew, 2003) concluded that these units are distal-margin in origin, and contain lithologies such as pelagic limestone, shale, chert, debris flow, lava, tuff, and volcaniclastic sediment of Triassic age (Monod, 1977; Özgül, 1997; Andrew and Robertson, 2002). The Beyşehir and Bozkir units, along with the Geyik Dağ, Hadim and Bozkir units, in this study are inferred to restore as a single contiguous Mesozoic continental platform. Using the tectonic facies concept (Robertson,

1994), a combination of all the Triassic sediments fits closest to a divergent setting, and has characteristics of both 'rift-related' and 'passive continental margin' tectonic facies.

Rift-related sedimentation is well documented in the Red Sea region. In southern Yemen (Gulf of Aden), the principal control on sedimentation was a series of basement highs which divided the rifted margin into a series of sub-basins (Watchorn et al., 1998). Subsidence rates were variable over a 20 Myr period, and climaxed with post-rift regional tectonic uplift and rift-shoulder erosion. Sediment accumulation during this period was of shallow-marine carbonates and clastics that interfingered with coastal alluvial and fluvial sediments. The thickness of sediment across the rifted margin is patchy, with the thickest sediment packages accumulating in regional 'troughs' between basement highs (Fig. 4.37). Sediments deposited during the post-rift tectonic uplift are the coarsest sediments in the sequence (Watchorn et al., 1998). Similar characteristics are seen along the north-eastern Gulf of Aden margin (Autin et al., 2007), and the eastern margin of the Gulf of Suez (McClay et al., 1998).

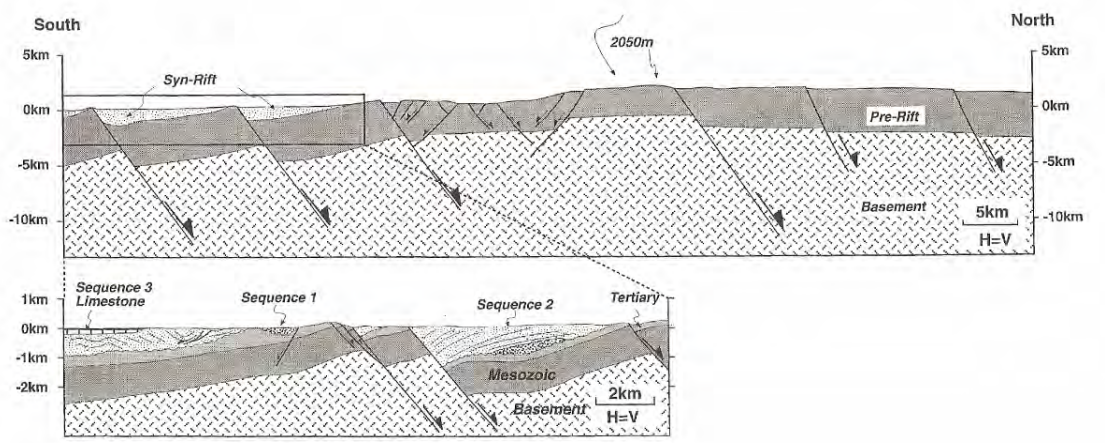

Fig. 4.37. Cross-section of part of the Gulf of Aden rifted margin, with syn-rift sediments accumulating in troughs between basement highs. Faults dip away from rift-basin in this section. From Watchorn et al. (1998).

In the northeastern Gulf of Aden (Dhofar region of southern Oman), basin evolution records Late Oligocene – Early Miocene rifting (Robertson and Bamakhalif, 2001). Following an original pulse of rifting and subsidence, flexural deformation of the continental margin uplifted the northern flank by up to 1500 m, resulting in the

deposition of shallow marine clastics, mainly limestone conglomerates. Following marine regression, red alluvial conglomerates accumulated on a resulting coastal plain. Typically within the central Taurides, a large unconformity at the base of the Çayır Formation is not observed. However, in the Hadim nappe at Çamlik (section 4.4.2.4), Upper Triassic sediments directly overlie Lower Triassic units (Monod, 1977; this study). Further documentation of pulsed rifting followed by rift-shoulder uplift in the Gulf of Aden is provided by fission-track data from northwestern Somalia (Abbate et al., 2001). Comparisons can be made between these examples from the Gulf of Aden, and the Triassic stratigraphy of the central Taurides. In western Crete, the Middle Carboniferous – Triassic succession is documented as representing a developing rift sequence (Robertson, 2006b), culminating in a phase of Late Triassic flexural related uplift and conglomerate deposition (Mana conglomerate). In the same study (Robertson, 2006b), evidence from the Sicily, Crete, Evia and the Pelaponese are consistent with Carboniferous – Triassic rifting with a pulse of uplift in the Middle to Late Triassic. These southern Mediterranean localities restore along strike from the Tauride platform in the Triassic, suggesting the two regions had a similar rift-related tectonic evolution.

Proximal deposits at the edge of a Miocene basin in the Sierra Espuna Mountains in southern Spain are composed of mixed marine carbonate and terrigenous sediments (Lonergan and Schreiber, 1993). Clastic sediments interfinger laterally and vertically with algal and coralline reef limestones. These sediments pass distally into fine-grained sediments. Sedimentation is thought to be controlled by faulting, although syn-sedimentary faults are not observed within the sequence.

Taking into consideration all of the data presented, it is proposed that the Triassic of the Geyik Dağ, Hadim nappe and Bolkar nappe represents a proximal rifted margin sequence. This is consistent with the increase in relative sedimentation rate for the Triassic, as shown in chapter 3 (section 3.4). Differential rift-block subsidence over a long period resulted in variable sediment thickness and facies associations across the margin. Episodes of subsidence and marine transgression resulted in the deposition of more distal sediments, such as mudstone. Episodes of platform stability and relative sea-level fall resulted in deposition of more proximal shallow-water sediments, such as

limestone. During the latest Triassic a pulse of rift-related flexural uplift caused the deposition of coarse terrestrial and marine deposits (Çayır Formation).

4.6.2.2 Comparisons with other Tethyan margins

Other well-documented Tethyan continental margins are comparable with the Central Tauride Triassic stratigraphy described in this chapter. The Eastern Tethys region runs laterally from the eastern Alps, through Greece, Turkey, the Middle East, and onto the Himalayas (Robertson, 2007). During the Mesozoic, it is documented that fragments of the south Tethyan (Gondwana) continental margin rifted and drifted towards Asia (Şengör et al., 1984; Robertson, 2007). Many of these rifted margins are now preserved in mountain belts throughout the Tethyan region.

The Antalya Complex is a heavily faulted and folded Mesozoic-Cenozoic continental margin (Woodcock and Robertson, 1981). A transition from proximal to distal units of a Triassic rifted margin are preserved to the SW of Antalya city (Robertson, 2007). The distal margin units contain turbidites, pelagic limestones, calciturbidites and radiolarian sediments. The proximal units (Kemer zone) are composed primarily of shallow-water limestone and dolomitic limestone that overlie pre-rift basement rocks (Woodcock and Robertson, 1981; Robertson, 2007). These carbonate facies are restored as rifted margins, bordering a Mesozoic oceanic basin. Combined with evidence of distal margin units from the Mamonia complex (S Cyprus), the Antalya represent pulsed rifting from Late Carboniferous – Middle Triassic, followed by continental break up in Latest Triassic – Early Jurassic time.

In the western Taurides (SW Turkey), the Menderes Massife and overlying Lycian nappes are another well documented Triassic rifted margin (Collins and Robertson, 1998; Robertson, 2007). The far-travelled Lycian nappes consist of variable proximal and distal continental margin, slope and oceanic units. Proximal units (Karadağ thrust sheet) consist of prerift basement (Carboniferous and Permian bioclastic limestone) overlain by Lower and Middle Triassic quartzarenites, algal limestone and bioclastic limestone (Collins and Robertson, 1998). Overlying these are Middle to Upper

Triassic shelf limestones, and Late Triassic lithic arenites and shales (Fig. 4.38). More distal units within the Lycian nappes consist of MOR-type lavas and redeposited deep-water carbonates (Collins and Robertson, 1998; Robertson, 2007). The proximal units of the Karadağ thrust sheet are comparable to the Triassic of the central Taurides discussed in this chapter. The Lycian nappes restore as a continental margin that rifted in the Triassic, with a full oceanic basin developed by the latest Triassic – Early Jurassic (Collins and Robertson, 1998; Robertson, 2007).

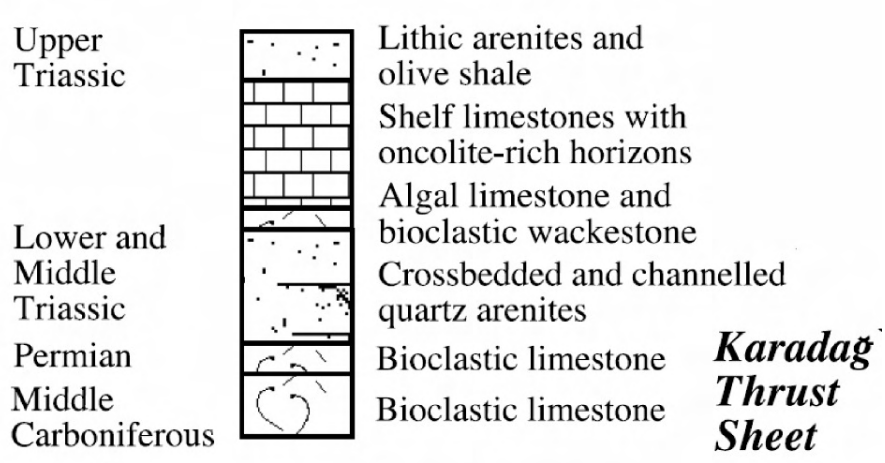

Fig. 4.38. Stratigraphy of the Karadağ thrust sheet, Lycian nappes, western Taurides. From Collins and Robertson (1998).

A rift to passive margin transition is well preserved in the Oman mountains (Glennie et al., 1973; Robertson, 2007). Prior to Cretaceous deformation, this region restores as a south Tethyan (Gondwana) continental margin during the Late Palaeozoic and Early Mesozoic, similar to the Tauride margin (Robertson, 2007). Rifting occurred from the Late Permian, with the proximal succession consisting of thin clastics and a thicker carbonate succession. Erosion during the Late Permian was a result of rift-related flexural rift-shoulder uplift (Stampfli et al., 2001; Robertson, 2007). The proximal rift experienced carbonate accumulation throughout the Mesozoic, whilst distal regions accumulated slope and abyssal plain sequences. This proximal – distal rift sequence is

comparable with the Triassic central Tauride units in the Beyşehir-Hoyran-Hadim nappes (Andrew and Robertson, 2002; Robertson, 2007).

In the western Tethys region, evidence of Late Triassic – Early Jurassic rifting is preserved in the Balkan region, and particularly the Pindos mountains. The northerly rifted margin of Adria is well exposed in these mountains between Albania and southern Greece. Evidence of pulsed rifting is observed in Late Palaeozoic – Early Mesozoic units, represented by a Phyllite-Quartzite unit (Robertson, 2006b; 2007). Facies evidence also suggests there was a later stage of rifting in the Late Triassic, which opened the Pindos ocean, followed by Mesozoic passive margin subsidence and deposition of a proximal carbonate platform (Robertson, 2007) (Fig. 4.39). A similar Triassic rifted margin is preserved northern Greece, represented by the Pelagonian microcontinent (south) and the Serbo-Macedonian microcontinent (north) (Robertson, 2007).

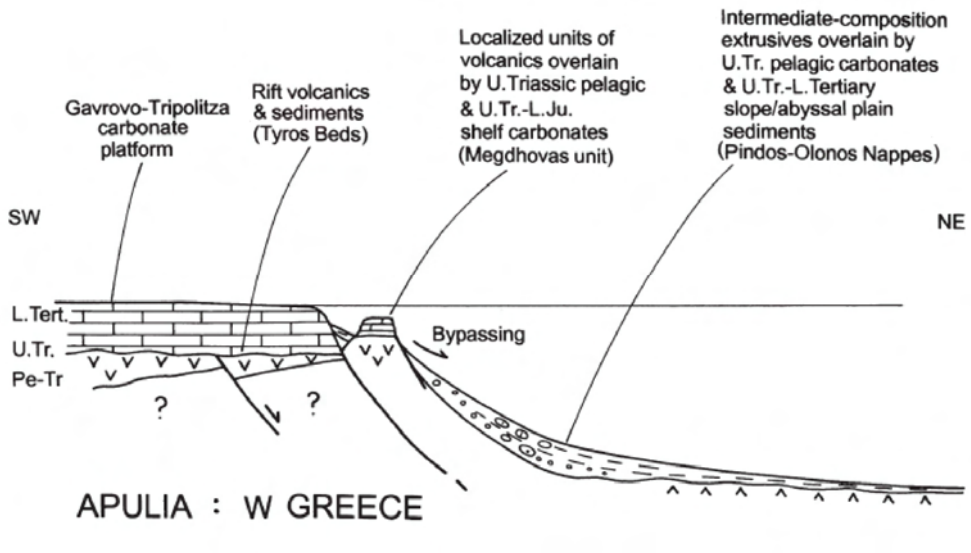

Fig. 4.39. Restored rifted – passive continental margin succession in Western Greece (Apulia). Proximal carbonate platform facies in the SW are comparable to those in the Tauride Platform. Figure from Robertson (2007).

Further afield in the Northern Indian Himalayas, a thick sedimentary sequence records Neo-Tethyan rifting between paleo-India and Cimmeria along the Gondwana margin (Gaetani and Garzanti, 1991). Rifting began in the Permian and continued until the Late Jurassic, as represented by regressive – transgressive sedimentary mega-

sequences and unconformities. Basal sandstones of Early Permian, Late Permian, Norian and Carnian are associated with oolitic sediments. These represent transgression during pulsed rifting along the margin. Nodular carbonates and shales, overlain by shallowing-upwards marls and platform carbonates, represent regression (Gaetani and Garzanti, 1991). This is very similar to the episodic subsidence and uplift observed in the central Taurides, as described in this chapter.

In summary, the southern Tethyan margin is preserved in a variety of regions throughout the Mediterranean, Arabian, Middle Eastern and Himalayan orogenic belts. Many examples document Early Mesozoic pulsed rifting along the Gondwanan margin, particularly in the Late Triassic and Early Jurassic. The proximal rifted margin facies are typically carbonate and siliciclastic platform sediments, which pass laterally into distal slope, abyssal plain and oceanic units. There are significant comparisons between the Triassic units observed in the Beyşehir-Hoyran-Hadim nappes and the other rifted margins documented.

4.6.3 Proposed new model

A regional unconformity exists within the autochthonous Geyik Dağ, and no units are exposed of Silurian to Early Triassic age. By contrast, in the Hadim and Bolkar nappes, there is a complete Palaeozoic succession from Devonian to Cretaceous. These three tectono-stratigraphic units are inferred to restore as parts of the same north-facing rifted continental margin during the Palaeozoic, from north to south: Bolkar unit, Hadim unit, Geyik Dağ unit. Regional topographic highs and lows could then have existed within the continental platform, with some rift-blocks being eroded, whilst others were sites of deposition.

Above the unconformity in the Geyik Dağ, and within the Hadim nappe and the Bolkar nappe, the Triassic stratigraphy (Monod, 1977; Önder, 1984; Özgül, 1984) comprises Early–Middle Triassic marine mudstones, limestones and sandstones, then Middle – Upper Triassic platform carbonates, in turn overlain by Late Triassic – Lower Jurassic Çayır Formation clastics. During the Triassic, the Tauride platform (including

the Konya complex) represented a north-facing subsiding rift. By the latest Triassic, extension-related flexural uplift caused the deposition of continental clastics in intra-platform basins, represented by the Çayır Formation (Fig. 4.40).

The source of the clastic sediment is seen as an uplifted fault block along the rifted margin to the north of the area studied. Studies of comparable rift shoulder uplift in the Red Sea and Gulf of Aden region (Watchorn et al., 1998; Abbate et al., 2001; Robertson and Bamakhalif, 2001; Autin et al., 2007) show that the topographically highest rift blocks can be closest to the newly forming oceanic basin, with sediment supply inland away from the rift shoulder.

In summary, the evidence suggests that the Tauride-Anatolide platform existed as a north-facing rifted margin at least from Triassic – Late Cretaceous (Fig. 4.40). The platform was hundreds of kilometres wide, as indicated by the combined lateral extent of the Beyşehir-Hoyran-Hadim nappes and autochthonous Geyik Dağ. Complex rift blocks created intra-platformal basins, resulting in variable erosion and deposition across the platform. During the Late Triassic–Early Jurassic, a pulse of rift-related flexural uplift caused erosion of the rift-flank and deposition of continental and shallow-marine clastics across a large area of the platform. The irregular topography of rift-blocks resulted in variable depositional environments and sediment provenance; however, the palaeocurrent data suggests that sediment was mainly derived from an uplifted block to the north, and transported southwards away from this topographic high (Fig. 4.40).

The platform had subsided by the Middle Jurassic and platform carbonates were deposited throughout the later Mesozoic. During the Late Cretaceous and Early Cenozoic, suturing of the Tethys ocean and emplacement of the Beyşehir-Hoyran-Hadim nappes was associated with regional compressional deformation throughout the Tauride platform.

Further evidence to support this model is provided in Appendix A, which is a draft of a manuscript for submission (Mackintosh & Robertson, in preparation). The manuscript includes sedimentary evidence provided in this chapter, along with structural evidence provided in chapter 5.

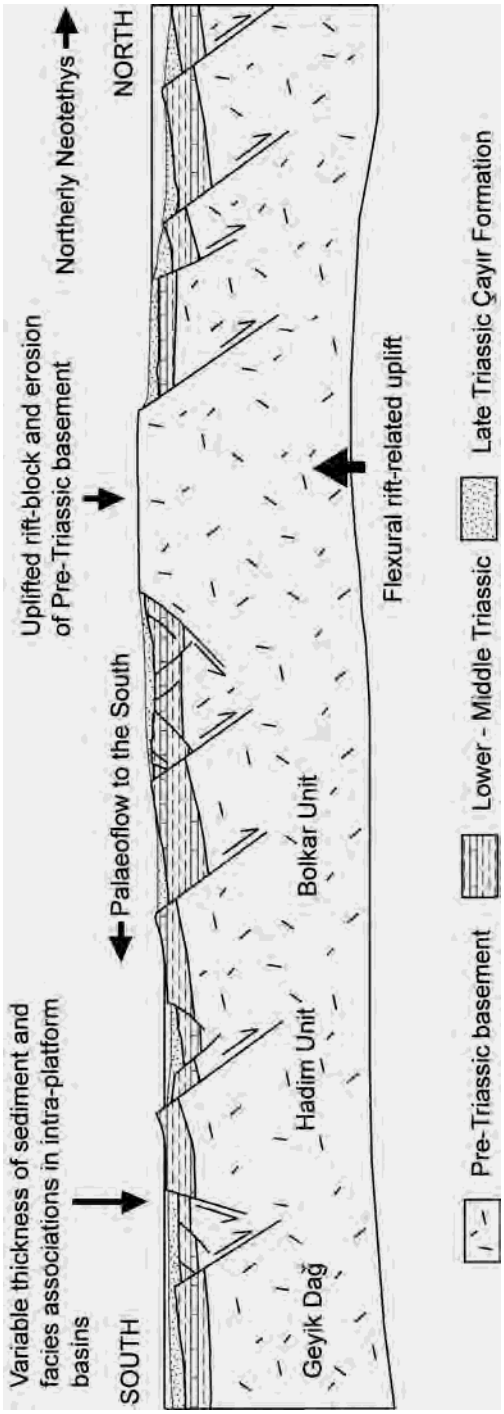

Fig. 4.40. Model of Late Triassic rift-related uplift of the Tauride platform. showing the relative positions of the Geyik Dağ, Hadim nappe and Bolkar nappe. The Beyşehir and Bozkir nappes would restore to a more distal position in rifted margin, adjacent to the Northerly Neotethys ocean.

4.7 Conclusions

1) Detailed sedimentary logging of the Triassic stratigraphy has allowed 4 facies associations to be identified for the Lower to Middle Triassic: (i) thick-bedded neritic carbonate and dolomite; (ii) medium-bedded shallow-marine clastics and carbonates; (iii) thin-bedded mudstone, shale and marly mudstone; (iv) interbedded mudstone, shale, sandstone, marly mudstone and carbonate.

2) Detailed sedimentary logging of the Upper Triassic stratigraphy (Çayır Formation) has allowed the following facies associations to be identified: (i) Coarse-grained conglomerate and sandstone; (ii) fine-grained mudstone and sandstone; (iii) calcareous sandstone, mudstone and limestone; (iv) limestone conglomerate and debris flow.

3) Variation in sediment thickness and laterally discontinuous facies associations indicate that the Tauride platform was divided into a series of topographically subdivided sub-basins during the Triassic.

4) During Lower to Middle Triassic, the depositional environment was shallow-marine, typically low energy, with facies ranging from proximal carbonates to more distal mudstones. During the Late Triassic, the depositional environment varied from shallow-marine to terrestrial, and an abundance of coarse-grained sediments indicative of a higher energy environment.

5) Palaeocurrent data from fifteen localities across the area show that sediment transport in the Çayır Formation was mainly from the north to the south, although flow was locally variable. This implies that a regional “basement” high existed to the north of the exposed Tauride platform during the Late Triassic.

6) The composition of conglomerates and sandstones in the Çayır Formation suggests that most of this material was derived from the Palaeozoic and Triassic stratigraphy of

the Tauride platform. There is an absence of sediment that could be derived from metamorphic or magmatic sources. Black chert within the Çayır Formation was probably derived from a Palaeozoic "basement" unit to the north of the area studied in detail (i.e. the Konya Complex).

7) Sedimentary evidence from the Triassic of the central Taurides is consistent with rifting followed by rift-related uplift, as seen in the Red Sea/Gulf of Aden region. The Triassic sediments were later transgressed by Jurassic platform carbonates, indicative of passive margin subsidence. The pulse of rift-related uplift was prior to, or during, final continental break-up to form northern Neotethyan ocean to the north.

8) No evidence has been found to support a previous hypothesis that a Palaeotethyan ocean finally closed in this area during the latest Triassic with emplacement of an Eurasian margin unit over a Gondwana-related ("Cimmerian") units. Instead, the evidence is consistent with Tethyan rifting during the Triassic.

5 Structural and emplacement history of the Tauride platform

5.1 Introduction

This chapter will investigate the emplacement of the Beyşehir-Hoyran-Hadim nappes, and the structural history of the Tauride platform. It has been documented that the thrust sheets were emplaced in Late Cretaceous – Early Cenozoic (Monod, 1977; Özgül, 1984; Andrew and Robertson, 2002). However, when carrying out detailed structural and sedimentological analysis of different autochthonous and allochthonous units, as in this study, extreme care must be taken to restore the components of the platform and rifted-margin back to their original pre-Cretaceous palinspastic setting.

Understanding the platform response to thrusting is important when interpreting stratigraphic relationships in the study area, including the identification and distinction between passive margin type sediments and syn-tectonic sediments. This also provides crucial new insight to the Late Cretaceous and Cenozoic tectonic setting of the Tauride platform, and the timing of closure of the Neo-Tethyan ocean. Furthermore, it increases our knowledge of collisional tectonic events.

The tectono-stratigraphic framework of the central Tauride mountains was discussed in chapter 2. The nappe stacking order in the northerly study area is not as complex as that in the south, but nevertheless requires careful consideration. This chapter takes each area separately and combines the results in the discussion. New data presented, largely for the Hadim and Bolkar nappe, follows on and develops previous work on the distal margin units of the study area (Andrew and Robertson, 2002). A summary of the distribution of the autochthonous and allochthonous units is shown in Fig. 5.1.

This chapter will test a previous structural model (Özgül, 1984) that was proposed for the Upper Cretaceous – Lower Cenozoic. In this model, the Beyşehir-Hoyran-Hadim nappes were restored based on in-sequence thrusting (further description of the model is given in section 5.4.2). This study will test this existing model through an integrated study of sedimentary and structural data.

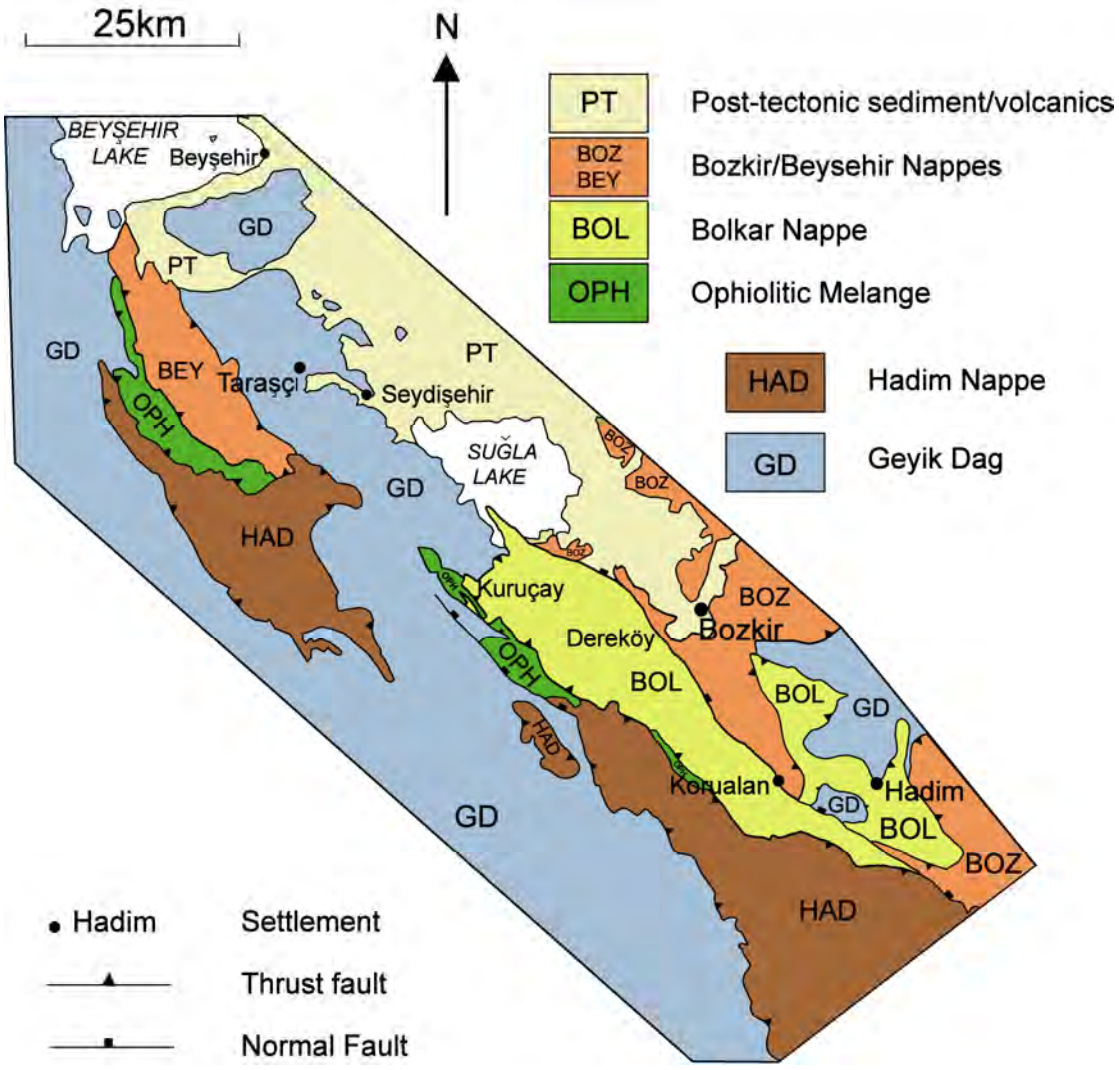

Fig. 5.1. Simplified tectonic map of the area studied, showing the distribution of the regional autochthon (Geyik Dağ) and the allochthonous tectonic units (Hadim, Bolkar, Bozkir/Beyşehir, and ophiolitic nappes) that are discussed in this chapter.

5.2 Thin-skinned vs. thick-skinned tectonics

Different emplacement styles have been suggested to explain variations in thrusting observed at compressional former passive margins. In many cases, as we shall see, not one process, but a combination of different processes operate at different times relating

to large-scale ophiolite obduction and nappe emplacement at continental margins. In the case of the Beyşehir-Hoyran-Hadim nappes, it has been documented that two phases of thrusting have occurred: (i) ophiolite obduction and emplacement of distal margin units took place in the Late Cretaceous; (ii) rethrusting of the ophiolite and distal margin units, along with emplacement of parts of the platform, occurred in the Early Cenozoic (Robertson, 2006a). As a result of this re-thrusting, the processes by which the ophiolite was initially emplaced are difficult to interpret. There are two well-documented styles of thrusting: thin-skinned and thick-skinned tectonics.

5.2.1 Thin-skinned tectonics

Thin-skinned tectonics in collisional zones occur when the basal / sole thrust is detached from the basement, allowing thrust faults to propagate at shallow depths, whilst the basement remains relatively undeformed (Coward, 1983; Park, 1988) (Fig. 5.2). The sedimentary cover and / or extrusive and near-surface volcanic and plutonic rocks, are involved in compressional faulting and tectonic thickening; however, the stronger crystalline basement is not cut by thrusts.

Thin-skinned thrust systems are shallow-rooted, and faults typically have a listric geometry, which flattens out at relatively shallow levels. These faults are thought to sole out on a 'decoupling horizon' which is linked to the origin of the thrust movement (Coward, 1983). Thrust faults emplace older and structurally lower material above younger and structurally higher material, along a series of ramps and flats (Park, 1988). The build up of stress at ramp-flat junctions causes resistance, and eventually a new fault propagates forward, carrying with it a now passive thrust fault in a piggy-back style. A series of active and passive thrust faults build up as a thrust wedge, otherwise known as a duplex structure. A combination of these duplex structures form classic thin-skinned thrust belts, for example the Rocky Mountains (Fig. 5.2, 2nd diagram). The basal thrust of a thin-skinned tectonic belt commonly occurs along a relatively weak horizon within the stratigraphic sequence (i.e. a décollement), such as a shale or evaporate layer, or a metamorphic boundary (Coward, 1983; Twiss and Moores, 1992). On a smaller scale, this weak horizon could be a bedding plane (Coward, 1983).

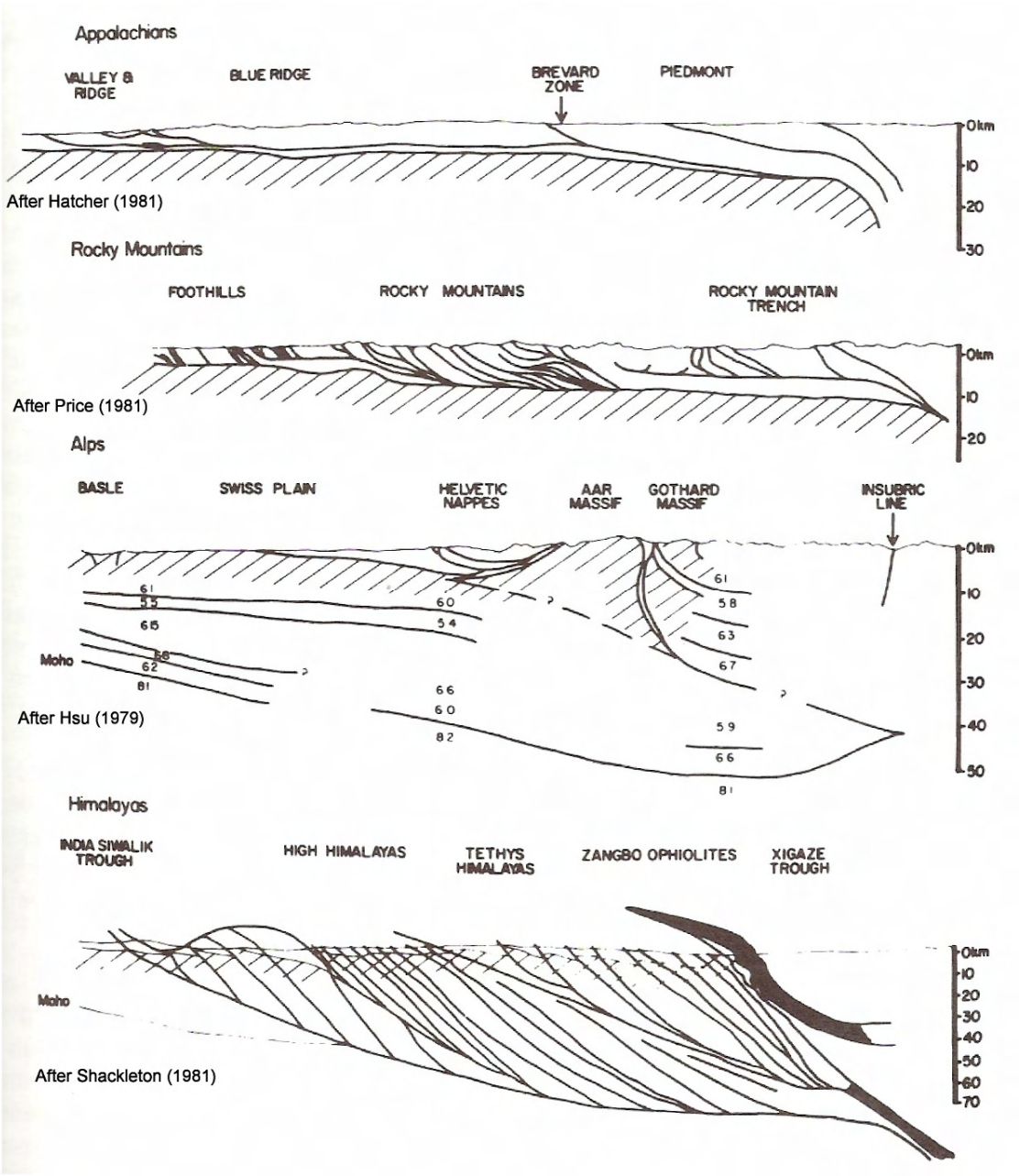

Fig. 5.2. Profile through 4 different thrust stacks showing thin-skinned tectonics (top two diagrams) and thick-skinned tectonics (bottom two diagrams). Figure taken directly from Park (1988), diagram originally produced in Soper and Barber (1982).

Thin-skinned tectonics are adequate at explaining the shortening of relatively shallow 'cover' within an orogenic belt; however, this does not account for shortening of the basement, and how displacement is accommodated in the lower crust and mantle lithosphere (Park, 1988).

5.2.2 Thick-skinned tectonics

Thick-skinned tectonics require basal thrust faults to propagate through crystalline basement towards the base of the crust (Park, 1988) (Fig. 5.2) . Rather than having a listric geometry, faults of thick-skinned systems are steeply dipping, and often planar in geometry. Thick-skinned tectonics involve nearly vertical faulting to significant depths, with very little horizontal displacement (Coward, 1983). However the term 'thick-skinned' may be used to imply the relative thickness of the fold and thrust zone, and whether or not it affects the crystalline basement.

Thick-skinned tectonics are involved in certain orogenic belts (e.g. Alps and Himalayas) to explain the exhumation of deep crustal rocks to the surface (Coward, 1983; Park, 1988). One possibility is that steeply dipping thrust faults act as a link between shallow-dipping or flat décollement horizons, and that a combination of shallow and steep faults transfer material from low to high levels within a thrust system (Mattauer, 1986). The energy required in thrusting is largely to combat gravity, in the processes of material uplift, resistance along the fault plane, or intra-rock strain (Coward, 1983). As a consequence, less energy is required in gently dipping, thin-skinned tectonic systems (e.g. foreland fold and thrust belts) than in steeply dipping thrust faults in a thick-skinned tectonic system (Coward, 1983). Steeply dipping faults that cut the basement are seen in recent seismic investigation of the Zagros folded belt (Mouthereau et al., 2007). In the same region, mid-crustal seismic activity in the Fars Arc provide strong evidence of basement deformation (Leturmy et al., 2007). An integrated petrological, structural and geodynamic study of the Zagros orogeny suggests that the main Zagros thrust is deep-rooted, possibly to Moho depths (Agard et al., 2007).

5.2.3 Combination of thin- and thick-skinned tectonics

Recently it has been appreciated that complex orogenic belts can be formed from a combination of thin- and thick-skinned tectonics (Calabrò et al., 2003; Molinaro et al., 2005). For example, in the Zagros fold-thrust belt, large scale folds and thrusts deform the Arabian shelf, which acts as a thin-skinned horizon above 'basement' (Molinaro et al., 2005). However, it is also documented that large scale reverse faults cut the pan-African basement, indicative of thick-skinned tectonics (Jackson and Fitch, 1981). A recent seismic investigation of the Zagros folded belt shows that active reverse faults cut down through the 'basement', and accommodate much of the shortening within the fold and thrust belt (Mouthereau et al., 2007). A study of the Fars Arc found that intense mid-crustal seismic activity was a consequence of basement deformation (Leturmy et al., 2007). The current thick-skinned deformation of the Zagros fold and thrust belt succeeded thin-skinned tectonics, illustrated by interference patterns which show early detachment folds are cut by younger oblique basement faults (Leturmy et al., 2007).

5.3 Alternative models of Beyşehir-Hoyran-Hadim nappe emplacement

Along with contrasting styles of tectonic regime (as documented above), it is also necessary to consider the continuing development of the thrust stack, which is especially significant during multi-phase thrusting. Typically, emplaced margins, as in the Tethyan realm, have been restored assuming in-sequence thrusting, which involves the restoration of higher thrust sheets to more distal locations within the margin (e.g. SW Turkey) (Robertson, 1993). However, recent work (Andrew and Robertson, 2002) shows that out-of-sequence thrusting is important in the restoration of the Central Tauride nappe stack. Elsewhere in the Tethyan region, out-of-sequence thrusting is also thought to be an important process, for example, in Oman, where deep-rooted continental margin rocks were exhumed during ophiolite obduction (Searle and Cox, 1999).

5.3.1 In-sequence

In-sequence thrusting is characterised by continual propagation of fault splays and ramps/flats into the footwall block, towards the foreland (Twiss and Moores, 1992), and is regarded as being the 'normal' style of faulting within a fold and thrust belt (Morley, 1988). Older rocks are emplaced on top of younger rocks during this process. An example of a thrust stack in the early stages of in-sequence thrusting is shown in Fig. 5.3a.

Within an in-sequence thrust belt, faults located close to the overriding plate are older than faults located close to the foreland, and there is a progressive younging of faults towards the foreland. Faults that are shallower in the thrust stack are also older in relation to faults towards the base of a thrust stack. The decrease in age of faulting and associated deformation towards the footwall block can be referred to as 'prograding deformation' (Twiss and Moores, 1992). This process commonly incorporates a syn-tectonic sedimentary foreland basin into the thrust stack, as the weaker sedimentary rocks act as an easy-slip horizon (e.g. Alpine and Apennine forelands).

5.3.2 Out-of-sequence

Out-of-sequence thrusting, in contrast, occurs when new faults develop towards the orogenic belt in the hanging wall, away from the foreland (Morley, 1988; Twiss and Moores, 1992). Out-of-sequence thrusting is not as common as in-sequence thrusting. During this process, younger rocks, which have originally been overthrust by older rocks, are re-thrust into higher structural positions (i.e. younger units on top of older units). An example of out-of-sequence thrusting is shown in Fig. 5.3b and Fig. 5.3c. In Fig. 5.3b, an in-sequence duplex thrust system is sandwiched between an older floor-thrust at the base and a younger roof-thrust at the top. The roof-thrust is the youngest fault, and a typical thrust scenario exists whereby older units are emplaced over younger units. Reactivation of a thrust within the duplex results in a new fault propagating through an overlying thrust sheet. In Fig. 5.3c, a new fault has emplaced the youngest thrust sheets (originally at the bottom of the nappe stack) into a structurally higher

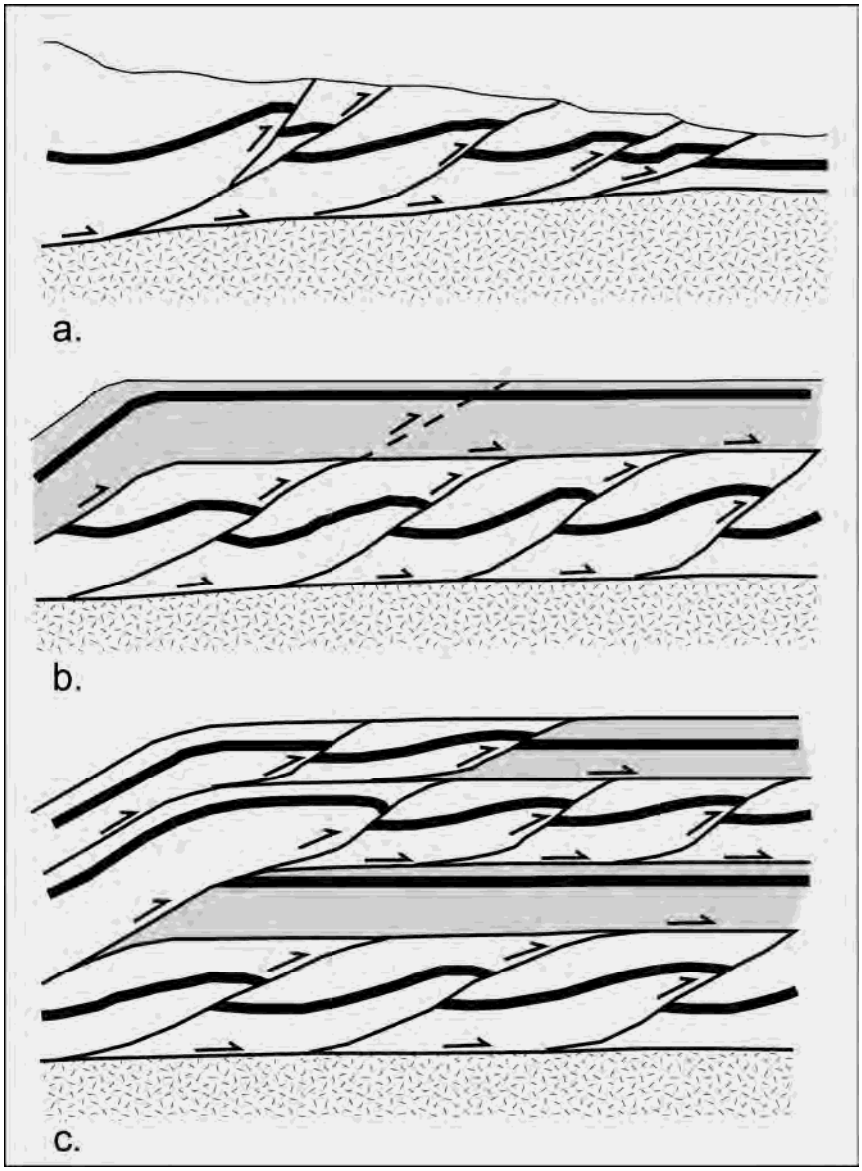

Fig. 5.3. a. Development of a thrust stack in its early stages by an in-sequence thrusting regime, and development of an imbricate thrust fan; b. A duplex thrust system whereby an older fault within the duplex is reactivated, and propagates through a younger overthrust; c. Significant thickening of thrust stack during out-of-sequence thrusting. Younger rocks, originally at the base of the stack, are re-thrust to higher structural positions.

position, resulting in younger units overlying older units. Also, significant re-thrusting of the older units has occurred in an out-of sequence fashion. In this scenario, out-of-sequence thrusting results in considerable thickening of the thrust stack.

During out-of-sequence thrusting, faults closer to the orogen are younger than those closer to the foreland. However, in-sequence propagation may be occurring simultaneously, and it is difficult to constrain fault ages due to their position in the thrust stack alone. Typically, out-of-sequence thrusts are formed by reactivation of older thrusts (as in Fig. 5.3), or through development of new faults in an already deformed thrust stack (Morley, 1988). The development of such thrusts may be as a result of pressure build-up within the thrust stack. Another possibility is that out-of-sequence thrusting occurs as a response to a change from thin- to thick-skinned tectonics.

5.4 Previous work

Structural interpretations of the Beyşehir-Hoyran-Hadim nappes were previously given by Monod (1977), Gutnic et al. (1979), Özgül (1976, 1983, 1984), MTA (2002), and most recently by Andrew (2003) and Andrew & Robertson (2002). A structural interpretation of the relatively autochthonous Geyik Dağ was also produced for the Beyşehir region (Monod & Akay, 1984). A review of previous studies is presented below.

5.4.1 Northern part of study area

The first recognition of the Beyşehir-Hoyran-Hadim nappes in the northerly study area resulted in a 1:200,000 scale map by Blumenthal (1947), with other works by the same author in the Beyşehir – Seydişehir region (Blumenthal, 1951; Blumenthal, 1956; Blumenthal, 1960-1963). The first detailed study of the nappe stack was by Monod (1977) who produced a 1:10,000 scale map of the region. Regional structural aspects were discussed by Gutnic et al. (1979). The initial work, particularly by Monod (1977), provided a regional stratigraphic and structural framework; however, the origin and regional geological context of the nappes was not discussed in detail. A more up-to-date 1:250,000 scale geological map of the region was published by the MTA (1997), but without explaining text.

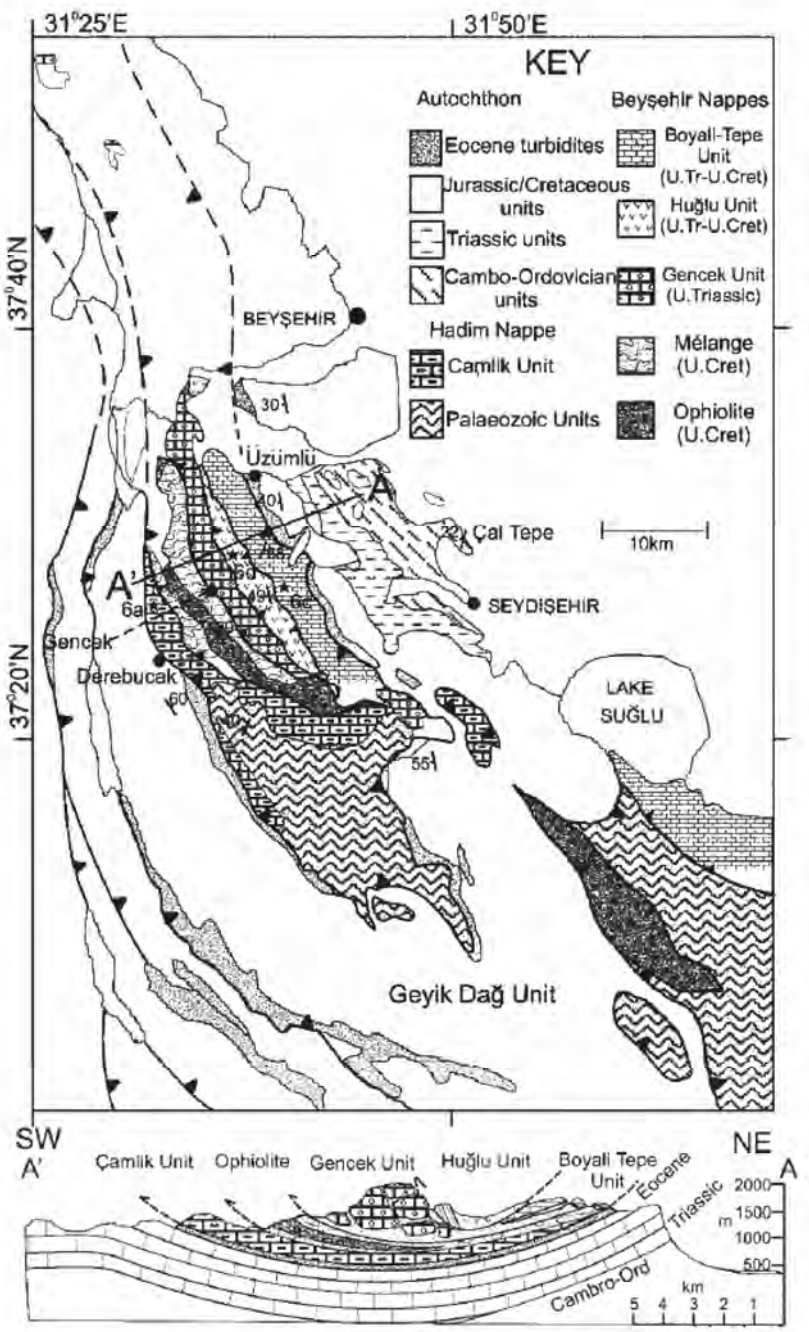

Fig. 5.4. Structural map and cross-section through the Beyşehir-Hoyran Hadim nappes near the towns of Beyşehir and Seydişehir. Note that in the cross-section, the Hadim nappe is represented by the Çamlik unit, and is at the lowest structural position within the thrust stack. Diagram from Andrew (2003).

Recent studies by Andrew (2003) and Andrew & Robertson (2002) provided extensive new information on the tectono-stratigraphic framework and the regional context of the Beyşehir-Hoyran-Hadim nappes. An excellent summary map and cross section through the nappe stack was given by Andrew (2003), as shown in Fig. 5.4. A summary of the nappe stacking order is shown in Fig. 5.5. Andrew (2003) concluded that there was evidence for three stages of deformation and emplacement of the Beyşehir-Hoyran-Hadim nappes:

First, compression during the Late Cretaceous emplaced the Gençek unit, Boyali-Tepe unit, Huğlu unit and the Ophiolitic Melange unit southwards onto the submerged Hadim nappe during Maastrichtian time. The Geyik Dağ unit was inferred to be further south and was not affected by the emplacement. The Upper Cretaceous allochthonous units are thought to be oceanic or distal margin in origin.

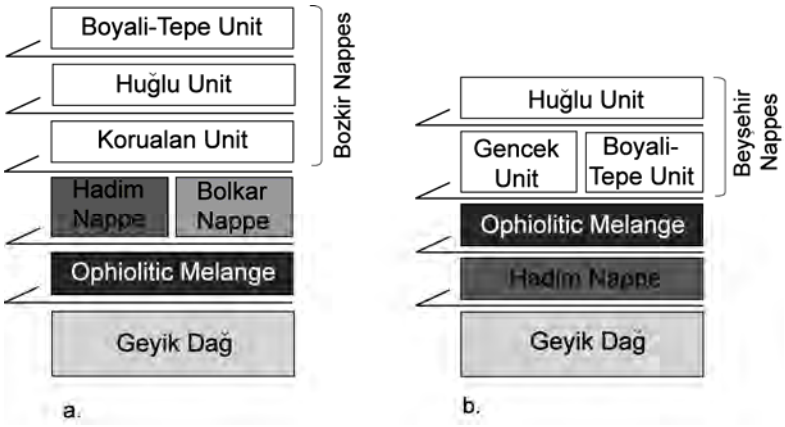

Fig. 5.5. Schematic representation of the nappe stacking area. a. Southerly study area near the towns of Hadim and Bozkir. b. Northerly study area near the towns of Beyşehir and Seydişehir.

Second, during the Early Tertiary, the Geyik Dağ autochthon experienced subsidence and collapse, represented by foredeep sediment accumulation during the Palaeocene to Lower / Middle Eocene. Emplacement of the Hadim nappe (part of the continental platform) occurred in the Middle Eocene, along with the allochthonous units emplaced during the Late Cretaceous. Andrew & Robertson (2002) conclude that the distal margin and ophiolitic units were emplaced by out-of-sequence thrusting. The final

stage of deformation described by Andrew (2003) was Miocene and younger Neotectonic extensional faulting.

It should be noted here that work on the ophiolitic melange unit was carried out previously by Andrew (2003), and it is not the intention here to study the stratigraphy or geochemistry of this unit in any further detail.

5.4.2 Southern part of study area

The first mapping and identification of structural units in the southerly study area was carried out by Blumenthal (1947, 1951, 1956, 1960-1963). The most detailed identification of allochthonous units, focusing mainly on detailed stratigraphy, was carried out by Özgül (1976, 1983, 1984, 1997). A geological map of the area was produced by the MTA (1997), and the most recent work on the tectono-stratigraphy of the area was completed by Andrew (2003) and Andrew & Robertson (2002). Only a basic structural map and cross-section through the nappe stack within the southern study area has previously been published, as shown in Fig. 5.6 (Özgül, 1976).

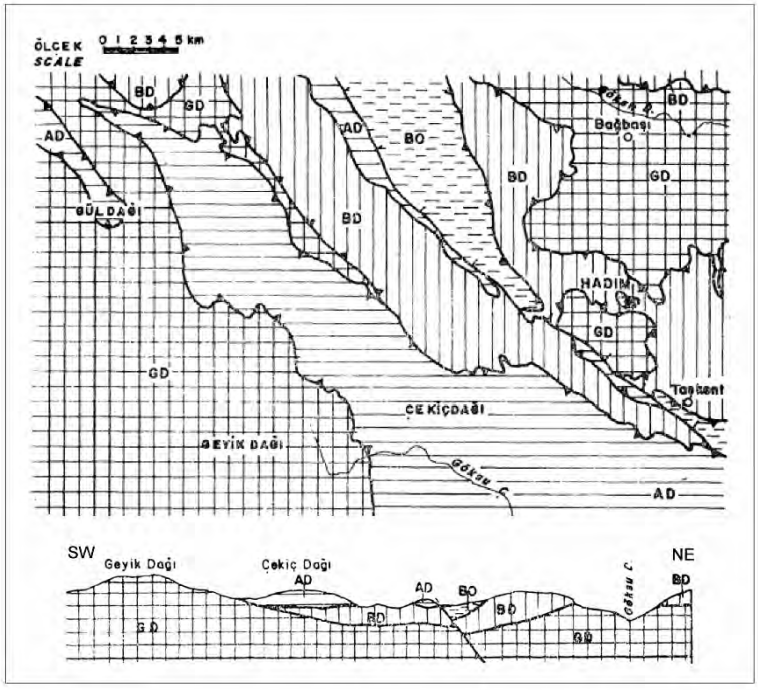

Fig. 5.6. Tectonic map and cross section of the area near the town of Hadim. Image from Özgül (1976).

The new information and cross-sections produced during this study suggest that the tectonic relationships are not as straightforward as previously assumed. A summary of the nappe stacking order is shown in Fig. 5.5a. Özgül (1984) introduced a model for nappe emplacement in the region which began with Upper Cretaceous emplacement of the Bozkir unit southwards onto the Bolkar unit and the Hadim unit (Fig. 5.7 - 1). A new oceanic basin (Dipsiz Göl) is then proposed to have formed in between the Geyik Dağ and Hadim unit during Late Senonian to Palaeocene time (Fig. 5.7 - 2). A second episode of compression during the Eocene (Ypresian – Lutetian) then sutured the inferred Dipsiz Göl basin, and emplaced it southwards onto the autochthonous Geyik Dağ platform, along with the Hadim, Bolkar and tectonically overlying Bozkir units (Fig. 5.7 - 3). This model assumes an in-sequence style of thrusting.

There are, however, problems with the supposed presence of the Dipsiz Göl oceanic basin. The model requires a rifted margin to have existed along the northern margin of the Geyik Dağ, and along the southern margin of the Hadim nappe, both during the Upper Cretaceous – Palaeocene. There is, however, no field evidence of these rifted margins (Andrew, 2003). The model also suggests that the Bozkir nappes were thrust southwards onto the Hadim unit during the Upper Cretaceous, but this structural relationship is not observed in the field. Finally, Özgül's model (1984) implies that the Dipsiz Göl ophiolite unit is at the base of the nappe stack, but in the Beyşehir region the Ophiolitic Melange tectonically overlies the Hadim nappe.

The recent work by Andrew (2003) and Andrew & Robertson (2002) infers a similar emplacement history to that documented above for the northerly study area: ophiolitic and distal margin units are emplaced in the Late Cretaceous; the Hadim and Bolkar units, plus the Late Cretaceous allochthonous units, are emplaced in the Early Tertiary. These authors inferred that the ophiolite, including the 'Dipsiz Göl' ophiolite formed in an oceanic supra-subduction zone setting followed by the Cretaceous emplacement onto the northern edge of the Tauride continental margin. Andrew & Robertson (2002) further inferred that the ophiolitic and distal margin units were finally emplaced by out-of-sequence thrusting during Early Cenozoic time (Middle Eocene).

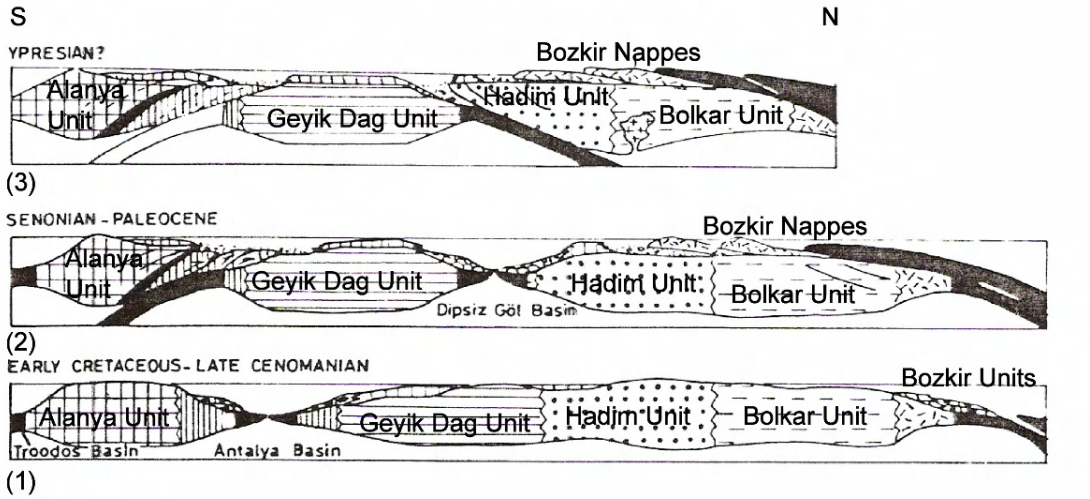

Fig. 5.7. Structural model of the tectonic evolution of the Central Taurides by Özgül (1984). Original diagram modified to highlight unit distribution.

Previous work in the both the northerly and southerly study areas left several key issues still to be resolved: (i) Were the Hadim and Bolkar nappes emplaced by in-sequence or out-of-sequence thrusting?; (ii) What is the reason for the difference in nappe stacking order between the northerly and southerly areas?; (iii) Where in the original rifted margin do the Hadim and Bolkar units restore palinspastically? The remainder of this chapter will attempt to answer these key questions.

5.5 Cross-sections through the nappe stack

The cross-sectional profile in the northerly study area, constructed by Andrew (2003) (Fig. 5.4), was field checked during this study. No reason was found to change or modify this cross-sectional interpretation of the nappe stacking order. The Hadim nappe, a tectonic unit composed of platform lithologies, is the lowermost allochthonous unit, and is emplaced directly onto the autochthonous Geyik Dağ (Fig. 5.4, Fig. 5.5). It is tectonically overridden by the ophiolitic melange unit, in turn overlain by the allochthonous Beyşehir nappes which are composed of distal margin lithologies.

The review of previous work in the area (section 5.4) indicated that the structural geology of the southerly study area has not been documented in such great detail. During this study, a series of traverses through the nappe stack were made in an attempt to clarify the regional structure.

A simplified tectonic map was constructed between the towns of Bozkir and Hadim using a recent geological map of the area (MTA, 2002) as a base map (Fig. 5.8). Traverses through the nappe stack focused particularly on contacts between different tectonic units, and the internal style and deformation observed. Five cross-sections through the nappe stack are documented in Fig. 5.9.

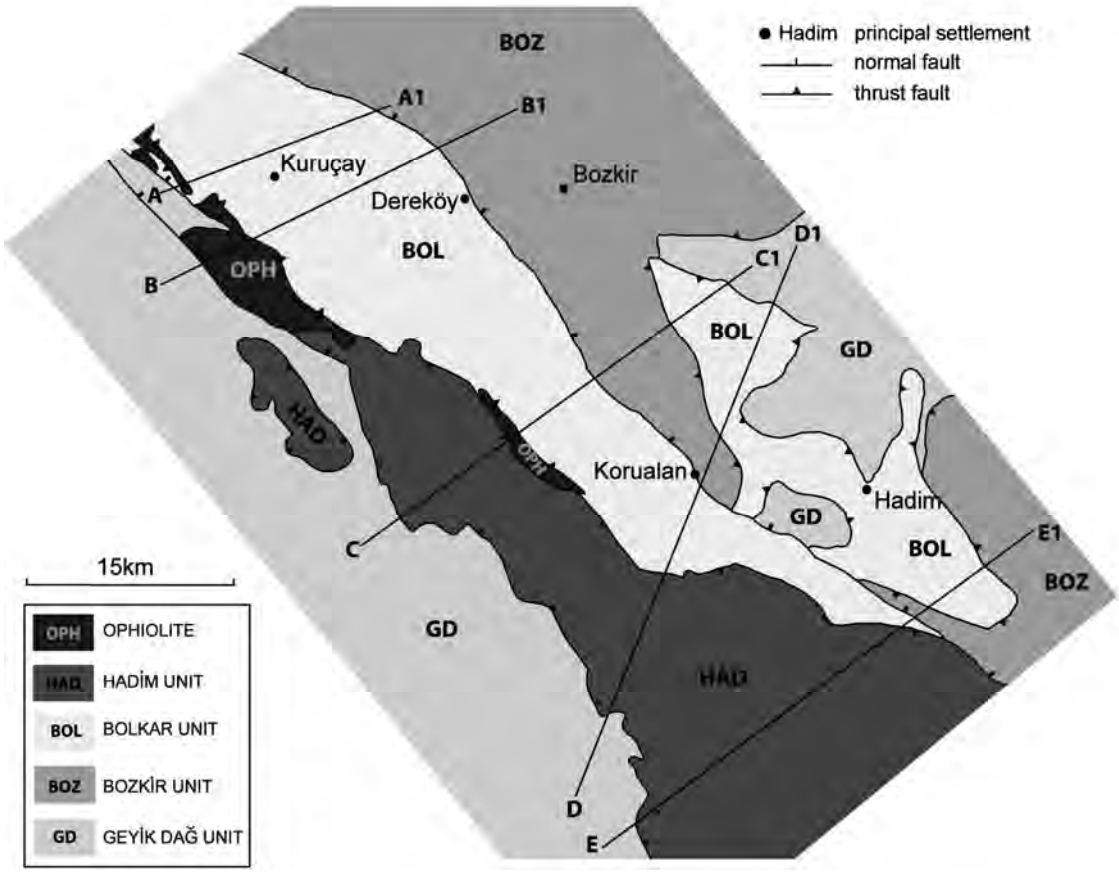

Fig. 5.8. Simplified tectonic map of the study area near the towns of Bozkir and Hadim. Lines of cross-section highlighted on this map are shown in Fig. 5.9.

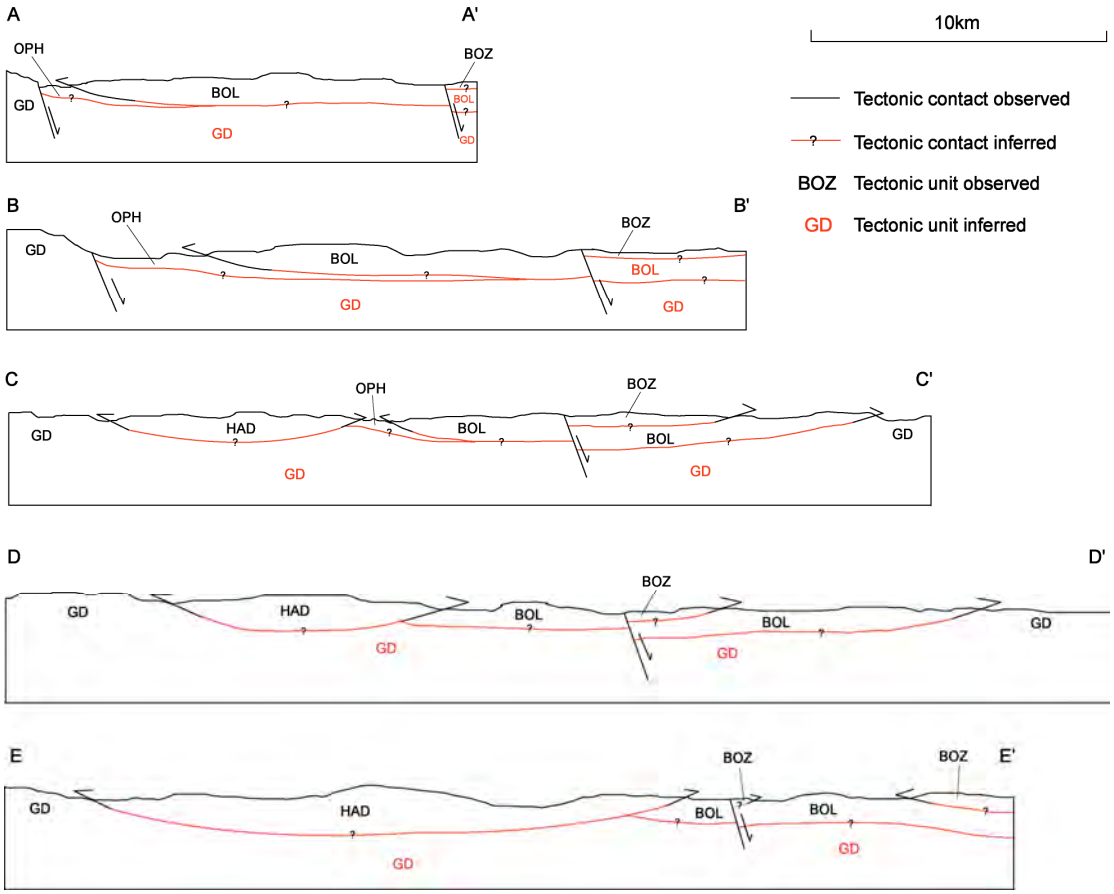

Fig. 5.9. Cross-sectional profiles through the nappe stack along the lines of section marked in Fig. 5.8. GD = Geyik Dağ; HAD = Hadim nappe; BOL = Bolkar nappe; BOZ = Bozkir nappes; OPH = ophiolitic melange. Note - lines/symbols in red are inferred, whilst those in black were observed in the field. Thrust barbs do not necessarily show direction of emplacement, but rather which unit is in the higher structural position.

From the observed tectonic contacts, a number of key relationships can be determined: (i) where present, the ophiolitic melange unit is at the bottom of the nappe stack, and is tectonically overlain by the Bolkar nappe and the Hadim nappe; (ii) where the Hadim and Bolkar nappes are in contact, the Hadim nappe is in a higher structural position; (iii) the Hadim nappe and Bolkar nappe are both seen to tectonically overlie the Geyik Dağ autochthon; (iv) the Bozkir nappes are always at the highest structural position, and are seen to overlie the Bolkar nappe; (v) a large normal fault, with a hanging wall to the northeast, is seen on all of the cross-sections and postdates the emplacement of the Hadim, Bolkar and Bozkir nappes.

Inferred contacts on the cross-sections are marked in red. In cross-section B-B', there is a possibility that the ophiolitic melange may actually be part of the Geyik Dag stratigraphy. However, as will be shown later in the chapter, there is no structural or sedimentological evidence to suggest that an ophiolite was emplaced directly onto the Geyik Dağ, and that the present relationship between the ophiolitic melange and the autochthon must be tectonic. These inferred contacts suggests that: (i) the ophiolitic melange unit, where present, appears to tectonically overlie the Geyik Dağ unit; (ii) the ophiolitic melange unit is laterally discontinuous, and localised within the nappe stack.

A number of key questions regarding the nappe stacking order arise from these cross-sections. Firstly, which tectonic unit underlies the ophiolitic melange unit? The sole of the ophiolitic nappe is not seen within the study area, and its distribution is somewhat limited. In cross section A-A', the ophiolitic melange unit is in the hanging wall of a normal fault which has an unknown amount of throw on it. The simplest restoration of this is that the ophiolitic unit tectonically overlies the Geyik Dağ autochthon. This tectonic relationship has not been documented elsewhere in the region, where there is no sedimentary or tectonic evidence to suggest that the ophiolitic unit was emplaced directly onto the Geyik Dağ. One possibility discussed later in this chapter is that the restoration of the ophiolitic melange and the Geyik Dağ platform relates to re-thrusting of the nappe stack (i.e. multi-phase thrusting).

It is also evident from the cross-section C-C' (Fig. 5.9) that the ophiolitic melange must be laterally discontinuous, as it would appear to be 'sandwiched' between the Geyik Dağ and the Bolkar / Hadim nappes in the southerly part of the cross-section; however, this ophiolite is absent at the same structural position in cross-sections D-D' and E-E'. There is also a fundamental question as to why the ophiolitic melange is at the base of the nappe stack in the southerly study area, whilst the Hadim nappe is the lowermost allochthonous unit in the northern study area.

Secondly, what is the relationship between the Hadim and Bolkar nappes? In cross-section C-C', the most obvious reconstruction is that the two units are part of a single allochthonous unit that has been locally folded into an anticline, with the

ophiolitic melange in the core of the anticline. However, in cross-sections D-D' and E-E', the Hadim nappe is clearly in a higher structural position, the contact of which is shown in Fig. 5.10. Regional tectonic evidence suggests that the nappes were all emplaced from the north/northeast to south/southwest (Monod, 1977; Özgül, 1984; Andrew, 2003), which leaves two possibilities: (i) that the Hadim nappe was always in a more southerly position, and that it has been back-thrust to its current position above the Bolkar nappe; (ii) the Hadim nappe was originally in a more northerly position, and has been thrust southwards over the top of the entire nappe stack (including the Bolkar nappe) to the current position. These questions will be addressed in subsequent sections of this chapter.

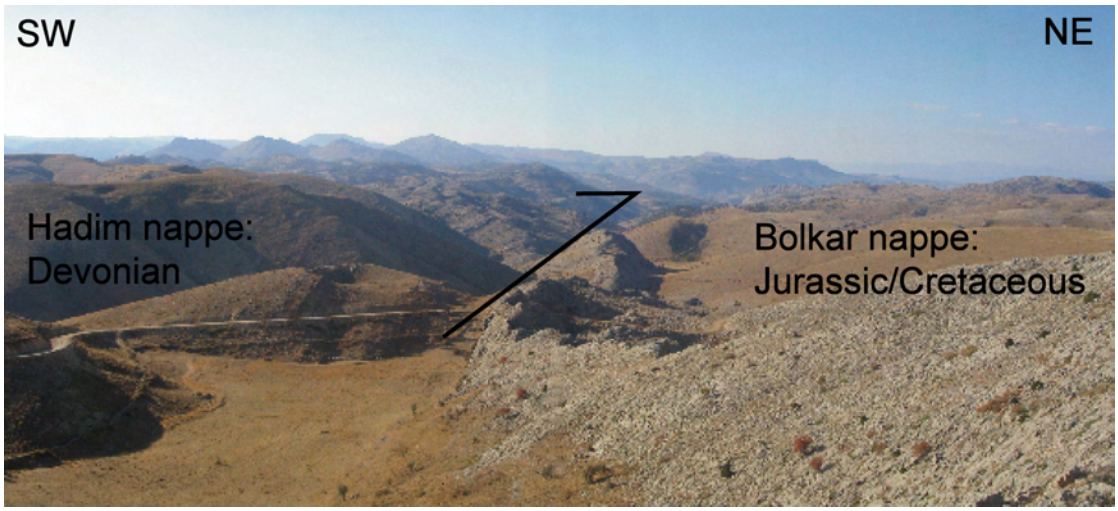

Fig. 5.10. Contact between the Hadim nappe and Bolkar nappe at the Ekinlik Yayla locality.

5.6 Regional structural trends

In the remainder of this chapter, each tectonostratigraphic unit will be described in detail, focusing on the degree and timing of deformation, structural data, and sedimentological characteristics. As the cross-sections through the nappe stack demonstrate (section 5.5), local tectonic contacts are critical in order to interpret the timing and nature of emplacement and structural evolution of the Tauride platform.

However, firstly it is worthwhile briefly introducing the regional trends within the study area before focusing on specific structural features in more detail.

5.6.1 Degree and timing of deformation

Regional deformation of the Geyik Dağ and Beyşehir-Hoyran-Hadim nappes is related to the emplacement of nappe stack in the Late Cretaceous – Early Cenozoic (e.g. Andrew, 2003). During this study, there was a lack of evidence to suggest pre-Cretaceous deformation in the study area, as suggested by previous authors (Monod and Akay, 1984). The degree of deformation is regionally determined by, firstly, the competency of individual sedimentary facies. For example, thick-bedded and massive carbonates are typically deformed in a brittle manor (e.g. faulting), whilst thin-bedded shales and siliciclastics are deformed in a more ductile manor (e.g. folding, shearing). Secondly, deformation is more intense adjacent to tectonic contacts, in particular the boundaries of regional allochthonous units. Zones of tectonic imbrication, found within individual nappes, are also intensely deformed. Finally, the northerly part of the study area is generally found to be more heavily deformed than in the south. This is attributed to the emplacement of the nappe stack from north to south, as suggested by previous authors (e.g. Andrew, 2003).

5.6.2 Structural data

Structural data, in particular fault planes and fold axial planes, were collected from throughout the study region. Data from individual localities will be discussed in section 5.8. However, Fig. 5.11 shows the combined data from regional tectonic contacts in the study area. Fault plane orientations are variable, however the dominant structural trend is NNW-SSE (Fig. 5.11a). Fold axial plane orientations are less variable, and show a strong WNW-ESE trend, indicating regional shortening on a N-S axis. The fold axial planes are consistent with emplacement of the nappes from north to south (e.g. Monod, 1977; Özgül 1984). It is likely that the fault data includes faults which are not related to

nappe emplacement (e.g. neotectonic faults); nevertheless, these data are consistent with the regional NW-SE orientation of the nappe stack (Fig. 5.1).

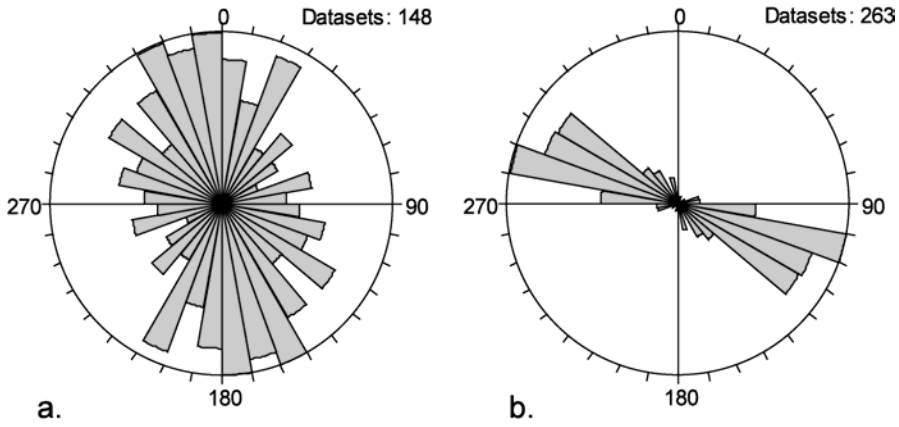

Fig. 5.11. a. Fault plane orientation from regional tectonic contacts in the study area. b. Fold axial plane orientations from regional tectonic contacts in the study area.

5.6.3 Sedimentology

Syn-tectonic sediments throughout the study area record the timing of nappe emplacement. Sediments were deposited in foredeep basins which developed ahead of the advancing nappe stack, and typically contain sediment that is derived from the overriding allochthonous units. Microfossils recovered from these sediments indicate that there were two phases of nappe emplacement, Late Cretaceous (Campanian – Maastrichtian) and Early Cenozoic (Palaeocene – Eocene). Sedimentary successions record the transition from low-energy shallow-water platform, to a higher energy hemi-pelagic and pelagic environment. The distribution of these sediments also helps to determine the direction of nappe emplacement, and will be discussed further in section 5.9.

The remainder of this chapter will discuss the local structural and sedimentological features in detail, which are critical to our understanding of the emplacement and structural evolution of the Tauride platform.

5.7 Degree and timing of deformation

The degree of deformation and metamorphism varies significantly between allochthonous and autochthonous Tauride platform units. This has implications for understanding the nature and timing of thrusting within the study area.

5.7.1 Geyik Dağ

Compression-related tectonics and deformation of Late Triassic age were in the past reported in the Geyik Dağ autochthon, especially near the towns of Beyşehir and Seydişehir (Monod and Akay, 1984). Several critical areas within the Central Taurides have been re-mapped in some detail (Fig. 5.12). The significance of these localities are also discussed in Appendix A, which is a manuscript for submission based on work presented here and in chapter 4.

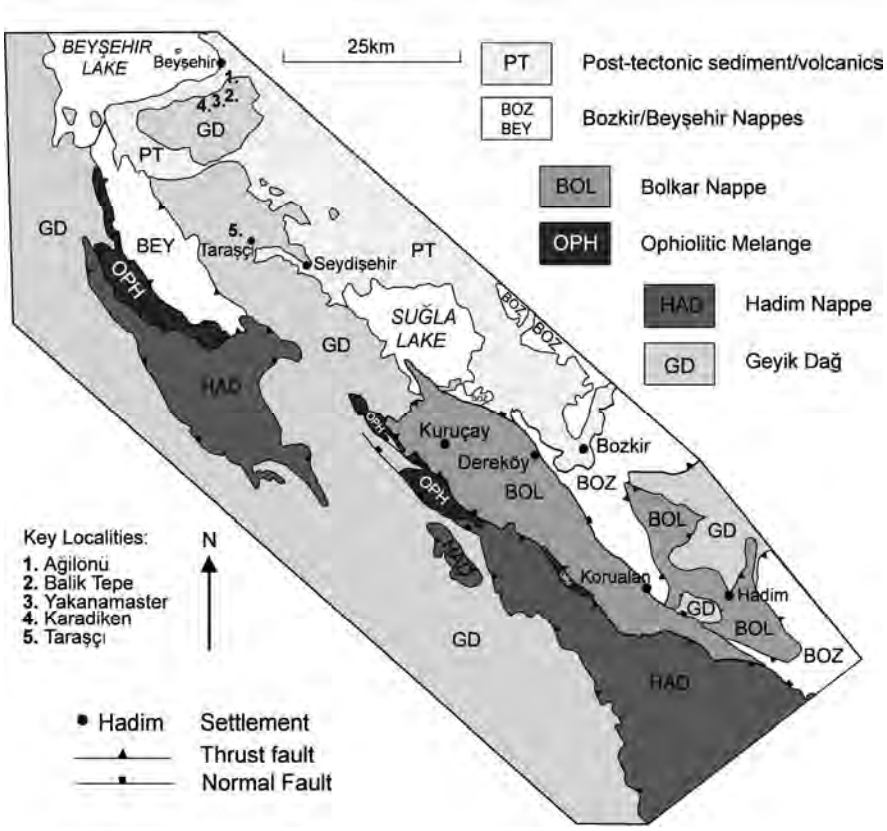

Fig. 5.12. Simplified structural map of the study area with key localities marked.

5.7.1.1 Locality 1: Ağılönü village (Fig. 5.12, Fig. 5.13a and b), GPS reference: 388500 4167500

The village of Ağılönü lies ~3 km south-east of Beyşehir within the autochthonous Geyik Dağ unit (Fig. 5.12, Fig. 5.13a and b). The stratigraphy consists of Cambrian dolomites (Çal Tepe Formation; Monod, 1977) and Ordovician shales (Seydişehir Formation; Monod, 1977), overlain by Jurassic siliciclastics and neritic carbonates (Sarakmana Limestone; Monod, 1977; Fig. 5.13c). The Cambrian sediments are medium to thick bedded, heavily recrystallised, nodular and beige-grey in colour. Locally, the succession dips gently towards the east (Fig. 5.13a, b, d). The dolomites are sheared and locally brecciated, especially near the contact with the overlying Ordovician sediments. Numerous low-angle faults, possibly reverse faults, cut the succession. Few sedimentary features are preserved.

Ordovician shales (Seydişehir Formation) are best exposed in a small quarry adjacent to Agilönü access road, 1 km south of Beyşehir (Fig. 5.13a). The Ordovician succession is made up of strongly sheared, foliated and folded micaceous shales, typically intercalated with thinly bedded (5-15 cm thick) quartzitic sandstones (Fig. 5.13c). The shales consist of brown and purple horizons, alternating on a 4-5 m scale. Quartzitic sandstone horizons are locally up to 1 m thick. They show evidence of brittle deformation and the formation of phacoidal blocks (up to 1.2 m in size) indicating layer-parallel extension (Fig. 5.14a). Less deformed beds retain clear sedimentary structures including flute casts, grooves and prod marks. These deposits could be turbidites, or possibly storm deposits. Trilobites found in the Seydişehir Formation elsewhere in the Taurides suggest the sedimentary setting is likely to be a continental shelf (Dean and Monod, 1990). Sedimentary structures preserved on the upper and lower surfaces of some beds indicate that parts of the succession have been overturned. The Ordovician units exhibit open parallel-folds on a 10-m scale, with axial planes trending NNW–SSE (Figs. Fig. 5.14b). The shales contain kink folds on a 5-10 cm scale.

Fold-vergence is predominantly to the west. Other deformation features in shales include normal and reverse faults with slickenside lineations (Fig. 5.14c), mineral

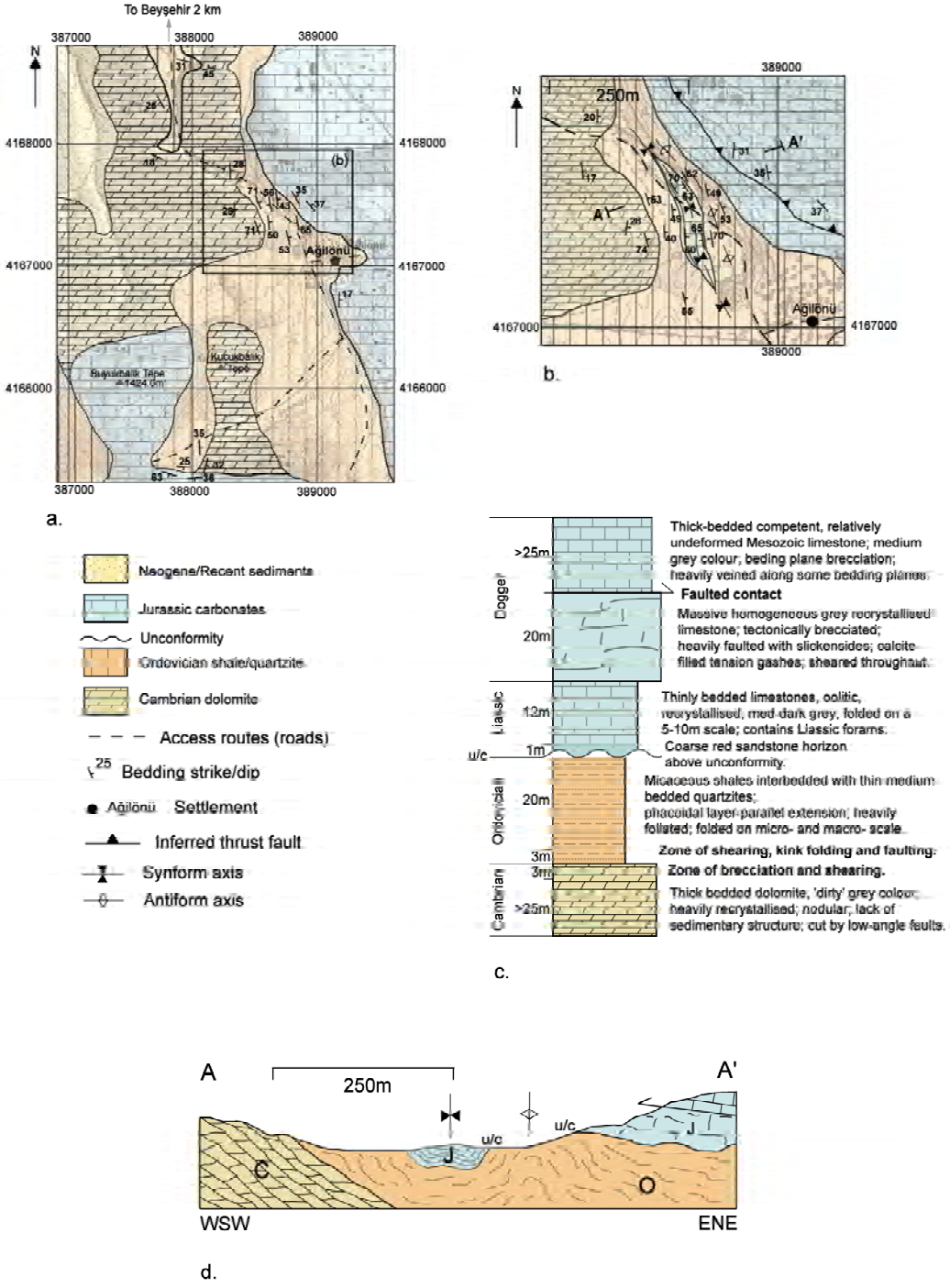

Fig. 5.13. a. Map of the Agilönü and Balik Tepe localities; b. Detailed map of the Agilönü locality; c. Simplified log showing stratigraphy at Agilönü; d. Cross-section A-A' through the Agilönü locality.

lineations interpreted as stretching lineations, and shear structures. All of the data display a dominantly NNW–SSE axial trend, implying ENE to WSW shortening when the fold vergence is taken into account (see section 5.8).

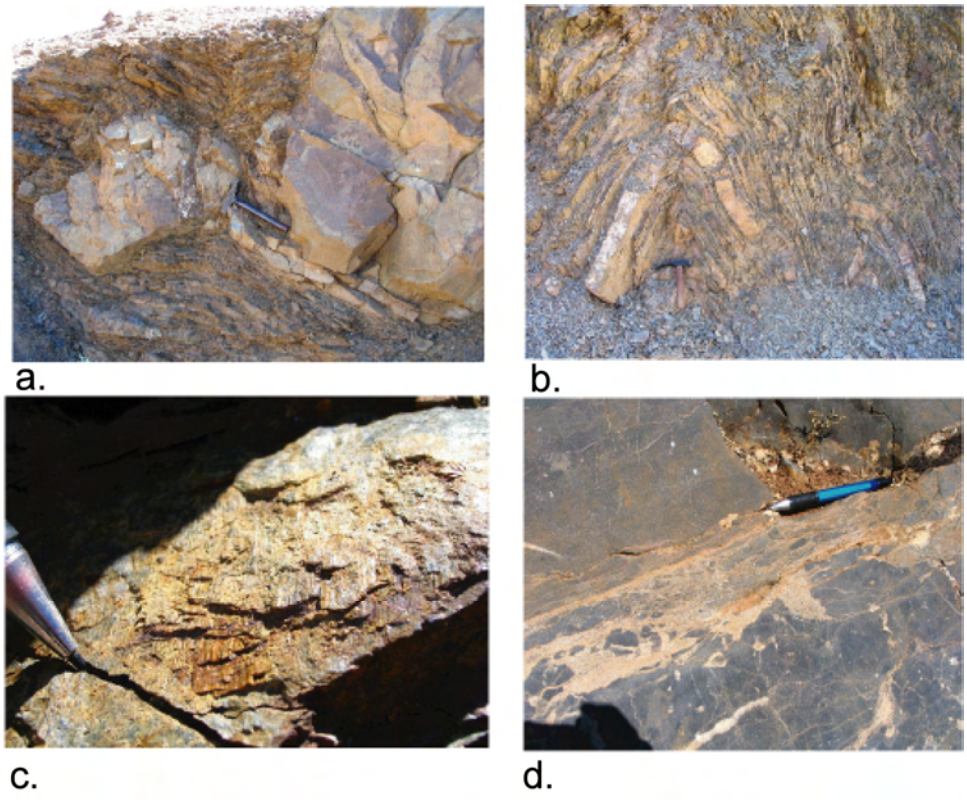

Fig. 5.14. a. Bedding parallel extension and formation of phacoidal sandstone blocks in Ordovician shale/quartzite succession at Agilönü locality; b. Ordovician shale/quartzites showing tight folding and deformation; c. Fault plane with slickensides within Ordovician shale/quartzites; d. Zone of tectonic brecciation within Middle Jurassic thick-bedded carbonates at the Agilönü locality.

The Ordovician sequence is locally tightly folded with a laterally discontinuous horizon of red quartzose sandstones and thin-bedded, recrystallised, medium-dark grey oolitic limestones (Fig. 5.13b, c). There is an abrupt change in lithology from shale-sandstone to oolitic limestone. Dating of benthic foraminifera (*Siphovalvulina variabilis* Septfontaine, *Amijiella amiji* [Henson], *Valvulina.* sp., *Thaumatoporella* parvovesiculifera [Raineri]) within the oolitic limestones indicates a Middle Liassic age, and confirms that a major unconformity exists between the Ordovician and Jurassic

successions, as in the Beyşehir - Seydişehir area generally (Monod, 1977). The uppermost part of the succession at this Agilönü locality is thick-bedded to massive, competent Mesozoic carbonate (Fig. 5.13c). The base of these carbonates (Sarakmana Limestone) was dated as "Lower Dogger" (Monod, 1977) and the succession as a whole was thought to be Jurassic (Monod and Akay, 1984). These units are in the topographically and structurally highest position within the mapping area (Fig. 5.13d). The lowermost carbonate beds have an irregular deformed contact with the underlying Ordovician sediments, above which the limestones are homogeneous. These are medium grey and heavily recrystallised, with few recognisable primary sedimentary features. Even bedding is barely recognisable in places. The limestones show strong structural deformation, including fault planes, bedding-parallel foliation, shear planes with associated small-scale folds, calcite-filled tension gashes, intense veining, bedding-parallel tectonic brecciation (Fig. 5.14d) and a weak boudinage.

Monod and Akay (1984) inferred that the Cambrian dolomites were thrust over the Ordovician shale/quartzite succession prior to the Jurassic, followed by erosion and transgression of the Jurassic Sarakmana Limestones. This would necessitate pre-Jurassic compression. However, the evidence can be interpreted differently.

Sedimentary structures within the Ordovician shale/quartzite succession show that the Cambro-Ordovician sequence has been tectonically inverted (overturned) in some places, whereas it remains the right way up in others (Fig. 5.13a, b, d). This is comparable with the relationships observed at Çal Tepe, near the town of Seydişehir (Monod, 1977) (Fig. 5.15).

The sharp planar nature of the contact between the Cambrian dolomite and the Ordovician shale/quartzite, together with associated tectonic brecciation and shearing adjacent to the contact, suggest that significant tectonic displacement has taken place between these two units. On the other hand, there is an absence of, for example, a basal conglomerate, or facies transition that would be expected along a stratigraphic unconformity.

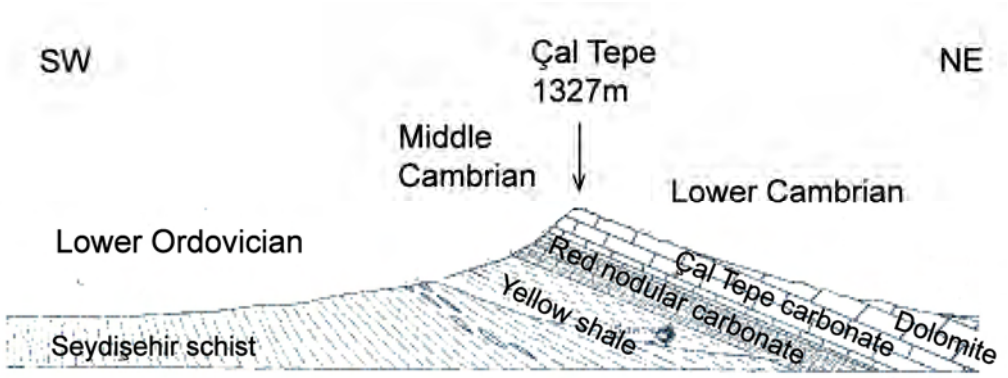

Fig. 5.15. Sketch showing the stratigraphic relationships at the Çal Tepe locality, near the town of Seydişehir. Reproduced from Monod, 1977.

The Ordovician sediments are unconformably overlain by thin-bedded Jurassic sandstones and oolitic limestones (Fig. 5.13c). Monod and Akay (1984) believed that the oldest Mesozoic rocks, of Middle Jurassic (Dogger) age, are represented by thick-bedded, to massive, units to the east of the study area (Fig. 5.13a–c). However, within the area mapped (Fig. 5.13a, b), limestones were found during this study to contain the Foraminifera *Siphovalvulina variabilis* Septfontaine, *Amijiella amiji* (Henson), *Valvulina.* sp., and *Thaumatoporella parvovesiculifera* (Raineri) of Middle Liassic age (N. İnan and K. Tasli, pers. comm., 2006). These Liassic sediments are folded and deformed to the same extent as nearby Ordovician sequences, suggesting that this deformation is younger than Liassic. Also, the contact between the Ordovician sequence and the Sarakmana Limestones is tectonic, as noted above, and both units exhibit very similar deformation (see section 5.8). The difference in competency between thick-bedded dolomites, thin-bedded shales/limestones, and massive to thick-bedded carbonates, has resulted in a variable style of deformation.

It can be inferred that the combined Cambrian – Jurassic sequence at locality 1 (Agilönü) experienced only one deformation event in post Early-Jurassic time that was related to Upper Cretaceous – Lower Cenozoic (Alpine) nappe emplacement. The Cambrian and Middle Jurassic carbonate units are deformed by brittle imbricate thrusting, with relatively little folding. By contrast, the Ordovician and Lower Jurassic

siliciclastic units were deformed in a more ductile fashion, with intense folding accommodating much of the strain.

5.7.1.2 Locality 2: Karadiken village (Fig. 5.12, Fig. 5.16a–c), GPS reference 380500 4164500

This locality, ~2 km to the south of Karadiken village (Fig. 5.12, Fig. 5.16a), exposes Ordovician shales/quartzite, unconformably overlain by Middle – Upper Triassic shales and Jurassic carbonates (Monod and Akay, 1984) (Fig. 5.16). The Ordovician sediments are similar to those at locality 1 (Agilönü), described above. Brown-weathering micaceous shales are again interbedded with thin-bedded quartzitic sandstones. The overlying Triassic sediments, identified by a deep red-purple colour, outcrop over an area 500 m² x 750 m² (Fig. 5.16a). These are dominantly shales interbedded with grey medium-grained quartzite, bioturbated grey limestone and purple sandstone. Locally, the purple colour has been leached out so that it can be difficult to distinguish Triassic and Ordovician sediments based on colour alone. However, the Ordovician is typically thinner bedded and contains no limestone. Both of these successions are heavily deformed, showing a variety of micro- and macro- scale folding and faulting, especially kink folds on a 2-10 cm scale. Fold axial planes dominantly trend NNW–SSE, with fold vergence towards the WSW, NE and NW (see section 5.8).

Fault planes dominantly trend NNW-SSE and WNW-ESE. Jurassic limestones are medium- to thick-bedded and heavily recrystallised. Bedding planes are often hard to distinguish. Jurassic carbonates are not tightly folded but strike/dip measurements are variable across the area (Fig. 5.16a).

Local topographic relationships suggest that the Ordovician is above the Triassic. However, detailed mapping of the local contacts between the Ordovician, Triassic and Jurassic units shows that the Ordovician in fact dips beneath the Triassic (Fig. 5.16a–c, Fig. 5.17, Fig. 5.18a). On the eastern margin of the mapped area, the contact dips steeply >60º, and is heavily deformed by kink folds and buckle folds within both units (Fig. 5.17). On the western margin of the mapped area the contact is less steeply dipping, and

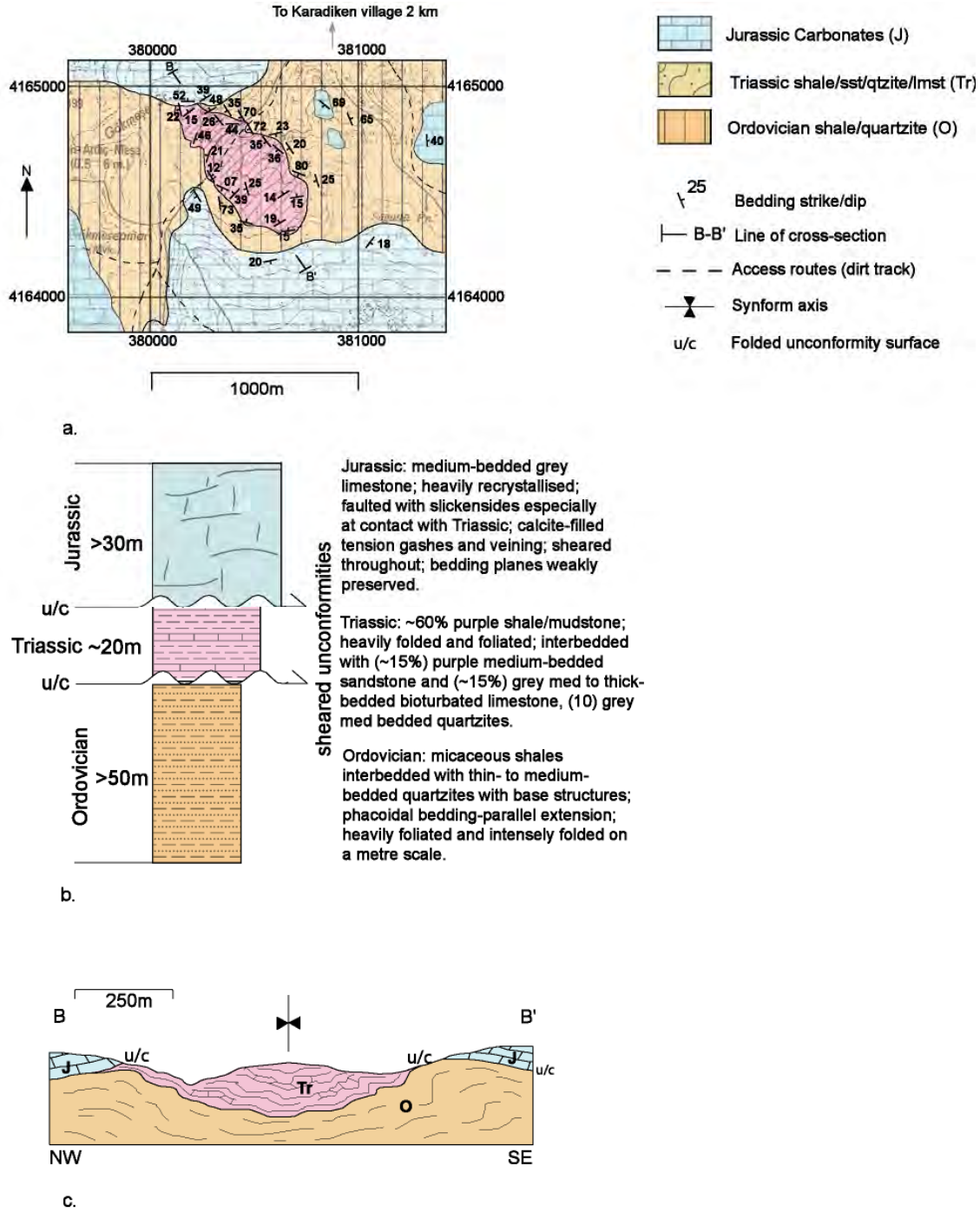

Fig. 5.16. a. Map of the Karadiken locality; b. Simplified log showing stratigraphy at Karadiken locality; c. Cross section B – B' through the Karadiken locality.

in some instances the units are flat-lying at the contact (Fig. 5.16a). Triassic sediments stratigraphically overlie Ordovician sediments at this locality.

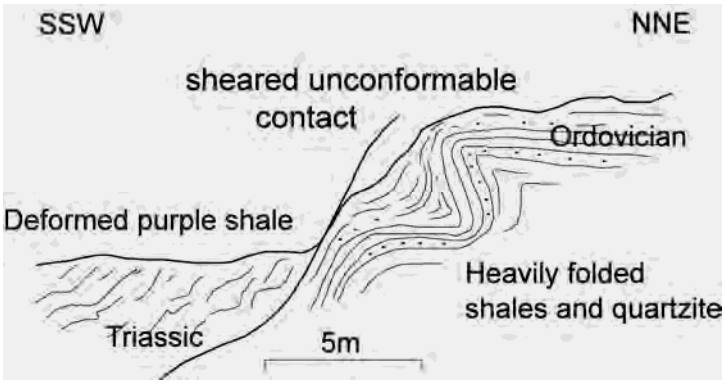

Fig. 5.17. Sketch of the contact between Ordovician and Triassic sediments at the Karadiken locality.

A contact between Ordovician–Triassic sediment and Jurassic limestone is observed towards the north of the mapped area (Fig. 5.16a). Medium-bedded Jurassic limestones are less deformed than the underlying Ordovician–Triassic shales, probably due to competency differences. The Ordovician–Triassic sediments at the contact are heavily cleaved and fractured, and dip beneath the Jurassic limestones with the same measured dip and strike (Fig. 5.16a, c). The planar nature of this contact suggests that it may be tectonic.

Monod and Akay (1984) believed that the Ordovician was thrust over the Triassic, and that the contact was then sealed and transgressed by Jurassic carbonates. This would again require a pre-Jurassic age of thrusting. However, re-mapping of this key locality shows that there is no tectonic contact between the Ordovician and Triassic sediments, but rather that this contact is a folded unconformity (Fig. 5.16c, Fig. 5.17, Fig. 5.18a). Displacement between these two units is restricted to minor bedding-parallel-slip between sediments of different competencies (i.e. shale and limestone). The Jurassic limestones unconformably transgress both the Ordovician and Triassic units,

although the planar nature of their contact suggests it may have experienced some tectonic reactivation, related to the competency difference.

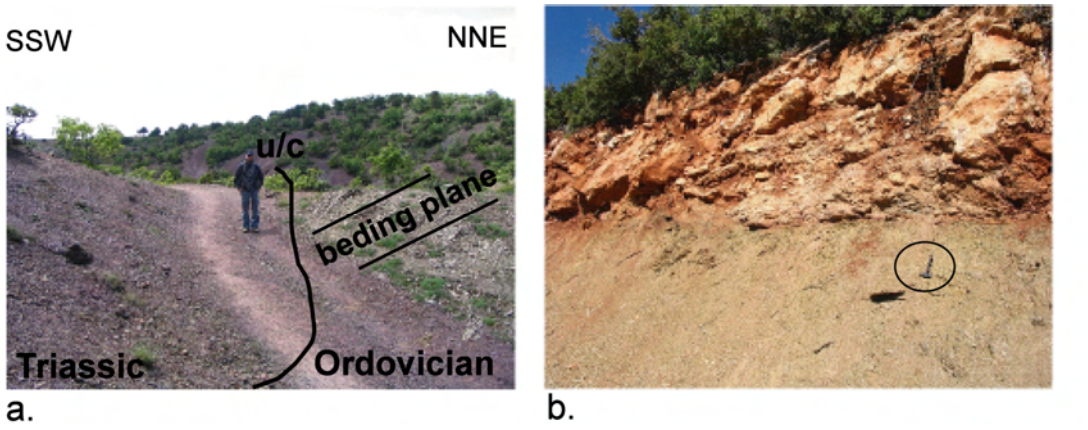

Fig. 5.18. a. Contact between Ordovician shale/quartzite and Triassic shale at the Karadiken locality; b. Sheared contact between Ordovician shale/quartzite (below) and Jurassic carbonates (above) at Yakanamaster locality. Contact was originally unconformable but has been reactivated at a later stage. Hammer for scale is circled.

This evidence, as at locality 1 (Agilönü), is consistent with an intact Palaeozoic–Mesozoic succession that was deformed during Late Cretaceous–Early Cenozoic time related to southward thrust emplacement of the Beyşehir-Hoyran-Hadim nappes. Again, there is no evidence to support latest Triassic "Cimmerian" compressional deformation.

Three other localities, not documented by Monod and Akay (1984), provide additional evidence that also supports a Late Cretaceous–Early Cenozoic age for regional deformation.

5.7.1.3 Locality 3: Yakanamaster (Fig. 5.12), GPS reference 386300 4166050

Located 6 km south of Beyşehir (Fig. 5.12), Cambrian–Ordovician and Jurassic sediments are exposed, as at locality 1 (Agilönü). There is further evidence of a tectonic contact between Ordovician shale/quartzite and Jurassic limestone.

Strongly folded Ordovician shales and quartzitic sandstones are separated from moderately deformed thick-bedded, to massive, Jurassic limestones (Fig. 5.18b). A thin

(3cm) horizon of highly sheared Ordovician shale with foliation-parallel slickenlines occurs at the contact. A distinctive 30 cm-thick zone of foliation is present in the Ordovician shales, parallel to adjacent Jurassic limestones. Quartzose sandstone beds within the Ordovician have undergone bedding-parallel extension generating phacoidal blocks. Folds, shear imbrication and slickensides within the Ordovician sediments all suggest a top-to-the-west movement (see section 5.8). The limestones exhibit a 10-20 cm-thick brecciated horizon adjacent to the contact. Sedimentary structures on the bases of some Ordovician beds indicate that part of the sequence is inverted, whilst other parts are the right way up.

The evidence indicates that competent Jurassic Limestones tectonically overlie incompetent Ordovician shales. Shearing and brecciation zones on either side of the contact show bedding-parallel slip. Ordovician beds are strongly deformed and inverted on local fold limbs. There are no sedimentary structures within the limestones to determine stratigraphic way-up. The most likely explanation is that Ordovician shale/sandstone is unconformably overlain by Jurassic Limestone, and that the contact has been tectonically reactivated during Late Cretaceous–Early Cenozoic (Alpine) deformation.

5.7.1.4 Locality 4: Balik Tepe (Fig. 5.12, Fig. 5.13a), GPS reference 387740 4165528

Balik Tepe is the highest peak (1424 m) in the study area, ~7km south of Beyşehir (Fig. 5.12, Fig. 5.13a). Unfortunately, exposure in the area is poor. Cambrian dolomites structurally overlie Ordovician shales/quartzose sandstones, and are then structurally overlain by Jurassic carbonates which form most of Balik Tepe. The Cambrian-Ordovician contact could be a thrust, or result from simple stratigraphic inversion. Where Cambrian dolomites and Jurassic limestones are seen in contact, heavy shearing and foliation are evident. Both units display calcite-filled tension gashes and localised tectonic brecciation. Locally, bedding planes display a mineral lineation related to layer-parallel extension.

Relationships in this area are comparable to those observed at locality 1 (Agilönü) and locality 3 (Yakanamaster). It is inferred that the Cambrian sequence was inverted related to Upper Cretaceous – Lower Cenozoic regional nappe emplacement. The planar contact between Palaeozoic and Jurassic units is unconformable, but was, therefore, reactivated during Alpine deformation.

5.7.1.5 Locality 5: Seydişehir-Tarasçi (Fig. 5.12), GPS reference 389870 4145750

The city of Seydişehir lies on the relatively autochthonous Tauride platform to the east of the Beyşehir-Hoyran-Hadim nappes (Fig. 5.12). A cross-section published by Monod (1977) through Çal Tepe, a prominent hill near Seydişehir, suggests that a thick Cambrian-Ordovician sequence has been folded and inverted in the east, so that Cambrian units are now in the highest structural position (Fig. 5.15). New mapping carried out in the west, near Taraşçı village (Fig. 5.12), now shows that the succession is the right way up, although heavily faulted and folded. An unconformable relationship between Ordovician and Triassic–Jurassic units is poorly exposed in a road section 250 m north of Taraşçı village (GR 389870 4145750).

The base of the Triassic succession consists of weakly foliated, variably coloured (purple to brown) micaceous sandy-shales. The thickness of the purple shales varies from 15-20 m in the road section, to 50-100 m to the west of Taraşçı village. The variable thickness of Triassic purple shales is consistent with deposition on an irregularly eroded Ordovician land surface, with the boundary between Ordovician and Triassic as an angular unconformity (Fig. 5.19). The shales pass up into thinly bedded (10-15 cm), moderately sheared, medium-dark grey recrystallised limestones, thickening upwards to medium-thick bedded over a 5-10 m interval. These beds contain nodules of black chert formed by diagenetic silica replacement. The sequence continues for >50 m and passes into thin-bedded microbial limestones, interbedded with shales and thick-bedded bioclastic limestones (Fig. 5.19).

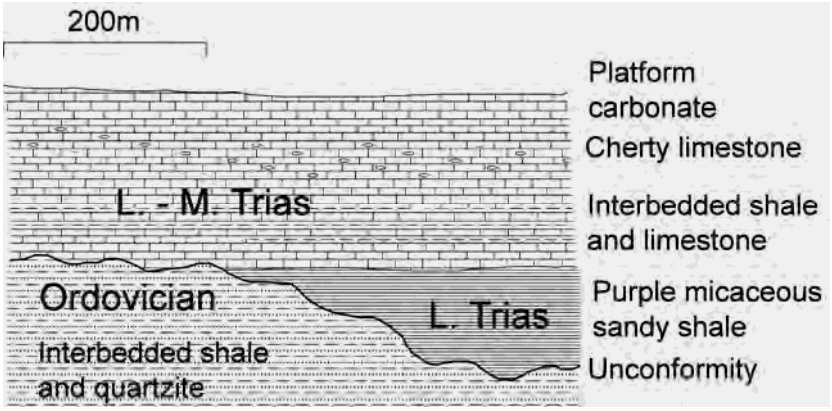

Fig. 5.19. Schematic diagram showing the stratigraphic relationships observed at Taraşçı village, near the town of Seydişehir.

The succession passes upwards into medium- to thick-bedded Triassic carbonates (Monod, 1977), interbedded with thin shale horizons, in all ~300 m thick. This is then transgressed by massive Jurassic carbonates, before being tectonically overlain by the Beysehir-Hadim nappes (Monod, 1977; MTA, 2002). The Triassic shales and limestones are regionally folded on a 10-50 m scale, but are more tightly folded locally on a 10 m scale. More competent massive Jurassic carbonates are not folded, but are heavily recrystallised. Complex structural relationships are present locally, with Jurassic carbonates of the autochthon overlain by imbricate slices of Ordovician turbidites near the base of the thrust stack.

The deformation is consistent with that elsewhere in the region. Competent thick-bedded and massive Jurassic carbonates are less deformed than thinner bedded more shaley and siliciclastic Lower Palaeozoic and Triassic lithologies. The most likely cause of this deformation is Upper Cretaceous - Lower Cenozoic emplacement of the Beyşehir-Hoyran-Hadim nappes.

In summary, structural study of the above key areas does not confirm the existence of a regional “Cimmerian” compressional deformation of latest Triassic age, but rather indicates that all of the deformation was of Late Cretaceous – Early Cenozoic age related to the regional southward thrusting of the Tethyan marginal and ophiolitic units of the Beyşehir-Hoyran-Hadim nappes.

5.7.1.6 Elsewhere in the Geyik Dağ

The degree and style of deformation was noted elsewhere in the Geyik Dağ. Intense folding and faulting, on a regional and outcrop scale, was observed in Ordovician shale and quartzite to the north of Hadim village. This was also documented by Özgül (1983), who described regional folding of Cambrian-Ordovician sediments near the village of Bağbaşi (Fig. 5.21a).

Elsewhere in the autochthonous platform, Lower Palaeozoic sediments are not exposed, and the common lithology observed is Jurassic – Cretaceous thick-bedded, to massive, platform carbonates. In most areas these carbonates are faulted and recrystallised (Fig. 5.21b) but folding and shearing, as seen in the Cambro-Ordovician sequence, was not observed. To the SW of the nappe stack, such as west of Derebuçak village, brittle deformation and imbrication of the autochthonous platform was observed. South and south-westerly propagating thrust faults are adjacent to small, elongate basins composed of siliciclastic turbidites of Eocene age that are interpreted as part of a foredeep (Özgül, 1976; Monod, 1977; Gutnic et al., 1979; Andrew, 2003). These are thought to represent brittle deformation and collapse of the autochthon during orogenic loading during emplacement of the Beyşehir-Hoyran-Hadim nappes (Andrew and Robertson, 2002); however, imbrication of the platform has not been described to the northeast of the nappe stack.

There are several key trends to note concerning the deformation within the Geyik Dağ autochthon: (i) The style of deformation varies between the lithologies of different competency, with thin-bedded shales and carbonates showing a more 'ductile' deformation in comparison to 'brittle' deformation of thick-bedded and massive carbonates; (ii) The degree of deformation varies between lithologies, with less competent shales and siliciclastics being deformed to a greater degree than competent carbonate units; (iii) Regional tectonic imbrication of the Tauride platform is only seen in thick massive Mesozoic carbonates to the southwest of the Beyşehir-Hoyran-Hadim nappe stack, where the thrusting has been dated as Eocene; (iv) The most severe

deformation of the autochthon is seen to the northwest of the nappe stack, adjacent to the Beyşehir-Hoyran-Hadim nappes.

A likely explanation of the deformation is that it was caused during the emplacement of the Beyşehir-Hoyran-Hadim nappe stack, previously documented as occurring between the Late Cretaceous and Early Cenozoic (Gutnic et al., 1979; Özgül, 1984; Andrew and Robertson, 2002). The thickness of the nappe stack is several kilometres in the northerly study area, and the compressional force on the underlying autochthon has caused collapse and imbrication of the platform towards the southwest during emplacement.

In summary, structural study of the above key areas does not confirm the existence of a regional "Cimmerian" compressional deformation of latest Triassic age, but rather indicates that all of the deformation was of Late Cretaceous – Early Cenozoic age related to the regional southward thrusting of the Tethyan marginal and ophiolitic units of the Beyşehir-Hoyran-Hadim nappes. See Appendix A for further discussion.

5.7.2 Hadim nappe

Deformation in the Hadim nappe tends to be related to outcrop and regional-scale 'brittle' faulting and imbrication of the exposed Palaeozoic and Mesozoic sequences. Intense shearing is noted at the leading edge (SW) of the nappe. Several examples can be demonstrated from both the northerly and southerly study areas.

In the northerly study area, faulting of the Palaeozoic and Triassic succession was observed at the village of Bademli. At the northeast of the village, a large normal fault, with a throw estimated at 150 m, juxtaposes Permian carbonates against Lower-Middle Carboniferous shales, quartzite and limestone. Adjacent to the fault is a zone of shearing and bedding disruption. At Derebuçak village, the leading edge of the Hadim nappe is folded into a WSW-verging recumbent anticline. The base of the thrust stack is exposed in a cutting beside a dam to the south of the village, exposing a 50m-thick succession of shearing and tectonic imbrication (Fig. 5.20).

Fig. 5.20. Leading edge of the Hadim nappe, south of Derebuçak village. Exposure created by development of new dam to the east of the picture. The limestones at the top of the picture are part of the Hadim nappe. Below this is a succession of sheared flysch deposits deposited in a foredeep basin on the Geyik Dag ahead of the emplaced nappe stack.

A Palaeozoic succession near Cevizli village exposes gentle open folding on an outcrop scale (20m). The sequence, exposed in a road cutting, is regularly interrupted by normal faulting with displacement ranging from 5-25 m. Near the village of Gumusdamla, Triassic shales, sandstones and limestone horizons are laterally truncated by faults near the western edge of the Hadim nappe. The type of fault was not ascertained; however, it is suspected to be reversed and related to emplacement of the nappe.

In the southerly study area, tectonic imbrication and thickening of the Triassic sequence is observed at Alanya road south (Fig. 5.21c). Adjacent to the northeast margin of the nappe, a 150 m sequence of Middle Triassic shale and limestone is stratigraphically repeated, with a zone of reversed faulting and shearing along the contact between the two sequences (Fig. 5.21c). A large reversed fault also cuts off the lowermost ~100 m of the Triassic sequence adjacent to the contact with the Bolkar nappe.

Near the town of Hadim (Fig. 5.8), the Carboniferous succession within the Hadim nappe, which is adjacent to the tectonic contact with the Bolkar nappe, is tectonically imbricated and thickened. Lower Carboniferous shales and quartzites, along with some Middle Carboniferous limestones, act as an easy-slip horizon within the Palaeozoic sequence. It is estimated that tectonic repetition of the sequence has resulted in a thickening of ~200 m adjacent to the nappe boundary. At this contact, Jurassic

carbonates of the Bolkar nappe are laterally variable in thickness due to the irregular tectonic contact with the Hadim nappe (Fig. 5.21d).

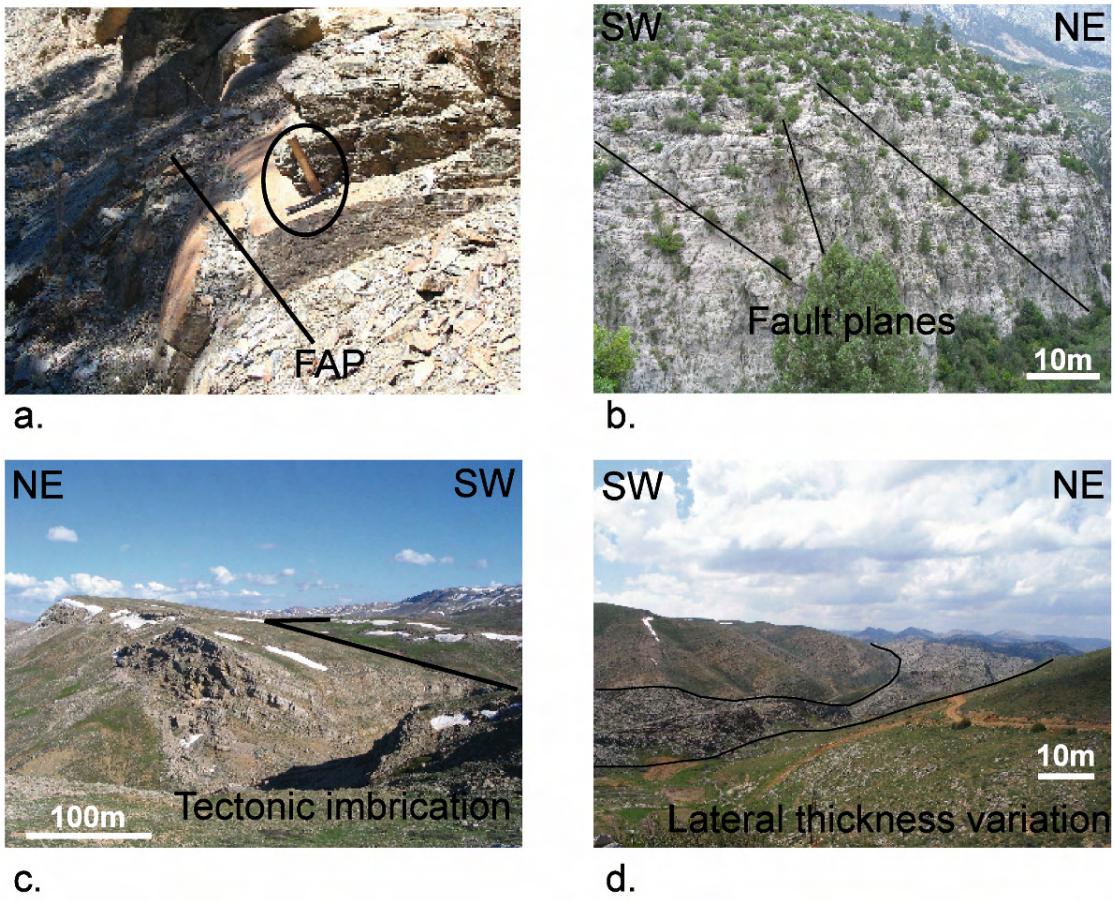

Fig. 5.21. a. Folded Ordovician shales and quartzites in the Geyik Dağ, near Bağbaşi village. Hammer circled for scale; b. Normal fault planes in Jurassic carbonates of the Geyik Dağ autochthon, in Uzumdere valley; c. Large-scale tectonic imbrication and stratigraphic thickening of Triassic sediments at Alanya Road; d. Lateral thickness variations in Jurassic carbonates as a result of tectonic emplacement of the Hadim nappe (SW in the photo).

In the Hadim nappe to the north of Beyreli village, Triassic shales and thin-bedded sandstone are gently folded on a 10m scale. Associated with these folds are low-angle faults, which are possibly originally thrusts, but which appear to have been reactivated to give a normal sense of movement. Conglomerate beds of Late Triassic age are also laterally discontinuous due to localised faulting.

To summarise, the Hadim nappe is relatively undeformed in comparison to other tectonic units within the study area. The main style of deformation is 'brittle', with much faulting and tectonic imbrication, especially near the nappe contacts. Shearing is also associated with these faulted zones. Any folding that was observed is localised and folds are gentle, open on a 10's of metre scale. At the leading edge of the nappe (SW), intense shearing and larger scale regional folding are seen within units at the base of the thrust sheet. This is localised along the nappe margin, and there is rarely evidence of overturned beds elsewhere in the Hadim nappe.

5.7.3 Bolkar nappe

The Bolkar nappe has previously been described as a coherent tectonic unit (Özgül, 1984; Özgül, 1997; Andrew and Robertson, 2002), similar to the Hadim nappe. During the course of this study, however, it was found to be intensely deformed and, in many areas, largely a broken formation. Intense, large-scale regional folding, previously not documented, was identified in this study, and uniquely (within the study area) the Bolkar nappe is metamorphosed at a low grade (Özgül, 1984; Özgül, 1997; Andrew and Robertson, 2002). Several key localities demonstrate the degree of deformation in the Bolkar nappe.

5.7.3.1 Sorkun – Dipsiz Göl section

A traverse through the Bolkar nappe to the west of Sorkun village (Fig. 5.22) shows that, far from being a coherent stratigraphic sequence, the Bolkar nappe comprises a disorganised arrangement of tectonically sheared and regionally folded units. Throughout the section, thrust faults dip to the east, indicating that the direction of movement was from the east to the west. Zones of thrusting are marked by intense shearing and localised folding. Regional folding was recognised in the form of a large-scale recumbent anticline, which is overturned to the west-southwest. A zone of imbricate thrusting at the leading edge of the nappe juxtaposes Palaeozoic and Triassic sediments against one and other, and an unknown amount of the stratigraphy may be tectonically missing in this region. It was very difficult to measure stratigraphic sections

in the area due to intense folding and faulting. Even lithologies that would be considered as relatively competent, such as Mesozoic limestone, were found to be folded and deformed. Critically, in the Sorkun village cross-section (Fig. 5.22) there is an unusual relationship whereby Cretaceous rocks appear to have been thrust southwards over Jurassic and Triassic rocks. This tectonic relationship, whereby younger rocks are thrust about older ones, is not typical of normal in-sequence thrusting, and instead is characteristic of complex thrust belts where out-of-sequence thrusting has taken place (Park, 1988).

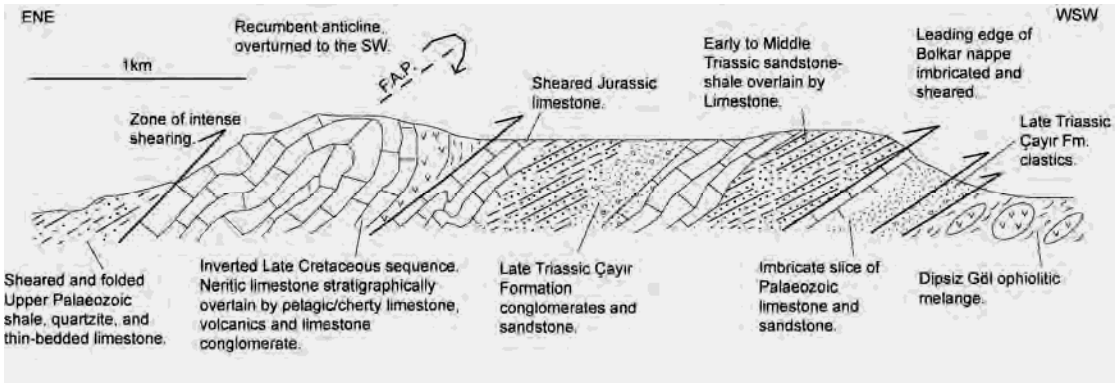

Fig. 5.22. Schematic cross-section through the Bolkar nappe between the village of Sorkun and Dipsiz Göl. This cross-section is along part of the line of transect B-B1 in Fig. 5.8. See text for full description.

5.7.3.2 Karabayir Yayla section

Another traverse through the Bolkar nappe at Karabayir Yayla, west of the village of Üçpınar, shows a similar degree and style of deformation (Fig. 5.23). To the east of the traverse, Devonian and Carboniferous shale, quartzite and limestone is tectonically imbricated and folded, and thrust to the southwest over a regionally folded Jurassic – Cretaceous sequence. These carbonates form a large recumbent anticline, overturned to the southwest (Fig. 5.24). These are, in turn, thrust southwards above a succession of sheared Middle to Late Triassic sediments, which is internally imbricated and tectonically thickened.

A stratigraphic break occurs to the SW of the traverse where Triassic sediments tectonically overlie Devonian quartzitic sandstone. This is not a typical thrust

relationship, and has implications for the style of thrusting which will be discussed later. Again, it is difficult to identify a continuous stratigraphic succession in any part of the traverse due to the disorganised nature of imbricate slices of lithologies of different ages. In this cross-section, Cretaceous rocks appear to have been thrust over Jurassic and Triassic rocks, which once more is not typical of in-sequence thrusting, and supports a complex out-of-sequence thrusting model.

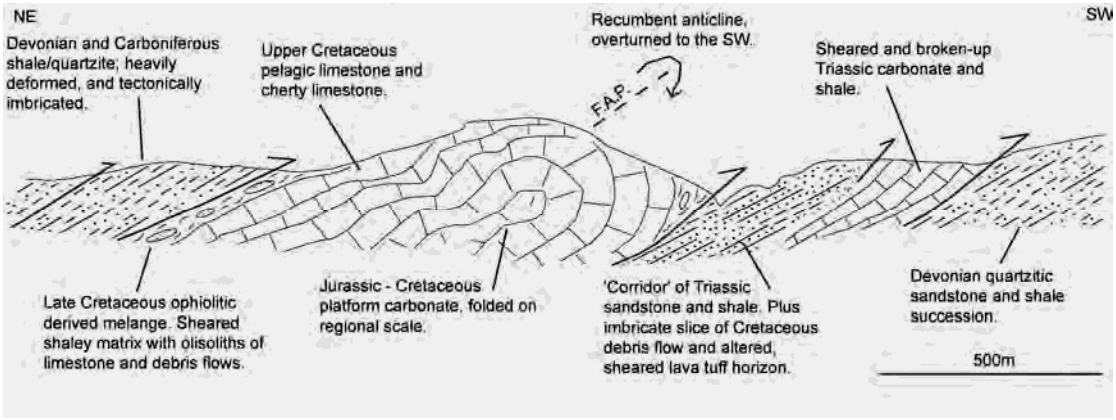

Fig. 5.23. Cross-section through the Bolkar nappe at Karabayir Yayla. This cross-section is along part of the line of transect C-C1 in Fig. 5.8. See text for full description.

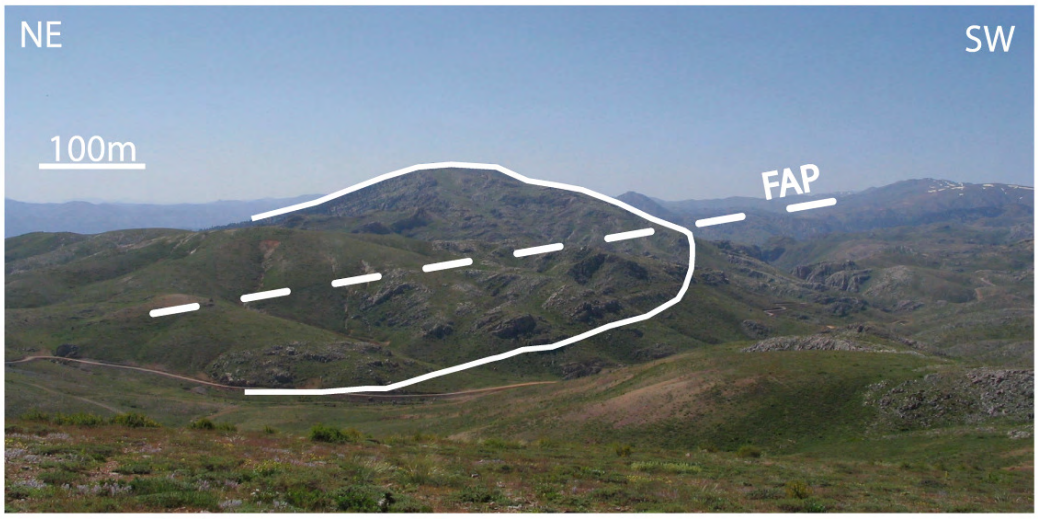

Fig. 5.24. Bolkar nappe deformation: Jurassic – Cretaceous carbonates forming a recumbent anticline, overturned to the SW in the Bolkar nappe at Karabayir Yayla. Similar deformation is observed elsewhere in the Bolkar nappe.

5.7.3.3 Other features of Bolkar nappe deformation

During this study, the intense degree of deformation within the Bolkar nappe was fully appreciated. Rather than being a coherent sequence of Late Palaeozoic and Mesozoic units, such as the Hadim nappe, the Bolkar nappe is a 'broken formation', where stratigraphic sequences are disorganised due to regional scale folding and faulting.

A common feature is laterally discontinuous bodies of a particular lithology. Competent and coherent Mesozoic limestone, in comparison to less competent shales, can form large 'rafts' within the nappe, ranging from 10 m (local) to 500m (regional) in size (Fig. 5.25a, Fig. 5.25b). Fig. 5.25a demonstrates this particularly well, and shows a 100 m-thick body of limestone pinching out laterally over a very small distance (~100m). These rafts constitute a regional tectonic melange.

Faulting occurs on a variety of scales. Fig. 5.25c shows a carbonate horizon that is cut by a series of, what appears to be, normal faults. However, the horizon package either side of these faults is not of the same thickness. Closer inspection of the contacts showed that the limestone horizon is actually a laterally discontinuous boudin which has been stretched and sheared. On a smaller scale, brittle faulting within competent lithologies was observed (Fig. 5.25d). Shear fabrics and flower structures are associated with the outcrop-scale faulting, suggesting that compressional and strike-slip tectonics were important during nappe emplacement.

Folding within the Bolkar nappe occurs both on regional and outcrop scales. Regional-scale folding is documented in the above, with recumbent anticlines highlighted in two traverses through the nappe. On an outcrop scale, folding is most pronounced near nappe contacts and imbricate thrusts. The degree of folding is influenced by lithology, with shales and less competent lithologies being heavily deformed. Vergence direction in overturned folds gives a good indication of the sense of shear, and consequently the direction of local emplacement (Fig. 5.26a). Adjacent to thrust faults, folds are often flattened and, in some cases, close to isoclinal, with parallel limbs (Fig. 5.26b). In Fig. 5.26b, a fold is highlighted in a layer of chert within a medium-bedded Palaeozoic limestone horizon. To deform such a competent lithology

must have required a significant amount burial and pressure in order to achieve this ductile form. Disharmonic kink folds on a smaller scale, with a random orientation of fold-axes are observed in Upper Cretaceous shales within the Bolkar nappe, adjacent to the tectonic contacts (Fig. 5.26c).

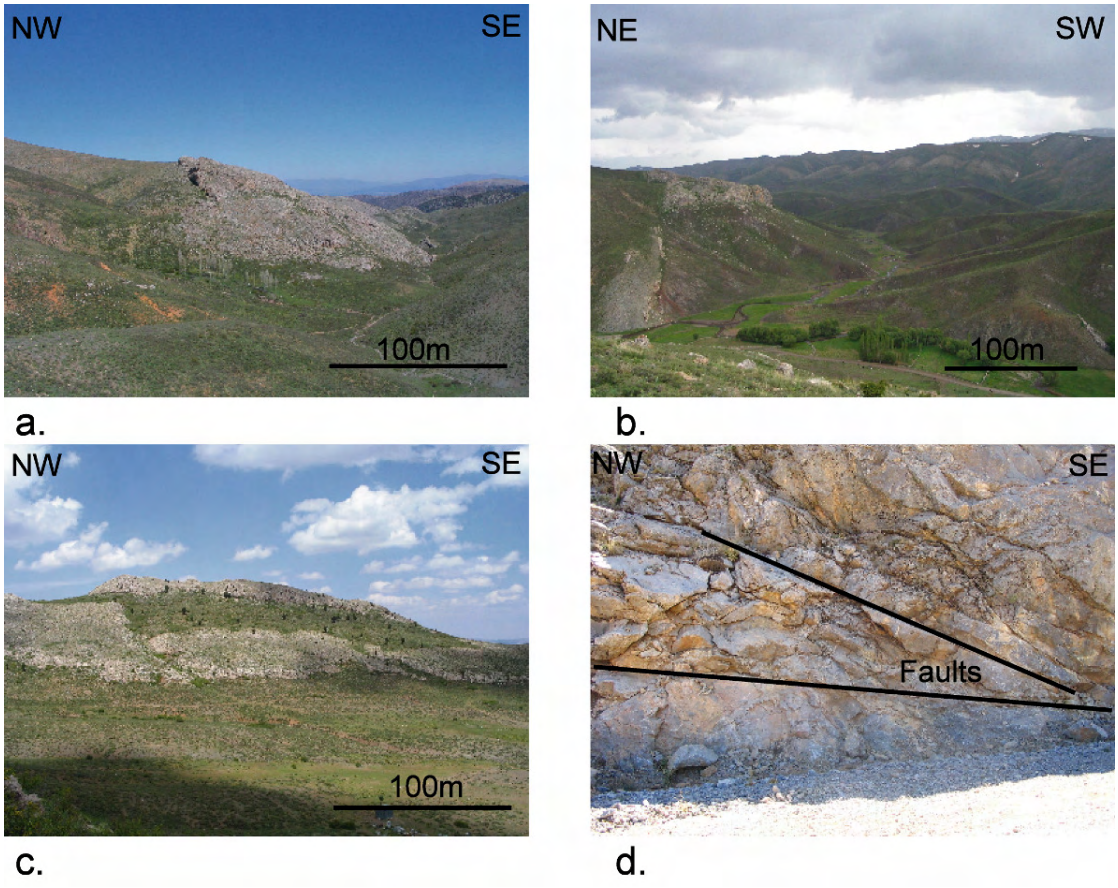

Fig. 5.25. a. Laterally discontinuous Mesozoic limestone 'raft' is a product of tectonic shearing and regional-scale boudinage; b. To the left of photograph are tectonic rafts of Mesozoic limestone at the base of a thrust sheet; c. Internal normal faulting within a laterally discontinuous horizon of Jurassic limestone; d. Outcrop-scale faulting with distinctive wedge-shaped shear package developed. Slickensides indicate thrusting to the NW at this locality.

Intense shearing of lithologies occurs adjacent to tectonic contacts and imbricate thrust faults. Lithologies lacking any primary stratigraphic relationship may be juxtaposed against one and other. For example, Fig. 5.26d shows a slice of Upper Cretaceous ophiolitic melange adjacent to a thin succession (10 m) of Upper Triassic Çayır Formation clastics. Both lithologies are heavily sheared. The bedding plane can be

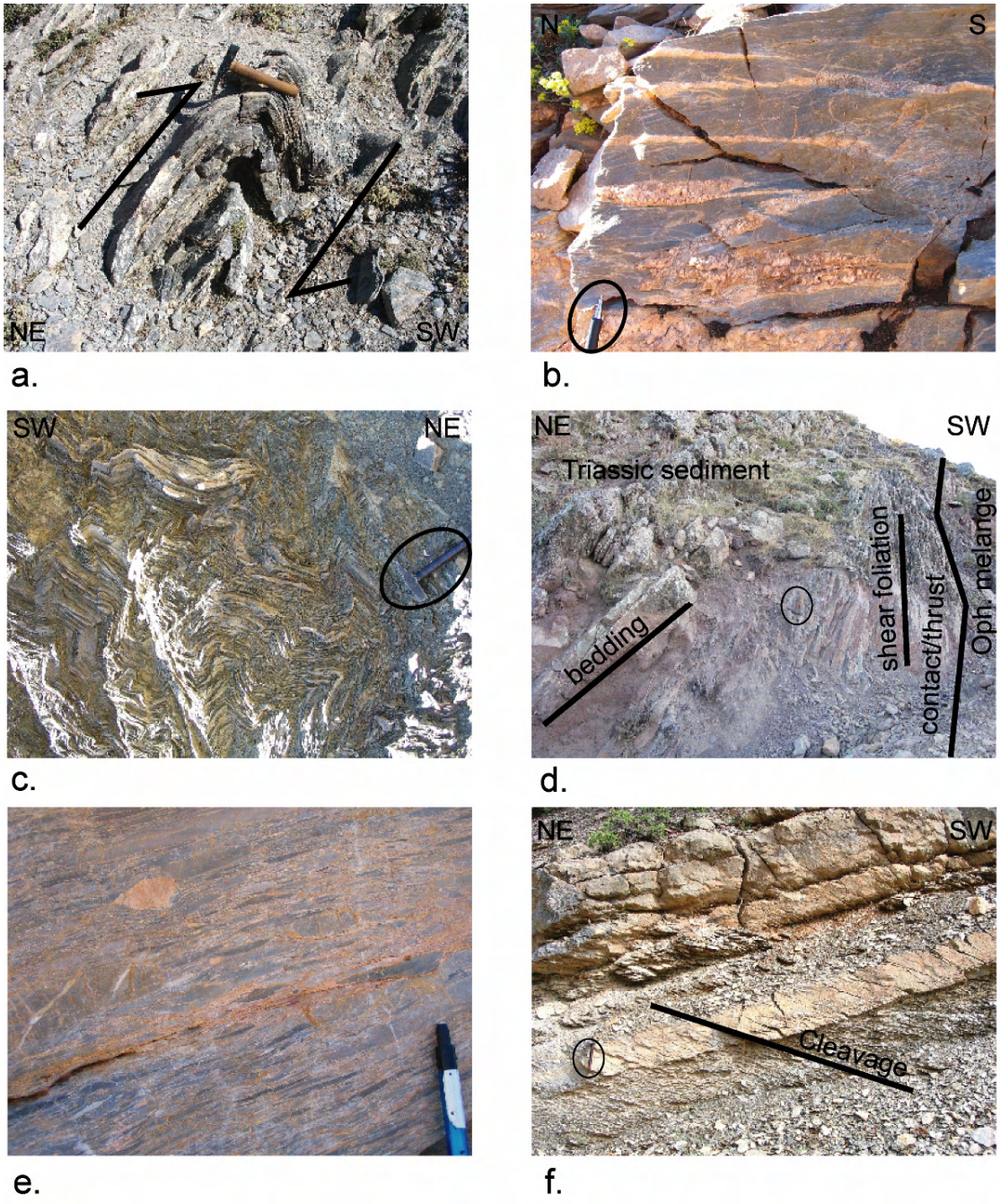

Fig. 5.26. a. Overturned folds within the Bolkar nappe giving sense of shear and emplacement direction of movement along thrust contacts; b. Near isoclinal folding observed in chert horizons within pelagic limestone in the Bolkar nappe. Pencil circled for scale; c. Disharmonic kink folds in Upper Cretaceous melange shale of the Bolkar nappe. Hammer circled for scale; d. Thrust / shear zone juxtaposing Triassic sediments against Upper Cretaceous ophiolitic melange. Bedding plane and shear foliation plane highlighted. Hammer circled for scale; e. Sheared limestone conglomerate showing elongate and flattened clasts. Chert nodule in top left of photo more competent and not elongated; f. Cleavage in Upper Palaeozoic limestone and shales. Hammer circled for scale.

seen to dip to the NE, but adjacent to the thrust contact a tectonic foliation has developed which is almost vertical. The slice of ophiolite melange is on the far right of the photograph.

Intense shearing of a limestone conglomerate bed adjacent to a imbricate thrust shows flattening and elongation of clasts (Fig. 5.26e). A replacement chert nodule, in the top left of the photograph, is not flattened because of its relative competency in relation to the limestone. A shear fabric envelopes this nodule. A secondary replacement chert, developed after the shearing, can be seen to exaggerate the shear foliation that has developed. A cleavage is developed in some Palaeozoic units adjacent to the eastern margin of the Bolkar nappe (Fig. 5.26f). The cleavage can be traced through alternating shale and limestone beds.

Finally, the Bolkar nappe is documented as displaying low-grade metamorphism (Özgül, 1976, 1984, 1997). Palaeozoic shales from near the sole of the Bolkar nappe in the Hadim region are intensely sheared and have a pronounced foliation. Devonian shales, in particular, are documented as showing initial greenschist metamorphism. According to Özgül (1997), shales contain the metamorphic minerals chlorite, muscovite, zeolite, epidote, and hornblende; the sediments observed during study were heavily deformed, and it was noted that they were micaceous.

To summarise, the Bolkar nappe is heavily deformed relative to other tectonic units within the study area. A combination of ductile and brittle deformation features are observed on an outcrop and regional scale, and locally the Bolkar nappe is metamorphosed at low-grade. Faulting, folding and shearing was common throughout, especially adjacent to nappe contacts and imbricate thrusts. Cleavage development and regional-scale stretching, elongation and boudinage were observed. Imbricate thrusting has resulted in a disorganised internal arrangement of the nappe. Contrary to previous investigations (e.g. Özgül, 1984), the Bolkar nappe is not a coherent unit, but largely a broken formation. Stratigraphic sections are difficult to interpret due to the chaotic internal nature of the nappe as a whole.

5.8 Structural data

Throughout this study, structural data were collected throughout the Beyşehir-Hadim nappe stack. This included fault plane orientation, slickensides, fold axial planes, fold vergence, stretching lineations, shear fabrics and tension gash orientation. The data provide insights into the direction of nappe emplacement, the principal axes of stress during emplacement, and how many phases of deformation occurred. In this section, structural data will be presented from 19 localities within the study area; the locations from which data were collected is shown in Fig. 5.27.

Localities that are considered particularly important in this study are those adjacent to regional-scale faults in the area. Two contacts of particular interest are between the Hadim nappe and the Bolkar nappe, and between the Hadim nappe and ophiolitic melange. As demonstrated in the cross-section profiles through the nappe stack (section 5.5), one alternative is that the Hadim unit was originally further north and has been emplaced over the top of the Bolkar nappe and ophiolitic melange into its current position; another alternative is that the Hadim nappe was backthrust to the northwest over the Bolkar nappe and ophiolitic melange.

5.8.1 Tectonic data

Fold axes, fold vergence, fault plane, slickenside lineation, mineral lineation, tension gash orientation, and shear fabric orientation data are presented in this section. All stereonet projections for the planes of fold axes, faults, shear fabrics and tension gashes are plotted as great circles in the lower hemisphere. Arrows on great circles represent slip direction (on faults) with the arrow corresponding to movement of the hangingwall block; strike slip faults are indicated by diverging arrows, with either a left-lateral or right-lateral sense. Fold vergence direction is plotted as an azimuth on a rose diagram. Mineral lineations are plotted as projections in the lower hemisphere.

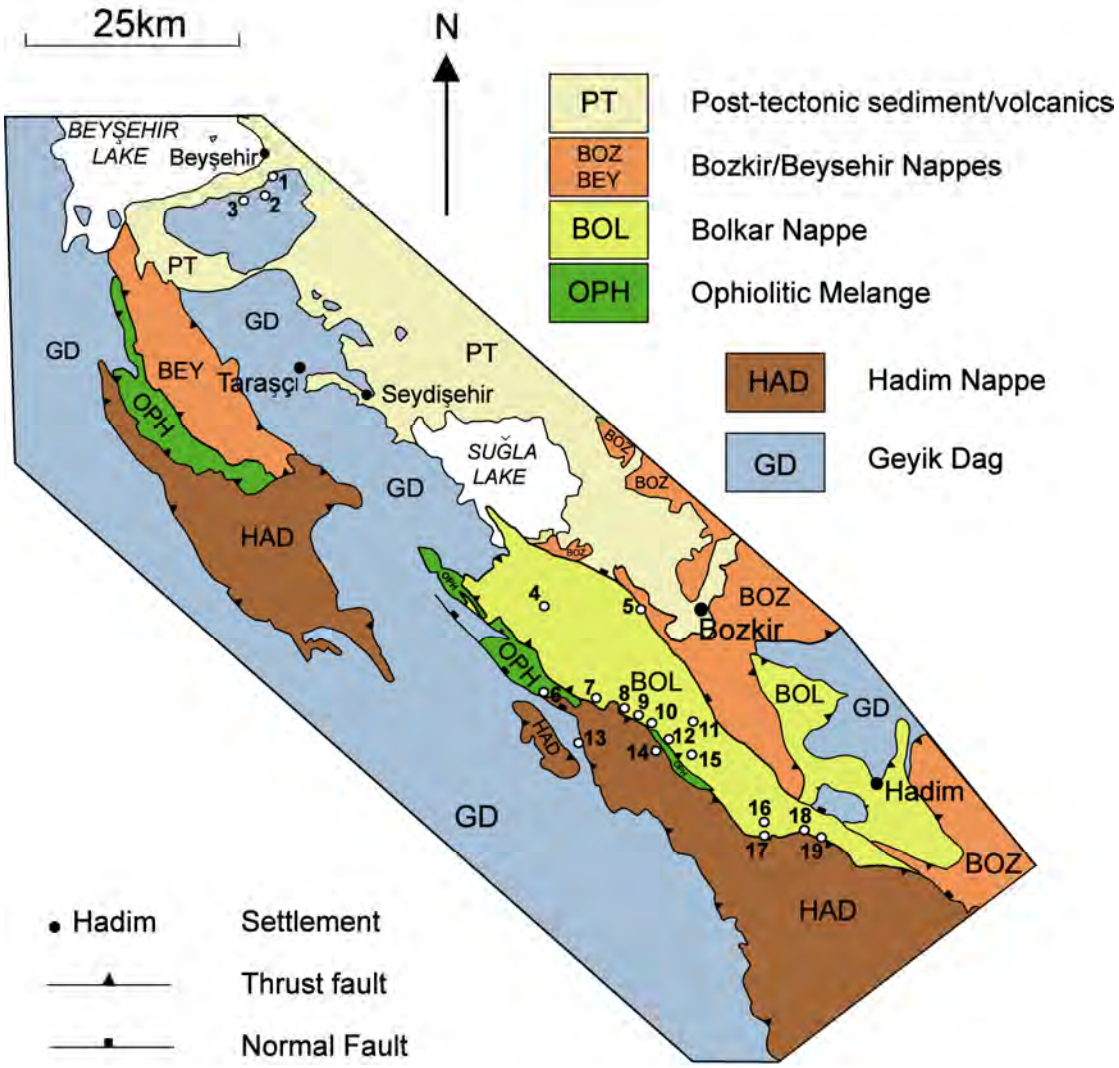

Fig. 5.27. Simplified structural map of the studied area. Localities: 1. Agilönü. 2. Yakanamaster. 3. Karadiken. 4. Dikilitaş Yayla. 5. Dereköy. 6. Sarapinar Yayla. 7. Oküz Çukuru. 8. Derence Dere. 9. Babuçcu Yayla. 10. Hocalar Yayla. 11. Karabayir Yayla. 12. Baybağan Yayla. 13. Gölbelen Tepe. 14. Küçüksu Tepe. 15. Elmaağaç Yayla. 16. Kuma Dere. 17. Sögüt Yayla. 18. Koyaardi. 19. Ekinlik Yayla.

5.8.2 Northern part of the study area

Within the northerly study area, structural data were collected from three localities (described in section 5.7.1).

5.8.2.1 Locality 1: Agilönü

Structural data from the Agilönü locality are shown in Fig. 5.28. Fold axial planes show a strong N-S orientation, with a lesser NW-SE trend. Vergence of these folds is primarily to the W and E, with a moderate NE trend also present. Fault planes are predominantly NW-SE to N-S trending, with a smaller number of faults orientated E-W. The majority of the NW-SW and N-S trending faults dip to the east. Kinematic indicators, in the form of slickensides, are marked in Fig. 5.28d by arrows which point in the direction of hanging-wall movement. These show that there are a variety of normal and reversed faults. Most faults that dip towards the west have a normal sense of displacement, whilst most of those that dip towards the east have a reversed sense of displacement. Mineral lineations, which are projected in Fig. 5.28e, show there are three clusters of data, trending W, NE, and S respectively. Finally, the planar orientation of calcite-filled tension gashes show a strong N-S to NW-SE orientation.

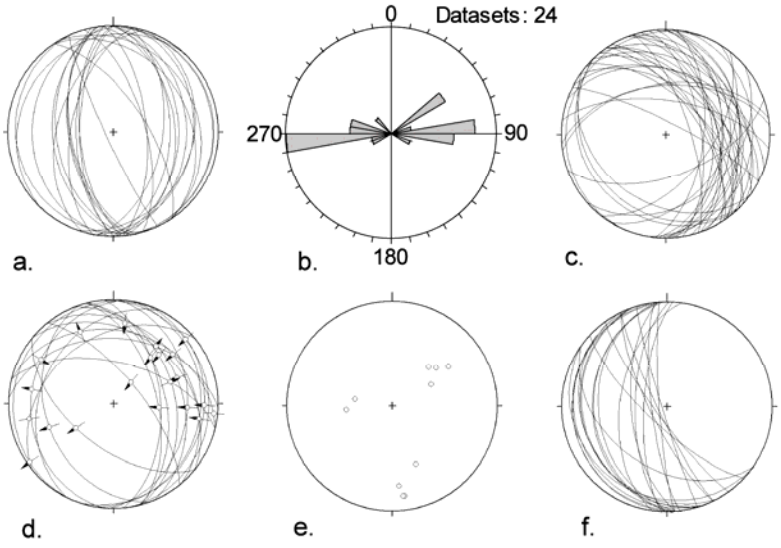

Fig. 5.28. Structural data from the Agilönü locality. a. Fold axial planes from Ordovician sediments. b. Fold vergence direction from Ordovician sediments. c. Fault planes from Ordovician sediments. d. Fault planes with slickensides from Ordovician sediments. e. Mineral lineations from Ordovician sediments. f. Tension gash orientations from Middle Jurassic sediments.

When all these data is considered, it can be seen that the principle direction of shortening is along a NE-SW to E-W axis. Fault data show that most reversed faults are dipping east, and that hanging wall movement is towards the west. When coupled with fold vergence data, and tension gash orientation, there is a bias towards top-to-the-west movement. The Beyşehir-Hadim nappe stack is found to the west of this locality, and it can, therefore, be inferred that the deformation of the Geyik Dağ autochthon at this locality was a result emplacement of the nappes to the W/SW.

5.8.2.2 Locality 2: Yakanamaster

Fold, fault and shear plane data were collected from the Yakanamaster locality (Fig. 5.29). Fault planes dip randomly, with a minor bias to W and S. Slickensides show fault movement of both normal and reverse nature, but with displacement along a E-W trending axis. The plane of shear fabrics dominantly trend NW-SE, with the majority dipping to the NE. Fold axial planes trend NW-SE and dip to the NE and SW. Fold vergence is predominantly towards the SW and W, with only a minor NE component. The data are similar to those observed at locality 1 (Agilönü). Principle shortening direction is along a NE-SW to E-W axis, and the data suggest top-to-the-W/SW emplacement. This is, again, consistent with the emplacement of the Beyşehir-Hadim nappes.

5.8.2.3 Locality 3: Karadiken

Structural data from Karadiken are shown in Fig. 5.30. Fold axial planes are strongly NW-SE and N-S trending, with variable angles of dip. A minor NE-SW trend is also seen. Fold vergence is towards the NE and SW, and a NW component is also evident. Fault planes are orientated E-W, N-S, and, to a lesser extent, NW-SE. The combined data are slightly more variable than at localities 1 and 2. A NE-SW to N-S shortening axis is inferred. There may also be a NW-SE component of strain, which could be related to an element of oblique compression. In general, most of the structural data at

this locality is consistent with emplacement of the Beyşehir-Hadim nappes to the W/SW, as seen at localities 1 and 2.

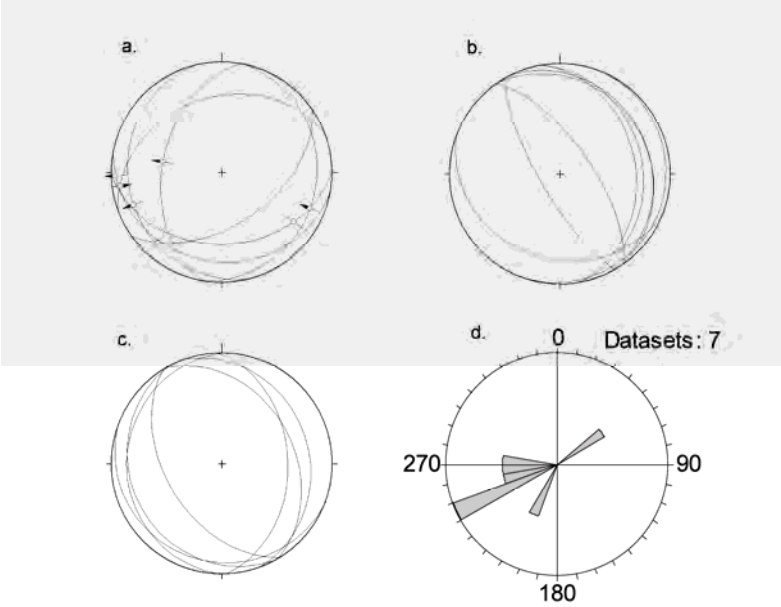

Fig. 5.29. Fold, shear plane, and fault data from Ordovician and Jurassic units (combined) at the Yakanamaster locality. a. Fault planes with slickensides; b. Shear fabric planes; c. Fold axial planes; d. Fold vergence direction.

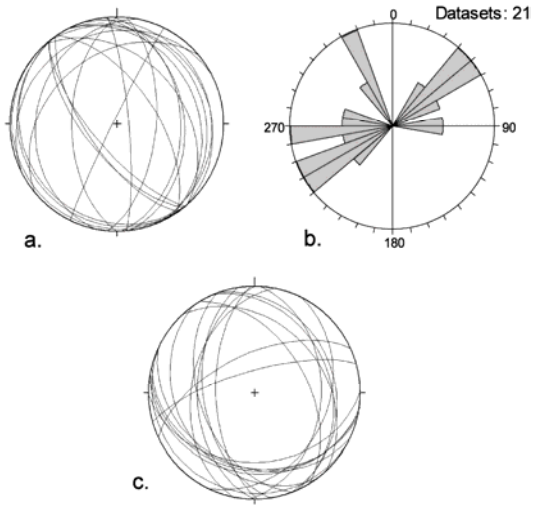

Fig. 5.30. Fold and fault data from Ordovician and Triassic units (combined) at the Karadiken locality. a. Fold axial planes; b. Fold vergence direction; c. Fault planes.

5.8.3 Southern part of the study area

In the southerly study area, structural data were collected from 16 localities. Rather than study the data by individual locality, they are grouped according to the tectonic contact and setting from which they were observed: (i) Hadim nappe – Bolkar nappe contact (7 localities); (ii) Hadim nappe – Geyik Dağ contact (1 locality); (iii) Hadim nappe – Ophiolitic melange contact (2 localities); (iv) Bolkar nappe – Ophiolitic melange contact (1 locality); (v) Bolkar nappe – Bozkir nappes contact (1 contact); (vi) Intra-Bolkar nappe (4 localities).

5.8.3.1 Hadim nappe – Bolkar nappe contact

This includes the following localities: 7 (Oküz Çukuru); 8 (Derence Dere); 9 (Babuçcu Yayla); 10 (Hocalar Yayla); 17 (Sögüt Yayla); 18 (Koyaardi); 19 (Ekinlik Yayla) (Fig. 5.27. Fault and fold data from these localities are shown in Fig. 5.31 and Fig. 5.32. Fold axial plane data (Fig. 5.31a-e) show a strong WNW-ESE and NW-SE trend. N-S trending planes occur at some localities, and occasionally a NE-SW trend. Fold vergence data (Fig. 5.31f-j) show that folds are predominantly N or S/SW verging; however, this is not exclusive and folds are seen to verge E and W as well.

In comparison to fold axial planes, fault planes are much more variable in orientation. At all localities shown there is a NW-SE trend, along with N-S and E-W trending faults. At one locality in particular (Fig. 5.32h), a strong NE-SW trend was observed. Where kinematic indicators are available, a variety of normal, reversed and strike slip faults were observed. Slickensides are not quite as random in orientation as the faults, with top-to-the-SW and top-to-the-N being the most common trends. There are also NW-SE trending slickensides at most localities, although these are less abundant.

The regional tectonic contact between the Hadim and Bolkar nappes trends in a NW-SE orientation, as seen on the simplified structural map (Fig. 5.27). This regional trend is clearly seen in the fault and fold data presented, with a large percentage of NW-SE trending structures. This suggests that the regional shortening orientation is in a NE-

SE plane. However, there are fault and fold orientations in other directions, particularly N-S and E-W. One thing that should noted is that the contact between the Hadim nappe and Bolkar nappe locally runs E-W (e.g. Loc. 17, Sögüt Yayla) (Fig. 5.27) and N-S (e.g. Loc. 8, Derence Dere) (Fig. 5.27).

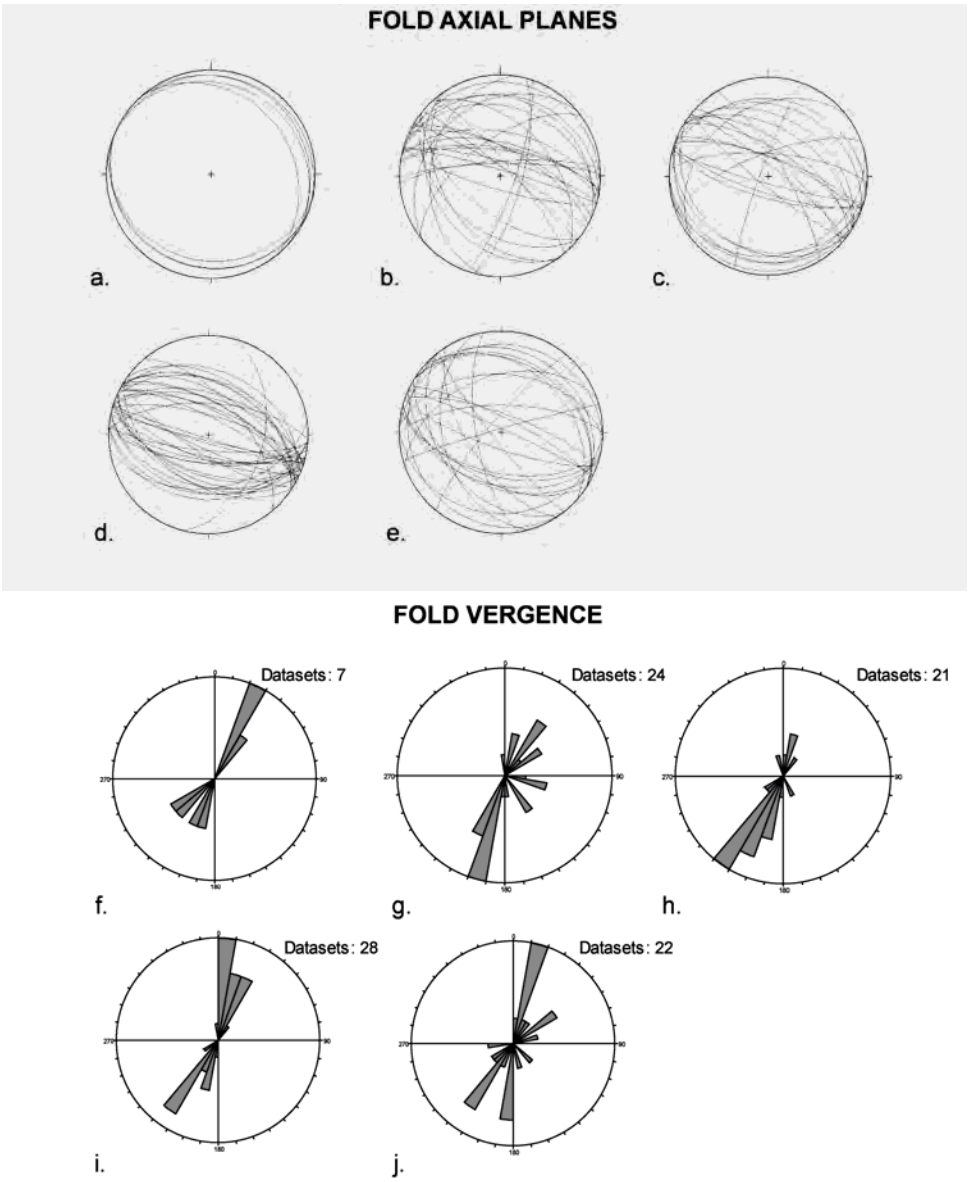

Fig. 5.31. Fold axial planes and fold vergence orientation from localities at the contact of the Hadim nappe and Bolkar nappe (see Fig. 5.27). a-e: Fold axial planes. f-j: Fold vergence. a. Loc. 7 (Oküz Çukuru); b. Loc. 8 (Derence Dere); c. Loc. 9 (Babuççu Yayla); d. Loc. 17 (Sögüt Yayla); e. Loc. 18 (Koyaardi); f. Loc. 7 (Oküz Çukuru); g. Loc. 8 (Derence Dere); h. Loc. 9 (Babuççu Yayla); i. Loc. 18 (Sögüt Yayla); j. Loc. 18 (Koyaardi).

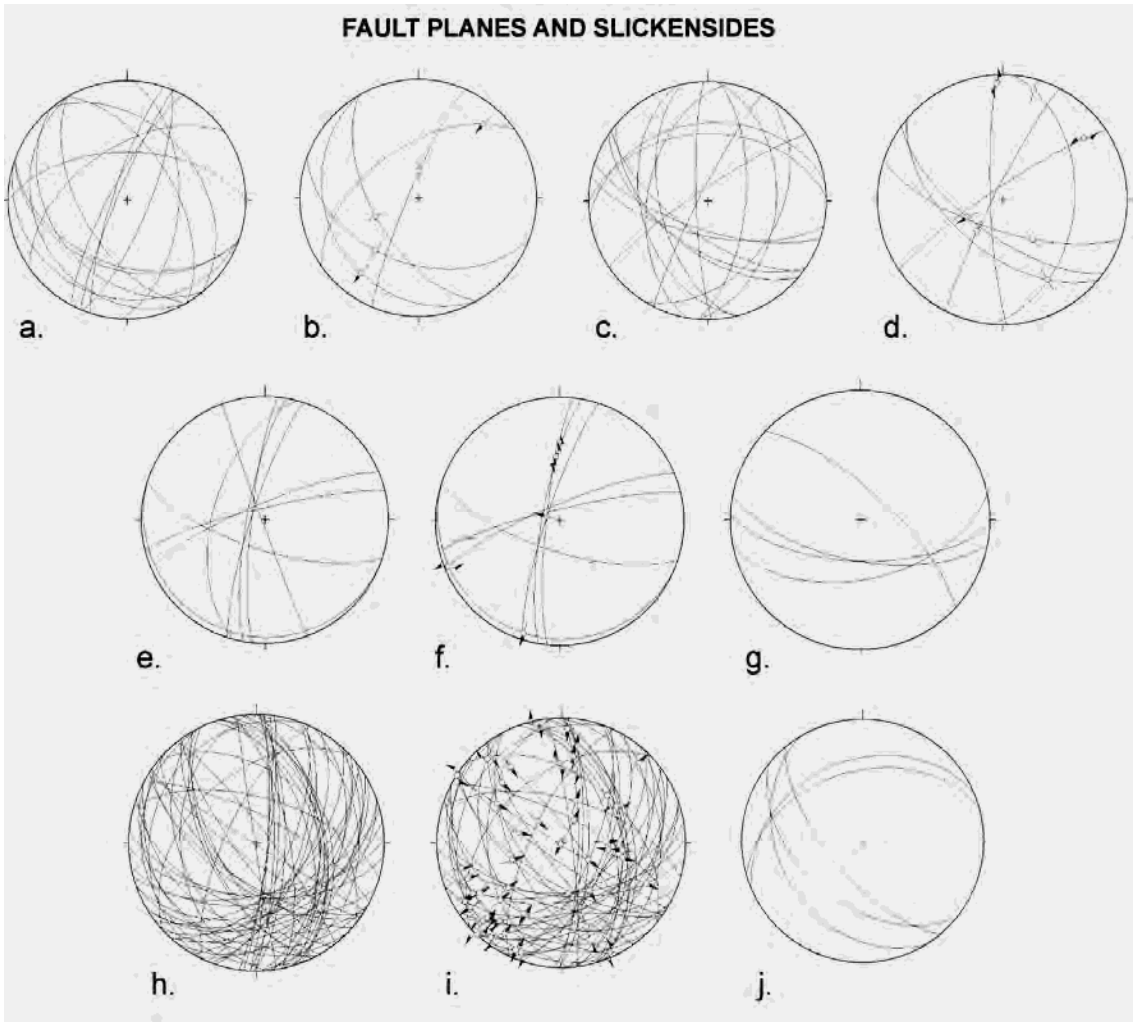

Fig. 5.32. Fault plane orientations and kinematic indicators from contact between Hadim nappe and Bolkar nappe. a. Fault planes, Loc. 7 (Oküz Çukuru). b. Fault planes with slickensides, Loc. 7 (Oküz Çukuru). c. Fault planes, Loc. 8 (Derence Dere). d. Fault planes with slickensides, Loc. 8 (Derence Dere). e. Fault planes, Loc. 10 (Hocalar Yayla). f. Fault planes with slickensides, Loc. 10 (Hocalar Yayla). g. Fault planes, Loc. 17 (Sögüt Yayla). h. Fault planes, Loc. 19 (Ekinlik Yayla). i. Fault planes with slickensides, Loc. 19 (Ekinlik Yayla). j. Fault planes, Loc. 18 (Koyaardi).

Taking this into consideration, it can be inferred that the contact between the Hadim nappe and Bolkar nappe has experienced compression along a NW-SE and W-E axis. However, there is likely to be an oblique component to this compression. There is not enough evidence to determine whether the Hadim nappe was emplaced from the north to

the south to its presently high level within the nappe stack, or whether it was 'backthrust' to the north over the Bolkar nappe.

5.8.3.2 Hadim Nappe – Geyik Dağ contact

There is only one data set for this contact; locality 13 (Gölbelen Tepe) (Fig. 5.33a). Fault planes run predominantly N-S to NW-SE orientation, with a single fault running perpendicular to this with a ENE-WSW trend. The faults were observed and measured from thick-bedded and massive limestones at the contact. The majority of the faults run parallel to the regional tectonic contact between the Hadim nappe and Geyik Dağ autochthon. Kinematic indicators were not seen on fault planes; however, it was noted that many of the faults are steeply dipping (Fig. 5.33a) and the local relationships observed suggest that most faults have a normal displacement. At this particular locality, it is likely that normal faulting occurred after original nappe emplacement, possibly as a result of neotectonic stress regimes, tectonic escape or orogenic collapse.

5.8.3.3 Hadim Nappe – Ophiolitic Melange contact

Fault data for this contact are found at two localities, 6 (Sarapinar Yayla) and 14 (Küçüksu Tepe) (Fig. 5.33b, c, d). At locality 6 (Fig. 5.33b), the dominant fault plane orientation is N-S, with a lesser number of faults trending E-W, NW-SE, and NE-SW. At locality 14 (Fig. 5.33c, d), all the faults have a NW-SE trend; nearly all of those faults dip to the NE. Kinematic indicators show a clear top-to-the-S/SW/W direction of movement. At both of these localities, the regional tectonic contact runs NW-SE. The variation in fault plane orientation, especially at locality 6, implies that there was oblique compression along the contact. Although limited, kinematic indicators do imply top-to-the-SW movement, so that back-thrusting of the Hadim nappe to the NE is still a possibility.

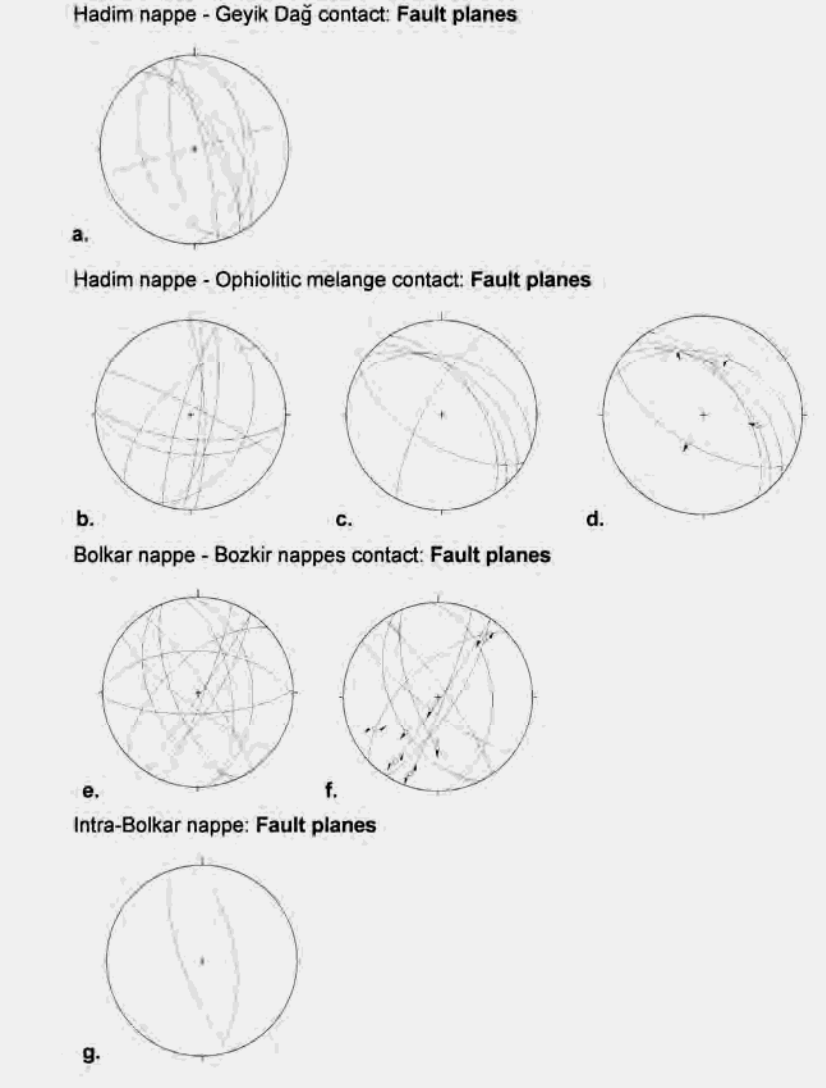

Fig. 5.33. Fault plane orientations and kinematic indicators from contact between: a. Hadim nappe and Geyik Dağ; b-d. Hadim nappe and Ophiolitic melange; e-f. Bolkar nappe and Bozkir nappes; g. Intra-Bolkar nappe. a. Fault planes, Loc. 13 (Gölbelen Tepe). b. Fault planes, Loc 6. (Sarapinar Yayla). c. Fault planes, Loc. 14. (Küçüksu Tepe). d. Fault planes with slickensides, Loc. 6 (Küçüksu Tepe). e. Fault planes, Loc. 5 (Dereköy). f. Fault planes with slickensides, Loc. 5. (Dereköy). g. Fault planes, Loc. 15. (Elmaağaç Yayla).

5.8.3.4 Bolkar Nappe – Ophiolitic Melange contact

Fold data for this tectonic contact was observed at locality 12 (Baybağan Yayla) (Fig. 5.34a, b). Fold axial planes are strongly orientated in a NW-SE plane, with a skew towards WNW-ESE. Most fold axial planes were seen to dip to the NE. Fault vergence

is predominantly to the SSW and SW, although some data suggests vergence to the NE. This locality provides the most convincing evidence of top-to-the-SW movement, as many of the folds recorded are overturned or recumbent giving a good sense of the shear direction along the contact. The Bolkar Nappe is in a structurally higher position than the ophiolitic melange along strike at Dipsiz Göl.

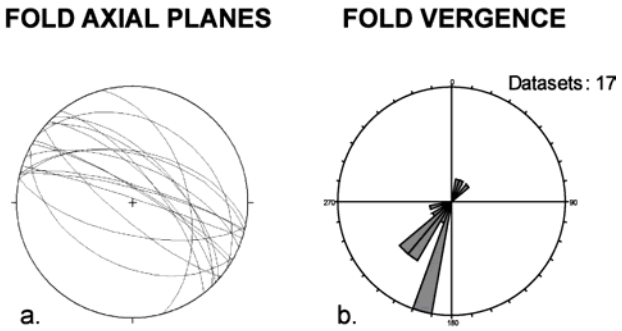

Fig. 5.34. Fold axial planes and fold vergence orientation from localities at the contact of the Bolkar nappe and Ophiolitic melange (see Fig. 5.27). a. Fold axial planes, Loc. 12 (Baybağan Yayla). b. Fold vergence, Loc. 12 (Baybağan Yayla).

5.8.3.5 Bolkar Nappe – Bozkir Nappes contact

Fault data for this tectonic contact was observed at locality 5 (Dereköy) (Fig. 5.33e, f). Faults at this locality do not exhibit a distinctly preferred orientation; however, more faults are orientated NW-SW than any other trend. Slickensides show that faults are either normal or strike-slip in nature. Normal faults are downthrown to the SW, whereas strike-slip faults are sinistral (left-stepping), and orientated in a SW-NE plane. These data do not reflect the regional tectonic regime of this contact, as it appears that the downthrown side should be to the NW. However, it does highlight the local variability that can be observed within a fault zone.

5.8.3.6 Intra-Bolkar nappe

Data from within the Bolkar nappe were collected at localities 4 (Dikilitaş Yayla), 11 (Karabayir Yayla), 15 (Elmaağaç Yayla), and 16 (Kuma Dere). Data for these localities are shown in Fig. 5.33g and Fig. 5.35. The localities where faults and fold data were collected are where imbricate thrusts were observed within the Bolkar nappe, which (as described in section 5.6) is largely a broken formation.

Fold axial planes (Fig. 5.35a-d) are orientated predominantly E-W and SE-NW, with a limited number of fold axes trending N-S or WSW-ENE. The axial planes dip at low angles, especially at locality 16 (Kuma Dere). Fold vergence (Fig. 5.35e-h) is more variable; however, there is an abundance of folds that verge SW and S. There is also a strong vergence towards the NE, and some measured orientations to the NW, N, and SE. Locality 16 (Kuma Dere), in particular, shows a strong S/SW fold vergence direction. Limited fault plane data show a NNW-SSE trend (Fig. 5.33g).

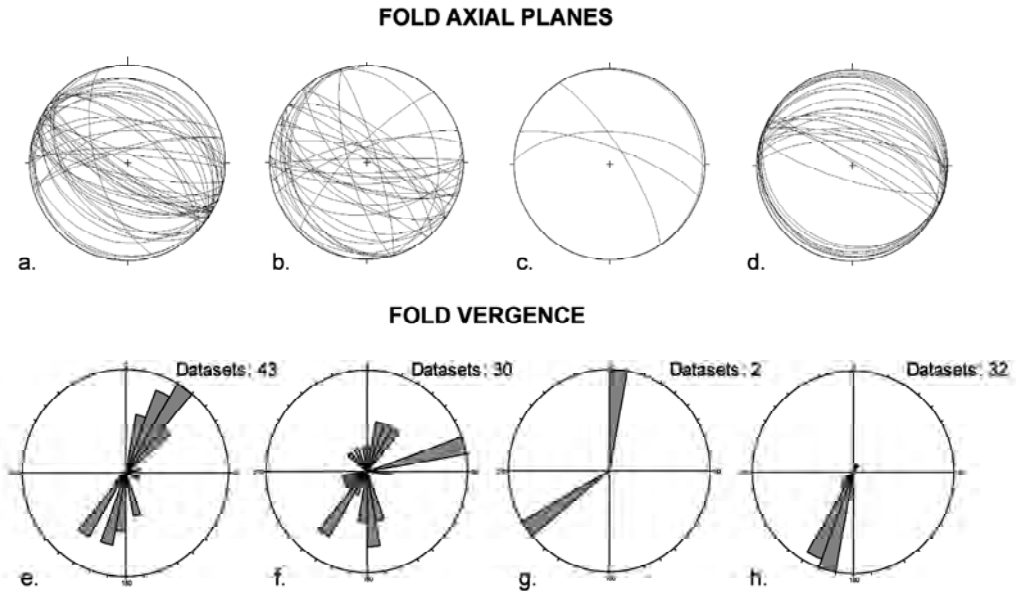

Fig. 5.35. Fold axial planes and fold vergence orientation from intra-Bolkar nappe localities (see Fig. 5.27). a-d: Fold axial planes. e-h: Fold vergence. a. Loc. 4 (Dikilitaş Yayla). b. Loc. 11 (Karabayir Yayla). c. Loc. 15 (Elmaağaç Yayla). d. Loc. 16 (Kuma Dere). e. Loc. 4 (Dikilitaş Yayla). f. Loc. 11 (Karabayir Yayla). g. Loc. 15 (Elmaağaç Yayla). h. Loc. 16 (Kuma Dere).

Intra-Bolkar nappe structural data imply a NE-SW orientation of compression, resulting in NW-SE trending structures. It is clear that although the internal faults / imbricate thrusts are not marked on the structural map (Fig. 5.27), they run more or less parallel to the Bolkar nappe tectonic contacts, and parallel to the regional NW-SE linear nature of the nappe itself. The internal deformation of the Bolkar nappe does suggest that the emplacement and deformation was caused by top-to-the-S/SW movement.

5.8.4 Summary of structural data

All of the structural data presented above are consistent with Upper Cretaceous and Lower Cenozoic emplacement of the Beyşehir-Hoyran-Hadim nappe stack throughout the Central Taurides. Despite local variation, fold axes, fold vergence, fault plane, slickenside lineation, mineral lineation, tension gashes and shear fabric orientations typically trend N-S, NW-SE, and W-E. These trends are consistent with the regional orientation of tectonic contacts between different allochthonous and autochthonous units within the study area. Kinematic indicators from faults (i.e. slickensides) and folds (fold vergence) imply a top-to-the-S/SW/W movement overall. However, along critical contacts, particularly that between the Hadim nappe and Bolkar nappe, the direction of motion cannot be directly inferred from the data available. Strong evidence of younger extensional and strike-slip faulting is observed, and hence faults and folds cannot be directly confirmed as being of Late Cretaceous – Early Cenozoic in age. It was also noted that structural data locally can conflict with regional tectonic trends, again possibly related to younger neotectonic faulting or post-emplacement tectonic collapse.

5.9 Stratigraphic / Sedimentological data

As is shown in the tectono-stratigraphic chapter (chapter 2), the Jurassic-Late Cretaceous stratigraphy in both the Geyik Dağ autochthon, and the Hadim and Bolkar nappes, is dominated by thick-bedded to massive platform carbonates. However, critical phases of subsidence of the platform occurred during the Late Cretaceous and Early Cenozoic. This section will document the stratigraphy and sedimentology of the autochthon and allochthonous units to help provide a temporal context for the emplacement of the Beyşehir-Hoyran-Hadim nappes.

5.9.1 Northerly study area

Within the northerly study area, the stratigraphy of the Geyik Dağ and Hadim nappe has been documented in detail (Monod, 1977; Gutnic et al., 1979; Andrew and Robertson, 2002). During this study key localities from the previous literature were field checked. Most of the stratigraphic data presented here represents a review of previous authors work.

5.9.1.1 Autochthonous Geyik Dag

A summary of the Geyik Dağ stratigraphy is shown in Fig. 5.36. The Jurassic to Cretaceous stratigraphy of the Geyik Dağ is dominated by thick-bedded to massive platform carbonates, which continue right up until the Early Cenozoic (Gutnic et al., 1979). The succession is mainly composed of grainstones and wackestones, with limited distinguishable fauna (Andrew, 2003). Bauxite horizons and stratigraphic gaps in the latest Cretaceous suggest that the platform experienced some emergence during this period (Monod, 1977). This implies that the platform experienced shallow, to very-shallow, marine conditions during most of the Late Cretaceous.

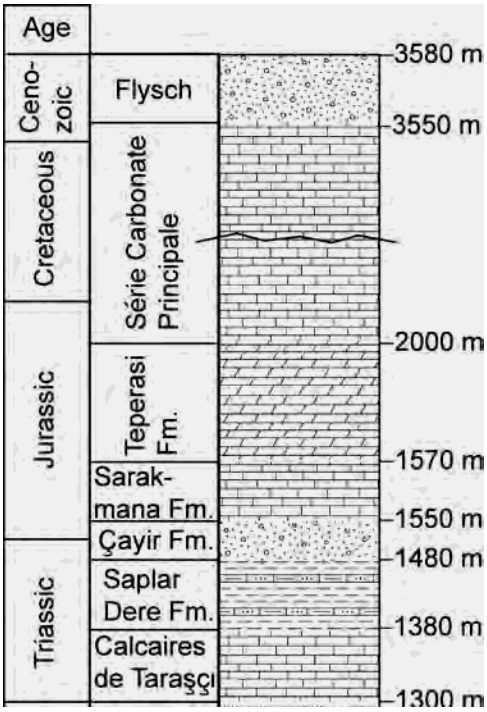

Fig. 5.36. Summary of Triassic, Jurassic and Cretaceous units in the Beyşehir – Seydişehir region.

The uppermost Cretaceous (Maastrichtian) to Palaeocene succession is composed of bioclastic limestones, grainstones and calcareous mudstones, which are laterally variable in thickness (Monod, 1977; Andrew, 2003). Overlying this are Lower to Middle Eocene limestones (~20 m) containing Nummulitic foraminifera (Fig. 5.37a), locally capped by a hardground horizon (Monod, 1977; Andrew, 2003). The top of the succession is composed of calcareous sandstone and siltstone turbidites, dated as Middle Eocene (Monod, 1977; Andrew, 2003) based on the presence of benthic foraminifera such as *Asterocyclina stellatus*. Locally, carbonate debris flows and conglomerates occur at the very top of the succession (Fig. 5.37b).

Detailed logging of the Early Cenozoic sequence was undertaken by Andrew (2003) near Üzümlü village. Middle Eocene clastics are interbedded with fissile mudstones on a 5-10 cm scale. Groove casts were observed on the underside of sandstone beds, which have planar contacts with mudstone beds. An overlying carbonate debris flow (150 m-thick) contains clasts 1 cm – 1 m in size composed of radiolarian

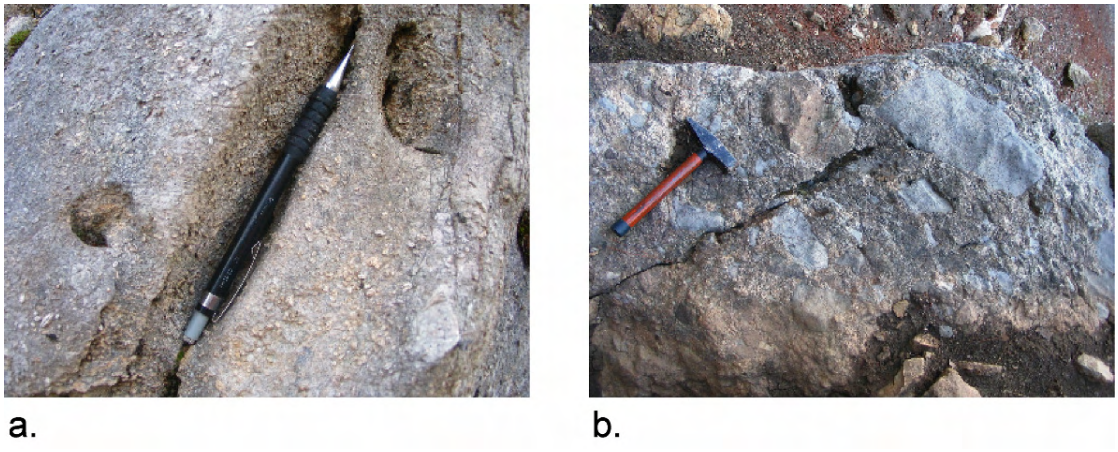

Fig. 5.37. a. Lower to Middle Eocene Nummulitic limestone from the Geyik Dağ autochthon, to the west of Derebuçak village. b. Carbonate debris flows of Middle Eocene age from the Geyik Dağ.

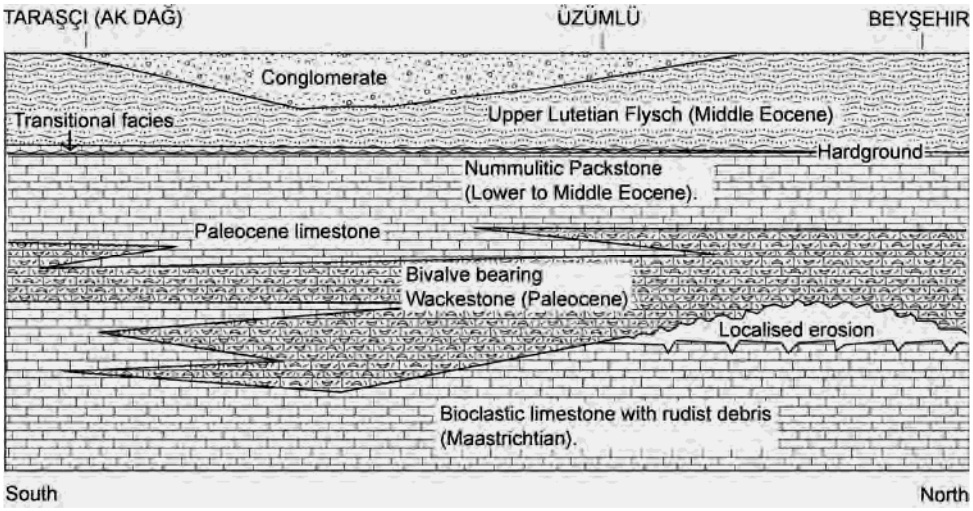

Fig. 5.38. Schematic diagram showing facies distribution of Upper Cretaceous and Lower Cenozoic sediments in the area between Beyşehir and Taraşçi. Diagram modified from Monod (1977).

chert, tuffs, volcanic and limestone clasts. These clasts were noted by Andrew (2003) to be of similar composition to lithologies within the overlying nappe stack.

This sedimentary sequence is tectonically overlain by the Hadim nappe, which is the lowermost allochthonous tectonic unit within the overriding nappe stack. A schematic diagram showing the detailed stratigraphy of the Upper Cretaceous and Lower Cenozoic (modified from Monod, 1977) is shown in Fig. 5.38. The sedimentary

sequence observed in the Geyik Dağ is indicative of a Jurassic – Upper Cretaceous shallow marine platform carbonate succession. However, in the Early Cenozoic, particularly the Eocene, the deposition of turbiditic sediments is indicative of subsidence of the platform and increased water depth.

5.9.1.2 Allochthonous Hadim nappe

Unlike the Geyik Dağ, the Hadim nappe does not contain any Cenozoic sediments. One possible reason for this is that the Hadim nappe is in a higher structural and topographic position within the nappe stack, and hence the uppermost part of the stratigraphy may have been eroded (i.e. all Cenozoic sediments eroded). However, another possibility is that the Hadim nappe did not experience any Cenozoic sedimentation due to its tectonic setting. This will be discussed later in the chapter.

Jurassic and Cretaceous units are dominated by platform carbonates. The Çamlik unit is a thick succession of neritic limestone and dolomite dated as Lower Jurassic – Upper Cretaceous age (Monod, 1977). The Late Triassic Çayır Formation grades into the Çamlik unit in a conformable manor. A transitional zone, which includes calcareous sandstone, packstone, grainstone, and silty marl, and locally dolomite, contains fragments of calcareous algae *Palaeodasycladus* sp. and *Girvanelles* of Middle – Early Jurassic age.

The transitional zone is ~100 m thick, and is overlain by a ~500 m succession of neritic carbonates, including oolitic limestone, pisolitic grainstone, bioclastic packstone and wackestone (Monod, 1977; Andrew, 2003). The lower 100 m of this sequence contains fragments of benthic foraminifera, such as *Lituolidae* and *Haurania.* This succession also contains fragments of bivalve, calcareous algae, and disarticulated shelly fauna (Monod, 1977; Andrew, 2003).

Above this, 200m of oosparite is overlain by micritic limestones containing the algae *Clypeines jurassica* dated as Upper Jurassic to Lower Cretaceous (Monod, 1977; Gutnic et al., 1979). Overlying this a ~150 m-thick succession of bioclastic calcarenite and breccia, containing bioclasts of rudist corals and Orbitoides, has been dated as Late Cretaceous (Monod, 1977). The uppermost sediments within this succession are micritic

limestone and coarse calciturbidites which contain neritic clasts. These sediments are <30 m thick, and have been found to contain pelagic foraminifera of Maastrichtian age (Monod, 1977).

Above this is the Zekeriya Formation that begins with red to cream coloured micritic limestone, containing Maastrichtian *Globotruncana* sp., a transitional facies (~10 m thick) between the Upper Senonian rudist-bearing limestones and turbiditic deposits (Monod, 1977; Özgül, 1997). The overlying coarse "flysch" deposits contain foraminiferal-bearing limestone blocks of Carboniferous and Permian age, as well as clasts of chert and volcanics (diabase, dolerite) set within a marl-sandstone matrix. Blocks are described as being several metres to 100 metres in size (Monod, 1977; Özgül, 1997). Directly above this, the sedimentary succession is tectonically overlain by allochthonous ophiolitic melange. It is not known what age the "flysch" matrix is; however, stratigraphic association suggests that it is Maastrichtian.

The sedimentary sequence described above is indicative of a stable, shallow-marine platform depositional environment from the Early Jurassic until the Late Cretaceous. The deposition of breccias and calciturbidites in the Late Cretaceous (including the Maastrichtian), and the identification of pelagic fauna, implies platform subsidence and an increase in water depth during this time.

5.9.2 Southerly study area

The Mesozoic and Cenozoic stratigraphy in the southerly study area has been documented in detail (Özgül, 1976; Özgül, 1984; Özgül, 1997; Andrew and Robertson, 2002). This work was field checked during this study.

5.9.2.1 Autochthonous Geyik Dağ

As described in the tectono-stratigraphic chapter (chapter 2), in the southerly study area the Geyik Dağ exhibits a regional unconformity between the Ordovician and Mesozoic – Cenozoic successions. Overlying this unconformity is a Middle Jurassic to Aptian – Cenomanian carbonate succession, known as the Polat Limestone, which is ~450-500 m

thick. This is largely composed of dolomitic limestone, dolomite, algal limestone and lagoonal limestone. Local benthic foraminiferal-bearing wackestone and packstone contain microfossils such as the benthic foraminifera *Alzonella* sp. (Middle Jurassic) and *Dukhania* sp. (Aptian – Cenomanian) (Özgül, 1984; Özgül 1997).

The Maastrichtian – Palaeocene Çataloluk Limestone overlies the Polat Limestone, which is up to ~150 m thick. This consists of a basal limestone conglomerate (~20 m), overlain by bioclastic rudist-bearing and reefal shallow-marine limestone (~100 m), in turn overlain by micritic limestone ~30 m thick (Özgül, 1984; Andrew, 2003). Only the uppermost 30 m of this succession is Palaeocene in age, as indicated by the presence of the coral *Actinacis* sp. and the foraminifera *Rotalia* sp. (Özgül, 1997).

Unconformably overlying this carbonate sequence is a "flysch" succession, which is up to 400 m thick in the type section (Andrew, 2003). Özgül (1997) has dated the base of this sequence as Palaeocene based on the identification of Nummulitic forams within a 30 m-thick limestone horizon. This is then overlain by lithiclastic sandstone (~ 200 m) and debris flows interbedded with limestone and shale. Clasts are composed of local sediment derived from the Upper Cretaceous and Palaeocene sequence of the Geyik Dağ, as well as far travelled "exotic" sediment such as radiolarian chert, volcanic clasts and Permian limestone (Özgül, 1997; Andrew 2003). An overlying debris-flow succession, <200 m thick, contains similar local and exotic clasts as above, and also phyllites and serpentinite (Andrew, 2003).

This succession is comparable with that of the Geyik Dağ succession of the northerly study area. Shallow-marine sedimentation dominates the Mesozoic succession, but by the Early Cenozoic, particularly Late Palaeocene to Eocene, deposition of turbidites and debris flows is indicative of subsidence of the platform and a change to a deeper water environment.

5.9.2.2 Allochthonous Hadim nappe

The Hadim nappe in the Hadim-Bozkir region consists of a relatively undeformed sequence of Devonian – Upper Cretaceous age (chapter 2). Transgressing the Late Triassic Çayır Formation clastics is a very thick (~800-1000 m) neritic limestone and

dolomitic limestone succession. The Liassic – Lower Cretaceous (~600 m) is dominated by grey dolomitic limestone and dolomite, overlain by packstone, wackestone and pelitic limestone containing algae and the foraminifera *Clipeina* sp., *Actinoporella* sp. and *Spirolina* sp.(Özgül, 1997). The top of this succession is dated as Cenomanian (Özgül, 1997), followed by a disconformity. Above this, Upper Cretaceous shallow-water rudist- and ostracod- bearing pelitic packstones, ~60 m thick, contain the foraminifera *Montcharmontia* sp. (Özgül, 1997).

The sedimentary sequence described above suggests that shallow-marine conditions dominated the post-Triassic Hadim unit succession. By the Late Cretaceous (Maastrichtian), the deposition of pelagic limestone and turbidites and debris flow deposits is indicative of platform subsidence and collapse.

It should be noted here that, in the southerly study area, no upper Cretaceous sediments were observed in the Hadim nappe during this study. Where studied by us, the Hadim nappe mainly exposes Upper Palaeozoic and Lower Mesozoic sediments; younger Mesozoic units are only found in areas to the SW of the study area of this project.

5.9.2.3 Allochthonous Bolkar nappe

The Bolkar nappe, like the Hadim nappe, contains Devonian to Cretaceous units (chapter 2); however, as mentioned earlier in this chapter the Bolkar Dağ is heavily deformed, by comparison. Overlying the Upper Triassic – Lower Jurassic Çayır Formation is a 600 m-thick succession of shallow-marine limestone, algal mudstone, wackestone, packstone, oolitic limestone and grainstone (Özgül, 1997). The succession typically contains bioclastic material (e.g. bivalves) and benthonic foraminifera (e.g. *Lenticulina* sp., *Pseudoeggerella* sp., *Favreina* sp.) giving an age range of Early Liassic to Late Malm (Özgül, 1997), although a continuous sequence is not present owing to intra-formational unconformities.

The overlying Cretaceous sequence, up to 200 m-thick, unconformably overlies the Jurassic sequence. The lowermost Cretaceous units are composed of interbedded

chert and pink packstone-wackestone containing *Tubiphytes morronensis*, amongst other benthic and planktonic foraminifera, dated as Cenomanian – Santonian in age (Özgül, 1997). Laterally this time period in places is represented by pelagic *Globotruncana*-bearing biomicrites (Özgül, 1984). Özgül (1984) has dated overlying interbedded wackestone, mudstone and calciturbidites as Campanian in age. The top of the Bolkar Dağ succession is marked by a flysch succession, < 200 m thick, beginning with interbedded limestone and shale, and passing up into a chaotic debris flow and tectonic melange (Özgül, 1997; Andrew, 2003). The debris flow matrix contains *Globotruncana bulloides* and *Globotruncana arca* of Maastrichtian age (Özgül, 1997; Andrew, 2003). A lithiclastic sandstone horizon is commonly found containing grains of carbonate, quartz, chert, and volcanics where the Bolkar nappe is overridden by the Hadim nappe, and where intra-Bolkar nappe imbricate thrusts exist. Although no dateable fauna were identified during this study, sediments of a near identical composition observed at Dipsiz Göl were found to contain large Nummulitic forams, dated as Palaeocene – Eocene (Özgül, 1984). By stratigraphic correlation it is suggested that these lithiclastic sandstones are they youngest sediments (Early Cenozoic) within the Bolkar nappe stratigraphy.

These data suggest that the Bolkar unit experienced shallow-marine platform carbonate deposition for most of the Jurassic – Cretaceous period. The unconformable relationship between the Jurassic and the Cretaceous units is indicative of emergence and possibly erosion of the platform during this time, although there are no related sedimentary deposits to confirm this. The platform then experienced pelagic conditions and deeper-water sedimentation from Campanian to Maastrichtian. Finally, lithiclastic sandstones and debris flows were deposited during the Palaeocene – Eocene.

5.9.3 Transition from Upper Cretaceous to Ophiolitic Melange

As shown in the regional cross-sections in section 5.5, the base of the allochthonous Ophiolitic Melange unit is not observed, and is inferred to tectonically overly the Geyik Dağ autochthon. Within the study area, regional-scale outcrops of ophiolitic rocks are rare, and are closely associated with Upper Cretaceous ophiolite-derived melange, for

example at Dipsiz Göl (Andrew, 2003). It has been inferred from this earlier study that oceanic lithosphere was emplaced onto the Tauride platform, the syn-tectonic ophiolitic melange developed ahead of the thrust front, which was in then tectonically overlain by the advancing ophiolitic slab (Andrew, 2003). Only local remnants of this slab remain, however the transitional facies from platform carbonate to ophiolite derived sediments is preserved locally in the Bolkar nappe.

During this study, several key localities were studied which provided insights into the transition from Lower Cretaceous neritic sedimentation, to Upper Cretaceous pelagic sedimentation, and finally to Upper Cretaceous ophiolite-derived sedimentation. Two logs through Upper Cretaceous sedimentary successions illustrate the relationships well (Fig. 5.39).

5.9.3.1 Sögüt Yayla

A measured section through the Upper Cretaceous succession at Sögüt Yayla (Fig. 5.39a) shows that the boundary between Cretaceous carbonates and Ophiolitic derived melange sediment is transitional. A thick neritic carbonate succession (at base of the log, Fig. 5.39a), several hundred metres thick (Özgül, 1997), is followed, above a sheared contact, by ~ 5m of sheared red shales. This is followed by ~20 m of micritic and oolitic limestone and then by chaotic debris flows (Fig. 5.40a). The debris flows contain clasts 2 - 40cm in size, which are sub-angular to sub-rounded, with a skew to sub-angular. These clasts are composed of a variety of dolomite, micritic limestone, pink pelagic limestone, quartzite and chert. The matrix is a poorly sorted purple-red sandy-silt. This is then overlain by micritic limestone which, up-sequence, contains abundant black and red chert nodules (Fig. 5.40b). A limestone conglomerate horizon above this (~10 m-thick) is exclusively composed of limestone clasts, but also replacement chert nodules. The top of the conglomerate is heavily sheared, and represents a faulted contact with overlying cherty limestone, ~10 m thick. This is, in turn, stratigraphically overlain by fine-grained pink pelagic limestone (Fig. 5.40c), which has yielded *Globotruncana* sp. of Campanian age (new data from this study; see section 5.9.4).

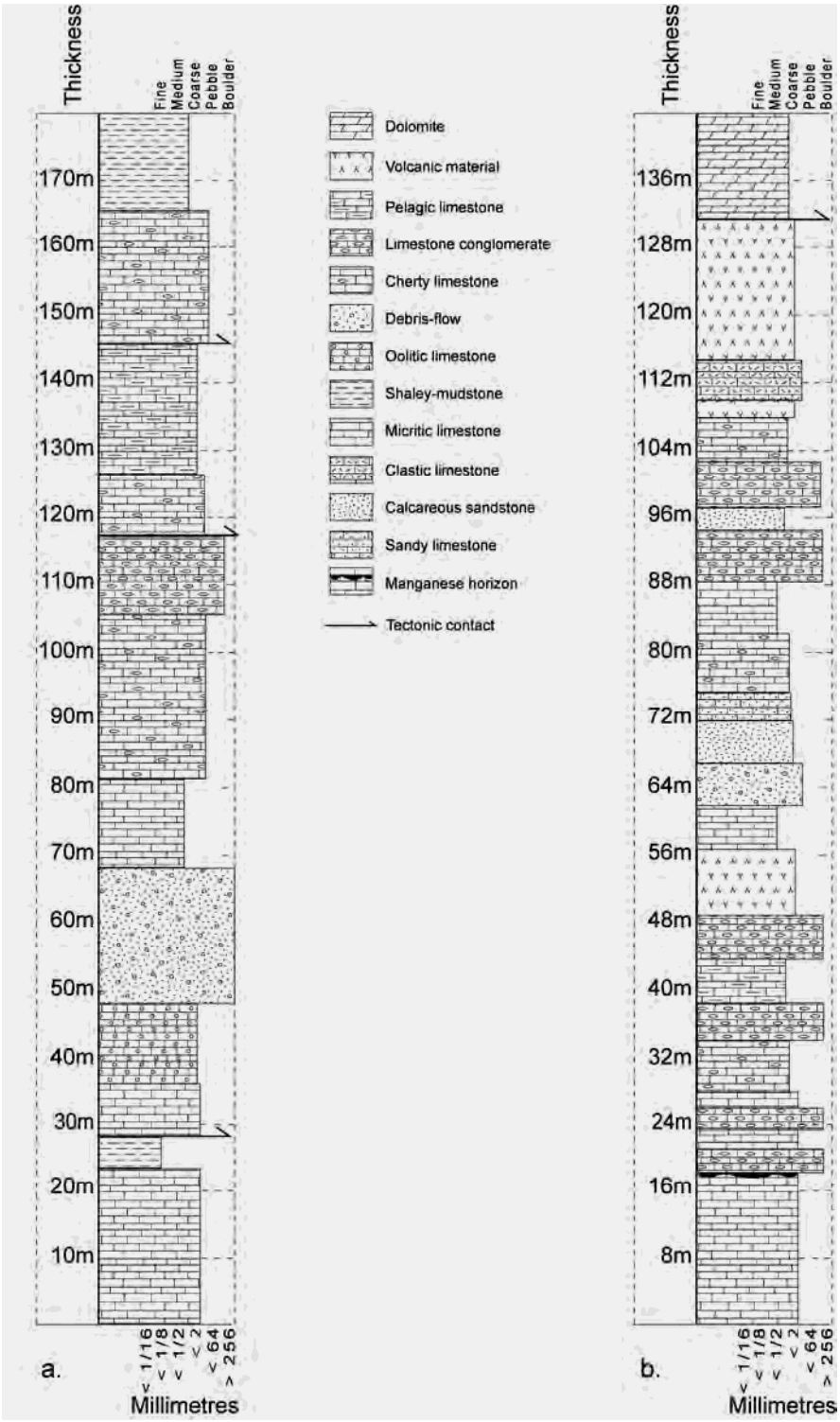

Fig. 5.39. a. Log through the Upper Cretaceous succession at Sögüt Yayla. b. Log through Upper Cretaceous succession at Dikilitaş Yayla.

The Upper Cretaceous pelagic limestone then 'grades' into ophiolitic melange over a 200 m interval. A large exotic block of limestone of unknown age, 300 m x 100 m in dimension, overlies the pink pelagic limestone. This is, in turn, overlain by pelagic limestone and volcaniclastic shales (Fig. 5.40d), composed of essentially ophiolite-derived sediment (further compositional information provided in section 5.9.5). The transition into ophiolitic melange is shown well in Fig. 5.40e.

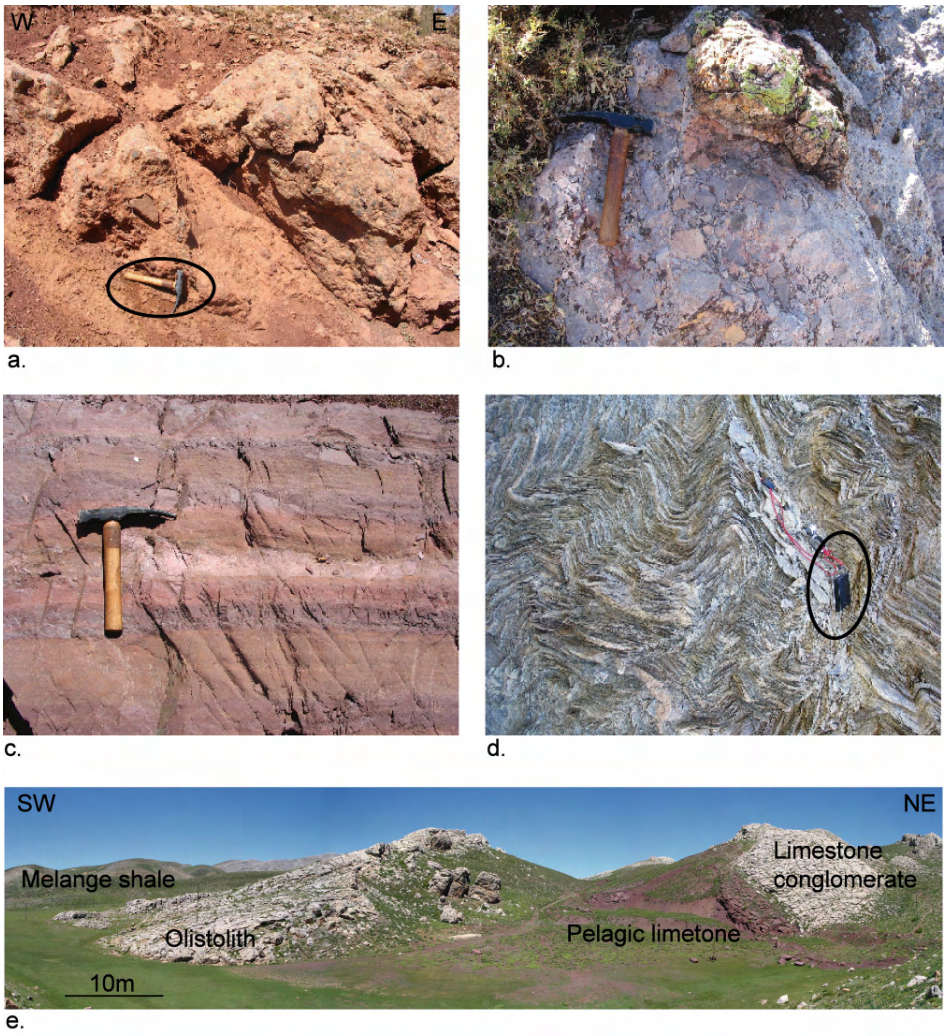

Fig. 5.40. a. Coarse debris-flow deposit. Hammer circled for scale. b. Replacement chert nodule within limestone conglomerate. c. Laminated pink pelagic limestone. d. Ophiolite-derived shale in the melange. Compass circled for scale. e. Transition through upper part of log at Sögüt Yayla (Fig. 5.39a).

The succession at Sögüt Yayla is the transition from Cretaceous shallow-marine platform sediments into ophiolitic melange. As the ophiolite was being emplaced, the platform was subsiding and sedimentation continued, resulting in the deposition of deeper water and coarser sediments. Faulting is closely associated with shale deposits, and this could be related to flexural loading of the platform as the ophiolite is being emplaced.

5.9.3.2 Dikilitaş Yayla

The log through Dikilitaş Yayla (Fig. 5.39b) was measured on the inverted limb of a regional recumbent anticline. The lowermost part of the succession are Mesozoic neritic carbonates (Fig. 5.39b), of inferred Early Cretaceous age based on stratigraphic relationships. The true thickness is several hundred metres, not shown on the measured log. A thin, but distinctive, horizon is a deep purple-black in colour (Fig. 5.41a), is very hard and forms an irregular bedding surface, which is interpreted as a manganese hardground representing a period of non-deposition and possibly erosion.

Above this distinctive horizon there is a change in lithology, with an incoming of limestone conglomerate, cherty limestone, and interbedded pelagic micritic limestone ~30 m-thick. Limestone conglomerates predominantly contain sub-angular to sub-rounded limestone clasts, set in a pink pelagic limestone matrix (Fig. 5.41b). The siliceous limestone includes recrystallised limestone with chert nodules (Fig. 5.41c), or with thin horizons (~15cm thick) of black bedded chert (Fig. 5.41d). The pelagic limestone is commonly a deep pink colour, similar in composition to the limestone conglomerate matrix.

Stratigraphically overlying is a distinctive, but poorly exposed, horizon of volcanogenic sedimentary material. This is composed of volcanogenic shale, with fragments of highly chloritised tuff. Fragments of vesicular basalt occur as clasts within the shaley matrix. Overlying this is a horizon of micritic limestone.

A coarse debris flow, composed of limestone, chert, basalt and volcaniclastic clasts / sediment, has a pelagic limestone matrix (Fig. 5.41e). The debris flow is poorly sorted and contains large angular clasts, particularly basalt. Limestone clasts are

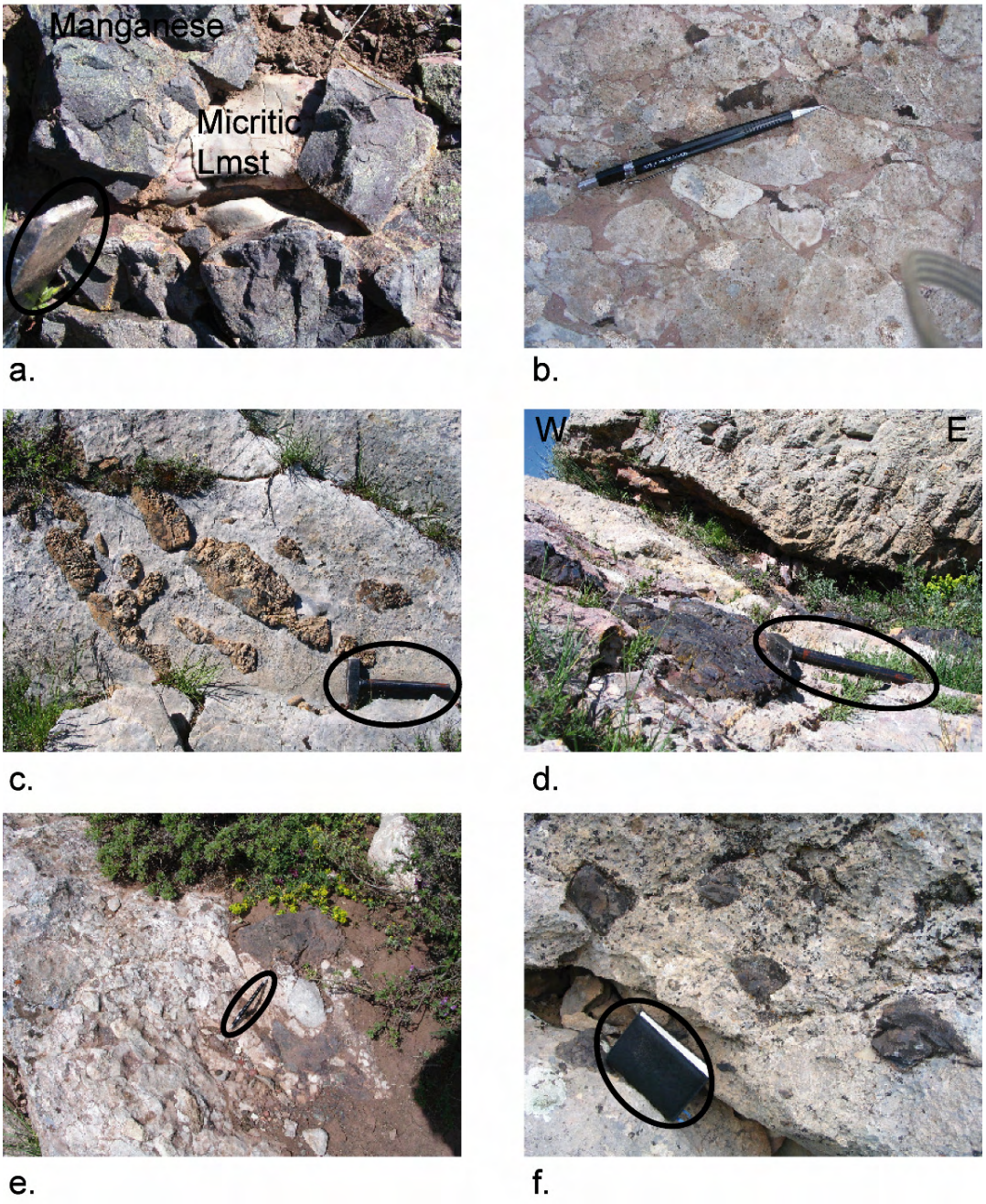

Fig. 5.41. a. Manganese horizon. Hammer tip circled for scale. b. Limestone conglomerate with pink pelagic limestone matrix. c. Replacement chert nodules within pelagic limestone. Hammer circled for scale. d. Bedded black chert horizon in pelagic limestone. Hammer circled for scale. e. Debris flow with limestone and vesicular basalt clasts. Basalt clast top right of circled pencil. f. Black angular vesicular basalt clasts within matrix of pelagic limestone. Notebook circled for scale.

generally more rounded. Terrigenous material (e.g. quartz) is absent from the unit. The debris flow grades up into a sandy-limestone composed of carbonate grains, pelagic limestone and highly altered green tuffaceous / basaltic grains. The overlying 40 m of the sequence is composed of alternating pelagic limestone, limestone conglomerate and clastic limestone, cherty limestone, lithoclastic sandstone, and rare volcaniclastic shale horizons. The contacts between each horizon were studied in detail and found to be conformable, not tectonic.

Limestone conglomerate horizons were found to contain sub-rounded to sub-angular clasts of vesicular basalt, up to 20 cm in size (Fig. 5.41f). The top of this stratigraphic sequence is defined by a ~20 m sequence of poorly exposed tuffaceous sediment, with blocks of vesicular basalt. The poor exposure made it difficult to determine if the basalt is interbedded with the volcaniclastic sediment as flows, or whether it represents olistoliths within a matrix. Granular dolomite then follows above a low-angle tectonic contact.

This succession at Dikilitaş Yayla shows a transition from Cretaceous neritic limestone to deeper water pelagic units and volcanic-derived sediment. The manganese horizon marks a change from shallow and deeper water environments. The presence of volcanic-derived material is consistent with the emplacement of ophiolitic melange unit during the Late Cretaceous. This locality also illustrates a gradational transition to ophiolitic melange.

5.9.4 New palaeontological dating

During this study, samples were collected for palaeontological dating in an attempt to constrain the timing of the onset of pelagic conditions and the subsidence of the platform in the Late Cretaceous. An analysis of microfossils was very kindly undertaken by Tethyan microfossil specialists at Mersin University, Turkey (Prof. Dr. Nurdan İnan and Doç. Dr. Kemal Tasli). Four samples of altered planktonic foraminifera identified as: (a) *Globotruncanita elevata* (BROTZEN); (b) *Globotruncana arca* (CUSHMAN); (c) *Globotruncanita* cf. *calcarata* (CUSHMAN); (d) *Globotruncana* gr. *linneiana* (D'ORBIGNY), are shown in Fig. 5.42. These microfossils came from the same pink

pelagic limestone horizon near the top of the Sögüt Yayla log (Fig. 5.39a), and date this horizon as Campanian. This indicates that pelagic conditions existed within the Bolkar unit by the Campanian – Maastrichtian. The pink pelagic limestone horizon mentioned above is an obvious stratigraphic marker within the sedimentary sequence along strike, owing to its obvious colour (Fig. 5.40c). Other samples of the same unit along strike at Ekinlik Yayla yielded *Globigerinelloides* sp., *Archaeoglobigerina* sp. and *Globotruncanidae* giving an age range of Campanian to Maastrichtian. Similarly, further north in the nappe stack at Baybağan Yayla, samples were found to contain *Rosita fornicata* (PLUMMER), *Globigerinelloides* sp. and *Archaeoglobigerina* sp., which were also dated as Campanian – Maastrichtian.

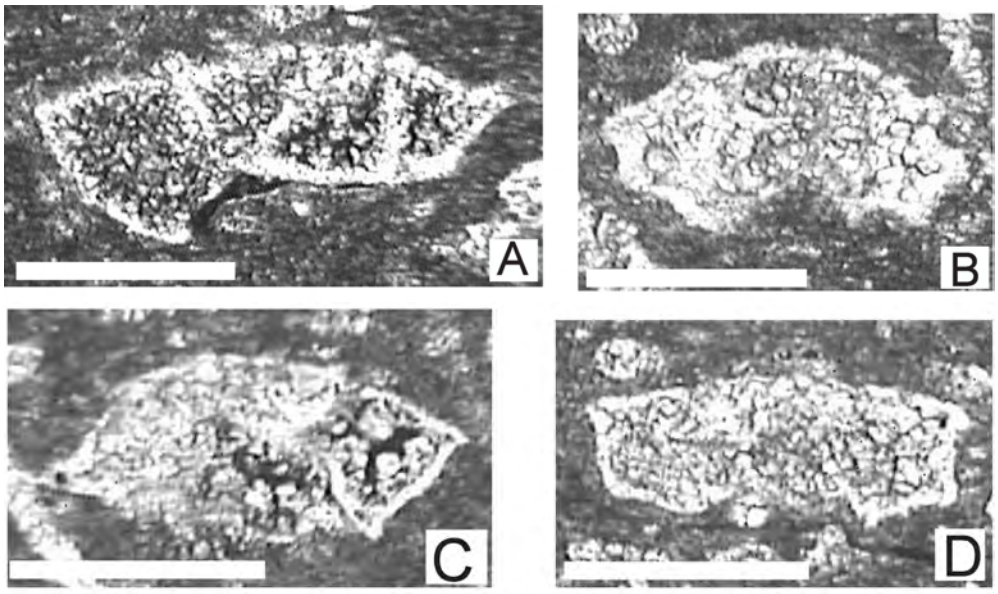

Fig. 5.42. Scale bar (white line) in each photomicrograph is 1mm in length. a. *Globotruncanita elevata* (BROTZEN). b. *Globotruncana arca* (CUSHMAN). c. *Globotruncanita* cf. *calcarata* (CUSHMAN). d. *Globotruncana* gr. *linneiana* (D'ORBIGNY).

At the Dikilitaş Yayla locality, a sample of pelagic clastic limestone overlying the manganese horizon near the base of the log (Fig. 5.39b), yielded *Globotruncana* gr. *linneiana* (D'ORBIGNY), Heterohelicidae (within reworked clasts), as well as rudistid shell fragments and echinoderm debris. This sample was also dated as Campanian –

Maastrichtian. The combined data convincingly dates the timing of the onset of pelagic conditions in the Bolkar unit as latest Cretaceous (Campanian – Maastrichtian).

5.9.5 Thin section analysis of syn-tectonic sediments

Thin-section analysis of Upper Cretaceous and Lower Cenozoic syn-tectonic sediments provides additional information on composition and provenance. Pelagic limestone that yielded Campanian – Maastrichtian aged microfossils is composed of very fine grained, red pelagic silty sediment (Fig. 5.43a). Pelagic foraminifera can be observed; however, the internal structure has been replaced by siliceous cement.

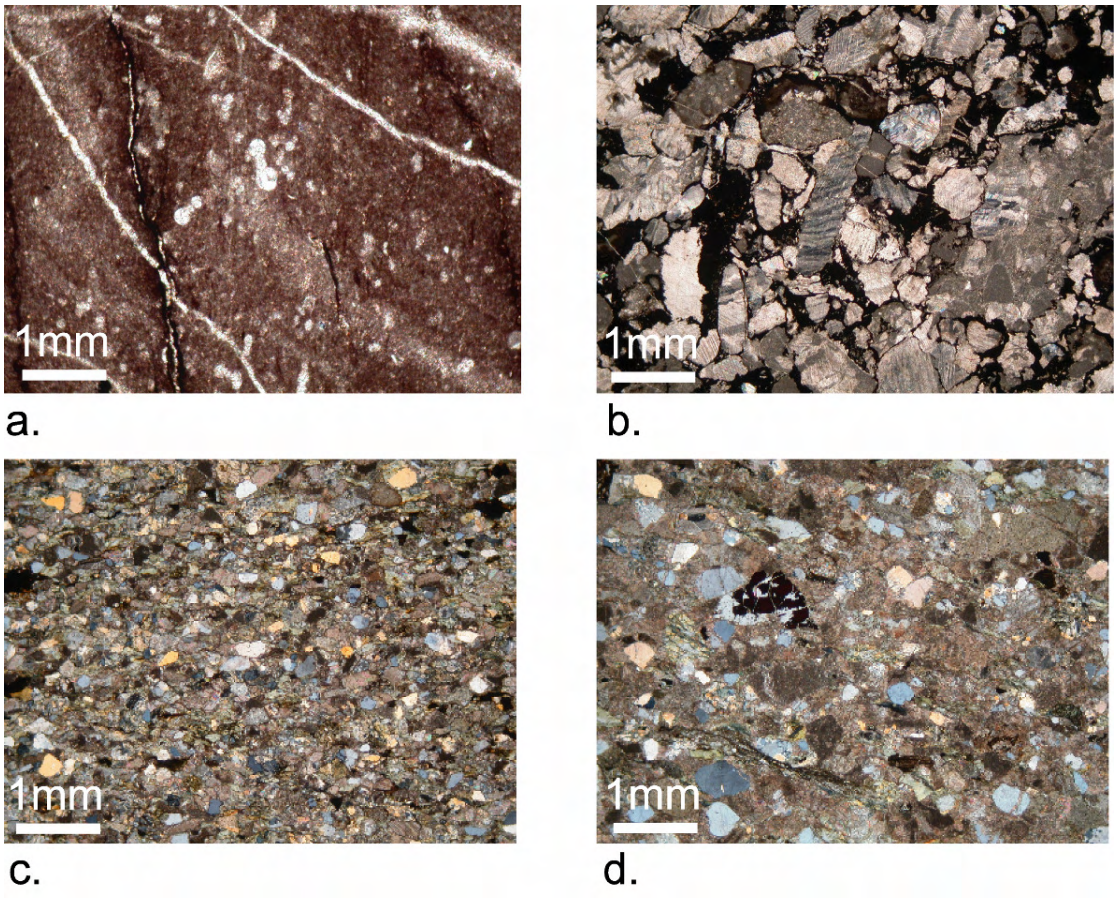

Fig. 5.43. Photomicrographs of syn-tectonic sediments. a. Campanian – Maastrichtian pelagic limestone containing siliceous microfossils. b. Maastrichtian calcareous sandstone containing reworked carbonate grains. c. and d. Palaeocene – Eocene lithoclastic sandstone.

The unit is heavily veined, with veins typically running in the same orientation as lamination. Calcareous sandstone beds, observed in the log at Dikilitaş Yayla (section 5.9.3.2), contain no observable terrigenous material, and are exclusively composed of carbonate grains (Fig. 5.43b). Samples of Palaeocene – Eocene syn-tectonic sediments observed in thin section are typically lithiclastic sandstone (Fig. 5.43c, d). Grains of varying composition are observed, including quartz, altered volcanic grains, carbonate and chert. The sandstone is cemented with a calcitic cement. This lithiclastic sediment was found to be evident beneath the nappe contact.

5.9.6 X-ray Fluorescence analysis of volcanic rocks

As described in previous sections of this chapter, the Upper Cretaceous of the Bolkar nappe contains volcanic rocks and volcanic-derived sediment. Volcanic-derived rocks, identified in the field as vesicular basalt and tuffs, are found as blocks within a large-scale volcano-sedimentary melange ('ophiolitic melange unit'), or as clasts within debris flow and conglomerate. There area also laterally continuous horizons of interbedded tuffs and vesicular basalts in the Upper Cretaceous stratigraphy near Sorkun village (see section 5.7.3.1). Samples of basaltic rocks were collected and analysed with the aim of using geochemical data to identify tectonic settings.

Seven samples were analysed using a high-quality X-ray fluorescence (XRF) technique for major and trace elements at the School of Geosciences, University of Edinburgh, as specified by Fitton et al. (1998). Data from the XRF analysis are listed in the Appendix.

A total alkali vs. silica (TAS) plot (Fig. 5.44a) shows that five of the samples are basic, whilst one is ultrabasic, and one is intermediate in composition. The samples all plot within the basalt, basaltic trachyandesite, and tephrite basanite fields. The AFM diagram (Fig. 5.44b) indicates that four of the samples fall into the tholeiitic basalt field, whilst three are calc-alkaline. A plot of Zr vs. P_2O_3 (Fig. 5.45d) also shows there is a mixture of alkaline and tholeiitic basalts present. Selected minor element data, plotted on tectonic discrimination diagrams (Fig. 5.45a-c), show that most samples plot in either the MORB (Mid Ocean Ridge Basalt) or WPB (Within Plate Basalt) fields. Most of the

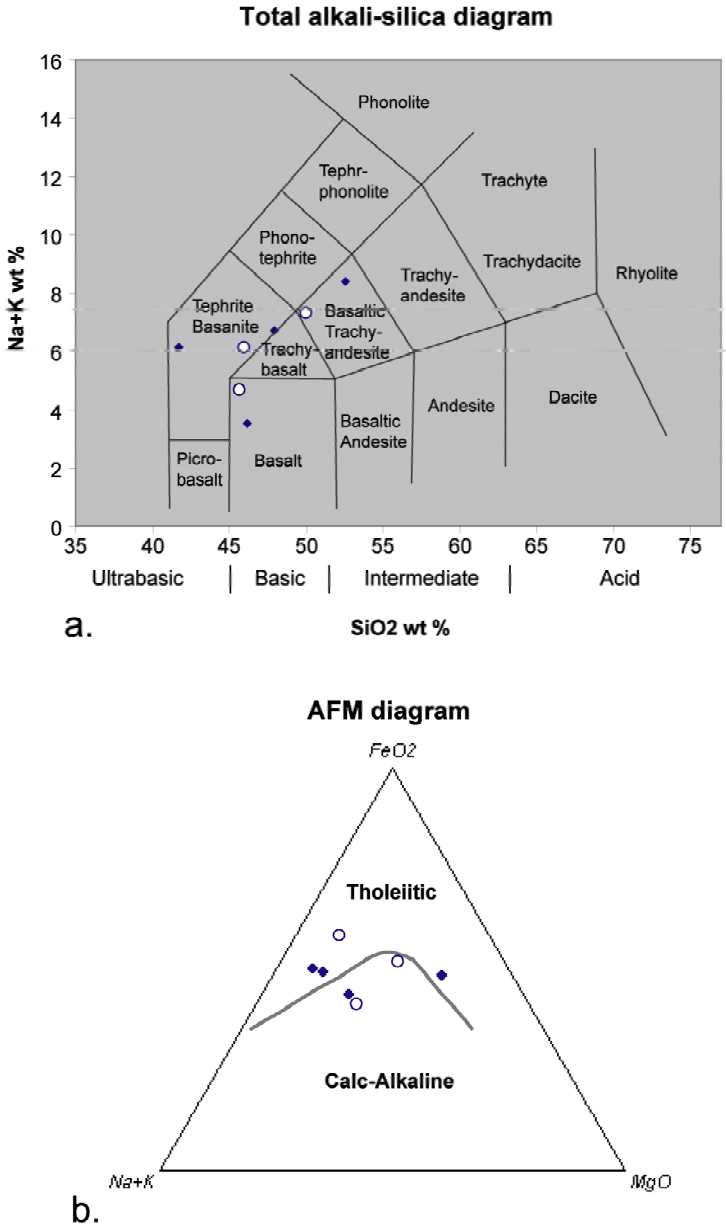

Fig. 5.44. Discrimination diagrams utilising XRF major-element analysis of volcanic rocks. Points marked by an open circle are samples from the ophiolitic melange; points marked by diamonds are samples from Upper Cretaceous stratigraphy of Bolkar nappe. a. Total alkali silica discrimination diagram; b. AFM diagram with Irvine and Baragar (1974) discrimination line for tholeiitic and calc-alkaline trends.

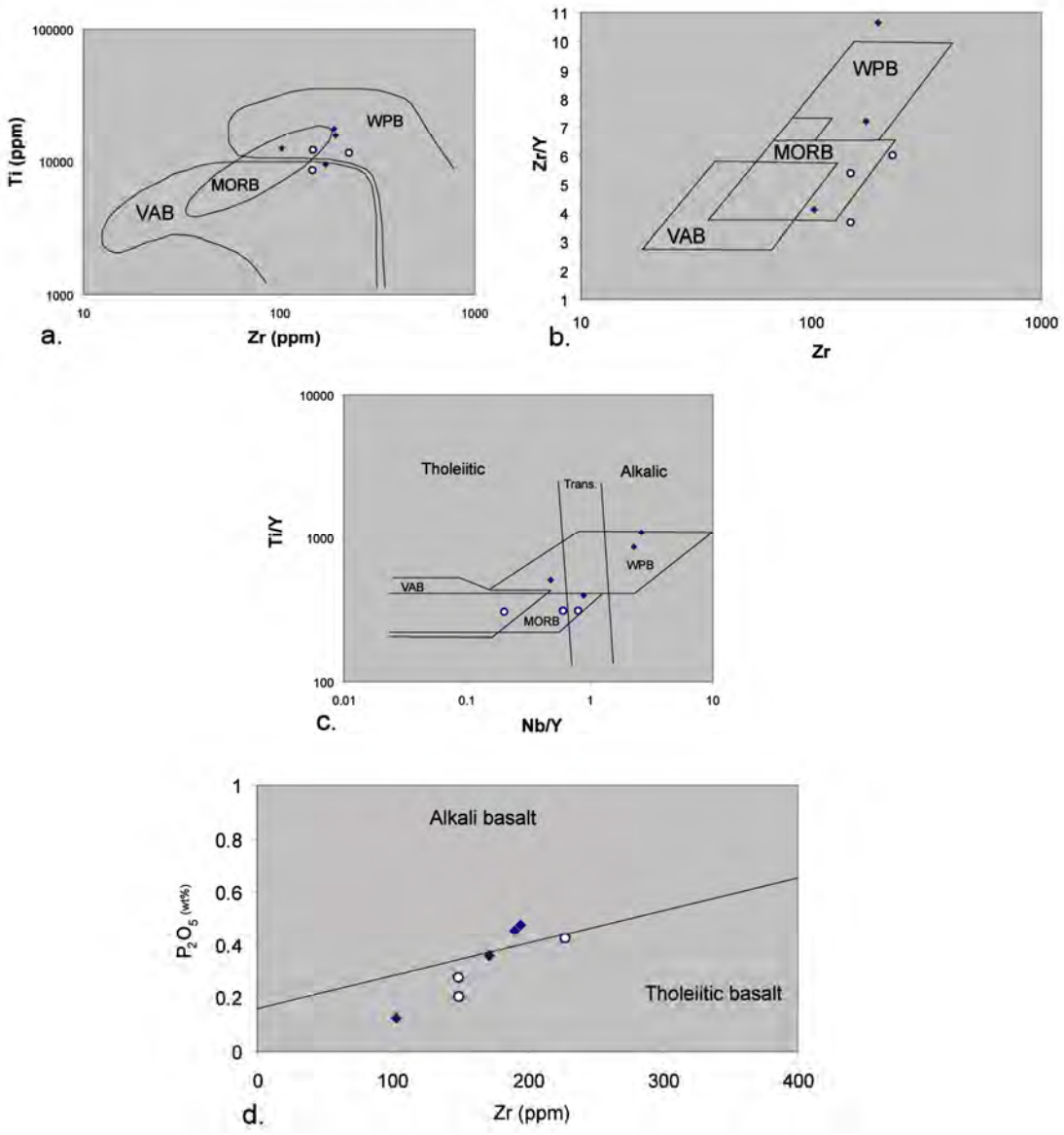

Fig. 5.45. Discrimination diagrams for basalt samples using selected major and minor elements. Points marked by an open circle are samples from the ophiolitic melange; points marked by diamonds are samples from Upper Cretaceous stratigraphy of Bolkar nappe. VAB – Volcanic Arc Basalt. MORB – Mid Ocean Ridge Basalt. WPB – Within Plate Basalt. a. Zr vs. Ti, after Pearce (1982); b. Zr vs. Zr/Y, after Pearce and Norry (1979); c. Nb/Y vs. Ti/Y, after Pearce (1982); d. Zr vs. P_2O_3, after Winchester and Floyd (1976).

samples from the volcano-sedimentary melange tend to plot close to the MORB field, but some plot in the WPB field. Samples from the Upper Cretaceous stratigraphy of the

Bolkar nappe tend to plot in the WPB field (Fig. 5.45a-c). Also, on the Zr vs. P_2O_3 plot, the melange basalts are all tholeiitic. It is likely that the blocks of basalt found in the volcano-sedimentary melange are from accreted oceanic crust (Andrew and Robertson, 2002). The laterally continuous horizons of basalt in the Upper Cretaceous stratigraphy is inferred from this study to have developed within the foredeep along with hemi-pelagic and pelagic limestones.

5.9.7 Summary of stratigraphic and sedimentary data

A review of previous literature on the stratigraphy of the Geyik Dağ and Beyşehir-Hoyran-Hadim nappes, combined with new field observations during this study, can be used to identify phases of subsidence of the Tauride platform. The Jurassic – Cretaceous of the Geyik Dağ, in both the northerly and southerly study areas, consists of a thick succession of platform carbonates, indicative of shallow-marine conditions. This is continuous into the Early Cenozoic, but in the Palaeocene – Eocene, the sequence consists of gravity deposits, including turbiditic sandstones and debris flows. This is indicative of a deeper marine depositional environment, including slope or hemi-pelagic conditions. Nummulitic forams found within calciturbidites indicate an age of Palaeocene to Middle Eocene for deposition of these sediments.

Within the allochthonous Hadim and Bolkar nappes, the Jurassic and the Early Cretaceous was characterised by a thick succession of shallow-marine platform carbonates. The presence of benthic foraminifera of Cenomanian and Santonian ages suggest that shallow-marine (shelf-type) conditions existed during this time. During the latest Cretaceous, hemipelagic and pelagic conditions existed in the Hadim and Bolkar units, as indicated by pelagic limestones, cherty limestone, limestone conglomerates and debris flows. Pelagic foraminifera date these deeper-water sediments as Campanian – Maastrichtian. Towards the top of the sequence, volcanic rocks and volcanic-derived sediments are found within the Upper Cretaceous stratigraphy of the Bolkar nappe, and using geochemical discrimination are interpreted as within-plate basalts. Blocks of basalt are typically mid-ocean-ridge type and possibly reflect accreted oceanic crust. These

volcanics are inferred to be have been tectonically overlain by an ophiolitic melange unit, in turn overlain by an ophiolitic slab; this relationship is only observed at Dipsiz Göl locality (Andrew, 2003). The transition from shallow-marine carbonates, to pelagic units, to ophiolitic melange is observed as being a gradational.

5.10 Discussion

In this chapter, a combination of new cross-sectional profiles, deformation data, structural data, stratigraphic and sedimentary evidence, along with a review of existing literature, is used to shed light on the structural history and emplacement of the Tauride platform. These data will now be reviewed, and by comparing this with concepts of orogenic thrusting (presented in sections 5.2 and 5.3), a model of tectonic break-up and emplacement of the Tauride platform will be proposed.

5.10.1 Cross sections through the nappe stack

This study focused on the nappe stacking order and regional tectonic associations in the southerly study area, as it was felt that the tectonic framework in the northerly study area had already been well documented (Andrew, 2003). However, it was found that there are aspects of the nappe stacking order which do not correlate between the northerly and southerly areas, namely the relative tectonic positions of the Hadim nappe and the ophiolitic melange unit. In the northerly study area, the Hadim nappe is at the base of the nappe stack, and is tectonically overlain by the ophiolitic melange. In the southerly study area, the ophiolitic melange is tectonically overlain by the Hadim nappe; however, the sole of the ophiolitic melange is not seen, and so it cannot be confirmed if this is the lowest allochthonous tectonic unit or not.

The above relationships suggest firstly that there must be lateral variations in the nature of emplacement of the Beyşehir-Hoyran-Hadim nappes. If the nappes were emplaced in a normal 'in-sequence' style, with more distal units (i.e. ophiolitic melange) emplaced onto more proximal units (i.e. Hadim and Bolkar nappes), it would be expected that the proximal units would be at the base of the nappe stack; this is indeed the case in the northerly study area, where the Hadim nappe is the lowermost unit.

However, in the southerly part of the study area a critical relationship is observed at Dipsiz Göl where ophiolitic melange (including remnant oceanic crust) is tectonically overlain by the Bolkar nappe which consists of platform-type lithologies of Palaeozoic and Mesozoic age. In this area, a simple in-sequence restoration of the nappe stack would result in 'pre-thrusting' (i.e. pre-Cretaceous) existence of a small oceanic basin sandwiched between the Geyik Dağ and Hadim and Bolkar platform units (Fig. 5.46a), as interpreted by Özgül (1984). This is unrealistic, however, as it would require the presence of two rifted margins on either side of an oceanic basin. In this study, and all previous studies, no evidence was found to suggest that a rifted margin existed in the Cretaceous stratigraphy of the Geyik Dağ, the Hadim nappe or the Bolkar nappe. Also, tectonic relationships observed at Sorkun (section 5.7.3.1) show Cretaceous rocks are tectonically overlying Jurassic and Triassic rocks. This is not typical of in-sequence thrusting, and strongly suggests that emplacement was more complex.

Having ruled out an in-sequence style of thrusting, an alternative is that the distal margin units (ophiolitic melange and Bozkir/Beyşehir nappes) were emplaced in an 'out-of-sequence' style (Andrew, 2003; Andrew & Robertson, 2002). It would appear that out-of-sequence thrusting is the only method by which ophiolitic melange could be positioned at the lowest level of the thrust stack, tectonically overlain by 'proximal' platform units (i.e. Hadim and Bolkar nappes). An out-of-sequence reconstruction would allow the presence of a single north-facing Mesozoic continental margin, represented by the Geyik Dağ, Hadim unit and Bolkar unit, passing northwards into distal margin and oceanic units, represented by the Bozkir unit and ophiolitic unit (Fig. 5.46b).

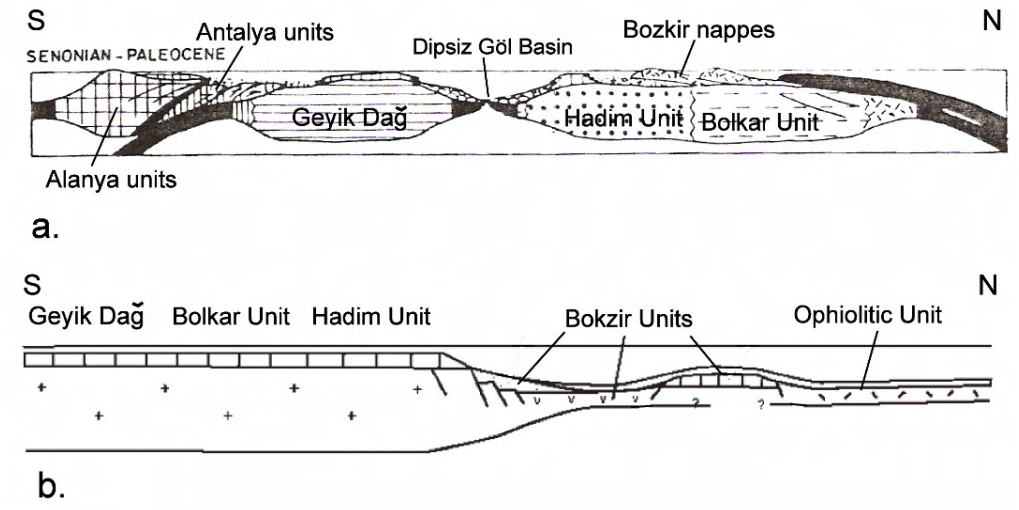

Fig. 5.46. a. In-sequence restoration of the nappe stack, resulting in a small oceanic basin separating the Geyik Dağ and Hadim units. Modified after Özgül (1984). b. Out-of-sequence restoration, resulting in a single north-facing rifted margin. Modified after Andrew and Robertson (2002).

Another key question concerning the nappe stacking order is the relationship between the Hadim and Bolkar nappes, especially which unit restores further to the north within the continental margin. Two critical cross-sections through the nappe stack (Fig. 5.9, D-D', E-E') show that the Devonian units of the Hadim unit overthrust Jurassic – Cretaceous units of the Bolkar unit (Fig. 5.10). This tectonic contact dips to the SW. If, as documented, the Hadim nappe was thrust towards the S/SW (Özgül, 1984; Andrew, 2003), it cannot cut down-sequence through the Bolkar nappe stratigraphy. Therefore, two possibilities exist: (i) the Hadim nappe was 'back-thrust' to the NE over the Bolkar nappe, during late-stage tightening of the nappe stack; (ii) or the Hadim nappe was emplaced to the SW over the top of the Bolkar nappe, and then the contact was tilted at a later stage related to post-thrusting neotectonic events or orogenic collapse.

5.10.2 Degree of Deformation

The degree of deformation within the study area is variable in relation to the age, type of lithology, and the tectonic unit. In the Geyik Dağ the most intense deformation was observed to the NE of the Beyşehir-Hoyran-Hadim nappe stack, whilst the autochthon to

the SW is generally less deformed. This is partly because in the SW the exposed Geyik Dağ succession is typically composed of competent Mesozoic carbonates, whilst in the NE, the exposed Palaeozoic units of the Geyik Dağ are less competent shales and quartzites. Critically, assuming the nappe emplacement was from N/NE to S/SW, the Geyik Dağ autochthon to the NE of the nappe stack would be severely deformed as it was overridden by the Beyşehir-Hadim nappes. The degree of deformation in the autochthon is highly dependent on the type of lithology and relative competency, with thin-bedded shales and sandstones displaying 'ductile' deformation, as opposed to more 'brittle' deformation in thick-bedded and massive carbonates. Regional tectonic imbrication of the Tauride platform is only seen to the SW of the nappe stack, caused by collapse of the foreland during thrusting. There is no evidence within the area studied that the Tauride platform experienced compressional deformation at any time during the Mesozoic prior to the Late Cretaceous. All of the deformation within the Geyik Dağ is consistent with a single deformation event, interpreted as the emplacement of the Beyşehir-Hoyran-Hadim nappes (see Appendix A for further discussion).

The Hadim nappe is relatively undeformed in comparison to some parts of the Geyik Dağ, with typically 'brittle' deformation consisting of faulting and imbrication. The Hadim nappe is most heavily deformed adjacent to tectonic contacts. Even in the northerly study area where the Hadim nappe is at the base of the whole thrust sequence, it is not intensely deformed. This poses the question as to why the Geyik Dağ is so heavily deformed relative to the overriding thrust sheets, wheras the Hadim nappe is not? A possible explanation is that the 'tectonic conditions' or 'style of thrusting' during emplacement of the Beyşehir-Hoyran nappe stack over the Hadim nappe were different to when the combined Beyşehir-Hoyran-Hadim nappes were emplaced over the Geyik Dağ. The nappes that override the Hadim nappe are ophiolitic melange and distal margin units, which are thought to have been emplaced during an initial phase of 'thin-skinned' or 'soft' collision in the Late Cretaceous (Andrew, 2003; Andrew and Robertson, 2002). The Hadim nappe, in contrast, may be related to 'thick-skinned' or 'hard' collision during final suturing of the Tethys ocean, and hence the forces affecting the underlying foreland may have been greater.

The Bolkar nappe, in contrast to the Hadim nappe, is intensely deformed throughout. Regional-scale folding, faulting, imbrication and low-grade metamorphism make stratigraphic investigation challenging. The Bolkar nappe is interpreted as a regional-scale broken formation, as opposed to a coherent tectonic unit, as assumed in previous studies (Özgül, 1984; Özgül, 1997). The Bolkar nappe and the Hadim nappe are likely to have formed parts of a continuous Tauride continental margin (Özgül, 1984; Andrew and Robertson, 2002). If so, another important question is why the Bolkar nappe is much more intensely deformed than the Hadim nappe? There are two possibilities.

Firstly, the Bolkar nappe is (locally) tectonically overlain by the Bozkir nappes, which are composed of distal margin units. During the emplacement of these nappes, in the Late Cretaceous (Andrew and Robertson, 2002), the Bolkar nappe may have been at the 'leading edge' of the foreland (i.e. in the north of the Tauride platform (Fig. 5.47a). The emplacement of the Bozkir nappes and ophiolite obduction onto the Bolkar unit has caused the intense deformation and low-grade metamorphism. The Hadim unit (and Geyik Dağ), located in a more southerly position relative to the Bolkar unit (Fig. 5.47a), would have been comparatively undeformed. At a later stage, the Bolkar and Hadim nappes were thrust southwards, carrying with them the previously overthrust Bozkir nappes in an in-sequence piggy-back thrusting style. The main problem with this model is the present tectonic contact between the Hadim and Bolkar nappes, with the Hadim nappe in a higher structural position. This would require that at some stage the Hadim nappe must have been backthrust to the N/NE over the Bolkar nappe.

A second option is that the Bolkar nappe was deformed by overthrusting of the Hadim nappe from a more northerly position into its present southerly position by out-of-sequence thrusting. In this scenario, the Hadim unit would have been located in a more northerly position within the pre-Cretaceous Tauride continental platform, with the Bolkar unit relatively further south (Fig. 5.47b). As the Hadim nappe was emplaced it caused deformation and metamorphism of the underlying Bolkar unit. There are, however, several problems with this model. Firstly, distal margin units (Bozkir nappes) are seen to tectonically overlie the Bolkar nappe, but not the Hadim nappe. If the Hadim

unit was originally in a more northerly position, it would be at the 'leading edge' of the foreland during Late Cretaceous nappe emplacement, and would be expected to be overlain by the Bozkir nappes. It is also likely that the Hadim unit would be heavily deformed by emplacement of the Bozkir nappes and ophiolitic melange, which it is not. However the evidence of rethrusting and out-of-sequence thrusting in the study area (Andrew and Robertson, 2002) means that the Bolkar nappes could have been relocated during later (thick-skinned) compressional events.

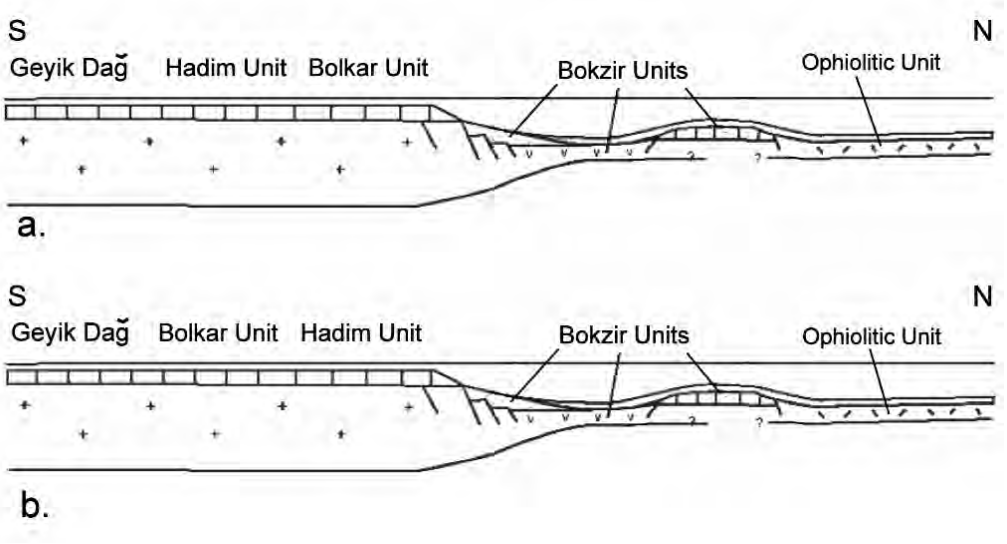

Fig. 5.47. a. Restoration of Tauride platform with the Bolkar unit in a northerly position relative to the Hadim unit. b. Alternative restoration with the Hadim unit in a northerly position relative to the Bolkar unit. Both diagrams modified from Andrew and Robertson (2002).

5.10.3 Evidence from structural data

To test the above alternatives, structural data were collected from key tectonic contacts in the studied area, as well as within autochthonous and allochthonous units away from tectonic contacts.

In the northerly study area, all structural data from the autochthonous Geyik Dağ indicate that the axis of shortening runs in a NW-SE to N-S orientation, with a top-to-the-W/SW direction of movement. This is entirely consistent with the regional orientation of the Beyşehir-Hoyran-Hadim nappe stack in the region, which trends in a NW-SE direction. Previous literature (e.g. Şengör and Yilmaz, 1981; Robertson and

Dixon, 1984) implies that the suturing of the Tethys ocean was along a W-E axis. This suggests either that the nappe emplacement in the studied area had an oblique component to it, or that there has been regional rotation of the Tauride units since the nappes were emplaced.

In the southerly study area, data from the contact between the Hadim nappe and Bolkar nappe show that shortening was along a NW-SE and E-W axis. Fold vergence and fault slickensides are indicative of top-to-the-north and top-to-the-south sense of displacement. Also, slickensides particularly show an oblique-slip component (Fig. 5.32; Fig. 5.33; Fig. 5.35). These data unfortunately do not give a definitive indication of the direction of movement along the contact between the Hadim and Bolkar nappes. The top-to-the-NE component of displacement would fit a 'backthrust' model (Fig. 5.48a), whilst the top-to-the-SW faulting fits the 'overthrust model' (Fig. 5.48b). One possible explanation is that the Hadim nappe overthrust the Bolkar nappe to the SW, and was then backthrust to the NE during a later stage of compression (e.g. final nappe stack tightening). Another option is that the Hadim nappe was backthrust to the NE, and then fault reversal and normal faulting caused hanging-wall downthrow to the SW during post-compression 'relaxation' of the nappe stack (the direction that the contact dips). Backthrusting has been documented as an important process throughout the Tethyan orogenic belt. In the Bolkar Dağı mountains, ~250 km east of the study area, the northern margin of the Tauride platform experienced shallow-water deposition until Late Cretaceous southward ophiolite emplacement (Jaffey and Robertson, 2001). Late Eocene closure of oceanic basins to the north then resulted in large-scale northwards backthrusting. In south central Turkey, the Mersin Melange and Mersin Ophiolite were emplaced from the north onto the Tauride platform, before being locally backthrust northwards during exhumation of the underlying carbonate platform (Parlak and Robertson, 2004). Further west in the Himalayas, the Zanskar shelf sediments of the north Indian continental margin were deformed in at least three phases: (i) Cretaceous – Palaeocene ophiolite emplacement deformation to the south; (ii) Palaeocene – Miocene continental collision and crustal shortening; and (iii) Pliocene – Pleistocene

backthrusting and rethrusting (Searle et al., 1997). These examples are comparable in both the style and timing of thrusting to the deformation observed in this study.

Another issue is that neotectonic faulting was observed during this study and is documented throughout the study region (Bozkurt, 2001). It is not apparent how many of the faults and folds measured were formed during Late Cretaceous and Early Cenozoic compression, and how many were formed by mainly extensional neotectonic processes.

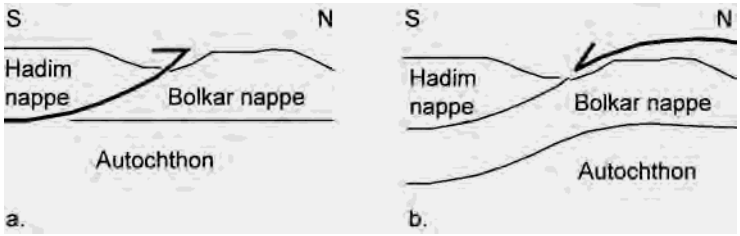

Fig. 5.48. Simplified diagrams showing alternative explanations of the tectonic contact between Hadim and Bolkar nappe. a. Hadim nappe is 'backthrust' to the N over the Bolkar nappe. b. Hadim nappe is emplaced to the S over the Bolkar nappe.

A likely example of neotectonic faulting was observed locally at the contact between the Hadim nappe and the Geyik Dağ at Gölbelen Tepe (Loc. 13, Fig. 5.27). Regionally, the tectonic contact is seen to be a thrust contact, with the Hadim nappe overlying the Geyik Dağ. However, at this locality, steeply dipping normal faults separate the two units, indicative of later stage extensional faulting. The faulted contact between the Bolkar nappe and Bozkir nappes (Loc. 5:Dereköy, Fig. 5.27) is also interpreted as a large neotectonic normal fault. The structural data from the contact are not consistent with the regional trend of the contact, which implies local variations in stress orientations.

Although somewhat limited, structural data from the contact between the Hadim nappe and ophiolitic melange do show top-to-the-SW movement. This would imply that the Hadim nappe was thrust to the SW over the ophiolitic melange during out-of-sequence thrusting. This seems to be the only realistic process by which the ophiolitic unit could end up at the base of the thrust stack. Further evidence for this comes from the contact between the Bolkar nappe and the ophiolitic melange unit. Fold vergence

there is almost exclusively to the S/SW, indicating that the Bolkar nappe was emplaced to the SW over the ophiolitic unit. Folds and faults near imbricate thrust faults within the Bolkar nappe also suggest a top-to-the-S/SW transport direction. Once again the only realistic process by which platform lithologies (Bolkar unit) could be thrust over distal margin units (ophiolitic melange) is by out-of-sequence thrusting.

5.10.4 Evidence from stratigraphic and sedimentological data

Information from the stratigraphy of the Late Mesozoic – Early Cenozoic of the Geyik Dağ, Hadim nappe and Bolkar nappe, provides crucial insights into the timing and nature of thrusting. The allochthonous Bolkar nappe preserves a classic transition from Cretaceous shallow-marine platform carbonates to pelagic sediments, and finally to ophiolitic melange. The facies and dating of pelagic limestone indicate that deep-water conditions prevailed during the Campanian to Maastrichtian. Limestones grade into volcaniclastic sediments which often contain clasts or blocks of volcanic rocks. XRF analysis of basalts from the volcano-sedimentary melange shows they are mainly of mid-ocean-ridge composition. These results agree with a recent investigation of the ophiolitic melange (Andrew, 2003). The WPB basalts were inferred by to be of a seamount or rifted-margin setting, whilst the MORB basalts were formed at a spreading rich above an intra-oceanic subduction zone (Andrew, 2003). Basalts from within the Upper Cretaceous stratigraphy are predominantly of within-plate-type, typically alkali basalts. They form laterally continuous horizons within the Upper Cretaceous stratigraphy of the Bolkar nappe, along with associated hemi-pelagic sediments are inferred to have formed in a foredeep basin prior to being overridden by the ophiolite in the Campanian – Maastrichtian times. Similar volcanism within a foredeep is observed on the Greek island of Evia, where localised volcanism is association with flexural upwarping of the carbonate platform during emplacement of Jurassic ophiolites (Robertson, 1991). In Oman, localised alkaline volcanism on the subsiding carbonate platform is interpreted as the result of flexural uplift and erosion during initial Late Cretaceous ophiolite emplacement resulted (Robertson, 2004).

Within the allochthonous Hadim nappe, the Upper Cretaceous stratigraphy is predominantly composed of shallow-marine carbonates. However, in the Maastrichtian, pelagic foraminifera and a succession of mixed carbonate and siliciclastic sediments are indicative of subsidence of the platform. Deeper-water sediments are only observed in the northerly study area, where they contain Palaeozoic and volcanic clasts and olistoliths. These are tectonically overlain by the Beyşehir-Hoyran nappes, and it is likely that the volcanogenic sediment in the 'flysch' was derived from the ophiolitic melange unit, which itself was shed from an accretionary prism of oceanic material. It is also known that the ophiolitic melange contains exotic Palaeozoic limestone blocks (Monod, 1977; Andrew, 2003). It is, therefore, likely that the Palaeozoic clasts observed in the Hadim nappe 'flysch' were eroded and re-deposited ('recycled') from the overriding thrust sheet during emplacement.

In the autochthonous Geyik Dağ, Upper Cretaceous shallow-marine carbonates, including local bauxite horizons, indicate that the platform experienced relative tectonic stability during this time. During the Palaeocene – Eocene, as dated by Nummulitic foraminifera, the deposition of turbidites and debris flows indicate subsidence and collapse of the platform, related to nappe emplacement (Andrew, 2003). The syn-emplacement clastic sediments contain ophiolitic and pelagic material, not present in the Geyik Dağ stratigraphy. This could have been derived from either: (i) the ophiolitic melange and Bozkir/Beyşehir nappes; (ii) the Late Cretaceous of the Bolkar and Hadim nappes.

Lithoclastic sandstone found at the very top of the Bolkar nappe sequence is very similar in composition to Palaeocene – Eocene sandstones identified at Dipsiz Göl, and also at the top of the Geyik Dağ sequence. This, is therefore, inferred to be related to the same emplacement event as that which caused subsidence of the Geyik Dağ.

The sedimentary evidence suggests that the Bolkar unit was locally at the leading edge (northerly) of the pre-Cretaceous Tauride platform. The Hadim unit would, thereby, be further south relative to the Bolkar nappe. However, the Hadim unit experienced variable subsidence during ophiolitic emplacement, as indicated by turbiditic accumulation in the northerly study area. The Geyik Dağ would be further to

the south than either of these units, and experienced little or no subsidence during this period. During the Palaeocene and Eocene, emplacement of the Hadim and Bolkar units southwards over the Geyik Dağ, along with emplaced ophiolitic and distal margin units, resulted in collapse and subsidence of the Geyik Dağ foreland, and subsequent sedimentation in a regional foredeep basin. Syn-tectonic sediments were also deposited adjacent to tectonic contacts between the Beyşehir-Hoyran-Hadim nappes, which were evidently re-thrust during this secondary phase of thrusting.

A comparable example of ophiolite emplacement in the eastern Mediterranean region is found in Greece. On the island of Evia, a Late Triassic – Early Jurassic platform carbonate succession is unconformably overlain by mudstones, tuffaceous sediments and radiolarian sediments (Baumgartner and Bernoulli, 1976; Robertson, 1991; Robertson, 2006a) (Fig. 5.49). These sediments were deposited in a foredeep basin, and record the collapse of the carbonate platform in response to loading of the allochthonous Evia ophiolite unit (Baumgartner and Bernoulli, 1976; Robertson, 1991). Overlying these sediments are debris-flows and an allochthonous oceanic-derived melange, that are interpreted as redeposition of material shed from the advancing thrust sheets (Robertson, 2006a). This melange is then tectonically overlain by the Evia ophiolite (Fig. 5.49).

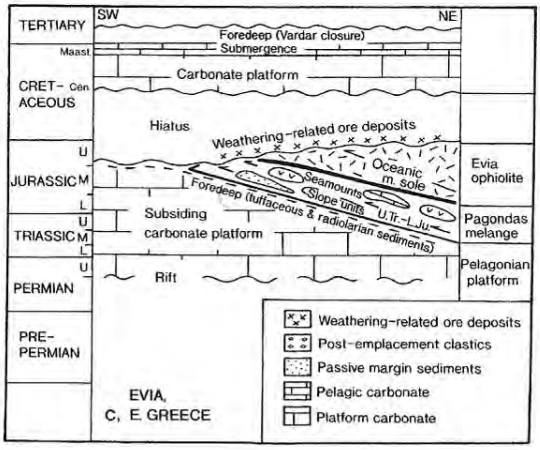

Fig. 5.49. Summary of the tectonostratigraphy of the Early – Mid Jurassic Evia ophiolite, eastern Greece. Diagram from Robertson (2006).

Similar uplift and collapse features are observed in Oman. The autochthonous carbonate platform underwent flexural uplift and erosion, associated with the loading of the advancing ophiolite (Robertson, 2006a). The uplifted margin then subsided, and a deepening-upwards succession of neritic to hemipelagic sediments were deposited. These were, in turn, overlain by chaotic debris flows and melange, associated with large-scale collapse of the platform (Robertson, 1987). In the Late Cretaceous platform of the Geyik Dağ, Hadim nappe and Bolkar nappe, stratigraphic discontinuities are present (Monod, 1977; Özgül, 1997), which could be representative of initial ophiolite loading.

5.10.5 Summary of emplacement and structural history of the platform

To recap, Özgül (1984) introduced a model for nappe emplacement in the region which began with Upper Cretaceous emplacement of the Bozkir unit southwards onto the Bolkar unit and Hadim unit (Fig. 5.7 - 1). A new oceanic basin (Dipsiz Göl) is then proposed to have formed in between the Geyik Dağ and Hadim unit during Late Senonian to Palaeocene time (Fig. 5.7 - 2). A second episode of compression during the Eocene (Ypresian – Lutetian) then sutured the inferred Dipsiz Göl basin, and emplaced it southwards onto the autochthonous Geyik Dağ platform, along with the Hadim, Bolkar and tectonically overlying Bozkir units (Fig. 5.7 - 3). A number of problems with this model were discussed in section 5.4.2. In light of the evidence presented in this chapter, a new model of the style of thrusting has been proposed, which provides a realistic restoration of the nappe stack to its pre-Cretaceous setting. Further implications of the evidence presented in this chapter can be found in Appendix A.

5.10.5.1 Thin-skinned emplacement of ophiolite and distal margin units.

The autochthonous Geyik Dağ and the allochthonous Beyşehir-Hoyran-Hadim nappes restore as a north-facing passive margin prior to the Late Cretaceous (Fig. 5.50a). During the Late Cretaceous (Campanian – Maastrichtian), the ophiolitic melange unit, along with distal margin units (Beyşehir and Bozkir nappes), were emplaced southwards onto the Tauride platform (Fig. 5.50b). Evidence suggests that locally this occurred by

in-sequence thrusting, resulting in distal margin units being emplaced directly above the Hadim unit, with the ophiolite being in the highest structural position (Fig. 5.50b) (Andrew and Robertson, 2002; Andrew, 2003). Laterally along the rifted margin, the ophiolitic unit was emplaced straight onto the Tauride platform, with the Beyşehir nappes emplaced above the ophiolite by out-of-sequence thrusting (as seen in the north of the study area, Fig. 5.4). The leading edge of the Tauride platform, the Bolkar unit, experienced subsidence and accumulation of syn-tectonic sediments, including volcaniclastic sediments, in a foredeep basin. The Bolkar unit experienced intense deformation and low-grade metamorphism as the allochthonous tectonic units were emplaced. Further south in the Tauride platform, the Hadim unit also experienced subsidence as part of the regional foredeep basin that had developed. The Hadim unit did not experience any significant deformation at this stage, possibly because the basal thrust of the overriding ophiolite separated the allochthonous and autochthonous units into discrete packages. Further south on the platform, the Geyik Dağ was unaffected by the emplacement of the ophiolitic and distal margin units, and stable shallow-water conditions continued during the Upper Cretaceous period. This episode of thrusting is considered to be a 'soft' collisional event, associated with ophiolitic melange emplacement.

Geochemical evidence from the ophiolite unit suggests it was formed in supra-subduction zone setting (Andrew and Robertson, 2002), where a spreading ridge formed above an intra-oceanic trench/subduction zone. This is consistent with other Neotethyan ophiolites, such as the Troodos and Oman ophiolites (Pearce et al., 1984). Ophiolite obduction was probably driven by collision of an intra-oceanic trench with the Tauride platform (Andrew, 2003), as documented for other Tethyan ophiolites, for example, the Lycian Nappes (Collins, 1997), Pozantı-Karsanti ophiolite (Polat and Casey, 1995; Parlak, 2000; Parlak et al., 2000). A structural and sedimentological study of the Maastrichtian – Late Eocene Ulukışla basin (S Turkey) found that initial Late Cretaceous ophiolite emplacement was a 'soft' collisional event (Clark and Robertson, 2002), comparable to this study.

5.10.5.2

Thick-skinned emplacement of platform units and distal margin units

During the Palaeocene – Eocene, the Hadim and Bolkar units were emplaced southwards onto the autochthonous Geyik Dağ unit (Fig. 5.50c). The Bozkir and Beyşehir nappes, and locally the ophiolitic melange, which were previously emplaced onto Tauride platform in the Late Cretaceous, were all carried in a piggy-back style on the back of the Hadim and Bolkar nappes. Laterally, however, the ophiolitic melange unit was re-thrust southwards directly onto the Geyik Dağ, and subsequently overridden by the Hadim and Bolkar nappes (Fig. 5.50d). This re- thrusting resulted in the ophiolitic melange unit ending up at the base of the resulting nappe stack. During this emplacement, the Geyik Dağ autochthon collapsed and a foredeep basin developed ahead of the thrust stack (Fig. 5.50d). The platform also underwent tectonic imbrication and southward propagating thrusts and associated 'flysch' basins developed to the south. The autochthonous platform, particularly Palaeozoic units, underwent intense deformation as the thick overriding nappe stack was emplaced. The Bolkar nappe experienced further internal deformation during emplacement, and locally Eocene clastic sediments were deposited along imbricate thrust contacts. During final tightening of the nappe stack, the Hadim nappe, which was in a southerly position relative to the Bolkar nappe, was locally backthrust towards the N/NE overriding the Bolkar nappe (Fig. 5.50d).

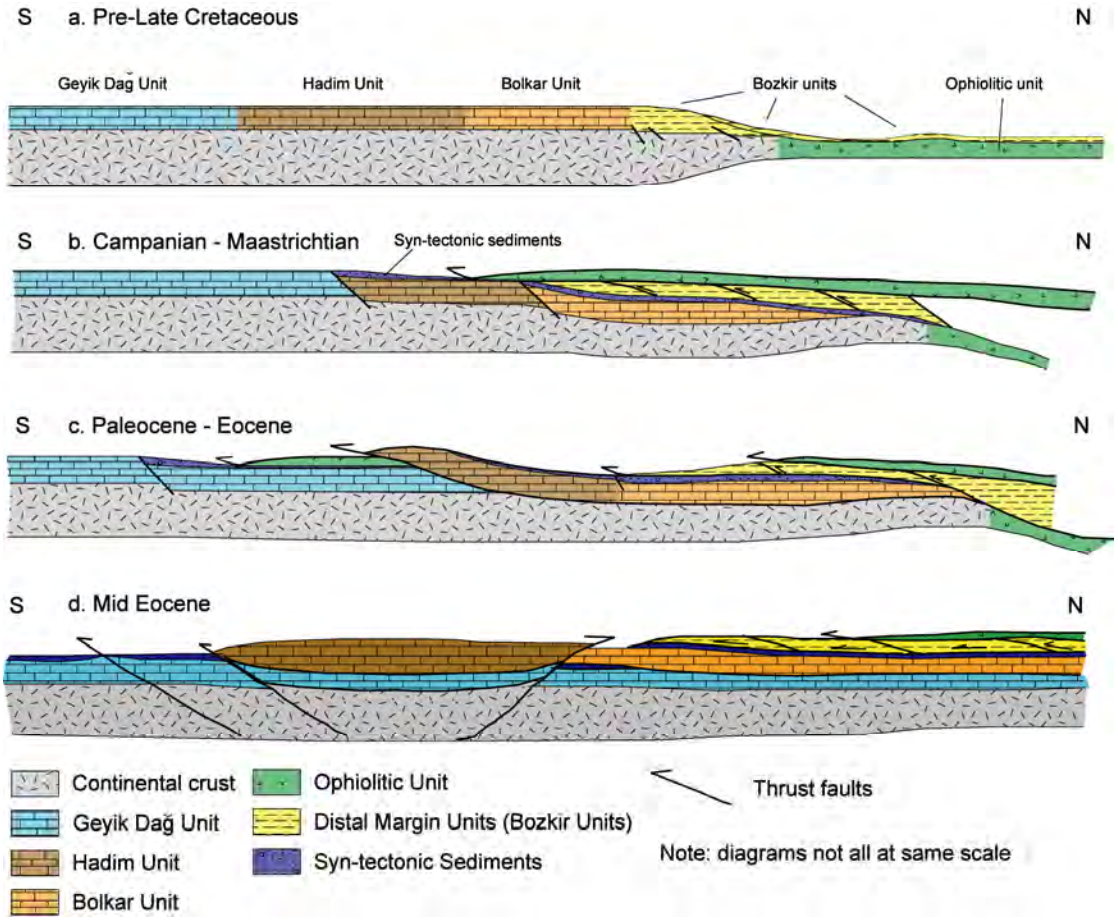

Fig. 5.50. Summary of emplacement and structural history of the Tauride platform. a. Pre-Late Cretaceous restoration of tectonic units. b. Campanian – Maastrichtian thin-skinned thrusting of ophiolitic and distal margin units. c. Palaeocene – Eocene thick-skinned emplacement of platform lithologies, and rethrusting of distal margin and ophiolitic units. d. Mid Eocene tectonic imbrication of foreland, and localised backthrusting between platform units.

5.11 Conclusions

(1) Cross-sectional profiles through the Beyşehir-Hoyran-Hadim nappes show that the stacking order is laterally variable. The relative structural positions of proximal, distal and ophiolitic units indicate that in-sequence and out-of-sequence thrusting occurred during emplacement, indicative of multiphase thrusting. Cross-sections suggest a top-to-the-south direction of emplacement, but locally top-to-the-north 'backthrusting' of the Hadim nappe over the Bolkar nappe is likely.

(2) Intense deformation of the Bolkar unit resulted from Upper Cretaceous emplacement of distal margin and ophiolitic units onto the leading edge of the Tauride platform. The Hadim unit and Geyik Dağ were then still further south within the Tauride platform, and remained undeformed during this thrusting episode. During the Palaeocene – Eocene, southward emplacement of the Hadim nappe and Bolkar nappe and rethrusting of ophiolitic and distal margin units took place, and the underlying Geyik Dağ autochthon was intensely deformed. To the SW of the nappe stack, tectonic imbrication of the Geyik Dağ occurred during the Palaeocene – Eocene.

(3) A study of several key areas does not confirm the existence of a regional "Cimmerian" compressional deformation of latest Triassic age, but rather indicates that all of the deformation was of Late Cretaceous – Early Cenozoic age related to the regional southward thrusting of the Tethyan marginal and ophiolitic units of the Beyşehir-Hoyran-Hadim nappes.

(4) Structural data from the study area suggest that the Beyşehir-Hoyran-Hadim nappes were emplaced towards the W/SW/S. The along strike variability could be indicative of oblique compression during thrusting; alternatively, there could have been regional rotation (unconstrained) of the Tauride units since emplacement. The Hadim nappe and Bolkar nappe were emplaced to the SW over the ophiolitic melange during out-of-sequence thrusting. Also, neotectonic faults are documented which may have locally

altered the primary tectonic contacts between the main allochthonous units. It is likely that the Hadim nappe was backthrust to the NE over the Bolkar nappe.

(5) The Bolkar unit, located to the north of the Tauride platform, experienced subsidence and deposition of pelagic sediments during Late Cretaceous (Campanian – Maastrichtian) emplacement of ophiolitic and distal margin units. The Hadim unit, further south, experienced variable subsidence during this time period, and accumulated a thinner sequence of ophiolitic melange-derived clastic sediments (e.g. turbidites and debris flows). The Geyik Dağ, the most southerly unit, was unaffected until the Palaeocene – Eocene emplacement of the Beyşehir-Hoyran-Hadim nappes, when collapse of the platform resulted in sedimentation in a regional foredeep basin. Syn-tectonic sediments were also deposited adjacent to tectonic contacts between the Beyşehir-Hoyran-Hadim nappes, which were re-thrust during this time.

(6) Combination all of the evidence suggests that the platform experienced initial Upper Cretaceous 'thin-skinned' emplacement of ophiolitic and distal margin units during 'soft' collision of the Tauride continental platform with a intra-oceanic trench. During the Palaeocene – Eocene, 'thick-skinned' emplacement of platform units, along with rethrusting of initially emplaced ophiolitic and distal margin units, was a result of 'hard' collision during final continental collision and suturing. A combination of post-orogenic collapse, tectonic escape, or a new neotectonic extensional regime may be the cause of normal and strike-slip faulting.

(7) A combination of in-sequence and out-of-sequence thrusting was responsible for the final nappe stacking order in the study area. This is apparent for both the initial Late Cretaceous and the later Early Cenozoic phases of thrusting. This has significant implications for restoration of thrust stacks throughout the Alpine-Tethys-Himalayan orogenic belt.

(8) Comparisons can be made between the style and timing of emplacement of the Beyşehir-Hoyran-Hadim nappes and other regions of the Tethyan orogen, such as Greece, W Turkey, Oman and the Himalayas.

6 Discussion

The aim of this thesis has been to investigate the tectonic and sedimentary evolution of the Tauride platform from the Late Palaeozoic to Early Mesozoic time, and to constrain the emplacement and structural history of the platform during the Late Cretaceous to Early Cenozoic. This chapter summarises the results presented in the preceding three chapters, and discusses some remaining issues. Appropriate references are found in the previous chapters and are not repeated here.

6.1 Late Palaeozoic evolution of the Tauride platform

The sedimentology and sedimentary geochemistry of Upper Palaeozoic rocks, presented in chapter 3, suggest that the Tauride platform experienced a passive margin evolution during this time. Devonian sandstones, shales and carbonates in the Hadim and Bolkar nappes were deposited on a shallow-marine shelf, with high frequency sea-level change in the Upper Devonian being an important control on sedimentary facies. Lower Carboniferous black shales were deposited in a relatively distal shelf setting during a prolonged time of global marine transgression, with phosphorite sediments probably being representative of increased organic productivity. Middle and Upper Carboniferous carbonates formed in a productive carbonate shelf setting, with coral assemblages and oolitic limestones being indicative of a shallow-water depth. Sandstone and mudstone horizons in the Upper Carboniferous are indicative of transgressive-regressive cycles, as indicated for this time period by global sea-level curves, related to southern hemisphere Gondwana glaciation. The Permian is represented by continuing shallow-marine carbonate production, with an increase in sedimentation rate possible related to rifting and subsidence along the Gondwana margin. The composition of the Upper Palaeozoic sediments suggests that provenance was from Tauride 'basement' units and other Pan-African outliers; there is no evidence of a local volcanic source in the Tauride platform. Regional evidence, notably the localised presence of volcanic rocks within the

autochthonous Sultan Dağ to the north of the Tauride platform, poses problems with the passive margin model. However, intra-plate volcanism is not necessarily related to local active margin processes (as seen, for example, in North Africa). It is also evident that the origin and nature of the Palaeozoic Konya Complex to the north of the study area is critical to understanding Tauride evolution. The details of the Konya Complex is outwith the scope of this study; however, it is now be briefly discussed to help assess the regional setting.

The Konya Complex, located in south Central Anatolia (chapter 1, Fig. 1.3), includes an assemblage of metamorphic rocks of Silurian – Mesozoic age (Özcan et al., 1988; Eren, 2001; Eren et al., 2004; Robertson and Ustaömer, submitted). A Silurian – Lower Carboniferous metamorphosed carbonate platform is locally cut by E-W trending diabase dykes. This is overlain by a Lower Carboniferous mélange containing blocks of Upper Palaeozoic limestone, chert, and volcanic-derived rocks, all set in a matrix of siliciclastic debris flows, turbidites and shales. The mélange is also associated with an interbedded sequence of volcaniclastic sediments (e.g. tuffs) and mainly basic to intermediate lavas. Overlying this is a Mid Permian – Mid Triassic sequence of carbonates and siliciclastics, in turn overlain by Upper Triassic – Cretaceous carbonate platform (Eren, 2001; Robertson and Ustaömer, submitted).

Four different tectonic models exist concerning the origin of the Konya Complex which are critical to test whether the Late Palaeozoic Gondwana margin was passive or active. In a first model (Fig. 6.1a), the complex is a back-arc rift related to southward subduction beneath the Gondwana margin (Özcan et al., 1988; Göncüoğlu et al., 2003; Göncüoğlu et al., 2007). In a second model (Fig. 6.1b), it is a fore-arc basin related to northward subduction-accretion beneath the Eurasian margin (Eren et al., 2004; Stampfli and Kozur, 2006). Thirdly, it could be an accretionary complex emplaced onto an extensional fore-arc basin during the Lower Carboniferous (Fig. 6.1c), possibly during southward subduction (Robertson and Ustaömer, submitted). Fourthly, it could be an exotic terrane, transported by right-lateral strike-slip to its present position in the pre-Middle Permian (Robertson and Ustaömer, submitted).

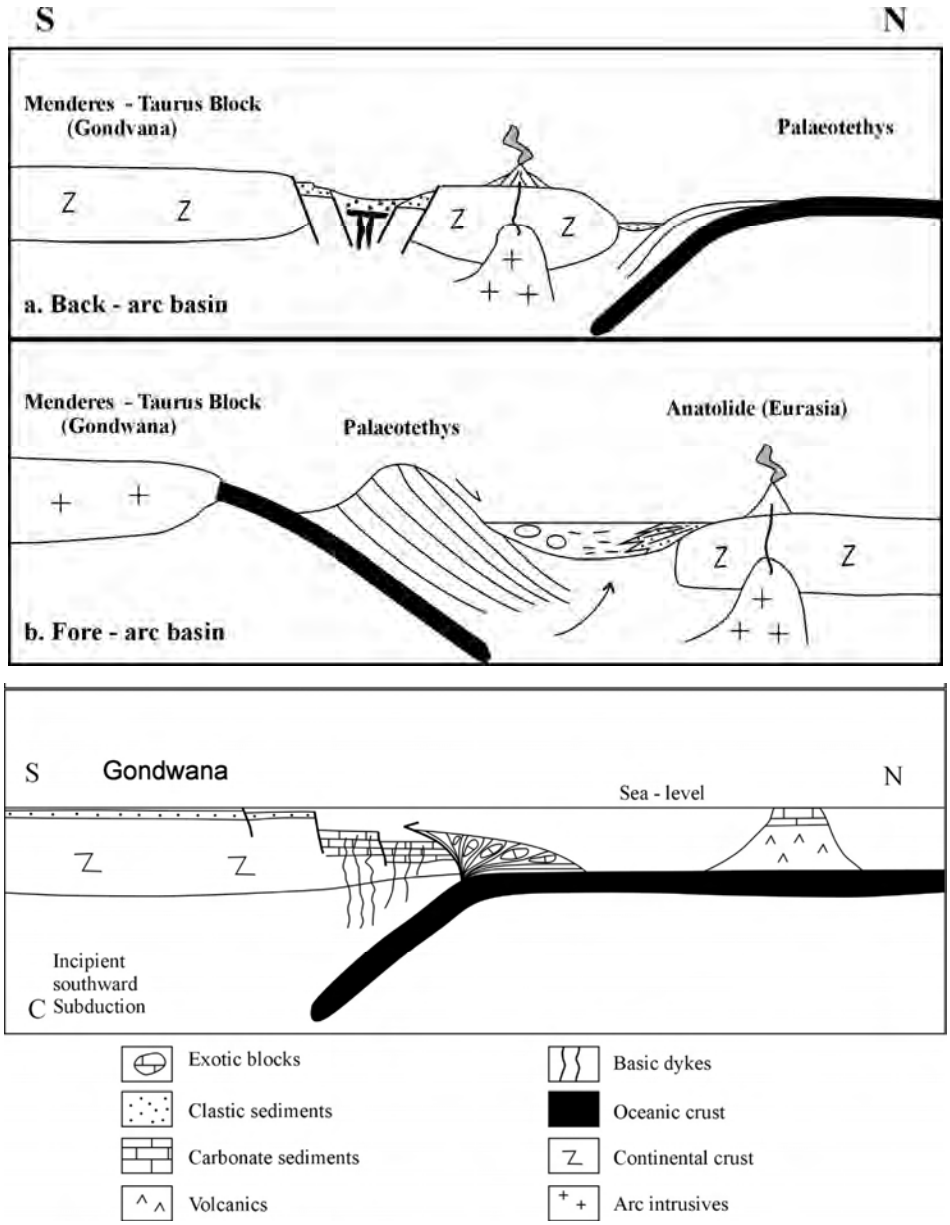

Fig. 6.1. Alternative tectonic models for the Konya Complex, from Robertson and Ustaömer (2008). a. Failed back-arc basin (Göncüoğlu et al., 2007); b. Fore-arc basin (Eren et al., 2004); c. Accretion to an extensional fore-arc .

A number of problems exist with each of the models described above. In the back-arc rift model (Fig. 6.1a), the Konya Complex is not stratigraphically comparable to other modern and ancient back-arc basins, especially the occurrence of mélange with large

blocks of lava, chert and carbonate. Problems with the northward subducting fore-arc model (Fig. 6.1b) are the mélange matrix is terrigenous rather than arc-derived, and some thick lavas in the Konya complex are in situ rather than being reworked blocks. Also, if the Konya Complex originated adjacent to the Eurasian margin, it must have sutured with the Tauride unit after it formed, i.e. Late Triassic (Stampfli et al., 2001; Stampfli and Borel, 2002). However, there is no evidence for this suturing, as shown in chapter 5 and Appendix A. In the accretionary/forearc model (Fig. 6.1c), the main problem is that there is no evidence in the adjacent Tauride platform units of southward subduction during the Lower Carboniferous, as shown in this study (chapter 3); however, this model cannot be excluded as the study area is well to the south of the possible active margin. Finally, in the terrane displacement model, there is no evidence of a strike-slip shear zone affecting the Konya Complex (Robertson and Ustaömer, submitted); once again, this model cannot be excluded, especially as a strike-slip could involve limited local deformation.

Active margin processes have been documented elsewhere along the north-Gondwana margin during the Late Palaeozoic. The mélange units of Karaburun (western Turkey) and Chios Island (Greece) are interpreted as a Late Carboniferous – Early Permian subduction-accretion complex that was then rifted in the Early Mesozoic (Robertson and Pickett, 2000). This mélange is thought to have formed during Late Palaeozoic trench-margin collision. Both accretion to Gondwana (Robertson and Pickett, 2000) and accretion to Eurasia (Zanchi et al., 2003) have been considered. Recent geochemical evidence from the islands of Chios, Inousses and Psara in the Aegean Sea, are interpreted to indicate that the Chios-Karaburun mélange represents a continental-margin arc formed along the Eurasian margin related to northward subduction of Palaeotethys during the Late Palaeozoic (Meinhold et al., 2007). On the other hand, the Permian cover succession has Gondwana-related rather than Eurasian fauna (e.g. Angiolini et al., 2005)

In southwestern Turkey, the Lycian Nappes include volcanic-sedimentary units of Carboniferous age (e.g. Collins, 1997; Kozur et al., 1998) . The Teke Dere unit has been interpreted as a subduction-accretion complex of Upper Carboniferous age, in

which deep-sea and volcaniclastic sediments were accreted and preserved, whilst oceanic crust was subducted (Kozur and Şenel, 1999). To the east, Late Palaeozoic deformation of the Arabian margin in Oman (e.g. Mann and Hanna, 1990) is possibly explained by active margin processes affecting the north Gondwana margin. Further west, zircon-dating of granites from Kithria Island (E. Crete, Greece) suggest that plutonism could have occurred along the north Gondwana margin during the Late Carboniferous, possibly related to southward subduction of Palaeotethys (Romano et al., 2006; Xypolias et al., 2006). With the evidence from the western Taurides and Aegean regions in mind, it is possible that southward subduction occurred along part of the Gondwana margin, to the west of the Konya Complex.

Palaeotethys is documented as closing in the Balkan region during the Lower Carboniferous Hercynian orogeny (Dercourt and Gaetani, 2000). It is estimated that ~1000km of strike-slip displacement may have accommodated large-scale Pangean terrane displacement, based on palaeomagnetic studies (Muttoni et al., 2003), which is supported by palaeontological evidence (Angiolini et al., 2007). The Konya Complex is transgressed by a continuous Permo-Triassic succession seen throughout the Tauride units. Therefore, it is likely to have been adjacent to the north Tauride platform by pre-Middle Permian time. However, there is simply not enough evidence to confirm either the accretionary/forearc model or the terrane displacement model.

This work restores the Hadim and Bolkar nappes as a shallow-marine continental shelf, between the Konya Complex and the Sultan Dağ, during the Early Carboniferous (Fig. 6.4 a, Fig. 6.5a). The Geyik Dağ, in a southerly location within the margin, was above sea level, and experienced net erosion throughout the Late Carboniferous. The cause of volcanism in the Sultan Dağ is still unclear, and requires further investigation.

6.2 Triassic evolution and "Cimmerian" uplift and deformation of the Tauride platform

Detailed sedimentary logging and facies analysis, presented in chapter 4, show that the Lower – Middle Triassic stratigraphy consists of shallow-marine mixed carbonate and

siliciclastic sediments. Sediment thickness and facies associations are laterally variable, suggesting that the Tauride platform was divided into a series of sub-basins during this time. Upper Triassic sequences are composed of coarser terrestrial and shallow-marine clastics and carbonates, again with variable lateral thickness and facies associations across the platform. Palaeocurrent data suggest that the regional flow in the Late Triassic was predominantly from north to south, indicative of a regional "basement" high to the north during this time. The composition of conglomerates and sandstones indicate that sediment source was mostly from the Palaeozoic and Triassic stratigraphy of the Tauride platform. Black chert clasts were probably derived partly from the Konya complex, further north in the Tauride platform; there is a lack of sediment that could have been derived from magmatic or metamorphic sources.

In chapter 4 (and Appendix A), the merits of several different tectonic models for the Triassic tectonic setting were discussed. There was no evidence to support a previous hypothesis that a Palaeotethyan ocean finally closed in this area during the latest Triassic, with emplacement of an Eurasian margin unit over Gondwana-related ("Cimmerian") units. However, "Cimmerian" tectonic events have been documented elsewhere along the Alpine-Himalayan suture zone, particularly in the Pontides (Turkey) (Yilmaz et al., 1997), the Caucuses and northern Iran (Zanchi et al., 2005; Balini et al., 2007; Berra et al., 2007a; Berra et al., 2007b; Golonka, 2007; Zanchi et al., 2007).

In the Alborz mountains, Iran, suturing between a "Cimmerian" terrane and the Eurasian margin is documented by a strong unconformity in the Triassic, below which basement rocks are heavily deformed in comparison to the cover sediments (Zanchi et al., 2005; Balini et al., 2007; Berra et al., 2007a). The Alam Formation (early Triassic) consists of shallow-marine tuffs and siliciclastics, whilst the Baqoroq Formation (Middle Triassic) consists of continental red clastics derived from an arc system to the north (Balini et al., 2007). The rocks are composed of reworked metamorphic-derived sediment, with a total thickness of >900 m. It is likely that this sedimentary sequence documents the collision of a continental fragment of Gondwana affinity with the Eurasian margin (Zanchi et al., 2005; Balini et al., 2007; Zanchi et al., 2007; A. Zanchi, Pers. Comm. 2007). There are three critical pieces of evidence seen in Iran, but not in

the central Taurides that are indicative of "Cimmerian" collision: (i) in Iran, there is a strong unconformity between 'basement' and Triassic rocks; (ii) the Triassic sediments in Iran contain abundant metamorphic and arc-derived material; (iii) the syn-tectonic sequence in Iran is over 900 m thick. This confirms that "Cimmerian" collision did occur further east in Tethys, but reinforces the likelihood that the Tauride platform was not involved in this event.

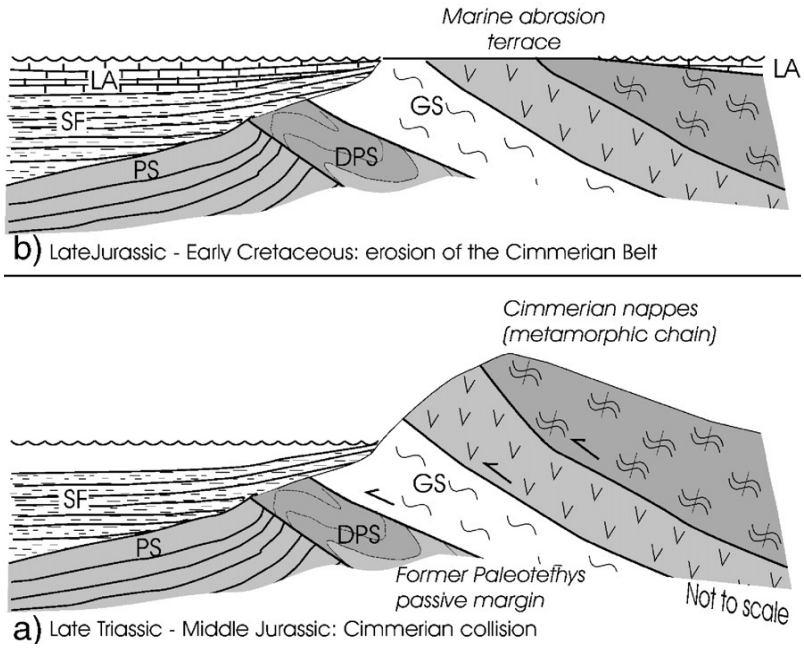

Fig. 6.2. Sketch showing the evolution of the Eastern Alborz mountains, Iran, during (a) Eo-Cimmerian orogenic events, and (b) post orogenic erosion of Cimmerian higher topography. Diagram from Berra et al. (2007b).

The sedimentary sequences observed in the central Tauride mountains are, in contrast to Iran, comparable to Triassic rifted margins elsewhere in the Tethyan realm (e.g. Oman, Greece, Arabia, Himalayas). It is proposed that stratigraphy of the central Taurides represent Early – Middle Triassic rifting followed by a pulse of Late Triassic rift-related flexural uplift, as seen, for example, in the Red Sea and Gulf of Aden region. The sequence was then transgressed by Jurassic platform carbonates, indicative of passive-margin subsidence. There are several models to explain this rifting episode.

Firstly, Göncüoğlu et al. (2003) infer the Tauride-Anatolide platform is located to the south of newly opening Izmir-Ankara Ocean, which itself is bordered to the north by an extinct magmatic arc (Sakarya Microcontinent) during the Late Triassic (Fig. 6.3a). Secondly, Okay et al. (2006) believe that the Apulia-Anatolide-Tauride block was separated from a thin 'Cimmerian' continental terrane by the Izmir-Ankara ocean (Fig. 6.3b) in the Late Triassic. Thirdly, Robertson et al. (2004) suggested that in the Mid – Late Triassic the northern Neotethys oceanic separated the Tauride-Anatolide platform from Çal rifted continental fragments in the west (Fig. 6.3c), whilst, fourthly, in Robertson (2006) the northerly continental fragment in the east is the Kirşehir-Massif (Fig. 6.3d). Fifthly, Andrew and Robertson (2002) suggest that the Tauride platform was separated from the Kirsehir-Nigde Massif by the Inner-Tauride Ocean (Fig. 6.3e). In each of these models, a continental fragment must have been adjacent to the northern Tauride margin (i.e. the Konya Complex) in the Permian, prior to rifting in the Triassic.

In model 1 (Göncüoğlu et al., 2003), the Sakarya unit is interpreted as an arc of Gondwana affinity, whilst in model 2 (Okay et al., 2006), it was located along the Eurasian margin by Late Palaeozoic time. The Sakarya zone is a high-grade metamorphic complex with a Palaeozoic basement of Carboniferous-Permian plutonic and metamorphic rocks and Triassic accretionary complexes (Okay et al., 2006). Triassic subduction-accretion is not described along the Gondwana margin, whilst it is well documented in the Pontides (e.g. Yilmaz et al., 1997). It is, therefore, likely that the Sakarya Unit is of Eurasian affinity.

In model 2 (Okay et al., 2006), break-up of the Palaeozoic Gondwana passive was associated with mafic magmatism as the Tauride-Anatolide block rifted from the Gondwana margin. It is tentatively suggested (Okay et al., 2006) that a sliver of the Tauride-Anatolide block, known as the 'Cimmerian continent', rifted in the Early Triassic and drifted northwards towards the Eurasian margin, opening the Izmir-Ankara ocean behind it to the south. However, the same authors also acknowledge that there is very little evidence of a 'Cimmerian' continental fragment in the Pontides.

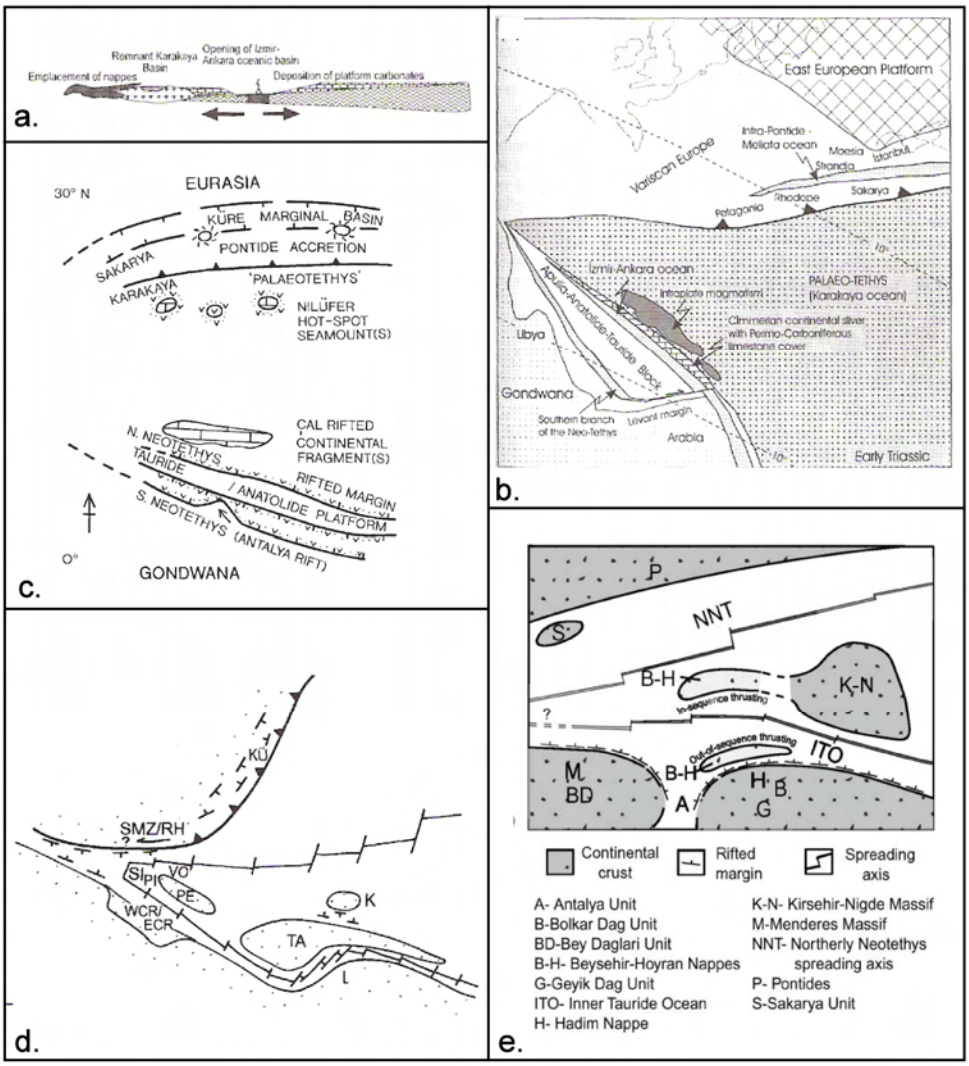

Fig. 6.3. Alternative tectonic reconstructions of the Tethys ocean for the Middle to Late Triassic. a. Göncüoğlu et al. (2003); b. Okay et al. (2006); c. Robertson et al. (2004); d. Robertson (2006); e. Andrew and Robertson (2002).

Perhaps a more plausible model is that a small ocean opened between the Tauride platform from the Kirşehir-Niğde massif (Andrew and Robertson, 2002). This terrane forms part of the high-grade metamorphic Central Anatolian crystalline complex (Whitney and Dilek, 1997), and is thought to be an extension of the Palaeozoic Tauride-Anatolide unit (Göncüoğlu et al., 1996-1997). The Kirşehir-Niğde massif can be restored as promontory of the Tauride margin prior to rifting (Andrew and Robertson, 2002), further east along the margin from the area in this study. The Triassic of the

Central Taurides can be explained by rifting of the Kirşehir-Niğde unit from the Tauride platform, forming of a new small oceanic basin to the north of the Konya Complex. Dating of oceanic-derived radiolarian cherts from the Izmir-Ankara suture zone provide evidence that an oceanic seaway was open to the north of the Tauride platform by the Late Triassic (Tekin et al., 2002; Göncüoğlu et al., 2006). Also, the Beyşehir-Hoyran nappes document Triassic rifting and Jurassic-Cretaceous passive margin subsidence to the north of the Tauride platform (Andrew, 2002; Andrew and Robertson, 2003). Proposed models for the Triassic tectonic setting is provided in Fig. 6.4b/c and Fig. 6.5b/c.

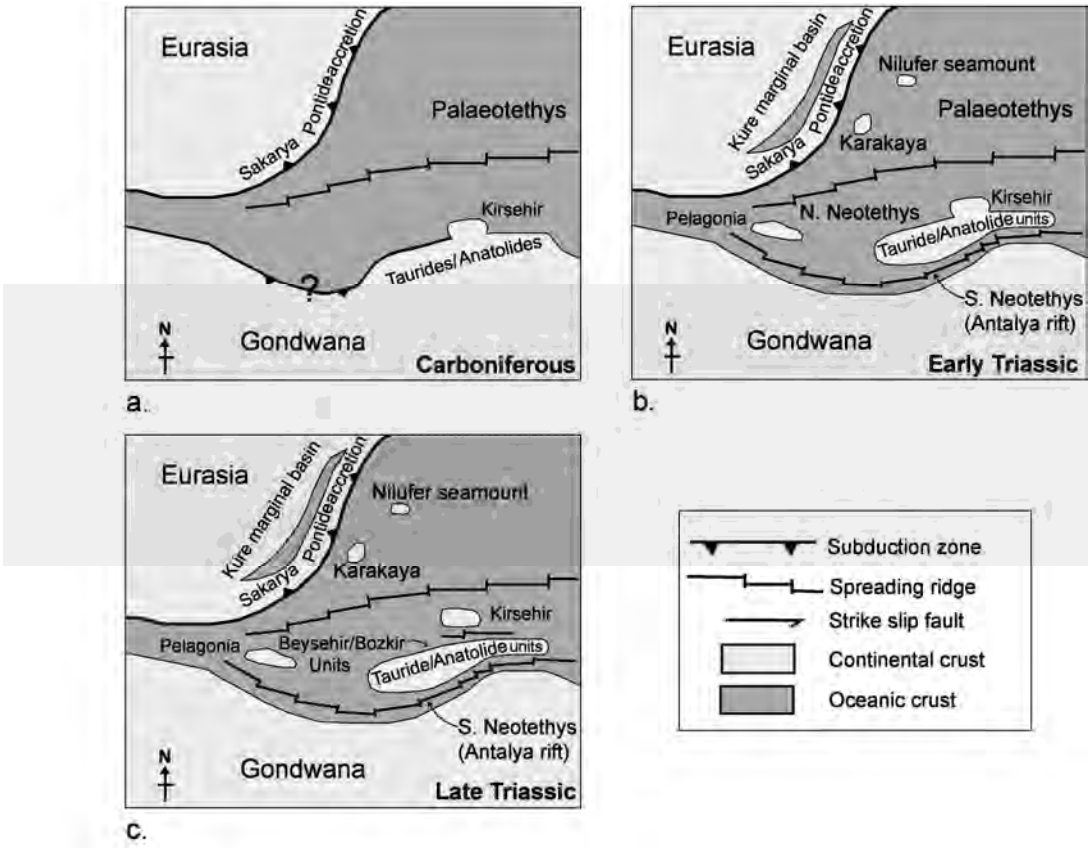

Fig. 6.4. Palaeotectonic maps of western Tethys in the Eastern Mediterranean region. a. Carboniferous; b. Early Triassic; c. Late Triassic.

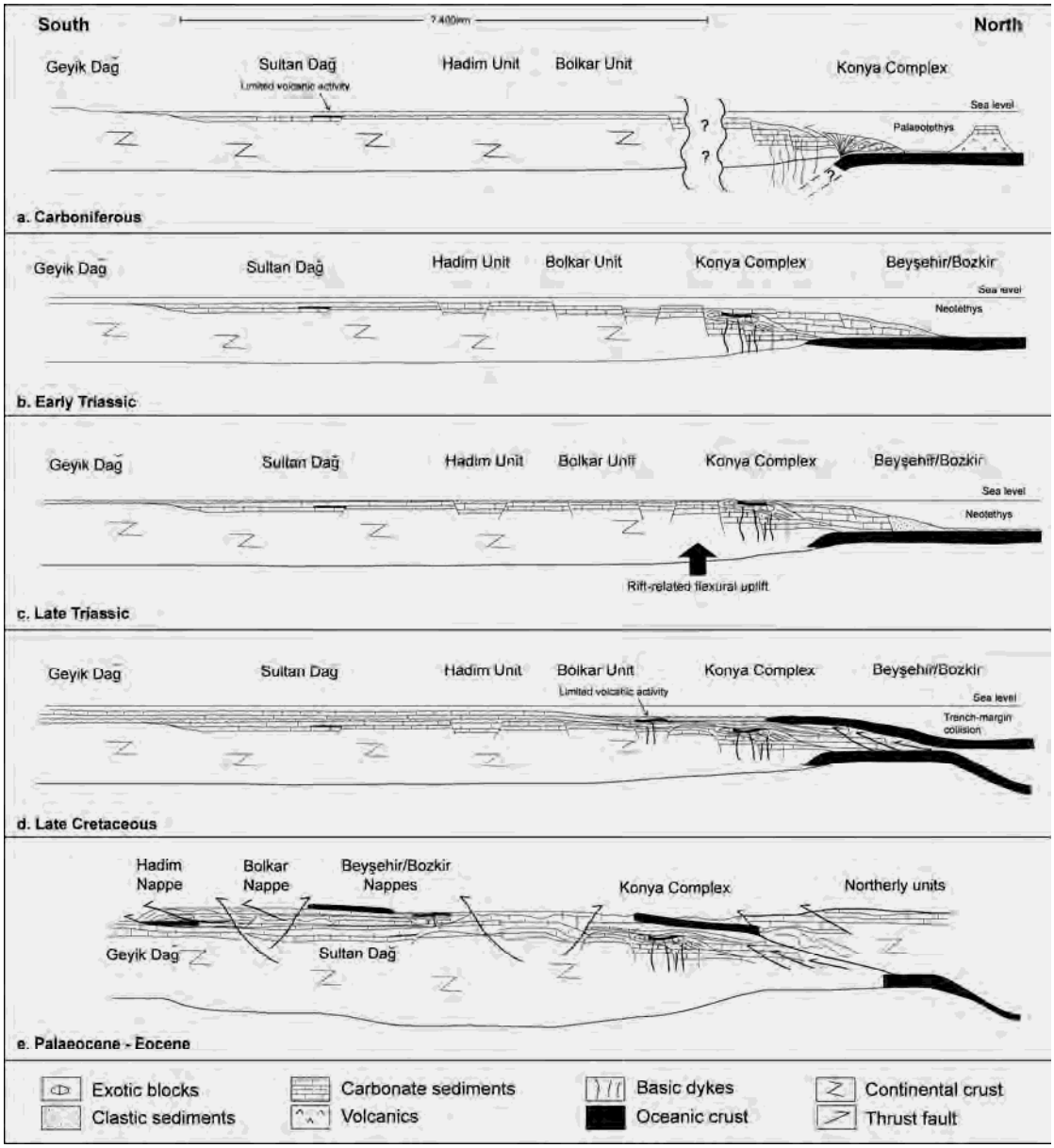

Fig. 6.5. Reconstructed cross-sections through the northern part of the Tauride platform. a. Carboniferous. The Konya Complex is left open to interpretation. Possible model shown is of southward subduction/accretion; b. Early Triassic; c. Late Triassic; d. Late Cretaceous; e. Early Cenozoic.

6.3 Emplacement and structural evolution

From the Jurassic – Middle Cretaceous, the Tauride platform experienced a subsiding passive margin evolution, with a thick succession of shallow-marine carbonates covering the Palaeozoic and Triassic of the Geyik Dağ and Sultan Dağ in the south, the Hadim and Bolkar units in the mid part of the platform (e.g. Monod, 1977; Ozgul, 1984), and the Konya Complex further north (Özcan et al., 1988; Eren, 2001). To the north of the Konya Complex, the Beyşehir/Bozkir units document the rifted margin evolution of the Tauride platform (Andrew and Robertson, 2002).

During the Late Cretaceous, the Beyşehir/Bozkir nappes, composed of rifted margin units and ophiolite, were emplaced southwards onto the Tauride continental platform. The ophiolite is locally found at the base of the Beyşehir-Hadim nappe stack (e.g. near Beyşehir and Seydişehir), indicating that thrusting was by out-of-sequence processes. This thrusting is represented in the Bolkar nappe by the deposition in a foredeep of Campanian – Maastrichtian pelagic limestones, turbidites, debris flows, volcaniclastic sediments, and finally ophiolitic mélange. The volcanic-derived rocks in the stratigraphy are possibly related to flexure of the continental margin as the ophiolite slab approached. During this emplacement the Bolkar nappe experienced intense deformation and low-grade metamorphism. The deformation and syn-tectonic sedimentation is also observed in the Late Cretaceous of Konya Complex, further north in the platform (Özcan et al., 1988; Eren, 2001; Andrew and Robertson, 2002; Eren et al., 2004; Robertson and Ustaömer, submitted). To the south of the platform, the Hadim nappe experienced some foredeep subsidence and accumulated pelagic sediments during this time; however, it was not deformed to the same degree as the Bolkar nappe and Konya Complex. In the southernmost part of the platform, the Geyik Dağ (and Sultan Dağ) were unaffected by the emplacement of the ophiolite and distal margin units, and shallow-water conditions prevailed until the Cenozoic. This emplacement is comparable with other regions of the Tethyan orogen, and is likely to represent thin-skinned ‘soft’ collision of continental margin with a intra-oceanic trench (Fig. 6.5d).

During the Palaeocene – Eocene the Hadim and Bolkar units were emplaced southwards onto the autochthonous Geyik Dağ, and the Beyşehir/Bozkir nappes were re-thrust southwards. Locally, the ophiolite unit was emplaced out-of-sequence, and was subsequently overridden by the Hadim and Bolkar nappes. During this emplacement the Geyik Dağ autochthon collapsed and a foredeep accumulated turbidites and gravity deposits ahead of the southward propagating thrust stack. The Geyik Dağ was deformed as the nappes were emplaced, whilst the Bolkar and Hadim nappes experienced further internal deformation during emplacement. During final Mid Eocene tightening of the nappe stack, the Hadim nappe was backthrust to the north over the Bolkar nappe. This second phase of emplacement is considered to be 'hard' collision; some 'thick-skinned' faults may propagate down to the crystalline basement of the Tauride platform (Fig. 6.5e). Structural data collected from the autochthonous and allochthonous units are consistent with Late Cretaceous – Early Cenozoic 'Alpine' deformation related to two-phase emplacement of the Beyşehir/Bozkir-Hadim nappe stack.

6.4 Wider implications and future work

This study provides new evidence concerning the Late Palaeozoic – Early Cenozoic tectonic development of the Tauride platform. It fills important gaps in knowledge of the geological development of the north Gondwana margin. A number of existing models have been critically tested and, in some cases, discounted, adding to the understanding of Tethyan ocean evolution. The palaeo-tectonic reconstructions of this study are critical for along-strike comparison of continental margin development, from the Balkans in the west to China in the east. The significance of out-of-sequence / in-sequence thrusting, and thin-skinned / thick-skinned tectonics, has implications for reconstructions, not only for the Alpine-Himalayan mountain belt, but also other orogenic belts across the world. Research in the eastern Mediterranean, such as this, addresses fundamental issues regarding tectonic processes, which constantly need 'updating' and critical testing. Investigations such as this show there are few set rules regarding large-scale tectonic processes, and continued investigation into orogenic belts is required to expand our

knowledge of the interactions between tectonics, sedimentation, magmatism and metamorphism. Hopefully this work will in future encourage further investigation of Eastern Mediterranean geology.

This study could be developed further by high-resolution stratigraphic investigation, using, for example, stable isotope and palaeontological investigation. The Beyşehir ophiolite requires dating in order to accurately compare it with other Turkish ophiolites. Further research is required on the origin of the Konya Complex, and its pre-Permian relationship (if any) to the Tauride platform. The Late Palaeozoic "active vs. passive" margin question could be tested on Anatolian terranes elsewhere in Turkey. The models of "Cimmerian" uplift also need to be tested in other Gondwana related terranes in the region. Palaeomagnetic investigation would contribute significantly to palaeo-tectonic reconstructions, and an investigation is currently in progress (Utrecht University). Fission track analysis could help to determine the burial and uplift of the Tauride units. An accurate study of the subsidence and sedimentation rates of Gondwana related terranes would also be of value.

7 Conclusions

(1) The Tauride platform, which restores as part of the northern margin of Gondwana continent during the Late Palaeozoic, experienced a passive margin evolution during the Devonian. Siliciclastic and carbonate sediments in the Hadim and Bolkar nappes were deposited on a shallow-marine shelf, with high frequency sea-level change in the Upper Devonian being seen as an important control of sedimentary facies. During this time, the Geyik Dağ autochthon was above sea-level and experienced net erosion, represented by a Ordovician – Triassic unconformity.

(2) Lower Carboniferous black shales were deposited in a relatively distal shelf setting during a time of global marine high-stand, with phosphorite sediments possibly representative of increased organic productivity. Compositional analysis suggests sediment provenance from the underlying Tauride "basement" and other Pan-African terranes. There is no clear sedimentary or structural evidence of an active margin setting along the Gondwana margin during the Carboniferous.

(3) Middle and Upper Carboniferous limestones formed in a productive carbonate shelf setting, with coral assemblages and oolitic limestones indicative of a shallow-water depth. Sandstone and mudstone horizons in the Upper Carboniferous are suggestive of transgressive-regressive cycles, as indicated for this time period by global sea-level curves.

(4) Carbonate deposition continued into the Permian, as represented by shallow-marine carbonate production, with an increase in inferred sedimentation rate possibly related to rifting of a Neotethyan ocean to the south (e.g. Antalya region).

(5) The Lower – Middle Triassic stratigraphy of the Geyik Dağ, Hadim nappe and Bolkar nappe consists of shallow-marine mixed carbonate and siliciclastic sediments.

Sediment thickness and facies associations are laterally variable, suggesting the Tauride platform was divided into a series of sub-basins during this time.

(6) Upper Triassic sequences are composed of coarser terrestrial to shallow-marine clastics and carbonates, with variable lateral thickness and facies associations across the platform. Palaeocurrent data suggest that the regional flow in the Late Triassic was predominantly from north to south, indicative of a regional "basement" high to the north during this time. The composition of conglomerates and sandstones suggest that sediment source was mostly from the Palaeozoic and Triassic stratigraphy of the Tauride platform.

(7) The Triassic stratigraphy of the central Taurides is interpreted to represent Early – Middle Triassic rifting followed by a pulse of Late Triassic rift-related flexural uplift, as seen, for example, in the Red Sea and Gulf of Aden region. There is no evidence of a "Cimmerian" continental collision event within the Taurides at this time.

(8) From Jurassic – Middle Cretaceous, the Tauride platform experienced a subsiding passive margin evolution, with a thick succession of shallow-marine carbonates covering the Palaeozoic and Triassic of the Geyik Dağ, Hadim nappe and Bolkar nappe.

(9) During the Late Cretaceous, the Beyşehir/Bozkir nappes, composed of distal margin and ophiolitic units, were emplaced southwards onto the Tauride continental platform, associated with the development of a Campanian – Maastrichtian age foredeep basin on the Bolkar unit. Flexure of the continental margin was accompanied by localised alkaline volcanism. During this emplacement the Bolkar nappe experienced intense deformation and low-grade metamorphism.

(10) During the Palaeocene – Eocene the Hadim and Bolkar units were emplaced southwards onto the autochthonous Geyik Dağ, together with rethrusting of the Beyşehir/Bozkir nappes. Locally, the ophiolite unit was emplaced out-of-sequence, and

was subsequently overridden by the Hadim and Bolkar nappes. The Geyik Dağ was deformed as the nappes were emplaced, and a foredeep basin developed to the south of the nappe stack. During final Mid Eocene tightening of the nappe stack, the Hadim nappe was backthrust to the northwards over the Bolkar nappe.

(11) This study of the Tauride units provides important new information on the tectonic development of the north Gondwana margin, contributing significantly to palaeo-tectonic reconstructions of the Tethyan ocean. The results have implications for studies of the Alpine-Himalayan orogenic belt and continental margins across the world.

References

Abbate, E., Balestrieri, M.L. and Bigazzi, G., 2001. Uplifted rift-shoulder of the Gulf of Aden in northwestern Somalia: palinspastic reconstructions supported by apatite fission-track data. In: Ziegler, P. A., Cavazza, W., Robertson, A. H. F., and Crasquin-Soleau, S. (eds). Peri-Tethys Memoir 6: Peri-Tethyan Rift / Wrench Basins and Passive margins, Mémoirs du Muséum national d'Histoire naturelle(186): 629-640.

Agard, P., Omrani, J., Jolivet, L., Whitechurch, H., Monié, P. and Vrielynck, B., 2007. Petrological, structural and geodynamic constraints for the Zagros Orogeny and regional-scale implications. Middle East Basins Evolution Programme, Abstract Volume, Paris Meeting, December 2007.

Al-Riyami, K. and Robertson, A.H.F., 2002. Mesozoic sedimentary and magmatic evolution of the Arabian continental margin, northern Syria: evidence from the Baer–Bassit Melange. Geological Magazine, 139(4): 395-420.

Allen, P.A. and Allen, J.R., 1990. Basin Analysis: Principles and Applications. Blackwell Sciences Limited, Oxford.

Andrew, T., 2003. Mesozoic to Early Tertiary tectonic-sedimentary evolution of the Northern Neotethys Ocean: evidence from the Beyşehir-Hoyran-Hadim Nappes, Southern Turkey. PhD Thesis, University of Edinburgh UK.

Andrew, T. and Robertson, A.H.F., 2002. The Beyşehir–Hoyran–Hadim Nappes: genesis and emplacement of Mesozoic marginal and oceanic units of the northern Neotethys in southern Turkey. Journal of the Geological Society, London, 159: 529–543.

Angiolini, L., Carabelli, L. and Gaetani, M., 2005. Middle Permian brachiopods from Greece and their palaeogeographical significance: new evidence for a Gondwanan affinity of the Chios Island Upper Unit. Journal of Systematic Palaeontology, 3: 169-185.

Angiolini, L., Gaetani, M., Muttoni, G., Stephenson, M.H. and Zanchi, A., 2007. Tethyan oceanic currents and climate gradients 300 m. y. ago. Geology, 35: 1071-1074.

Arzani, N., 2005. The fluvial megafan of Abarkoh Basin (Central Iran): an example of flash-flood sedimentation in arid lands. From: Harvey, A.M., Mather, A.E., & Stokes, M. (eds) 2005 Alluvial Fans: Geomorphology, Sedimentology, Dynamics. Geol. Soc. London, Spec. Pub., 251: 41-59.

Autin, J., Leroy, S., d'Acremont, E., Beslier, M.-O., Ribodetti, A., Courrèges, E., Perrot, J. and Bellahsen, N., 2007. Structure and evolution of the north-eastern Gulf of Aden margin. European Geosciences Union 2007, Geophysical Research Abstracts, 9.

Balini, M., Nicora, A., Berra, F., Garzanti, E., Mattei, M., Zanchi, A., Bollati, I., Levera, M., Salamati, R. and Mossavari, F., 2007. The Triassic stratigraphic succession of Nakhlak (Central Iran), record of an active margin. Geophysical Research Abstracts, Vol. 9, European Geosciences Union, Vienna 2007.

Baumgartner, P.O. and Bernoulli, D., 1976. Stratigraphy and radiolarian fauna in a Late Jurassic - Early Cretaceous section near Achladi (Evoia, Eastern Greece). Eclogae Geologicae Helvetiae, 69(601-626).

Berra, F., Zanchi, A., Mattei, M., Marinoni, N. and Nawab, A., 2007a. Stratigraphy across the Cimmerian unconformity in Eastern Alborz (Neka Valley, Iran): Late Cretaceous glauconitic facies as indicator of a geodynamic event Geophysical Research Abstracts, Vol. 9, European Geosciences Union, Vienna 2007.

Berra, F., Zanchi, A., Mattei, M. and Nawab, A., 2007b. Late Cretaceous transgression on a Cimmerian high (Neka Valley, Eastern Alborz, Iran): A geodynamic event recorded by glauconitic sands. Sedimentary Geology, 199: 189-204.

Blumenthal, M., 1947. Geologie der Taurusketten im hinterland von Seydişehir und Beyşehir. Maden tetkik ve Arama Report, D 2.

Blumenthal, M., 1951. Récherches géologiques dans les Taurus occidental dans l'arriere-pays d'Alanya. Maden Tetkik ve Arama Report, D 5.

Blumenthal, M., 1956. Les chaines bordières du Taurus au sud-ouest di bassin de Karaman-Konya et le problème stratigraphique de la formation schisto-radiolaritique. Bulletin of Maden Tetkik ve Arama Report, D 5.

Blumenthal, M., 1960-1963. Le Système structural du Taurus sud-anatolien. Livre Mémoire. P. Fallot, Paris: 611-662.

Bosworth, W. and McClay, K.R., 2001. Structural and stratigraphic evolution of the Gulf of Suez Rift, Egypt: a synthesis. In Ziegler, P., Cavazza, W., Robertson, A.H.F., & Crasquin-Soleau, A. (eds) Peri-Tethyan Rift/Wrench Basins and Passive Margins. Peri-Tethys Memoire, 6: 567-606.

Bozkurt, E., 2001. Noetectonics of Turkey - a synthesis. Geodinamica Acta, 14: 3-30.

Calabrò, R.A., Corrado, S., Di Bucci, D., Robustini, P. and Tornaghi, M., 2003. Thin-skinned vs. thick-skinned tectonics in the Matese Massif, Central-Southern Apennines (Italy). Tectonophysics, 377(3-4): 269-297.

Caplan, M.L. and Bustin, R.M., 1999. Devonian–Carboniferous Hangenberg mass extinction event, widespread organic-rich mudrock and anoxia: causes and consequences. Palaeogeography, Palaeoclimatology, Palaeoecology, 148(4): 187-207.

Clark, M. and Robertson, A.H.F., 2002. The role of the Early Tertiary Ulukışla Basin, southern Turkey, in suturing of the Mesozoic Tethys ocean. Journal of the Geological Society, 159: 673-690.

Collins, A., 1997. Tectonic evolution of the Lycian Taurides. PhD Thesis, University of Edinburgh, Edinburgh, UK.

Collins, A. and Robertson, A.H.F., 1998. Processes of Late Cretaceous to Late Miocene episodic thrust-sheet translation in the Lycian Taurides, SW Turkey. Journal of the Geological Society, London, 155: 759–772.

Coward, M.P., 1983. Thrust tectonics, thin skinned or thick skinned, and the continuation of thrusts to deep in the crust. Journal of Structural Geology, 5(2): 113-123.

Crowley, T.J. and Baum, S.K., 1991. Estimating Carboniferous sea-level fluctuations from Gondwanan ice extent. Geology, 19(10): 975-977.

Dalrymple, R.A., 2005. The Offshore transport of mud: why it doesnt happen and the stratigraphic implications. Abstract of Oral Presentation, The Geological Society of America, Annual Meeting, Salt Lake City, Oct. 16-19.

Dalziel, I.W.D., 1997. Neoproterozoic-Paleozoic geography and tectonics: Review, hypothesis, environmental speculation. Geological Society of America Bulletin, 109(1): 16-42.

Dean, W.T. and Monod, O., 1970. The Lower Palaeozoic stratigraphy and the faunas of the Taurus Mountains near Beyşehir, Turkey. Bulletin of the British Museum (Natural History), Geology, 15: 411-426.

Dean, W.T. and Monod, O., 1990. Revised stratigraphy and relationships of Lower Palaeozoic rocks, eastern Taurus Mountains, south central Turkey. Geological Magazine, 127(4): 333-347.

Demirkol, C., 1981. Sultandağ kuyezbatısının jeolojisi ve Beyşehir-Hoyran Napları ile ilişkileri. Unpublished M.T.A. report, Project no. TBAG-382, Ankara.

Demirkol, C., 1982. Yalvac-Aksehir Dolayinin Stratigrafisi ve Bati Toroslarla Denestirimi. PhD Thesis, Cukurova Universitesi Turkey.

Demirtaşlı, E., 1984a. Stratigraphic evidence of Variscan and early Alpine tectonics in Southern Turkey. In Dixon, J. E. & Robertson A. H. F. (eds) The Geological Evolution of the Eastern Mediterranean. Geological Society, London, Special Publication, 17: 129-145.

Demirtaşlı, E., 1984b. Stratigraphy and tectonics of the area between Silifke and Anamur, Central Taurus Mountains. In Tekeli, O. and Göncüoglu, M. C. (eds) Geology of the Taurus belt. Proceedings of the International Symposium. MTA, Ankara: 101-118.

Dercourt, J. and Gaetani, M., 2000. Peri-Tethys Palaeogeographical Atlas, 2000.

Dercourt, J., Ricou, L.E. and Vrielynck, B., 1993. Atlas Tethys Palaeoenvironmental Maps. Beicip-Franlab(1993).

Dercourt, J., Zonenshain, L.P., Ricou, L.E., Kazmin, V.G., Le Pichon, X., Knipper, A.L., Grandjacquet, C., Sbortshikov, I.M., Geyssant, J., Lepvrier, C., Pechersky, D.H., Boulin, J., Sibuet, J.-C., Savostin, L.A., Sorokhtin, O., Westphal, M., Bazhenov, M.L., Lauer, J.P. and Biju-Duval, B., 1986. Geological evolution of the Tethys belt from the Atlantic to the Pamirs since the Lias. Tectonophysics, 123: 241-315.

Einsele, G., 1992. Sedimentary Basins: Evolution, facies and sediment budget. Springer-Verlag, Berlin Heidelberg, 628 pp.

Eren, Y., 2001. Polyphase Alpine deformation at the northern edge of the Menderes-Taurus block, North Konya, Central Turkey. Journal of Asian Earth Sciences, 19: 737-749.

Eren, Y., Kurt, H., Rosselet, F. and Stampfli, G., 2004. Palaeozoic deformation and magmatism in the northern area of the Anatolide block (Konya), witness of the Palaeotethys active margin. Eclogae Geologicae Helvetiae, 97(2): 293-306.

Fitton, J.G. and Dunlop, H.M., 1985. The Cameroon Line, West Africa, and its bearing on the origin of oceanic and continental alkali basalts. . Earth and Planetary Science Letters, 72: 23-38.

Fitton, J.G., Saunders, A.D., Larson, L.M., Hardarson, B.S. and Norry, M.S., 1998. Volcanic rocks of the southeastern Greenland margin. In: Saunders, A. D., Larsen, H. C., Wise, S. W. (eds) Proceedings of the Ocean Drilling Program, Scientific Results, 152. Ocean Drilling Program, College Station, TX: 331-350.

Fraiser, M.L. and Bottjer, D.J., 2007. When bivalves took over the world. Paleobiology, 33(3): 397-413.

Gaetani, M. and Garzanti, E., 1991. Multicycle history of the Northern India continental margin (northwestern Himalayas). AAPG Bulletin, 75: 1427-1446.

Glennie, K.W., Boeuf, M.G.A., Hughes Clarke, M.W., Moody-Stuart, M., Pilaar, W.F.H. and Reinhardt, B.M., 1973. Late Cretaceous nappes in the Oman Mountains and their geologic significance. AAPG Bulletin, 57: 5-27.

Golonka, J., 2007. Late Triassic and Early Jurassic palaeogeography of the world. Palaeogeography, Palaeoclimatology, Palaeoecology, 244(1-4): 297-307.

Göncüoğlu, M.C., Çapkinoğlu, Ş., Gürsü, S., Noble, P., Turhan, N., Tekin, U.K., Okuyucu, C. and Göncüoğlu, Y., 2007. The Mississippian in the Central and Eastern Taurides (Turkey): constraints on the tectonic setting of the Tauride-Anatolide Platform. Geologica Carpathica, 58(5): 427-442.

Göncüoğlu, M.C., Direk, K. and Kozlu, H., 1996-1997. Pre-alpine and alpine terranes in Turkey: explanatory notes on the terrane map of Turkey. Annales Geologique de Pays Hellenique, 37: 1-3.

Göncüoğlu, M.C., Göncüoğlu, Y., Kozur, H. and Kozlu, H., 2004. Palaeozoic stratigraphy of the Geyik Dag Unit in the Eastern Taurides (Turkey): new age data and implications for Gondwanan evolution. Geologica Carpathica, 55(6): 433-447.

Göncüoğlu, M.C. and Kozlu, H., 2000. Early Palaeozoic Evoltuion of the NW Gondwanaland: Data from Southern Turkey and Surrounding regions. Gondwana Research, 3(3): 315-324.

Göncüoğlu, M.C., Turhan, N., Şentürk, K., Özcan, A., Uysal, Ş. and Yalınız, M.K., 2000. A geotraverse across northwestern Turkey: tectonic units of the Sakarya region and their tectonic evolution. In Bozkurt, E., Winchester, J. A. & Piper, J. D. A. (eds) Tectonics and Magmatism in Turkey and the Surrounding Area. Geological Society, London, Special Publication, 173: 139-161.

Göncüoğlu, M.C., Turhan, N. and Tekin, K., 2003. Evidence for the Triassic rifting and opening of the Neotethyan Izmir-Ankara Ocean and discussion on the presence of Cimmerian events at the northern edge of the Tauride-Anatolide Platform, Turkey. Bollettino della Societa Geologica Italiana Roma, Special publication, volume 2: 203-212.

Göncüoğlu, M.C., Yalınız, M.K. and Tekin, U.K., 2006. Geochemistry, tectono-magmatic discrimination and radiolarian ages of basic extrusives within the Izmir-Anakra suture belt (NW Turkey): Time constraints for the Neotethyan evolution. Ofioliti, 31(1): 25-38.

Gradstein, 2004. A Geological Time Scale. Cambridge University Press, Cambridge.

Gromet, L.P., Haskin, L.A., Korotev, R.L. and Dymek, R.F., 1984. The "North American shale composite": Its compilation, major and trace element characteristics. Geochimica et Cosmochimica Acta, 48(12): 2469-2482.

Guiraud, R., Issawi, B. and Bosworth, W., 2001. Phanerozoic history of Egypt and surrounding areas. In Ziegler, P., Cavazza, W., Robertson, A.H.F., & Crasquin-Soleau, A. (eds) Peri-Tethyan Rift/Wrench Basins and Passive Margins. Peri-Tethys Memoire, 6: 469-509.

Gürsu, S. and Göncüoğlu, M.C., 2001. Geology of the late Pre-Cambrian rocks in Sandikli Area: Implications for the Pan-African Evolution in NW Gondwana. 4th International Symposium on Eastern Mediterranean Geology, 12th - 25th May, Isparta, Turkey.

Gürsu, S., Göncüoğlu, M.C. and Bayhan, H., 2004. Geology and Geochemistry of the Pre-Lower Cambrian Rocks in Sandikli Area: Implications for the Pan-African evolution of NW Gondwanaland. Gondwana Research, 7(4): 923-935.

Gutnic, M., Monod, O., Poisson, A. and Dumont, J., 1979. Géologie des Taurides Occidentales (Turquie). Societé Géologique de France, Mémoir, 137: 1-112.

Hallam, A., 1984. Pre-Quaternary sea-level changes. Annual Review of Earth and Planetary Sciences, 12: 205-243.

Hallam, A., 1992. Phanerozoic sea-level changes. Columbia University Press, New York.

Hallam, A. and Wignall, P.B., 1999. Mass extinctions and sea-level changes. Earth Science Reviews, 48(4): 217-250.

Hamilton, 1836. Research in Asia Minor. 1 and 2, London.

Jackson, C.A.L., Gawthorpe, R.L., Carr, I.D. and Sharp, I.R., 2005. Normal faulting as a control on the stratigraphic development of shallow marine syn-rift sequences: the Nukhul and Lower Rudeis Formations, Hammam Faraun fault block, Suez Rift, Egypt. Sedimentology, 52(2 %R doi:10.1111/j.1365-3091.2005.00699.x): 313-338.

Jackson, J.A. and Fitch, T., 1981. Basement faulting and the focal depths of the larger earthquakes in the Zagros mountains (Iran). Geophysical Journal of the Royal Astronomical Society, 64: 561-586.

Jaffey, N. and Robertson, A.H.F., 2001. New sedimentological and structural data from the Ecemis Fault Zone, southern Turkey: implications for its timing and offset and the Cenozoic tectonic escape of Anatolia. Journal of the Geological Society, 158(2): 367-378.

James, N.P., 1984. Introduction to carbonate facies models. in: Walker, R. G. (editor). Facies Models (2nd Edition). Geoscience Canada Reprint, series 1: 209-211.

Johnson, H.D. and Baldwin, C.T., 1986. Shallow Siliciclastic Seas. In: Reading, H. G. (editor). Sedimentary Environments and Facies, Blackwell Scientific Publications, Oxford: 229-282.

Kozur, H. and Göncüoğlu, M.C., 2000. Mean features of the pre-Variscan development in Turkey. Acta Universitatis Carolinae-Geologica, 42: 456-464.

Kozur, H. and Şenel, M., 1999. Carboniferous oceanic sequences in the Lycian nappes of southern Turkey. In XIV ICCP, International Congress on the Carboniferous-Permian, Calgary, p. 79.

Kozur, H., Senel, M. and Tekin, K., 1998. First Evidence of Hercynian Lower Carboniferous Flyschoid Deep-Water Sediments in the Lycian Nappes, Southwestern Turkey. Geologia Croatica, 51(1): 15-22.

Leturmy, P., Molinaro, M. and Frizon de Lamotte, D., 2007. Geometry and chronology of basement faulting in the Fars Arc: A view from structural and morphological analysis. Middle East Basins Evolution Programme, Abstract Volume, Paris Meeting, December 2007.

Lonergan, L. and Schreiber, B.C., 1993. Proximal deposits at a fault-controlled basin margin, Upper Miocene, SE Spain. Journal of the Geological Society, 150: 719-727.

Machent, P.G., Taylor, K.G., Macquaker, J.H.S. and Marshall, J.D., 2007. Patterns of early post-depositional and burial cementation in distal shallow-marine sandstones: Upper Cretaceous Kenilworth Member, Book Cliffs, Utah, USA. Sedimentary Geology, 198: 125-145.

Mackintosh, P.W. and Robertson, A.H.F., submitted. Structural and sedimentary evidence from the northern margin of the Tauride platform: testing models of Late Triassic "Cimmerian" uplift and deformation in southern Turkey. Tectonophysics(Special publication: Tectonic evolution of Tethys.).

Mann, A. and Hanna, S.S., 1990. The tectonic evolution of pre-Permian rocks, Central and Southeastern Oman Mountains. In. Robertson, A.H.F., Searle, M.P., Ries, A.C. (Eds). The Geology and Tectonics of the Oman Mountains, Geological Society Special Publication, 49: 307-325.

Márquez, L., 2005. Foraminiferal fauna recovered after the Late Permian extinctions in Iberia and the westernmost Tethys area. Permian-Triassic Transition in Spain: A multidisciplinary approach, 229(1-2): 137-157.

Mather, A.E. and Hartley, A., 2005. Flow events on a hyper-arid alluvial fan: Quebrada Tambores, Salar de Atacama, northern Chile. From: Harvey, A.M., Mather, A.E., & Stokes, M. (eds) 2005 Alluvial Fans: Geomorphology, Sedimentology, Dynamics. Geol. Soc. London, Spec. Pub., 251: 9-29.

Mattauer, M., 1986. Intracontinental subduction, crust-mantle décollement and crustal-stacking wedge in the Himalaya's and other collision belts. In Coward, M. P. and Ries, A. (eds). Collisional tectonics. Geological Society, London, Special Publication 19: 37-50.

McClay, K.R., Nichols, G.J., Khalil, S.M., Darwish, M. and Bosworth, W., 1998. Extensional tectonics and sedimentation, eastern Gulf of Suez, Egypt. In Purser, B. H., and Bosence, D. W. J (eds) Sedimentation and Tectonics of Rift Basins: Red Sea-Gulf of Aden. Chapman & Hall, London.

McLennan, S.M., Taylor, S.R. and Hemming, S.R., 2006. Composition, differentiation, and evolution of continental crust: constraints from sedimentary rocks and heat flow. In: Brown, M. and Rushmer, T. (eds), Evolution and Differentiation of the Continental Crust, Cambridge University Press, pp. 92-134. .

Meert, J.G. and Van Der Voo, R., 1997. The Assembly of Gondwana 800-550 Ma. Journal of Geodynamics, 23(3/4): 223-235.

Meinhold, G., Kostopoulos, D. and Reischmann, T., 2007. Geochemical constraints on the provenance and depositional setting of sedimentary rocks from the islands of Chios, Inousses and Psara, Aegean Sea, Greece: implications for the evolution of Palaeotethys. Journal of the Geological Society, 164(1145-1163).

Miall, A.D., 1985. Architectural-element analysis: a new method of facies analysis applied to fluvial deposits. Earth Science Review, 22: 261-308.

Miall, A.D., 1996. The Geology of Fluvial Deposits. Springer - Verlag Berlin Heidelberg, 582 pp.

Miller, K.G., Kominz, M.A., Browning, J.V., Wright, J.D., Mountain, G.S., Katz, M.E., Sugarman, P.J., Cramer, B.S., Christie-Blick, N. and Pekar, S.F., 2005. The Phanerozoic Record of Global Sea-Level Change. Science, 310(5752): 1293-1298.

Molinaro, M., Leturmy, P., Guezou, J.-C., Frizon de Lamotte, D. and Eshraghi, S.A., 2005. The structure and kinematics of the southeastern Zagros fold-thrust belt, Iran: From thin-skinned to thick-skinned tectonics. Tectonics, 24(TC3007): doi:10.1029/2004TC001633.

Monod, O., 1977. Récherches géologique dans les Taurus occidental au sud de Beyşehir (Turique). PhD Thesis, Université de Paris-Sud, Orsay, France.

Monod, O. and Akay, E., 1984. Evidence for a Late Triassic - Early Jurassic orogenic event in the Taurides. In Dixon, J. E. & Robertson A. H. F. (eds) The Geological Evolution of the Eastern Mediterranean. Geological Society, London, Special Publication, 17: 113-122.

Morley, C.K., 1988. Out of Sequence Thrusts. Tectonics, 7: 539-561.

Mossman, D.J., Gauthier-Lafaye, F. and Jackson, S.E., 2005. Black shales, organic matter, ore genesis and hydrocarbon generation in the Paleoproterozoic Franceville Series, Gabon. Precambrian research, 137(3-4): 253-272.

Mouthereau, F., Lacombe, O., Bellahsen, N., Tensi, J., Dissez, L., De Boisgrollier, T., Navabpour, P., Kargar, S. and Khadivi, S., 2007. Style, sequence and mechanisms of deformation in the Zagros Folded Belt (Fars Area). Middle East Basins Evolution Programme, Abstract Volume, Paris Meeting, December 2007.

MTA, 2002. General Directorate of Mineral Research and Exploration - Geological Map of Turkey 1:500,000, Ankara.

Muttoni, G., Kent, D.V., Garzanti, E., Brack, P., Abrahamsen, N. and Gaetani, M., 2003. Early Permian Pangea `B' to Late Permian Pangea `A'. Earth and Planetary Science Letters, 215(3-4): 379-394.

Okay, A.I., Satır, M. and Siebel, W., 2006. Pre-Alpide Palaeozoic and Mesozoic orogenic events in the Eastern Mediterranean region. From: Gee, D.G. & Stephenson, R.A. (eds) European Lithosphere Dynamics. Geological Society, London, Memoirs, 32: 389-405.

Önder, F., 1984. Some concepts on the stratigrpahical and environmental investigation on the Triassic rocks of Central Taurus Mountains. In Tekeli, O. and Göncüoğlu, M. C. (eds) Geology of the Taurus belt, MTA, Ankara: 91-99.

Özcan, A., Göncüoğlu, M.C., Turan, N., Uysal, Ş., Şentürk, K. and Işık, A., 1988. Late Paleozoic evolution of the Kütahya-Bolkardağ belt. Middle East Technical University (METU) Journal of Pure and Applied Sciences, 21(1-3): 211-220.

Özgül, N., 1976. Some geological aspects of the Taurus orogenic belt (Turkey). Bulletin of the Geological Society of Turkey, 19: 65-78.

Özgül, N., 1983. Geology of the Central Taurus: field guide book. International Symposium on the Geology of the Taurus belt, 26-29 September 1983, Ankara, Turkey.

Özgül, N., 1984. Stratigraphy and tectonic evolution of the Central Taurides. In Tekeli, O. and Göncüoğlu, M. C. (eds) Proceedings of the International Symposium on the Geology of the Taurus belt, MTA, Ankara: 77-90.

Özgül, N., 1997. Bozkir Hadim Taşkent Dolayinda yer alan tektono-stratigraphic briliklerin Stratigrafisi, (translated into English by Fatih Karaoğlan, Çukurova Universitesi). MTA Dergisi, 119: 113-174.

Park, R.G., 1988. Geological structures and moving plates. Chapman & Hall, London.

Parlak, O., 2000. Geochemistry and significance of dyke swarms in the Pozanti–Karsanti ophiolite (Southern Turkey). Turkish Journal of Earth Sciences, 24: 29-38.

Parlak, O., Höck, V. and Delaloye, M., 2000. Suprasubduction zone origin of the Pozanti–Karsanti ophiolite (southern Turkey) deduced from whole-rock and mineral chemistry of the gabbroic cumulates. In Bozkurt, E., Winchester, J. A. & Piper, J. D. A. (eds) Tectonics and Magmatism in Turkey and the Surrounding Area. Geological Society, London, Special Publication.

Parlak, O. and Robertson, A.H.F., 2004. The ophiolite-related Mersin Melange, southern Turkey: its role in the tectonic–sedimentary setting of Tethys in the Eastern Mediterranean region. Geological Magazine, 141(3): 257–286.

Pearce, J.A., 1982. Trace element characteristic of lavas from destructive plate boundaries. . In: Thorpe, R. S. (ed.) Andesites. Wiley, Chichester: 525-548.

Pearce, J.A., Lippard, S.J. and Roberts, S., 1984. Characteristics and tectonic significance of supra-subduction zone ophiolites. In: Kokelaar, B.P. & Howells, M. F. (eds) Marginal Basin Geology. Geological Society, Special Publication, 16: 77-94.

Pearce, J.A. and Norry, M.J., 1979. Petrogenetic implications of Ti, Zr, Y and Nb variations in volcanic rocks. . Contributions to Mineralogy and Petrology, 69(33-47).

Pemberton, S.G. and Frey, R.W., 1982. Trace fossil nomenclature and the Planolites-Palaeophycus dilemma. Journal of Paleontology, 56(4): 843-881.

Pickett, E., 1994. Tectonic evolution of the Palaeotethys ocean in NW Turkey. PhD Thesis, University of Edinburgh UK.

Polat, A. and Casey, J.F., 1995. A structural record of the emplacement of the Pozanti-Karsanti ophiolite onto the Menderes-Tauride block in the Late Cretaceous, eastern Taurides, Turkey. Journal of Structural Geology, 17: 1673-1688.

Ramos, A., Sopena, A. and Perez-Arlucea, M., 1986. Evolution of Buntsandstein fluvial sedimentation in the northwest Iberian Ranges (Central Spain). Journal of Sedimentary Petrology, 56: 862-875.

Reading, H.G., 1986. Sedimentary Environments and Facies. Blackwell Scientific Publications, Oxford, 615 pp.

Ricou, L.E., 1996. The plate tectonic history of the past Tethys ocean. In Nairn, A. E. M., Ricou, L. E., Vreilynck, B. and Dercourt, J. (eds) The Ocean Basins and Margins, 8, The Tethys Ocean. Plenum, New York, 3-62.

Robertson, A.H.F., 1987. Late Cretaceous chemical sediments related to a carbonate platform foreland basin transition in the Oman mountains. Sedimentary Geology, 57(1-15).

Robertson, A.H.F., 1991. Origin and emplacement of an inferred Late Jurassic subduction-accretion complex, Euboea, eastern Greece. Geological Magazine, 128: 27-41.

Robertson, A.H.F., 1993. Mesozoic-Tertiary sedimentary and tectonic evolution of Neotethyan carbonate platforms, margins and small ocean basins in the Antalya complex, S. W. Turkey. In Frostick, L. E., and Steel, R. (eds), Special Publication International Association of Sedimentologists, 20: 415-465.

Robertson, A.H.F., 1994. Role of the tectonic facies concept in orogenic analysis and its application to Tethys in the Eastern Mediterranean region. Earth-Science Reviews, 37: 139-213.

Robertson, A.H.F., 2004. Development of concepts concerning the genesis and emplacement of Tethyan ophiolites in the Eastern Mediterranean and Oman regions. Earth Science Reviews, 6: 331-387.

Robertson, A.H.F., 2006a. Contrasting modes of ophiolite emplacement in the Eastern Mediterranean region. In Gee, D. G. & Stephenson, R. A. (eds) 2006. European Lithosphere Dynamics. Geological Society, London, Memoirs,, 32: 233-259.

Robertson, A.H.F., 2006b. Sedimentary evidence from the south Mediterranean region (Sicily, Crete, Peloponnese, Evia) used to test alternative models for the regional tectonic setting of Tethys during Late Palaeozoic - Early Mesozoic time. In: Robertson, A.H.F. & Mountrakis, D. (eds) 2006. Tectonic development of the Eastern Mediterranean region. Geological Society, London, Special Publications, 260: 91-154.

Robertson, A.H.F., 2007. Overview of tectonic settings related to the rifting and opening of Mesozoic ocean basins in the Eastern Tethys: Oman, Himalayas and Eastern Mediterranean regions. In Karner, G. D., Manatschal, G., and Pinheiro, L. M. (eds) Imaging, Mapping and Modelling Continental Lithosphere Extension and Breakup. Geological Society, London, Special Publication, 282: 325-388.

Robertson, A.H.F. and Bamakhalif, K.A.S., 2001. Late Oligocene-early Miocene rifting of the northeastern Gulf of Aden: basin evolution in Dhofar (southern Oman). In: Ziegler, P. A., Cavazza, W., Robertson, A. H. F., and Crasquin-Soleau, S. (eds). Peri-Tethys Memoir 6: Peri-Tethyan Rift / Wrench Basins and Passive margins, Mémoirs du Muséum national d'Histoire naturelle (186): 641-670.

Robertson, A.H.F., Clift, P.D., Degnan, P.J. and Jones, G., 1991. Palaeogeographic and Palaeotectonic evolution of the Eastern Mediterranean Neotethys. Palaeogeography, Palaeoclimatology, Palaeoecology, 87: 289-343.

Robertson, A.H.F. and Dixon, J.E., 1984. Introduction: aspects of the geological evolution of the Eastern Mediterranean. In Dixon, J. E. & Robertson A. H. F. (eds) The Geological Evolution of the Eastern Mediterranean. Geological Society, London, Special Publication, 17: 1-74.

Robertson, A.H.F. and Mountrakis, D., 2006. Tectonic development of the Eastern Mediterranean region: an introduction. In: Robertson, A.H.F. & Mountrakis, D.

(eds) 2006. Tectonic development of the Eastern Mediterranean region. Geological Society, London, Special Publications, 260: 539-556.

Robertson, A.H.F. and Pickett, E.A., 2000. Palaeozoic-Early Tertiary Tethyan evolution of melanges, rift and passive margin units in the Karaburun Peninsula (western Turkey) and Chios Island (Greece). In Bozkurt, E., Winchester, J. A. & Piper, J. D. A. (eds) Tectonics and Magmatism in Turkey and the Surrounding Area. Geological Society, London, Special Publication, 173: 43-82.

Robertson, A.H.F. and Ustaömer, T., submitted. Role of Carboniferous subduction-accretion in tectonic development of the Konya Complex and related units in central and southern Turkey. Submitted, 2008.

Robertson, A.H.F., Ustaömer, T. and Mackintosh, P.W., 2007. Sedimentary evidence for the tectonic development of the Konya complex, central Turkey. *in prep.*

Robertson, A.H.F., Ustaömer, T., Pickett, E.A., Collins, A.S., Andrew, T. and Dixon, J.E., 2004. Testing models of Late Palaeozoic - Early Mesozoic orogeny in Western Turkey: support for an evolving open-Tethys model. Journal of the Geological Society, London, 161: 501-511.

Rollinson, H., 1993. Using geochemical data: evaluation, presentation, interpretation. Longman Publishing Group, UK.

Romano, S.S., Brix, M.R., Dorr, W., Fiala, J., Krenn, E. and Zulauf, G., 2006. The Carboniferous to Jurassic evolution of the pre-Alpine basement of Crete: constraints from U-Pb abd U-(Th)-Pb dating of orthogneiss, fission-track dating of zircon, structural and petrological data. In: Robertson, A.H.F. and Mountrakis, D. (Eds.), Tectonic Development of the Eastern Mediterranean Region. Geol.Soc. Special Publication, 260: 69-90.

Scasso, R.A. and Castro, L.N., 1999. Cenozoic phosphatic deposits in North Patagonia, Argentina: Phosphogenesis, sequence-stratigraphy and paleoceanography. Journal of South American Earth Sciences, 12(5): 471-487.

Schmidt, S., Jouanneau, J.-M., Weber, O., Lecroart, P., Radakovitch, O., Gilbert, F. and Jézéquel, D., 2007. Sedimentary processes in the Thau Lagoon (France): From seasonal to century time scales. Estuarine, Coastal and Shelf Science, 72: 534-542.

Scotese, C.R., Boucot, A.J. and McKerrow, W.S., 1999. Gondwanan palaeogeography and palaeoclimatology. Journal of African Earth Sciences, 28(99-114).

Searle, M.P., Corfield, R.I., Stephenson, B. and McCarron, J., 1997. Structure of the North Indian continental margin in the Ladakh-Zanskar Himalayas: implications for the timing of obduction of the Spontang Ophiolite, India-Asia collision and deformation events in the Himalaya. Geological Magazine, 134(3): 297-316.

Searle, M.P. and Cox, J., 1999. Tectonic setting, origin, and obduction of the Oman Ophiolite. Geol Soc Am Bull, 111(1): 104-122.

Sellwood, B.W., 1986. Shallow-marine Carbonate Environments. In: Reading, H. G. (editor). Sedimentary Environments and Facies: 283-342.

Şengör, A.M.C., Gorur, N. and Sungurlu, O., 1984. Tectonics of the Mediterranean Cimmerides: nature and evolution of the western termination of Palaeotethys. In Dixon, J. E. & Robertson A. H. F. (eds) The Geological Evolution of the Eastern Mediterranean. Geological Society, London, Special Publication, 17: 77-112.

Şengör, A.M.C. and Yılmaz, Y., 1981. Tethyan Evolution of Turkey: A plate tectonic approach. Tectonophysics, 75: 181-241.

Soper, N.J. and Barber, A.J., 1982. A model for the deep structure of the Moine thrust zone. Journal of the Geological Society, London, 139: 127-138.

Stampfli, G. and Kozur, H., 2006. Europe from the Variscan to the Alpine cycles. In: Gee, D.G., Stepherson, R.A. 2006. European Lithosphere Dynamics, Geological Society, London, Memoir, 32: 43-56.

Stampfli, G.M., 2000. Tethyan oceans. In Bozkurt, E., Winchester, J. A. & Piper, J. D. A. (eds) Tectonics and Magmatism in Turkey and the Surrounding Area. Geological Society, London, Special Publication, 173: 1-23.

Stampfli, G.M. and Borel, G.D., 2002. A plate tectonic model for the Paleozoic and Mesozoic constrained by dynamic plate boundaries and restored synthetic oceanic isochrons. Earth and Planetary Science Letters, 196: 17-33.

Stampfli, G.M., Mosar, J., Favre, P., Pellevuit, A. and Vannay, J.-C., 2001. Permo-Mesozoic evolution of the western Tethys realm: the Neo-Tethys East Mediterranean Basin connection. In Ziegler, P., Cavazza, W., Robertson, A.H.F., & Crasquin-Soleau, A. (eds) Peri-Tethyan Rift/Wrench Basins and Passive Margins. Peri-Tethys Memoire, 5: 51-108.

Tamura, T. and Masuda, F., 2003. Shallow-marine fan delta slope deposits with large-scale cross-stratification: the Plio-Pleistocene Zaimokuzawa formation in the Ishikari Hills, northern Japan. Sedimentary Geology, 158(3): 195-207.

Tekeli, O., Aksay, A., Ürgün, B.M. and Işik, A., 1984. Geology of the Aladağ Mountains. In Tekeli, O. and Göncüoglu, M. C. (eds) Proceedings of the International Symposium on the Geology of the Taurus belt, MTA, Ankara.

Tekin, U.K., 1999. Biostratigraphy and Systematics of Late Middle to Late Triassic Radiolarians from the Taurus Mountains and Ankara Region, Turkey. Geologisch-Palaeontologische Mitteilungen Innsbruck, 5: 1-296.

Tekin, U.K., Göncüoğlu, M.C. and Turhan, N., 2002. First evidence of Late Carnian radiolarians from the Izmir–Ankara suture complex, central Sakarya, Turkey: implications for the opening age of the Izmir–Ankara branch of Neo-Tethys. Geobios, 35: 127-135.

Tomašových, A., 2004. Microfacies and depositional environment of an Upper Triassic intra-platform carbonate basin: the Fatric Unit of the West Carpathians (Slovakia). Facies, 50: 77-105.

Tucker, M.E., 1985. Shallow-marine carbonate facies and facies models. In Brenchley, P. J., & Williams, B. P. J. (eds) Sedimentology: Recent Developments and Applied Aspects. Geological Society, London, Special Publications., 18: 147-169.

Tucker, M.E., 1991. Sedimentary Petrology: an introduction to the origin of sedimentary rocks, second edition. Blackwell Sciences Ltd, 260 pp.

Turan, A., 2000. Structural characteristics of the area between Korualan and Bagbasi: Hadim-Konya. Dokuz Eylül Üniversitesi (Izmir) Department of Science and Engineering, 2(3): 51-65.

Twiss, R.J. and Moores, E.M., 1992. Structural Geology. W. H. Freeman and Co., New York.

Ustaömer, T. and Robertson, A.H.F., 1993. A Late Palaeozoic-Early Mesozoic marginal basin along the actives sourthern continental margin of Eurasia: Evidence from the central Pontides (Turkey) and adjacent regions. Geological Journal, 28(3-4): 219-238.

Van Steenwinkel, M., 1992. The Devonian–Carboniferous boundary: comparison between the Dinant Synclinorium and the northern border of the Rhenish State Mountains. Ann. Soc. Geol. Belg., 115: 665-671.

Warme, J.E., 1988. Jurassic carbonate facies of the central and eastern High Atlas Rift, Morocco. In: The Atlas system of Morocco: studies on its geodynamic evolution. Springer Berlin / Heidelberg.

Watchorn, F., Nichols, G.J. and Bosence, D.W.J., 1998. Rift-related sedimentation and stratigraphy, southern Yemen (Gulf of Aden). In Purser, B. H., and Bosence, D. W. J (eds) Sedimentation and Tectonics of Rift Basins: Red Sea-Gulf of Aden. Chapman & Hall, London: 165-189.

Whitney, D.L. and Dilek, Y., 1997. Core Complex development in Central Anatolia, Turkey. Geology, 25(11): 1023-1026.

Wilson, J.L., 1975. Carbonate Facies in Geologic History. Springer-Verlag, New York. , 471 pp.

Winchester, J.A. and Floyd, P.A., 1976. Geochemical magma type discrimination; application to altered and metamorphosed basic igneous rocks. Earth and Planetary Science Letters, 28: 459-469.

Wippern, J., 1962. Die Bauxite der Taurus und ihre tektonische Stellung. Bulletin of Mineral Resources Exploration (Turkey), 62: 74-82.

Woodcock, N.H. and Robertson, A.H.F., 1981. Wrench and thrust tectonics along a Mesozoic–Cenozoic continental margin: Antalya Complex, SW Turkey. Journal of the Geological Society, London, 139(2): 147-163.

Wright, V.P. and Vanstone, S.D., 2001. Onset of Late Palaeozoic glacio-eustasy and the evolving climates of low latitude areas: a synthesis of current understanding. Journal of the Geological Society, 158(4): 579-582.

Xypolias, P., Dörr, W. and Zulauf, G., 2006. Late Carboniferous plutonism within the pre-Alpine basement of the External Hellenides (Kithira, Greece): evidence from U–Pb zircon dating. Journal of the Geological Society, London, 163(3): 539-547.

Yilmaz, Y., Tüysüz, O., Yiğitbas, E., Gen, S.C. and Şengör, A.M.C., 1997. Geology and tectonic evolution of the Pontides. In: Robinson, A. G. (ed) Regional and Petroleum Geology of the Black Sea and Surrounding Region. American Association of Petroleum Geologists, Memoirs, 68(183-226).

Zanchi, A., Balini, M., Berra, F., Garzanti, E., Mattei, M., Muttoni, G., Zanchetta, S., Nicora, A., Bollati, I. and Mossavari, F., 2007. The Cimmerian evolution of the Nakhlak-Anarak area (Central Iran) and its bearing for the reconstruction of the history of the Eurasian margin. Geophysical Research Abstracts, Vol. 9, European Geosciences Union, Vienna 2007.

Zanchi, A., Berra, F., Mattei, M., Zanchetta, S., Nawab, A. and Sabouri, J., 2005. The Early Mesozoic Cimmerian orogeny in the Alborz mountains, Iran. Geophysical Research Abstracts, Vol. 7, European Geosciences Union, Vienna 2005.

Zanchi, A., Garzanti, E., Larghi, C., Angiolini, L. and Gaetani, M., 2003. The Variscan orogeny in Chios (Greece): Carboniferous accretion along a Palaeotethyan active margin. Terra Nova, 15(3): 213-223.

Ziegler, A.M., Hulver, M.L. and Rowley, D.B., 1997. Permian world topography and climate. In Martini, I.P., ed., Late glacial and postglacial environmental changes: Quaternary, Carboniferous–Permian, and Proterozoic. Oxford, Oxford University Press: 111-146.

Appendix A

Structural and sedimentary evidence from the northern margin of the Tauride platform: testing models of Late Triassic “Cimmerian” uplift and deformation in southern Turkey.

This is the first draft of a complete manuscript that has been jointly written for publication by myself and Alastair Robertson for a special edition of *Tectonophysics* on ‘The tectonic evolution of Tethys in the eastern Mediterranean region’ (Robertson, A. H. F., Parlak, O., Koller, F. (eds.), 2008). At the time of completion of this thesis, the manuscript was under review and it is likely that the final publication will be significantly edited. The paper addresses the issue of Late Triassic “Cimmerian” uplift of the Tauride platform. New structural and sedimentary evidence, presented elsewhere in this thesis, is used to test alternative models of the Late Triassic tectonic setting of the Tauride platform.

Appendix A

Alternative models of the Late Triassic tectonic setting

A critical issue in the reconstruction of the Tethys ocean is the nature and significance of a supposed latest Triassic “Cimmerian” tectonic event. Apparent evidence for this is recorded in the tectonic-sedimentary evolution of the Tauride platform. It is generally accepted that the relatively autochthonous Tauride platform and associated thrust sheets restore as a north-facing passive margin, at least during Jurassic–Cretaceous time (Şengör and Yılmaz, 1981; Robertson and Dixon, 1984; Stampfli et al., 2001; Andrew and Robertson, 2002; Robertson et al., 2004; Okay et al., 2006). However, the Triassic and earlier tectonic setting of these Tauride units is contentious. Three contrasting tectonic models involve Permian–Triassic closure of a Palaeozoic Tethys, followed by opening of a Mesozoic Tethys.

In a first model (Stampfli, 2000; Stampfli et al., 2001; Stampfli and Borel, 2002), following Late Permian – Early Triassic rifting of a Cimmerian block, the Tauride platform and the Anatolide block collided in latest Triassic time during a regional “Cimmerian” orogeny. This resulted in the development of a foreland basin on Tauride crust and over-thrusting of the Anatolide block, associated with thrusting and folding. Palaeotethys closed by the latest Triassic, resulting in a suture zone between the Tauride and Anatolide terranes (Fig. 1a, Fig. 2a).

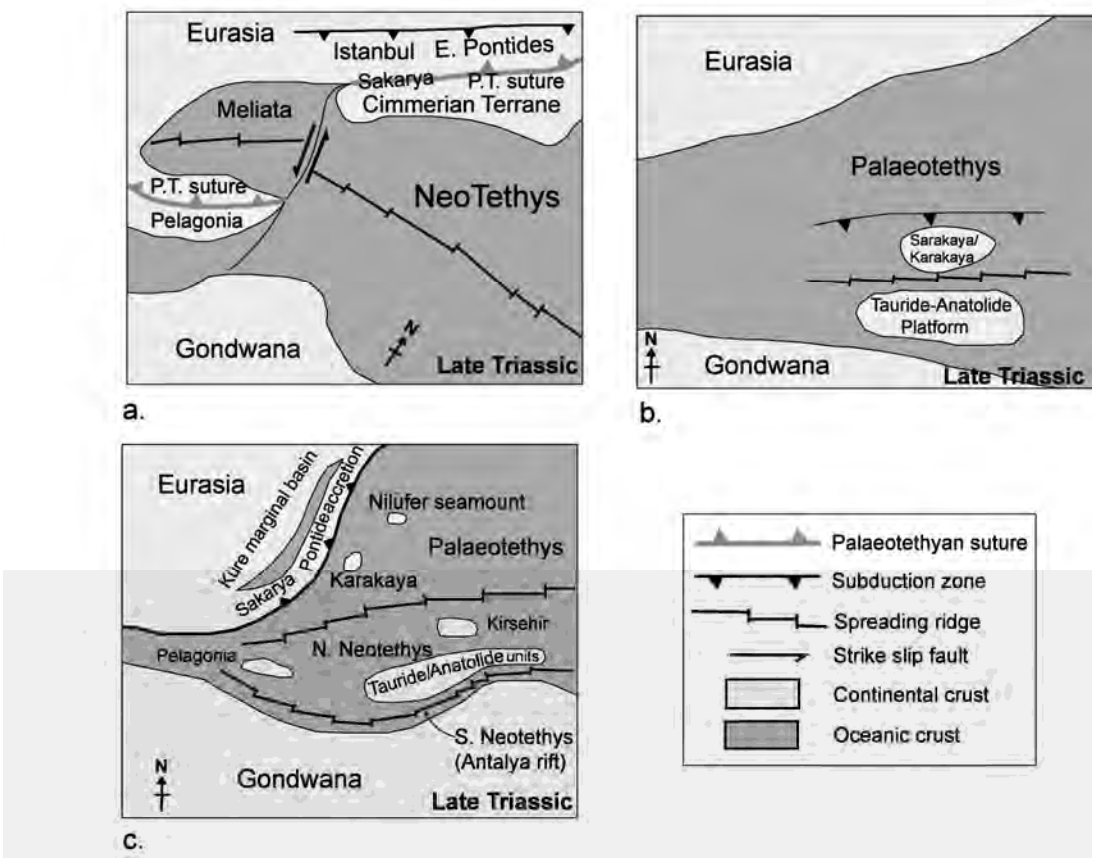

Fig. 1. Schematic tectonic models of Late Triassic Tethys, showing the relative locations of the Tauride and Anatolide units. a. Model 1, based on Stampfli (2000). b. Model 2, based on Göncüoğlu et al. (2003). c. Model 3, based on Robertson et al. (2004).

In a second model (Göncüoğlu et al., 2003), following Late Palaeozoic inferred southward subduction beneath Gondwana, a combined Tauride–Anatolide platform and Palaeozoic continental arc terrane (Sakarya terrane) was bordered to the north by a Palaeozoic Tethys during the late Permian. During the Early Triassic, Palaeotethys continued to subduct southwards, initiating opening of a back-arc basin and rift-related uplift of the northern part of the Tauride–Anatolide platform. Continentally derived clastics were deposited on the Tauride platform during this Early Triassic phase of rifting. Rifting continued, and by the Late Triassic (Fig. 1b, Fig. 2b) the Taurides–Anatolides were completely separated from the Sakarya terrane by a northerly strand of the Neo-Tethys (Izmir-Ankara ocean). Platform carbonates were deposited on the Tauride–Anatolide platform during Late Triassic–Cretaceous time.

In a third model (Robertson et al., 2004) a combined Tauride–Anatolide platform was separated from Gondwana by a small oceanic basin to the south during the Triassic (Southern Neo-Tethys). Further north, continental fragments drifted across Palaeotethys (e.g. Çal unit of the Karakaya complex) until they collided with the Eurasian active margin prior to latest Triassic. The Taurides-Anatolide unit, however, remained in a southerly location and experienced a rift-related Triassic evolution. Uplift is inferred to have resulted from stress transmission through the northerly oceanic crust, from the Late Triassic “Cimmerian” collision along the Eurasian margin; this possibly resulted in reversal of normal faults and inversion during the Late Triassic (Fig. 1d, Fig. 2c). Alternatively, a pulse of rift-related flexural uplift could have caused clastic sedimentation during the latest Triassic (Fig. 2d).

The main differences between these three models concern the origin of the “Anatolide platform” (Gondwanian or Eurasian); the polarity of subduction during the Triassic, and whether collision and suturing of separate Tauride and Anatolide continental blocks took place during the latest Triassic.

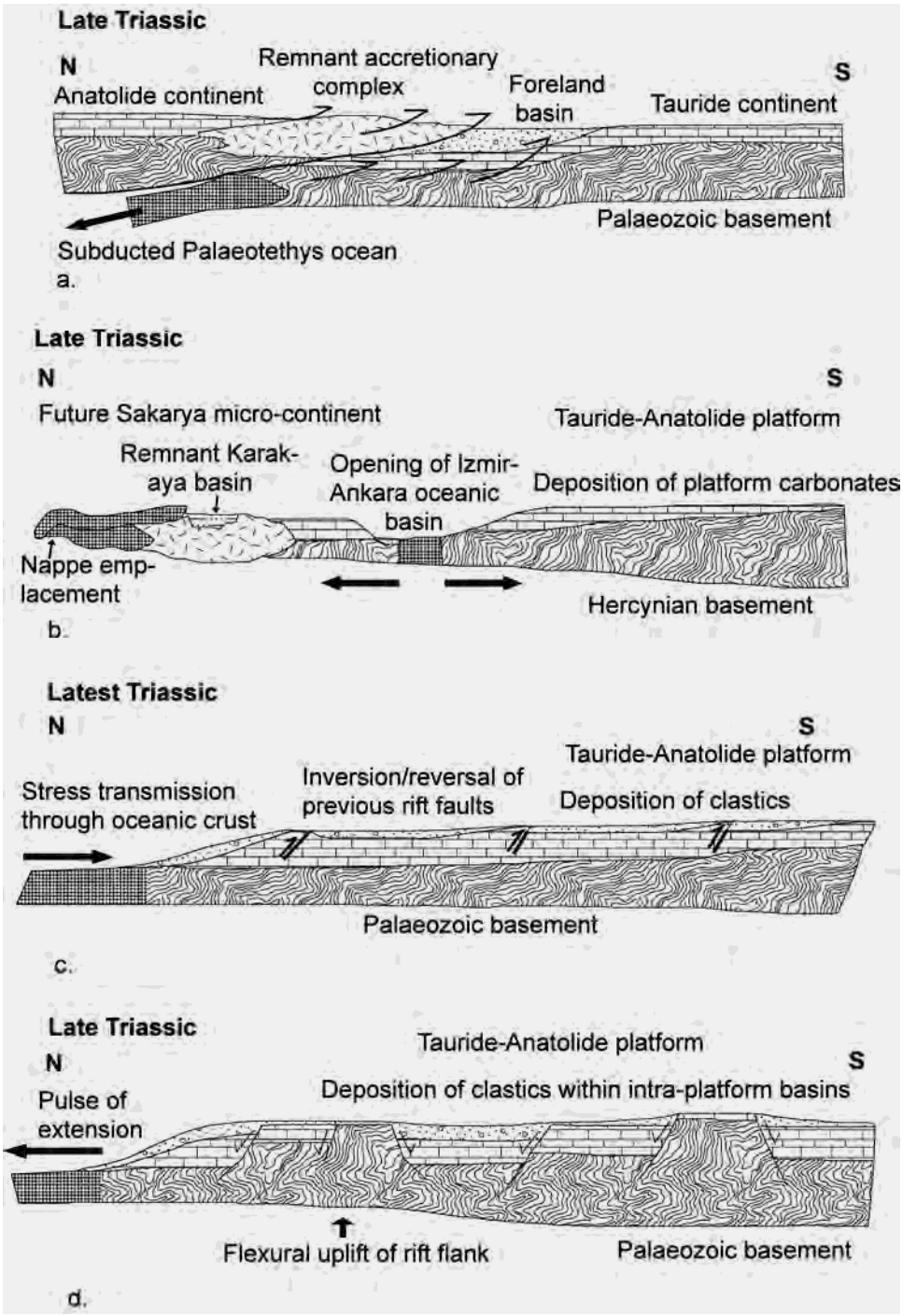

Fig. 2. Alternative models of Late Triassic uplift of the Tauride platform. a. After Stampfli & Borel, 2002. b. After Göncüoglu et al., 2003. c. After Robertson et al., 2004. d. After Mackintosh and Robertson, 2007.

Previous work

A field-based study of the Tauride units by Monod and Akay (1984) provided apparent evidence of Late Triassic uplift and deformation of the Tauride platform. Three localities were reported to show pre-Jurassic deformation within the Tauride autochthon. The timing of this supposed thrusting was determined by dating of Jurassic limestones (Monod, 1977; Gutnic et al., 1979), combined with stratigraphic and structural relationships.

In addition, sedimentary evidence was described throughout the Tauride units that apparently supported a Late Triassic to Early Jurassic uplift event. The Çayır Formation, a distinctive succession of red clastic sediments, was identified at nine localities, extending from the Greek Island of Chios in the west, to the Bolkar Dağ in the east (Fig. 3). Dating of the Çayır Formation was determined by local stratigraphic relationships, and limited palaeontological data from some localities. The dates for the clastics ranged from latest Triassic–Middle and Upper Liassic, and when combined with the limited available structural evidence, were taken to support a latest Triassic “Cimmerian” compressional event. Recently, the existence of “Cimmerian” deformation has been questioned (Göncüoğlu et al., 2003; Okay et al., 2006) but without presenting new evidence. New sedimentary and structural data are presented here that support an extensional rift-related setting (Fig. 2d) for the Taurides throughout Triassic time, and preclude any need for a latest Triassic regional compressional event.

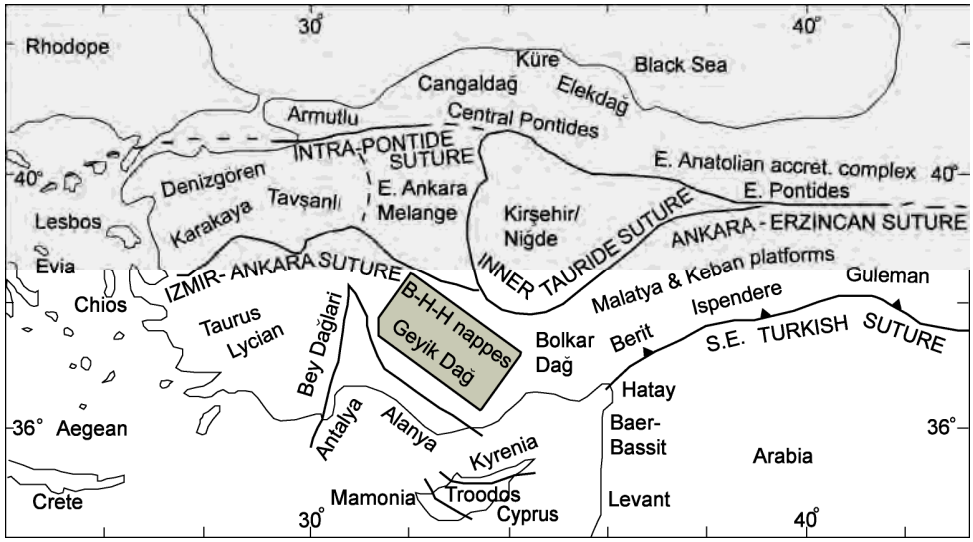

Fig. 3. The main tectonic zones in the Eastern Mediterranean region, with the study area in the Central Taurides highlighted (shaded box). 'B-H-H' stands for 'Beyşehir-Hoyran-Hadim'. Modified from Robertson et al. (2006).

Regional Geology

We have conducted extensive fieldwork within the central Taurides between the towns of Beyşehir in the north-west and Hadim in the south-east (Fig. 5.12). The relatively autochthonous Tauride platform, the Geyik Dağ, is tectonically overlain by the Beyşehir-Hoyran-Hadim nappes (Blumenthal, 1947; Monod, 1977; Özgül, 1984; Andrew and Robertson, 2002). The nappes consist of platform, marginal and deep-marine sediments, together with ophiolitic rocks (Fig. 5). The marginal and deep oceanic units were termed the Beyşehir nappes in the north-west (Monod, 1977), whereas in the south-east they were termed the Bozkir nappes (Özgül, 1984) (Fig. 6). The Hoyran nappes refer to contrasting margin-related units further northwest in the Isparta angle (outwith the scope of this work). The Hadim nappe is a regional-scale thrust sheet of Upper Palaeozoic–Mesozoic passive margin-related sedimentary rocks that lies between the autochthonous Tauride platform (Geyik Dağ) below, and the distal margin units (Beyşehir nappes), above. In addition, the regional scale Bolkar nappe consists of Upper Palaeozoic–Mesozoic passive margin lithologies that are mainly highly deformed. Recent work showed that the autochthon and the nappe stack can be restored as a north-facing Mesozoic passive margin bordering Tethyan oceanic crust to the north (Andrew and

Robertson, 2002). This was followed by initial compression-related tectonic events during Late Cretaceous time. The Geyik Dağ restores to a southerly position within the Mesozoic platform, whereas the Hadim and Bolkar units restore further north, closer to the northern Neotethys ocean (Özgül, 1984; Andrew and Robertson, 2002; this study)

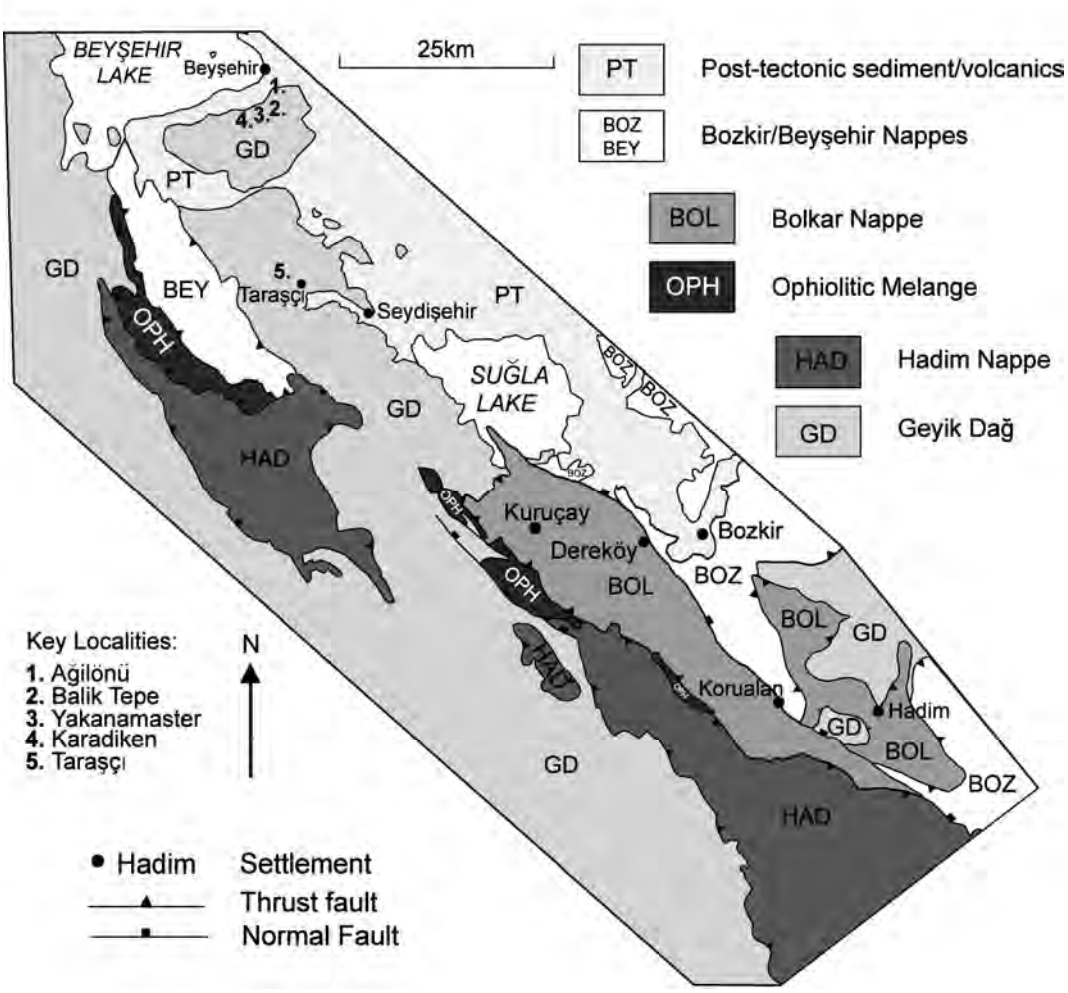

Fig. 4. Simplified structural map of the study area with key localities marked.

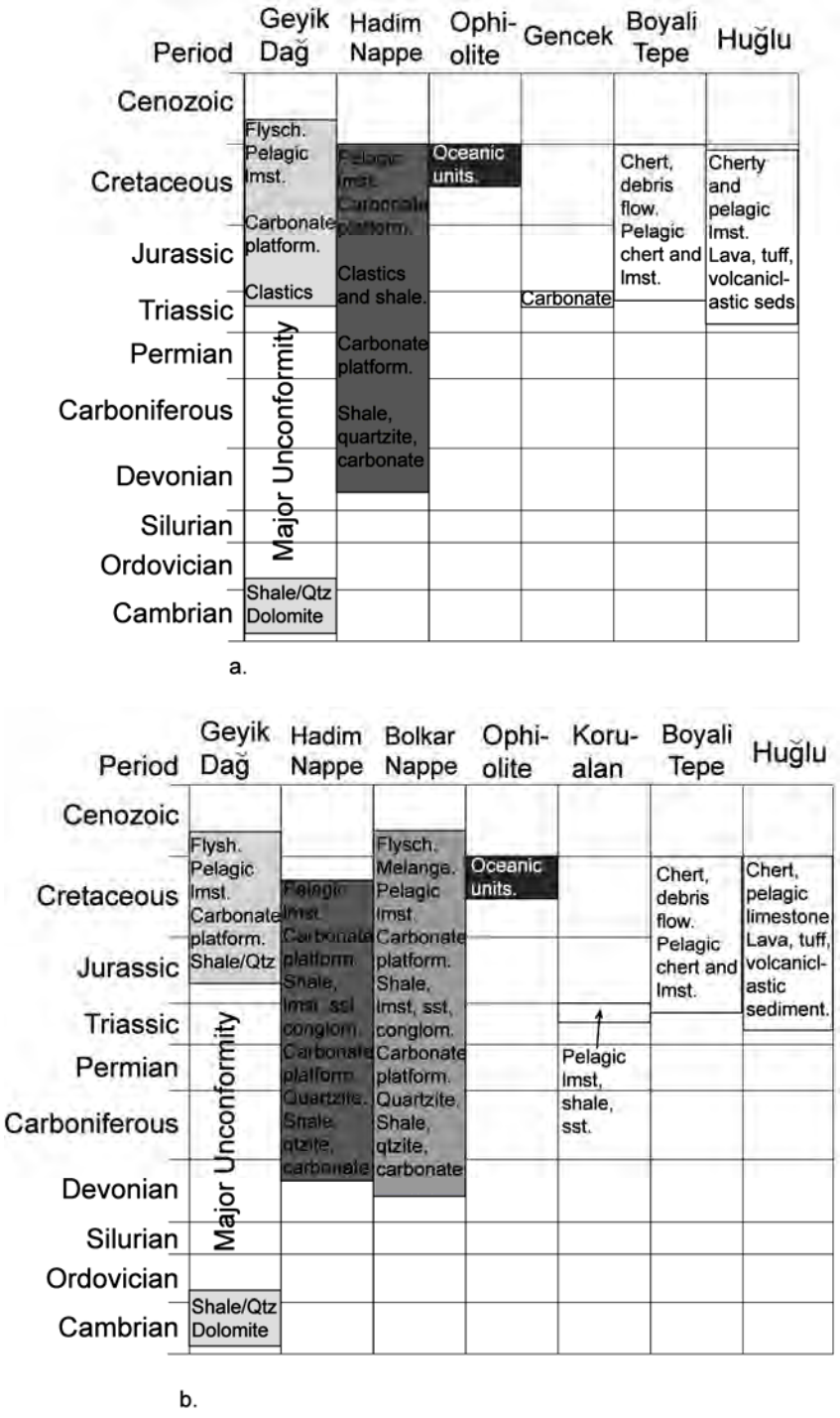

Fig. 5. Simplified representation of the tectonic units and their primary lithologies within the studied area. a. The northerly part of the mapping area (after Monod, 1977). b. The southerly part of the mapping area (after Özgül, 1984). Geological timescale based on Palmer, A. R. and Geissman, J. (1999).

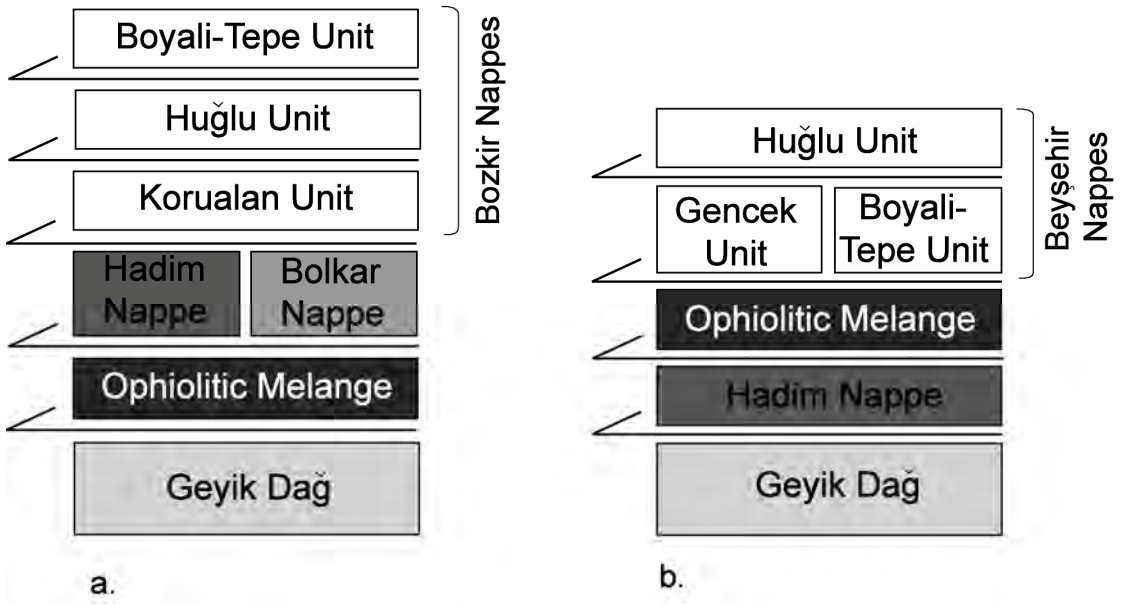

Fig. 6. Schematic representation of the nappe stacking order. a. The north-west of the study area (after Monod, 1977). b. The south-west of the study area (after Özgül, 1984).

Structural evidence

If the Tauride platform had been involved in latest Triassic "Cimmerian" collisional uplift, as in model 1 (Fig. 2a), compressional deformation would be expected in a foreland setting, now represented by the Geyik Dağ, and the Hadim and Bolkar nappes. Compression-related tectonics of Late Triassic age were in the past reported from the Central Taurides, especially near the towns of Beyşehir and Seydişehir (Monod and Akay, 1984). Several critical areas within the Central Taurides have been re-mapped in some detail.

Locality 1: Ağılönü village (Fig. 5.12, Fig. 5.13a and b), GPS reference: 388500 4167500

The village of Ağılönü lies ~3 km south-east of Beyşehir within the autochthonous Geyik Dağ unit (Fig. 5.12, Fig. 5.13a and b). The stratigraphy consists of Cambrian dolomites (Çal Tepe Formation; Monod, 1977) and Ordovician shales (Seydişehir Formation; Monod, 1977), overlain by Jurassic siliciclastics and neritic carbonates (Sarakmana Limestone; Monod, 1977; Fig. 5.13c). The Cambrian sediments are medium to thick bedded, heavily recrystallised, nodular and beige-grey in colour. Locally, the succession

dips gently towards the east (Fig. 5.13a, b, d). The dolomites are sheared and locally brecciated, especially near the contact with the overlying Ordovician sediments. Numerous low-angle faults, possibly reverse faults, cut the succession. Few sedimentary features are preserved.

Ordovician shales (Seydişehir Formation) are best exposed in a small quarry adjacent to Agilönü access road, 1 km south of Beyşehir (Fig. 5.13a). The Ordovician succession is made up of strongly sheared, foliated and folded micaceous shales, typically intercalated with thinly bedded (5-15 cm thick) quartzitic sandstones (Fig. 5.13c). The shales consist of brown and purple horizons, alternating on a 4-5 m scale. Quartzitic sandstone horizons are locally up to 1 m thick. They show evidence of brittle deformation and the formation of phacoidal blocks (up to 1.2 m in size) indicating layer-parallel extension (Fig. 5.14a). Less deformed beds retain clear sedimentary structures including flute casts, grooves and prod marks. These deposits could be turbidites, or possibly storm deposits. Trilobites found in the Seydişehir Formation elsewhere in the Taurides suggest the sedimentary setting is likely to be a continental shelf (Dean and Monod, 1990). Sedimentary structures preserved on the upper and lower surfaces of some beds indicate that parts of the succession have been overturned. The Ordovician units exhibit open parallel-folds on a 10-m scale, with axial planes trending NNW–SSE (Figs. Fig. 5.14b, Fig. 9a). The shales contain kink folds on a 5-10 cm scale.

Fold-vergence is predominantly to the west (Fig. 9b). Other deformation features in shales include normal and reverse faults with slickenside lineations (Fig. 5.14c, Fig. 9c, d), mineral lineations (Fig. 9e) interpreted as stretching lineations, and shear structures. All of the data display a dominantly NNW–SSE axial trend, implying ENE to WSW shortening when the fold vergence is taken into account.

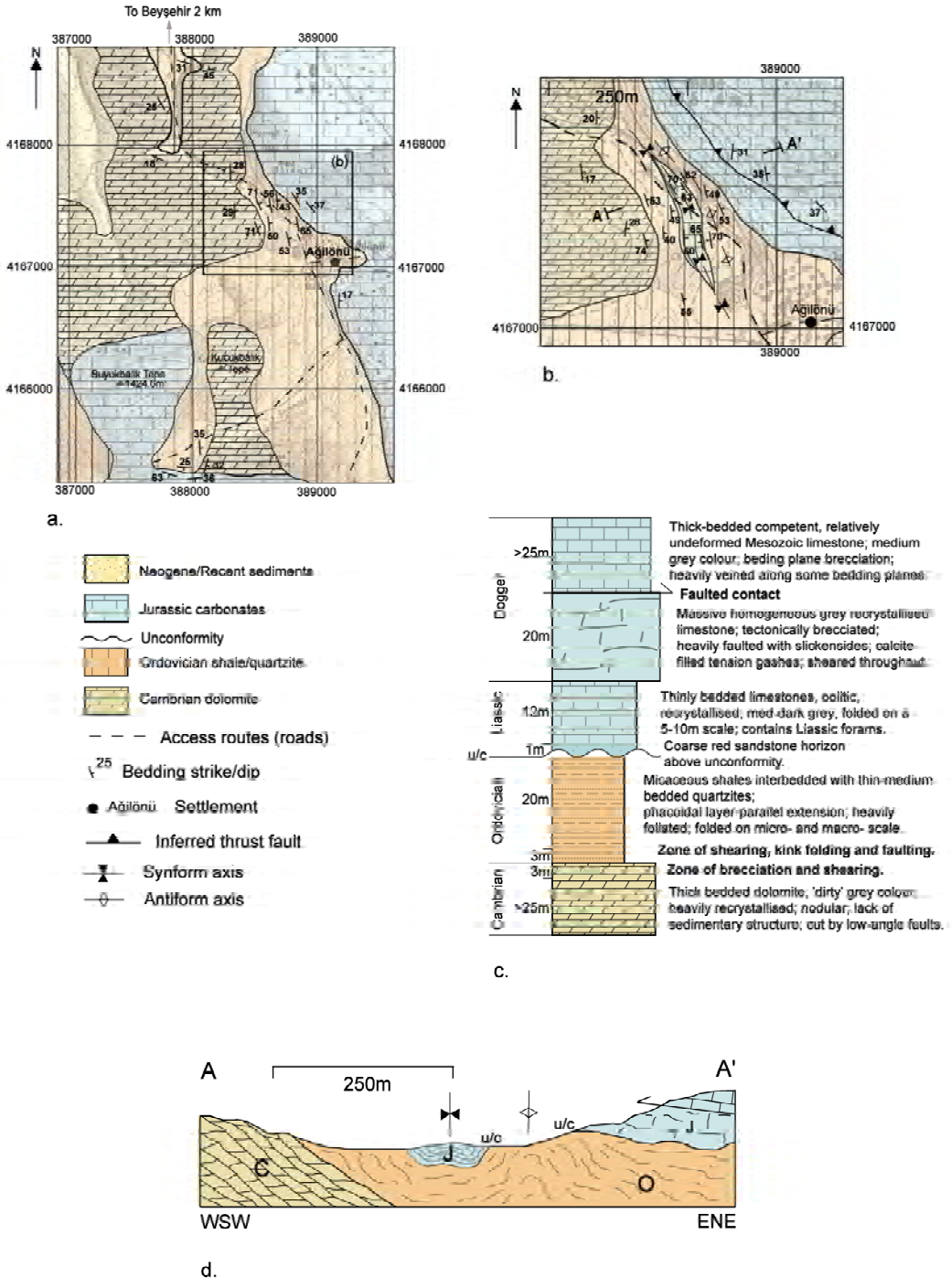

Fig. 7. a. Map of the Agilönü and Balik Tepe localities; b. Detailed map of the Agilönü locality; c. Simplified log showing stratigraphy at Agilönü; d. Cross-section A-A' through the Agilönü locality.

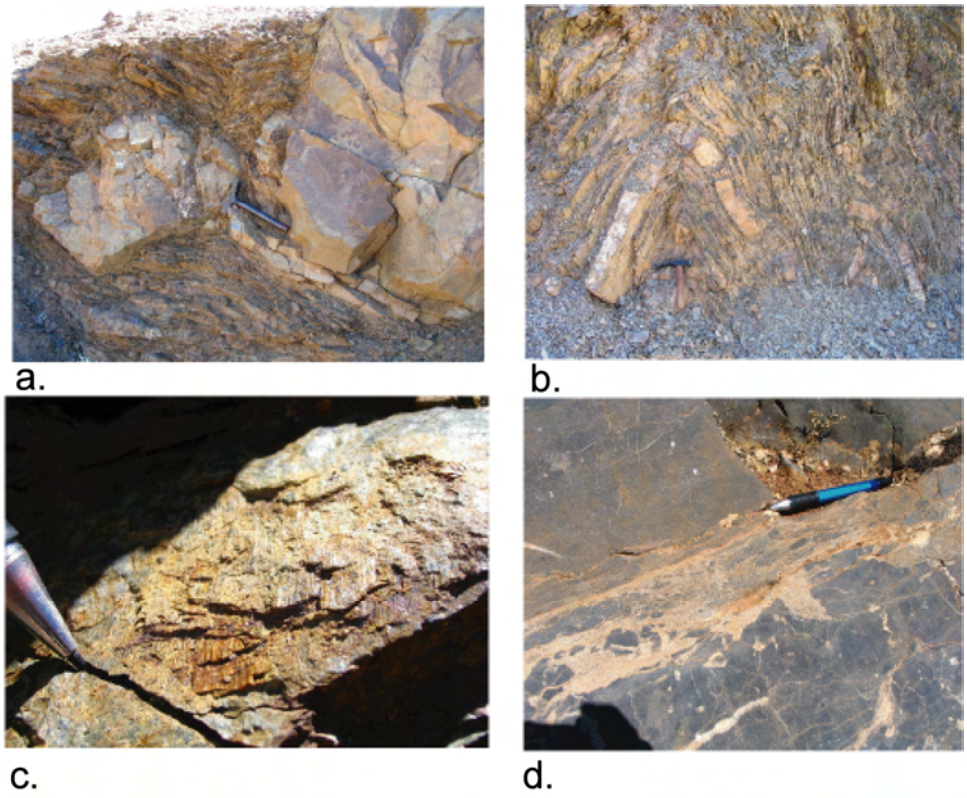

Fig. 8. a. Bedding parallel extension and formation of phacoidal sandstone blocks in Ordovician shale/quartzite succession at Agilönü locality; b. Ordovician shale/quartzites showing tight folding and deformation; c. Fault plane with slickensides within Ordovician shale/quartzites; d. Zone of tectonic brecciation within Middle Jurassic thick-bedded carbonates at the Agilönü locality.

The Ordovician sequence is locally tightly folded with a laterally discontinuous horizon of red quartzose sandstones and thin-bedded, recrystallised, medium-dark grey oolitic limestones (Fig. 5.13b, c). There is an abrupt change in lithology from shale-sandstone to oolitic limestone. Dating of benthic foraminifera (*Siphovalvulina variabilis* Septfontaine*, Amijiella amiji* [Henson], *Valvulina.* sp., *Thaumatoporella* parvovesiculifera [Raineri]) within the oolitic limestones indicates a Middle Liassic age, and confirms that a major unconformity exists between the Ordovician and Jurassic successions, as in the Beyşehir - Seydişehir area generally (Monod, 1977). The uppermost part of the succession at this Agilönü locality is thick-bedded to massive, competent Mesozoic carbonate (Fig. 5.13c). The base of these carbonates (Sarakmana Limestone) was dated as “Lower Dogger” (Monod, 1977) and the succession as a

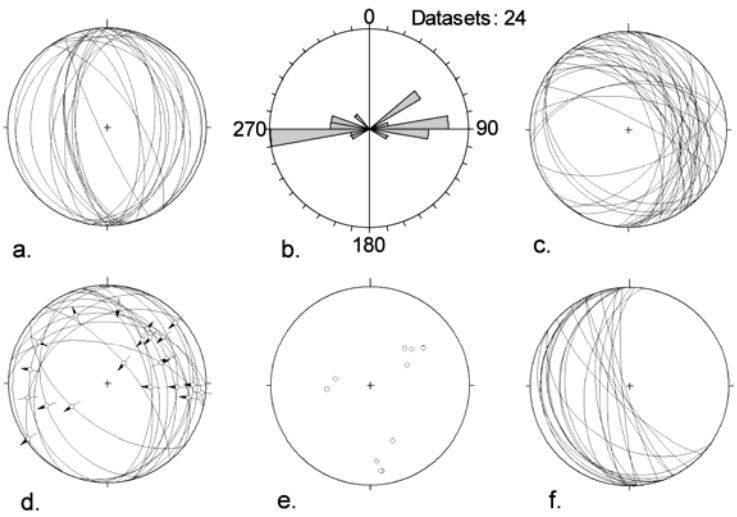

Fig. 9. Structural data from the Agilönü locality. a. Ordovician fold axial planes; b. Ordovician fold vergence direction; c. Ordovician fault planes; d. Ordovician fault planes with slickenlines; e. Ordovician mineral lineations; f. Middle Jurassic tension gash orientations.

whole was thought to be Jurassic (Monod and Akay, 1984). These units are in the topographically and structurally highest position within the mapping area (Fig. 5.13d). The lowermost carbonate beds have an irregular deformed contact with the underlying Ordovician sediments, above which the limestones are homogeneous. These are medium grey and heavily recrystallised, with few recognisable primary sedimentary features. Even bedding is barely recognisable in places. The limestones show strong structural deformation, including fault planes, bedding-parallel foliation, shear planes with associated small-scale folds, calcite-filled tension gashes (Fig. 9f), intense veining, bedding-parallel tectonic brecciation (Fig. 5.14d) and a weak boudinage.

Monod and Akay (1984) inferred that the Cambrian dolomites were thrust over the Ordovician shale/quartzite succession prior to the Jurassic, followed by erosion and transgression of the Jurassic Sarakmana Limestones. This would necessitate pre-Jurassic compression. However, the evidence can be interpreted differently.

Sedimentary structures within the Ordovician shale/quartzite succession show that the Cambro-Ordovician sequence has been tectonically inverted (overturned) in some places, whereas it remains the right way up in others (Fig. 5.13a, b, d). This is comparable with

the relationships observed at Çal Tepe, near the town of Seydişehir (Monod, 1977) (Fig. 5.15).

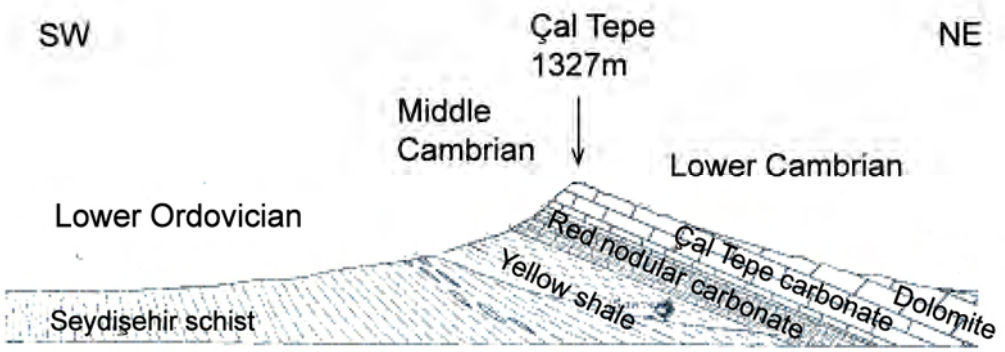

Fig. 10. Sketch showing the stratigraphic relationships at the Çal Tepe locality, near the town of Seydişehir. Reproduced from Monod, 1977.

The sharp planar nature of the contact between the Cambrian dolomite and the Ordovician shale/quartzite, together with associated tectonic brecciation and shearing adjacent to the contact, suggest that significant tectonic displacement has taken place between these two units. On the other hand, there is an absence of, for example, a basal conglomerate, or facies transition that would be expected along a stratigraphic unconformity.

The Ordovician sediments are unconformably overlain by thin-bedded Jurassic sandstones and oolitic limestones (Fig. 5.13c). Monod and Akay (1984) believed that the oldest Mesozoic rocks, of Middle Jurassic (Dogger) age, are represented by thick-bedded, to massive, units to the east of the study area (Fig. 5.13a–c). However, within the area mapped (Fig. 5.13a, b), limestones were found during this study to contain the Foraminifera *Siphovalvulina variabilis* Septfontaine*, Amijiella amiji* (Henson), *Valvulina.* sp., and *Thaumatoporella parvovesiculifera* (Raineri) of Middle Liassic age (N. İnan and K. Tasli, pers. comm., 2006). These Liassic sediments are folded and deformed to the same extent as nearby Ordovician sequences, suggesting that this deformation is younger than Liassic. Also, the contact between the Ordovician sequence and the Sarakmana Limestones is tectonic, as noted above, and both units exhibit very similar deformation (Fig. 9a–f). The difference in competency between thick-bedded dolomites, thin-bedded

shales/limestones, and massive to thick-bedded carbonates, has resulted in a variable style of deformation.

It can be inferred that the combined Cambrian – Jurassic sequence at locality 1 (Agilönü) experienced only one deformation event in post Early-Jurassic time that was related to Upper Cretaceous – Lower Cenozoic (Alpine) nappe emplacement. The Cambrian and Middle Jurassic carbonate units are deformed by brittle imbricate thrusting, with relatively little folding. By contrast, the Ordovician and Lower Jurassic siliciclastic units were deformed in a more ductile fashion, with intense folding accommodating much of the strain.

Locality 2: Karadiken village (Fig. 5.12, Fig. 5.16a–c), GPS reference 380500 4164500

This locality, ~2 km to the south of Karadiken village (Fig. 5.12, Fig. 5.16a), exposes Ordovician shales/quartzite, unconformably overlain by Middle – Upper Triassic shales and Jurassic carbonates (Monod and Akay, 1984) (Fig. 5.16). The Ordovician sediments are similar to those at locality 1 (Agilönü), described above. Brown-weathering micaceous shales are again interbedded with thin-bedded quartzitic sandstones. The overlying Triassic sediments, identified by a deep red-purple colour, outcrop over an area 500 m² x 750 m² (Fig. 5.16a). These are dominantly shales interbedded with grey medium-grained quartzite, bioturbated grey limestone and purple sandstone. Locally, the purple colour has been leached out so that it can be difficult to distinguish Triassic and Ordovician sediments based on colour alone. However, the Ordovician is typically thinner bedded and contains no limestone. Both of these successions are heavily deformed, showing a variety of micro- and macro- scale folding and faulting, especially kink folds on a 2-10 cm scale. Fold axial planes dominantly trend NNW–SSE (Fig. 12a), with fold vergence towards the WSW, NE and NW (Fig. 12b).

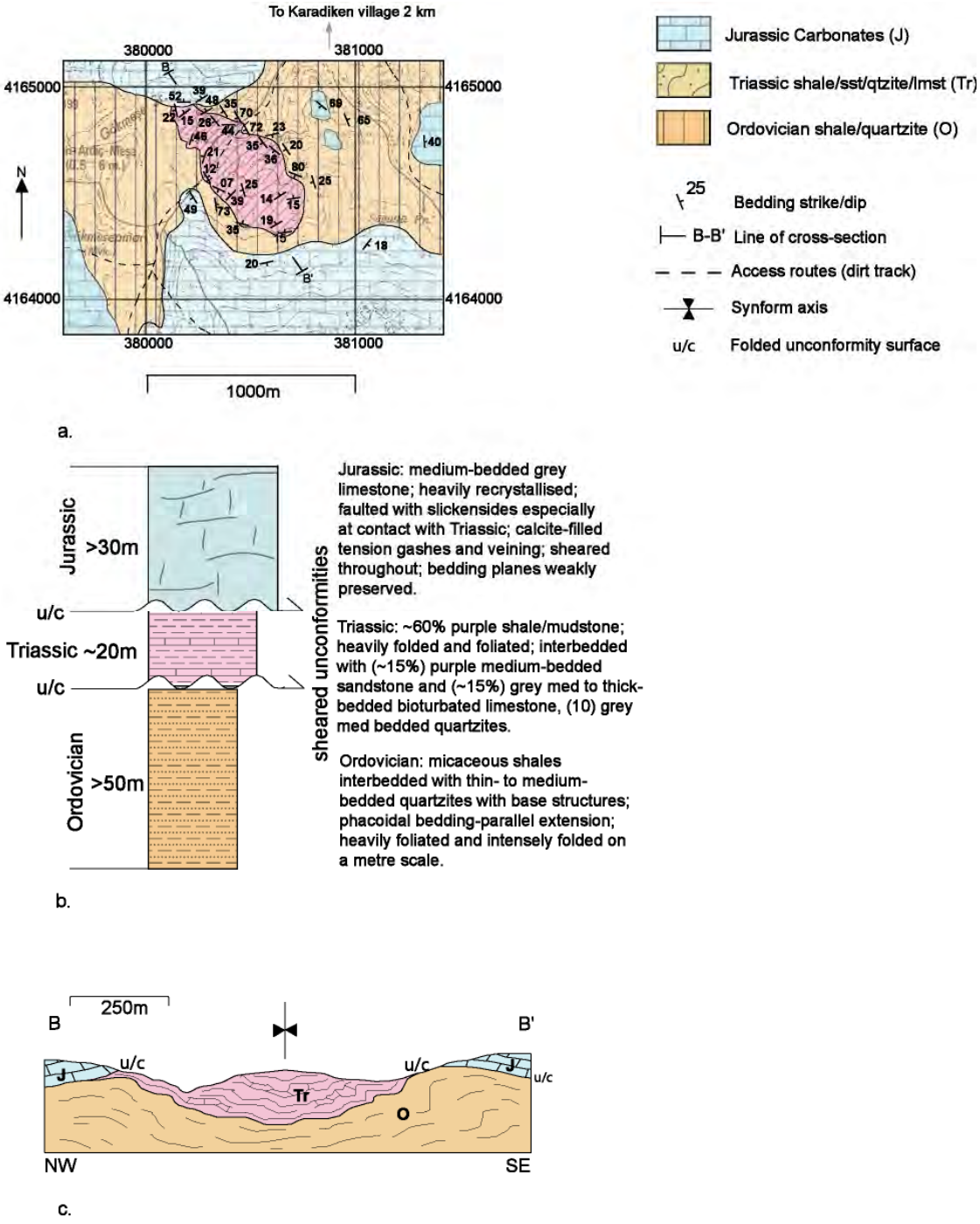

Fig. 11. a. Map of the Karadiken locality; b. Simplified log showing stratigraphy at Karadiken locality; c. Cross section B – B' through the Karadiken locality.

Fault planes dominantly trend NNW-SSE and WNW-ESE (Fig. 12c). Jurassic limestones are medium- to thick-bedded and heavily recrystallised. Bedding planes are often hard to

distinguish. Jurassic carbonates are not tightly folded but strike/dip measurements are variable across the area (Fig. 5.16a).

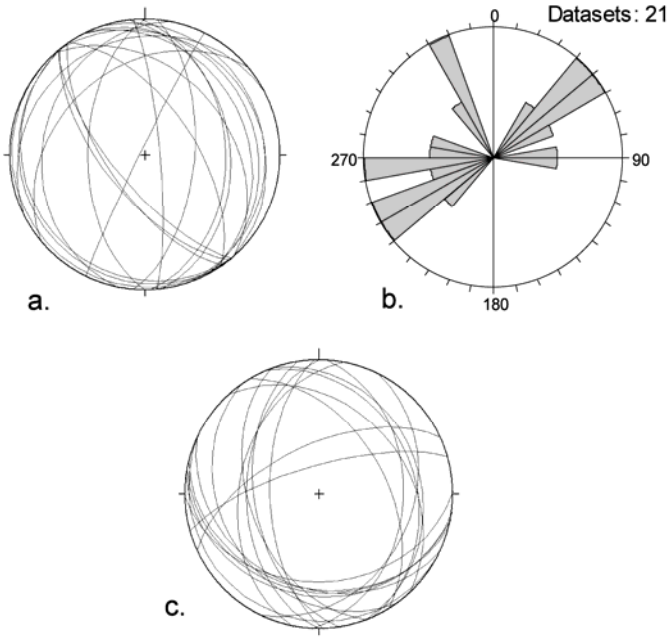

Fig. 12. Fold and fault data from Ordovician and Triassic units (combined) at the Karadiken locality. a. Fold axial planes; b. Fold vergence direction; c. Fault planes.

Local topographic relationships suggest that the Ordovician is above the Triassic. However, detailed mapping of the local contacts between the Ordovician, Triassic and Jurassic units shows that the Ordovician in fact dips beneath the Triassic (Fig. 5.16a–c, Fig. 5.17, Fig. 5.18a). On the eastern margin of the mapped area, the contact dips steeply >60º, and is heavily deformed by kink folds and buckle folds within both units (Fig. 5.17). On the western margin of the mapped area the contact is less steeply dipping, and in some instances the units are flat-lying at the contact (Fig. 5.16a). Triassic sediments stratigraphically overlie Ordovician sediments at this locality.

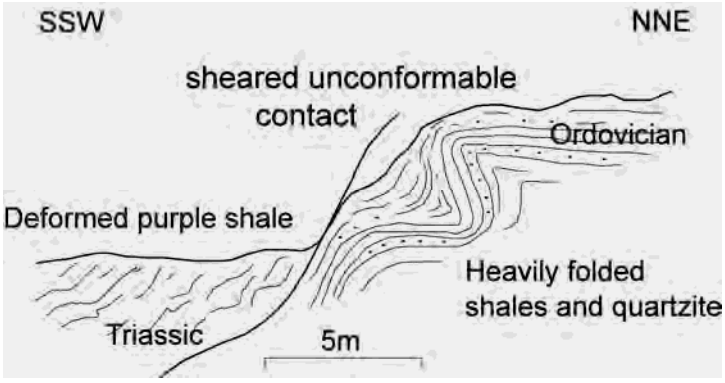

Fig. 13. Sketch of the contact between Ordovician and Triassic sediments at the Karadiken locality.

A contact between Ordovician–Triassic sediment and Jurassic limestone is observed towards the north of the mapped area (Fig. 5.16a). Medium-bedded Jurassic limestones are less deformed than the underlying Ordovician–Triassic shales, probably due to competency differences. The Ordovician–Triassic sediments at the contact are heavily cleaved and fractured, and dip beneath the Jurassic limestones with the same measured dip and strike (Fig. 5.16a, c). The planar nature of this contact suggests that it may be tectonic.

Monod and Akay (1984) believed that the Ordovician was thrust over the Triassic, and that the contact was then sealed and transgressed by Jurassic carbonates. This would again require a pre-Jurassic age of thrusting. However, re-mapping of this key locality shows that there is no tectonic contact between the Ordovician and Triassic sediments, but rather that this contact is a folded unconformity (Fig. 5.16c, Fig. 5.17, Fig. 5.18a). Displacement between these two units is restricted to minor bedding-parallel-slip between sediments of different competencies (i.e. shale and limestone). The Jurassic limestones unconformably transgress both the Ordovician and Triassic units, although the planar nature of their contact suggests it may have experienced some tectonic reactivation, related to the competency difference.

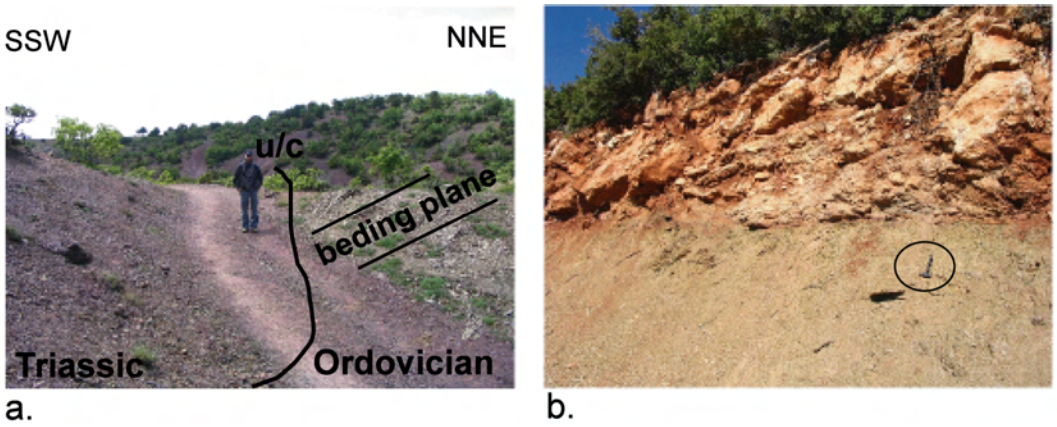

Fig. 14. a. Contact between Ordovician shale/quartzite and Triassic shale at the Karadiken locality; b. Sheared contact between Ordovician shale/quartzite (below) and Jurassic carbonates (above) at Yakanamaster locality. Contact was originally unconformable but has been reactivated at a later stage. Hammer for scale is circled.

This evidence, as at locality 1 (Agilönü), is consistent with an intact Palaeozoic–Mesozoic succession that was deformed during Late Cretaceous–Early Cenozoic time related to southward thrust emplacement of the Beyşehir-Hoyran-Hadim nappes. Again, there is no evidence to support latest Triassic "Cimmerian" compressional deformation.

Three other localities, not documented by Monod and Akay (1984), provide additional evidence that also supports a Late Cretaceous–Early Cenozoic age for regional deformation.

Locality 3: Yakanamaster (Fig. 5.12), GPS reference 386300 4166050

Located 6 km south of Beyşehir (Fig. 5.12), Cambrian–Ordovician and Jurassic sediments are exposed, as at locality 1 (Agilönü). There is further evidence of a tectonic contact between Ordovician shale/quartzite and Jurassic limestone.

Strongly folded Ordovician shales and quartzitic sandstones are separated from moderately deformed thick-bedded, to massive, Jurassic limestones (Fig. 5.18b). A thin (3cm) horizon of highly sheared Ordovician shale with foliation-parallel slickenlines occurs at the contact. A distinctive 30 cm-thick zone of foliation is present in the Ordovician shales, parallel to adjacent Jurassic limestones. Quartzose sandstone beds within the Ordovician have undergone bedding-parallel extension generating phacoidal blocks. Folds, shear imbrication and slickensides within the Ordovician sediments all

suggest a top-to-the-west movement (Fig. 15a–d). The limestones exhibit a 10-20 cm-thick brecciated horizon adjacent to the contact. Sedimentary structures on the bases of some Ordovician beds indicate that part of the sequence is inverted, whilst other parts are the right way up.

The evidence indicates that competent Jurassic Limestones tectonically overlie incompetent Ordovician shales. Shearing and brecciation zones on either side of the contact show bedding-parallel slip. Ordovician beds are strongly deformed and inverted on local fold limbs. There are no sedimentary structures within the limestones to determine stratigraphic way-up. The most likely explanation is that Ordovician shale/sandstone is unconformably overlain by Jurassic Limestone, and that the contact has been tectonically reactivated during Late Cretaceous–Early Cenozoic (Alpine) deformation.

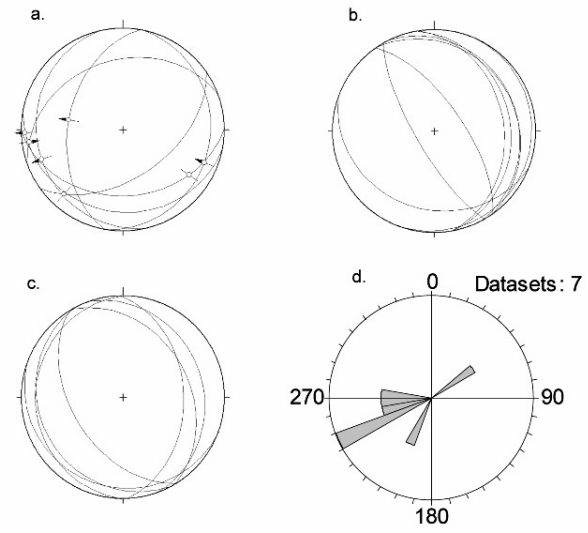

Fig. 15. Fold, shear plane, and fault data from Ordovician and Jurassic units (combined) at the Yakanamaster locality. a. Fault planes with slickensides; b. Shear fabric planes; c. Fold axial planes; d. Fold vergence direction.

Locality 4: Balik Tepe (Fig. 5.12, Fig. 5.13a), GPS reference 387740 4165528

Balik Tepe is the highest peak (1424 m) in the study area, ~7km south of Beyşehir (Fig. 5.12, Fig. 5.13a). Unfortunately, exposure in the area is poor. Cambrian dolomites

structurally overlie Ordovician shales/quartzose sandstones, and are then structurally overlain by Jurassic carbonates which form most of Balik Tepe. The Cambrian-Ordovician contact could be a thrust, or result from simple stratigraphic inversion. Where Cambrian dolomites and Jurassic limestones are seen in contact, heavy shearing and foliation are evident. Both units display calcite-filled tension gashes and localised tectonic brecciation. Locally, bedding planes display a mineral lineation related to layer-parallel extension.

Relationships in this area are comparable to those observed at locality 1 (Agilönü) and locality 3 (Yakanamaster). It is inferred that the Cambrian sequence was inverted related to Upper Cretaceous – Lower Cenozoic regional nappe emplacement. The planar contact between Palaeozoic and Jurassic units is unconformable, but was, therefore, reactivated during Alpine deformation.

Locality 5: Seydişehir-Tarasçi (Fig. 5.12), GPS reference 389870 4145750

The city of Seydişehir lies on the relatively autochthonous Tauride platform to the east of the Beyşehir-Hoyran-Hadim nappes (Fig. 5.12). A cross-section published by Monod (1977) through Çal Tepe, a prominent hill near Seydişehir, suggests that a thick Cambrian-Ordovician sequence has been folded and inverted in the east, so that Cambrian units are now in the highest structural position (Fig. 5.15). New mapping carried out in the west, near Taraşçı village (Fig. 5.12), now shows that the succession is the right way up, although heavily faulted and folded. An unconformable relationship between Ordovician and Triassic–Jurassic units is poorly exposed in a road section 250 m north of Taraşçı village (GR 389870 4145750).

The base of the Triassic succession consists of weakly foliated, variably coloured (purple to brown) micaceous sandy-shales. The thickness of the purple shales varies from 15-20 m in the road section, to 50-100 m to the west of Taraşçı village. The variable thickness of Triassic purple shales is consistent with depostion on an irregularly eroded Ordovician land surface, with the boundary between Ordovician and Triassic as an angular unconformity (Fig. 5.19). The shales pass up into thinly bedded (10-15 cm), moderately sheared, medium-dark grey recrystallised limestones, thickening upwards to

medium-thick bedded over a 5-10 m interval. These beds contain nodules of black chert formed by diagenetic silica replacement. The sequence continues for >50 m and passes into thin-bedded microbial limestones, interbedded with shales and thick-bedded bioclastic limestones (Fig. 5.19).

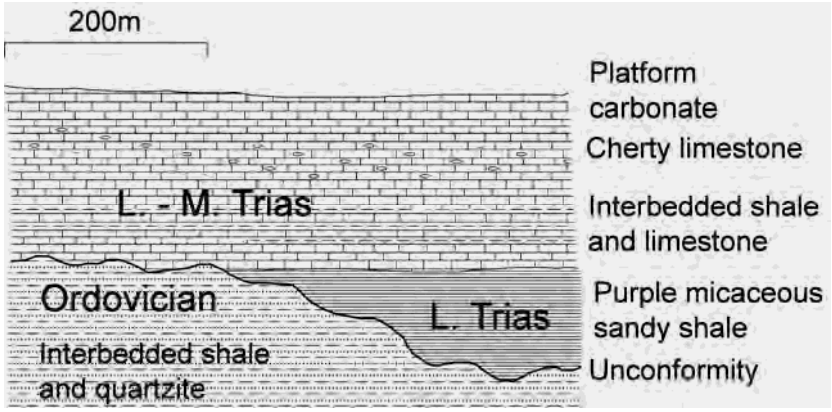

Fig. 16. Schematic diagram showing the stratigraphic relationships observed at Taraşçı village, near the town of Seydişehir.

The succession passes upwards into medium- to thick-bedded Triassic carbonates (Monod, 1977), interbedded with thin shale horizons, in all ~300 m thick. This is then transgressed by massive Jurassic carbonates, before being tectonically overlain by the Beysehir-Hadim nappes (Monod, 1977; MTA, 2002). The Triassic shales and limestones are regionally folded on a 10-50 m scale, but are more tightly folded locally on a 10 m scale. More competent massive Jurassic carbonates are not folded, but are heavily recrystallised. Complex structural relationships are present locally, with Jurassic carbonates of the autochthon overlain by imbricate slices of Ordovician turbidites near the base of the thrust stack.

The deformation is consistent with that elsewhere in the region. Competent thick-bedded and massive Jurassic carbonates are less deformed than thinner bedded more shaley and siliciclastic Lower Palaeozoic and Triassic lithologies. The most likely cause of this deformation is Upper Cretaceous - Lower Cenozoic emplacement of the Beyşehir-Hoyran-Hadim nappes.

In summary, structural study of the above key areas does not confirm the existence of a regional "Cimmerian" compressional deformation of latest Triassic age, but rather indicates that all of the deformation was of Late Cretaceous – Early Cenozoic age related to the regional southward thrusting of the Tethyan marginal and ophiolitic units of the Beyşehir-Hoyran-Hadim nappes.

Sedimentary evidence

Additional critical evidence for the Late Triassic tectonic setting of Tauride platform is provided by a succession of red clastic sediments known as the Çayır Formation (Monod and Akay, 1984). This formation has been correlated laterally across southern Turkey, from the island of Chios (Greece) in the west to the Bolkar Dağ in the east, and has been inferred to have accumulated close to the Triassic–Jurassic boundary (Monod and Akay, 1984). The character of these sediments, predominantly conglomerates and sandstones that interrupt a largely shallow-marine carbonate Mesozoic succession, was cited as evidence for uplift and erosion related to compression.

In model 1 (Fig. 2a), the Çayır sediments were derived from "Cimmerian" uplift resulting from continental collision (Stampfli, 2000; Stampfli et al., 2001). The Çayır sediments were seen as the molasse fill of a foreland basin related to southward overthrusting of an "Anatolide" terrane (Stampfli and Borel, 2002). In model 2 (Fig. 2b), a main pulse of rift-related flexural uplift occurred during the Early Triassic, with Late Triassic–Jurassic clastic sedimentation being attributed to continued extension along faults within the Tauride-Anatolide platform. In model 3 (Fig. 2c), the sediments were deposited after stratigraphic inversion of Triassic extensional faults in the Tauride platform, related to stress transmission through the northerly Neotethyan oceanic crust from the Eurasian Late Triassic collisional margin to the north. In the model proposed here (Fig. 2d) sediment was eroded from the rift flank during a pulse of flexural uplift in the Late Triassic, and was deposited in one, or several, basins within the Tauride unit.

During this study the sedimentology of the Çayır Formation was studied at fifteen localities within the autochthonous Tauride platform and the allochthonous Hadim and Bolkar nappes (Fig. 4.8).

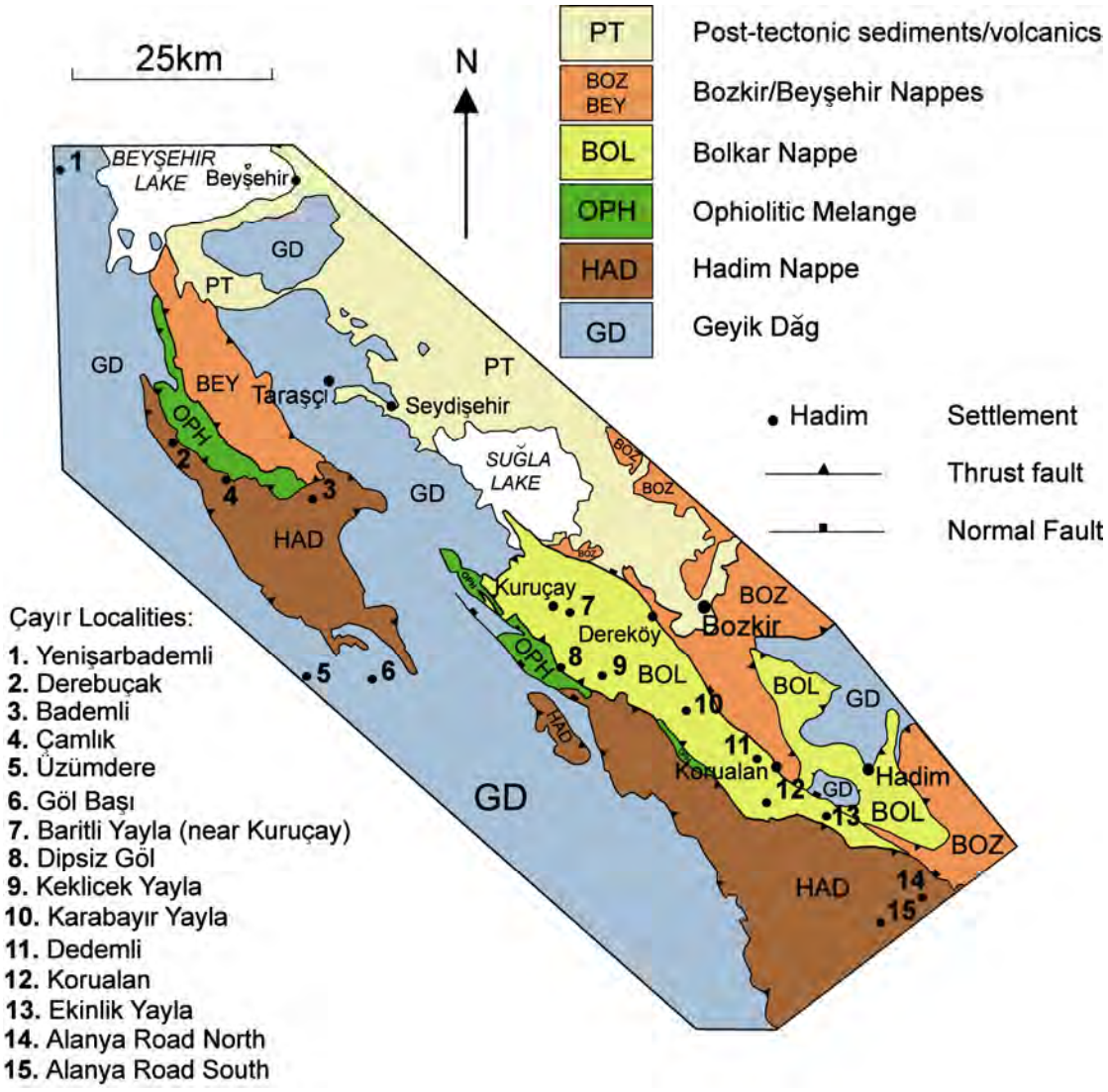

Fig. 17. Simplified tectonic map of the study area showing the location of studied Çayır Formation successions documented in section 4.5.2.

Age

Determining the age of the Çayır Formation is difficult owing to a sparcity of datable fossils. Monod and Akay (1984) cited ages ranging from Late Triassic to Middle Jurassic, based on local stratigraphic relationships and limited palaeontological data (e.g. Foraminifera *Triasina hantkeni* of Upper Norian age; Algae *Paleodasycladus*

mediterraneus of Middle to Upper Liassic age). Özgül (1997) inferred a general Anisian-Norian age, beacause limestones overlying the clastics were dated as Norian-Rhaetian, and hence the Çayır sediments were inferred to be younger. In the Hadim nappe, clastic facies of the Çayır Formation pass conformably into Upper Liassic limestones and dolomites (Gutnic et al. 1979). The base of the Çayır Formation typically rests unconformably on Upper Triassic shallow-marine platform carbonates at a locality 15 km south of Taşkent village (Önder, 1984). A recent geological map of the region indicates the Çayır Formation as Late Rhaetian – Early Liassic in age (MTA, 2002); however, evidence on what this is based on is unavailable. During this work fossiliferous limestone horizons in the mid-part of the succession yielded the benthic foraminifera *Siphovalvulina variabilis* Septfontaine, *Amijiella amiji* (Henson), *Orbitopsella primaeva* (Henson), *Planiinvoluta* sp., *Valvulina* sp., *Thaumatoporella parvovesiculifera* (Raineri), implying a Middle Liassic age (N. İnan and K. Taslı, pers. comm., 2007).

Sedimentary facies

Where observed in this study, the Çayır Formation is typically a fining upward succession, <200 m thick, of continental clastics and shales intercalated with shallow-marine limestones (Fig. 18, Fig. 4.20a-d) (see chapter 4 for complete review of Late Triassic sedimentology). The basal part of the Çayır Formation is usually composed of coarse conglomerates and sandstones (Fig. 4.20b). At some localities conglomerates are not present and the succession as a whole is represented by a fine-grained sandstone/shale succession. Shales and limestones become more abundant upwards, and typically passes into Jurassic shallow-marine platform carbonates in the sequences (Fig. 18).

Several key depositional environments can be identified from detailed facies analysis, as outlined below. Laterally discontinuous lens-shaped conglomerate bodies are interbedded with planar cross-bedded sandstone and less abundant mudstone horizons. These sediments are found towards the base of the sequence of this facies

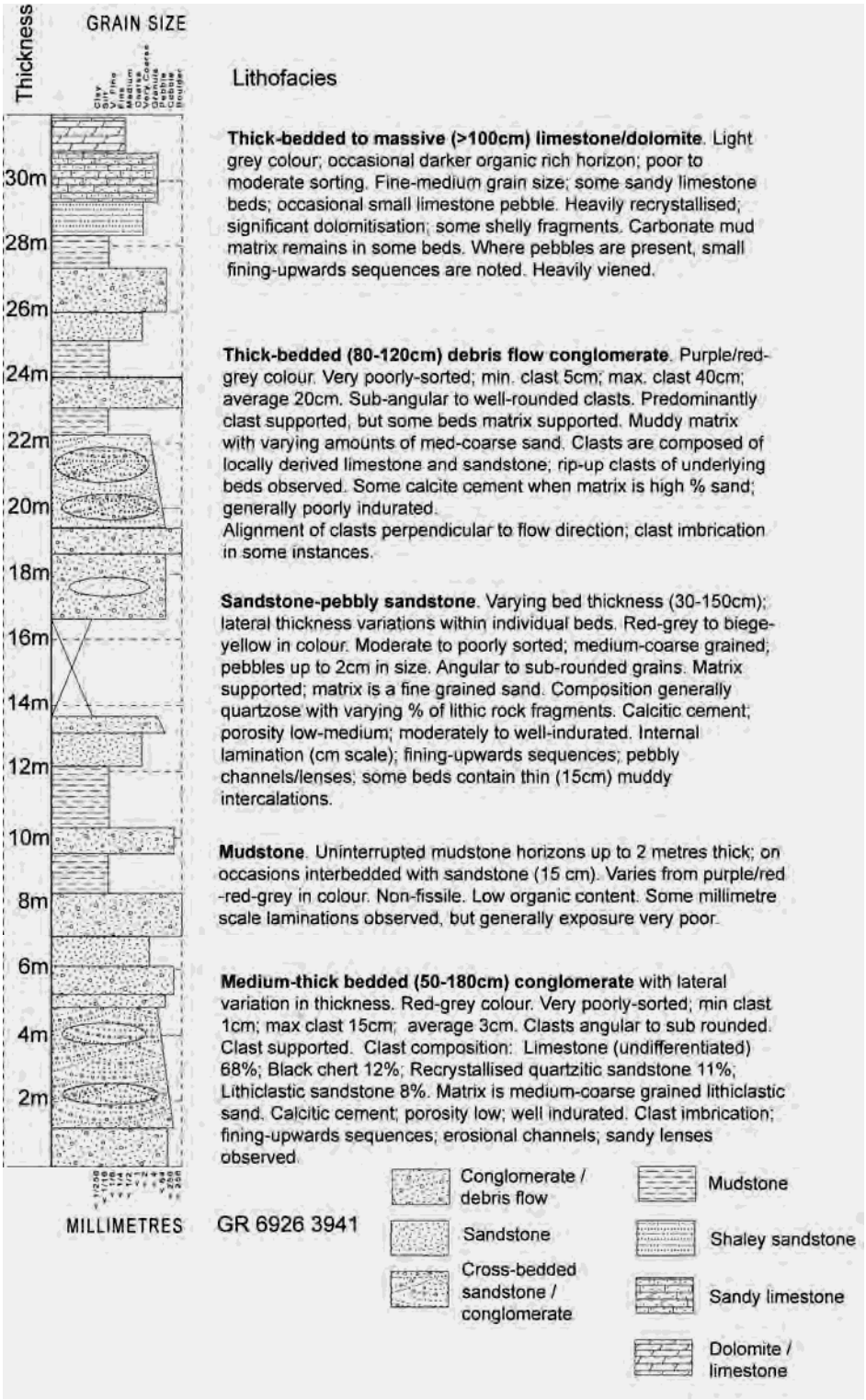

Fig. 18. Representative log of the Çayır Formation, from the sequence east of Derebuçak village, 50km SW of Beyşehir.

association, and are interpreted as a terrestrial braided-river environment. In some cases, coarser and less well sorted sediments, with a higher percentage of angular clasts, are thought to represent terrestrial alluvial fan deposits. Some conglomerate successions contain exclusively limestone clasts, and are set in a marine mudstone matrix, which suggests they may be related to submarine debris flows and channels. The thickness of all of these coarse clastic deposits varies considerably along strike. Medium- to thick-bedded sandstones are interbedded with fine-grained mudstones and medium-bedded shallow-marine limestones. Towards the top of the Çayır Formation, these interbedded sediments are typically transgressed by thick-bedded shallow-marine platform carbonates. This facies association is interpreted as a marginal shallow-marine environment, with significant clastic input. Fine-grained mudstones are interbedded with irregular, thin-bedded, medium-grained sandstones >40m thick. This facies association, known at only two localities, represents terrestrial/coastal overbank deposits. Facies relationships are summarised in Fig. 4.31.

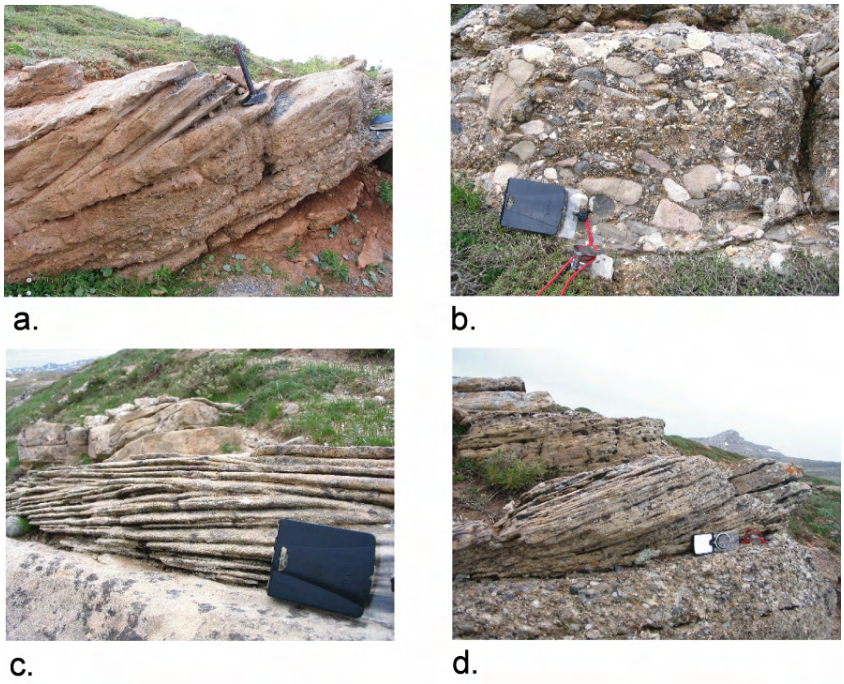

Fig. 19. Typical sedimentary facies and sedimentary structures of the Çayır Formation. a. Planar cross-bedded sandstone/conglomerate; b. Clast-imbricated conglomerate; c. Cross-laminated sandstone; d. Trough cross-bedded sandstone/conglomerate.

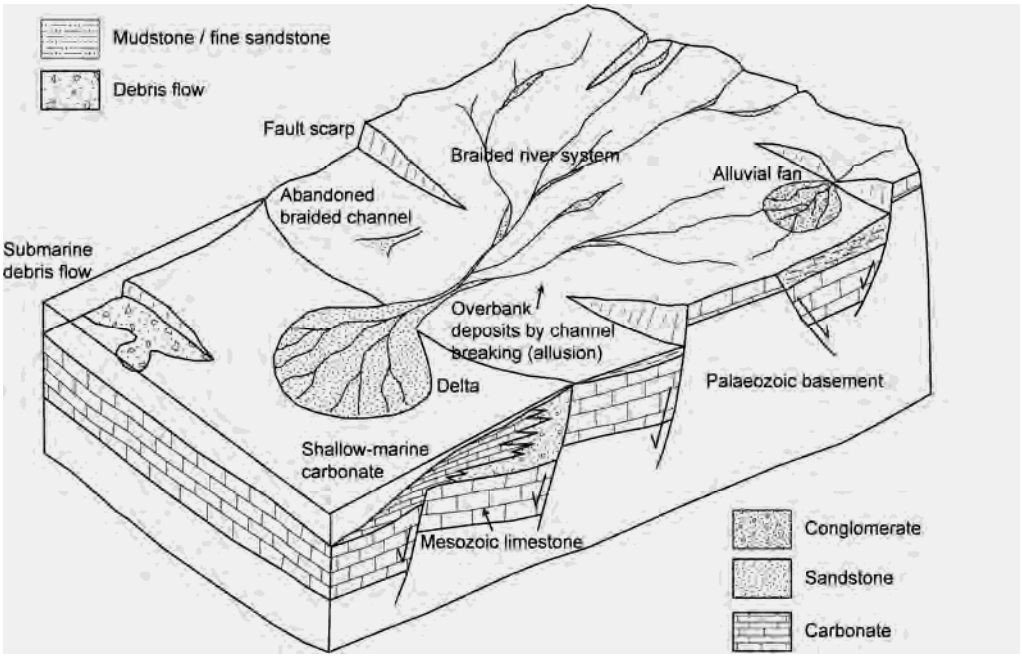

Fig. 20. Schematic diagram illustrating the range of depositional environments in which the Çayır Formation sediments were deposited.

Palaeocurrent evidence

Palaeocurrent data was collected at 15 localities, as shown in Fig. 4.19. Direction indicators are exhibited in the form of cross-bedding, cross-lamination, primary current lineation, and clast imbrication (Fig. 4.20a-d). Although the results are locally variable, the consolidated data clearly indicate a flow from the north (Fig. 4.19o). This does not in itself discriminate between any of the three alternative models, although the simple model of a rifted margin passing into a more distal setting northward can be ruled out.

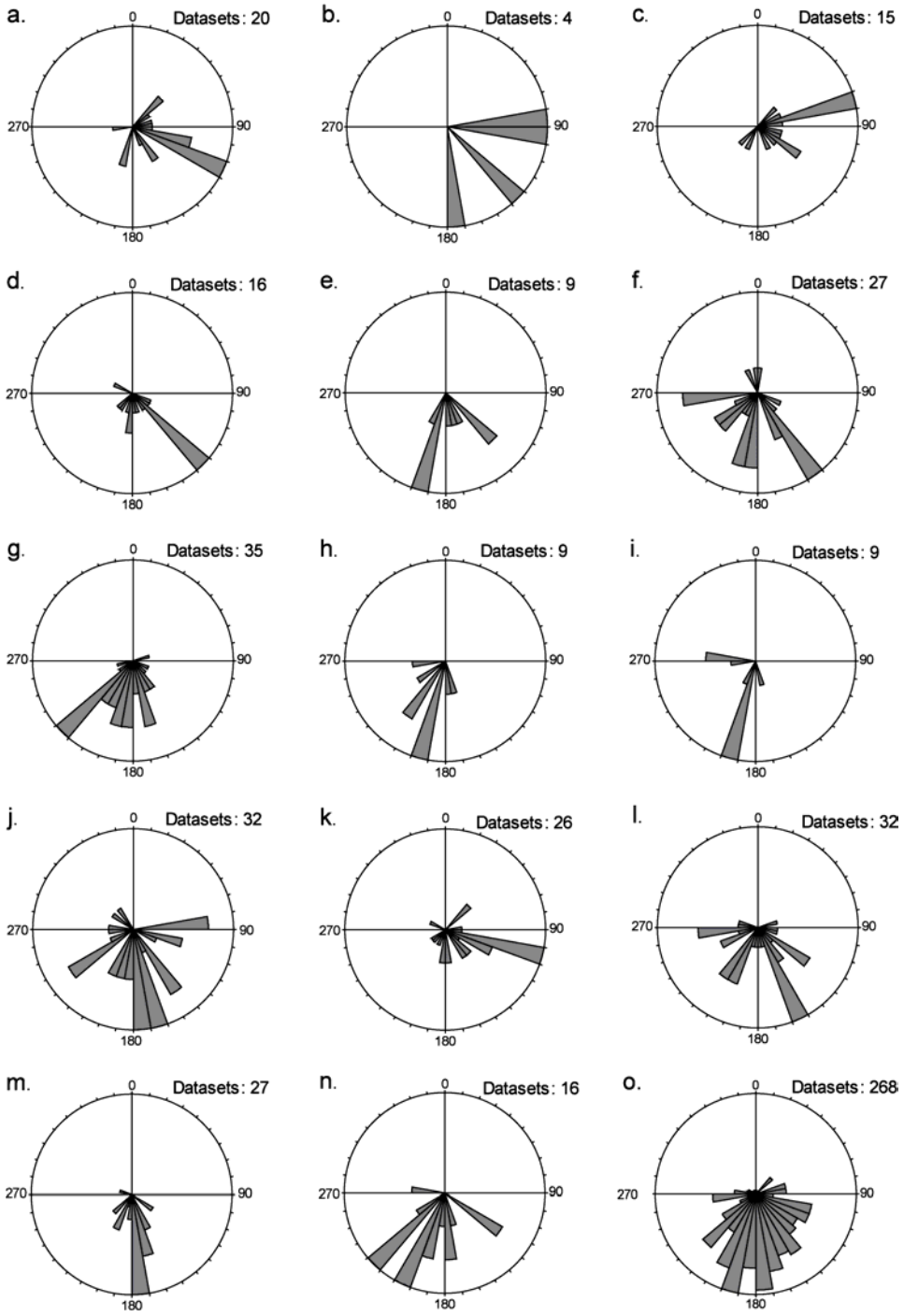

Fig. 21. Palaeocurrent data from the Çayır Formation. a. Locality 2: Derebuçak; b. Locality 3: Bademli; c. and d. Locality 4: Üzümdere 1 and 2; e. Locality 6: Göl Başı; f. Locality 9: Keklicek Yayla; g. and h. Locality 14: Alanya road north 1 and 2; i. – n. Locality 15: Alanya road south 1 – 6; o. Consolidated data from 14 localities.

Sediment composition

To determine the provenance of the Cayir Formation, the composition of conglomerate clasts in the field was investigated (Fig. 4.21, Fig. 4.22), and sandstone composition in the laboratory using thin sections was determined (Fig. 4.23, Fig. 25).

In decreasing order of abundance, the sedimentary rocks identified as clasts within conglomerates in the field are: light grey recrystallised limestone, well-indurated recrystallised quartzose sandstone (quartzite), dark grey recrystallised limestone, red limestone, micritic limestone, weakly-lithified quartzose sandstone, black chert (“lydite”), wackestone, crystalline white limestone, dolomite, oolitic limestone (Fig. 4.21, Fig. 4.22). In addition, a small numbers of clasts were found of altered metamorphic/volcanic rock (e.g. mica schist, basalt), limestone breccia, quartz vein, and packestone. In thin section (Fig. 4.23, Fig. 25), the grains identified, in decreasing order of abundance, are: monocrystalline quartz, polycrystalline quartz, microcrystalline quartz, sheared composite quartz, altered light limestone, altered dark limestone, micritic limestone, altered feldspar, radiolarian chert. In addition, a small number of altered metamorphic/volcanic grains were observed.

The age of the clasts can rarely be determined directly from evidence of fossils within them. Radiolarians present within chert grains are recrystallised and have not been dated. Micritic limestone clasts locally contain the bivalve *Halobia* sp. that indicates a Triassic age. Also, the large foraminifera *Fusulinia* sp. in some limestone clasts suggests a Palaeozoic, possibly Permian age. In addition, the ages of the clasts and grains can be inferred by a lithological correlation with the various successions exposed in the area. This allows the following inferences: the micritic limestone, red limestone, dolomite and light grey limestones (including wackestone, oolitic limestone, packestone) were derived from the Triassic succession subjacent the Çayır Formation; the weakly-lithified sandstones came from middle part of the Triassic succession; the dark fusilinid-bearing limestones were derived from the Permian shallow-water carbonate succession, locally exposed in the Taurides (Özgül, 1984) and the Konya area further north (Özcan et al., 1988; Robertson et al., 2007b). The well-indurated quartzose sandstone,

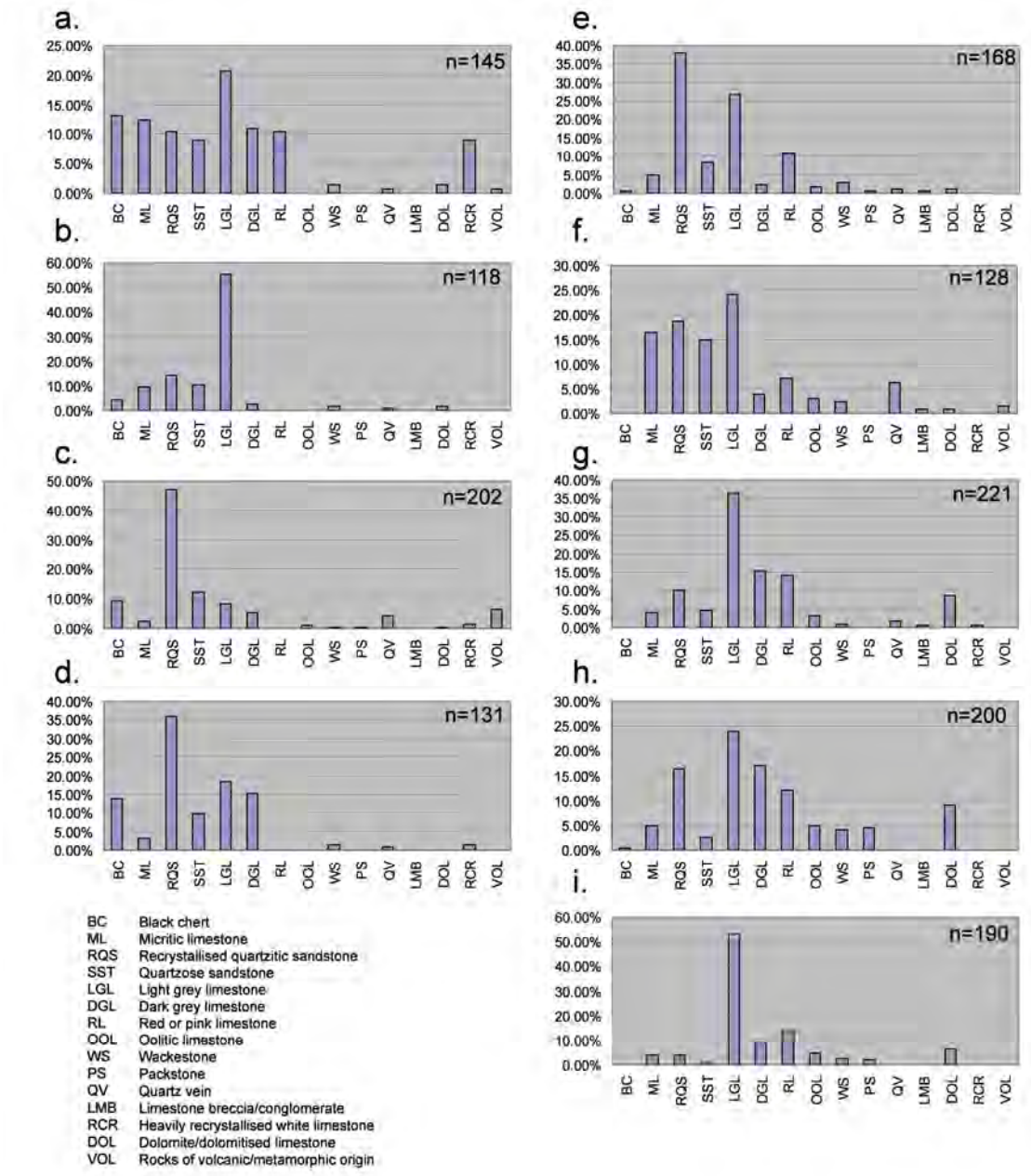

Fig. 22. Clast count data for the Çayır Formation. a. Locality 2: Derebuçak. b. Locality 3: Bademli. c. and d. Locality 5: Üzümdere 1 and 2. e. Locality 8: Dipsiz Göl. f. Locality 9: Keklicek Yayla. g. Locality 11: Dedemli. h. and i. Locality 12: Korualan 1 and 2.

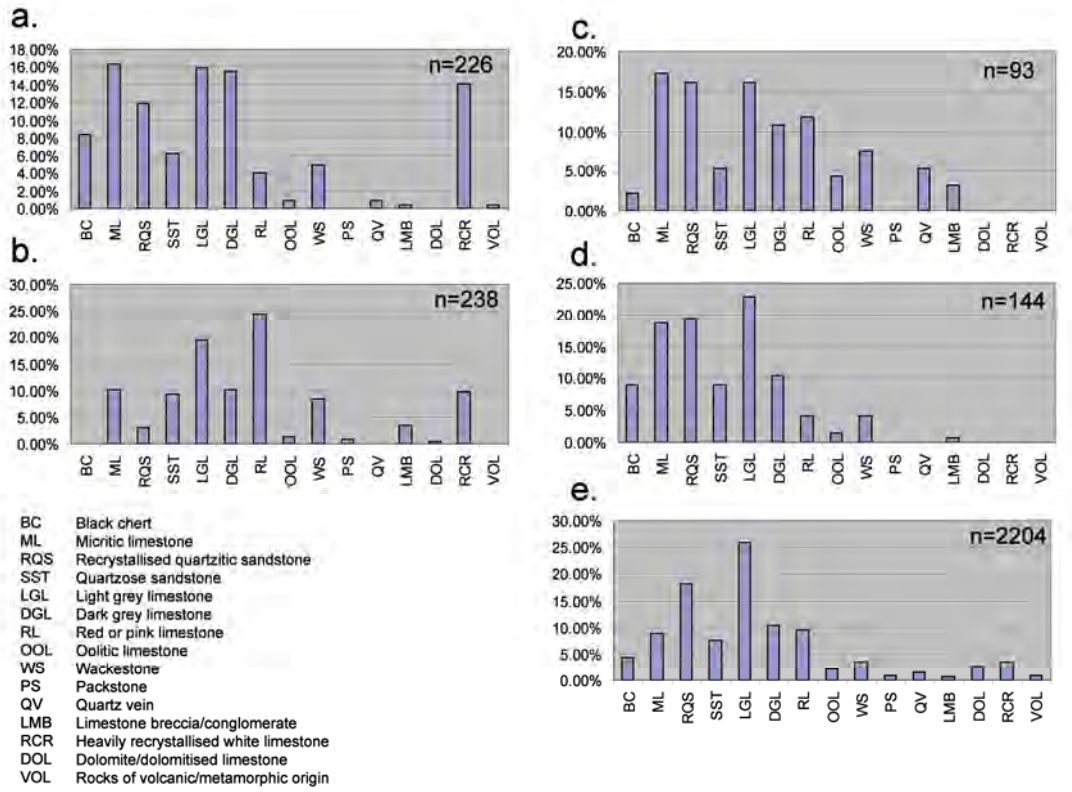

Fig. 23. Clast count data for the Çayır Formation. a. and b. Locality 14: Alanya road north 1 and 2. c. and d. Locality 15: Alanya road south 1and 2. e. Combined data from all localities documented.

crystalline white limestone and quartz veins are known in the Cambrian-Ordovician succession exposed in the north (Seydişehir–Beyşehir area) and also further south in the Tauride autochthon (Geyik Dağ). There are also thick successions of well-indurated quartzose sandstone within the Carboniferous and Permian sequences of the allochthonous Hadim nappe and Bolkar nappe (Monod, 1977; Özgül, 1984). Black chert (lydite) of Carboniferous age is known in the Konya area beneath a Permo-Triassic unconformity (Özcan et al., 1988; Eren et al., 2004). Finally, metamorphic rocks (e.g. mica schist) are locally found in the Precambrian “basement” of the Taurides, as exposed in the Sultan Dağ further west (Gutnic et al., 1979).

Crucially, there is an absence of clastic material that could have been related to closure of an oceanic basin during the Triassic, including arc volcanic and plutonic rocks, accreted deep-sea sediments, ophiolitic rocks (e.g. serpentinite), and metamorphic

material. Instead, all of the sedimentary material could have come from Tauride units, including the pre-Triassic of the Konya area further north.

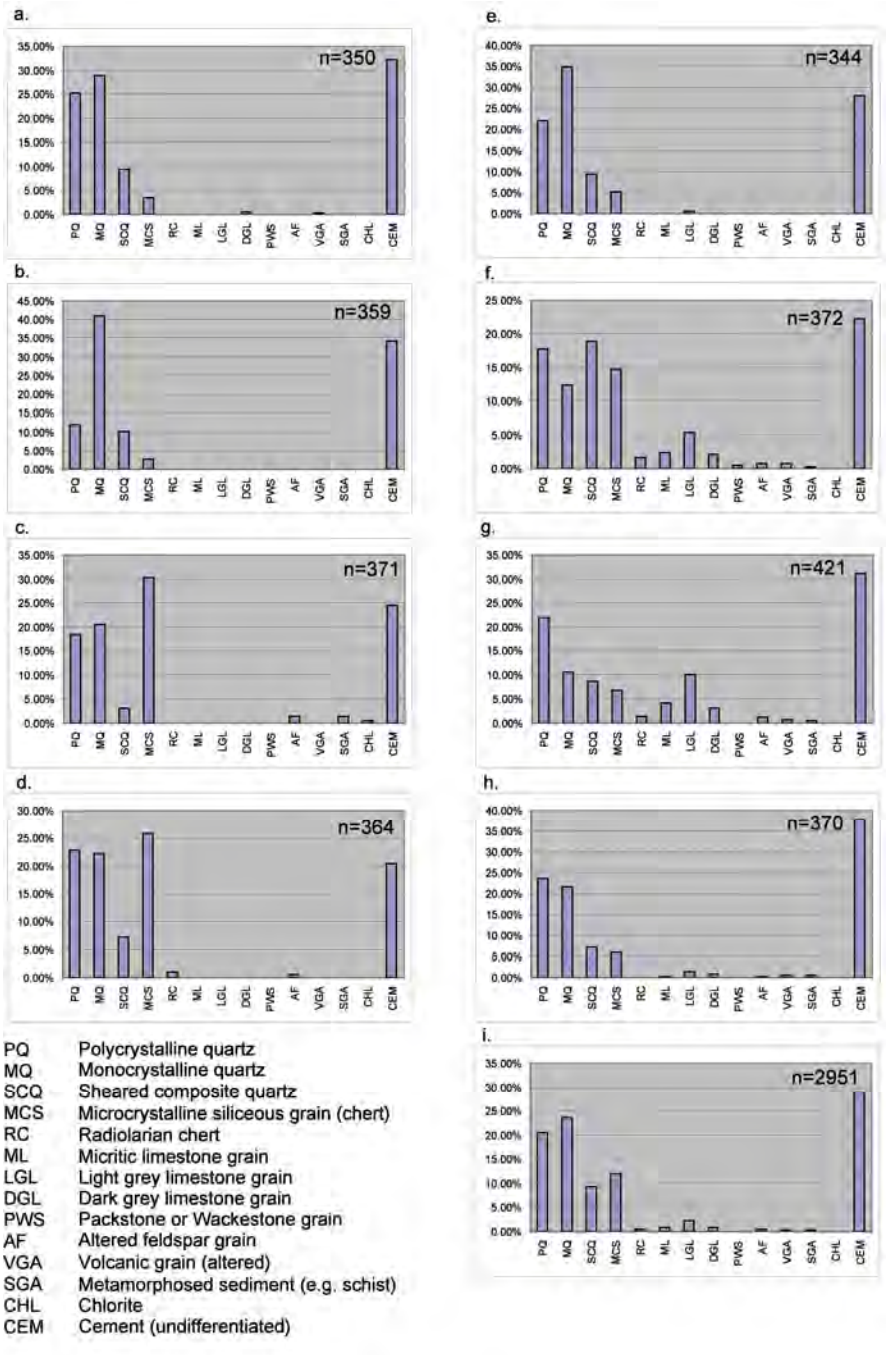

Fig. 24. Point count data for the Çayır Formation. a. Locality 2: Derebuçak; b. Locality 3: Bademli; c. Locality 5: Üzümdere; d. Locality 6: Göl Başı; e. Locality 9: Keklicek Yayla; f. Locality 14: Alanya road north; g. and h. Locality 15: Alanya road south; i. Combined data from all localities documented.

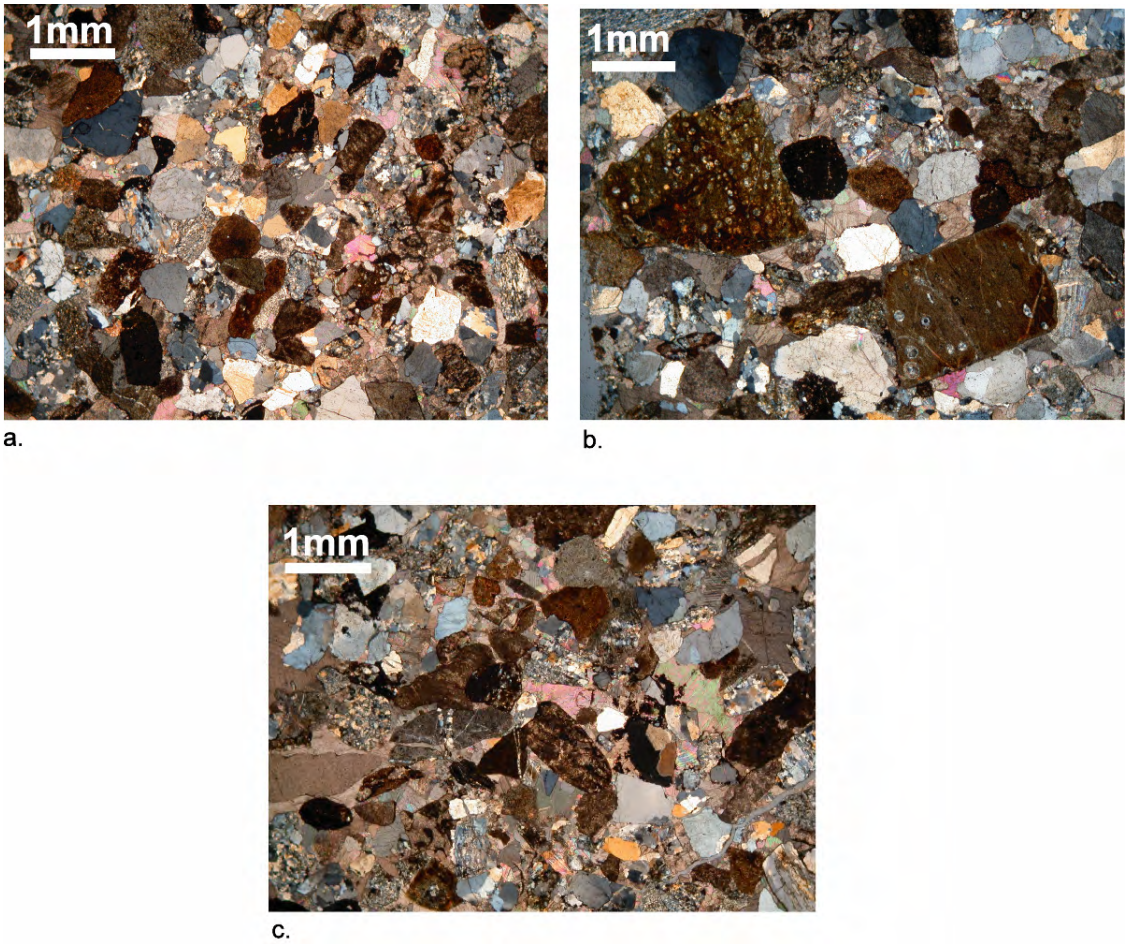

Fig. 25. Photomicrographs of typical Çayır Formation lithiclastic sandstone, showing grains of radiolarian chert, quart and altered carbonate.

Sediment provenance

In model 1 (Stampfli et al., 2001) (Fig. 2a), sediment would have been derived mainly from the north, i.e. from the supposed “Anatolide” terrane, which it is assumed was thrust southwarda over the Tauride unit to form a flexural foreland basin. The “Anatolide” terrane would then be in a structurally and topographically high position as - in typical collisional settings, e.g. the western Taiwan foreland basin (Covey, 1986). It would thus be expected to act as an erosional high and supply clastic sediment to the newly formed flexural basin to the south. However, some sediment could also have been derived from an inferred forebulge in the south, especially at an early stage when the foreland would have been flexurally uplifted and eroded. In model 2 (Göncüoğlu et al.,

2003) (Fig. 2b), the sediment could have been derived from the north or the south equally, since the basin formed by continental rifting with margins both to the south (Tauride unit) and the north (Sakarya unit). However, the newly formed Izmir-Ankara oceanic basin could have acted as a barrier to sediment derived from the north after the ocean opened. Assuming the ocean was already opening from Middle – Late Triassic, the Tauride platform would have been the more likely source of sediment. In model 3 (Robertson et al., 2004) (Fig. 2c), the sediment would initially have been derived from the south, since it is assumed that the Tauride margin rifted in the Triassic opening a Mesozoic oceanic basin to the north. However, a northerly derivation is also possible if a pulse of compression-related reversed faulting had taken place. In model 4 (Fig. 2d), the sediment could be derived from the north or the south, but provenance would be exclusively from the Tauride platform and any associated "basement" units.

Discussion

No one piece of structural or sedimentological evidence is conclusive in determining the Late Triassic tectonic setting; however, a review of all the evidence presented above allows a number of key issues to be resolved.

Structural setting

There is no evidence within the area studied that the Tauride platform experienced compressional deformation at any time during the Mesozoic prior to the Late Cretaceous. The new structural evidence, faunal data and stratigraphic observations suggest that the deformation, where observed, was associated with closure of the northern Neotethyan ocean and the Late Cretaceous and Early Cenozoic southward overthrusting of the Beyşehir-Hoyran-Hadim nappes.

In model 1 (Stampfli, 2000; Stampfli et al., 2001; Stampfli and Borel, 2002) (Fig. 1a, Fig. 2a) continental collision between Tauride and "Anatolide" units would have been expected to cause significant compressional thrusting and folding within the footwall represented by the Tauride platform. A suture zone should exist between the two units, which has not been identified in the Taurides. However, the critical area between the

unmetamorphosed Tauride units in the Beyşehir region and metamorphosed Mesozoic equivalents further north in the Konya region is covered by the younger Bozkir nappes and Cretaceous ophiolitic units, as well as Cenozoic sediments and volcanics. As a consequence, the presence of a suture cannot be directly disproved for this area alone. Further west in the Sultan Dağ massif, Palaeozoic metamorphic rocks of the supposed Palaeotethyan unit ("Hun terrane") are exposed in direct tectonic contact with the late Precambrian basement of the Taurides but without any intervening exposed suture of Middle – Late Triassic age, as predicted by this model.

In model 2 (Göncüoğlu et al., 2000; 2003) (Fig. 1b, Fig. 2b), all the deformation should be extensional, as is indeed inferred. In this model, a backarc basin opened along the northern margin of the future Tauride platform during Late Palaeozoic time, and then closed associated with compressional deformation and regional metamorphism prior to Permian time. This was followed by re-opening of the İzmir-Ankara ocean to the north during Middle – Late Triassic time. The continent that rifted away was the Sakarya zone, which is assumed to have always been located along the Gondwana margin. By contrast, in a favoured interpretation the northern margin of the Tauride platform, including Permian shelf carbonates, rifted away, while the Sakarya zone already formed part of the Eurasian margin far to the north (Robertson et al., 2004; Okay et al., 2006).

In model 3 (Robertson et al., 2004) (Fig. 1c, Fig. 2c), it was assumed that the Triassic setting was generally extensional, related to opening of northern Neotethys, but that a pulse of compression took place during latest Triassic time, possibly recording stress transition from the "Cimmerian" orogeny affecting the Eurasian margin during the time. This interpretation assumed that the evidence of compression reported by Monod and Akay (1984) was correct. However, the information presented in this paper does not confirm the existence of any Triassic compressional deformation.

Sedimentary setting

In model 1 (Stampfli, 2000; Stampfli et al., 2001; Stampfli and Borel, 2002) (Fig. 1a, Fig. 2a) the Çayır Formation should have accumulated in a foreland basin associated with suturing of Palaeotethys. A flexural forebulge unconformity would then be expected

within the Tauride platform, but this has not been observed. Also, a deepening- and coarsening-upward sequence would be expected, as in typical foreland basin settings (Covey, 1986), but this is not seen either. Since the sediments are coarse, commonly conglomeratic, a proximal setting would need to be envisaged. It would be expected that the sediment would have been mainly derived from the inferred over-riding Eurasian plate, represented by Sakarya zone, for example, including Late Palaeozoic granitic rocks and Triassic meta-clastic sediments (Yilmaz et al., 1997). Derivation of material from an intervening suture zone would also be likely (e.g. basalt, serpentinite, Triassic chert). However, the clast composition indicates that sediment was largely derived from the underlying Tauride platform.

A complicating aspect is the source of the common black chert in the Çayır Formation. The only known possible source of the black chert is from an area of Palaeozoic rocks that underlies a metamorphosed Mesozoic carbonate platform succession in the Konya region to the north of the area studied. This Mesozoic carbonate platform is generally interpreted as a metamorphosed equivalent of the Tauride platform further south (Şengör and Yılmaz, 1981; Göncüoğlu et al., 2003; Robertson et al., in prep.; Robertson, 2007b). This 'basement' unit includes Palaeozoic platform carbonates, terrigenous clastic sediments, alkaline volcanics and black chert. The chert ranges from quite well preserved with clearly visible radiolarians in thin section, to recrystallised fine-grained quartzite. A similar range of textures is seen in the black chert clasts within the Çayır Formation. One apparent problem with this 'basement' unit as the source of the chert pebbles as that few, if any, volcanic grains were observed in the Çayır Formation (Fig. 4.21, Fig. 4.22, Fig. 4.23), whereas volcanic rocks are widespread in the Konya 'basement' unit. A possible explanation is that black chert is extremely durable, and hence could be transported long distances without breaking down, in contrast, for example, to basic lava. This is clearly demonstrated by study of the Triassic basal conglomerate above the 'basement' in the Konya area (unpublished data). Black chert clasts are common there, whereas only a small amount of chert exists in the rocks exposed beneath. The chert has been effectively concentrated in the overlying conglomerate. Such preferential preservation of chert is confirmed by studies of modern beach deposits, for example in southern Cyprus where chert is greatly over-represented

compared to the rocks exposed on the island (Garzanti et al., 2000). Another aspect is that the black chert cannot have been derived from the present exposures of the Palaeozoic 'basement' as there are covered by a continuous succession of shallow-water carbonates from the Middle Triassic to the Early Cretaceous (Göncüoğlu et al., 2003). However, it is possible that the chert came from part of the 'basement' that is no longer exposed, for example, from beneath the area of younger units exposed between the Tauride platform and the Palaeozoic 'basement' in the Konya area.

In model 2 (Göncüoğlu et al., 2003) (Fig. 1b, Fig. 2b), the İzmir-Ankara ocean rifted in the Lower Triassic and began to open by the Middle Triassic when shelf carbonates accumulated on the 'basement' units to the north of the Tauride platform (e.g. in the Konya area). If spreading simply began by the Middle Triassic the margin would be expected to be undergoing passive margin subsidence by Late Triassic-Early Jurassic time when the Çayır Formation was accumulating, with no obvious source of coarse-grained sediment. Upper Triassic platform carbonate across the study area also suggests that subsidence had not started by this time. This suggests that final continental break-up and onset of sea-floor spreading might have been delayed until after the Middle – Late Triassic.

In model 3 (Robertson et al., 2004) (Fig. 1c, Fig. 2c), seafloor spreading could have begun during the Middle – Late Triassic, as in model 2, but there was then a pulse of uplift related to the inversion of rift faults, triggered by collision-related events along the Eurasian margin to the north. Comparable far-field stress transmission and associated deformation has been documented in, for example, the Tanganyika-Rukwa-Malawi rift segment in the east African rift system (Delvaux, 2001), where stress was transmitted from the Gondwana margin over long distances through continental lithosphere. This could have resulted in uplift of a block of 'basement', including black chert, adjacent to the Tauride platform, thus providing a source of black chert. No regional compression need be recorded, however, as the Tauride platform remained far from the collision zone. This model remains as a possibility but without independent supporting evidence.

The alternative that we favour is that rift-related faulting persisted in the area until Late Triassic-Early Jurassic time when the Çayır Formation was deposited (Fig. 2d). Collins and Robertson (1997) previously inferred that the northern branch of the

Mesozoic Neotethys started to open during the Late Triassic, based on the presence of Late Triassic T-MORB-type basalt within the Lycian nappes. Also, a Carnian age has been obtained from radiolarian cherts associated with transitional MORB from the İzmir-Ankara suture zone (Central Sakarya zone) (Tekin et al., 2002; Göncüoğlu et al., 2006). This evidence proves that a deep-water, volcanically active basin existed by the Late Triassic and thus that rifting long pre-dated the Early Jurassic, unlike some earlier models (e.g. Şengör and Yılmaz, 1981). The presence of Late Triassic radiolarians does not by itself prove the existence of normal ocean crust in any area, however. There is still no proof that normal sea-floor spreading had begun by Middle – Late Triassic time. For example, in the Lycian nappes Triassic T-MORB is stratigraphically overlain by shallow marine carbonates (Collins, 1997). Studies of the North Atlantic and the Alps, for example, show that final continental break-up was preceded by a long period when crustal extension was occurring without magmatism (e.g. Manatschal et al., 2007). MORB was extruded immediately prior to and during final continental break-up, as confirmed by recent deep drilling of the Newfoundland margin (e.g. Robertson, 2007a). It is, therefore, possible that rift faulting remained active until final onset of normal sea-floor spreading, sometime during latest Triassic to earliest Jurassic time.

An additional possibility is that the source area of the black chert in the Çayır Formation was introduced from an exotic terrane that was juxtaposed with the Tauride margin, possibly by strike-slip faulting during Mid-Triassic Jurassic time. Stampfli and Borel (2002) inferred that a source terrane was transposed south-westwards away from Iranian units in the Mid-Triassic, followed by docking with a "Cimmerian" continental fragment i.e. the Taurides during latest Triassic time. The possibility of a source area being introduced by strike-slip is difficult to evaluate. However, strike-slip and collisional processes are inconsistent with the evidence of a rift-related settting along the northern margin of the Tauride platform as a whole (e.g. Göncüoğlu et al., 2003; Robertson, 2007b).

Proposed new model

A regional unconformity exists within the autochthonous Geyik Dağ, and no units are exposed of Silurian to Early Triassic age. By contrast, in the Hadim and Bolkar

nappes, there is a complete Palaeozoic succession from Devonian to Cretaceous. These three tectono-stratigraphic units are inferred to restore as part of the same north-facing rifted continental margin during the Palaeozoic. Regional topographic highs and lows could then have existed within the continental platform, with some rift-blocks being eroded, whilst others were sites of deposition.

Above the unconformity in the Geyik Dağ, and within the Hadim nappe and Bolkar nappe, the Triassic stratigraphy (Monod, 1977; Önder, 1984; Özgül, 1984) comprises Early–Middle Triassic marine mudstones, limestones and sandstones, then Middle – Upper Triassic platform carbonates, in turn overlain by Late Triassic – Lower Jurassic Çayır Formation clastics. During the Triassic, the Tauride platform (including the Konya complex) represented a north-facing subsiding rift. By the latest Triassic, extension-related flexural uplift caused the deposition of continental clastics in intra-platform basins, represented by the Çayır Formation.

The source of the clastic sediment is seen as an uplifted fault block along the rifted margin to the north of the area studied. Studies of comparable rift shoulder uplift in the Red Sea and Gulf of Aden region (Watchorn et al., 1998; Abbate et al., 2001; Robertson and Bamakhalif, 2001; Autin et al., 2007) show that the topographically highest rift blocks can be closest to the newly forming oceanic basin, with sediment supply inland away from the rift shoulder.

In summary, the evidence suggests that the Tauride-Anatolide platform existed as a north-facing rifted margin at least from Triassic – Late Cretaceous. The platform was hundreds of kilometres wide, as indicated by the combined lateral extent of the Beyşehir-Hoyran-Hadim nappes and autochthonous Geyik Dağ. Complex rift blocks created intra-platformal basins, resulting in variable erosion and deposition across the platform. During the Late Triassic–Early Jurassic, a pulse of rift-related flexural uplift caused erosion of the rift-flank and deposition of continental and shallow-marine clastics across a large area of the platform. The irregular topography of rift-blocks resulted in variable depositional environments and sediment provenance; however, the palaeocurrent data suggests that sediment was mainly derived from an uplifted block in the north, and transported southwards away from this topographic high.

The platform had subsided by the Middle Jurassic and platform carbonates were deposited throughout the later Mesozoic. During the Late Cretaceous and Early Cenozoic, suturing of the Tethys ocean and emplacement of the Beyşehir-Hoyran-Hadim nappes was associated with regional compressional deformation throughout the Tauride platform.

Conclusions

1) Structural evidence (faulting and folding) does not support the existence of Late Triassic "Cimmerian" compressional tectonics within the Tauride platform. The entire Cambrian-Ordovician sequence has been deformed regionally, with a NW – SE axis of compression. All of the faulting and folding observed is consistent with Late Cretaceous and Early Cenozoic deformation related to closure of the Northern Neotethys, to the north of the area studied.

2) Available palaeontological evidence suggests that the Çayır Formation, a sequence of reddish coloured clastic continental/shallow-marine sediments, accumulated during Middle Triassic (Anisian) –Middle Liassic.

3) The Çayır Formation is a typically fining-upwards sequence with coarsest sediments at the base. The clastics overlie Middle – Upper Triassic platform carbonates and shales/sandstones, commonly with a low-angle angular discordance. The top of the formation is transgressed by massive Mesozoic platform carbonates.

4) Several different depositional environments are inferred from sedimentological evidence from the Çayır Formation (i.e. terrestrial braided river; alluvial fan; terrestrial/coastal overbank, deltaic and submarine channel).

5) Combined palaeocurrent data from 15 localities across the area show that sediment transport in the Çayır Formation was mainly from the north to the south, although flow was locally variable. This implies that a regional high was established to the north of the exposed Tauride platform during the Middle Triassic – Early Jurassic time.

6) The compositions of conglomerates and sandstones in the Çayır Formation suggests that this material was derived from the Palaeozoic and Triassic stratigraphy of the Tauride platform. There is a lack of sediment that could be derived from a metamorphic or magmatic source. Black chert within the Çayır Formation was probably derived from an Palaeozoic "basement" unit to the north of the area studied in detail.

7) Sedimentary evidence from the Çayır Formation is consistent with rift-related uplift, as seen in the Red Sea/Gulf of Aden region. The fining-upwards sequence, transgressed by carbonates, can be explained by a pulse of rift-related uplift prior to, or during, final continental break-up to form northern Neotethyan ocean.

8) No evidence has been found to support a previous hypothesis that a Palaeotethyan ocean finally closed in this area during the latest Triassic with emplacement of an Euarasian margin unit over a Gondwana-related ("Cimmerian") units. Instead, the evidence is consistent with Tethys in this region remaining open until Late Mesozoic-Early Cenozoic time

References

Abbate, E., Balestrieri, M.L. and Bigazzi, G., 2001. Uplifted rift-shoulder of the Gulf of Aden in northwestern Somalia: palinspastic reconstructions supported by apatite fission-track data. In: Ziegler, P. A., Cavazza, W., Robertson, A. H. F., and Crasquin-Soleau, S. (eds). Peri-Tethys Memoir 6: Peri-Tethyan Rift / Wrench Basins and Passive margins, Mémoirs du Muséum national d'Histoire naturelle(186): 629-640.

Andrew, T. and Robertson, A.H.F., 2002. The Beyşehir–Hoyran–Hadim Nappes: genesis and emplacement of Mesozoic marginal and oceanic units of the northern Neotethys in southern Turkey. Journal of the Geological Society, London, 159: 529–543.

Autin, J., Leroy, S., d'Acremont, E., Beslier, M.-O., Ribodetti, A., Courrèges, E., Perrot, J. and Bellahsen, N., 2007. Structure and evolution of the north-eastern Gulf of Aden margin. European Geosciences Union 2007, Geophysical Research Abstracts, 9.

Collins, A., 1997. Tectonic evolution of the Lycian Taurides. PhD Thesis, University of Edinburgh, Edinburgh, UK.

Collins, A. and Robertson, A.H.F., 1997. Lycian melange, southwestern Turkey: An emplaced Late Cretaceous accretionary complex. Geology, 25: 255-258.

Covey, M., 1986. The evolution of foreland basins to steady state: evidence from the western Taiwan foreland basin. In Allen, P. and Homewood, P. (eds) Foreland Basins. Special publication of the International Association of Sedimentologists, 8: 77-90.

Dean, W.T. and Monod, O., 1990. Revised stratigraphy and relationships of Lower Palaeozoic rocks, eastern Taurus Mountains, south central Turkey. Geological Magazine, 127(4): 333-347.

Delvaux, D., 2001. Tectonic and Palaeostress evolution of the Tanganyika-Rukwa-Malawi rift segment, East African Rift System. . In: Ziegler, P. A., Cavazza, W., Robertson, A. H. F., and Crasquin-Soleau, S. (eds). Peri-Tethys Memoir 6: Peri-Tethyan Rift / Wrench Basins and Passive margins, Mémoirs du Muséum national d'Histoire naturelle(186): 545-566.

Garzanti, E., Andò, S. and Scutellà, M., 2000. Actualistic Ophiolite Provenance: The Cyprus Case. The Journal of Geology, 108: 199-218.

Göncüoğlu, M.C., Turhan, N., Şentürk, K., Özcan, A., Uysal, Ş. and Yalınız, M.K., 2000. A geotraverse across northwestern Turkey: tectonic units of the Sakarya region and their tectonic evolution. In Bozkurt, E., Winchester, J. A. & Piper, J. D. A. (eds) Tectonics and Magmatism in Turkey and the Surrounding Area. Geological Society, London, Special Publication, 173: 139-161.

Göncüoğlu, M.C., Turhan, N. and Tekin, K., 2003. Evidence for the Triassic rifting and opening of the Neotethyan Izmir-Ankara Ocean and discussion on the presence of Cimmerian events at the northern edge of the Tauride-Anatolide Platform, Turkey. Bollettino della Societa Geologica Italiana Roma, Special publication, volume 2: 203-212.

Göncüoğlu, M.C., Yalınız, M.K. and Tekin, U.K., 2006. Geochemistry, tectono-magmatic discrimination and radiolarian ages of basic extrusives within the Izmir-Anakra suture belt (NW Turkey): Time constraints for the Neotethyan evolution. Ofioliti, 31(1): 25-38.

Gutnic, M., Monod, O., Poisson, A. and Dumont, J., 1979. Géologie des Taurides Occidentales (Turquie). Societé Géologique de France, Mémoir, 137: 1-112.

Manatschal, G., Muntener, O., Lavier, L.L., Minshull, T.A. and Peron-Pinvidic, G., 2007. Observations from the Alpine Tethys and Iberia Newfoundland margins pertinent to the interpretation of continental breakup. In Karner, G. D., Manatschal, G., and Pinheiro, L. M. (eds) Imaging, Mapping and Modelling Continental Lithosphere Extension and Breakup. Geological Society, London, Special Publication, 282.

Monod, O., 1977. Récherches géologique dans les Taurus occidental au sud de Beyşehir (Turique). PhD Thesis, Université de Paris-Sud, Orsay, France.

Monod, O. and Akay, E., 1984. Evidence for a Late Triassic - Early Jurassic orogenic event in the Taurides. In Dixon, J. E. & Robertson A. H. F. (eds) The Geological Evolution of the Eastern Mediterranean. Geological Society, London, Special Publication, 17: 113-122.

MTA, 2002. General Directorate of Mineral Research and Exploration - Geological Map of Turkey 1:500,000, Ankara.

Okay, A.I., Satır, M. and Siebel, W., 2006. Pre-Alpide Palaeozoic and Mesozoic orogenic events in the Eastern Mediterranean region. From: Gee, D.G. & Stephenson, R.A. (eds) European Lithosphere Dynamics. Geological Society, London, Memoirs, 32: 389-405.

Önder, F., 1984. Some concepts on the stratigrpahical and environmental investigation on the Triassic rocks of Central Taurus Mountains. In Tekeli, O. and Göncüoğlu, M. C. (eds) Geology of the Taurus belt, MTA, Ankara: 91-99.

Özgül, N., 1984. Stratigraphy and tectonic evolution of the Central Taurides. In Tekeli, O. and Göncüoğlu, M. C. (eds) Proceedings of the International Symposium on the Geology of the Taurus belt, MTA, Ankara: 77-90.

Özgül, N., 1997. Bozkir Hadim Taşkent Dolayinda yer alan tektono-stratigraphic briliklerin Stratigrafisi, (translated into English by Fatih Karaoğlan, Çukurova Universitesi). MTA Dergisi, 119: 113-174.

Robertson, A.H.F., 2007a. Geochemical evidence for the sedimentary and diagenetic development of the Mesozoic - Early Cenozoic Newfoundland rifted margin, Northwest Atlantic (Ocean drilling program Leg 210, Site 1276). In: Tucholke, B.E., Sibuet, J.-C., and Klaus, A. (Eds.) Proceedings of the Ocean Drilling Program, Scientific Results Volume 210.

Robertson, A.H.F., 2007b. Overview of tectonic settings related to the rifting and opening of Mesozoic ocean basins in the Eastern Tethys: Oman, Himalayas and Eastern Mediterranean regions. In Karner, G. D., Manatschal, G., and Pinheiro, L. M. (eds) Imaging, Mapping and Modelling Continental Lithosphere Extension and Breakup. Geological Society, London, Special Publication, 282: 325-388.

Robertson, A.H.F. and Bamakhalif, K.A.S., 2001. Late Oligocene-early Miocene rifting of the northeastern Gulf of Aden: basin evolution in Dhofar (southern Oman). In: Ziegler, P. A., Cavazza, W., Robertson, A. H. F., and Crasquin-Soleau, S. (eds). Peri-Tethys Memoir 6: Peri-Tethyan Rift / Wrench Basins and Passive margins, Mémoirs du Muséum national d'Histoire naturelle (186): 641-670.

Robertson, A.H.F. and Dixon, J.E., 1984. Introduction: aspects of the geological evolution of the Eastern Mediterranean. In Dixon, J. E. & Robertson A. H. F. (eds) The Geological Evolution of the Eastern Mediterranean. Geological Society, London, Special Publication, 17: 1-74.

Robertson, A.H.F., Ustaömer, T., Pickett, E.A., Collins, A.S., Andrew, T. and Dixon, J.E., 2004. Testing models of Late Palaeozoic - Early Mesozoic orogeny in Western Turkey: support for an evolving open-Tethys model. Journal of the Geological Society, London, 161: 501-511.

Şengör, A.M.C. and Yılmaz, Y., 1981. Tethyan Evolution of Turkey: A plate tectonic approach. Tectonophysics, 75: 181-241.

Stampfli, G.M., 2000. Tethyan oceans. In Bozkurt, E., Winchester, J. A. & Piper, J. D. A. (eds) Tectonics and Magmatism in Turkey and the Surrounding Area. Geological Society, London, Special Publication, 173: 1-23.

Stampfli, G.M. and Borel, G.D., 2002. A plate tectonic model for the Paleozoic and Mesozoic constrained by dynamic plate boundaries and restored synthetic oceanic isochrons. Earth and Planetary Science Letters, 196: 17-33.

Stampfli, G.M., Mosar, J., Favre, P., Pellevuit, A. and Vannay, J.-C., 2001. Permo-Mesozoic evolution of the western Tethys realm: the Neo-Tethys East Mediterranean Basin connection. In Ziegler, P., Cavazza, W., Robertson, A.H.F., & Crasquin-Soleau, A. (eds) Peri-Tethyan Rift/Wrench Basins and Passive Margins. Peri-Tethys Memoire, 5: 51-108.

Tekin, U.K., Göncüoğlu, M.C. and Turhan, N., 2002. First evidence of Late Carnian radiolarians from the Izmir–Ankara suture complex, central Sakarya, Turkey: implications for the opening age of the Izmir–Ankara branch of Neo-Tethys. Geobios, 35: 127-135.

Watchorn, F., Nichols, G.J. and Bosence, D.W.J., 1998. Rift-related sedimentation and stratigraphy, southern Yemen (Gulf of Aden). In Purser, B. H., and Bosence, D. W. J (eds) Sedimentation and Tectonics of Rift Basins: Red Sea-Gulf of Aden. Chapman & Hall, London: 165-189.

Yilmaz, Y., Tüysüz, O., Yiğitbas, E., Gen, S.C. and Şengör, A.M.C., 1997. Geology and tectonic evolution of the Pontides. In: Robinson, A. G. (ed) Regional and Petroleum Geology of the Black Sea and Surrounding Region. American Association of Petroleum Geologists, Memoirs, 68(183-226).

Appendix B

X-ray fluorescence.

Whole rock chemical analysis was carried out by x-ray fluorescence at the School of Geosciences, University of Edinburgh. Techniques were used as described by Fitton et al. (1985; 1998).

Approximately 50 g of rock was crushed, and any alteration or veining was removed. The sample was then ground to a fine-grained uniform powder in a tungsten carbide tema mill for two minutes. Powder was then dried in an oven overnight.

For major element analysis, measured quantities of lithium flux were added to previously ignited powder samples. These were fused at 1100ºC then pressed into glass discs. The samples were analysed using standard procedures on the Edinburgh University Phillips 1280 wavelength dispersive sequential X-ray fluorescence spectrometer.

For minor element analysis, powder was pressed into pellets after mixing the powder with a binding agent, and compressing to 8 tons using a hydraulic press. These were analysed using the same spectrometer as described above.

Sample name Jan-20	Measurement date	Measurement time	Sum of conc. (%)	Result type	SiO2 -- (%)	Al2O3 Al (%)	Fe2O3 Fe (%)	MgO Mg (%)	CaO Ca (%)	Na2O Na (%)
T30	13/11/2006	17:47	100	Concentration	52.52	15.69	10.05	1.62	5.46	7.93
T31	13/11/2006	18:10	100	Concentration	41.74	12.7	11.12	1.86	11.16	4.99
T34	13/11/2006	18:22	100	Concentration	45.65	13.4	10.72	5.35	11.56	3.36
T50	13/11/2006	18:44	100	Concentration	46.02	16.26	7.55	1.62	12.89	5.77
T51	13/11/2006	18:54	100	Concentration	49.93	17.2	8.47	3.71	7.87	5.93
V1	05/01/2006	20:25	100	Concentration	46.19	12.94	11.15	8.4	9.03	3.36
V2	05/01/2006	20:51	100	Concentration	47.96	18.02	7.38	3.92	5.89	5.89
S1	05/01/2006	17:28	100	Concentration	41.04	14.91	5.26	1.96	15.52	0.97
S2	05/01/2006	17:53	100	Concentration	38.43	10.49	4.09	1.01	22.05	0.48
S3	05/01/2006	18:19	100	Concentration	29.81	8.99	3.51	1.38	28.52	0.42
S4	05/01/2006	18:44	100	Concentration	56.35	22.29	7.44	1.42	0.64	0.84
S5	05/01/2006	19:09	100	Concentration	38.83	7.44	2.94	0.68	25.21	0.29
S6	05/01/2006	19:35	100	Concentration	38.87	8.27	3.33	0.83	23.82	0.34
S7	05/01/2006	20:00	100	Concentration	32.77	5.2	2.18	0.66	30.76	0.15
S8	13/11/2006	19:06	100	Concentration	60.31	18.94	7.72	2.24	0.59	0.67
XX4	05/01/2006	21:41	100	Concentration	2.81	1.1	0.79	1.75	50.79	-0.01
XX14	05/01/2006	22:07	100	Concentration	94.5	0.2	0.08	0.21	2.32	-0.05
V4	05/01/2006	21:16	100	Concentration	22.72	9.8	7.44	0.76	29.75	0.12
PWM-K1	13/11/2006	17:47	100	Concentration	91.8	3.09	2.02	0.42	-0.15	-0.35
LW11	15/11/2006	15:06	100	Concentration	51.58	15.57	10.09	6.78	9.37	3.23
LW12	15/11/2006	15:16	100	Concentration	50.18	15.64	10.2	6.84	10.42	3.36

	K2O K (%)	TiO2 Ti (%)	MnO Mn (%)	P2O5 P (%)	Zn Zn (ppm)	Cu Cu (ppm)	Ni Ni (ppm)	Cr Cr (ppm)	V V (ppm)	Ba Ba (ppm)	Sc Sc (ppm)
T30	0.461	2.108	0.052	0.124	190	164.9	69.7	221.6	167.3	103.5	22.5
T31	1.173	2.969	0.067	0.455	181.7	128.5	161.2	373.6	234.2	106.6	24.1
T34	1.357	2.047	0.204	0.2	103.2	41.2	58	137.4	371	122.6	45.5
T50	0.379	1.421	0.104	0.277	45	25.7	51.6	91.1	171.3	76.9	27.6
T51	1.389	1.928	0.135	0.425	73.9	12.7	54.7	86.3	196.2	160.6	21.9
V1	0.166	2.623	0.121	0.478	94.6	45.5	272.1	497	230.6	78.8	20
V2	0.844	1.585	0.047	0.357	193	21.8	103.1	184.4	200.4	96.7	29.4
S1	2.487	0.662	0.046	0.079	40.8	15.9	28.7	95.6	111	274.1	11.8
S2	1.931	0.53	0.038	0.158	98.1	18.3	31.1	84.2	100.5	266.7	6
S3	1.826	0.379	0.044	0.064	71.9	23.2	24.4	52.1	69.5	216.9	1.7
S4	3.795	0.981	0.023	0.122	125.3	38.3	44.8	115	138.1	637.2	28
S5	1.784	0.471	0.024	0.091	18.4	17.4	22.3	66.7	72.6	136.6	0.1
S6	1.992	0.523	0.024	0.113	20.5	16.3	21.3	65.9	74	195.2	1.2
S7	1.238	0.324	0.027	0.15	23.5	14.8	20.5	54.9	51.5	141.9	-6.3
S8	2.877	0.865	0.064	0.137							
XX4	0.336	0.064	0.088	0.075	10.3	10.4	20.3	8.4	33.1	133.2	-19
XX14	0.055	0.013	0.002	0.008	-0.3	4.7	-13.9	-1.8	-1.7	57.4	-1.3
V4	1.57	0.465	0.031	20.727	38.4	19.3	34.6	63.4	115.4	253.3	-3.3
PWM-K1	1.009	0.248	0.004	0.037							
LW11	0.492	1.027	0.163	0.048							
LW12	0.066	0.988	0.175	0.048							

	U U2 (ppm)	Rb Rb1 (ppm)	Th Th (ppm)	Pb Pb (ppm)	Nb(ZYN2) Nb (ppm)	Zr Zr1 (ppm)	Y Y (ppm)	Sr Sr (ppm)	La La (ppm)	Ce Ce (ppm)	Nd Nd (ppm)
T30	1	13.1	0.1	4.2	12	103	25.1	375.6	1.6	9.1	8.2
T31	1	24.7	2.5	1.7	42.9	190.6	16.3	214.7	17.8	50.8	26.3
T34	0.7	20.3	0.8	0.3	8.4	149.2	40.7	190.9	4.6	23.9	17.2
T50	0.8	9.4	0.6	1.8	17.4	149.2	27.8	268.5	10	31	16.4
T51	0.5	24.4	1.2	1.6	30.4	227.9	37.8	190.6	14.1	40.5	21.6
V1	1.3	2.3	2.8	1.8	41.4	194.9	18.3	357.3	21.8	51.8	25.7
V2	1.7	22.4	1.2	4.6	21.4	172.2	23.9	110	7.3	17.3	12.6
S1	2.4	97.4	13.9	20.3	19.2	124.7	26.1	482.2	48.2	96.3	40.7
S2	2.2	72.5	10.6	18.9	14.9	101.6	25.9	414.2	44.3	80.5	37.2
S3	2.2	68.3	7.2	8.9	9.2	93.7	14.9	507.4	29.1	54.5	26.6
S4	3.3	164.3	15.9	14.8	19.8	167.1	34.1	89.5	58.7	110.9	49
S5	1.8	54.7	7.8	19.1	12.2	130.5	23.8	282.5	37.1	68.6	34.8
S6	1.6	60.7	8	20.1	13	139	25.4	314.2	35.7	71.8	34.3
S7	1.3	40.8	5.4	10.2	8.1	92.5	19.7	346.4	29.5	52.6	25.5
S8											
XX4	0.8	11.3	1.5	5.1	1.5	9.8	10.7	549.5	15.9	27.9	13.6
XX14	0.7	2.7	0.1	0.1	0.4	1	-0.1	24.6	-1.4	0.8	0.1
V4	17.9	49.3	24	15.9	10.5	120.1	404.2	822.7	217.7	403.1	254.7